Towards matter-wave experiments with biomolecules: Generation and detection of neutral biomolecular beams

Inauguraldissertation

zur

Erlangung der Würde eines Doktors der Philosophie

vorgelegt der

Philosophisch-Naturwissenschaftlichen Fakultät

der Universität Basel

von

Jonas Martin Schätti

aus Basel BS, Schweiz

Basel, 2019

Genehmigt von der Philosophisch-Naturwissenschaftlichen Fakultät

auf Antrag von

Prof. Dr. Marcel Mayor

Prof. Dr. Thomas R. Ward

Basel, den 21.05.2019

Prof. Dr. Martin Spiess

Dekan

Acknowledgments

First I would like to thank my supervisor Dr. Valentin Köhler for asking me to do the Ph.D. in his group. Without him, I would never have come in touch with the exciting field of matter-wave interference. Furthermore, I would like to thank him for the great support during the 4.5 years of my time in his group.

I want to thank Prof. Dr. Marcel Mayor for making this project possible as my Ph.D. examiner and as the faculty responsible professor. His advice, support, suggestions and creative input enabled the succesful conclusion of my PhD work.

I want to thank Prof. Dr. Thomas R. Ward for his commitment to being the co-examiner and for hosting me in his labs during my Ph.D.

I am grateful to Prof. Dr. Markus Arndt for being the external expert, without him and the collaboration with his group this thesis would not have been possible.

A big thank you goes to all the people who contributed to this thesis; there were so many that I cannot mention all of them here. I thank Dr. Ugur Sezer and Dr. Joseph Cotter for the collaboration on the evaporable peptides. Dr. Ugur Sezer and Philipp Rieser for the laser desorption/photoionization experiments. Dr. Maxime Debiossac and Moritz Kriegleder for the collaboration during the photocleavable project and Dr. Lukas Felix for the synthesis of the first photocleavable building block. Dr. Joseph Cotter, Dr. Lukas Mairhofer, Dr. Stefan Gerlich and Yaakov Fein for trying everything to make matter-wave interference with peptides possible. Dr. Armin Shayeghi for advice and his drive during all the collaborations with Arndt group.

I want to thank Dr. Hendrik Mallin, Juliane Klehr and Jaicy Vallapurackal for the help with the biological part of this thesis.

Thanks go to Fadri Christoffel for proofreading the experimental part of this thesis.

I want to thank the analytical team: Dr. Heinz Nadig, Dr. Michael Pfeffer and Sylvie Mittelheisser for measuring HRMS; PD. Dr. Daniel Häussinger, Dr. Thomas Müntener and Daniel Joss for helping with NMR problems and for keeping the NMR working nicely the whole time.

Thanks to the Werkstatt team for their support and a special thanks to Philipp Knöpfel for building an evaporation chamber for us.

I would like to thank the administrative team (Claudia Wirth, Andreas Baumgartner, Michéle Wegmann, Isa Worni, Ester Stalder, Beatrice Erismann, Brigitte Howald)

I want to thank the Swiss Nanoscience Institute (SNI) for funding.

I want to thank all the people from all the groups I was part of during my Ph.D. I enjoyed the time with all of you in the

Ward group: Isabel, Daniel, Yoann, Holly, Ali, Yasu, Ryan, Jo, Joan, Alain, Fadri, Brett, Nico, Boris, Corentin, Valerio, Alina, Jaicy, Valérie, Amanda, Juliane, Tillmann, Martina, Miriam, Sascha, Vincent, Hendrik, Michela, Emeline, Fabian, Shuke, Jingming, Yi, Raphael, Nobutaka, Marc, Ewa, Maxime, Christian

Mayor group: Eric, Thomas, David, Loïc, Rajesh, Almudena, Alfredo, Erich, Laurent, Lorenzo, Patrick, Peter, Linda, Florian, Ksenia, Tomáš, Yves, Kevin, Michal, Ina, Manuel, Viktor, Mario, Prince, Lukas, Lukas, Michel, Sylvie

Arndt group: Ugur, Maxime, Armin, Moritz, Philipp, Georg, Philipp, Joe, Sebastian, Christian, Yaakov, Stefan, Lukas

and the SNI PhD school: Jan, Mina, Thomas, Deepika, Claudio, Christina, Marietta, Svenja, Panagiotis, Mirko, Wojciech, Lujun, David, Paolo, Noah, Shubham, Shabnam, Stefano, Luc, Lukas, Mehdi, Joanan David, Toshiya, Lukas, Thomas, Jann, Claudio, Luca, Tamara,Tomaz, Nora, Ian, Clevin, Arne, Davide, Yushuke.

Finally, yet importantly I would like to thank my family for their support during the whole time towards my Ph.D.

Outline of the thesis

This thesis summarizes the work performed from January 2015 – April 2019 as part of a collaboration between the Köhler group (University of Basel), Marcel Mayor (University of Basel) and the Arndt group (University of Vienna). The author JS designed experiments in collaboration with the Arndt group and performed synthesis and protein production at the University of Basel. The evaporation tests and laser desorption post-ionization studies, as well as the photocleavage experiments, were performed by the Arndt group with some assistance from the author during two research stays in Vienna for one and two weeks, respectively. Parts of this thesis have been published in peer reviewed journals.

Aim of the thesis

The thesis aimed to identify chemical modifications for biomolecules such as peptides and proteins to make these amenable for matter-wave interference experiments. Crucial for matter-wave interference experiments are charge neutral biomolecular beams, which had previously only been successfully formed for small peptides in a limited number of studies. Accordingly, a main focus of the thesis was set on the formation of such beams in close collaboration with M. Arndt's group in Vienna. A second difficulty arises from the fact that neutral molecules are not detectable with common mass spectrometer detectors, i.e. electron multipliers. Consequently the ionization of neutral protein beams in high vacuum was a second central point of the presented studies.

Various methods and approaches were investigated whereby the contribution of the author was concentrated on the design, synthesis and expression of the constructs for interrogation in matter-wave experiments. A summary of the individual chapters is followed by a short and selective introduction to MS-based methods for the study of biomolecules in the gas-phase.

Summary of individual chapters

Chapter 1.

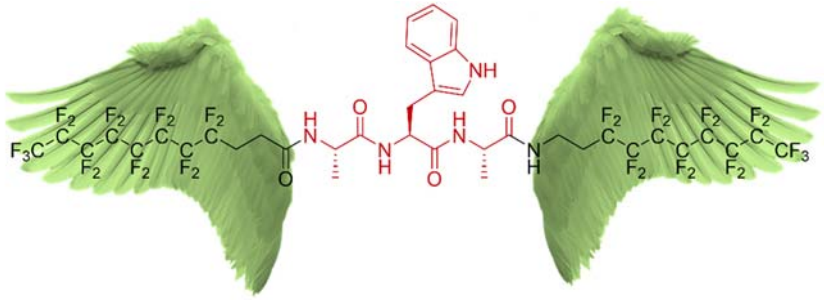

Tripeptides (Ala-Trp-Ala and sequence isomers) were chemically modified to reduce their intermolecular interactions and to enable their thermal evaporation. The attachment of fluor-inated alkyl chains to the N- and C-terminus of the peptides was identified as a suitable modification in this respect. Permethylation of all NH- groups together with charge removal at the termini by acetylation and amidation, respectively, also improved the volatility, but was accompanied by increased fragmentation. The thermally formed neutral peptide beam was then ionized by electron impact, or VUV photo-ionization (157 nm) and the two ionization methods compared. Electron impact led to strong peptide fragmentation and a weak signal for intact peptide ions. In contrast, VUV ionization produced much 'cleaner' spectra, where - apart from the intact peptide ion - only fragments of the tryptophan sidechain, i.e. the indole and the skatole cation, were observed. Thermal evaporation of a significantly larger construct, based on $(Trp\text{-}Lys)_4$-Trp where every lysine side chain and the N-terminus were amidated with fluorinated alkyl chains, was not successful and resulted in decomposition.

Chapter 2.

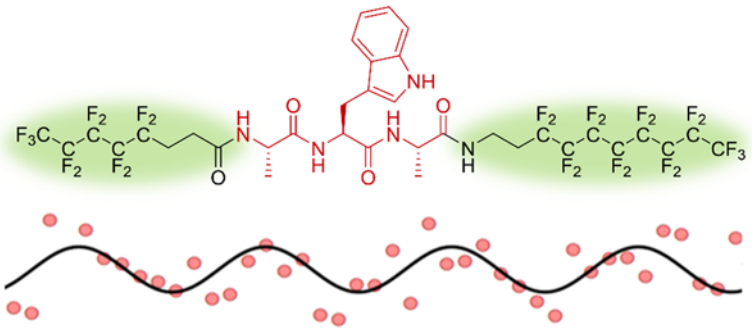

Introduction to matter-wave interference experiments. The progress in matter-wave interference since its inception is briefly summarized with a focus on the work performed in the group of Markus Arndt, University of Vienna. Matter-wave interference experiments on functionalized tripeptides are presented.[1] The first ever measured interference pattern of a peptide was recorded on the Kapitza–Dirac–Talbot–Lau interferometer (KDTLI). Interference pattern of sequence isomers were observed with the newly built long baseline Universal Matter-wave Interferometer (LUMI) – an extended version of the KDTLI. Attempts to distinguish two sequence isomers in an interference experiment based on their differences in polarizability are discussed.

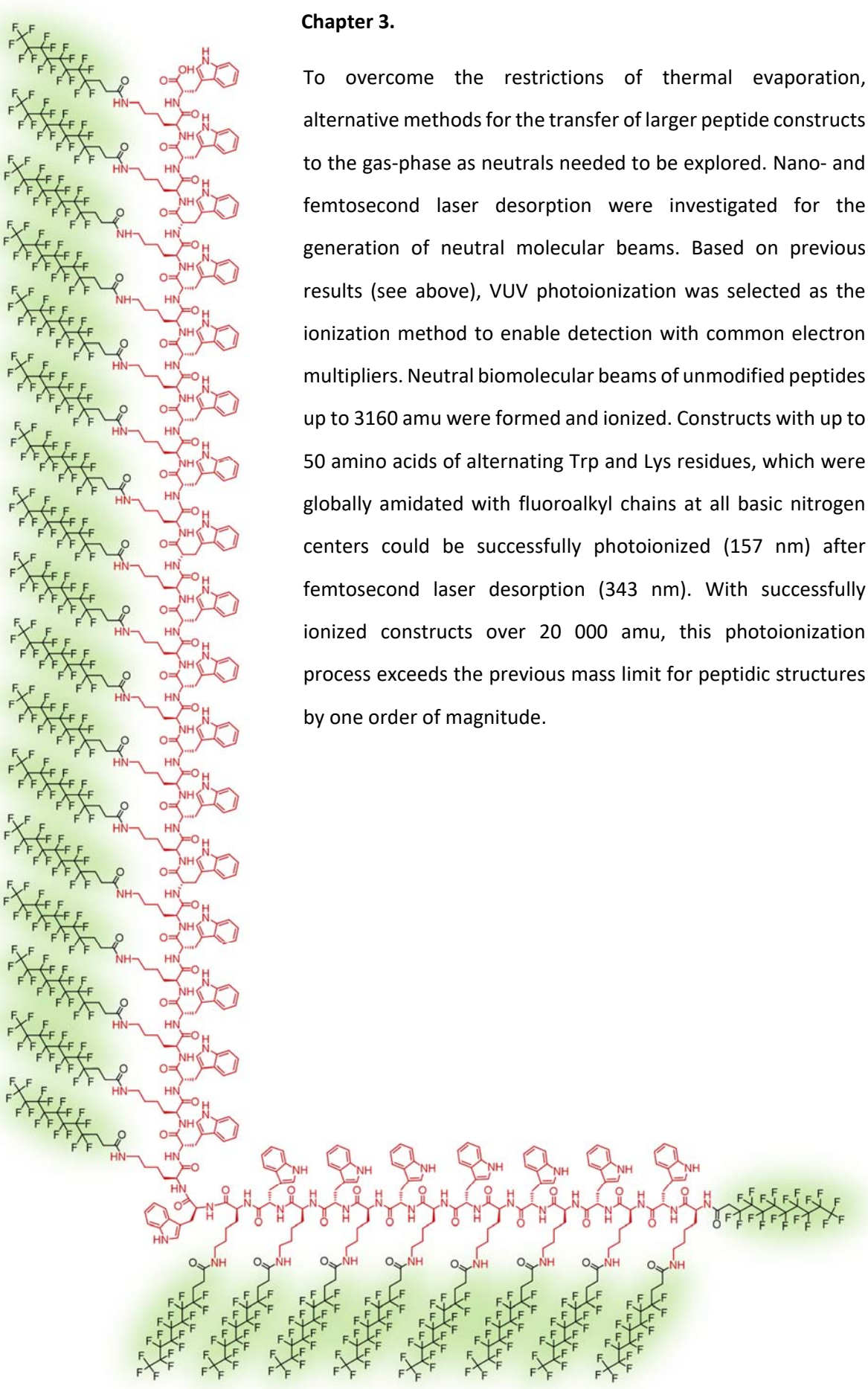

Chapter 3.

To overcome the restrictions of thermal evaporation, alternative methods for the transfer of larger peptide constructs to the gas-phase as neutrals needed to be explored. Nano- and femtosecond laser desorption were investigated for the generation of neutral molecular beams. Based on previous results (see above), VUV photoionization was selected as the ionization method to enable detection with common electron multipliers. Neutral biomolecular beams of unmodified peptides up to 3160 amu were formed and ionized. Constructs with up to 50 amino acids of alternating Trp and Lys residues, which were globally amidated with fluoroalkyl chains at all basic nitrogen centers could be successfully photoionized (157 nm) after femtosecond laser desorption (343 nm). With successfully ionized constructs over 20 000 amu, this photoionization process exceeds the previous mass limit for peptidic structures by one order of magnitude.

Chapter 4.

Inspired by the successful laser desorption/photoionization experiments performed with tryptophan-rich peptide constructs, tryptophan-rich tags were genetically added to ubiquitin and the ribosomal protein S6 to make these proteins amenable to photoionization after laser desorption. No protein cations could be observed after femtosecond laser desorption followed by VUV ionization when applying the optimized conditions described in chapter 3. It remains unclear whether desorption or ionization or both are responsible for the failure of the experiment.

Chapter 5.

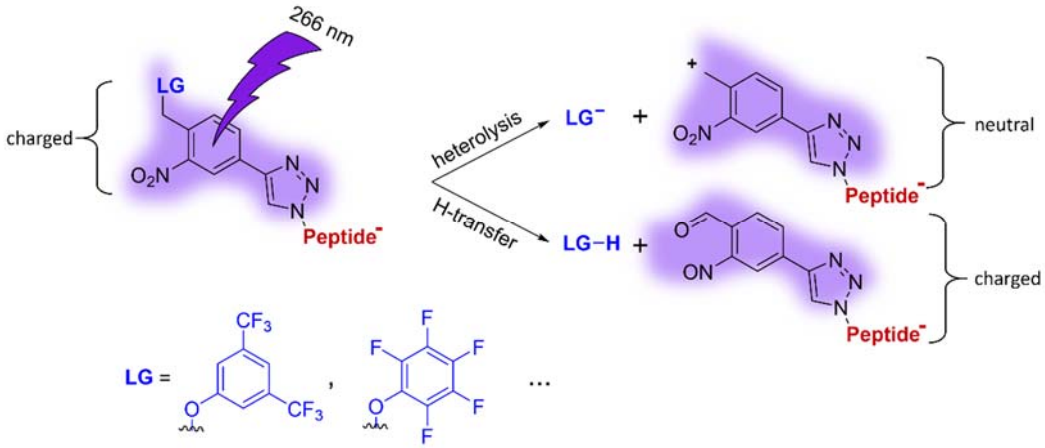

As an alternative to the laser desorption/photoionization strategies, the formation of a neutral molecular beam by photocleavage of electrosprayed ions was investigated. Peptides with up to 12 amino acids were functionalized with a photocleavable tag. The tag consists of an *ortho*-nitroarylether with a 3,5-bis(trifluoromethyl)phenol as a leaving group. Upon irradiation of the peptide anion with 266 nm light the ether bond breaks and liberates the phenolate/phenol and a peptide fragment. Two cleavage mechanisms were observed: (i) bond cleavage under heterolysis leading to a charged phenolate and a neutral zwitterionic peptide fragment; (ii) bond cleavage under H-transfer in analogy to solution phase behavior. In the latter case, a neutral phenol fragment and a charged peptide fragment are formed. The influence of the leaving group and the peptide length on the cleavage mechanism were investigated. With increasing chain length the mechanism under H-transfer, which was not observed for tripeptides, becomes dominant, rendering the method already unsuitable for the neutralization of peptides with nine amino acids (see also chapter 6).

Chapter 6.

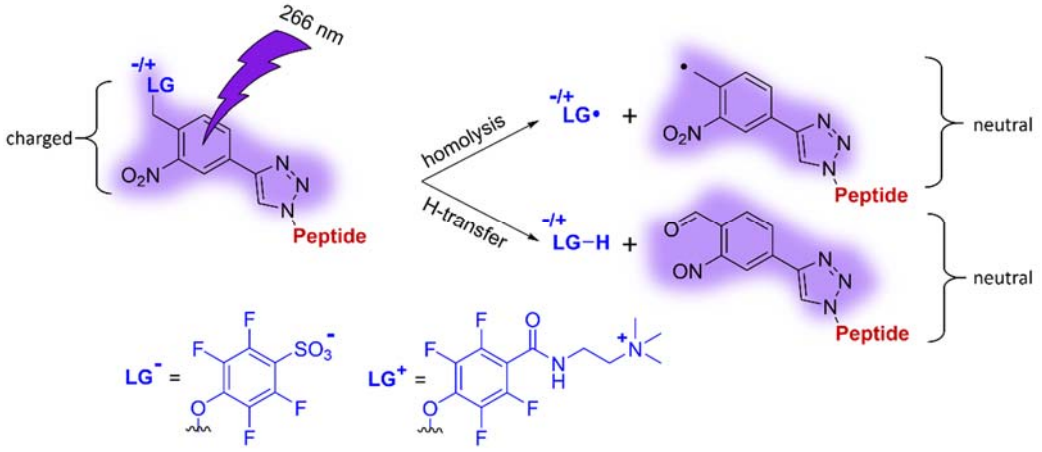

By introduction of a permanent charge ($-SO_3^-$, $-NMe_3^+$) on the phenol leaving group neutralization of larger peptides and even insulin was realized. Intriguingly, the new photocleavable constructs cleave under bond homolysis and under H-transfer, but not under heterolysis in contrast to the constructs described in chapter 5. Starting from a singly charged ion, independent of the mechanism a neutral peptide moiety can be generated by photocleavage. Starting from multiple charged species photoinduced charge reduction can be performed – in this case, both moieties - peptide and the leaving group - remain charged and can be detected by mass spectrometry. In combination with charge reduction by an ionized buffer gas this method enabled the neutralization of insulin constructs.

Chapter 7.

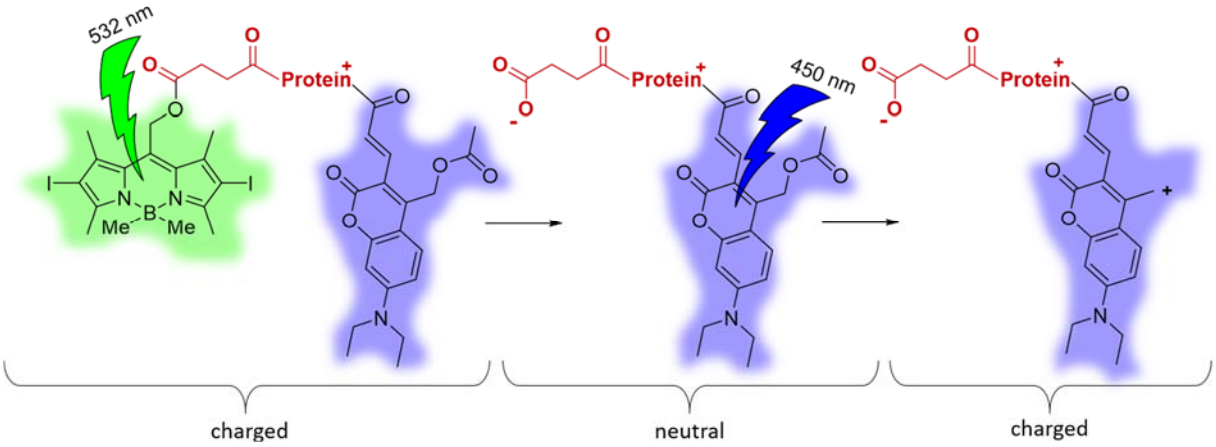

New photocleavable tags for cleavage under visible light irradiation were identified to prevent competitive absorbance from aromatic amino acid side chains of the peptide or protein. Two model compounds for orthogonal tags were synthesized, an aminocoumarin and a BODIPY based one, which cleave in solution upon irradiation at 450 nm and 532 nm, respectively. Employing two wavelength-orthogonal tags on the same biomolecule should allow to i) first neutralize the biomolecule at a longer wavelength and ii) subsequently reionize at a shorter wavelength for MS detection. The first set of coumarin and BODIPY based cleavable model compounds has been prepared and awaits testing of its gas-phase cleavage behavior.

Table of Contents

Publications and unpublished work

Introduction. Mass spectrometry related methods for the study of biomolecules in the gas-phase

Although the goal of this thesis was to generate and detect neutral protein beams for interference experiments, all studies involved elements of mass spectrometry. To illustrate the wider research context, a few selected methods related to the gas-phase study of biomolecules as ionic species are briefly presented in the following.

Exploration of larger biomolecules in the gas-phase passed a major milestone in 1988 with the report on Matrix-Assisted Laser Desorption Time Of Flight mass spectrometry (MALDI-TOF) for cytochrome-c and other small proteins by the group of Koichi Tanaka.[1] One year later John B. Fenn showed that Electrospray Ionization Mass Spectrometry (ESI-MS) was also capable of producing monodisperse protein ions in the gas-phase. [2] ESI-MS has the advantage that it can be easily coupled to liquid chromatography.[3] In 2002 both group leaders were awarded the noble prize in chemistry. Mostly based and enabled by these two methods, MALDI and ESI, a new field of research started to develop in the last three decades – namely the investigation of protein properties in the gas phase in addition to their mass. While MALDI is producing predominantly singly charged ions, mainly multiple charged ions are formed in the case of ESI for larger biomolecules. Around the year 2000, Lloyd M. Smith presented a method to generate singly charged protein ions with an electrospray ion-source in combination with an ionized buffer gas. In the so-called Charge Reduction Electrospray Mass Spectrometry (CREMS) a neutralization chamber is placed between the ESI nozzle and the entrance of the mass spectrometer., In this chamber, the multi-charged ions are charge-reduced by proton-transfer with ionized gas molecules of inverse charge. The neutralization gas itself, which is typically air, can be ionized by either α-particles or by corona discharge.[4-5]

Fragmentation-based methods were designed to obtain information about the amino acid sequence and to some extent posttranslational modifications.[6] In a typical protocol, the protein is first digested into smaller peptides by a protease, the fragments are separated on-line by HPLC, and further fragmentation follows in the mass spectrometer. This fragmentation can be either initiated by collision with buffer gas molecules (collision-induced dissociation),[7-10] by absorption of electrons (electron capture dissociation)[11-13] or by absorption of multiple infrared photons (infrared multiphoton dissociation).[14-17] Light of shorter wavelength than infrared has also been employed in so-called light-induced fragmentation.[18-20]

Selective labeling of the protein of interest before digestion with an isobaric tag enables a quantitative comparison of protein concentrations in complex samples, e.g., before and after induction of expression. To accomplish this, the protein in the mixtures to be compared is labeled with complementary isobaric tags from a set. An isobaric tag consists of a reporter group, a balance group and a functional group for the modification of the protein. When the modified peptide/protein is fragmented by CID, the reporter group provides a characteristic signal. By introducing heavy isotopes into the reporter group, fragments of different mass will be formed, if complementary isobaric labels with isotopomeric reporter groups are employed. The total mass of the peptide/protein is balanced by the balance group, hence the term isobaric. The samples labeled with complementary isobaric tags are then combined, digested, the relevant fraction separated chromatographically and the peak of interest mass-selected and fragmented. By comparing the integrals of the isotopomeric reporter groups the relative protein/peptide concentration can be determined. By addition of a reference sample of known concentration the unknown amount of peptide/protein can be quantified.[21-23]

Performing an H/D exchange before digestion can provide information on the 3-D solution structure of the protein. Acidic protons on the surface of the protein will exchange much faster than those buried inside.[24] H/D exchange experiments can also be performed on the whole protein in the gas-phase by collision with D_2O to investigate the structure within the mass spectrometer.[25-27] Thanks to the development of native MS, where near physiological conditions are applied for sample injection, it is now possible to maintain and study intermolecular interactions in the gas-phase.[28-29]

Native MS was the starting point for several new techniques to gain information about the tertiary and quaternary structure of proteins in the gas-phase. By performing IR spectroscopy in the gas-phase, different bands were observed for amide bonds in dependence of the secondary structure element they are part of. This can be exploited to determine the content of a secondary structural element in the protein.[30,31] With Ion-Mobility-Spectrometry-Mass Spectrometry (IMS-MS) the cross-section of the protein, and therefore to a certain extent its shape, can be investigated by analyzing the time the ion needs to pass a chamber with buffer gas.[32-34] IMS-MS has also been employed to study the dynamics of molecules in the gas-phase.[35]

The phenomenon of Förster Resonance Energy Transfer (FRET) is employed as an alternative method to gain information about the 3-D structure of proteins. It is widely exploited in solution measurements,[36] but can also be applied in the gas-phase.[37-39] For FRET measurements the molecule of interest is regio-selectively tagged with two fluorophores, one donor and one acceptor fluorophore. The molecule is irradiated at the absorbance maximum of the donor, which results in its electronic excitation. The energy is then transferred to the acceptor, and the acceptor finally releases a portion of the energy as a photon of longer wavelength. The distance between donor and acceptor can be

estimated by the efficiency of the process, i.e. the quantum yield.[22] Whereas FRET is used to determine long distances (25-75 Å), fluorescence quenching can be employed for shorter distances.[40] Besides the so far mentioned methods there are fragmentation based methods to gain information about the tertiary structure of proteins in the gas-phase. In so-called action FRET, the excitation of the donor leads to fragmentation of an acceptor in dependence on the distance between them.[41] Other excitation energy transfer mechanisms can be employed similarly to FRET to accomplish fragmentation at shorter distances (0-25 Å).[42]

The goal of this thesis was to implement matter-wave interferometry (see Chapter 2) as a sensitive tool to investigate biomolecules in the gas-phase.[43] In contrast to the methods outlined above, matter-wave interference experiments rely on neutral molecular beams, because charged species would interact too strongly with the gratings and would not give rise to interference patterns. The ability to form controlled and cold neutral beams of biomolecules would not only open the door for interference experiments but also for classical deflectometry[44-45] or the investigation of controlled gas phase reactions.[46-47] The transfer of neutral biomolecules into the gas phase is - somewhat surprisingly - much less investigated, and their detection is not as easily accomplished as for their charged equivalents. Within the context of this thesis three methods for the generation of neutral bio-molecular beams were developed (Figure 1): (a) Thermal evaporation; (b) nano- and femtosecond laser desorption; (c) neutralization of electro sprayed ions by photocleavage.

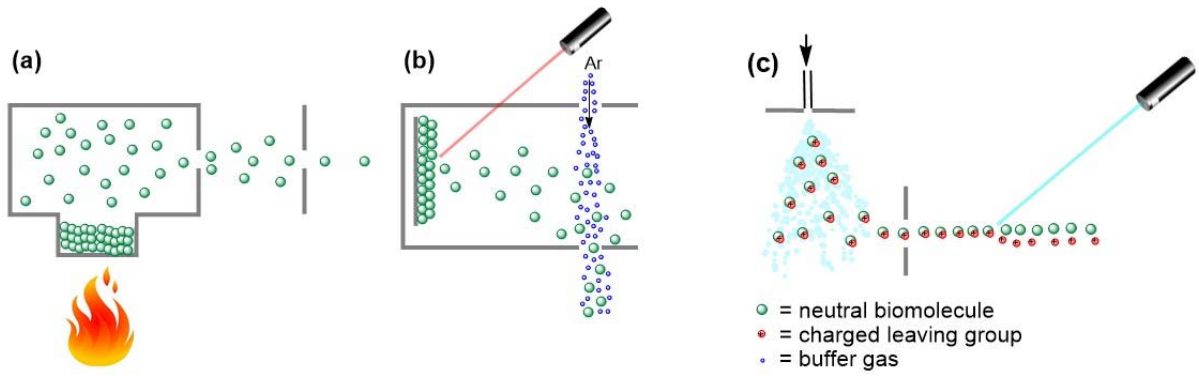

Figure 1. Methods for the generation of neutral molecular beams investigated in this thesis. (a) Thermal evaporation of modified peptides in an oven; (b) nano- and femtosecond laser desorption of modified and unmodified peptides; (c) neutralization of electrosprayed peptides and proteins by photocleavage.

The detection of the neutral molecules formed was investigated (Figure 2): (a) by electron impact ionization; (b) by photoionization (157 nm); (c) and by the indirect proof of neutrals after the photocleavage event by detection of a charged leaving group fragment.

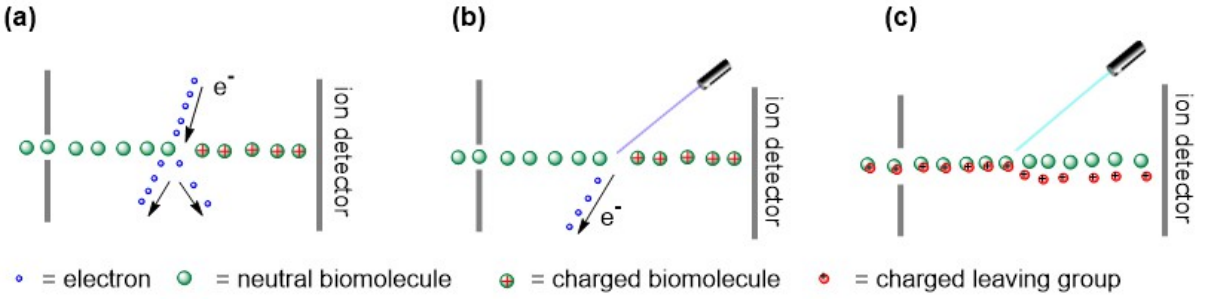

Figure 2. Methods for the detection of the neutral molecular beams investigated within the scope of this thesis. (a) Electron-impact ionization; (b) VUV photoionization (157 nm); (c) the indirect proof of neutrals after the photocleavage event by detection of a charged leaving group (compare Figure 1c). The last method could potentially also be employed for the ionization of neutrals.

The ability to control the charge state of a protein in the gas-phase, which can be realized by the controlled photocleavage of a tagged protein as described in chapter 6, is intriguing, considering that the charge state has a significant impact on the tertiary and quaternary structure.[32] However, due to time and resource limitations, such structural investigations have not been conducted yet and will have to be revisited at a later stage of the project.

References

1. T. Yoshida; K. Tanaka; Y. Ido; S. Akita; Y. Yoshida, Detection of High Mass Molecular Ions by Laser Desorption Time-of-Flight Mass Spectrometry. *J. Mass Spectrom. Soc. Jpn.* **1988,** *36* (2), 59-69.
2. J. Fenn; M. Mann; C. Meng; S. Wong; C. Whitehouse, Electrospray ionization for mass spectrometry of large biomolecules. *Science* **1989,** *246* (4926), 64-71.
3. C.-K. Lim; G. Lord, Current Developments in LC-MS for Pharmaceutical Analysis. *Biol. Pharm. Bull.* **2002,** *25* (5), 547-557.
4. D. D. Ebeling; M. S. Westphall; M. Scalf; L. M. Smith, Corona Discharge in Charge Reduction Electrospray Mass Spectrometry. *Anal. Chem.* **2000,** *72* (21), 5158-5161.
5. M. Scalf; M. S. Westphall; L. M. Smith, Charge Reduction Electrospray Mass Spectrometry. *Anal. Chem.* **2000,** *72* (1), 52-60.
6. K. Breuker, Raw protein from the top down. *Nat. Chem.* **2018,** *10*, 114.
7. R. A. Yost; C. G. Enke, Selected ion fragmentation with a tandem quadrupole mass spectrometer. *J. Am. Chem. Soc.* **1978,** *100* (7), 2274-2275.
8. R. S. Johnson; S. A. Martin; K. Biemann; J. T. Stults; J. T. Watson, Novel fragmentation process of peptides by collision-induced decomposition in a tandem mass spectrometer: differentiation of leucine and isoleucine. *Anal. Chem.* **1987,** *59* (21), 2621-2625.
9. J. M. Wells; S. A. McLuckey, Collision-Induced Dissociation (CID) of Peptides and Proteins. In *Methods Enzymol.*, Academic Press: **2005**; Vol. 402, pp 148-185.
10. S. A. McLuckey, Principles of collisional activation in analytical mass spectrometry. *J. Am. Soc. Mass. Spectrom.* **1992,** *3* (6), 599-614.
11. R. Bakhtiar; Z. Guan, Electron Capture Dissociation Mass Spectrometry in Characterization of Peptides and Proteins. *Biotechnol. Lett.* **2006,** *28* (14), 1047-1059.

12. R. A. Zubarev; N. L. Kelleher; F. W. McLafferty, Electron Capture Dissociation of Multiply Charged Protein Cations. A Nonergodic Process. *J. Am. Chem. Soc.* **1998,** *120* (13), 3265-3266.
13. R. A. Zubarev; N. A. Kruger; E. K. Fridriksson; M. A. Lewis; D. M. Horn; B. K. Carpenter; F. W. McLafferty, Electron Capture Dissociation of Gaseous Multiply-Charged Proteins Is Favored at Disulfide Bonds and Other Sites of High Hydrogen Atom Affinity. *J. Am. Chem. Soc.* **1999,** *121* (12), 2857-2862.
14. A. R. Ledvina; M. V. Lee; G. C. McAlister; M. S. Westphall; J. J. Coon, Infrared multiphoton dissociation for quantitative shotgun proteomics. *Anal. Chem.* **2012,** *84* (10), 4513-4519.
15. J. S. Brodbelt; J. J. Wilson, Infrared multiphoton dissociation in quadrupole ion traps. *Mass Spectrom. Rev.* **2009,** *28* (3), 390-424.
16. D. P. Little; J. P. Speir; M. W. Senko; P. B. O'Connor; F. W. McLafferty, Infrared Multiphoton Dissociation of Large Multiply Charged Ions for Biomolecule Sequencing. *Anal. Chem.* **1994,** *66* (18), 2809-2815.
17. Y. Hashimoto; H. Hasegawa; K. Yoshinari; I. Waki, Collision-Activated Infrared Multiphoton Dissociation in a Quadrupole Ion Trap Mass Spectrometer. *Anal. Chem.* **2003,** *75* (3), 420-425.
18. J. P. Reilly, Ultraviolet photofragmentation of biomolecular ions. *Mass Spectrom. Rev.* **2009,** *28* (3), 425-447.
19. J. S. Brodbelt, Photodissociation mass spectrometry: new tools for characterization of biological molecules. *Chem. Soc. Rev.* **2014,** *43* (8), 2757-2783.
20. T.Ly; R. R. Julian, Ultraviolet Photodissociation: Developments towards Applications for Mass-Spectrometry-Based Proteomics. *Angew. Chem. Int. Ed.* **2009,** *48* (39), 7130-7137.
21. A. Thompson; J. Schaefer; K. Kuhn; S. Kienle; J. Schwarz; G. Schmidt; T. Neumann; C. Hamon, Tandem mass tags: A novel quantification strategy for comparative analysis of complex protein mixtures by MS/MS. *Anal. Chem.* **2003,** *75* (8), 1895-1904.
22. P. L. Ross; Y. N. Huang; J. N. Marchese; B. Williamson; K. Parker; S. Hattan; N. Khainovski; S. Pillai; S. Dey; S. Daniels; S. Purkayastha; P. Juhasz; S. Martin; M. Bartlet-Jones; F. He; A. Jacobson; D. J. Pappin, Multiplexed protein quantitation in Saccharomyces cerevisiae using amine-reactive isobaric tagging reagents. *Mol. Cell. Proteomics* **2004,** *3* (12), 1154-1169.
23. N. Rauniyar; J. R. Yates, Isobaric Labeling-Based Relative Quantification in Shotgun Proteomics. *J. Proteome Res.* **2014,** *13* (12), 5293-5309.
24. T. E. Wales; J. R. Engen, Hydrogen exchange mass spectrometry for the analysis of protein dynamics. *Mass Spectrom. Rev.* **2006,** *25* (1), 158-170.
25. F. W. McLafferty; Z. Guan; U. Haupts; T. D. Wood; N. L. Kelleher, Gaseous Conformational Structures of Cytochrome c. *J. Am. Chem. Soc.* **1998,** *120* (19), 4732-4740.
26. M. J. Chalmers; S. A. Busby; B. D. Pascal; G. M. West; P. R. Griffin, Differential hydrogen/deuterium exchange mass spectrometry analysis of protein-ligand interactions. *expert rev. proteomic.* **2011,** *8* (1), 43-59.
27. I. A. Kaltashov; C. E. Bobst; R. R. Abzalimov, H/D exchange and mass spectrometry in the studies of protein conformation and dynamics: is there a need for a top-down approach? *Anal. Chem.* **2009,** *81* (19), 7892-7899.
28. A. C. Leney; A. J. R. Heck, Native Mass Spectrometry: What is in the Name? *J. Am. Soc. Mass. Spectrom.* **2017,** *28* (1), 5-13.
29. A. A. Rostom; P. Fucini; D. R. Benjamin; R. Juenemann; K. H. Nierhaus; F. U. Hartl; C. M. Dobson; C. V. Robinson, Detection and selective dissociation of intact ribosomes in a mass spectrometer. *Proc. Natl. Acad. Sci. USA* **2000,** *97* (10), 5185-5190.
30. J. Oomens; N. Polfer; D. T. Moore; L. van der Meer; A. G. Marshall; J. R. Eyler; G. Meijer; G. von Helden, Charge-state resolved mid-infrared spectroscopy of a gas-phase protein. *Phys. Chem. Chem. Phys.* **2005,** *7* (7), 1345-1348.
31. J. L. Alonso; O. V. Boyarkin; P. Carcabal; E. J. Cocinero; R. C. Dunbar; M. P. Gaigeor; E. Gloaguen; J. C. Lopez; M. Mons; J. Oomens; A. L. Patrick; N. C. Polfer; A. M. Rijs; T. R. Rizzo; R. Spezia; M. S. de Vries, *Gas-Phase IR Spectroscopy and Structure of Biological Molecules*. Springer International Publishing: **2015**.

32. D. E. Clemmer; M. F. Jarrold, Ion Mobility Measurements and their Applications to Clusters and Biomolecules. *J. Mass Spectrom.* **1997,** *32* (6), 577-592.
33. R. Cumeras; E. Figueras; C. E. Davis; J. I. Baumbach; I. Gràcia, Review on ion mobility spectrometry. Part 1: current instrumentation. *Analyst* **2015,** *140* (5), 1376-1390.
34. R. Cumeras; E. Figueras; C. E. Davis; J. I. Baumbach; I. Gràcia, Review on ion mobility spectrometry. Part 2: hyphenated methods and effects of experimental parameters. *Analyst* **2015,** *140* (5), 1391-1410.
35. T. Wyttenbach; N. A. Pierson; D. E. Clemmer; M. T. Bowers, Ion Mobility Analysis of Molecular Dynamics. *Annu. Rev. Phys. Chem.* **2014,** *65* (1), 175-196.
36. T. Förster, Zwischenmolekulare Energiewanderung und Fluoreszenz. *Ann. Phys.* **1948,** *437* (1-2), 55-75.
37. M. F. Czar; R. A. Jockusch, Sensitive probes of protein structure and dynamics in well-controlled environments: combining mass spectrometry with fluorescence spectroscopy. *Curr. Opin. Struct. Biol.* **2015,** *34*, 123-134.
38. A. S. Danell; J. H. Parks, FRET measurements of trapped oligonucleotide duplexes. *Int. J. Mass spectrom.* **2003,** *229* (1), 35-45.
39. M. F. Czar; F. Zosel; I. Konig; D. Nettels; B. Wunderlich; B. Schuler; A. Zarrine-Afsar; R. A. Jockusch, Gas-Phase FRET Efficiency Measurements To Probe the Conformation of Mass-Selected Proteins. *Anal. Chem.* **2015,** *87* (15), 7559-7565.
40. A. T. Iavarone; D. Duft; J. H. Parks, Shedding Light on Biomolecule Conformational Dynamics Using Fluorescence Measurements of Trapped Ions. *J. Phys. Chem. A* **2006,** *110* (47), 12714-12727.
41. S. Daly; F. Poussigue; A.-L. Simon; L. MacAleese; F. Bertorelle; F. Chirot; R. Antoine; P. Dugourd, Action-FRET: Probing the Molecular Conformation of Mass-Selected Gas-Phase Peptides with Förster Resonance Energy Transfer Detected by Acceptor-Specific Fragmentation. *Anal. Chem.* **2014,** *86* (17), 8798-8804.
42. N. G. Hendricks; N. M. Lareau; S. M. Stow; J. A. McLean; R. R. Julian, Bond-Specific Dissociation Following Excitation Energy Transfer for Distance Constraint Determination in the Gas Phase. *J. Am. Chem. Soc.* **2014,** *136* (38), 13363-13370.
43. P. Geyer; U. Sezer; J. Rodewald; L. Mairhofer; N. Dörre; P. Haslinger; S. Eibenberger; C. Brand; M. Arndt, Perspectives for quantum interference with biomolecules and biomolecular clusters. Phys. Scr. **2016,** *91* (6).
44. R. Antoine; P. Dugourd; D. Rayane; E. Benichou; M. Broyer; F. Chandezon; C. Guet, Direct measurement of the electric polarizability of isolated C60 molecules. *J. Chem. Phys.* **1999,** *110* (19), 9771-9772.
45. R. Antoine; I. Compagnon; D. Rayane; M. Broyer; P. Dugourd; N. Sommerer; M. Rossignol; D. Pippen; F. C. Hagemeister; M. F. Jarrold, Application of molecular beam deflection time-of-flight mass spectrometry to peptide analysis. *Anal. Chem.* **2003,** *75* (20), 5512-5516.
46. Y.-P. Chang; K. Dlugolecki; J. Kuepper; D. Roesch; D. Wild; S. Willitsch, Specific Chemical Reactivities of Spatially Separated 3-Aminophenol Conformers with Cold Ca+ Ions. *Science* **2013,** *342* (6154), 98-101.
47. M. C. Heaven, Turn the Molecule This Way for a Faster Reaction. *Science* **2013,** *342* (6154), 46-47.

Chapter 1. Tailoring the volatility and stability of oligopeptides

J. Schätti; U. Sezer; S. Pedalino; J.P. Cotter; M. Arndt; M. Mayor; V. Köhler;
J. Mass Spectrom., **2017**, *52*, 550-556.

Outline of the author's contribution

U. Sezer and the author J. Schätti contributed equally to this work. J. Schätti synthesized and characterized the molecular compounds, U. Sezer and S. Pedalino designed and conducted the volatilization experiment with subsequent photoionization, J. P. Cotter designed and performed the volatilization experiment with subsequent electron-impact ionization. J. Schätti helped to conduct the molecular beam experiments during a one week stay in Vienna. U. Sezer., S. Pedalino, J. P. Cotter and J. Schätti analyzed the data. V. Köhler, M. Arndt and M. Mayor conceived and supervised the experiments. U. Sezer, J. Schätti, V. Köhler, and M. Arndt wrote the paper, with all authors reviewing it.

Tripeptides with different modifications to improve their volatility were synthesized. The unmodified peptides were produced by Fmoc Solid Phase Peptide Synthesis (SPPS). The modification with fluorinated alkyl chains was achieved by coupling $CF_3(CF_2)_nCH_2CH_2COOH$ to the N-terminus while the peptide was still attached to the resin. The fluorinated alkyl chain on the C-terminus was introduced by solution phase peptide coupling of $NH_2CH_2CH_2(CF_2)_7CF_3$ to the peptide. Permethylation of the peptide was a challenging reaction. Suitable conditions for the reaction were deprotonation by treatment with a dimsyl-solution followed by methylation with an excess of methyl iodide. Furthermore, a $(Trp\text{-}Lys)_4$-Trp nonapeptide functionalized with fluorinated alkyl chains was synthesized (see also chapter 3).

Research article

Journal of MASS SPECTROMETRY

Received: 23 April 2017 Revised: 8 June 2017 Accepted: 8 June 2017 Published online in Wiley Online Library

(wileyonlinelibrary.com) DOI 10.1002/jms.3959

Tailoring the volatility and stability of oligopeptides

J. Schätti,[a] U. Sezer,[b] S. Pedalino,[b] J. P. Cotter,[b] M. Arndt,[b]* M. Mayor[a,c] and V. Köhler[a]*

Amino acids are essential building blocks of life, and fluorinated derivatives have gained interest in chemistry and medicine. Modern mass spectrometry has enabled the study of oligo- and polypeptides as isolated entities in the gas phase, but predominantly as singly or even multiply charged species. While laser desorption of neutral peptides into adiabatically expanding supersonic noble gas jets is possible, UV–VIS spectroscopy, electric or magnetic deflectometry as well as quantum interferometry would profit from the possibility to prepare thermally slow molecular beams. This has typically been precluded by the fragility of the peptide bond and the fact that a peptide would rather 'fry', i.e. denature and fragment than 'fly'. Here, we explore how tailored perfluoroalkyl functionalization can reduce the intermolecular binding and thus increase the volatility of peptides and compare it to previously explored methylation, acylation and amidation of peptides. We show that this strategy is essential and enables the formation of thermal beams of intact neutral tripeptides, whereas only fragments were observed for an extensively fluoroalkyl-decorated nonapeptide. © 2017 The Authors. *Journal of Mass Spectrometry* Published by John Wiley & Sons Ltd.

Keywords: fluorination; molecular beams; peptides; thermal evaporation; vuv ionization

Introduction

Since the early days of Otto Stern[1] and Immanuel Estermann,[2] neutral molecular beams have played a key role in fundamental studies of physics and physical chemistry.[3–5] Experiments with isolated molecules in the gas phase have laid the ground for high-precision spectroscopy,[6,7] molecule and cluster deflectometry[8–10] and for an improved understanding of chemical reactions with quantum state control.[11,12] Modern molecular beam experiments have allowed setting new bounds on the electric dipole moment of the electron[13,14] and enabled the observation of quantum interference with clusters and molecules,[15,16] even with masses exceeding 10′000 amu.[17] Modern research in molecular beam methods has recently focused on obtaining improved control over the motional and internal states of polyatomic molecules using selectors,[18,19] electrical,[20–24] magnetic[25] and mechanical[26] decelerators as well as laser cooling of dimers and trimers.[27–29] Polyatomic particles were even successfully trapped at mK temperatures.[22,26,30,31] Complementary to that, there has been a growing effort to prepare neutral beams of large molecules. Our present contribution addresses the question how to bring complex biomolecular building blocks into the gas phase.[32] D. Gross and G. Grodsky reported on the sublimation and decomposition of unmodified amino acids and certain dipeptides in 1955.[33–38] Methylation and acylation of peptides have already been investigated in the late 60s and early 70s in combination with electron impact mass spectrometry (EI-MS) as a means for increased volatility in sequence analysis of unknown proteins.[39–41] Here, we aim at preparing neutral continuous beams of peptides at low velocity as required for spectroscopy, deflectometry and quantum interferometry or even nanostructuring using soft-landing of individual biomolecules on surfaces. Even though one may argue that biomolecules are most naturally studied in an aqueous environment, it is meaningful to start from isolated species to which one may later add an increasing number of water molecules to compare their physical data with quantum chemical models.[42,43] Additionally, gas phase studies of biomolecules enable the elucidation of intrinsic folding preferences without interference of solvents or other molecules.[44–47]

While some biomolecules or biomolecular moieties – such as nucleobases and some vitamins – can be readily sublimated or evaporated[48] oligopeptides, proteins and oligonucleotides will rather fragment than fly when heated. To suppress fragmentation, one may reduce the heating time or add collisional cooling, once the molecules are airborne. Both ideas have been earlier explored for biomolecules injected into supersonic noble gas jets.[43,49,50] This way, neutral intact macromolecules can be volatilized, but at the expense of being 300–1000 m/s fast, depending on the gas type and temperature. In contrast, velocities down to several 10 m/s have been achieved in buffer gas cooled sources[51] for molecules up to stilbene or using laser-induced acoustic desorption even for molecules beyond 10′000 amu.[52,53] However, the generation of thermally slow neutral beams of oligopeptides, which we take here as examples of relevant but fragile biomolecules, poses a considerable challenge.

* *Correspondence to: Markus Arndt, University of Vienna, Faculty of Physics, Boltzmanngasse 5, Vienna 1090, Austria. E-mail: markus.arndt@univie.ac.at*
Valentin Köhler, University of Basel, Department of Chemistry, Basel 4056, Switzerland. E-mail: valentin.koehler@unibas.ch

a *University of Basel, Department of Chemistry, Basel 4056, Switzerland*

b *University of Vienna, Faculty of Physics, Boltzmanngasse 5, 1090, Vienna, Austria*

c *Karlsruhe Institute of Technology, Institute for Nanotechnology, Hermann-von-Helmholtz-Platz 1, 76344, Eggenstein-Leopoldshafen, Germany*

Journal of MASS SPECTROMETRY

Fluorination has gained increasing attention in medicinal chemistry over the last 50 years.[54,55] Around 20% of all pharmaceuticals contain at least one carbon–fluorine bond. Fluorine modification of single amino acids, peptides and proteins substantially alters their properties and provides new opportunities for peptide and protein design.[56,57] The strong electron-withdrawing effect of fluorine lowers the pk_a value of proximal protons, affects hydrogen bonding and – despite the high polarization of the individual carbon fluorine bond – perfluoroalkyls exhibit a low overall dipole moment due to their inherent geometry. The very low polarizability of perfluoroalkyls results in very weak intermolecular dispersion forces and consequently low boiling points compared to hydrocarbons of similar mass.[58]

In our present work, we focus on the question how to derivatize biomolecular structures such that their sublimation enthalpy is reduced and their thermal stability increased. Perfluoroalkyl functionalization of individual molecules is expected to reduce the binding to neighbouring particles and surfaces because earlier studies have shown that it enhances the volatility of large organic compounds.[17,59–61] Here, we apply this strategy for the first time to oligopeptides and study its influence on their volatility.

Flying rather than frying the peptide

The volatility of the first model system, namely the tripeptide alanine–tryptophan–alanine (AWA) was compared in various

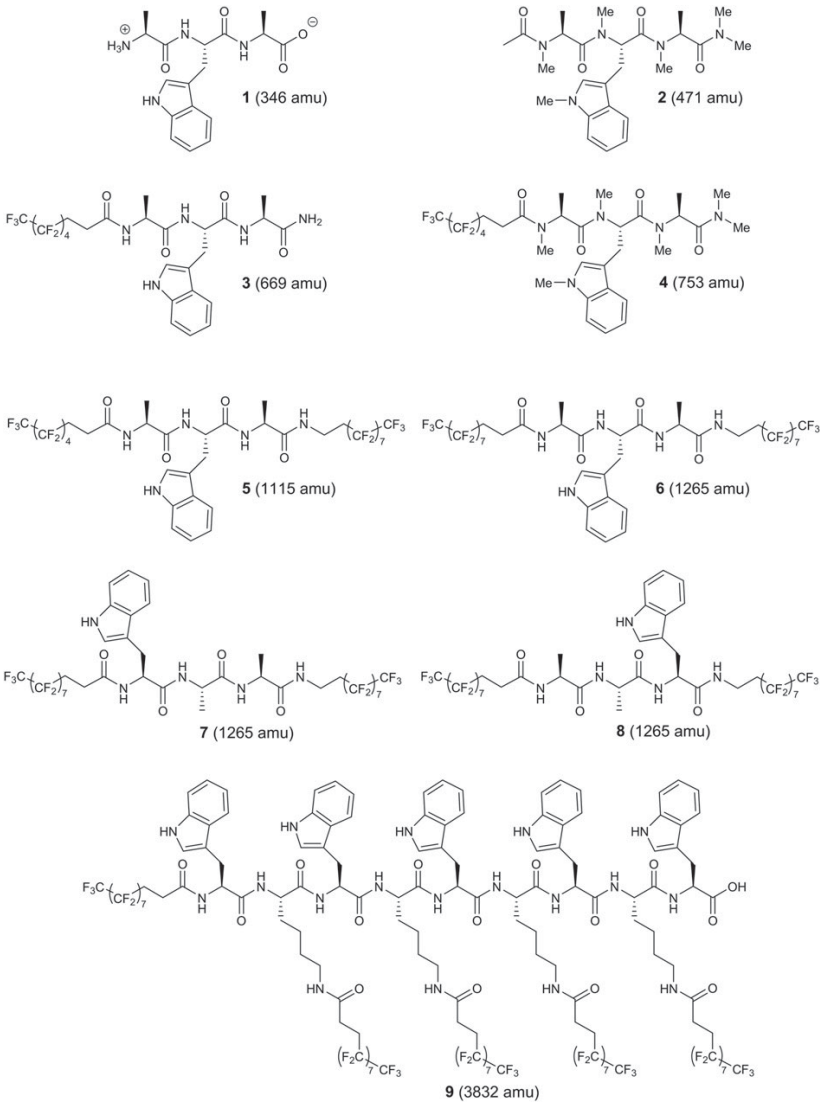

Figure 1. Gallery of peptides **1**–**9** with increasing molecular weight employed in this study. Tripeptides **1**–**8** resulted from variation of the Ala-Trp-Ala motif: charges and hydrogen bond donors present in parent tripeptide **1** were removed by acylation, methylation and amidation in derivative **2**; one perfluoroalkyl chain was introduced at the *N*-terminus by acylation and the *C*-terminus amidated in derivative **3**; **4** was obtained by methylation of **3**; fluorinated alkyl chains of different or equal length were introduced at the *N*- and *C*-terminus by acylation and amidation, respectively, in derivative **5** and **6**; **7** and **8** are sequence isomers of **6**; high Trp and fluoroalkyl content realized by alternating Trp and Lys followed by acylation of the lysine side chains and the *N*-terminus as exemplified in peptide **9**.

Journal of MASS SPECTROMETRY

modifications, i.e. in its native, methylated or perfluoroalkyl modified form including acylation and amidation of the termini, respectively, as shown in Fig. 1.

All peptides were volatilized in a resistively heated oven whose temperature was monitored on its outside and inside with an absolute uncertainty of ±5 K. The sublimated or evaporated molecules passed a differential pumping stage before they entered the probe chamber, where they were ionized (see Fig. 2). For selected compounds, electron impact ionization (E_{impact} = 70 eV) in quadrupole mass spectrometry (EI-QMS) was compared with vacuum-ultraviolet (VUV) photoionization (λ = 157 nm, τ = 10 ns) in time-of-flight mass spectrometry (TOF-MS) to distinguish ionization induced from thermal decomposition processes.

Results

We started by comparing the native tripeptide **1** with its methylated derivative **2** where internal charges were removed by acetylation and amidation of the termini (Fig. 3). Upon evaporation of **1** at varying source temperatures up to T = 595 K, only molecular fragments were detected, both in EI-QMS and VUV-TOF-MS. Three major fragments were observed that were tentatively assigned to the loss of the C-terminal alanine (H_2N-$CH(CH_3)$-COOH) possibly resulting from thermal diketopiperazine formation ($C_{14}H_{15}N_3O_2$, 257 amu)[62,63] as well as two common tryptophan fragments[64] which were observed in all following mass spectra: the indole cation ($C_8H_6N^+$, 116 amu) and the skatole cation ($C_9H_8N^+$, 130 amu).

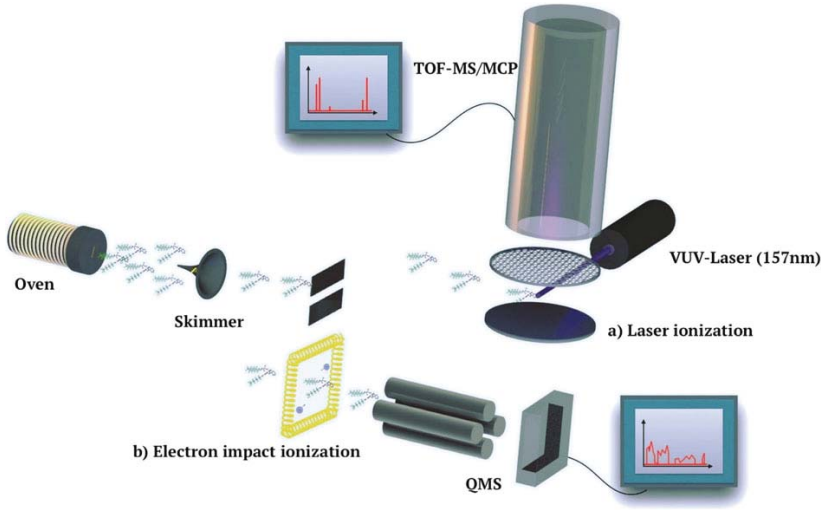

Figure 2. Experimental scheme for the volatilization/ionization tests. The peptides were heated in a ceramic cell with an aperture of 3 × 0.05 mm^2. The molecular beam reached the mass spectrometer through two differential pumping stages, separated by one skimmer and one slit of 3 mm as the relevant dimension. Under heat load, the pressure in the three chambers was 1 × 10^{-5}, 3 × 10^{-6} and 1.5 × 10^{-7} mbar, respectively. Pulsed photoionization of the molecular beam was combined with time-of-flight mass spectrometry (panel (a)). Alternatively, continuous electron impact ionization (b) was combined with a quadrupole mass spectrometer. Because both spectrometers were optimized for high transmission, their mass resolution is limited to about 2% with a calibration uncertainty of 5% across the entire mass range.

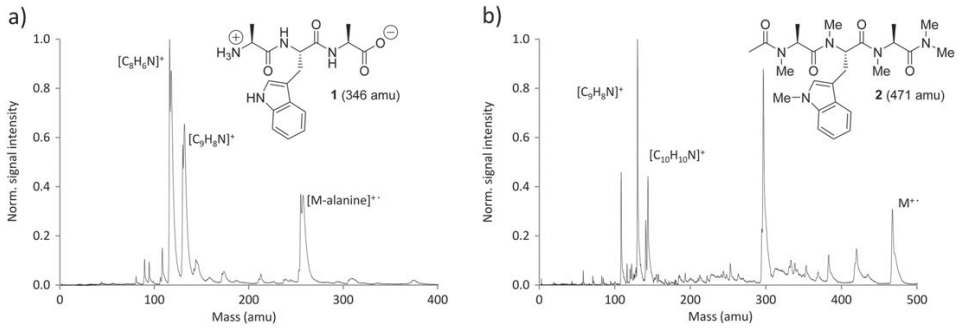

Figure 3. Panel (a) shows the mass spectrum of the native tripeptide Ala-Trp-Ala **1** after evaporation at 595 K and VUV postionization with a pulse intensity of I_{ion} = 2.9(3)MW/cm^2. The native biomolecule (346 amu) falls apart under these conditions, and the following main fragments are observed: the indole cation ($C_8H_6N^+$, 116 amu), the skatole cation ($C_9H_8N^+$,130 amu) and a signal that is tentatively assigned to a cationic Ala-Trp diketopiperazine fragment ($C_{14}H_{15}N_3O_2^+$, 257 amu). The spectrum was calibrated to the indole cation ($C_8H_6N^+$, 116 amu). (b) Under similar experimental conditions, but at lower temperature (T = 525 K), the mass spectrum of the methylated tripeptide 2 displays the intact parent ion at 471 amu. (b). Fragments include the *N*-methyl indole cation ($C_9H_8N^+$,130 amu) and the *N*-methylated skatole cation ($C_{10}H_{10}N^+$, 144 amu) as well as several unidentified species. The spectrum was calibrated to the *N*-methyl indole cation ($C_9H_8N^+$,130 amu).

As reported in the literature, the removal of internal charges and hydrogen bond donors – through acylation of the *N*-terminus, amidation of the *C*-terminus and methylation of all nitrogen atoms – reduces the intermolecular binding and increases the volatility of the peptides.[39] Indeed, evaporation of **2** permitted the observation of intact molecular ions (m = 471 amu), already at 525 K (see Fig. 3(b)).

Earlier studies with stable organic molecules showed that their volatility and stability can be enhanced by functionalization with perfluoroalkyl chains.[65] The high electronegativity of fluorine reduces the polarizability-to-mass ratio in the compound and redistributes electron density slightly to the outside of the neutral molecule. Pictorially speaking, this functionalization aims at 'wrapping' the peptide in a protective fluorinated shell. Even though the particle is technically not encapsulated, the attachment of the chains is assumed to be beneficial.

This hypothesis was verified for derivative **3** of the thermolabile tripeptide AWA. Upon heating to 548 K and exposure to VUV-TOF mass spectrometry with laser settings equal to those used for the native peptide **1**, a substantial parent peak was observed (Fig. 4(a)) corroborating our design hypothesis. It was also noted that VUV photoionization is softer than electron impact ionization (Fig. 4(b)).[66] This was apparent in the substantially reduced number of fragments and the higher parent-to-fragment ratio shown in Fig. 4(a).

A dense mass spectrum was observed upon photoionization of a thermal beam of the methylated derivative **4**, which carries one fluoroalkyl chain introduced by acylation of the *N*-terminus (Fig. 5(a)). Intact parent molecules were detected over the entire temperature range from 467 to 585 K. Based on this positive trend, additional perfluoroalkylation by amidation of the *C*-terminus was investigated in the absence of *N*-methylation. The mass spectrum of the peptide derivative **5** is shown in Fig. 5(b). The parent peak (m = 1115 amu) appears at 548 K, reaches its maximum at 586 K and now clearly dominates the spectrum. A similar but less pronounced effect is observed with the non-*N*-methylated peptide **3**, which carries only one fluoroalkyl chain (Fig. 4(a)). This corroborates the hypothesis that perfluoroalkylation enhances the volatility of the peptides and stabilizes them against thermal and photo-induced dissociation whereas *N*-methylation seems to promote fragmentation.

To elucidate whether peptide stability and detectability are sequence dependent, the three perfluoroalkylated compounds **6**, **7** and **8** were synthesized, which differ only in the order of the three amino acid residues. Their VUV-TOF mass spectra are shown in Fig. 6(a–c). The strongest parent signal is found in the temperature

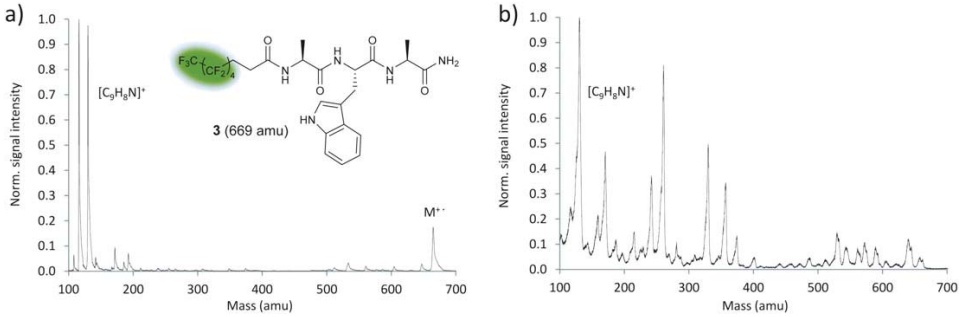

Figure 4. VUV-TOF *versus* EI-QMS. (a) VUV-TOF mass spectrum of a thermal perfluoroalkyl functionalized peptide beam (**3**), recorded at T = 548 K. A strong parent peak (m = 669 amu) is observed and accompanied by the indole cation ($C_8H_6N^+$, 116 amu) and skatole cation ($C_9H_8N^+$, 130 amu). The spectrum was calibrated to the indole cation ($C_8H_6N^+$, 116 amu). (b) In contrast, the EI-QMS spectrum at 70-eV electron energy yields a pronounced fragment spectrum under otherwise identical boundary conditions. The spectrum was calibrated to the skatole cation ($C_9H_8N^+$, 130 amu). The green highlight indicates the fluoroalkyl-tag. [Colour figure can be viewed at wileyonlinelibrary.com]

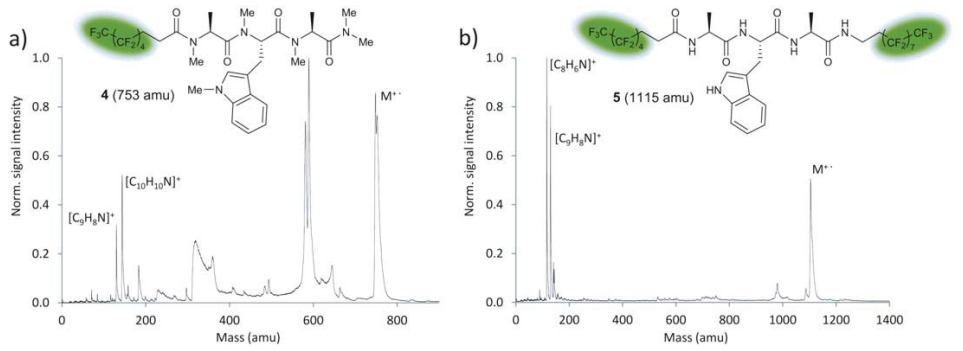

Figure 5. (a) VUV-TOF mass spectrum of a thermal beam of perfluoroalkyl functionalized and methylated tripeptide **4** at T = 552 K and I_{ion} = 2.9(3) MW/cm^2. We observe the methylated skatole cation ($C_{10}H_{10}N^+$, 144 amu) and the *N*-methyl indole cation ($C_9H_8N^+$, 130 amu) as well as unidentified fragments. The spectrum was calibrated to the *N*-methyl indole cation ($C_9H_8N^+$,130 amu). (b) A second perfluoroalkyl chain adds to the molecular mass but results in a relatively clean mass spectrum of the non *N*-methylated peptide **5** (compare also Fig. 4(a)). The spectrum was calibrated to the indole cation ($C_8H_6N^+$, 116 amu). [Colour figure can be viewed at wileyonlinelibrary.com]

Journal of MASS SPECTROMETRY

range of 575–585 K and for the highest photoionization intensity $I_{ion} = 2.9(3)\text{MW/cm}^2$. In all three cases, we find a dominant parent peak (**1265** amu) and a simple mass pattern with the indole and skatole cation ($C_8H_6N^+$, 116 amu and $C_9H_8N^+$, 130 amu, respectively) as prominent fragments (Fig. 6(a–c)). Interestingly, the Trp-Ala-Ala sequence isomer **6** led to additional unidentified fragments over 600 amu compared to the other two sequence permutations **7** and **8** (Fig. 6(a)).

To probe the thermal contribution to fragmentation, we have studied the mass spectrum of **8** as a function of the source temperature (see Fig. 6(e)). Both the parent peak and its fragments rise in a constant relation with increasing temperature, up to 615 K, where the parent molecule finally disintegrates. This suggests that the molecules remain stable up to this temperature and that the fragments are predominantly due to the ionization process.

Because perfluoroalkyl functionalization substantially increases the molecular volatility,[65] it is intriguing to test the mass limit of this method. The ideal model analyte would (i) have a high fluoroalkyl content and (ii) include a high tryptophan content for efficient photo-ionization. Compound **9** fulfils these requirements and was heated in the same setup (Fig. 2), under high vacuum. The resulting VUV-TOF-mass spectrum (Fig. 6(d)) contains no intact parent molecule.

In order to test for the presence of an intact parent fraction in the neutral molecular beam, we have collected the evaporated material on a glass slide next to the oven. This sample was post-analysed in a commercial MALDI instrument and did not show any intact parent peak, suggesting that the functionalized nonapeptide did not reach the glass slide as an intact entity in sufficient quantities.

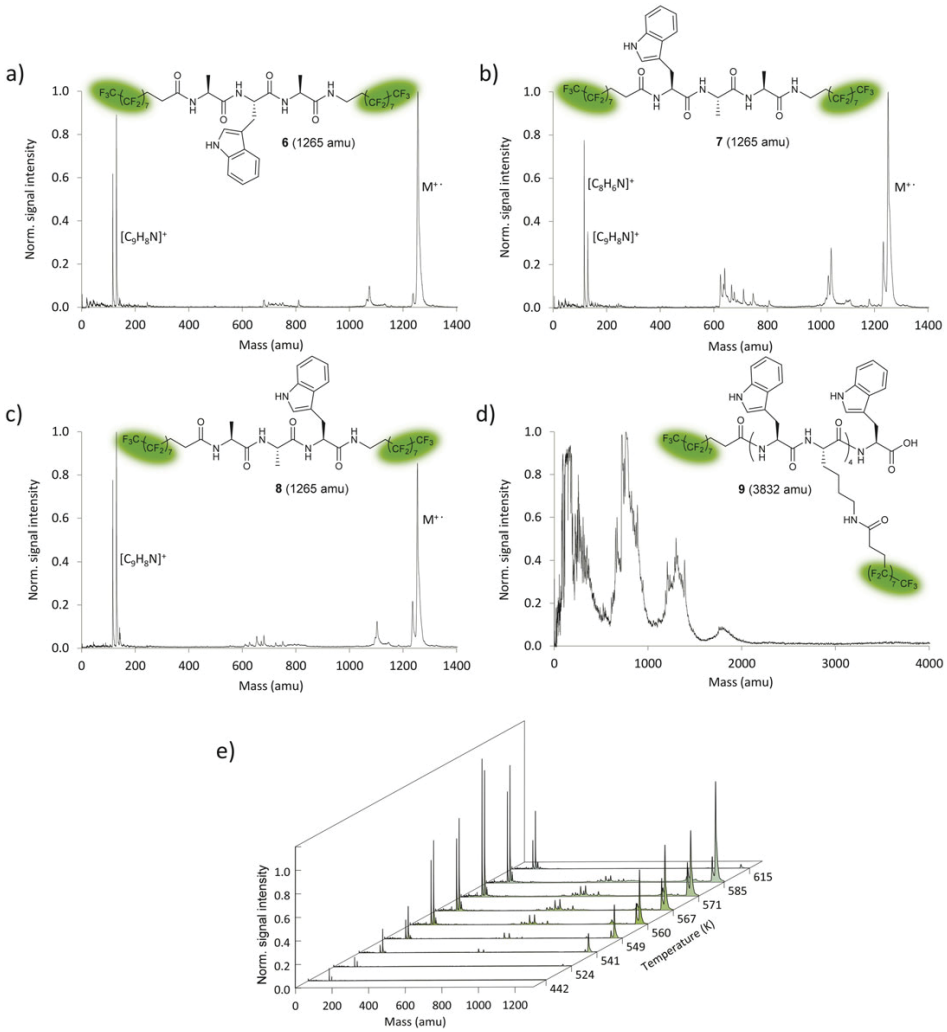

Figure 6. (a–c) Sequence isomers of tripeptide derivative with perfluoroalkyl decorated termini. Mass spectra for **6**, **7** and **8** are very similar, although a higher proportion of fragments is observed for **7**. Spectra were calibrated to the indole cation ($C_8H_6N^+$, 116 amu). The indole cation is not indicated in (a) and (c) for improved clarity. (d) No intact ion was detected for highly perfluoroalkyl decorated Trp-Lys oligomer **9** after thermal evaporation and photoionization. (e) Variation of the oven temperature leads to an increase of both the parent signal and the fragments of compound **8**. Significant thermal decomposition is observed at 615 K. [Colour figure can be viewed at wileyonlinelibrary.com]

Discussion

By comparing the mass spectra of all tailored peptides depicted in Fig. 1 and assuming similar photoionization efficiency for compounds **1**–**8**, it can be seen that compounds **6**, **7** and **8** produce the most intense thermal beams and VUV-TOF mass signals with a small proportion of fragments, even though they are 3.6 times more massive than the free AWA tripeptide alone. This observation can be attributed to reduced intermolecular interactions resulting from the removal of internal charges and the low polarizability of the perfluoroalkyl chains. The chain length of the perfluoroalkyl decoration, although not investigated in detail, seemed to play a minor but significant role with a more pronounced parent ion peak for compound **6** (C- and N-terminal C_8F_{17}) in comparison to compound **5**, which carries a shorter perfluoroalkyl chain (C_5F_{11}) at the N-terminus (Figs 5(b) and 6(a)). For compound **4** which has only one short perfluoroalkyl chain (C_5F_{11}), the relative intensity of the indole and skatole fragment ions *versus* the parental ion is significantly increased (Fig. 4(a)) although little additional fragments were observed. Interestingly, sequence isomers with identical decoration of perfluoroalkyl groups exhibited different degrees of fragmentation with the Trp-Ala-Ala sequence isomer being the most fragile in the series.

N-methylation appears to promote fragmentation in combination with fluoroalkyl chains or without (Figs 3(b) and 5(a)). In contrast, already a single perfluoroalkyl chain with native N—H bonds in the peptide delivers significantly cleaner spectra than *N*-methylated compounds.

The parent–fragment ratio does also depend on the ionization mechanism. Many mass spectrometry experiments use electron impact ionization with energies of 70 eV for optimum sensitivity. However, the excess of electron energy can open a variety of fragmentation channels.[67] In contrast, VUV photoionization at 157 nm (7.90 eV) was confirmed as a soft ionization technique,[66] whenever the peptide chain contained one or more tryptophan units.

Even though derivatization changes the geometry and chemical response of the molecule, we argue that our method can serve many practical purposes. In recent years, substantial research effort has been dedicated to evaluate, understand and explore the effects and benefits of fluorination in biochemistry, medicine and pharmacology.[54–57,68] Studying fluoroalkyl derivatized molecules in the gas phase with an increasing number of hydration layers shall soon allow to systematically study the change of their electro-optical properties in quantum interferometry experiments.[43] Furthermore, it allows the preservation of native N—H functionality and thereby investigation of intramolecular interactions which might well reflect those of native peptides in the absence of solvent or other molecules.[44,45]

Methods

Synthesis and characterization of peptide constructs are detailed in the Supporting Information. Figures 3–5 and 6(a–d) were generated with Microsoft Excel 2010 using the 'Scatter with Smooth Lines' function. Figure 6e was prepared with Origin 9.2.214.

Acknowledgments

We thank the FP7 Ideas: European Research Council for support under grant agreement no 320694, the Austrian Science Fund (W1210-25) and the Swiss Nanoscience Institute at the University of Basel, project P1403. We thank Jan Pac for support in early measurements and the Mass Spectrometry Center of the University of Vienna for MALDI-MS. We thank PD Dr. Daniel Häussinger, University of Basel, for the NMR spectra of compound **9**. JPC gratefully acknowledges a Vienna Quantum Fellowship.

Author contribution statement

J.S. and U.S. contributed equally to the work. J.S. synthesized and characterized the molecular compounds, U.S. and S.P designed and conducted the volatilization experiment with subsequent photoionization, J.C. designed and conducted the volatilization experiment with subsequent electron-impact ionization, U.S., S.P. and J.C. analysed the data. V.K., M.A. and M. M. conceived and supervised the experiments. U.S., J.S., V.K. and M.A. wrote the paper, with all authors reviewing it.

Additional information

There are no additional accession codes; the authors declare to have no competing financial interests.

References

[1] O. Stern. Eine direkte Messung der thermischen Molekularstrahlgeschwindigkeit. *Z. Phys.* **1920**, *2*, 49.
[2] I. Estermann, O. Stern. Diffraction of molecular beams. *Z. Phys.* **1930**, *61*, 95.
[3] S. Y. T. van de Meerakker, H. L. Bethlem, G. Meijer. Taming molecular beams. *Nat. Phys.* **2008**, *4*, 595.
[4] M. Henini. *Molecular Beam Epitaxy: From Research to Mass Production*. Elsevier Science: Oxford, **2012**.
[5] G. Scoles, D. Bassi, U. Buck, D. C. Laine. *Atomic and Molecular Beam Methods. 1*. Oxford University Press: New York, **1988**.
[6] C. J. Bordé, S. Avrillier, A. Van Lerberghe, C. Salomon, D. Bassi, G. Scoles. Observation of optical Ramsey fringes in the 10 μm spectral region using a supersonic beam of SF6. *J. Phys. Colloq* **1981**, *42*, C8-15-C18-19.
[7] S. Eibenberger, J. Doyle, D. Patterson. Enantiomer-specific state transfer of chiral molecules. *arXiv:1608.04691v1 [physics.chem-ph] 15 Aug 2016* **2016**.
[8] R. Antoine, P. Dugourd, D. Rayane, E. Benichou, M. Broyer, F. Chandezon, C. Guet. Direct measurement of the electric polarizability of isolated C_{60} molecules. *J. Chem. Phys.* **1999**, *110*, 9771.
[9] R. Antoine, I. Compagnon, D. Rayane, M. Broyer, P. Dugourd, G. Breaux, F. C. Hagemeister, D. Pippen, R. R. Hudgins, M. F. Jarrold. Electric dipole moments and conformations of isolated peptides. *Eur. Phys. J. D* **2002**, *20*, 583.
[10] W. A. de Heer, V. V. Kresin. In *Handbook of Nanophysics, Clusters and Fullerenes*. (K. D. Sattler Ed.). CRC Press: Boca Raton, **2010** 10.11.
[11] M. Kirste, X. Wang, H. C. Schewe, G. Meijer, K. Liu, A. van der Avoird, L. M. C. Janssen, K. B. Gubbels, G. C. Groenenboom, S. Y. T. van de Meerakker. Quantum-state resolved bimolecular collisions of velocity-controlled OH with NO radicals. *Science* **2012**, *338*, 1060.
[12] S. Willitsch, M. T. Bell, A. D. Gingell, S. R. Procter, T. P. Softley. Cold reactive collisions between laser-cooled ions and velocity-selected neutral molecules. *Phys. Rev. Lett.* **2008**, *100*, 043203.
[13] J. J. Hudson, B. E. Sauer, M. R. Tarbutt, E. A. Hinds. Measurement of the electron electric dipole moment using YbF molecules. *Phys. Rev. Lett.* **2002**, *89*, 023003.
[14] J. Baron, W. C. Campbell, D. DeMille, J. M. Doyle, G. Gabrielse, Y. V. Gurevich, P. W. Hess, N. R. Hutzler, E. Kirilov, I. Kozyryev, B. R. O'Leary, C. D. Panda, M. F. Parsons, E. S. Petrik, B. Spaun, A. C. Vutha, A. D. West. Order of magnitude smaller limit on the electric dipole moment of the electron. *Science* **2014**, *343*, 269.
[15] W. Schöllkopf, J. P. Toennies. Nondestructive mass selection of small Van der Waals clusters. *Science* **1994**, *266*, 1345.

Journal of MASS SPECTROMETRY

[16] P. Haslinger, N. Dörre, P. Geyer, J. Rodewald, S. Nimmrichter, M. Arndt. A universal matter-wave interferometer with optical ionization gratings in the time domain. *Nat. Phys.* **2013**, *9*, 144.
[17] S. Eibenberger, S. Gerlich, M. Arndt, M. Mayor, J. Tüxen. Matter-wave interference of particles selected from a molecular library with masses exceeding 10 000 amu. *Phys. Chem. Chem. Phys.* **2013**, *15*, 14696.
[18] T. Rieger, T. Junglen, S. A. Rangwala, P. W. H. Pinkse, G. Rempe. Continuous loading of an electrostatic trap for polar molecules. *Phys. Rev. Lett.* **2005**, *95*, 173001.
[19] T. Junglen, T. Rieger, S. A. Rangwala, P. W. H. Pinkse, G. Rempe. Slow ammonia molecules in an electrostatic quadrupole guide. *Eur. Phys. J. D* **2004**, *31*, 365.
[20] S. Y. T. van de Meerakker, H. L. Bethlem, N. Vanhaecke, G. Meijer. Manipulation and control of molecular beams. *Chem. Rev.* **2012**, *112*, 4828.
[21] J. Küpper, F. Filsinger, G. Meijer. Manipulating the motion of large neutral molecules. *Faraday Discuss.* **2009**, *142*, 155.
[22] C. E. Heiner, D. Carty, G. Meijer, H. L. Bethlem. A molecular synchrotron. *Nat. Phys.* **2007**, *3*, 115.
[23] H. L. Bethlem, F. M. H. Crompvoets, R. T. Jongma, S. Y. T. van de Meerakker, G. Meijer. Deceleration and trapping of ammonia using time-varying electric fields. *Phys. Rev. A* **2002**, *65*, 053416.
[24] H. L. Bethlem, G. Berden, G. Meijer. Decelerating neutral dipolar molecules. *Phys. Rev. Lett.* **1999**, *83*, 1558.
[25] E. Narevicius, C. G. Parthey, A. Libson, M. F. Riedel, U. Even, M. G. Raizen. Towards magnetic slowing of atoms and molecules. *New J. Phys.* **2007**, *9*.
[26] S. Chervenkov, X. Wu, J. Bayerl, A. Rohlfes, T. Gantner, M. Zeppenfeld. Continuous centrifuge decelerator for polar molecules. *Phys. Rev. Lett.* **2014**, *112*, 013001.
[27] E. S. Shuman, J. F. Barry, D. DeMille. Laser cooling of a diatomic molecule. *Nature* **2010**, *467*, 820.
[28] J. Barry, Yale (New Haven), **2013**.
[29] V. Zhelyazkova, A. Cournol, T. E. Wall, A. Matsushima, J. J. Hudson, E. A. Hinds, M. R. Tarbutt, B. E. Sauer. Laser cooling and slowing of CaF molecules. *Phys. Rev. A* **2014**, *89*, 053416.
[30] B. Englert, M. Mielenz, C. Sommer, J. Bayerl, M. Motsch, P. Pinkse, G. Rempe, M. Zeppenfeld. Storage and adiabatic cooling of polar molecules in a microstructured trap. *Phys. Rev. Lett.* **2011**, *107*.
[31] M. Zeppenfeld, B. G. U. Englert, R. Glockner, A. Prehn, M. Mielenz, C. Sommer, L. D. van Buuren, M. Motsch, G. Rempe. Sisyphus cooling of electrically trapped polyatomic molecules. *Nature* **2012**, *491*, 570.
[32] J.-P. Schermann. *Spectroscopy and Modeling of Biomolecular Building Blocks*. Elsevier, **2007**.
[33] D. Gross, G. Grodsky. The sublimation of amino acids and peptides. *J. Am. Chem. Soc.* **1955**, *77*, 1678.
[34] V. G. Badelin, E. Y. Tyunina, A. V. Krasnov, V. V. Tyunina, N. I. Giricheva, A. V. Girichev. Mass spectrometry study of the sublimation of aliphatic dipeptides. *Russ. J. Phys. Chem. A* **2012**, *86*, 457.
[35] V. V. Tyunina, A. V. Krasnov, E. Y. Tyunina, V. G. Badelin, G. V. Girichev. Enthalpy of sublimation of natural aromatic amino acids determined by Knudsen's effusion mass spectrometric method. *J. Chem. Thermodyn.* **2014**, *74*, 221.
[36] V. V. Tyunina, A. V. Krasnov, V. G. Badelin, G. V. Girichev. Enthalpy of sublimation of hydroxyl-containing amino acids: Knudsen's effusion mass spectrometric study. *J. Chem. Thermodyn.* **2016**, *98*, 62.
[37] C. G. de Kruif, J. Voogd, J. C. A. Offringa. Enthalpies of sublimation and vapour pressures of 14 amino acids and peptides. *J. Chem. Thermodyn.* **1979**, *11*, 651.
[38] D. P. Glavin, J. L. Bada. Isolation of amino acids from natural samples using sublimation. *Anal. Chem.* **1998**, *70*, 3119.
[39] B. C. Das, S. D. Gero, E. Lederer. N-methylation of N-acyl oligopeptides. *Biochem. Biophys. Res. Commun.* **1967**, *29*, 211.
[40] H. R. Morris, D. H. Williams, R. P. Ambler. Determination of the sequences of protein-derived peptides and peptide mixtures by mass spectrometry. *Biochem. J.* **1971**, *125*, 189.
[41] P. Roepstorff, R. K. Spear, K. Brunfeldt. Mass spectrometric sequence determination of permethylated peptide mixtures. *FEBS Lett.* **1971**, *15*, 237.
[42] M. S. de Vries, P. Hobza. Gas-phase spectroscopy of biomolecular building blocks. *Annu. Rev. Phys. Chem.* **2007**, *58*, 585.
[43] P. Geyer, U. Sezer, J. Rodewald, L. Mairhofer, N. Dörre, P. Haslinger, S. Eibenberger, C. Brand, M. Arndt. Perspectives for quantum interference with biomolecules and biomolecular clusters. *Phys. Scripta* **2016**, *91*, 063007.
[44] P. S. Walsh, K. N. Blodgett, C. McBurney, S. H. Gellman, T. S. Zwier. Inherent conformational preferences of Ac-Gln-Gln-NHBn: sidechain hydrogen bonding supports a β-turn in the gas phase. *Angew. Chem. Int. Ed.* **2016**, *55*, 14618.
[45] H. Fricke, G. Schaefer, T. Schrader, M. Gerhards. Secondary structure binding motifs of the jet cooled tetrapeptide model Ac-Leu-Val-Tyr(Me)-NHMe. *Phys. Chem. Chem. Phys.* **2007**, *9*, 4592.
[46] H. Fricke, A. Funk, T. Schrader, M. Gerhards. Investigation of secondary structure elements by IR/UV double resonance spectroscopy: analysis of an isolated beta-sheet model system. *J. Am. Chem. Soc.* **2008**, *130*, 4692.
[47] M. F. Jarrold. Peptides and proteins in the vapor phase. *Annu. Rev. Phys. Chem.* **2000**, *51*, 179.
[48] G. Grégoire. In *Nucleic Acids in the Gas Phase*. (V. Gabelica Ed.). Springer: Heidelberg, **2014** 21.
[49] M. Dey, F. Moritz, G. H. Atkinson, J. Grotemeyer, E. Schlag. Molecular beams of polyenes: retinals and beta-carotene. *J. Chem. Phys.* **1991**, *95*, 4584.
[50] G. Meijer, M. S. de Vries, H. E. Hunziker, H. R. Wendt. Laser desorption jet-cooling of organic molecules cooling characteristics and detection sensitivity. *Appl. Phys. B Lasers Opt.* **1990**, *51*, 395.
[51] J. Piskorski, D. Patterson, S. Eibenberger, J. M. Doyle. Cooling, spectroscopy and non-sticking of trans-stilbene and Nile Red. *Chem Phys Chem* **2014**, *15*, 3800.
[52] U. Sezer, L. Wörner, J. Horak, L. Felix, J. Tüxen, C. Götz, A. Vaziri, M. Mayor, M. Arndt. Laser-induced acoustic desorption of natural and functionalized biochromophores. *Anal. Chem.* **2015**, *87*, 5614.
[53] A. V. Zinovev, I. V. Veryovkin, J. F. Moore, M. J. Pellin. Laser-driven acoustic desorption of organic molecules from back-irradiated solid foils. *Anal. Chem.* **2007**, *79*, 8232.
[54] Y. Zhou, J. Wang, Z. Gu, S. Wang, W. Zhu, J. L. Acena, V. A. Soloshonok, K. Izawa, H. Liu. Next generation of fluorine-containing pharmaceuticals, compounds currently in Phase II–III clinical trials of major pharmaceutical companies: new structural trends and therapeutic areas. *Chem. Rev.* **2016**, *116*, 422.
[55] K. Müller, C. Faeh, F. Diederich. Fluorine in pharmaceuticals: looking beyond intuition. *Science* **2007**, *317*, 1881.
[56] E. N. G. Marsh. Fluorinated proteins: from design and synthesis to structure and stability. *Acc. Chem. Res.* **2014**, *47*, 2878.
[57] Y. Tang, G. Ghirlanda, W. A. Petka, T. Nakajima, W. F. DeGrado, D. A. Tirrell. Fluorinated coiled-coil proteins prepared in vivo display enhanced thermal and chemical stability. *Angew. Chem. Int. Ed.* **2001**, *40*, 1494.
[58] P. Kirsch. *Modern Fluoroorganic Chemistry*. Wiley-VCH Verlag GmbH & Co. KGaA: Weinheim, **2013** 1.
[59] L. Felix, U. Sezer, M. Arndt, M. Mayor. Synthesis of highly fluoroalkyl-functionalized oligoporphyrin systems. *Eur. J. Org. Chem.* **2014**, 6884.
[60] J. Tüxen, PhD. thesis, University of Basel (Basel), **2012**.
[61] D. O'Hagan. Understanding organofluorine chemistry. An introduction to the C—F bond. *Chem. Soc. Rev.* **2008**, *37*, 308.
[62] N. Lichtenstein, S. Hestrin, E. Dimant, H. Brzoza. Behavior of peptides when heated in β-naphthol. *J. Am. Chem. Soc.* **1938**, *60*, 560.
[63] E. Drabik, A. Jeziorna, U. Bienias, K. Trzeciak-Karlikowska, T. Pawlak, P. Paluch, M. J. Potrzebowski. Study of the mechanism of thermal chemical processes in the crystals of YAF tripeptides by means of mass spectrometry and solid state NMR. *J. Phys. Chem. B* **2013**, *117*, 13481.
[64] F. Piuzzi, I. Dimicoli, M. Mons, B. Tardivel, Q. Zhao. A simple laser vaporization source for thermally fragile molecules coupled to a supersonic expansion: application to the spectroscopy of tryptophan. *Chem. Phys. Lett.* **2000**, *320*, 282.
[65] U. Sezer, P. Schmid, L. Felix, M. Mayor, M. Arndt. Stability of high-mass molecular libraries: the role of the oligoporphyrin core. *J. Mass Spectrom.* **2015**, *50*, 235.
[66] L. Hanley, R. Zimmermann. Light and molecular ions: the emergence of vacuum UV single-photon ionization in MS. *Anal. Chem.* **2009**, *81*, 4174.
[67] K. Vékey. Internal energy effects in mass spectrometry. *J. Mass Spectrom.* **1996**, *31*, 445.
[68] D. O'Hagan, C. Schaffrath, S. L. Cobb, J. T. Hamilton, C. D. Murphy. Biochemistry: biosynthesis of an organofluorine molecule. *Nature* **2002**, *416*, 279.

Supporting information

Additional Supporting Information may be found online in the supporting information tab for this article.

Chapter 2. Matter-wave interference of modified tripeptides

Outline of the author's contribution

The author J. Schätti wrote a summary of the history of matter-wave interference, which comprises the first part of the chapter. J. Schätti participated in the design and synthesized and characterized the molecular compounds. The first interference experiments of a peptide were performed by J. P. Cotter and L. Mairhofer on the KDTLI. Further interference measurements, as well as the determination of the electric susceptibility, were performed by S. Gerlich and Y. Fein.

The synthesis of the tripeptides modified with fluorinated alkyl chains was scaled up to 1.5 g each. Three new pairs of sequence isomeric tripeptides were synthesized following previously described methods.[1-2] In the case of the Lys-Trp-Gly sequence isomers, the two fluorinated alkyl chains at the N-terminus and the lysine side chain were introduced in a single solution phase acylation reaction.

Introduction to matter-wave interference

Interference is a phenomenon that occurs when two or more waves superimpose. The superposition results in the addition of their amplitudes. Constructive interference is observed when waves are in phase, whereas destructive interference occurs when the waves are out of phase.[3] Thomas Young demonstrated the wave behavior of light In the so-called "Young's double slit experiment" at the beginning of the 19th century, which was in contrast to the prevailing view of the particulate nature of light suggested by Isaac Newton (Figure 1).[4-6] With the discovery of the photoelectric effect by H. Hertz[7] and P. Lenard,[8-9] namely the emission of electrons from the surface of illuminated material, an alternative theory for the nature of light was needed. The kinetic energy of the emitted electrons is not dependent on the amplitude, as was expected, if light would only have wave properties, but on the wavelength of the light.[7-9] Taking this into account Albert Einstein proposed in the year 1905 the particulate nature of light.[10]

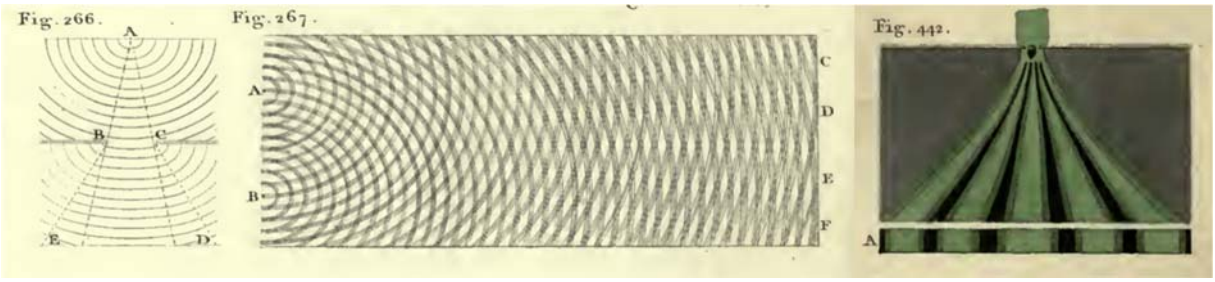

Figure 1. Original drawings by Thomas Young copied from "A course of lectures on natural philosophy and the mechanical arts".[3] (left) The propagation of a wave after passing through a small slit. (center) Two waves are diverging from two point sources A and B and overlay constructively or destructively. (right) Interference pattern on a screen behind a double slit when coherent light passes through.[3]

While certain experimental findings support the wave nature of light, others can only be explained if light is considered to consist of a beam of particles. This seemingly paradoxical behavior has been termed the wave-particle dualism by Louis de Broglie. He proposed particle-wave dualism, not only for light but for all particles[11] – expressed in his famous formula [1], which relates the wavelength to the impulse of a particle. It just took a few years until the wave nature of electrons,[12] neutrons,[13] helium atoms,[14] and even dihydrogen molecules[14] was demonstrated by their diffraction at a crystal lattice.

$$\lambda = \frac{h}{p} = \frac{h}{m \times v} \qquad [1]$$

The first electron interference spectra observed in a double slit experiment similar to the one performed by Thomas Young was published in the year 1961 by Claus Jönsson.[15] Analogous experiments with sodium atoms[16] and diatomic sodium (Na_2)[17] followed. In the year 1999, the group of Markus Arndt reported another breakthrough in matter-wave interference. They generated an

interference pattern from a beam of evaporated C_{60} buckminsterfullerene molecules thereby increasing the mass limit and the number of atoms for more than one order of magnitude. They adapted the experimental setup of Young's experiment to enable interference experiments with molecules. The interferometer developed by the Arndt group consists of five main components as shown in Figure 2b. C_{60}-molecules were evaporated in an oven, which they leave through a nozzle to form a plume of particles. Out of this plume, a molecular beam is selected by two collimation slits 10 µm wide and 1 m apart. Subsequently, the molecular beam passes a silicon nitride (SiN_x) grating (grating period 100 nm) placed 10 cm behind the second collimation slit, and the C_{60}-molecules are finally thermally ionized after another 1.25 m by a visible argon-ion laser . Finally, the fullerene ions were focused on a BeCu conversion electrode, and the emitted electrons were detected by a secondary electron multiplier. The interference pattern was observed by scanning the molecular beam with the ionization laser at micrometer resolution (Figure 2c).[18]

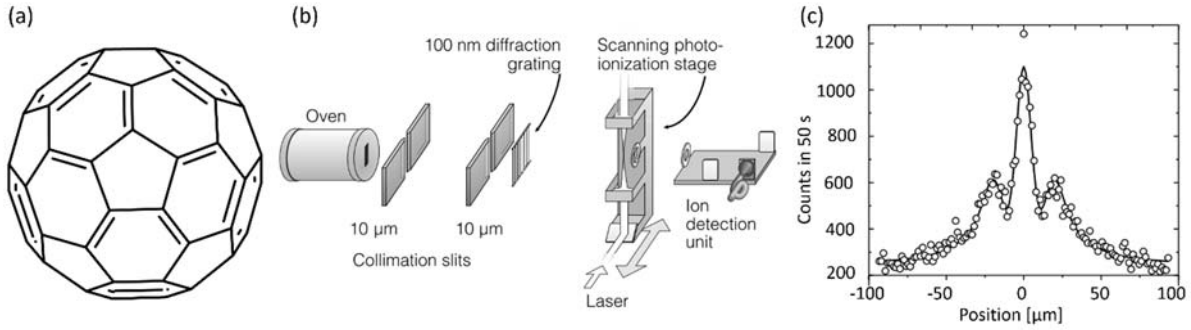

Figure 2. (a) C_{60}-Buckminsterfullerene employed in the experiment. (b) The experimental set-up used by the Arndt group for the interference measurement of C_{60} consisting of an oven, two collimation slits, a diffraction grating, an ionization laser, and a detector unit. (c) The interference pattern of C_{60} molecules. Adapted by permission from *Nature*: *Nature,* **1999,** *401*, 680-682.[18]

The contrast of the interference pattern could be significantly improved by the introduction of a gravitational velocity selection into the molecular beam.[19] This setup was adapted by the Arndt group in 2012. In these experiments, phthalocyanine derivates were employed (1298 amu, Figure 3). The molecular beam was produced by laser-induced evaporation of the molecules from a glass plate. The fluorescent properties of phthalocyanines enabled to monitor the build-up of the interference pattern in real time by fluorescence microscopy (Figure 3).[20] One remaining problem was that the Van der Waals interactions between the molecular beam and the silicon nitride grating led to lower contrast of the interference pattern and the possibility of blocked gratings. This problem can be addressed by replacing the SiN_x grating by a standing light wave. Pyotr Kapitza and Paul Dirac proposed already in the year 1933 the scattering of particles at a standing light wave,[21] which was later experimentally demonstrated for sodium atoms by David E. Pritchard[22] and electrons by Hermann Batelaan.[23]

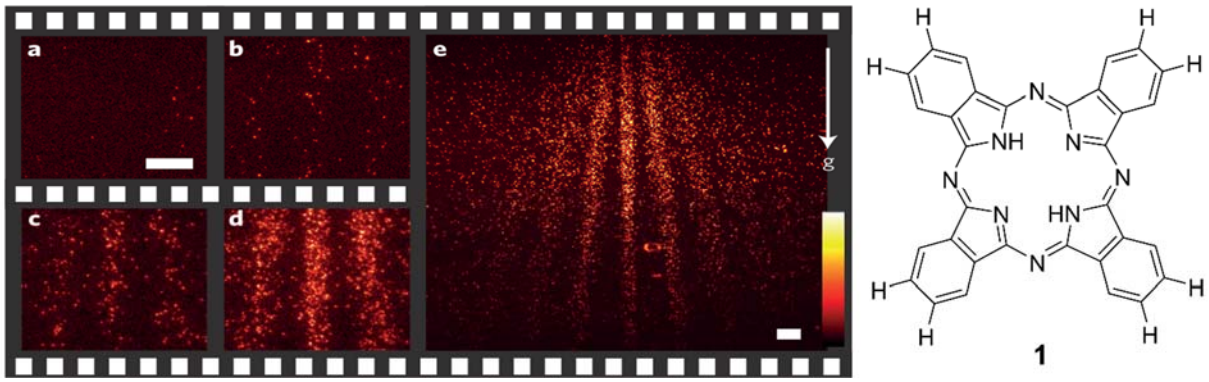

Figure 3. (left) Observed fluorescence images of phthalocyanine molecules deposited on a glass slide. (a) Before deposition of the molecules, (b) after 2 min, (c) after 20 min, (d) after 40 min, (e) after 90 min exposure to the diffracted molecular beam; (right) phthalocyanine molecule used in the study. Reprinted by permission from *Nature*: *Nat. nanotechnol.* **2012**, *7*, 297-300.[20]

Another limitation for high mass particles is that with increasing mass (reduced de Broglie wavelength) the grating period needs to get smaller and smaller. By the use of the so-called Talbot-Lau concept, the required grating period only scales with $\sqrt{\lambda}$ instead of λ. The Talbot-Lau interferometer is built up out of three identical gratings. The first one produces transverse coherence of the molecular beam; the second one acts as a diffraction grating. The diffraction at the second grating generates a self-image of the second grating at the position of the third mask if they are spaced by the Talbot length $L_T = d^2/\lambda$, where d is the period of the grating and λ is the wavelength. By moving the third grating perpendicular to the beam, the interference pattern can be converted into position dependent beam intensity after the third grating. The replacement of the mechanical diffraction grating with a standing light wave leads to the so called Kapitza–Dirac–Talbot–Lau Interferometer (KDTLI).[24-26] The setup of a KDTL interferometer is shown in Figure 4.[18] With this experimental setup, it was possible to measure interference patterns of tetraphenyl porphyrins decorated with fluorinated alkyl chains with a molecular weight exceeding 10 000 amu. The molecular beam was produced by evaporation of the molecules in an oven. Out of the formed molecular plume molecules with a defined velocity were selected by three slits D_1-D_3 through their free fall in the gravitational field. In between slits D_2 and D_3, the molecules pass first a SiN_x grating G_1 which leads to a spatial coherence of the beam. Then they are passing a standing light wave G_2 which acts as a diffracting grating. The second SiN_x grating G_3 serves the same function as described above for the Talbot-Lau interferometer: When the slits of G_3 are positioned where constructive interference occurs more molecules will pass the grating compared to a position where destructive interference occurs. Finally, the molecules were ionized by either electron impact ionization or photoionization, and the ions detected by a quadrupole mass spectrometer. Detection of the ions by mass spectrometry has the advantage that interference patterns can also be observed with impure samples and compound libraries.[18]

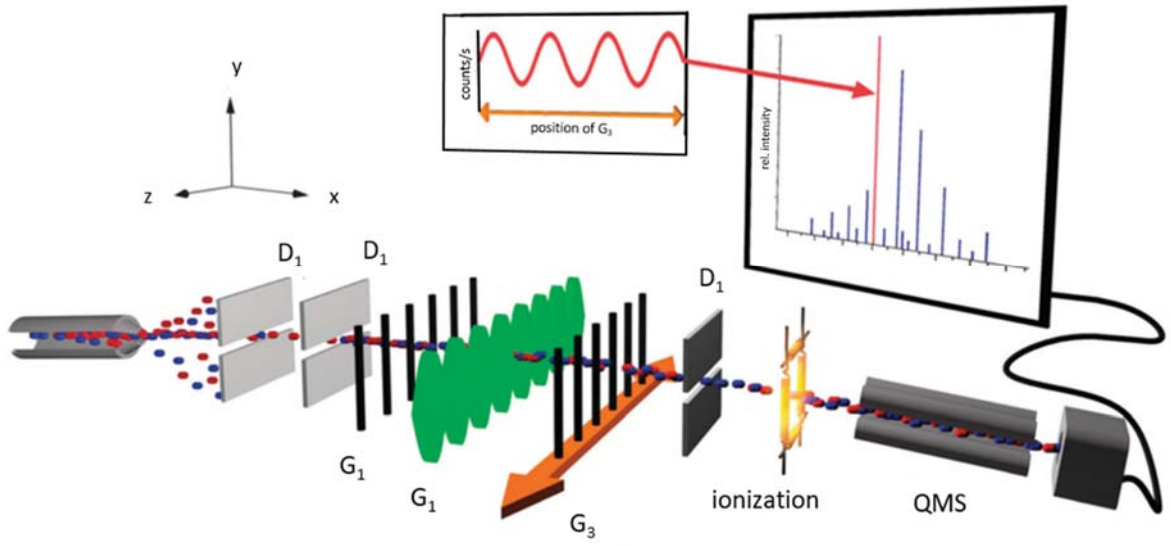

Figure 4. The KDTLI consists of an oven; three velocity selector slits D_1-D_3, three gratings with periods of 266 nm G_1-G_3; G_1 and G_3 are SiN_x gratings whereas G_2 is a standing light wave; G_3 can be moved along the z-axis. Further on there is an ionization source (electron impact- or photo-ionization) and a quadrupole mass spectrometer for detection. Reprinted by permission from *Nature*: *Nat. commun.* **2011,** *2*, 263.[18]

To demonstrate the potential of matter-wave interferometry for metrological applications the Arndt group showed that the discrimination between constitutional isomers by analysis of the fringe shifts of the interference patterns is possible if an external field is applied. To that effect, they implemented a pair of electrodes between G_1 and G_2 to generate an electrical force field across the molecular beam (Figure5). This electrical field now affects the phase of the matter-wave and leads to a shift (Δx_3) of the interference pattern parallel to the grating. The shift (Δx_3) is proportional to the electric susceptibility of the investigated molecule and can accordingly vary for different constitutional isomers given a sufficient difference in electric susceptibility. This was demonstrated for the two molecules shown in Figure 5, which both have the same molecular mass of 1592 amu but differ in their polarizability by around 10%.[27]

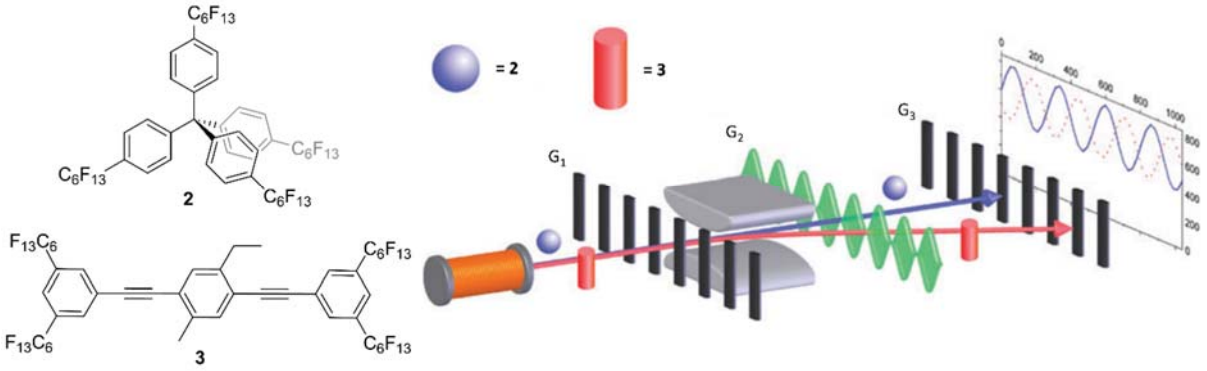

Figure 5. (left) The two constitutional isomers used for this study. (right) The adapted KDTLI setup with an implemented electrical force field between G_1 an G_2. Reproduced from Ref. 27 with permission from The Royal Society of Chemistry.[27]

Matter-wave interference with modified tripeptides

So far all large molecules used for matter-wave interference experiments were tailor-made molecules with optimized properties. They were designed in a way that they can be i) thermally evaporated without decomposition and ii) easily detected after the interference experiment. Since high mass regimes were within reach after the first proof of concept studies, the attention was drawn towards interference experiments with more relevant molecules, namely biomolecules such as peptides and proteins. To show and investigate the wave behavior of biomolecules is of particular interest because they are fundamental components of every known living being and provide complex molecular function. Due to their strong intermolecular interactions such as hydrogen bonds and their low thermal stability, peptides and proteins are not suitable for evaporation in an oven. Accordingly, different strategies to obtain neutral bio-molecular beams had to be investigated. Two alternative approaches were explored: i) reduction of intermolecular interactions by extensive chemical modification to increase the volatility of peptides[1, 28] ii) a limited chemical modification to neutralize electro-sprayed ions via charge-reduction by photocleavage.[29]

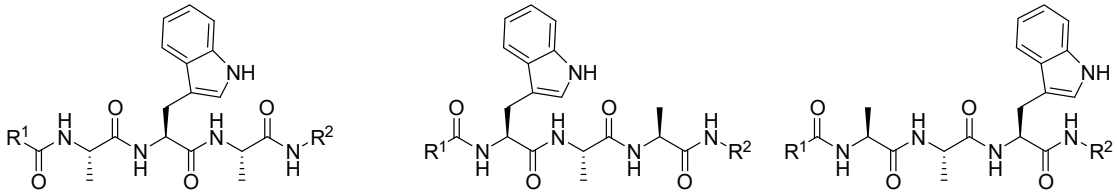

4 R^1= $(CH_2)_2(CF_2)_7CF_3$, R_2= $(CH_2)_2(CF_2)_4CF_3$
5 R^1= R^2 = $(CH_2)_2(CF_2)_7CF_3$

6 R^1= R^2 = $(CH_2)_2(CF_2)_7CF_3$

7 R^1= R^2 = $(CH_2)_2(CF_2)_7CF_3$

Figure 6. Three sequence isomers of the modified Ala-Trp tripeptides used in the first interference experiments with peptides.

By attaching two fluorinated alkyl chains to the C- and N- terminus of tryptophan-containing tripeptides consisting of tryptophan and two alanine residues (Figure 6), they become volatile enough to be evaporated thermally.[1] With peptide **4** the first ever measured interference pattern of a peptide was observed on the KDTL-interferometer with the experimental setup shown in Figure 4.[18] This spectrum is presented in Figure 7.

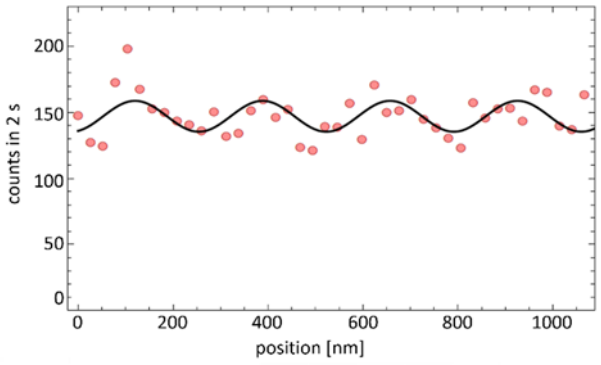

Figure 7. Interference pattern measured for **4** with the KDTLI setup presented in Figure 4. Interference experiments were performed by Joseph Cotter and Lukas Mairhofer.

Inspired by the experiments by Martin F. Jarrold and coworkers which demonstrated, that sequence isomers of the unmodified zwitterionic tripeptide Trp-Tyr-Gly can be distinguished by deflection mass spectrometry,[30] it was attempted to identify the three sequence isomers **5-7** by means of interferometry (compare also Figure 5).[27] The interference experiments were performed on the new Long baseline Universal Matter-wave Interferometer (LUMI). The newly built LUMI has a similar set-up as the KDTLI, but a distance of 1 m in between the different gratings, compared to 10.5 cm for the KTDLI. The longer distance enables an up to 100 × improved sensitivity in molecule metrology to be achieved. The interference pattern for isomers **5** and **7** are presented in Figure 8. It was not possible to generate a stable molecular beam by evaporation for peptide **6**, and therefore no interference could be measured. The poor signal/noise in the interference experiments of tripeptides is likely due to electron impact ionization. As observed in previous studies[1] electron impact leads to strong fragmentation of the peptides whereas under photoionization (157 nm) a strong signal for the intact molecular ion can be observed. Photoionization is currently not applicable for interference experiments due to the low puls frequency of the available ionization lasers in Vienna which translates to a low count rate.

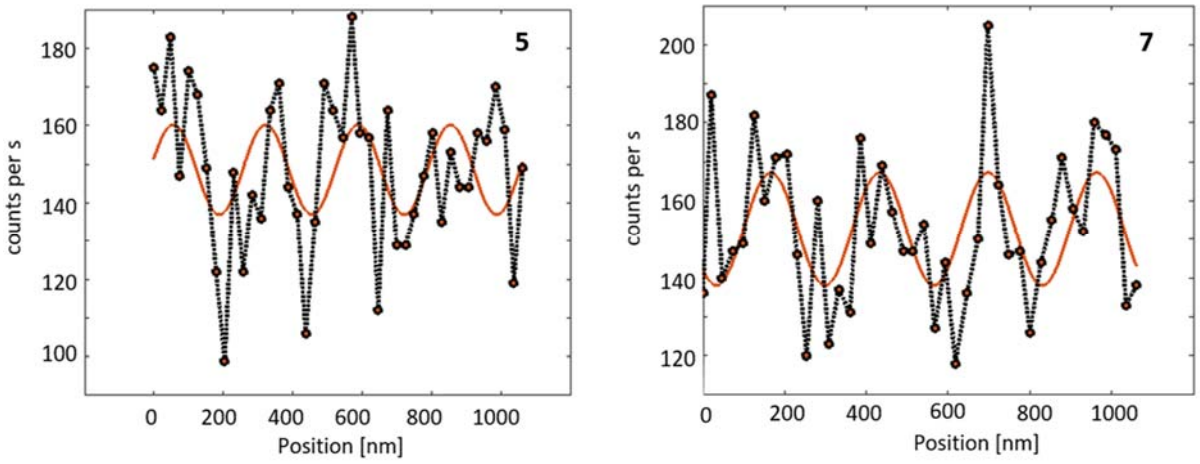

Figure 8. Interference spectra of the three sequence isomers **5** and **7**. Interference experiments performed by Stefan Gerlich and Yaakov Fein.

Unfortunately, the contrast of the interference pattern for the two isomers **5** and **7** was not over 10%. It was only possible to determine the deflection at different voltages for compounds **4** and **5**, which have the same peptide sequence and differ only in the length of the fluorinated chain R_2. The signal of **7** was not stable enough and therefore it was not possible to measure the interference pattern at different voltages. For peptide **4** and **5** a deflection at different voltages could be measured (e.g., about 800 nm at 1500 V for **5**). This corresponds to an electric susceptibility of 264 A^3 for both of them.

Other sets of sequence isomeres (Figure 9) were synthesized and tested in the setup described above. **8** and **9** contain Trp, Gly, and Lys with a fluorinated chain sitting at the N-terminus and the lysine side

chain. **10** and **11** consist of Trp, Tyr, and Gly with fluorinated chains attached to N- and C-terminus. Finally, **12** and **13** were sequence isomeres of Ala, Pro, and Trp. It was not possible to record good quality interference patterns for any of these, due to their low thermal stability or their low tolerance towards electron impact ionization and they were not further investigated.

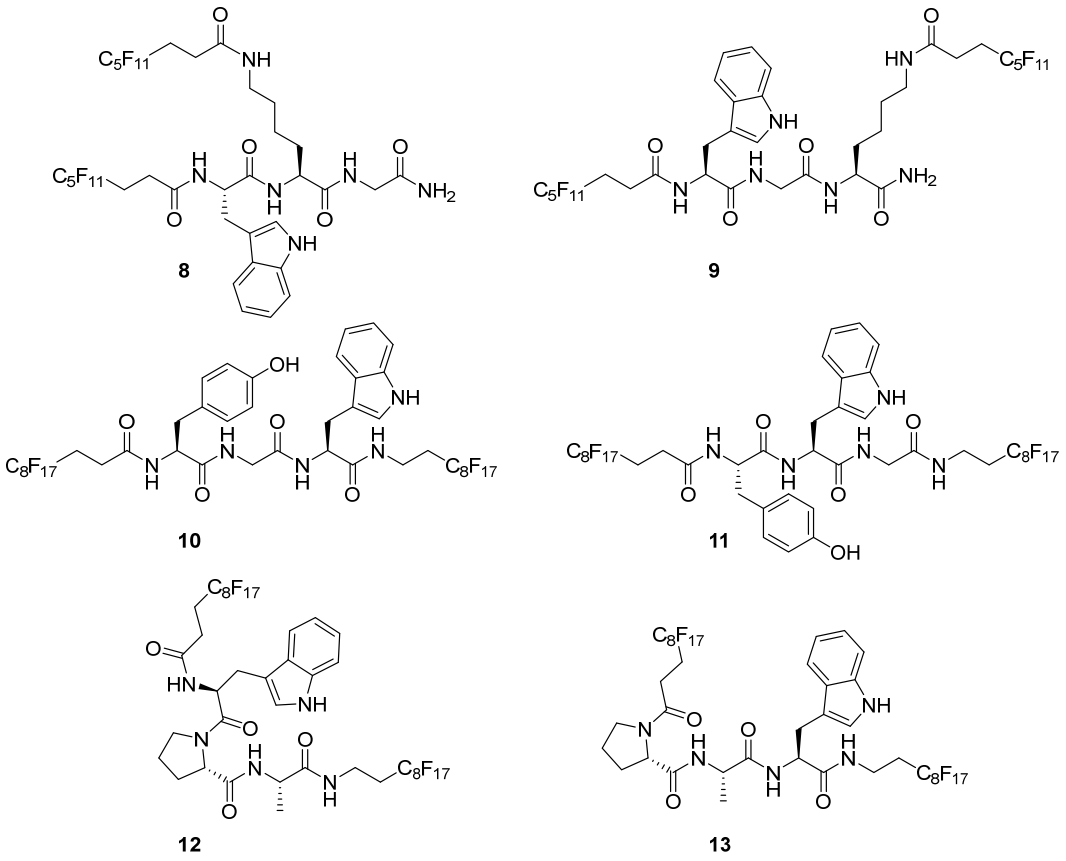

Figure 9. Additional pairs of sequence isomers tested for thermal evaporation followed by matter-wave interference. **8** and **9** contain Lys, Trp, and Gly; **10** and **11** Tyr, Gly, and Trp; **12** and **13** Trp, Pro and Ala.

References

1. J. Schätti; U. Sezer; S. Pedalino; J. P. Cotter; M. Arndt; M. Mayor; V. Köhler, Tailoring the volatility and stability of oligopeptides. *J. Mass Spectrom.* **2017,** *52* (8), 550-556.
2. L. Malik; J. Nygaard; R. Hoiberg-Nielsen; L. Arleth; T. Hoeg-Jensen; K. J. Jensen, Perfluoroalkyl Chains Direct Novel Self-Assembly of Insulin. *Langmuir* **2012,** *28* (1), 593-603.
3. D. Meschede, Optik, Licht und Laser; Vieweg Teubner In Gwv Fachverlage: Wiesbaden. **2008**.
4. T. Young, II. The Bakerian Lecture. On the theory of light and colours. *Philos. Trans. R. Soc.* **1802,** *92*, 12-48.
5. T. Young, *A course of lectures on natural philosophy and the mechanical arts*. J. Johnson: London :, **1807**; Vol. 1.
6. I. Newton, Opticks or, a Treatise of the Reflections, Refractions, Inflections, and Colours of Light. **1704**.
7. H. Hertz, Ueber einen Einfluss des ultravioletten Lichtes auf die electrische Entladung. *Ann. Phys.* **1887,** *267* (8), 983-1000.
8. P. von Lenard, On cathode rays. *Nobel Lecture* **1906**.
9. B. R. Wheaton, Philipp Lenard and the Photoelectric Effect, 1889-1911. *Hist. Stud. Nat .Sci.* **1978,** *9*, 299-322.

10. A. Einstein, Über einen die Erzeugung und Verwandlung des Lichtes betreffenden heuristischen Gesichtspunkt. *Ann. Phys.* **1905,** *322* (6), 132-148.
11. L. De Broglie, Waves and Quanta. *Nature* **1923,** *112*, 540.
12. C. Davisson; L. H. Germer, The Scattering of Electrons by a Single Crystal of Nickel. *Nature* **1927,** *119*, 558.
13. H. von Halban; P. Preiswerk, Preuve experimental de Ia diffraction des neutrons. *C.R. Acad. Sci. Paris* **1936,** *203*, 73-5.
14. I. Estermann; O. Stern, Beugung von Molekularstrahlen. *Z. Phys.* **1930,** *61* (1), 95-125.
15. C. Jönsson, Elektroneninterferenzen an mehreren künstlich hergestellten Feinspalten. *Z. Phys.* **1961,** *161* (4), 454-474.
16. O. Carnal; J. Mlynek, Young's double-slit experiment with atoms: A simple atom i nterferometer. *Phys. Rev. Lett.* **1991,** *66* (21), 2689-2692.
17. M. S. Chapman; C. R. Ekstrom; T. D. Hammond; R. A. Rubenstein; J. Schmiedmayer; S. Wehinger; D. E. Pritchard, Optics and Interferometry with with Na_2 Molecules *Phys. Rev. Lett.* **1995,** *74* (24), 4783-4786.
18. M. Arndt; O. Nalrz; J. Vos-Andreae; C. Keller; G. Van Der Zouw; A. Zellinger, Wave-particle duality of C60 molecules. *Nature* **1999,** *401* (6754), 680-682.
19. M. Arndt; O. Nairz; J. Petschinka; A. Zeilinger, High contrast interference with C60 and C70. *C. R. Acad. Sci., Ser. IV: Phys., Astrophys.* **2001,** *2* (4), 581-585.
20. T. Juffmann; A. Milic; M. Mullneritsch; P. Asenbaum; A. Tsukernik; J. Tuxen; M. Mayor; O. Cheshnovsky; M. Arndt, Real-time single-molecule imaging of quantum interference. *Nat. Nanotechnol.* **2012,** *7* (5), 297-300.
21. P. L. Kapitza; P. A. M. Dirac, The reflection of electrons from standing light waves. *Math. Proc. Camb. Philos. Soc.* **1933,** *29* (2), 297-300.
22. P. J. Martin; B. G. Oldaker; A. H. Miklich; D. E. Pritchard, Bragg scattering of atoms from a standing light wave. *Phys. Rev. Lett.* **1988,** *60* (6), 515-518.
23. D. Freimund; K. Aflatooni; H. Batelaan, Observation of the Kapitza-Dirac effect. *Nature* **2001,** *413* (6852), 142-143.
24. S. Gerlich; L. Hackermueller; K. Hornberger; A. Stibor; H. Ulbricht; M. Gring; F. Goldfarb; T. Savas; M. Mueri; M. Mayor; M. Arndt, A Kapitza-Dirac-Talbot-Lau interferometer for highly polarizable molecules. *Nat. Phys.* **2007,** *3* (10), 711-715.
25. S. Gerlich; S. Eibenberger; M. Tomandl; S. Nimmrichter; K. Hornberger; P. J. Fagan; J. Tuxen; M. Mayor; M. Arndt, Quantum interference of large organic molecules. *Nat. Commun.* **2011,** *2*, 263.
26. S. Eibenberger; S. Gerlich; M. Arndt; M. Mayor; J. Tuxen, Matter-wave interference of particles selected from a molecular library with masses exceeding 10,000 amu. *Phys. Chem. Chem. Phys.* **2013,** *15* (35), 14696-700.
27. J. Tüxen; S. Gerlich; S. Eibenberger; M. Arndt; M. Mayor, *Quantum interference distinguishes between constitutional isomers*. 2010; Vol. 46, p 4145-7.
28. J. Schätti; P. Rieser; U. Sezer; G. Richter; P. Geyer; G. G. Rondina; D. Häussinger; M. Mayor; A. Shayeghi; V. Köhler; M. Arndt, Pushing the mass limit for intact launch and photoionization of large neutral biopolymers. *Commun. Chem.* **2018,** *1* (1), 93.
29. M. Debiossac; J. Schatti; M. Kriegleder; P. Geyer; A. Shayeghi; M. Mayor; M. Arndt; V. Kohler, Tailored photocleavable peptides: fragmentation and neutralization pathways in high vacuum. *Phys. Chem. Chem. Phys.* **2018**.
30. R. Antoine; I. Compagnon; D. Rayane; M. Broyer; P. Dugourd; N. Sommerer; M. Rossignol; D. Pippen; F. C. Hagemeister; M. F. Jarrold, Application of molecular beam deflection time-of-flight mass spectrometry to peptide analysis. *Anal. Chem.* **2003,** *75* (20), 5512-5516.

Chapter 3. Pushing the mass limit for intact launch and photo-ionization of large neutral biopolymers

J. Schätti; P. Rieser; U. Sezer; G. Richter; P. Geyer; G. G. Rondina; D. Häussinger; M. Mayor; A. Shayeghi; V. Köhler; M. Arndt, *Chem. Commun.,* **2018,** *1 (1)*, 93.

Outline of the author's contribution

The experiments were conceived by M. Arndt, V. Köhler, M. Mayor, U. Sezer, and A. Shayeghi. The molecular design and synthesis were realized by J. Schätti, V. Köhler, and M. Mayor. The nanosecond experiments were realized by U. Sezer, P. Rieser, and P. Geyer. The femtosecond experiments were realized by P. Rieser., G. Richter., and A. Shayeghi. Data analysis was performed by J. Schätti, U. Sezer, G. Richter, P. Rieser, A. Shayeghi and M. Arndt. NMR experiments were carried out and analyzed by J. Schätti with the help of D. Häussinger. Molecular dynamics simulations were designed and analyzed by A. Shayeghi, G. G. Rondina, and M. Arndt and realized by G. G. Rondina. The manuscript was written by M. Arndt, V. Köhler and J. Schätti with contributions from all authors.

A variety of polypeptides with up to 50 amino acids were synthesized by means of a peptide synthesizer. The challenging purification of the produced $(WK)_n$ oligomers was performed by preparative HPLC with varying success. $(WK)_n$ constructs with fluorinated alkyl chains attached to all lysine side chains were produced in a one-step reaction by global amidation of the unmodified peptide with the NHS-ester of $CF_3(CF_2)_nCH_2CH_2COOH$. In an alternative approach, the lysine side-chain was amidated with the fluorinated alkyl group prior to solid phase peptide synthesis. This approach worked well for short peptides of up to ten amino acids, but could not be applied for longer peptides. The second approach led to decreasing coupling yields with increased peptide length, which was likely due to the poor solubility of the resin-bound peptide.

COMMUNICATIONS CHEMISTRY

ARTICLE

https://doi.org/10.1038/s42004-018-0095-y OPEN

Pushing the mass limit for intact launch and photoionization of large neutral biopolymers

Jonas Schätti[1], Philipp Rieser[2], Ugur Sezer[2], Georg Richter[2], Philipp Geyer[2], Gustavo G. Rondina[3], Daniel Häussinger[1], Marcel Mayor[1,4,5], Armin Shayeghi[2], Valentin Köhler[1] & Markus Arndt[2]

Since their first discovery by Louis Dunoyer and Otto Stern, molecular beams have conquered research and technology. However, it has remained an outstanding challenge to isolate and photoionize beams of massive neutral polypeptides. Here we show that femtosecond desorption from a matrix-free sample in high vacuum can produce biomolecular beams at least 25 times more efficiently than nanosecond techniques. While it has also been difficult to photoionize large biomolecules, we find that tailored structures with an abundant exposure of tryptophan residues at their surface can be ionized by vacuum ultraviolet light. The combination of these desorption and ionization techniques allows us to observe molecular beams of neutral polypeptides with a mass exceeding 20,000 amu. They are composed of 50 amino acids – 25 tryptophan and 25 lysine residues – and 26 fluorinated alkyl chains. The tools presented here offer a basis for the preparation, control and detection of polypeptide beams.

[1] Department of Chemistry, University of Basel, 4056 Basel, Switzerland. [2] Faculty of Physics, University of Vienna, Boltzmanngasse 5, 1090 Vienna, Austria. [3] Eduard-Zintl-Institut für Anorganische und Physikalische Chemie, Technische Universität Darmstadt, 64287 Darmstadt, Germany. [4] Institute of Nanotechnology, Karlsruhe Institute of Technology, Hermann-von-Helmholtz-Platz 1, 76344 Eggenstein-Leopoldshafen, Germany. [5] Lehn Institute of Functional Materials (LIFM), Sun Yat-Sen University (SYSU), XinGangXi Road 135, 510275 Guangzhou, P.R. China. [6] Faculty of Physics, University of Vienna, Boltzmanngasse 5, A-1090 Vienna, Austria. Correspondence and requests for materials should be addressed to V.Köh. (email: valentin.koehler@unibas.ch) or to M.A. (email: markus.arndt@univie.ac.at)

Molecular beam science was started at the beginning of the last century[1] to explore the foundations of physics in early tests of the kinetic theory of gases and in the first matter–wave diffraction of atoms and diatomic molecules[2]. Since then, free molecular beams have found diverse applications ranging from atomic clocks[3] and high-resolution molecular spectroscopy[4], over cluster deposition[5] to nanoparticle metrology[6,7] and modern tests of fundamental quantum optics[8–12]. Even functionalized silicon nanocrystals[8] and silver-sulfur nanoparticles[9] have been thermally transferred as neutral particles into high vacuum.

In recent years, unsolvated biomolecules have attracted interest[13–15] since beam experiments allow one to extract intrinsic electronic or structural information of molecules free from any perturbing interactions with a local environment. While charged molecules have been successfully trapped in vacuum for spectroscopy[16], photodissociation[17,18], or photodetachment studies[19], many electronic, magnetic, and optical properties are particularly interesting for neutral particle beams[20]. Beams of isolated molecules[21] were also essential for the analysis of optical[16] and electronic properties of oligopeptides[22] and vitamins[23].

Extending such experiments to large biopolymers and biomimetic particles requires novel methods for transferring them into the gas phase and for detecting them efficiently as well as mass-selectively. While some amino acids[24], nucleotides[25], and functionalized tripeptides[26] can be sublimated or evaporated, large peptides and proteins typically decompose in thermal sources. Nanosecond laser desorption can reduce the heat load and an adiabatically expanding noble gas[27] can cool and carry the molecules toward their subsequent analysis[28]. However, for more than 20 years, it has remained a challenge to desorb and photoionize biopolymers with masses exceeding 2,000 amu[29,30].

Several arguments have been put forward to explain this observation: For instance, internal state relaxation competes with multi-photon ionization[29,31]. This can be reduced using femtosecond ionization[32] but dissipation to non-ionizing states still often dominates in large biopolymers. Single-photon ionization (SPI) can avoid the intermediate levels and close such relaxation channels but it requires typically a photon energy >10 eV, which is beyond the reach of sufficiently intense table-top laser sources[33,34]. Tryptophan (Trp) is the only natural amino acid that can be ionized by a single photon of 7.89 eV as emitted by vacuum ultraviolet (VUV) F_2 lasers.

Gramicidin D and a number of other antibiotic peptides[22] owe their ionization properties to their Trp residues[35]. The role of Trp as an ionizable moiety has been shown for amino acid clusters up to Trp_{30}, which can be abundantly detected using 157.6 nm light[36]. In contrast, photoionization of large covalently bound polypeptides has remained a challenge. A model for the reduced photoionization yield, based on the assumption of rapid electron recapture within the molecule, predicted an exponential decrease with particle mass[31] and negligible efficiency for peptides beyond 2,000 amu, as observed in many experiments so far. We therefore hypothesized that ionization might still be possible if a high number of chromophores could be exposed to vacuum.

Here we show that polypeptides with alternating Trp residues and lysine residues that are amidated with fluoroalkyl chains can be efficiently laser desorbed and postionized. Femtosecond laser desorption enables >25 times higher material economy when compared to nanosecond methods. Polypeptides exceeding 20,000 amu were successfully desorbed and postionized.

Results

Peptide design. Based on these reasonings, we have designed and synthesized five model compounds (see Fig. 1) to build on the antibiotic polypeptide gramicidin D (**1**), which was among the most massive neutral biomolecules in previous beam experiments. Commercial gramicidin D is composed of 15 amino acids, and the most abundant A1 form (molecular weight 1882 amu) contains four Trp residues. Our first tailored model system, decatryptophan Trp_{10} (**2**), contains more than double the number of chromophores at a comparable mass. Since peptide solubility decreases with the number of Trp residues, Trp_{10} represents a practical upper bound to the chain length for a quantitative synthesis of such molecules. The second model compound combines good solubility with high Trp content by alternating Trp with lysine to Ac-$(Lys\text{-}Trp)_5$-OH (**3**). This sequence of alternating amino acids is scalable to long peptides. Compound (**4**) displays the same $(Trp\text{-}Lys)_n$ motif as (**3**) for $n = 10$ and each NH_2 has been amidated with a fluorinated alkyl chain. The total mass therefore exceeds that of gramicidin already by a factor of 4.5. The high fluorine content is intended to reduce intermolecular interactions and to enhance volatility.

In order to maximize the molecular weight at constant Trp ratio, we synthesized the model polymers (**5**) and (**6**) with $n = 14$ and $n = 25$ blocks of $(Lys\text{-}Trp)_n$. They were functionalized in the same way as (**3**). Peptide (**6**) holds 1,960 atoms in 50 amino acid building blocks with a total mass of 20,201 amu. It resembles a protein in macromolecular architecture and mass. The molecules were prepared by standard solid-phase peptide chemistry under Fmoc protection[37]. Fluorinated alkyl groups were introduced by amidation with the respective *N*-hydroxysuccinimide ester after cleavage from the resin[38].

From short-pulse to ultrafast laser desorption of heavy polypeptides. The molecular beam apparatus is sketched in Fig. 2. Analyte powder is picked up by a felt wheel, which transfers a thin layer of molecules onto a counter-rotating glassy carbon wheel. This layer is desorbed by a pulsed focused laser beam[39]. Different desorption lasers were used to answer different questions. Model compounds (**1**)–(**3**) were desorbed by short-pulse infrared laser light (7 ns, 1064 nm, $4–6 \times 10^7$ W cm^{-2}) to explore the role of the Trp content. A quantitative assessment of the importance of the laser pulse duration was realized using gramicidin D (**1**). The high-mass peptides (**4**) and (**5**) show the influence of fluoroalkyl functionalization. They were volatilized using ultraviolet nanosecond pulses (7 ns, 266 nm, $5–8 \times 10^7$ W cm^{-2}). The most massive polypeptide (**6**) was desorbed using *ultrafast*, ultraviolet laser desorption (292 fs, 343 nm) with peak intensities around 5×10^{11} W cm^{-2}.

Once detached from the surface, the analyte molecules are immediately entrained by the atomic carrier gas (argon or neon) that is released by a valve with about 20 µs opening time. The neutral peptides fly 75 cm in high vacuum, across two differentially pumped vacuum chambers. They are then photoionized by a laser pulse at 157 nm to be extracted and detected by orthogonal time-of-flight mass spectrometry.

Influence of the Trp content and fluoroalkyl chains. Figure 3 compares a set of three tailored polypeptides with gramicidin D (**1**), which formed a molecular beam strong enough to saturate the detector after VUV postionization. Assuming that a high Trp content correlates with a high ionization cross-section, we have desorbed decatryptophan (**2**) but find additional fragmentation (For enlarged spectra and peak assignments, see Supplementary Figures 33–38). Substituting half of the Trp residues by lysine units enhances the solubility, facilitates the peptide synthesis and enables soft volatilization with reduced fragmentation, as shown for peptide (**3**). Compound (**4**) is built on this insight and raises the mass by more than a factor of five compared to (**3**), using

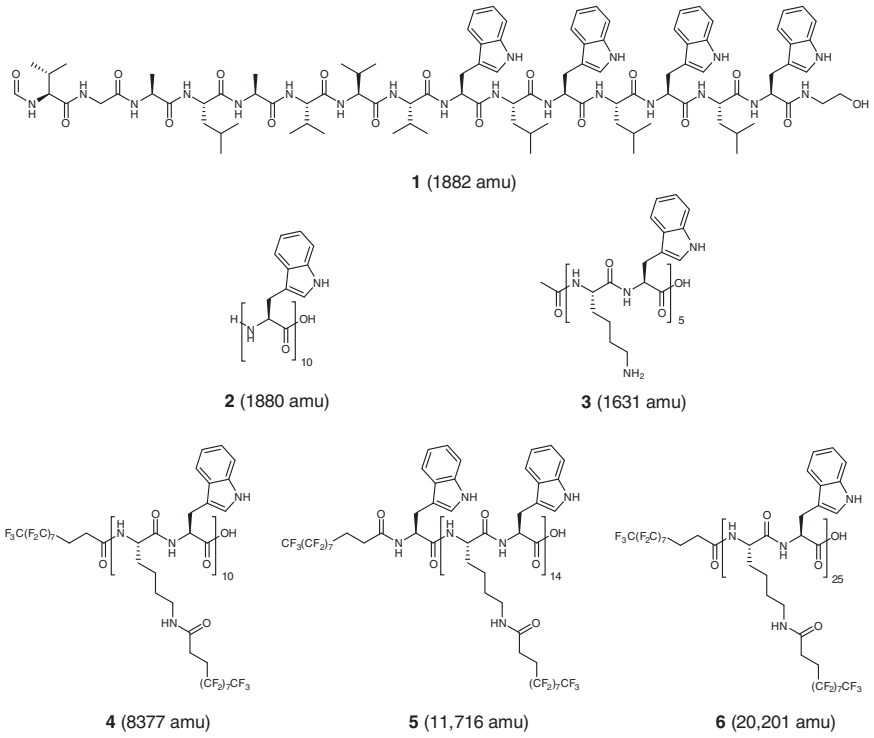

Fig. 1 Iterative design of high mass oligopeptides for molecular beam experiments. Gramicidin A1, as shown here (**1**) is the principal component of commercial gramicidin D. Decatryptophan (**2**) has the highest tryptophan-to-mass ratio of all peptides in our study. Alternating Trp with Lys as in (**3**) provides better solubility and synthetic scalability. The molecular mass and the volatility can be enhanced by capping the NH_2 groups with CO $(CH_2)_2(CF_2)_7CF_3$ groups as in (**4**)–(**6**). (**5**) extends (**4**) to $n = 14$, with a total of 29 amino acids. (**6**) extends (**5**) to $n = 25$, i.e., it contains 50 amino acids. It is functionalized to increase its molecular weight to 20,201 amu and to expose copious amounts of tryptophan to the vacuum

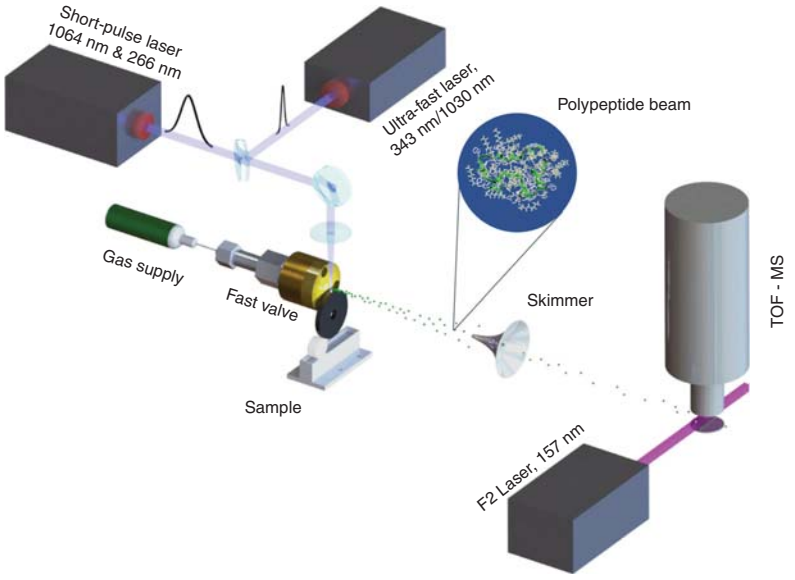

Fig. 2 Molecular beam machine to launch and detect neutral polypeptides. Short or ultrashort laser pulses can be used to desorb the analyte molecules from a powder coated onto a rotating carbon wheel. The individualized polypeptides are entrained by an adiabatically expanding noble gas jet. The molecular beam enters the differentially pumped ionization chamber where a vacuum ultraviolet (VUV) laser pulse (ca. 1 mJ and 10 ns) ionizes it for subsequent analysis by a time-of-flight mass spectrometer (TOF-MS).

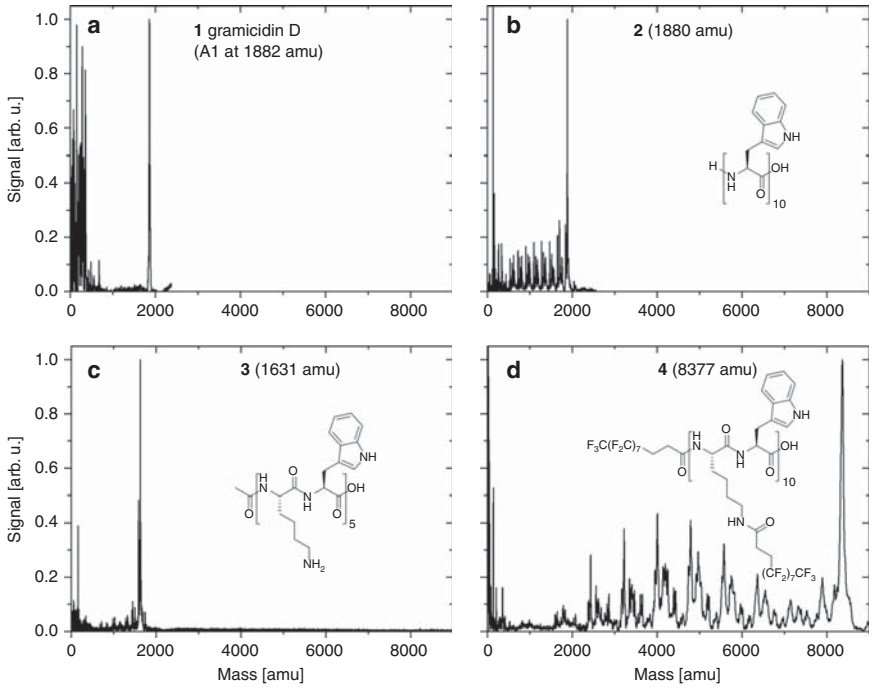

Fig. 3 Nanosecond desorption and VUV ionization of functional polypeptides (**1**)-(**4**). Gramicidin D (**1**) serves as a reference molecule for desorption/postionization experiments. Decatryptophan (**2**) has the highest tryptophan-to-mass ratio and lowest solubility in our series of unmodified peptides. Peptide (**3**) improves on that by substituting every second Trp by Lys. (**4**) is the first step on a new path toward neutral bio-inspired nanoparticle beams and toward a better understanding of the conditions for biopolymer ionization

fluoroalkyl functionalization. Even though peptide (**4**) exhibits more fragments than (**3**), it demonstrates that high-mass peptides can be tailored for neutral molecular beam experiments and be photoionized by VUV laser light.

We have verified the robustness of the mass spectra for various UV nanosecond desorption and ionization energies using compound (**4**) (8377 amu) and oligopeptide (**P7**, Supplementary Figures 41–43, Supplementary Table 2, Supplementary Notes 3–5) (12,320 amu). While we find a threshold behavior followed by saturation for the desorption process (Supplementary Figures 41 and 42 and Supplementary Table 2), the ion yield grows continuously with the ionization energy for the available range of laser pulse energies (Supplementary Figure 43).

On the importance of ultrafast desorption. At a pulse energy of up to 3 mJ, the Q-switched nanosecond laser beam was focused into a spot of 2 mm diameter and reached a peak intensity of about 10^7 W cm^{-2}. This value is comparable to threshold values in matrix-assisted laser desorption ionization (MALDI) experiments[40]. However, several MALDI studies have shown that only a fraction of 10^{-4}–10^{-7} of all desorbed material contributes to the final ion signal[41]. Similarly, in our experiments a substantial fraction of the material is released as nano- and microparticles, which visibly coat the vacuum chamber and are thus lost for the molecular beam.

This indicates an opportunity for substantial improvements and one is led to believe that ultrafast desorption might increase the desorption efficiency, since the absorbed heat will spread less before the pulse energy is transferred and molecules are ejected. This idea has caught on in recent mass spectrometric experiments that combined femtosecond laser desorption with electrospray postionization under atmospheric conditions[42,43]. Here we explore the benefits of ultrafast laser light on biomolecular layers in high vacuum, followed by rapid injection into an adiabatically expanding argon beam. Our ultrafast lasers cover pulse energies up to 80 µJ at 1030 nm and up to 40 µJ at 343 nm with a pulse duration down to 292 fs. We have characterized this idea using gramicidin D (**1**) because of its abundant commercial availability. The robustness of the qualitative form of the mass spectra was first tested for a wide range of desorption conditions, now including femtosecond light (Supplementary Table 2 and Supplementary Figure 40). Comparing then ultrafast desorption at 1030 and 343 nm for comparable pulse durations (292 fs) and energies (15 µJ, on the sample), we find the high UV photon energy (3.6 eV) to be essential for peptide desorption. The energy threshold at this wavelength amounts to about 10 µJ focused in a near-Gaussian waist of ca. 100 µm diameter, i.e., 100 mJ cm^{-2} or 3×10^{11} W cm^{-2} .

Most importantly, the femtosecond pulses improve the sample life time by a factor of >25 in comparison to nanosecond desorption. This is documented in Fig. 4a, where the molecular beam signal is traced as a function of time, while the laser is irradiating the same sample spot with a rate of 100 Hz. The hypothesis that ultrafast desorption favors individualized molecules over the formation of nanoparticles is also corroborated by the fact that the source chamber remains visibly clean.

Figure 4b might suggest that, for the chosen parameters, a laser pulse duration of 10–20 ps already achieves this goal. Reducing the duration by another factor of 33, from 10 ps to 300 fs, the signal decreases by only about a factor of 2. This is consistent with the assumption that most particles depart already as isolated molecules. Reducing the laser pulse length at constant energy and thus increasing the peak intensity may foster multiphoton processes that reduce the molecular beam signal.

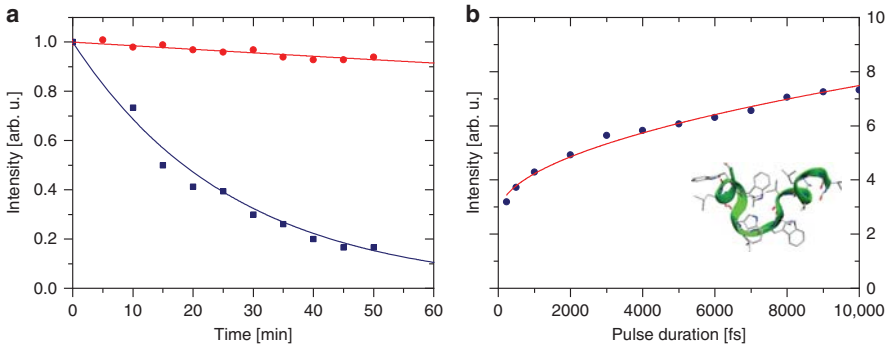

Fig. 4 Molecular beam strength and desorption efficiency as a function of laser pulse duration. **a** Desorption economy: Gramicidin D was desorbed from a thin film. We compare the longevity of a typical sample spot under ultrafast desorption (300 fs at 343 nm, 15 μJ red full circles and line) and short pulse desorption (7 ns at 355 nm, 3 mJ, blue full squares and line). For the same surface area of 100 × 100 μm^2, femtosecond irradiation yields approximately the same initial molecular beam signal but at substantially longer sample life time. The solid lines are exponential fits to the data, with a decay constant of τ_{ns} = 27 and τ_{fs} = 676 min. **b** Desorption laser pulse duration: When varying the pulse duration of infrared light (1030 nm, 40 μJ on 100 × 100 μm^2) irradiating gramicidin D (see inset), we find a smooth increase in the number of detected molecules when the pulse duration is ramped through a factor of 25. The solid line is a square root fit to guide the eye

Improving the material economy by up to two orders of magnitude is a precious advantage in experiments with rare materials, but how would the tremendous laser intensity increase of ultrafast desorption affect the fragmentation pattern? Figure 5 illustrates that ultraviolet desorption can generate a neutral and photoionizable beam of the high-mass peptide (**5**) in both the nanosecond and the femtosecond mode. Comparable integrated signals and fragmentation patterns were obtained; however, at 100 times lower pulse energy, 200 times higher peak intensity and 2 orders of magnitude reduced material consumption in the femtosecond case.

Further exploring the scalability of our new synthesis, desorption, and detection methods, Fig. 6 shows that even the most massive polypeptide in this series can be transferred into a beam of neutral molecules that can be postionized using 157 nm VUV light. This is noteworthy since compound (**6**) is about an order of magnitude more massive than other biopolymers whose photoionization has been reported in the literature so far.

To explore the role of the molecular structure and folding on the exposure of the Trp chromophores to vacuum, canonical-ensemble molecular dynamics simulations were performed for different temperatures. While even at low temperatures a plethora of stretched and coiled structures can stably coexist, we explore the extreme case, starting from the stretched state. While molecule (**6**) can initially extend over >7 nm, our numerical simulations show that it collapses within <100 ps into an energetically more favorable coiled-up tertiary structure upon heating, regardless of the initial state, which is kinetically trapped at low temperature. As a measure of compactness, the average radius of gyration $\langle R_G \rangle$ was calculated as a function of temperature. Figure 7a traces the collapse toward an equilibrium end-to-end distance of about 2 nm beyond $T > 350$ K and $\langle R_G \rangle \simeq$ 1.5 nm. One might worry that the close conformation might bury most chromophores and render photoionization difficult. To obtain an estimate for the exposure of all moieties to vacuum, we have calculated the solvent accessible surface area for the entire molecule as well as for its relevant components, i.e., the Trp and Lys residues as well as the fluoroalkyl chains. Figure 7b shows that the exposed surface area of Trp remains essentially constant over the 0-400 K temperature range and Trp residues are still abundantly exposed to vacuum even in the collapsed state. This can facilitate the escape of electrons after photoionization and distinguishes these Trp-rich polypeptides from many natural proteins (Computational details can be found in the Supplementary Note 2).

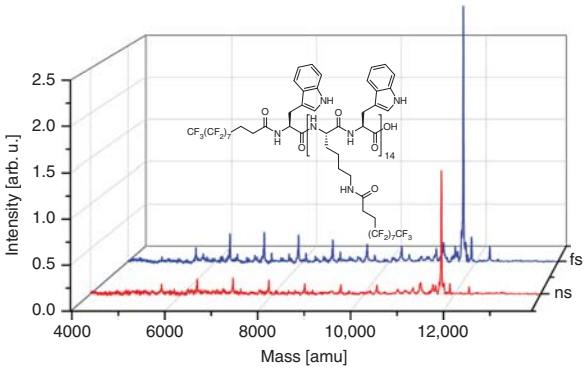

Fig. 5 Mass spectra of the polypeptide (**5**) in comparison between nanosecond and femtosecond desorption. Desorption conditions: short-pulse: $\lambda = 355$ nm, $E = 3$ mJ, $\tau = 7$ ns (red line, foreground). Ultrashort pulse: $\lambda = 343$ nm, $E = 15$ μJ, $\tau = 292$ fs (blue line, background). The different desorption conditions change the desorption efficiency but hardly influence the fragmentation pattern. For peak assignments, see Supplementary Figure 37

Polymer length and desorption/detection efficiency. While earlier papers had speculated that there might be an exponential decrease in the ionization efficiency with increasing mass of the biopolymer, the compounds of our present study were explicitly tailored to avoid this: the number of ionizable Trp chromophores increases in proportion with the polymer length and the simulations show that for all tested circumstances they are arranged abundantly on the molecular surface. While the absorption and ionization probability should thus remain constant with increasing polymer length, the dependence of the volatilization on chain length is less obvious. On the one hand, the equally increasing number of perfluoroalkyl chains reduces the potential stacking of aromatic rings and increase the mass/polarizability or mass/dipole moment ratios. This was already the idea and success of earlier high-mass molecular quantum optics experiments[12]. However, desorbing a given mass and volume of biopolymers

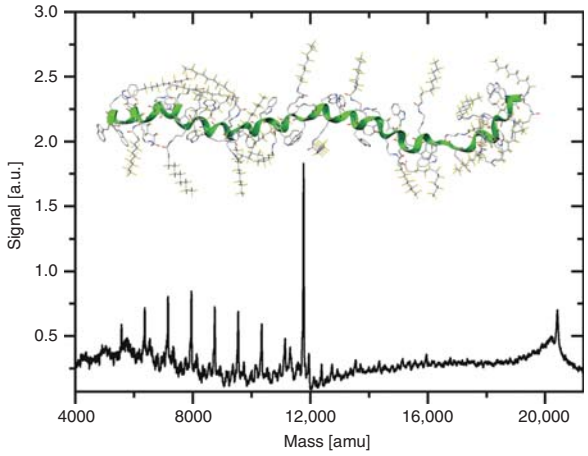

Fig. 6 A neutral molecular beam of massive functionalized polypeptides. A mixture of model peptides (**5**) and (**6**) was prepared in a ratio of 15 mg:140 mg and exposed to ultraviolet femtosecond desorption ($\lambda = 343$ nm, $\tau =$ 292, 15 μJ in 100×100 μm^2). Even compound (**6**) stands out with good signal-to-noise ratio, proving the successful neutral launch and VUV postionization of this massive polypeptide. The fragments are assigned to the cleavage of Trp-Lys(fluoroalkyl) groups (as in Fig. 5) and are also found in the MALDI spectra of the same compounds (Supplementary Figures 24 and 28, see also Supplementary Figures 38 and 39)

must result in 10 times fewer clicks for compound (**6**) at about 20,000 amu compared to gramicidin at not even 2,000 amu. Finally, the secondary electron multiplication efficiency inside the time-of-flight mass spectrometer (TOF-MS) strongly depends on the velocity rather than the kinetic energy of the incident ions. While all molecules are accelerated by the same 16 kV voltage, they reach different velocities, whose influence is critical but not exactly determined for this particular molecular species. This makes it impossible to provide a clear functional dependence. However, we do not observe any substantial decay in signal/noise across the biopolymer mass range of 3,832–12,320 amu.

Discussion

Our study shows that a combined approach of synthetic design and ultrafast desorption enables *the soft launch* of neutral high-mass polypeptides up to the complexity of small proteins into *neutral* molecular beams and their successful soft photoionization. This could be achieved for bio-inspired nanoparticles composed of 50 amino acids and exceeding 20,000 amu, i.e., an order of magnitude higher than seen on native peptides. The functionalized polypeptide (**6**) is 350% more massive and contains 250% more atoms than insulin (51 residues, 5803 amu, 788 atoms).

Exploiting bio-mimetic growth principles, the tailored compounds can be synthesized with atomically defined composition and structure. It seems possible to ligate two or more of these chains to design bio-mimetic molecules with defined mass and atomic sequence to much higher masses, in future.

The peptide design focused on the abundant inclusion of Trp, which is the only natural amino acid compatible with single-photon VUV postionization using table top laser sources at 157 nm. The high Trp abundances also ensures that these chromophores will be exposed to vacuum, even in coiled-up peptides. This has been crucial for the successful in situ mass analysis of the initially neutral molecular beam. For the largest polypeptide in our series, ultrafast ultraviolet desorption was essential. And even for peptides up to 2,000 amu, fs-desorption was >25 times more material efficient than nanosecond methods. Ultrafast desorption therefore promises to also improve on mass spectrometry in combination with novel ionization methods. Intriguing progress on native proteins had been reported using electrospray post-ionization before[43,44].

The high susceptibility of Trp-rich peptides to VUV SPI will also be of importance for advanced macromolecular matter–wave experiments where photo-depletion gratings[45,46] provide novel beam splitters for complex biomolecular matter–waves. Polypeptides exceeding 20,000 amu are therefore interesting candidates for the next generation of matter–wave interference experiments, which can cope with de Broglie wavelengths as small as 50 fm.

Methods

Sample preparation and desorption. A homogeneous distribution of the molecules is established by first dissolving them and loading a felt wheel, which rubs against the counter-rotating glassy carbon wheel[39]. For the nanosecond desorption of compound (**4**), the sample was premixed with Trp in a ratio of 1:20. This procedure was not necessary for the femtosecond experiments. The Vienna TOF-MS was calibrated to the Swiss MALDI TOF results via a linear transformation using all sizeable peaks of the mass distribution of (**5**) and (**6**) up to 20,000 amu.

Four different laser types were compared in the desorption experiments (See Supplementary Table 2 for detailed conditions of every single experiment):

Short-pulse ultraviolet light, emitted by the fourth harmonic of the flash-lamp pumped *Innolas Spitlight 400*: wavelength $\lambda = 266$ nm, duration $\tau_d = 7 \pm 2$ ns.

Short-pulse ultraviolet light, emitted by an *EKSPLA* "*NT200 OPO*" laser: $\lambda =$ 355 nm, $\tau_d = 7 \pm 2$ ns, $E = 1.5$ mJ.

Ultrafast infrared light, emitted by *a TOPAG* "*Carbide*" fs-fiber laser: $\lambda = 1030$ nm, $\tau_d = 292$ fs–10 ps, $E_d < 40$ μJ on the sample

Ultrafast ultraviolet light, *343* nm, *ultrafast* pulse, emitted by a *TOPAG* "*Carbide*" fs-fiber laser: $\lambda = 343$ nm, $E = 40$ μJ.

Supersonic expansion and molecular beam velocity. A noble gas jet is released by an Even–Lavie valve[47] with a backing pressure between 2 and 50 bar and a pulse duration of 20–22 μs. The experiments were performed using argon or neon with a purity of 99.999%. The gas and the polypeptides travel through a differentially pumped vacuum chamber, separated by a 3-mm skimmer, 55 cm behind the source and 20 cm from the ionization region. During operation at 100 Hz, the residual pressure is ca. 5×10^{-5} mbar in the source chamber and 5×10^{-7} mbar or 2×10^{-8} mbar in the detector chamber, for the nanosecond tests on (**1**)–(**4**) and the fs-tests on (**5**) and (**6**), respectively. For gramicidin D (**1**), we observe a mean velocity of 590 m s^{-1} with a full width at half maximum of 80 m s^{-1}. The absence of any major velocity slip and the width of the distribution suggest that the number of collisions suffices to thermalize the translational energy spread of gramicidin to a temperature of 18 K. This is a lower limit to the expected rotational and vibrational temperature of this peptide.

Ion detection. The peptides were ionized by light from a fluorine laser (*Coherent Excistar*) with $\lambda = 157$ nm, $\tau_i = 10$ ns, $E_i = 1$–2 mJ, $A = 3 \times 3$ mm^2 and analyzed using an orthogonal TOF-MS (Kaesdorf München). Model compounds (**1**)–(**4**) were detected using an orthogonal TOF-MS $\Delta m{:}m = 1{:}500$ and baseline corrected. For (**5**)–(**6**), we used an orthogonal reflectron TOF-MS ($\Delta m{:}m = 1{:}500$). Both spectrometers accelerate the ions by 16 kV and count them by electron multiplication using a triple-stack of multi-channel plates. Figure 4: Every point was integrated 5 times over 1000 mass spectra. Figure 6: Each spectrum contained 10^6 points and was smoothed using a running average of 100 points (SI).

Synthetic procedures and characterization of compounds. See Supplementary Methods and Supplementary Note 1, Supplementary Table 1, Supplementary Figures 1–32.

Computational details. See Supplementary Note 2.

Laser desorption/photoionization mass spectra and conditions. See Supplementary Figures 33–39, 40, 42, 43 and Supplementary Notes 3–5, Supplementary Table 2.

Influence of the desorption laser wavelength and pulse length on the character of the mass spectrum. See Supplementary Note 3 and Supplementary Figure 40.

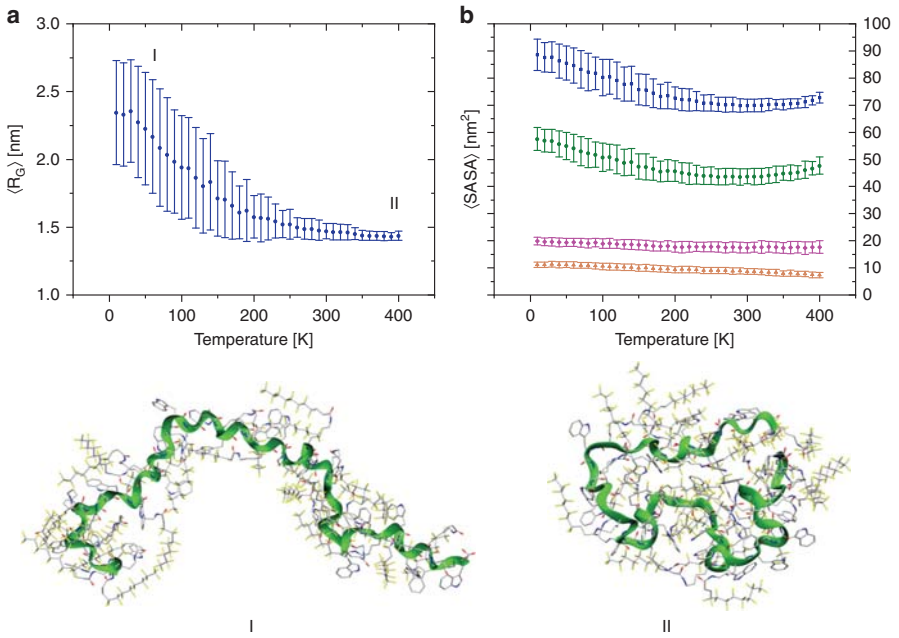

Fig. 7 Structural parameters obtained with canonical-ensemble molecular dynamics simulations. **a** Temperature dependence of the radius of gyration $\langle R_G \rangle$ of polypeptide (**6**). Even when starting from a stretched state, the molecule rapidly coils into a closed tertiary structure with increasing temperature. **b** The average solvent accessible surface area ⟨SASA⟩ quantifies the exposure of different parts of the molecule, here to vacuum. The total area (blue squares) decreases with increasing temperature, as expected but slowly increases beyond 300 K because of the increased exposure of the fluoroalkyl chains (green circles). The tryptophan residues (magenta diamonds) remain almost fully exposed at all temperatures, while the lysine surface (orange triangles) shrinks slightly. Error bars correspond to the standard deviation of the mean.

Influence of the desorption energy/fluence. See Supplementary Note 4 and Supplementary Figure 41.

Influence of the ionization energy/fluence on the normalized mass peak. See Supplementary Note 5 and Supplementary Figures 42 and 43.

Data availability

All relevant data are available from the authors upon reasonable request.

Received: 19 September 2018 Accepted: 16 November 2018
Published online: 10 December 2018

References

1. Stern, O. Zur Methode der Molekularstrahlen. I. *Z. Phys.* **39**, 751–763 (1926).
2. Estermann, I. & Stern, O. Beugung von Molekularstrahlen. *Z. Phys.* **61**, 95–125 (1930).
3. Rabi, I. I., Millman, S., Kusch, P. & Zacharias, J. R. The molecular beam resonance method for measuring nuclear magnetic moments. The magnetic moments of $_3Li^6$, $_3Li^7$and $_9F^{19}$. *Phys. Rev.* **55**, 526–535 (1939).
4. Bordé, C. J. et al. Observation of optical Ramsey fringes in the 10 μm spectral region using a supersonic beam of SF_6. *J. Phys. Coll.* **42**, C8-15–C8-18 (1981).
5. Barth, J. V., Costantini, G. & Kern, K. Engineering atomic and molecular nanostructures at surfaces. *Nature* **437**, 671–679 (2005).
6. de Heer, W. A. The physics of simple metal clusters: experimental aspects and simple models. *Rev. Mod. Phys.* **65**, 611–676 (1993).
7. Schmidt, M., Kusche, R., Issendorff, B. V. & Haberland, H. Irregular variations in the melting point of size-selected atomic clusters. *Nature* **393**, 238–240 (1998).
8. Schöllkopf, W. & Toennies, J. P. Nondestructive mass selection of small Van der Waals clusters. *Science* **266**, 1345–1348 (1994).
9. Chapman, M. S. et al. Optics and interferometry with Na_2 molecules. *Phys. Rev. Lett.* **74**, 4783–4786 (1995).
10. Arndt, M. et al. Wave-particle duality of C60 molecules. *Nature* **401**, 680–682 (1999).
11. Akoury, D. et al. The simplest double slit: interference and entanglement in double photoionization of H2. *Science* **318**, 949–952 (2007).
12. Hornberger, K., Gerlich, S., Haslinger, P., Nimmrichter, S. & Arndt, M. Colloquium: quantum interference of clusters and molecules. *Rev. Mod. Phys.* **84**, 157–173 (2012).
13. Scherman, J.-P. *Spectroscopy and Modelling of Biomolecular Building Blocks* (Elsevier, Amsterdam, 2008).
14. Jarrold, M. F. Peptides and proteins in the vapor phase. *Annu. Rev. Phys. Chem.* **51**, 179–207 (2000).
15. Meyer, T., Gabelica, V., Grubmüller, H. & Orozco, M. Proteins in the gas phase. *Wires Comp. Mol. Sci.* **3**, 408–425 (2013).
16. Laure, J. et al. Ultraviolet spectroscopy of peptide and protein polyanions in vacuo: signature of the ionization state of tyrosine. *J. Am. Chem. Soc.* **129**, 8428–8429 (2007).
17. Viglino, E., Shaffer, C. J. & Turecek, F. UV/Vis action spectroscopy and structures of tyrosine peptide cation radicals in the gas phase. *Angew. Chem. Int. Ed.* **55**, 7469–7473 (2016).
18. Brodbelt, J. S. Photodissociation mass spectrometry: new tools for characterization of biological molecules. *Chem. Soc. Rev.* **43**, 2757–2783 (2014).
19. Gabelica, V. et al. Electron photodetachment dissociation of DNA polyanions in a quadrupole ion trap mass spectrometer. *Anal. Chem.* **78**, 6564–6572 (2006).
20. Antoine, R. et al. Electric susceptibility of unsolvated glycine-based peptides. *J. Am. Chem. Soc.* **124**, 6737–6741 (2002).
21. Grotemeyer, J., Bösel, U., Walter, K. & Schlag, E. W. Biomolecules in the gas phase. 1. Multiphoton-ionization mass spectrometry of native chlorophylls. *J. Am. Chem. Soc.* **108**, 4233–4234 (1986).
22. Antoine, R. et al. Application of molecular beam deflection time-of-flight mass spectrometry to peptide analysis. *Anal. Chem.* **75**, 5512–5516 (2003).
23. Mairhofer, L. et al. Quantum-assisted metrology of neutral vitamins in the gas phase. *Angew. Chem. Int. Ed.* **56**, 10947–10951 (2017).
24. Weinkauf, R., Schermann, J. P., de Vries, M. S. & Kleinermanns, K. Molecular physics of building blocks of life under isolated or defined conditions. *Eur. Phys. J. D* **20**, 309–316 (2002).
25. Gabelica, V. *Nucleic Acids in the Gas Phase* (Springer, Heidelberg, New York, Dordrecht, London, 2014).
26. Schätti, J. et al. Tailoring the volatility and stability of oligopeptides. *J. Mass Spectrom.* **52**, 550–556 (2017).

27. Meijer, G., de Vries, M. S., Hunziker, H. E. & Wendt, H. R. Laser desorption jet-cooling of organic molecules cooling characteristics and detection sensitivity. *Appl. Phys. B* **51**, 395–403 (1990).
28. Grotemeyer, J., Boesl, U., Walter, K. & Schlag, E. W. Biomolecules in the gas phase. II. Multiphoton ionization mass spectrometry of angiotensin I. *OMS Lett.* **21**, 595–597 (1986).
29. Schlag, E., Grotemeyer, J. & Levine, R. Do large molecules ionize? *Chem. Phys. Lett.* **190**, 521–527 (1992).
30. Becker, C. H. & Wu, K. J. On the photoionization of large molecules. *J. Am. Soc. Mass Spectrom.* **6**, 883–888 (1995).
31. Schlag, E. W. & Levine, R. D. Ionization, charge separation, charge recombination, and electron transfer in large systems. *J. Phys. Chem.* **96**, 10608–10616 (1992).
32. Weinkauf, R., Aicher, P., Wesley, G., Grotemeyer, J. & Schlag, E. W. Femtosecond versus nanosecond multiphoton ionization and dissociation of large molecules. *J. Phys. Chem.* **98**, 8381–8391 (1994).
33. Akhmetov, A., Moore, J. F., Gasper, G. L., Koin, P. J. & Hanley, L. Laser desorption postionization for imaging MS of biological material. *J. Mass Spectrom.* **45**, 137–145 (2010).
34. Hanley, L. & Zimmermann, R. Light and molecular ions: the emergence of vacuum UV single-photon ionization in MS. *Anal. Chem.* **81**, 4174–4182 (2009).
35. Hanley, L. et al. 7.87eV postionization of peptides containing tryptophan or derivatized with fluorescein. *Appl. Surf. Sci.* **252**, 6723–6726 (2006).
36. Marksteiner, M. et al. Gas-phase formation of large neutral alkaline-earth metal tryptophan complexes. *J. Am. Soc. Mass Spectrom.* **19**, 1021–1026 (2008).
37. Chan, W. C. & White, P. D. *Fmoc Solid Phase Peptide Synthesis* (Oxford University Press, Oxford, 2000).
38. Malik, L. et al. Perfluoroalkyl chains direct novel self-assembly of insulin. *Langmuir* **28**, 593–603 (2011).
39. Gahlmann, A. P., Sang, T. & Zewail, A. H. Structure of isolated biomolecules by electron diffraction-laser desorption: uracil and guanine. *J. Am. Chem. Soc.* **131**, 2806–2808 (2009).
40. Hillenkamp, F., Karas, M., Beavis, R. C. & Chait, B. T. Matrix-assisted laser desorption/ionization mass spectrometry of biopolymers. *Anal. Chem.* **63**, 1193A–1203A (1991).
41. Knochenmuss, R. & Zenobi, R. MALDI ionization: the role of in-plume processes. *Chem. Rev.* **103**, 441–452 (2003).
42. Brady, J. J., Judge, E. J. & Levis, R. J. Mass spectrometry of intact neutral macromolecules using intense non-resonant femtosecond laser vaporization with electrospray post-ionization. *Rapid Commun. Mass Spectrom.* **23**, 3151–3157 (2009).
43. Brady, J. J., Judge, E. J. & Levis, R. J. Nonresonant femtosecond laser vaporization of aqueous protein preserves folded structure. *Proc. Natl Acad. Sci. USA* **108**, 12217–12222 (2011).
44. Cui, Y. et al. Molecular imaging and depth profiling of biomaterials interfaces by femtosecond laser desorption postionization mass spectrometry. *ACS Appl. Mater. Interfaces* **5**, 9269–9275 (2013).
45. Haslinger, P. et al. A universal matter-wave interferometer with optical ionization gratings in the time domain. *Nat. Phys.* **9**, 144–148 (2013).
46. Dörre, N. et al. Photofragmentation beam splitters for matter-wave interferometry. *Phys. Rev. Lett.* **113**, 233001 (2014).
47. Bahat, D., Cheshnovsky, O., Even, U., Lavie, N. & Magen, Y. Generation and detection of intense cluster beams. *J. Phys. Chem.* **91**, 2460–2462 (1987).

Acknowledgements

This project has received funding from the European Research Council (ERC) under the European Union's Horizon 2020 research and innovation program (Grant Nr. 320694), the Austrian Science Fund (FWF) within program W1210-N25, the Swiss National Science Foundation 200020-178808), and the Swiss Nanoscience Institute (P1403). The computational results were obtained using the Vienna Scientific Cluster (VSC); PRO-BIOTIQUS 70918. A.S. acknowledges funding by the (FWF) within the Lise-Meitner fellowship M 2364. G.G.R. is thankful for funding from the Brazilian National Council for Scientific and Technological Development (206729/2014-6). We gratefully acknowledge the loan of a *Carbide* femtosecond laser by TOPAG Germany and a *Monaco* fs-laser from Coherent Inc. Germany.

Author contributions

The experiments were conceived by M.A., V.K., M.M., U.S. and A.S. The molecular design and synthesis was realized by J.S., V.K. and M.M. The nanosecond experiments were realized by U.S., P.R. and P.G. The femtosecond experiments were realized by P.R., G.R., and A.S. Data analysis was performed by J.S., U.S., G.R., P.R., A.S. and M.A. NMR experiments were carried out and analyzed by J.S. and D.H. Molecular dynamics simulations were designed and analyzed by A.S., G.G.R. and M.A. and realized by G.G. R. The manuscript was written by M.A., V.K. and J.S. with contributions from all authors.

Additional information

Supplementary information accompanies this paper at https://doi.org/10.1038/s42004-018-0095-y.

Competing interests: The authors declare no competing interests.

Reprints and permission information is available online at http://npg.nature.com/reprintsandpermissions/

Publisher's note: Springer Nature remains neutral with regard to jurisdictional claims in published maps and institutional affiliations.

Chapter 4. Gene-encoded tryptophan-rich tags and synthetic tags for protein photoionization

Outline of the author's contribution

The genetically engineered protein constructs of ubiquitin and the ribosomal protein S6 from *Thermus thermophilu*s were designed by the author J. Schätti together with V. Köhler. Codon optimization for the constructs was performed by J. Schätti together with H. Mallin. Protein expression, purification, and characterization were conducted by J. Schätti under the guidance of H. Malin, J. Klehr and J. Vallapurackal. Desorption/postionization tests were performed by U.Sezer and A. Shayeghi. Chemical modification of insulin was performed by the author.

The genes for 24 different protein constructs were designed, and their expression attempted in *E.coli*. Expression levels were estimated by SDS-PAGE, and the proteins were additionally characterized by UPLC-MS. The two wild type variants of ubiquitin and the ribosomal protein S6 from *Thermus thermophilus* were purified by heat treatment. For the purification of the most promising mutant, namely a ubiquitin construct with five tryptophan residues attached to its C-terminus, a purification method based on selective precipitation was developed. In a separate study insulin was modified with naphthyl- and pyrenyl-groups by reaction with the NHS-esters of the corresponding acetic acids. Again the hope was that such tags would facilitate photoionization. The modified insulin derivates could be obtained in good yield after preparative HPLC purification. For all systems mentioned here, photoionization failed so far.

Proteins for laser desorption/photoionization experiments

Laser desorption appeared to be a promising approach for the generation of neutral molecular beams of proteins following the successful desorption and post-ionization of tailor-made high-mass tryptophan-rich polypeptides decorated with fluorinated chains. Molecules of up to 20 kDa were successfully desorbed as neutrals into the gas-phase and subsequently photoionized.[1] Laser desorption of singly charged protein ions is routine in MALDI. It has been reported that during the MALDI desorption process mostly neutral molecules are volatilized.[2-3] Accordingly, it was assumed that photo-ionization and hence detection would be the limiting factor for successful interference experiments with natural proteins. The transfer of neutral unmodified peptides, such as gramicidin, into the gas-phase, has been demonstrated by the Arndt group[1] and even larger unmodified peptides were sucessfully laser desorbed and photoionized such as a peptide where ten lysine and tryptophan residues are alternated (experimental part)[4]

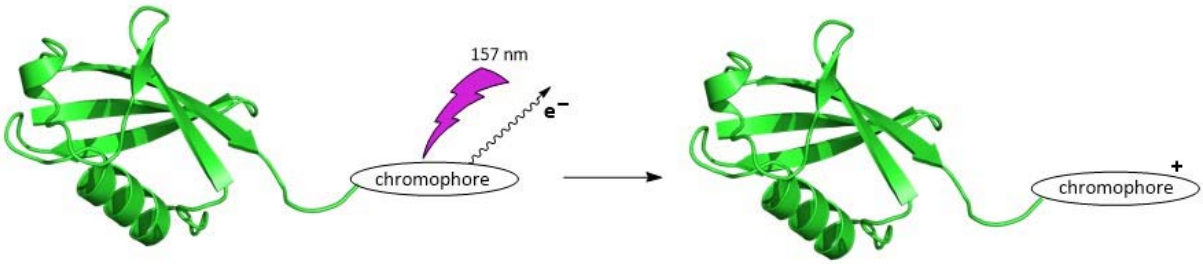

Figure 1. Photoionization of a protein modified with a chromophore. The chromophore can be either introduced by chemical modification or genetic engineering of the protein. The electron-rich tag is supposed to facilitate the photoionization process.

To make proteins accessible to photoionization they need a suitable chromophore to absorb light and enable electron detachment (Figure 1). Photoionization of large and flexible biomolecules is not a trivial task and is potentially complicated by i) energy redistribution, i.e. competitive heating of the molecule, and ii) electron recapture processes. Both effects likely contribute to the exponentially decreasing efficiency of photoionization with increasing mass.[5-7] Until recently it was believed that an approximate limit of 2 kDa for the photoionization of biomolecules by VUV could not be overcome. The group of M. Arndt showed with constructs synthesized in the context of this thesis that tryptophan-rich modified peptides can be successfully photoionized up to 20 kDa. A beneficial factor for the success of the experiment was considered to be a high chromophore density at the surface of the peptide. Chromophores can be posttranslationally attached to natural proteins by chemical methods or amino acid (aa) based natural chromophores (Trp, Tyr) can be introduced by genetic engineering. Both approaches were investigated.

Chemical modification of insulin with naphthalene and pyrene chromophores

Initially, we explored the chemical modification of human insulin (**1**) as a small model protein (5 kDa, see experimental part for amino acid sequence) with the NHS-ester of 1-pyrenylacetic acid (**2**) and 1-naphthalene acetic acid (**3**), respectively. The insulin modification was performed in aq. Na_2CO_3-buffer (pH 8.5, 0.1 M) with acetonitrile or THF as a cosolvent to solubilize the NHS-ester. A large excess of the NHS-ester (75 eq.) was employed. In the case of pyrenylacetic acid this lead to the formation of predominantly triply modified insulin **4** which was isolated with a yield of 14% by preparative HPLC. When the same conditions were applied for the derivatization with the NHS ester of naphthalene acetic acid (**3**) six-fold modified insulin was obtained. The highly modified insulin species could be partially hydrolyzed under acidic conditions to yield triply modified insulin **5** with a yield of 30% (see experimental part). The position of modification were presumably the two N-termini of insulin as well as Lys B29, but this assumption was never fully confirmed. Reduction of the disulfide bonds, followed by UPLC-MS for the case of pyrenyl modified insulin reveal one modification on the A-chain and two on the B-chain (see experimental part). Laser desorption/photoionization tests (desorption by short-pulse infrared laser light (7 ns, 1064 nm, 32 mJ); post-ionization by 266 nm light (frequency quadrupled Nd:YAG laser) of these constructs were performed by Ugur Sezer, but the detection of intact protein failed.

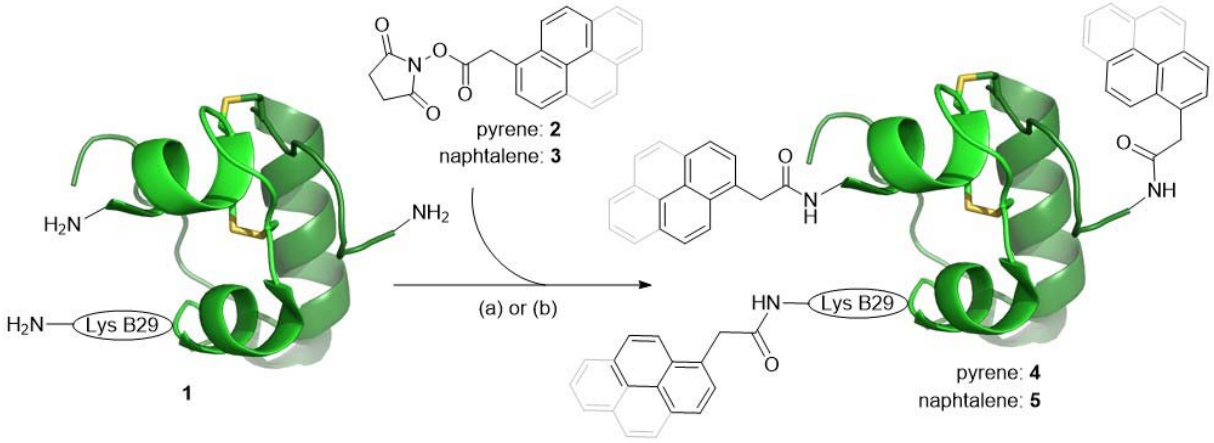

Figure 2. Insulin modification with 1-naphthylacetyl and pyrenylacetyl groups, respectively. (a) Pyrenylacetyl modification: 75.0 eq. 1-pyrenylacetic acid NHS ester, aq. Na_2CO_3 (pH 8.5, 0.1 M) : THF (1 : 1), rt, 2 h. (b) Naphthylacetyl modification: i) 75.0 eq. naphthalene acetic acid NHS ester, aq. Na_2CO_3 (pH 8.5, 0.1 M) : MeCN (3 : 2), rt, 2 h; ii) addition of TFA (2.5 mL), rt, 15 min; iii) addition of aq. NH_3 (5 mL, 32%), rt, 2 min; iv) pH adjusted to 7 with aq. HCl.

Genetically encoded tryptophan-rich tags for ubiquitin and the ribosomal protein S6 from *Thermus thermophilus*

Encouraged by the successful laser-desorption/photoionization of large tryptophan-rich peptide constructs,[1] the introduction of gene-encoded tryptophan-rich tags at the C- or N-termini of model proteins was investigated. Advantages of genetically introduced tags, compared to chemical modification of proteins, include scalability and the defined location of the chromophore at one of the termini of the protein. The method provides direct access to a single fully defined species, whereas chemical modification methods frequently lead to mixtures of modified species. Today many recombinant proteins are produced on a gram scale in various organisms such as *E.coli*. Accordingly, we tried to introduce a suitable number of tryptophan residues as photoionizable chromophores to either the C- or N-terminus of model proteins in the hope to maintain good expression levels while introducing favorable photoionization properties to the protein. For the presented study ubiquitin (**Ubi**) and the ribosomal protein S6 from *Thermus thermophilus* (**S6**) were selected. Both of them are small proteins (76 aa, 8557 amu and 101 aa, 11973 amu, respectively), known to be easily expressed in *E.coli*, have a compact, well-defined structure and are remarkably heat stable.[8-9] It was hypothesized that the heat stability of the wild type proteins might translate to the engineered constructs and would enable purification by heat treatment. Different tag sequences were introduced to the recombinant protein, containing at least five tryptophan residues. The tags consisted either of tryptophan only (**Ubi-3**, **S6-3**, **Ubi-7**, **Ubi-14**, **Ubi-15**) or contained additionally other amino acids for improved solubility to mitigate detrimental effects on protein expression.[10-11] Apart from **Ubi-14** and **Ubi-15,** all new protein constructs were designed to have their photoionization tag attached to the C-terminus. A C-terminal modification was expected to affect protein expression less than modification at the N-terminus where the ribosomal protein synthesis begins. Simultaneously the two R→K mutants (all arginine residues were converted to lysine residues in ubiquitin and S6, respectively) were prepared for chemical modification (see above) and are displayed on the SDS-gels, but were not studied further. All constructs are listed in Table 1. Gene constructs encoding for the different ubiquitin and S6 mutants were purchased from *GeneScript* in a pET24a plasmid with kanamycin resistance (see experimental part, Table S2 for gene sequences). The plasmids were transformed into competent *E.coli* cells (BL21) and protein expression was performed in ZYP autoinduction media (see experimental part for details). Protein expression was qualitatively analyzed for the 24 different constructs by SDS-PAGE of the cell suspension as shown in Figure 3.

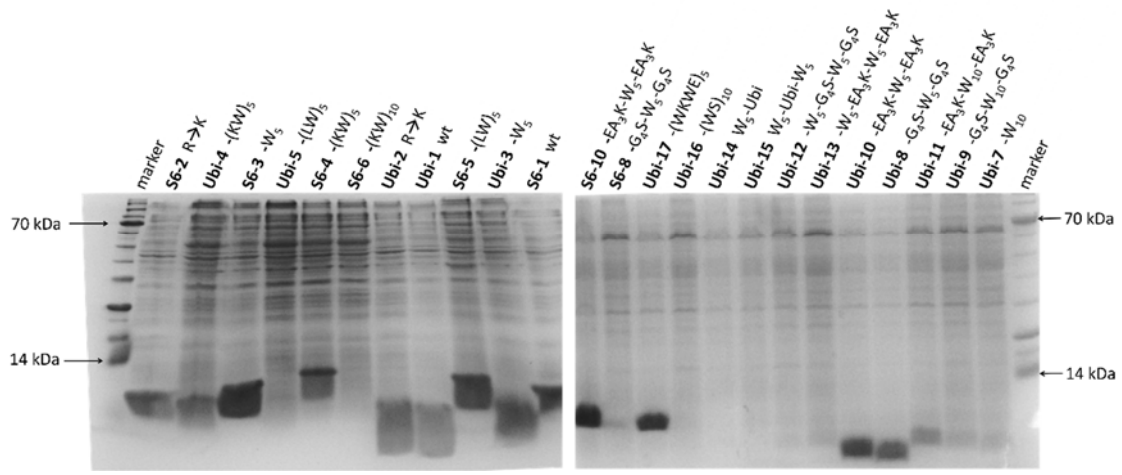

Figure 3 Coomassie-stained SDS-PAGE of the cell suspension of all 24 ubiquitin and S6 constructs.

Out of the 24 constructs, 14 expressed well in *E.coli* and 9 of these at least partially in soluble form according to SDS-PAGE analysis of the supernatant (Table 1 and Figure 4). The other ten constructs were either only expressed at deficient levels or not expressed at all. Incorporation of the tag at the N-terminus of the wild type was not successful as judged by the observed expression levels for constructs **Ubi-14** and **Ubi-15**. It seems reasonable that protein expression which begins with a poorly soluble sequence is less advantageous than solubilizing a poorly soluble tag with a fully formed soluble protein. No expression was further observed for **S6-6**, which might be explained by the antibiotic character of Trp/Lys rich motifs,[12] which could lead to enhanced plasmid secretion. The other constructs where expression failed (**Ubi-5**, **Ubi-7**, **S6-8**, **Ubi-9**, **Ubi-12**, **Ubi-13**, **Ubi-16**) had either long oligotryptophan sequences (W_{10} or W_5-XXXXX-W_5) or contained a motif where tryptophan was alternated with hydrophobic leucine residues. Remarkably **Ubi-11** - ubiquitin with a W_{10} motif flanked by an EAAAK motif on either side could be expressed in soluble form, albeit at a low expression level.

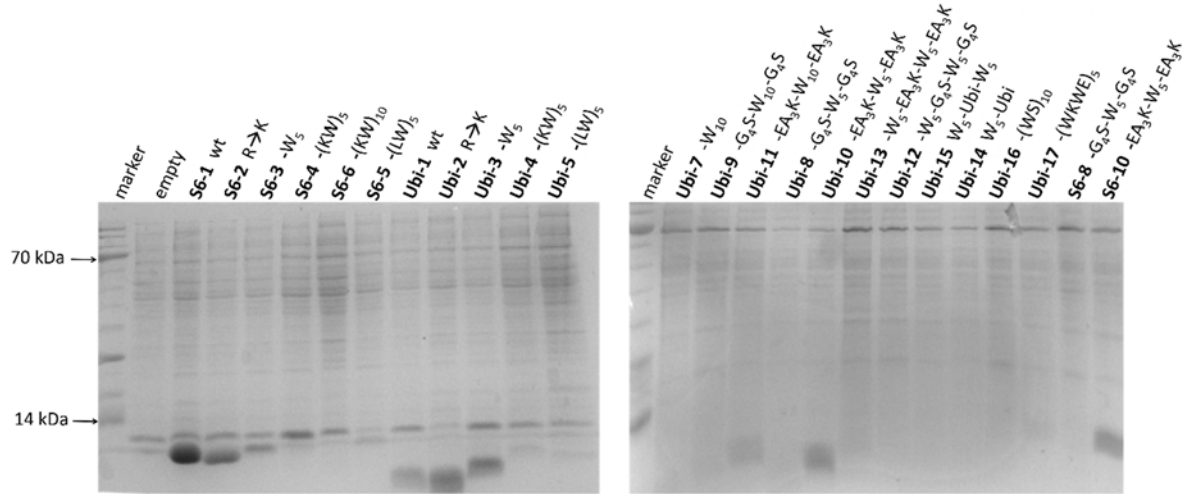

Figure 4. Coomassie-stained SDS-PAGE of the soluble fraction for all 24 constructs.

Besides the two wild type proteins and the R→K mutants (**Ubi-1**, **S6-1**, **Ubi-2,** and **S6-2**) five tryptophan enriched constructs were expressed in soluble form (**Ubi-3**, **S6-3**, **Ubi-10**, **S6-10,** and **Ubi-11**, Figure 4). Ubiquitin with five C-terminal tryptophan residues (**Ubi-3)** was selected for further studies based on its high expression level and good solubility. The two wild type proteins have high thermal stability and can be purified by heating of the cell-free extracts for 30 min to 70 °C for ubiquitin or 80 °C for S6, respectively. The heat treatment denatures other less heat stable proteins in the cell-free extracts, which can subsequently be removed by centrifugation (see Figure 5a). This purification procedure leads unfortunately also to complete precipitation of ubiquitin and S6 constructs containing tryptophan-rich tags. For the most promising candidate Ubi-W_5 the time and temperature dependence of the precipitation was investigated in more detail (see Figure 5b). The best trade-off conditions, in terms of yield vs. purification, was identified in this screen as heating to 60°C for 15 min. The heat treatment could be extended to 30 min to improve the purification effect without a dramatic loss of material (data not shown).

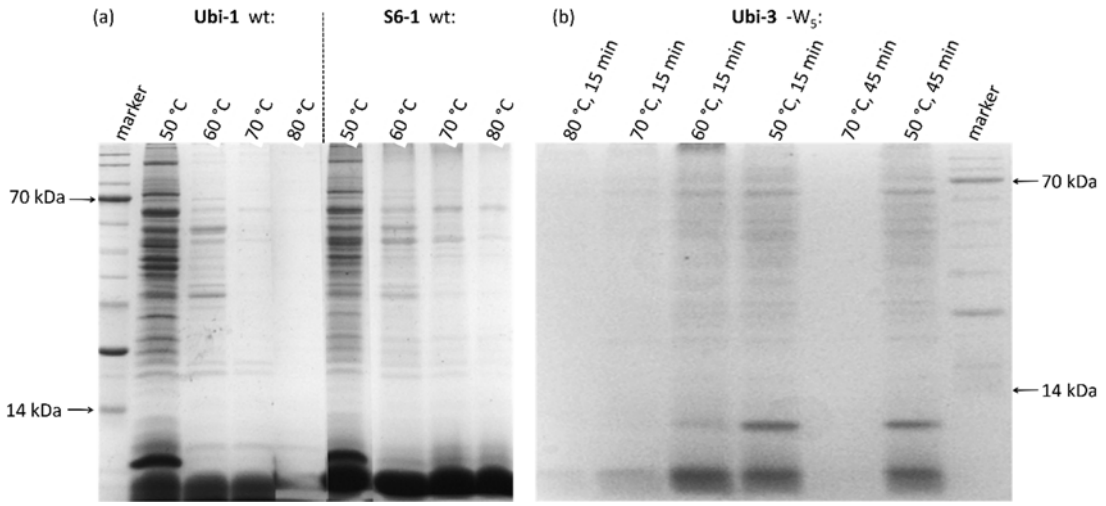

Figure 5. (a) Coomassie-stained SDS-PAGE of heat-treated cell-free extracts containing wild type **S6-1** and **Ubi-1**, respectively. Heat treatment was performed for 30 minutes at various temperatures. (b) Coomassie-stained SDS-PAGE of cell-free extracts of the tryptophan tagged ubiquitin (**Ubi-3**) over 15 or 45 min at different temperatures.

The purity of the heat treated **Ubi-3** was considered to be in an acceptable range, according to SDS-PAGE, and the proteins were dialyzed against Milli-Q water. For the wild type proteins, a yield of 120 mg and 210 mg of protein were obtained from a two-liter fermentation for S6 and ubiquitin, respectively. The purity of the obtained wild type proteins was considered to be high according to SDS-PAGE and revers phase UPLC chromatograms (see experimental part). The same procedure for the Ubi-W_5 construct leads to unexpected precipitation during dialysis. SDS-PAGE of the precipitate showed improved purity of **Ubi-3** (Figure 6a).

#	construct	expressed	soluble	#	construct	expressed	soluble
Ubi-1	Ubiquitin (WT)	✓	✓	**S6-1**	S6 (WT)	✓	✓
Ubi-2	Ubi R→K	✓	✓	**S6-2**	S6 R→K	✓	✓
Ubi-3	Ubi-W_5	✓	✓	**S6-3**	S6-W_5	✓	(✓)
Ubi-4	Ubi-$(KW)_5$	✓	X	**S6-4**	S6-$(KW)_5$	✓	X
Ubi-5	Ubi-$(LW)_5$	X	X	**S6-5**	S6-$(LW)_5$	X	X
-	-	-	-	**S6-6**	S6-$(KW)_{10}$	X	X
Ubi-7	Ubi-W_{10}	X	X	-	-	-	-
Ubi-8	Ubi-GGGGS-W_5-GGGGS	✓	X	**S6-8**	S6-GGGGS-W_5-GGGGS	X	X
Ubi-9	Ubi-GGGGS-W_{10}-GGGGS	X	X	-	-	-	-
Ubi-10	Ubi-EAAAK-W_5-EAAAK	✓	✓	**S6-10**	S6-EAAAK-W_5-EAAAK	✓	✓
Ubi-11	Ubi-EAAAK-W_{10}-EAAAK	✓	✓	-	-	-	-
Ubi-12	Ubi-W_5-GGGGS-W_5-GGGGS	X	X	-	-	-	-
Ubi-13	Ubi-W_5-EAAAK-W_5-EAAAK	X	X	-	-	-	-
Ubi-14	W_5–Ubi	X	X	-	-	-	-
Ubi-15	W_5–Ubi-W_5	X	X	-	-	-	-
Ubi-16	Ubi-$(WS)_{10}$	X	X	-	-	-	-
Ubi-17	Ubi-$(WKWE)_5$	✓	X	-	-	-	-

Table 1. Expression and solubility (yes/no) of all ubiquitin and S6 constructs. Blank entries - not all possible combinations were tested.

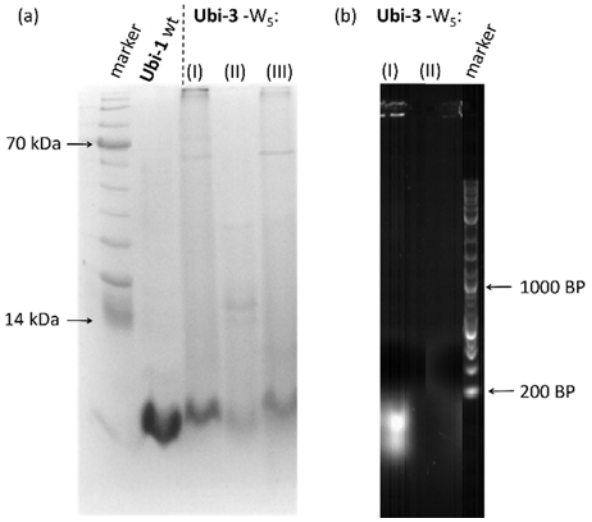

Figure 6: (a) Coomassie-stained SDS-PAGE of ubiquitin with five tryptophan residues at the C- terminus (**Ubi-3)** after dialysis: (1) **Ubi-3** precipitated from an 8 M urea solution during dialysis against Milli-Q water; (2) remaining soluble proteins not precipitated during dialysis; (3) **Ubi-3** purified by heat treatment (60 °C for 30 min) and subsequent precipitation during dialysis against Milli-Q water. (b) Ethidium bromide stained agarose gel of **Ubi-3** purified by precipitation (I) and after further purification by a DNA extraction columns (II).

The UV/Vis spectra of the purified **Ubi-3** construct indicate the presence of DNA-fragments in the precipitate, which was confirmed by ethidium bromide staining after electrophoresis on an agarose gel (Figure 6b). Commercial DNA miniprep cartridges could efficiently remove the DNA fragments, but

the cost was prohibitive for large scale purifications. Alternatively, extra DNAse could be added to the cell-free extracts to form smaller DNA-fragments which could be removed by dialysis. This approach was not investigated in the scope of this thesis.

The laser desorption/photoionization experiments performed under the optimized conditions (ultraviolet femtosecond desorption (λ =343 nm, τ= 292, 15 µJ in 100 × 100 µm2) followed by photoionization at 157 nm) as performed for the perfluoroalkyl modified $(Trp\text{-}Lys)_n$ peptides,[1] was unsuccessful. It remains unclear whether desorption or photoionization was the limiting factor.

References

1. J. Schätti; P. Rieser; U. Sezer; G. Richter; P. Geyer; G. G. Rondina; D. Häussinger; M. Mayor; A. Shayeghi; V. Köhler; M. Arndt, Pushing the mass limit for intact launch and photoionization of large neutral biopolymers. *Commun. Chem.* **2018,** *1* (1), 93.
2. R. Knochenmuss; R. Zenobi, MALDI Ionization: The Role of In-Plume Processes. *Chem. Rev.* **2003,** *103* (2), 441-452.
3. C. D. Mowry; M. V. Johnston, Simultaneous detection of ions and neutrals produced by matrix-assisted laser desorption. *Rapid Commun. Mass Spectrom.* **1993,** *7* (7), 569-575.
4. The results for the laser desorption/photoionization of this construct have not been published. The desorption/photoionization can be found in the experimental part of chapter 4, the synthesis is described in the experimental part of chapter 3.
5. E. W. Schlag; J. Grotemeyer; R. D. Levine, Do large molecules ionize? *Chem. Phys. Lett.* **1992,** *190* (6), 521-7.
6. E. W. Schlag; R. D. Levine, Ionization, charge separation, charge recombination, and electron transfer in large systems. *J. Phys. Chem.* **1992,** *96* (26), 10608-16.
7. C. H. Becker; K. J. Wu, On the photoionization of large molecules. *J. Am. Soc. Mass. Spectrom.* **1995,** *6* (10), 883-888.
8. E. Ozkaynak; D. Finley; M. J. Solomon; A. Varshavsky, The yeast ubiquitin genes: a family of n atural gene fusions. *EMBO J.* **1987,** *6* (5), 1429-39.
9. M. Kurnik; L. Hedberg; J. Danielsson; M. Oliveberg, Folding without charges. *Proc. Natl. Acad. Sci. USA* **2012,** *109* (15), 5705-10.
10. X. Chen; J. L. Zaro; W.-C. Shen, Fusion protein linkers: Property, design and functionality. *Adv. Drug Deliv. Rev.* **2013,** *65* (10), 1357-1369.
11. V. P. Reddy Chichili; V. Kumar; J. Sivaraman, Linkers in the structural biology of protein–protein interactions. *Protein Sci.* **2013,** *22* (2), 153-167.
12. L. Jin; X. Bai; N. Luan; H. Yao; Z. Zhang; W. Liu; Y. Chen; X. Yan; M. Rong; R. Lai; Q. Lu, A Designed Tryptophan- and Lysine/Arginine-Rich Antimicrobial Peptide with Therapeutic Potential for Clinical Antibiotic-Resistant Candida albicans Vaginitis. *J. Med. Chem.* **2016,** *59* (5), 1791-1799.

Chapter 5. Tailored photocleavable peptides: fragmentation and neutralization pathways in high vacuum

M. Debiossac; J. Schätti; M. Kriegleder; P. Geyer; A. Shayeghi; M. Mayor; M. Arndt; V. Kohler, *Phys.Chem.Chem.Phys.,* **2018***, 20,* 11412-11417.

Outline of the author's contribution

M. Debiossac and the author J. Schätti contributed equally to the work. J. Schätti synthesized and characterized the molecular compounds. The initial alkyne carrying photocleavable building block was first synthesized by L. Felix in the course of his PhD-thesis.[87] M. Debiossac, M. Kriegleder, and P. Geyer designed and conducted the photocleavage experiments in the gas-phase. A. Shayeghi performed ab initio molecular dynamics (AIMD) simulations. The data were analyzed by M. Debiossac, M. Kriegleder, J. Schätti, M. Arndt and V. Köhler. M. Debiossac, J. Schätti, V. Köhler, and M. Arndt wrote the paper, with all authors reviewing it.

Several 6-azido-lysine containing peptides (3-12 amino acids) were synthesized by SPPS. A set of seven different nitroarylether photocleavable tags with an alkyne substituent were synthesized. The click reaction between the peptide and the tags gave, after preparative HPLC purification, rise to a considerable variety of modified peptides to test in gas-phase photocleavage experiments.

PCCP

PAPER

View Article Online
View Journal | View Issue

Cite this: *Phys. Chem. Chem. Phys.*, 2018, **20**, 11412

Tailored photocleavable peptides: fragmentation and neutralization pathways in high vacuum†

M. Debiossac, ‡[a] J. Schätti,‡[b] M. Kriegleder,[a] P. Geyer,[a] A. Shayeghi,[a] M. Mayor,[bcd] M. Arndt *[a] and V. Köhler *[b]

Received 14th February 2018,
Accepted 23rd March 2018

DOI: 10.1039/c8cp01058g

rsc.li/pccp

Photocleavable tags (PCTs) have the potential for excellent spatio-temporal control over the release of subunits of complex molecules. Here, we show that electrosprayed oligopeptides, functionalized by a tailored *ortho*-nitroarylether can undergo site-specific photo-activated cleavage under UV irradiation (266 nm) in high vacuum. The comparison of UV photodissociation (UVPD) and collision-induced dissociation (CID) points to the thermal nature of the cleavage mechanism, a picture corroborated by the temperature dependence of the process. Two competing photodissociation pathways can be identified. In one case a phenolate anion is separated from a neutral zwitterion. In the other case a neutral phenol derivative leaves a negatively charged peptide behind. To understand the factors favoring one channel over the other, we investigate the influence of the peptide length, the nature of the phenolic group and the position of the nitro-group (*ortho vs. para*). The observed gas phase cleavage of a *para*-nitro benzylic ether markedly differs from the established behavior in solution.

1 Introduction

The charge state of peptides and proteins affects their chemical and biological behavior through intermolecular electrostatic interactions as well as by modulation of their geometry and folding, electronic and vibrational energy structure,[1] and their electro-optical or collisional[2,3] properties. Spectroscopic studies of biomolecules in the gas phase are interesting as they specifically allow identifying the role of matrix effects.[4–6]

The combination of both aspects, *i.e.* charge control of biomolecules in the gas phase is relevant for molecular trapping,[7,8] optical[9] and photo-electron spectroscopy,[10,11] as well as for electron or femto-second X-ray diffraction.[12,13] Several methods for charge manipulation have been studied in the past, such as atomic collisions,[14] chemical reactions,[15] and low-energy electron attachment.[16]

Laser-induced processes are intriguing since they are compatible with ultra-high vacuum requirements, can achieve high efficiency and combine high spatial resolution with sub-nanosecond timing. UV electron photodetachment (ED) has recently been successfully demonstrated on insulin polyanions,[17] however, in complex molecules it competes with photodissociation (PD).[18]

It has been shown that photocleavage can be optimized using tailored tag molecules that respond to UV light[19,20] and visible light,[21] also for peptides with ionization energies exceeding the photon energies of table-top lasers.[22] The heterolytic removal of the leaving group (LG) from a singly charged photo-tagged peptide anion is a promising strategy for the controlled generation of neutral zwitterions in the gas phase[23] (Scheme 1) and can be relevant for proteomics.[24–26]

Our work aims at developing tools that enable the generation of continuous beams of neutral, slow and internally cold peptides and proteins for matter-wave interferometry.[27] Such controlled beams are valuable for fundamental tests of quantum physics, enable new measurements of molecular electronic,[28] optical and magnetic properties,[29,30] as well as optical and infrared spectroscopy under controlled interaction-free conditions.[31]

Here, we study tailored oligopeptides with a photocleavable tag in an electrospray mass spectrometer,[32] aiming at the controlled charge removal from singly charged anions by photodissociation (PD) at a tailored cleavage point.[33] For that purpose, we have synthesized non-aromatic oligopeptides containing between three and twelve amino acids (**1–4**), and a covalently attached photocleavable tag (PCT) with a leaving group that is supposed to split off upon absorption of one or several UV photons (Scheme 1 and ESI†). We have synthesized the four different LGs (**a–d**) to

[a] *Faculty of Physics, University of Vienna, VCQ, Boltzmanngasse 5, A-1090 Vienna, Austria. E-mail: markus.arndt@univie.ac.at*
[b] *Department of Chemistry, University of Basel, Mattenstrasse 24a, BPR 1096, CH-4058 Basel, Switzerland. E-mail: valentin.koehler@unibas.ch*
[c] *Institute of Nanotechnology (INT), Karlsruhe Institute of Technology (KIT), Hermann-von-Helmholtz-Platz 1, D-76344 Eggenstein-Leopoldshafen, Germany*
[d] *Lehn Institute of Functional Materials (LIFM), Sun Yat-Sen University (SYSU), Xingang Rd. W., Guangzhou, China*

† Electronic supplementary information (ESI) available: Details concerning the chemical synthesis and NMR characterization of the molecules, the data analysis, computational details and additional discussions. See DOI: 10.1039/c8cp01058g

‡ These authors contributed equally to this work.

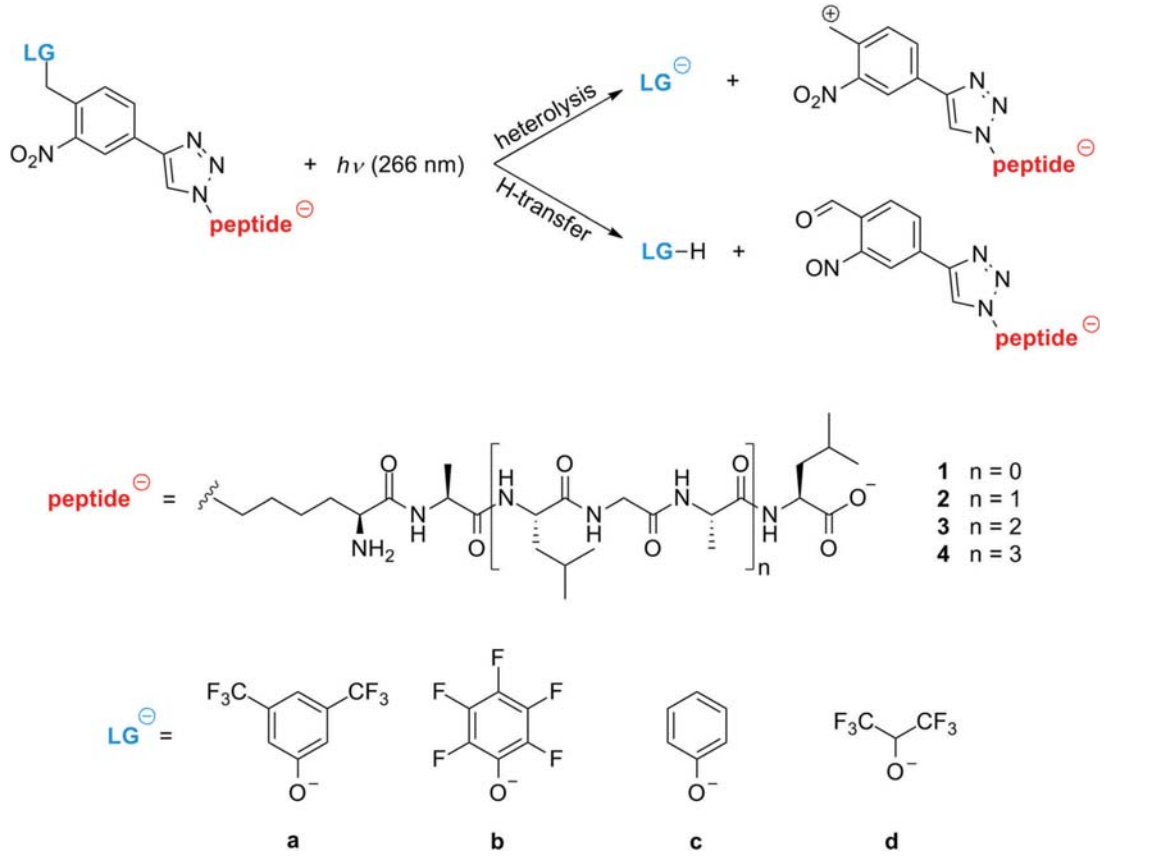

Scheme 1 Photocleavable tags (PCT), reaction scheme, oligopeptides and leaving groups (LG) used in this study. Upon irradiation with 266 nm UV light the functionalized peptides can undergo either heterolytic cleavage or dissociation with simultaneous proton transfer. The functionalized peptides differ in their amino acid sequence Lys-Ala-(Leu-Gly-Ala)$_n$-Leu and in their leaving group (LG) **1a**, **1b**, **1c**, **1d**. The index n = 0–3 labels the oligopeptides from a tripeptide **1a** to the dodecapeptide **4a**.

investigate their influence on the cleaving efficiency and in all cases the aromatic PCT is designed to be the dominant UV absorber in the tagged peptide.

The experiments are performed using a customized ESI-Q-TOF mass spectrometer, as shown in Fig. 1. The electro-sprayed ions are guided into high vacuum by a stack of ring electrodes. They are mass-selected by a quadrupole ion filter, temperature-controlled by the buffer-gas in the first hexapole ion guide (marked in blue in Fig. 1), photo-activated by UV laser light inside the second hexapole ion guide (without buffer gas, marked in red) and detected using a time-of-flight mass spectrometer. A pulse-tube cooler was fitted to the first hexapole, allowing to set a temperature of between T = 60–300 K. Pulsed ultraviolet laser light (λ = 266 nm, 10 ns, <1 mJ per pulse) was aligned to be collinear and counter-propagating to the ion beam.

2 Results and discussion

Fig. 2a and b show the UVPD (a) and CID (b) mass spectra of the tripeptide **1a**. The fragment at 229 u/e results from heterolytic cleavage of the leaving group **a**. Both mass spectra show the desired LG-anion **a** as the only fragment, suggesting that UVPD and CID follow a similar mechanism.

Fig. 2c and d trace the UV photodepletion efficiency for the tripeptide **1a** as a function of the laser fluence and for two different molecular temperatures. The molecules interact with a buffer gas at 300 K (c) or 60 K (d) prior to the PD experiments. We define the UVPD efficiency as $1 - S/S_0$. It measures the reduction of the parent ion signal in the presence (S) or absence (S_0) of the UV light. Its dependence on the laser fluence F is derived from kinetic rate equations[21,34]

$$1 - S/S_0 = 1 - \alpha + \alpha(1 + \gamma\sigma F)e^{-\sigma F} \quad (1)$$

with α as the spatio-temporal overlap between the UV laser beam and the ion beam, γ the fraction of two-photon processes and σ the PD cross section as a lower bound to the absolute absorption cross section (see Fig. S1, ESI†). The temperature of the buffer gas determines whether one (γ = 0) or at least two photons (γ = 1) are needed to deplete the parent ion signal. From Fig. 2a we extract α = 0.4 ± 0.1 and σ = 0.4 ± 0.1 Å^{-2}.

View Article Online

PCCP Paper

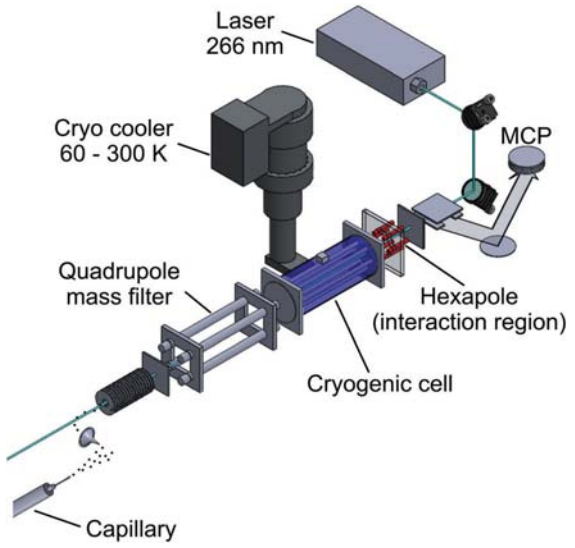

Fig. 1 Experimental setup. Ions are sprayed and mass-selected in a 2D quadrupole filter (MS1) and temperature controlled in the cryogenic hexapole ion guide before interacting with short (10 ns) 266 nm laser pulse inside the second hexapole guide.

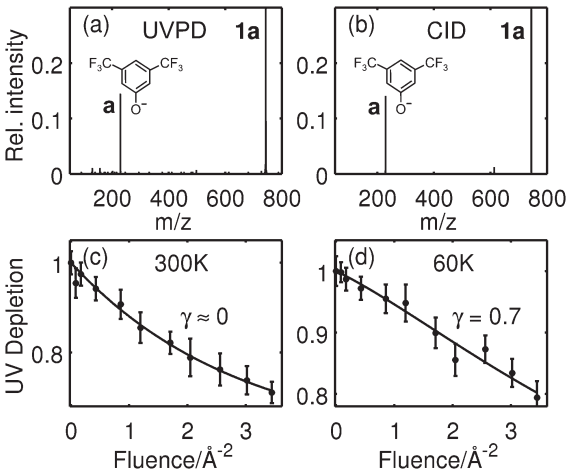

Fig. 2 (a and b) The UVPD and CID mass spectra of the tripeptide **1a** (m = 744 u/e) show one and the same fragment **a** at m/z = 229 u/e. The CID spectrum was recorded at an ion energy of 28 eV in collision with room temperature argon atoms. (c and d) Temperature dependence of the photodepletion efficiency: at a molecular temperature of 300 K, the UVDP curve can be fitted by a pure exponential decay, corresponding to a single-photon process (c). At $T \simeq 60$ K a large fraction of molecules must absorb two or more photons before they fragment.

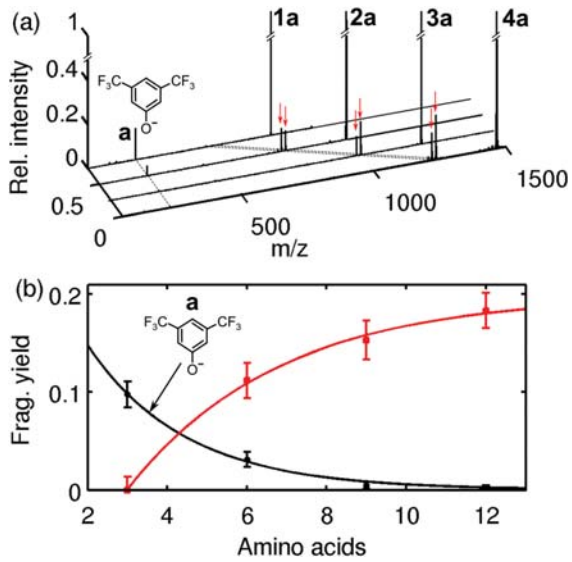

Fig. 3 (a) UVPD mass spectra for peptides **1a–4a** for maximum laser fluence of 3.3 Å^{-2}. The fragment at 229 u/e results from heterolytic cleavage of the LG. Red arrows indicate the fragments formed due to proton transfer dissociation (M-LG-H and M-LG-H-16). (b) Fragment yield for LG **a** (dark circles) and for fragments due to proton transfer dissociation (red squares) as a function of the peptide length. Points and error bars represent experimental values, full lines display curve fitting using the exponential depletion function.

While single-photon cleavage prevails at 300 K, the data are best fitted by a 70% probability for a two-photon process when the molecules are 60 K cold.

This suggests that the cleavage process depends on the molecular heat capacity, which increases with peptide length (Fig. 3). More photons are then required for heterolytic cleavage to occur on the experimental time scale (Fig. S3, ESI†). This hypothesis is corroborated by the observation that the character of the dissociation changes with peptide length. Fig. 3a shows that for the tripeptide **1a** heterolytic cleavage of the LG-anion **a** at 229 u/e is the only observed dissociation channel. However, for all longer oligopeptides we find the additional channel involving the transfer of a proton, which results in the separation of a neutral leaving group LG-H from a negatively charged peptide (Fig. 3b and Scheme 1). While the hexapeptide **2a** still shows partial heterolysis, the longer peptides **3a** and **4a** dissociate exclusively under proton transfer, with the fragment at m/z = (M − 230) u/e. The proton transfer reaction is always accompanied by the formation of a second fragment at m/z = (M − 246) u/e.

In contrast to that we have never observed proton transfer in our collision induced dissociation experiments (Fig. S5, ESI†). Instead, the CID spectrum of the hexa- and nonapeptide **2a** and **3a** yield about 5% of heterolytic cleavage at 300 K, and the nonapeptide spectrum shows the appearance of some backbone fragments.

A systematic variation of the leaving group **a**, **b**, **c**, **d** at the tripeptide **1**, confirmed our design hypothesis that the electron withdrawing fluorine substituents stabilize the negative charge on the LG phenolates and enable heterolytic cleavage. We correlate the heterolytic cleavage efficiencies with density functional theory (DFT) calculations (ESI†) to shed light on our experimental findings. Initial conformations used in DFT calculations are modeled in terms of chemical constitution and further locally relaxed using manually created conformations. Short *ab initio*

molecular dynamics (AIMD) simulations at 300 K further helped us to explore the potential energy surface (PES) for candidates while the electronic potential is provided by DFT at the PBE0/3-21G level of theory. Several conformational candidates are further locally optimized at 0 K at the PBE0/Def2TZVP[35,36] level and lowest energy conformations are used in the following calculations. The energetics of the photocleavage process is addressed by relating heterolytic bond dissociation energies (BDE),[37] vertical electron detachment energies (VDE),[38] fragment yields and pK_a values. Additionally, mean thermal energies are estimated from calculated vibrational spectra in the harmonic approximation (Table S1, ESI†).

Even though the energy of a single 266 nm photon (4.7 eV) is smaller than the BDE of **1a** (6.9 eV), it adds to a mean thermal energy of 1.4 eV at 300 K and thus to a total internal energy of 6.1 eV, which is close enough to the BDE for fragmentation to occur after some intra-molecular reorganization. At lower temperature, here at 60 K, the total internal energy of 4.8 eV is far below the BDE value. This is consistent with the observation in Fig. 2b that at 60 K two or more photons are required in most cases. Electron detachment cannot be entirely excluded, given the computed VDE values of 4.6 eV, especially since the experimental fragment collection efficiency is not exactly known.

Apparently, for some LGs heterolytic cleavage becomes less probable than a dissociation involving proton transfer (**1c**). Heterolytic cleavage must leave a zwitterionic peptide behind which might be favored by the formation of a tropylium cation. Preliminary DFT calculations (ESI†) indicate that this structure is of comparable stability to the corresponding benzyl cation. It remains, however, an open task to model detailed reaction pathways and to evaluate the barriers for the intermediates. We also find that the trend in fragmentation yields for compounds **1a–1d** (Fig. 4a), correlate with the pK_a values of the protonated leaving groups LG-H (Table S1, ESI†), even though the latter also include ion solvation energies.

To compare the optical response of the tripeptides **1** with different LGs, time-dependent density functional theory (TDDFT) calculations were performed at the same level of theory as before, involving 100 excited states. Gaussian convolutions to the calculated line spectra show strong absorption around 250 nm for **1a–1d** (Fig. 4b). Electronic excitation analysis based on natural transition orbitals (NTO)[39] confirms that the UV light excites the PCT rather than the peptide. We also find that the absorption spectra do not significantly change upon exchange of the LG.

The photocleavage of *o*-nitrobenzylethers and related nitroaryls in solution is well documented in the literature.[40,41] Since cleavage of the 2-phenoxy-methyl-nitrobenzene can already be realized with electrons and atoms of the photolinker, that is without the involvement of solvent molecules, site-specific dissociation should also be possible in the gas phase,[33] as seen in our experiments.

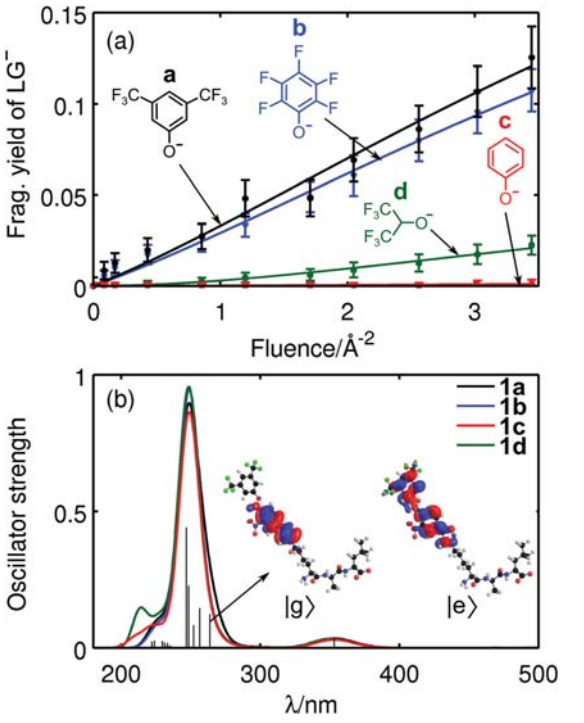

Fig. 4 (a) LG fragment yield of the functionalized tripeptide **1** as a function of the laser fluence. The four difference curves correspond to the same PCT core with four different leaving groups (**a**, **b**, **c** and **d**). (b) The oscillator strength of the tripeptides **1a–1d** is obtained by TDDFT. For simplicity we show a Gaussian convolutions to the line spectrum only for peptide **1a**. The arrow points to the NTOs with the largest eigenvalue for the transition close to 266 nm. For the particular LG **a** the calculations find efficient charge transfer from the absorbing PCT towards the LG in the transition from the ground state |g⟩ to the excited state |e⟩.

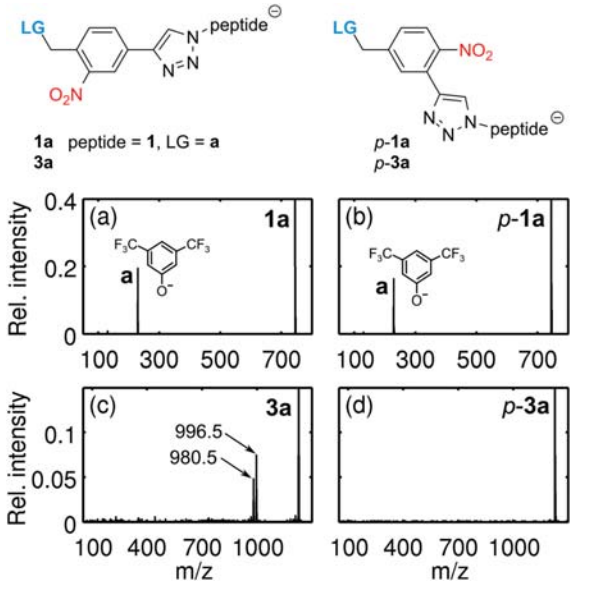

Fig. 5 Effect of nitro-group position on photocleavage efficiency. Heterolysis in the tripeptide is little affected by moving the nitro-group to the *para*-position of the LG (a and b) whereas cleavage under proton transfer is suppressed in the nonapeptide (c and d).

To decipher the role of the nitro group, isomers of the tripeptide **1a** and the nonapeptide **3a**, (*p*-**1a**, *p*-**3a**) were synthesized with the nitro-group in the *para*-position of the benzylic ether function (Fig. 5). We find that *p*-**1a** and **1a** cleave with a comparable heterolytic efficiency, corroborating the thermal nature of the process. This is markedly different from the behavior in solution (DMSO-d_6) where irradiation of *p*-**1a** at 254 nm does not yield any cleavage, while it does for **1a** (Fig. S8, ESI†). However, the modified nonapeptide *p*-**3a** does not cleave under conditions where **3a** dissociates. This indicates that the proton transfer pathway resembles the accepted solution phase mechanism[42] and can be suppressed by repositioning the nitro group. The heterolytic channel, on the other hand, is too slow for the *para*-functionalized nonapeptides. For the short peptides **1a–1b**, the sum of photon (4.7 eV) and thermal energies ($\approx$1.3 eV) is sufficient to release a negatively charged LG, and the heterolytic mechanism is observed. For larger peptides, however, the heterolytic process seems less favourable and the proton transfer pathway takes over, which sensitively depends on the proximity of the NO_2 to the leaving group.

3 Conclusions

Our results demonstrate that photocleavable peptides can efficiently and selectively be cleaved in the gas-phase using UV light. The tailored peptides undergo different dissociation mechanisms depending on the nature of the LG, the size of the peptides, the molecular temperature and the position of the nitro group within the PCT.

We have demonstrated that small peptides can undergo thermally assisted heterolytic photocleavage in the gas phase while longer oligopeptides follow a dissociation path presumably involving proton transfer to the LG, more closely resembling the solution phase mechanism. This insight can contribute to the design of new peptide labels for proteomics.[19,43]

Photoactive groups have recently been studied for applications in solution and optimized response to a desired wavelength.[42,44] In our current work we have explored the influence of peptide size and the nature of the LG on the heterolytic photocleavage efficiency in the gas phase. Since our longest oligopeptides preferentially follow a PD mechanism with proton transfer, neutralization of large polypeptides or eventually proteins in the gas phase may require the charge to be stabilized on the leaving group. Our current experiments were targeting non-aromatic peptides where we can avoid an absorption competition between the tag and the aromatic chromophores. Future experiments will explore red-shifted tags, which will then be applicable to aromatic peptides, also.

Both the neutral and the charged dissociation pathways are interesting and useful for gaining optical control over the motional states of molecules. Photocleavage can be realized with high spatial control and very precise timing. This technique may be used for post-neutralizing singly charged anion beams, which have been previously guided and cooled in a buffer gas environment. The optically induced gas phase photo-depletion of the parent peak is also promising for realizing coherent beam splitters based on photo-depletion of a molecular beam with nanometer resolution.[45] This will become important for quantum optics and metrology experiments with complex neutral biomolecules.

Conflicts of interest

There are no conflicts to declare.

Acknowledgements

This project has received funding from the European Research Council (ERC) under the European Union's Horizon 2020 research and innovation programme (Grant No. 320694), the Swiss National Science Foundation (200020-159730), and the Swiss Nanoscience Institute at the University of Basel (P1403). We are thankful to M. C. Böhm for computational advice and M. Kerschbaum for support in the ESI measurements. We thank N. Münch und D. Häussinger for NMR experiments. The computational results were obtained using the Vienna Scientific Cluster (VSC).

Notes and references

1 M. F. Jarrold, *Annu. Rev. Phys. Chem.*, 2000, **51**, 179–207.
2 M. Schennach and K. Breuker, *Angew. Chem., Int. Ed.*, 2014, **53**, 164–168.
3 O. S. Skinner, F. W. McLafferty and K. Breuker, *J. Am. Soc. Mass Spectrom.*, 2012, **23**, 1011–1014.
4 T. Meyer, V. Gabelica, H. Grubmüller and M. Orozco, *Wiley Interdiscip. Rev.: Comput. Mol. Sci.*, 2013, **3**, 408–425.
5 P. S. Walsh, K. N. Blodgett, C. McBurney, S. H. Gellman and T. S. Zwier, *Angew. Chem., Int. Ed.*, 2016, **55**, 14618–14622.
6 C. Baldauf and M. Rossi, *J. Phys.: Condens. Matter*, 2015, **27**, 493002.
7 F. Bierau, P. Kupser, G. Meijer and G. von Helden, *Phys. Rev. Lett.*, 2010, **105**, 133402.
8 A. Ostendorf, C. B. Zhang, M. Wilson, D. Offenberg, B. Roth and S. Schiller, *Phys. Rev. Lett.*, 2006, **97**, 243005.
9 M. Guidi, U. J. Lorenz, G. Papadopoulos, O. V. Boyarkin and T. R. Rizzo, *J. Phys. Chem. A*, 2009, **113**, 797–799.
10 J. M. Weber, I. N. Ioffe, K. M. Berndt, D. Löffler, J. Friedrich, O. T. Ehrler, A. S. Danell, J. H. Parks and M. M. Kappes, *J. Am. Chem. Soc.*, 2004, **126**, 8585–8589.
11 M. Vonderach, O. T. Ehrler, K. Matheis, P. Weis and M. M. Kappes, *J. Am. Chem. Soc.*, 2012, **134**, 7830–7841.
12 H. N. Chapman, P. Fromme, A. Barty, T. A. White, R. A. Kirian, A. Aquila, M. S. Hunter, J. Schulz, D. P. DePonte, U. Weierstall, R. B. Doak, F. R. N. C. Maia, A. V. Martin, I. Schlichting, L. Lomb, N. Coppola, R. L. Shoeman, S. W. Epp, R. Hartmann, D. Rolles, A. Rudenko, L. Foucar, N. Kimmel, G. Weidenspointner, P. Holl, M. Liang, M. Barthelmess, C. Caleman, S. Boutet, M. J. Bogan, J. Krzywinski, C. Bostedt, S. Bajt, L. Gumprecht, B. Rudek, B. Erk, C. Schmidt, A. Hömke, C. Reich, D. Pietschner, L. Strüder, G. Hauser,

H. Gorke, J. Ullrich, S. Herrmann, G. Schaller, F. Schopper, H. Soltau, K. Kühnel, M. Messerschmidt, J. D. Bozek, S. P. Hau-Riege, M. Frank, C. Y. Hampton, R. G. Sierra, D. Starodub, G. J. Williams, J. Hajdu, N. Timneanu, M. M. Seibert, J. Andreasson, A. Rocker, O. Jönsson, M. Svenda, S. Stern, K. Nass, R. Andritschke, C. Schröter, F. Krasniqi, M. Bott, K. E. Schmidt, X. Wang, I. Grotjohann, J. M. Holton, T. R. M. Barends, R. Neutze, S. Marchesini, R. Fromme, S. Schorb, D. Rupp, M. Adolph, T. Gorkhover, I. Andersson, H. Hirsemann, G. Potdevin, H. Graafsma, B. Nilsson and J. C. H. Spence, *Nature*, 2011, **470**, 73–77.

13 T. Gorkhover, S. Schorb, R. Coffee, M. Adolph, L. Foucar, D. Rupp, A. Aquila, J. D. Bozek, S. W. Epp, B. Erk, L. Gumprecht, L. Holmegaard, A. Hartmann, R. Hartmann, G. Hauser, P. Holl, A. Hömke, P. Johnsson, N. Kimmel, K. Kühnel, M. Messerschmidt, C. Reich, A. Rouzée, B. Rudek, C. Schmidt, J. Schulz, H. Soltau, S. Stern, G. Weidenspointner, B. White, J. Küpper, L. Strüder, I. Schlichting, J. Ullrich, D. Rolles, A. Rudenko, T. Möller and C. Bostedt, *Nat. Photonics*, 2016, **10**, 93–97.

14 P. Schanen, D. Yang, R. Weinkauf and E. Schlag, *Int. J. Mass Spectrom. Ion Processes*, 1997, **167**, 447–470.

15 J. L. Stephenson and S. A. McLuckey, *J. Am. Chem. Soc.*, 1996, **118**, 7390–7397.

16 X. Pan, P. Cloutier, D. Hunting and L. Sanche, *Phys. Rev. Lett.*, 2003, **90**, 208102.

17 L. Joly, R. Antoine, A.-R. Allouche, M. Broyer, J. Lemoine and P. Dugourd, *J. Am. Chem. Soc.*, 2007, **129**, 8428–8429.

18 J. A. Stearns, S. Mercier, C. Seaiby, M. Guidi, O. V. Boyarkin and T. R. Rizzo, *J. Am. Chem. Soc.*, 2007, **129**, 11814–11820.

19 J. S. Brodbelt, *Chem. Soc. Rev.*, 2014, **43**, 2757–2783.

20 R. Antoine and P. Dugourd, *Phys. Chem. Chem. Phys.*, 2011, **13**, 16494–16509.

21 M. Bouakil, A. Kulesza, S. Daly, L. MacAleese, R. Antoine and P. Dugourd, *J. Am. Soc. Mass Spectrom.*, 2017, **28**, 2181–2188.

22 A. R. Milosavljevic, C. Nicolas, J. Lemaire, C. Dehon, R. Thissen, J.-M. Bizau, M. Réfrégiers, L. Nahon and A. Giuliani, *Phys. Chem. Chem. Phys.*, 2011, **13**, 15432–15436.

23 W. D. Price, R. A. Jockusch and E. R. Williams, *J. Am. Chem. Soc.*, 1998, **120**, 3474–3484.

24 T. Ly and R. R. Julian, *J. Am. Chem. Soc.*, 2008, **130**, 351–358.

25 D. A. Polasky, F. Lermyte, M. Nshanian, F. Sobott, P. C. Andrews, J. Loo and B. T. Ruotolo, *Anal. Chem.*, 2018, **90**, 2756–2764.

26 R. Hodyss, H. A. Cox and J. Beauchamp, *J. Am. Chem. Soc.*, 2005, **127**, 12436–12437.

27 T. Juffmann, H. Ulbricht and M. Arndt, *Rep. Prog. Phys.*, 2013, **76**, 086402.

28 L. Mairhofer, S. Eibenberger, J. P. Cotter, M. Romirer, A. Shayeghi and M. Arndt, *Angew. Chem., Int. Ed.*, 2017, **56**, 10947.

29 S. Eibenberger, S. Gerlich, M. Arndt, J. Tüxen and M. Mayor, *New J. Phys.*, 2011, **13**, 043033.

30 J. Tüxen, S. Gerlich, S. Eibenberger, M. Arndt and M. Mayor, *Chem. Commun.*, 2010, **46**, 4145–4147.

31 J. Rodewald, P. Haslinger, N. Dörre, B. A. Stickler, A. Shayeghi, K. Hornberger and M. Arndt, *Appl. Phys. B: Lasers Opt.*, 2017, **123**, 3.

32 J. B. Fenn, M. Mann, C. K. Meng, S. F. Wong and C. M. Whitehouse, *Mass Spectrom. Rev.*, 1990, **9**, 37–70.

33 U. Sezer, P. Geyer, M. Kriegleder, M. Debiossac, A. Shayeghi, M. Arndt, L. Felix and M. Mayor, *Beilstein J. Nanotechnol.*, 2017, **8**, 325.

34 J. Friedrich, S. Gilb, O. T. Ehrler, A. Behrendt and M. M. Kappes, *J. Chem. Phys.*, 2002, **117**, 2635–2644.

35 C. Adamo and V. Barone, *J. Chem. Phys.*, 1999, **110**, 6158–6170.

36 F. Weigend and R. Ahlrichs, *Phys. Chem. Chem. Phys.*, 2005, **7**, 3297–3305.

37 S. J. Blanksby and G. B. Ellison, *Acc. Chem. Res.*, 2003, **36**, 255–263.

38 J. M. Herbert and M. Head-Gordon, *J. Phys. Chem. A*, 2005, **109**, 5217–5229.

39 R. L. Martin, *J. Chem. Phys.*, 2003, **118**, 4775–4777.

40 P. Sebej, T. Solomek, L. Hroudna, P. Brancova and P. Klan, *J. Org. Chem.*, 2009, **74**, 8647–8658.

41 T. Šolomek, S. Mercier, T. Bally and C. G. Bochet, *Photochem. Photobiol. Sci.*, 2012, **11**, 548–555.

42 P. Klán, T. Šolomek, C. G. Bochet, A. Blanc, R. Givens, M. Rubina, V. Popik, A. Kostikov and J. Wirz, *Chem. Rev.*, 2012, **113**, 119–191.

43 Q. Enjalbert, M. Girod, R. Simon, J. Jeudy, F. Chirot, A. Salvador, R. Antoine, P. Dugourd and J. Lemoine, *Anal. Bioanal. Chem.*, 2013, **405**, 2321–2331.

44 M. J. Hansen, W. A. Velema, M. M. Lerch, W. Szymanski and B. L. Feringa, *Chem. Soc. Rev.*, 2015, **44**, 3358–3377.

45 N. Dörre, J. Rodewald, P. Geyer, B. von Issendorff, P. Haslinger and M. Arndt, *Phys. Rev. Lett.*, 2014, **113**, 233001.

Chapter 6. Ionic tags for photo-induced charge control andneutralization of proteins in the gas phase

J. Schätti; M. Kriegleder; M. Debiossac; M. Kerschbaum; Philipp Geyer; Armin Shayeghi; Marcel Mayor; Markus Arndt; Valentin Köhler;

Outline of the author's contribution

J. Schätti and V. Köhler designed the charged photocleavables. J. Schätti synthesized and characterized the molecular compounds. M. Kriegleder, M. Debiossac, P. Geyer and J. Schätti performed the photocleavage experiments in the gas-phase. M. Kerschbaum, M. Kriegleder, and M. Debiossac built and tested the corona discharge neutralizer used for the charge reduction of the modified insulin. A. Shayeghi performs ab initio molecular dynamics (AIMD) simulations, which are not included in this thesis and analyse the data with all authors. V. Köhler, M. Arndt and M. Mayor conceived and supervised the experiments. J. Schätti, M. Debiossac, V. Köhler, and M. Arndt wrote the draft of the paper.

A cationic and an anionic nitroarylether based photocleavable tag were synthesized, and the previously described peptides (Chapter 5) were modified with these tags. Azido acetic acid was coupled to the trimethylsilylacetylene moiety of the tags, followed by the formation of an NHS-ester. With this NHS-esters the modification of insulin with photocleavable tags was investigated under physiological conditions as well as in organic solvents.

The results presented in this chapter are published in Chemistry Communications:

Chem. Commun., **2019**, 55, 12507-12510.[1]

Ionic tags for photo-induced charge control and neutralization of proteins in the gas phase

Jonas Schätti, Moritz Kriegleder, Maxime Debiossac, Michael Kerschbaum, Philipp Geyer, Armin Shayeghi, Marcel Mayor, Markus Arndt, Valentin Köhler

Abstract. Electrosprayed and mass selected peptides equipped with *ortho*-nitroarylether tags that carry a permanent charge on their leaving group (LG) undergo selective cleavage in high vacuum upon irradiation with 266 nm light. The charge bias on the fluoroaryl-leaving group was realized by either a sulfonate (**neg-LG**) or tetraalkylammonium group (**pos-LG**) and led after cleavage to loss of a negatively or positively charged leaving group fragment. Two major cleavage mechanisms were observed – cleavage under H-transfer and bond homolysis, both giving rise to a charge reduced peptide moiety in positive or negative ion mode, respectively. In contrast to previous designs these tags enable the neutralization of medium sized peptides and large amino acid condensates. Selective charge reduction of a variety of charge states of a labelled insulin molecule by one charge was realized. Importantly the neutralization of insulin could also be accomplished. To achieve this, lowly charged species were first enriched by collision with an ionized buffer gas, before the singly charged ion of the insulin derivative was mass selected and charge depleted by photocleavage. This allows us to demonstrate here for the first time the position-and time controlled, charge-reduction and neutralization of mass-selected insulin in high vacuum.

Introduction

Controlling the charge state of biomolecules in the gas phase

Already thirty years ago, electrospray ionization (ESI-MS)[2] and matrix-assisted laser desorption ionization (MALDI) [3-4] were established as efficient ways of transferring charged macromolecules into the gas phase for mass spectrometry. ESI excels in producing continuous beams of highly charged and even massive biomolecules under mild conditions and it is readily coupled with on-line separation methods, i.e. high performance liquid chromatography. MALDI transfers short pulses of macromolecules into the gas phase, that are mostly singly charged.

Both techniques complement each other and have become essential in biomolecular analysis. A high charge-per-mass value determines the molecular velocity in time-of-flight mass spectrometry (TOF-MS) and thus the secondary electron emission efficiency and sensitivity of the instrument while a low charge value and a narrow charge distribution can simplify the mass spectrum of complex molecular mixtures.[5]

Interestingly, even though studies suggest that a substantial fraction of molecules in ESI and MALDI emerge as neutrals,[6] the controlled preparation of neutral mass-selected peptides and proteins has remained a grand challenge up to now. Such neutral beams are expected to open a new window to electric and magnetic beam deflection,[7-8] action-free single-photon recoil spectroscopy [9-10] as well as the field of molecular quantum optics.[11]

We recently reported on the cleavage behaviour of electrosprayed and mass selected short peptides equipped with photo-cleavable tags in high vacuum monitored by a TOF-MS operated in negative ion mode.[12] The tags comprised an *ortho*-nitroarylether unit which underwent ether-cleavage upon irradiation and released a leaving group e.g. a charge-neutral bis(trifluoromethyl)-substituted phenol (**neu-LG**-H). Two competing cleavage mechanisms, namely bond heterolysis or cleavage under H-transfer were observed. While cleavage under H-transfer maintains the negative charge on the peptide fragment, heterolysis releases a neutral zwitterionic peptide fragment and a negatively charged leaving group (**neu-LG**$^-$**,** Figure 1).[12]

Parameters that affect the bias of one cleavage mechanism over the other such as peptide length and nature of the leaving group were identified. Extending the peptide length from 3 to 9 amino acids changed the cleavage behaviour from exclusively heterolytic to exclusive cleavage under H-transfer.[12] To overcome the limitation in peptide length for charge control, we envisioned to study the effect of charge decorated leaving groups, which should enable charge removal under non-heterolytic mechanisms. We based the design on our previous study and selected a fluorinated phenol as a template. Leaving group **pos-LG** is equipped with a positively charged tetraalkylammonium group while the **neg-LG** contains a negatively charged sulfonate. The new leaving groups have been combined with a set of tri- and nonapeptides **1**-**4**. In contrast to the previously investigated constructs with **neu-LG**, none of the new compounds cleaved under bond heterolysis. The new constructs undergo either cleavage under H-transfer or show previously unobserved bond homolysis. Both pathways lead to charge removal from the peptide when charged leaving groups **neg-LG** or **pos-LG** are employed. The charge-reduction-methodology is applicable to small proteins such as insulin, while the previous approach was limited to hexapeptides.

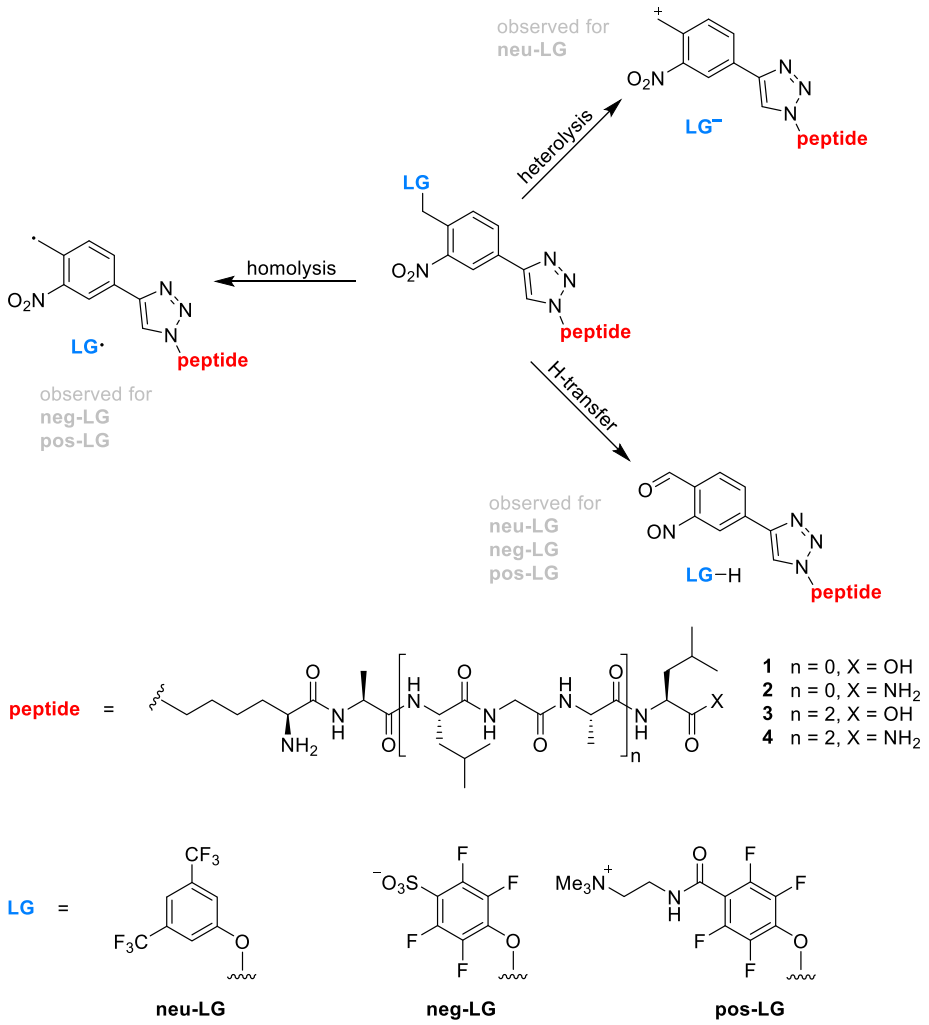

Figure 1. Cleavage mechanisms of *ortho*-nitroarylether-modified electrosprayed peptides upon irradiation with UV light (266 nm) in high vacuum. Constructs with LGs that carry a permanent charge ($-SO_3^-$, $-NMe_3^+$) cleave under bond homolysis or H-transfer, while constructs without a permanent charge on the leaving group cleave under H-transfer or bond heterolysis. The following factors determine if a neutral, positively or negatively charged peptide fragment is formed: i) initial charge of the peptide-LG-conjugate, ii) cleavage mechanism, iii) charge of the leaving group.

Photo-induced and collisional cleavage in ESI-TOF spectrometry

The experiment is built on top of a commercial quadrupole ESI TOF machine. The peptides are volatilized using micro-electrospray and aerodynamically guided into high vacuum to be selected by a quadrupole mass filter. They pass on to a hexapole ion guide for collisional cooling and/or dissociation in a dilute Argon buffer gas. The remaining ions fly on to be analysed by a high-resolution time-of-flight mass spectrometer.

The machine is customized in various ways:[13] the electrospray ion source is equipped with a DC plasma discharge inside an additional inlet chamber, to achieve efficient charge reduction of the peptides in bi-polar air.[14] A Stirling cooler is mounted to the hexapole ion guide to tune the gas temperature between 60 – 300 K. The beam of a short-pulse (10 ns) ultraviolet (266 nm) laser is aligned collinearly with the ion beam and induces photo-cleavage, right behind the collision cell.

Results and Discussion

The irradiation of **1-neg-LG** and **3-neg-LG** sprayed and monitored in negative ion mode resulted in clean LG formation without any additional peaks other than the parent and the leaving group signal (Figure 2). Low relative counts of the negatively charged peptide moiety compared to the LG-signal confirmed that the negative charge of the peptide resided mainly on the leaving group as intended by design. The remaining peptide fragment is consequently charge-neutral, which renders it invisible for mass-spectrometric-analysis. Examination of the leaving group signal revealed that cleavage occured simultaneously under homolysis and H-transfer at a ratio of around 2:1 to 1:1.

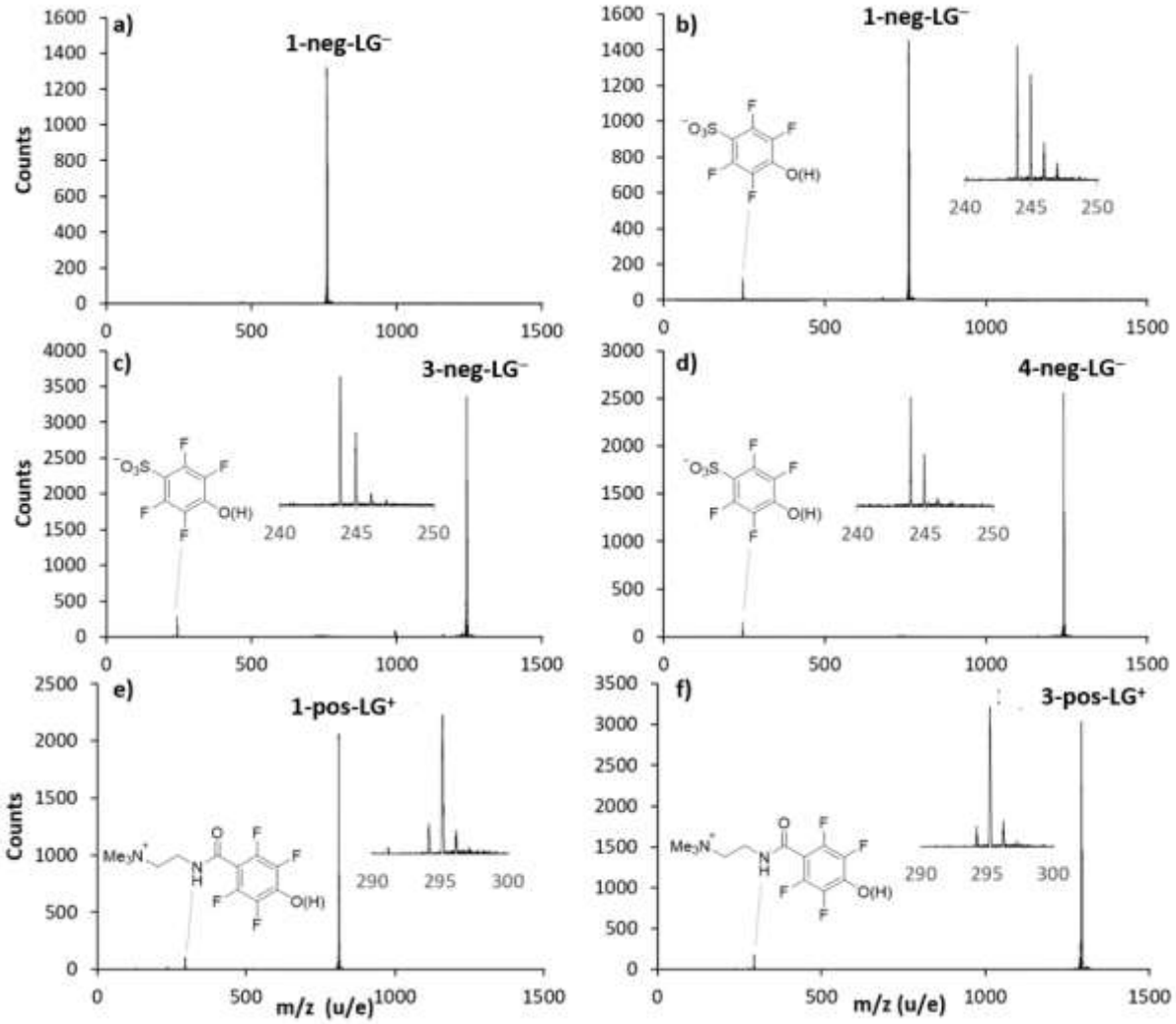

Figure 2. TOF-mass spectra of electrosprayed and mass-selected peptide constructs upon photocleavage with 266 nm laser light. a) Control: **1-neg-LG**⁻ without irradiation b) **1-neg-LG**⁻c) **3-neg-LG**⁻ d) **4-neg-LG**⁻ e) **1-pos-LG**⁻ f) **3-pos-LG**⁻. The insets are a zoom of the LG fragment signal. In c) a small signal at 997 m/z indicates formation of a charged peptide fragment resulting from charge location on the C-terminus instead of the sulfonate group. This signal is not visible when the carboxylate terminus of the peptide is replaced by an amide in **4-neg-LG**⁻ (panel d). In e) a very small signal at 236 m/z indicates loss of NMe_3 from the leaving group. Insets are a zoom of the leaving group signal.

Ions **1-pos-LG**⁺ and **3-pos-LG**⁺ which carry a positive charge on their leaving group and have been recorded in positive ion mode also cleave efficiently upon irradiation. Analysis of the fragment pattern

shows that the constructs cleave preferentially under H-transfer and only to a smaller extent under homolysis at a ratio of around 5:1. Additionally the loss of NMe_3 can be observed from both the parent peak and the leaving group fragment. The absence of a peptide fragment indicates again the formation of a neutral species (Figure 2). Further insight into the fate of the peptide fragment was gathered by mass-selecting and irradiating the doubly charged species of **3-neg-LG**$^{2-}$ and **3-pos-LG**$^{2+}$ which hold an additional charge on the peptide moiety. In these cases one charge remains on the peptide moiety whereas the other charge is located on the leaving group. Both fragments become observable by TOF-MS (see SI).

Homolytic cleavage, which leaves a radical on the peptide fragment, did generally not result in any observable further fragmentation, indicating that such pathways are slow on the time scale of the experiment. Somewhat surprising was the absence of heterolytic cleavage for constructs with **pos-LG**, which would generate an overall charge-neutral LG fragment (**pos-LG**$^{-}$) and a positively charged peptide fragment.

CID of singly charged **1-pos-LG**$^{+}$ and **3-pos-LG**$^{+}$ shows mainly loss of the NMe_3 fragment at low collision gas energy (20 - 30 eV). With increasing collision gas energy multiple fragments are observable whereby the LG-fragment constitutes only a minor signal until it becomes dominant and eventually the only fragment at high collision energies (70 eV, see SI). The LG-fragment appears hereby exclusively after loss of NMe_3 and is apparantly only formed under H-transfer. A similar trend is observed when doubly charged **3-pos-LG**$^{2+}$ is subjected to CID with increasing collision gas energy whereby substantial fragmentation occurs already at 20 eV. Surprisingly only the LG-fragment (minus NMe_3) is observed at high collision energy, suggesting that other charge carrying fragments do not reach the detector or are below the mass cut-off of 90 amu. **1-neg-LG** on the other hand showed mainly formation of the leaving group at 30 eV and little fragmentation.

In order to explore if the methodology is also applicable to biomolecules of higher mass, insulin was derivatized with tags holding either negatively or positively charged leaving groups. In each case a threefold modified species (**neg-Ins** or **pos-Ins**, respectively) was isolated after treatment with NHS-ester derivatives of the charged photocleavable tags and preparative HPLC (Figure 3). The localization of the tags was not experimentally verified, however the most likely attachement sites are the two N-termini of insulin and the only lysine-side chain of insulin (B29).

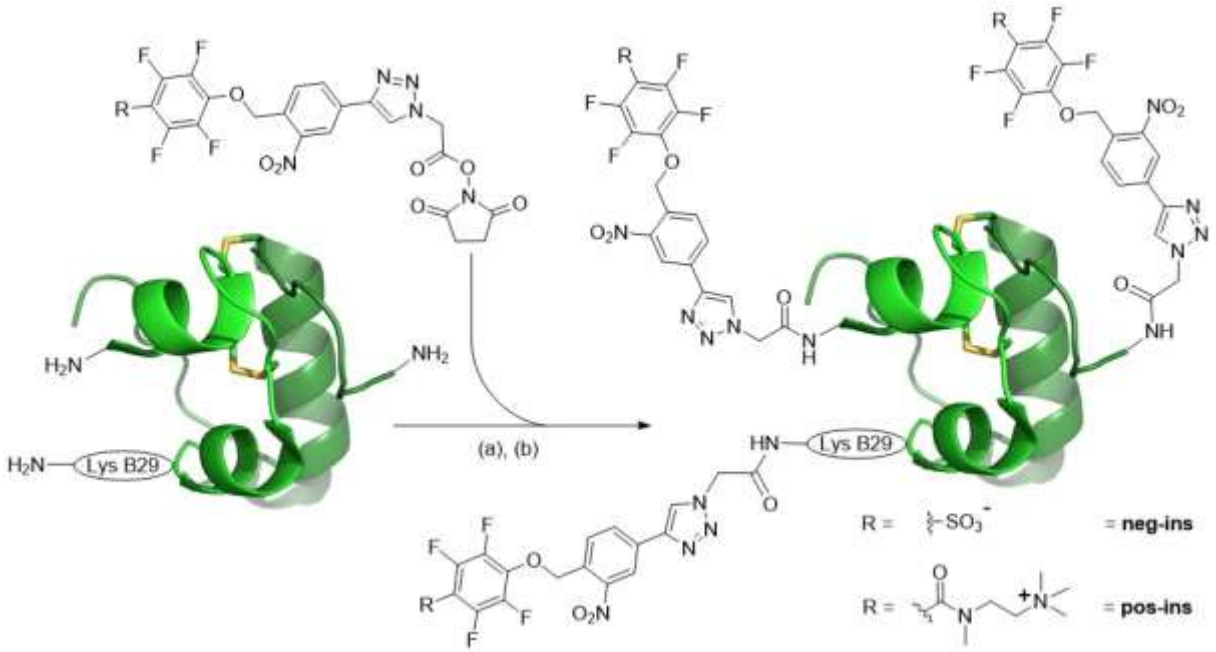

Figure 3. Insulin modification with a photo cleavable tag carrying a neg-LG or pos-LG, respectively. (a) For introduction of pos-LG: 3.0 eq. NHS-ester (formed *in situ*), DMF, rt, 2 h; (b) for introduction of neg-LG: 4.0 eq. NHS-ester (formed *in situ*), DMF, rt, 2 h.

Photocleavage was realized for charge states -1 to -7 in negative ion mode with **neg-ins** and from +3 to +7 in positive ion mode with **pos-ins**. All investigated charge states led to efficient release of the charged leaving group fragment upon irradiation, yielding a charge state reduced insulin moiety without additional fragmentation. The ratio of H-transfer vs. homolytic reflects the observations for the model compounds (the ratio was ca. 1 : 1). For negatively charged insulin species photocleavage was in competition with electron detachment, whereby photocleavage was the far more efficient process (Figure 4, left, signal a (photocleavage) vs. b (electron detachment).

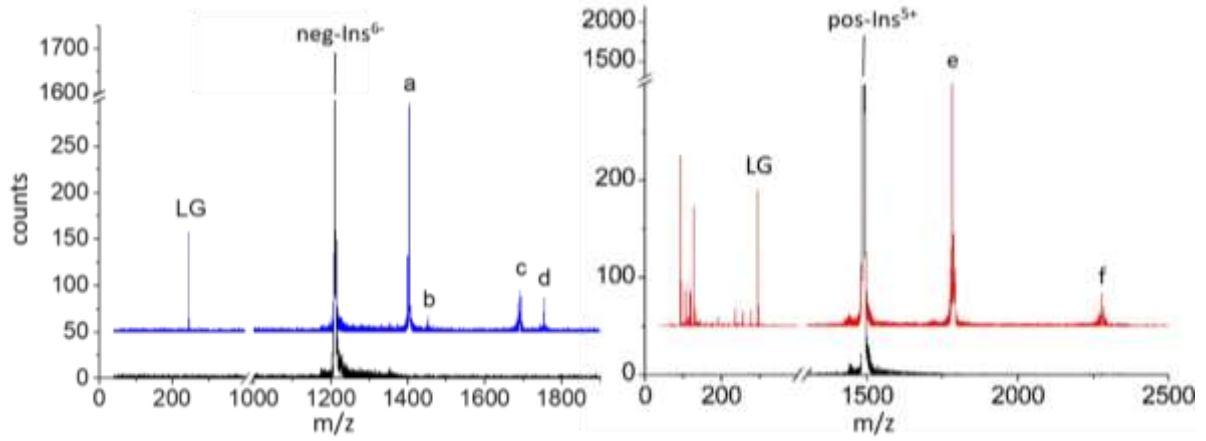

Figure 4. Exemplary mass spectra of mass-selected, labeled insulin before and after irradiation. black line – spectrum before irradiation, blue/red line – spectrum after irradiation. LG = leaving group signal, a = [**neg-Ins** -LG]$^{5-}$, b = [**neg-Ins**]$^{5-}$ (electron detachment), c = [**neg-Ins** -2 LG]$^{4-}$, d = [**neg-Ins** -LG]$^{4-}$ (photocleavage and electron detachment), e = [pos-Ins –LG]$^{4+}$, f = [pos-Ins -2 LG]$^{3+}$.

The cleavage efficiency showed a moderate charge state dependency based on depletion data (integral of the parent signal without irradiation / integral of the parent signal after irradiation, Figure 5).

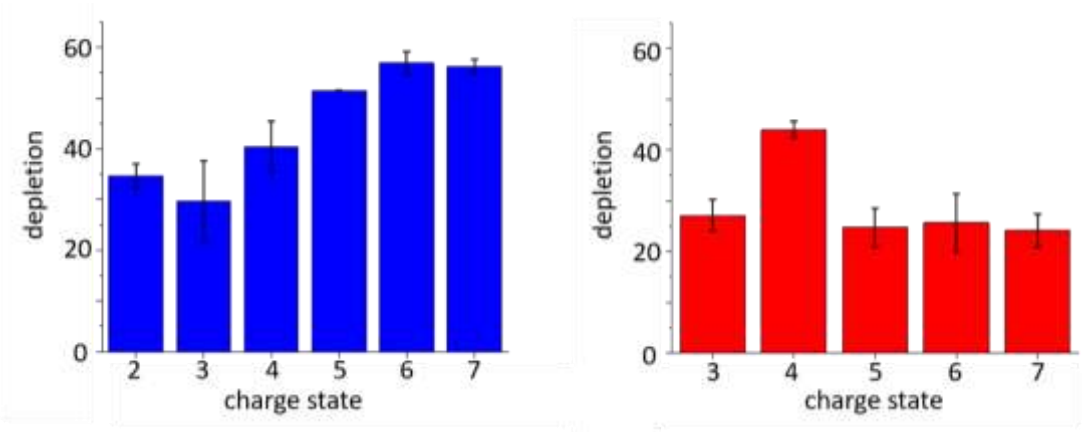

Figure 5. Depletion efficiency in dependence of the charge state. Plotted is the ratio of the integrals in percent = (integral of the parent signal without irradiation / integral of the parent signal after irradiation) × 100%; (blue) depletion efficiency for negative charge states 2-7; (red) depletion efficiency for positive charge states 3-7. The mean value of two measurements is displayed. The limiters of the errorbars indicate the values of the individual measurements.

Neutralization of insulin was possible following charge reduction with an ionizing buffer gas. Upon irradition of the singly negatively charged species **neg-Ins**$^-$ the signal of the LG appeared and the depletion efficiency was around 10%. Evidence is in this case only indirect since the neutral particles can not be detected with common mass spectrometry detectors (Figure 6).

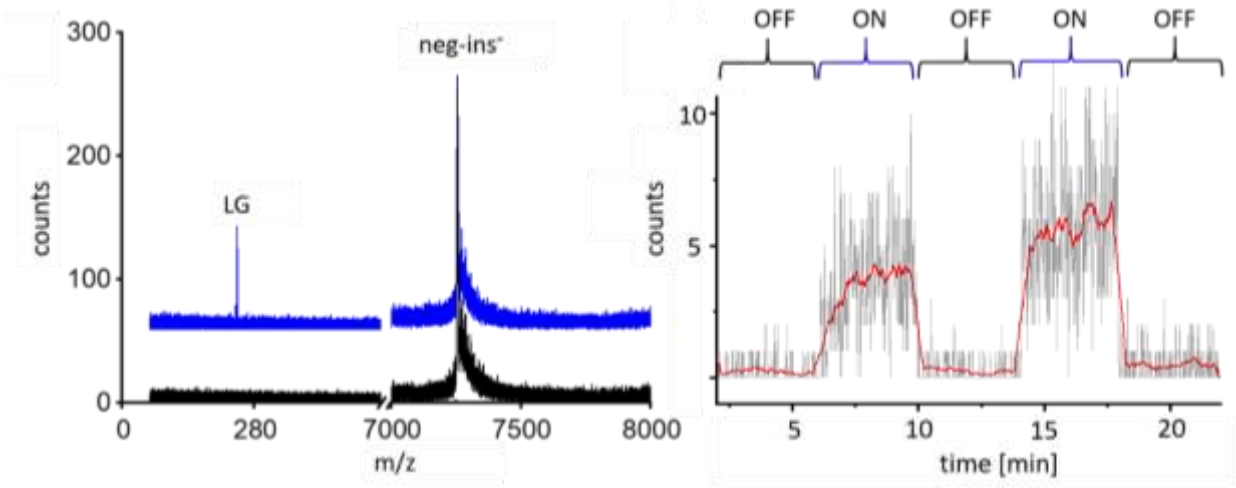

Figure 6. (left) Mass spectra of mass selected singly negatively charged **neg-ins** before (black) and after irradiation (blue). The observation of the LG indicates the formation of a neutral insulin. (right) Leaving group signal over time; the signal appears only when the laser is on; (red line) time-averaged counts over 30 sec.

It is noteworthy that insulin contains 4 tyrosine and 3 phenylalanine residues which compete for 266 nm photons with the photocleavable tags. A comparison of their combined extinction coefficients in solution (ca. 4300 $M^{-1}cm^{-1}$)[15] with the combined extinction coefficient of the nitroarylgroups (> 12000 $M^{-1}cm^{-1}$) indicates that absorption nevertheless occurs predominantly at the photocleavable tags. Furthermore indicates the lack of additional signals that the disulfide bridges are not affected by the photocleavage process.[16]

CID of insulin at 30 eV kinetic energy with argon as the collision gas led to clean formation of the leaving group and the charge reduced species. An exemplary CID spectrum is shown in Figure 7. Although CID might also serve to neutralize singly charged insulin species, the method is likely less suitable for the generation of collimated neutral beams since the collision event is expected to disperse the particles.

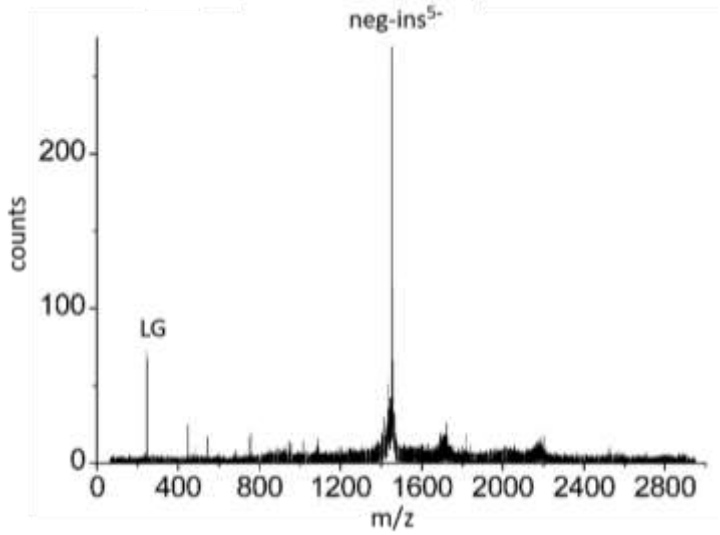

Figure 7. Exemplary CID spectrum of mass-selected **neg-Ins**$^{5-}$ at 30 eV collision energy with argon as a collision gas.

Conclusion

Photocleavable tags based on nitroaryl ethers which carry a permanent charge enable efficient charge reduction and neutralization of large, electrosprayed peptides. Especially the positively charged tags need to be engineered further to prevent loss of NMe_3 which leads to a dilution of the signal. This could likely be accomplished by changing the nature of the linker between fluorinated phenolate and the trimethylalkyl ammonium group. For a more general method the photocleavable group would need to respond efficiently to light of a wavelength that is outside of the absoption profile of proteins (>300 nm).

References

1. J. Schätti; M. Kriegleder; M. Debiossac; M. Kerschbaum; P. Geyer; M. Mayor; M. Arndt; V. Köhler, Neutralization of insulin by photocleavage under high vacuum. *Chem. Commun.* **2019,** *55* (83), 12507-12510.
2. J. B. Fenn; M. Mann; C. K. Meng; S. F. Wong; C. M. Whitehouse, Electrospray Ionization for Mass Spectrometry of Large Biomolecules. *Science* **1989,** *246*, 64-71. M. Karas; F. Hillenkamp, Laser Desorption Ionization of Proteins with Molecular Mass Exceeding 10,000 Daltons. *Anal. Chem.* **1988,** *60*, 2299-2301.
3. K. Tanaka; H. Waki; Y. Ido; S. Akita; Y. Yoshida; T. Yoshida, Protein and Polymer Analyses up to *m/z* 100 000 by Laser Ionization Time-of-flight Mass Spectrometry. *Rap. Comm. Mass Spectr.* **1988,** *2*, 151-153.
4. L. M. Smith, Is charge reduction in ESI really necessary? *J. Am. Soc. Mass Spectrom.* **2008,** *19* (5), 629-631.
5. R. Knochenmuss; R. Zenobi, MALDI Ionization: The Role of In-Plume Processes. *Chemical Reviews* **2003,** *103* (2), 441-452.
6. R. Antoine; P. Dugourd, Visible and ultraviolet spectroscopy of gas phase protein ions. *Phys. Chem. Chem. Phys.* **2011,** *13* (37), 16494-16509.
7. R. Antoine; I. Compagnon; D. Rayane; M. Broyer; P. Dugourd; N. Sommerer; M. Rossignol; D. Pippen; F. C. Hagemeister; M. F. Jarrold, Application of Molecular Beam Deflection Time-of-Flight Mass Spectrometry to Peptide Analysis. *Anal. Chem.* **2003,** *75*, 5512 - 5516.
8. S. Eibenberger; X. Cheng; J. P. Cotter; M. Arndt, Absolute absorption cross sections from photon recoil in a matter-wave interferometer. *Phys. Rev. Lett.* **2014,** *112*, 250402
9. J. Rodewald; P. Haslinger; N. Dörre; B. A. Stickler; A. Shayeghi; K. Hornberger; M. Arndt, New avenues for matter-wave-enhanced spectroscopy. *Appl. Phys. B* **2016,** *123* (1).
10. M. Arndt, De Broglie's meter stick: Making measurements with matter waves. *Phys. Today* **2014,** *67* (5), 30-36.
11. M. Debiossac; J. Schatti; M. Kriegleder; P. Geyer; A. Shayeghi; M. Mayor; M. Arndt; V. Kohler, Tailored photocleavable peptides: fragmentation and neutralization pathways in high vacuum. *Physical Chemistry Chemical Physics* **2018**.
12. M. Debiossac; J. Schätti; M. Kriegleder; P. Geyer; A. Shayeghi; M. Mayor; M. Arndt; V. Köhler, Tailored photocleavable peptides: fragmentation and neutralization pathways in high vacuum. *Phys. Chem. Chem. Phys.* **2018,** *20*, 11412--11417.
13. B. L. Frey; Y. Lin; M. S. Westphall; L. M. Smith, Controlling gas-phase reactions for efficient charge reduction electrospray mass spectrometry of intact proteins. *J. Am. Soc. Mass. Spectrom.* **2005,** *16* (11), 1876-87.
14. https://omlc.org/spectra/PhotochemCAD/html/092.html.
15. Y. M. Fung; F. Kjeldsen; O. A. Silivra; T. W. Chan; R. A. Zubarev, Facile disulfide bond cleavage in gaseous peptide and protein cations by ultraviolet photodissociation at 157 nm. *Angew Chem Int Ed Engl* **2005,** *44* (39), 6399-403.

Chapter 7. Wavelength-dependent photocleavage with visible light for neutralization followed by post-ionization

Outline of the author's contribution

J. Schätti and V. Köhler identified new potential tags for photocleavage under visible light irradiation and designed first test compounds. J. Schätti synthesized and characterized the molecular compounds.

Two published photocleavable chromophore motifs were synthesized, namely a BODIPY- and an aminocoumarin-based one and derivatives for gas phase photocleavage experiments were prepared.[1,2] The described procedure for the synthesis of the BODIPY core was modified for scale-up. With this building block in hand, two new derivatives of the cleavable were synthesized to test gas-phase cleavage in positive and negative ion mode. Four derivatives of the coumarin-based cleavable with different leaving groups (acetate or 3,5-bis(trifluoromethyl)phenolate) and a carboxylic acid or tetraalkylammonium group were synthesized to enable measurements in both ion modes.

Design of the new photocleavable system

Although insulin was successfully neutralized in the gas-phase by photocleavage of designed nitrobenzyl ether groups, this approach for protein-ion neutralization is limited by potential competitive absorption of the protein scaffold. Furthermore, does this approach not address the detection of neutrals, required for various experiments and in particular for interference experiments. Photocleavage of *ortho*-nitroarylethers can be performed at a wavelength of up to 350 nm, although the cleavage efficiency is likely to drop towards higher wavelength as judged by solution phase and theoretical studies.[3] The *ortho*-nitroarylether group shows an absorbance maximum at around 250 nm and a second, much smaller, maximum around 350 nm.[4] Attempts to enable efficient cleavage at higher wavelength by shifting the absorption maximum through the introduction of electron donating groups at the nitroaryl-group had only limited success. Calculations point to non-productive excitation decay at higher wavelengths for 4,5-methylenedioxy-nitrobenzyl compounds.[3] Intense laser light in the given wavelength region from a relatively affordable tabletop laser light source can be provided by the 4th harmonic of an Nd:YAG laser, which produces light at 266 nm. However, aromatic amino acid side chains of tryptophan and tyrosine display significant absorption at 266 nm. Light absorption by tryptophan and tyrosine leads to undesired competitive heating of the protein and possibly even additional fragmentation. The generation of neutral protein molecules in the gas-phase, i.e. insulin, has so far only been proven indirectly, namely by detection of the charged leaving group fragment liberated in the neutralization process (see chapter 6).

Alternative photocleavable systems need to be identified and applied. These need to fulfill the following criteria: i) cleavage must proceed under liberation of a charged leaving group fragment ii) efficient cleavage must proceed at wavelengths above 300 nm to avoid competitive absorbance by amino acid side chains of the protein (e.g. frequency doubled Nd:YAG laser, 532 nm). Additionally, the new tags need to be stable during the process of production of singly charged ions, namely electrospray ionization and charge reduction with an ionized buffer gas,[5] and the attachment to the protein should be simple (e.g. by amidation with a NHS-ester derivative).

Photocleavage can potentially not only be employed for the neutralization of a molecule, but also for ionization if the tag is appropriately designed. Consequently, two sequential photocleavage events could first neutralize the molecule and then reionize it for detection. To circumvent competition between neutralization and post-ionization processes by photocleavage, the introduction of a second, wavelength-orthogonal tag is proposed. A protein tagged with two orthogonal photocleavable tags (PCT), could potentially first be neutralized with green light (e.g., from a frequency doubled Nd:YAG laser, 532 nm). The green laser light would only cleave the PCT absorbing in this wavelength region and would leave the other one intact. Subsequently, the neutral protein could be post-ionized using

blue light (e.g. a frequency doubled Ti-sapphire laser, 450 nm) to cleave the second tag and reestablish a net-charge on the protein. Alternatively, the photocleavage of the second tag could also be investigated under employment of a frequency tripled Nd:YAG laser (355 nm) which could be easier implemented in the setup as it stands at the moment in Vienna. The absorbance of the aminocoumarin based tags is limited at 355 nm, however. The concept is sketched in Figure 1 under the assumption of a heterolytic cleavage mechanism for both PCTs.

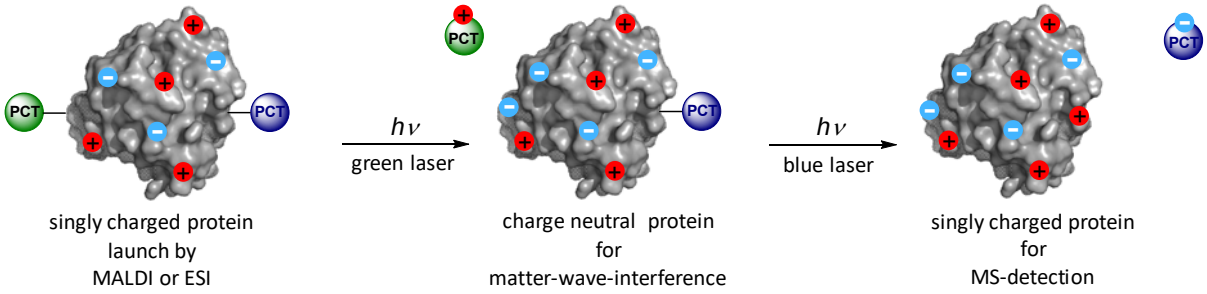

Figure 1. Photocleavage for photoneutralization followed by photo(re)ionization. A heterolytic cleavage mechanism is assumed for both PCTs.

Two wavelength-orthogonal chromophores, which fulfill these criteria in solution experiments, were identified by means of literature research.[6-9] The tag for cleavage by green light is a BODIPY based chromophore and has an absorbance maximum of 536 nm. It was developed and studied in solution by the group of Petr Klán.[7] They observed efficient heterolytic cleavage of a C-O bond that could well be incorporated in a future tag design. Their BODIPY derivate cleaved with a quantum yield of 25% upon irradiation with green light in solution.[7]

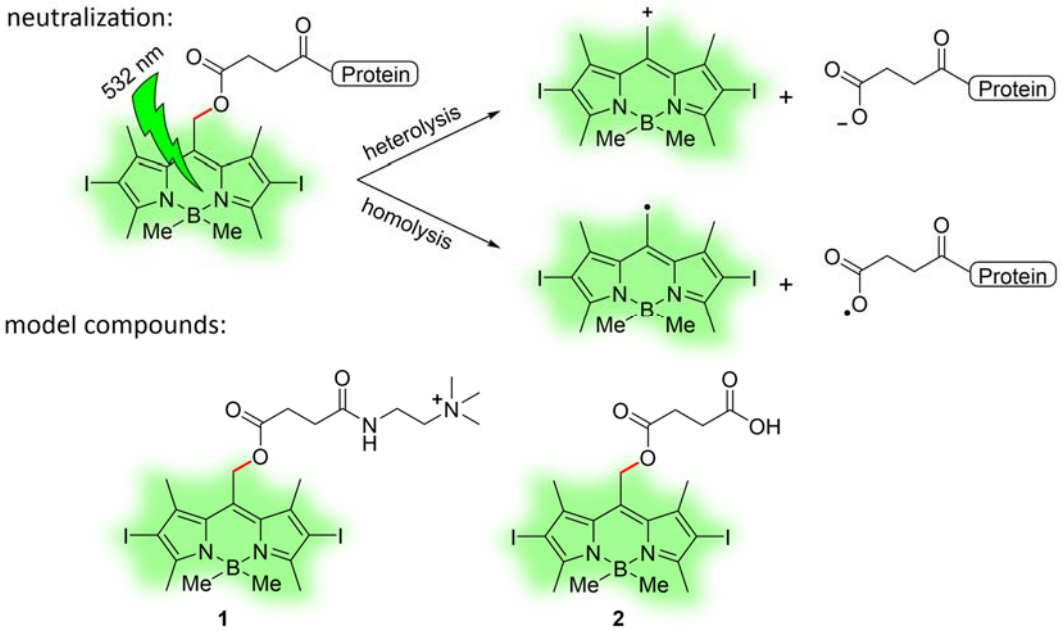

Figure 2. BODIPY based PCT and possible protein linkage. The C-O bond drawn in red underwent cleavage in solution phase studies of related small molecule constructs reported in the literature upon irradiation with green light under a heterolytic mechanism.[7] (top) Proposed protein labeling with the chromophore motif. While heterolysis of the C-O bond was observed for model compounds in solution, gas-phase cleavage might also occur under bond homolysis. (bottom) Model compounds synthesized for first gas-phase photocleavage tests.

Gas-phase cleavage studies are needed to elucidate potential cleavage mechanisms. It was previously observed that the photocleavage behavior of nitroarylethers differed substantially in the gas-phase compared to established solution phase behavior. Furthermore, different cleavage mechanisms played a role depending on the peptide length and the nature of the leaving group (chapter 5).[4] Figure 2 (top) illustrates a possible strategy to attach BODIPY based photocleavable tags to proteins. When heterolytic cleavage occurs, an additional negative charge is generated on the protein. If the starting point is an overall species with a single cationic charge, then this mechanism would lead to a charge neutral protein. A hypothetical heterolytic cleavage of model compound **1** can serve to illustrate the concept. The introduction of additional, 'permanent' charges such as tetraalkylammonium or sulfonate groups, which would be required if homolytic cleavage dominates, is considered to be quite demanding. However, a range of water-soluble charged BODIPY derivatives have been reported, and various strategies for the elaboration and modification of the BODIPY motif have been developed.[10-12] For the initial investigation of the cleavage behavior two complementary model compounds for tests in positive (compound **1**) or negative ion mode (compound **2**), respectively, were synthesized. Both BODIPY constructs tended to be somewhat sensitive and decomposed easily.

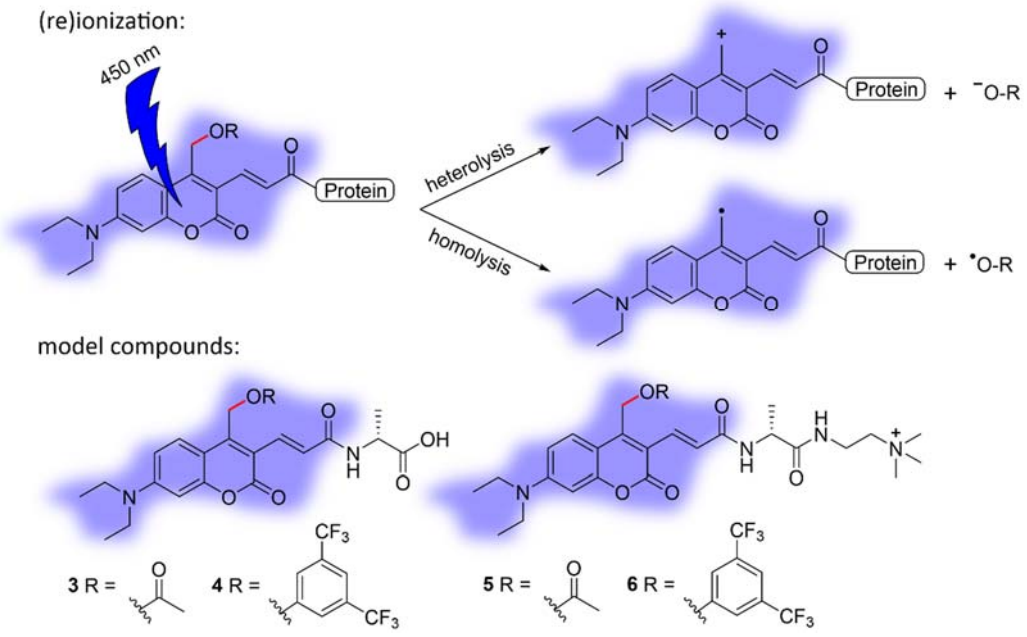

Figure 3. (top) The 7-Diethylaminocoumarin photocleavable motif adapted from literature reports[13] and possible protein linkage of the chromophore. The C-O bond drawn in red underwent cleavage in solution phase studies of related small molecule constructs with blue light under a heterolytic mechanism.[13] (bottom) Model compounds synthesized for first gas-phase photocleavage tests.

As a second cleavable motif, a 7-diethylaminocoumarin[13] based chromophore with an absorption maximum of 450 nm and almost no absorbance at 532 nm was chosen. This photocleavable group was developed by Graham C. R. Ellis-Davies and coworkers as a photochemical protecting group for the

controlled release of bioactive compounds *in vivo*. Upon irradiation with blue light, the C-O bond marked in red in Figure 3 is cleaved heterolytically in solution for related small molecule constructs.[6, 8] As for the BODIPY based photocleavable tag, homolytic C-O bond breakage needs to be considered in the gas-phase. A possible protein attachment of the photocleavable coumarin tag is depicted in Figure 3. The 7-diethylaminocoumarin derived constructs differ fundamentally from the BODIPY ones. Whereas the BODIPY unit is lost upon photocleavage, the aminocoumarin dye ejects a leaving group fragment, but the chromophore itself remains bound to the protein. Therefore heterolytic C-O bond cleavage leads to the formation of a new positive charge on the protein fragment and makes this construct ideal for (re)ionization. In contrast to the BODIPY dyes the introduction of an additional charge on the leaving group, which would be needed should homolytic cleavage dominate, could be easily realized in analogy to the *ortho*-nitroarylether based PCTs (Chapter 6). Furthermore, the aminocoumarin motif also offers the option to link the protein to the leaving group, which would result in an inverted net-charge transfer to the protein moiety upon heterolytic cleavage (Figure 4).

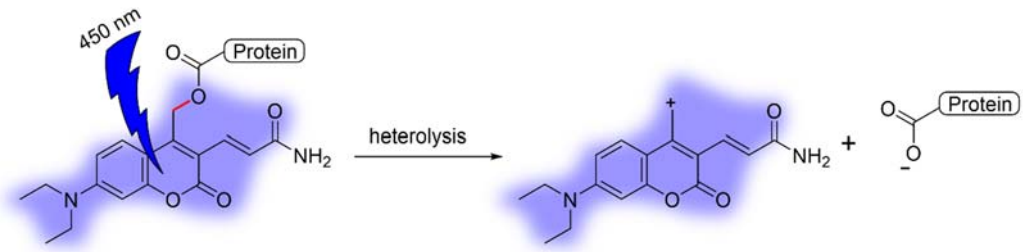

Figure 4. Alternative linkage of the aminocoumarin-based chromophore. In this case bond heterolysis would lead to the formation of a negative charge on the protein fragment.

For initial photocleavage tests of the aminocoumarin tag in the gas-phase, four model compounds **3-6** were synthesized. These carry either an acetate or 3,5-bis(trifluoromethyl)phenolate as a leaving group and a negative or positive charge on the moiety intended to carry the peptide. The latter feature enables cleavage experiments in positive or negative ion mode, respectively. Photocleavage experiments of the model compounds were not performed in the scope of this thesis.

Synthesis

The BODIPY cleavable was synthesized following a slightly modified procedure to the one reported by Gonzalo Cosa[1] and Petr Klán.[7] The BODIPY motif **7** was formed from 2,4-dimethylpyrrole, 2-chloro-2-oxoethyl acetate by condensation followed by coordination of the two pyrrole nitrogen atoms to the boron center upon addition of BF_3 etherate. The acetyl protecting group was removed with LiOH in a water/THF mixture (1:1). After deprotection, the fluorine substituents at the boron center were replaced by methyl groups upon reaction with MeMgBr. The first three steps were performed in a manner without chromatographic purification in contrast to the described protocol by G. Cosa[1] and P. Klán.[7] Chromatographic purifications of the intermediates **7** and **8** on gramm scale was not successful.

However, **7** and **8** could be partially purified by precipitation from acetonitrile upon addition of water and were used as such in the following step. Compound **9** was isolated after column chromatography with a yield of 7% over three steps compared to a published yield of 35% for a small scale synthesis (<0.2 g for each step) where each intermediate was purified by chromatography.[1, 7] The two iodine atoms were introduced by reaction with *N*-Iodosuccinimide.[7] **10** could be easily coupled to Fmoc-alanine as described by Petr Klán.[7] Unfortunately Fmoc-deprotection of **11** under various conditions (see experimental part for details) led to decomposition. The use of Boc-protected amino acids instead of Fmoc-protected ones was not investigated because **10** decomposes rapidly under the acidic conditions typically applied for Boc-deprotection. As an alternative strategy **10** was treated with succinic anhydride to obtain the first model compound **2** in 69% yield. The positive charged model compound **1** could be obtained by coupling **2** to NH_2-CH_2-CH_2-NMe_3^+under standard peptide coupling conditions with a yield of 32%.

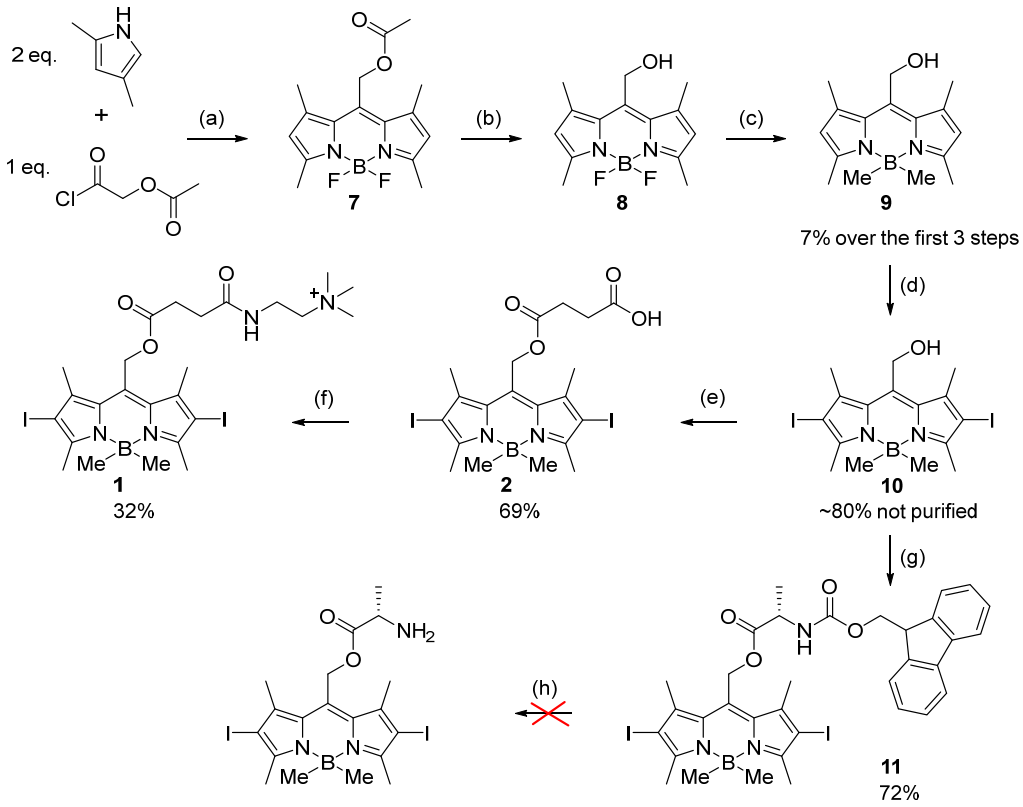

Scheme 1. Synthesis of the two BODIPY based model compounds **1** and **2**. (a) i) CH_2Cl_2 , 40 °C, 5 h. ii) 4.0 eq. DIPEA, rt, 15 min. iii) 4.0 eq. $BF_3{\cdot}Et_2O$, rt, 1 h. (b) 3.0 eq. LiOH, THF/H_2O (1:1), rt, 3 h. (c) 10 eq. MeMgI, Et_2O, rt, 1 h. (d) 1.95 eq. *N*-iodosuccinimide, THF, 0 °C, 5 h. (e) 10 eq. Succinic anhydride, 10 eq. DIPEA, $CHCl_3$, 50 °C, 1 h. (f) 3.0 eq. NH_3-CH_2-CH_2-$NMe_3^{2+}I^-$ TFA^-, 3.0 eq. EDC, 0.1 eq. DMAP, 6.0 eq. DIPEA, DMF, rt, 3 h. (g) 2.0 eq. Fmoc-Ala-OH, 2.0 eq. EDC, 0.1 eq. DMAP, CH_2Cl_2, rt, 2.5 h. (h) Different conditions were tried but always lead to decomposition of the compound instead of Fmoc-deprotection; see experimental part for deprotection conditions.

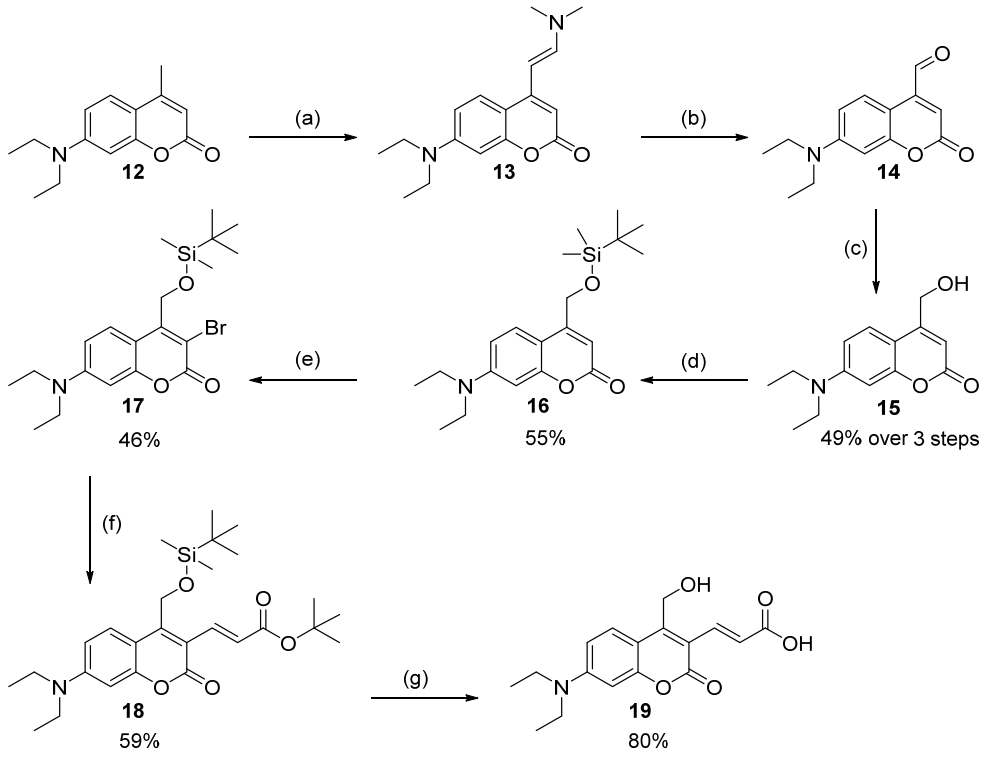

Scheme 2. Synthesis of of the 7-Diethylaminocoumarin-2-acrylic acid derivate **19** according to known procedures.[2, 6] (a) 2 eq. DMF-DMA, DMF, reflux, overnight. (b) 3 eq. $NaIO_4$, H_2O/THF (1:1), rt, 2 h. (c) 2 eq. $NaBH_4$, THF, 0°C → rt, 2 h. (d) 1.2 eq. TBDMS-Cl, CH_2Cl_2, 0°C → rt, 4 h. (e) 1.2 eq. NBS, MeCN, 0°C → rt, 1 h. (f) 3 eq. *tert*-butyl acrylate, 1.7 eq. LiCl, 1.1 eq. tetrabutylamoniumchlorid, 3 eq. $NaHCO_3$, 0.1 eq. $Pd(OAc)_2$, DMF, reflux, 1 h. (g) i) TFA, rt, 30 min, ii) 5 eq. TBAF, THF, 6 h.

The first steps of the synthesis of the coumarin-based photocleavable (**12** to **15**) followed published protocols by Michael W. Göbel.[2] The steps towards **18** were achieved by protocols from Graham C. R. Ellis-Davies.[6] Starting from 7-diethylamino-4-methylcoumarin (**12**), the formation of the enamine **13** was accomplished by condensation with DMF-DMA. The crude product was oxidized to the corresponding aldehyde **14** with $NaIO_4$, and the crude aldehyde **14** was reduced to the corresponding alcohol **15** with $NaBH_4$. Over these three sequential steps, a yield of 49% was obtained compared to 71% reported in the literature.[2] The alcohol was protected with TBDMS-Cl and it followed the bromination of **16** with NBS to yield **17**. A Heck reaction with *tert*-butyl acrylate led to the formation of **18** with 59% yield (lit. yield 68%).[6] In contrast to the protocol from Ellis-Davies,[6] where only the carboxylic acid was deprotected, a sequential deprotection of the carboxylic acid and the alcohol without intermediate workup was performed to give **19** in good yield (80%). The carboxylic acid **19** was then coupled under standard peptide coupling conditions with EDC to alanine *tert*-butyl ester. With **20** in hand, two different leaving groups were introduced. i) An acetate leaving group was installed by esterification of the primary alcohol employing EDC and DMAP for the coupling in analogy to procedures described by Ellis-Davies and coworkers[6] ii) a 3,5-bis(trifluoromethyl)phenol leaving group was introduced by Mitsunobu reaction in analogy to the nitroarylether PCTs with an isolated yield of 34%.

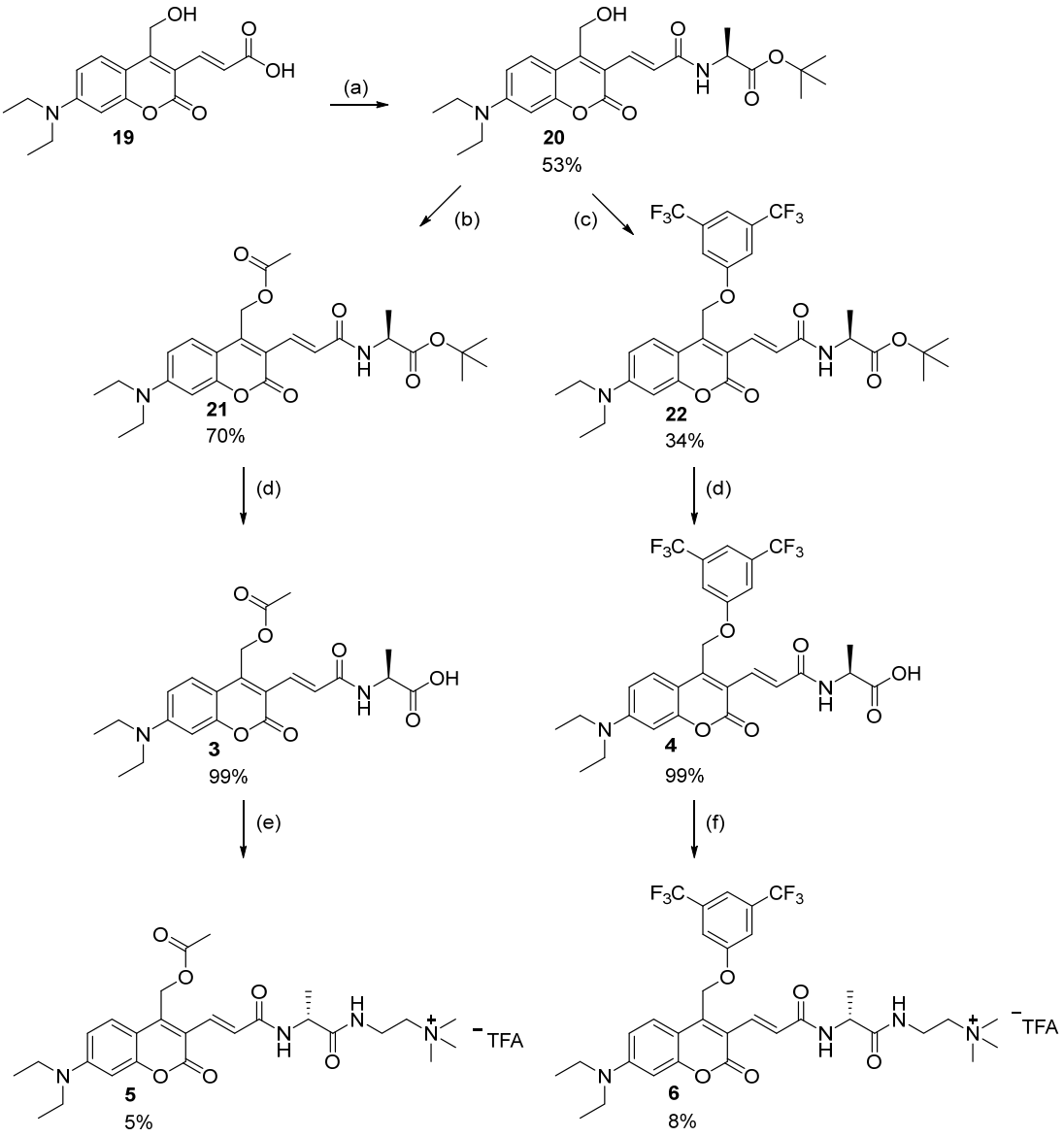

Scheme 3. Synthesis of the four coumarin-based model compounds **3-6**: (a) 1.0 eq. *tert-butyl L*-alanine, 1.2 eq. EDC, 2.0 eq. DIPEA, CH_2Cl_2/MeCN (1:1), rt, 5 h. (b) 3.0 eq. Acetic acid, 3.0 eq. EDC, 0.1 eq. DAMP, CH_2Cl_2, rt, 3 h. (c) 2.0 eq. 3,5-bis(trifluoromethyl)phenol, 6.0 eq. DIAD, 6.0 eq. PPh_3, THF, 0°C, 3 h. (d) TFA/ CH_2Cl_2 (1:1), rt, 30 min, (e) 1.2 eq. NH_3-CH_2-CH_2-$NMe_3^{2+}I^-TFA^-$, 1.2 eq. EDC, 4.0 eq. DIPEA, DMF, rt, 3 h. (f) 2. eq. NH_3-CH_2-CH_2-$NMe_3^{2+}I^-TFA^-$, 2.0 eq. HBTU, 4.0 eq. DIPEA, DMF, rt, 3 h.

Subsequently, the *tert*-butyl ester group of **21** and **22** were deprotected with TFA/CH_2Cl_2 (1:1) to give the first two photocleavable test compounds **3** and **4** in almost quantitative yield. To prepare test compounds **5** and **6** for cleavage experiments in the positive ion mode, the alanine moiety was coupled to NH_2-CH_2-CH_2-NMe_3^+ with EDC (for **3**) respectively HBTU (for **4**). Compounds **5** and **6** were obtained in low isolated yields of 5% and 8%, respectively, although reaction monitoring by UPLC-MS indicated full conversion of the starting materials. NH_2-CH_2-CH_2-NMe_3^+ was produced according to known procedures by permethylation of Boc-NH-CH_2-CH_2-NH_2 followed by Boc deprotection.[14]

References

1. K. Krumova; G. Cosa, Bodipy Dyes with Tunable Redox Potentials and Functional Groups for Further Tethering: Preparation, Electrochemical, and Spectroscopic Characterization. *J. Am. Chem. Soc.* **2010,** *132* (49), 17560-17569.
2. W. Timo; G. Markus; G. Christian; P. Thomas; G. Michael, Synthesis of a Cytidine Phosphoramidite with Protected Nitroxide Spin Label for EPR Experiments with RNA. *Eur. J. Org. Chem.* **2017,** *2017* (3), 491-496.
3. K. Schaper; M. Etinski; T. Fleig, Theoretical investigation of the excited states of 2-nitrobenzyl and 4,5-methylendioxy-2-nitrobenzyl caging groups. *Photochem. Photobiol.* **2009,** *85* (5), 1075-1081.
4. M. Debiossac; J. Schatti; M. Kriegleder; P. Geyer; A. Shayeghi; M. Mayor; M. Arndt; V. Kohler, Tailored photocleavable peptides: fragmentation and neutralization pathways in high vacuum. *Phys. Chem. Chem. Phys.* **2018**.
5. D. D. Ebeling; M. S. Westphall; M. Scalf; L. M. Smith, Corona Discharge in Charge Reduction Electrospray Mass Spectrometry. *Anal. Chem.* **2000,** *72* (21), 5158-5161.
6. J. P. Olson; M. R. Banghart; B. L. Sabatini; G. C. R. Ellis-Davies, Spectral Evolution of a Photochemical Protecting Group for Orthogonal Two-Color Uncaging with Visible Light. *J. Am. Chem. Soc.* **2013,** *135* (42), 15948-15954.
7. T. Slanina; P. Shrestha; E. Palao; D. Kand; J. A. Peterson; A. S. Dutton; N. Rubinstein; R. Weinstain; A. H. Winter; P. Klan, In search of the perfect photocage: structure-reactivity relationships in meso-methyl BODIPY photoremovable protecting groups. *J. Am. Chem. Soc.* **2017,** *139* (42), 15168-15175.
8. J. P. Olson; H.-B. Kwon; K. T. Takasaki; C. Q. Chiu; M. J. Higley; B. L. Sabatini; G. C. R. Ellis-Davies, Optically Selective Two-Photon Uncaging of Glutamate at 900 nm. *J. Am. Chem. Soc.* **2013,** *135* (16), 5954-5957.
9. K. Sitkowska; B. L. Feringa; W. Szymański, Green-Light-Sensitive BODIPY Photoprotecting Groups for Amines. *J. Org. Chem.* **2018,** *83* (4), 1819-1827.
10. G. Fan; L. Yang; Z. Chen, Water-soluble BODIPY and aza-BODIPY dyes: synthetic progress and applications. *Front. Chem. Sci. Eng.* **2014,** *8* (4), 405-417.
11. A. Loudet; K. Burgess, BODIPY Dyes and Their Derivatives: Syntheses and Spectroscopic Properties. *Chem. Rev.* **2007,** *107* (11), 4891-4932.
12. A. Kamkaew; K. Burgess, Aza-BODIPY dyes with enhanced hydrophilicity. *Chem. Commun.* **2015,** *51* (53), 10664-10667.
13. R. S. Givens; M. Rubina; J. Wirz, Applications of p-hydroxyphenacyl (pHP) and coumarin-4-ylmethyl photoremovable protecting groups. *Photochem. Photobiol. Sci.* **2012,** *11* (3), 472-488.
14. A. Saha; S. Panda; S. Paul; D. Manna, Phosphate bioisostere containing amphiphiles: a novel class of squaramide-based lipids. *Chem. Commun.* **2016,** *52* (60), 9438-9441.

Summary and Outlook

Three different methods for the generation of neutral biomolecular beams were investigated: (i) thermal evaporation; (ii) laser desorption (iii) and the neutralization of electrosprayed ions by photocleavage. The generation of neutral biomolecules in the gas phase could be accomplished with all three methods. (i)Tryptophan-containing tripeptides, which were modified with fluorinated alkyl chains on the C- and N-terminus, were evaporated as neutral molecules from an oven. The tripeptides left the oven through a pinhole and formed a neutral molecular beam. The neutrals were susequently ionized by either electron impact or VUV-ionization. (ii) $(Trp\text{-}Lys)_n$ polypeptides decorated with fluorinated alkyl chains at every lysine side chain and the N-terminus with a molecular weight of up to 20 201 Da were volatilized by femtosecond laser desorption into a cold buffer gas. The desorbed neutral peptides were ionized by a 157 nm fluorine laser for detection. (iii) Electrosprayed peptide ions were neutralized in the gas phase by photocleavage of a tailored *ortho*-nitroarylether tag after irradiation with 266 nm light. Employing 3,5-bis(trifluoromethyl)phenol as a leaving group, allowed charge neutralization only for tri- and hexapeptides, where heterolytic bond cleavage of the arylether bond occurs. Longer peptides cleaved under H-transfer and therefore no charge reduction of the peptide fragment was observed. By introducing a permanent charge (as a tetraalkylammonium or sulfonate group, respectively) on the leaving group, neutralization of longer peptides could be realized by photocleavage. The neutralization of human insulin modified with three negatively charged photocleavable tags was accomplished by charge reduction with an ionized buffer gas followed by charge depletion by photocleavage.

The first interference patterns of peptides were observed for thermally evaporated functionalized peptides in the KDTLI as well as the LUMI. The implementation of the other two sources for neutral biomolecular beams in matter-wave experiments, namely laser desorption and charge neutralization, has not been accomplished yet and remains a future goal. To realize their implementation, the molecular beam density needs to be improved for both methods. For the femtosecond laser desorption/photoionization process the desorption conditions as well as the photoionization process would likely need to be rendered more efficient. For the charge reduction of electrosprayed ions, a higher flux of neutral biomolecules could be accomplished by a more powerful cleavage laser source. With such a laser in hand, the ion beam could be irradiated orthogonally instead of in a collinear fashion, which would additionally provide higher spatial and temporal control of the process. Such laser sources are commercially available. So far the formation of neutral particles by photocleavage has only been proven indirectly through the detection of the charged leaving group fragment after cleavage. To make this method applicable for matter-wave interference experiments, detection of the

neutral peptides/proteins after diffraction is required. This could be realized by the implementation of a wavelength orthogonal photocleavable tag. By combining two subsequent photocleavage events, the ions could first be neutralized by cleavage at longer wavelength before being reionized at shorter wavelength. Once the diffration experiments can be established for only moderately modified, real-world biomolecules, the methodology will be probed to address questions related to their gas-phase structures.

Experimental part and supplementary information files

If not stated otherwise the following general information applies. Chemicals were purchased from *Sigma Aldrich*, *Fluorochem*, *Apollo Scientific* and used as received unless otherwise noted. UPLC experiments were performed with *an Acquity UPLC-H Class Bio* from *Waters* equipped with a PDA and an SQ detector 2 with the following column: *ACQUITY UPLC*, *HSS T3* 1.8 µm, 2.1 x 100 mm. Solvents were water and acetonitrile, respectively, each containing 0.1% formic acid, later on, referred to as (A) and (B). The flow rate was set to 0.61 mL/min and the column temperature to 40 °C. Method 1: 0 min – 90% A; 1 min – 90% A; 6 min – 100% B; 7.5 min – 100% B. Method 2: 0 min – 90% A; 1 min – 90% A; 4 min – 100% B; 7.5 min – 100% B. Method 3: 0 min – 65% A; 1 min – 65%; 7 min – 40% A. Mass detection was performed in scan mode for positive ions (cone voltage 40 V, desolvation temperature: 600°C). A *Waters Prep LC 4000 System* equipped with a *Waters 2487: Dual λ Absorbance Detector* was used for preparative separations with the following column: *Agilent: XDB-C18*, 21.2 x 150 mm, 5 µm. Ultrapure water was prepared by means of an Ultra Ionic system from *Milli-Q*. HRMS experiments were conducted on a *Bruker maXis 4G*. NMR experiments were performed at 20°C on *Bruker Avance III* NMR spectrometers operating at 600 or 500 MHz proton frequency.Both NMR spectrometers were equipped with inverse dual-channel broadband probe heads with *z*-gradients. ^{13}C shifts were determined by 2D NMR experiments (HMBC and HMQC). ^{1}H and ^{13}C signals were assigned by 2D NMR (COSY, HMBC, HMQC).

Chapter 1. Tailoring the volatility and stability of oligopeptides

J. Schätti; U. Sezer; S. Pedalino; J.P. Cotter; M. Arndt; M. Mayor; V. Köhler;
J. Mass Spectrom., **2017**, *52*, 550-556.

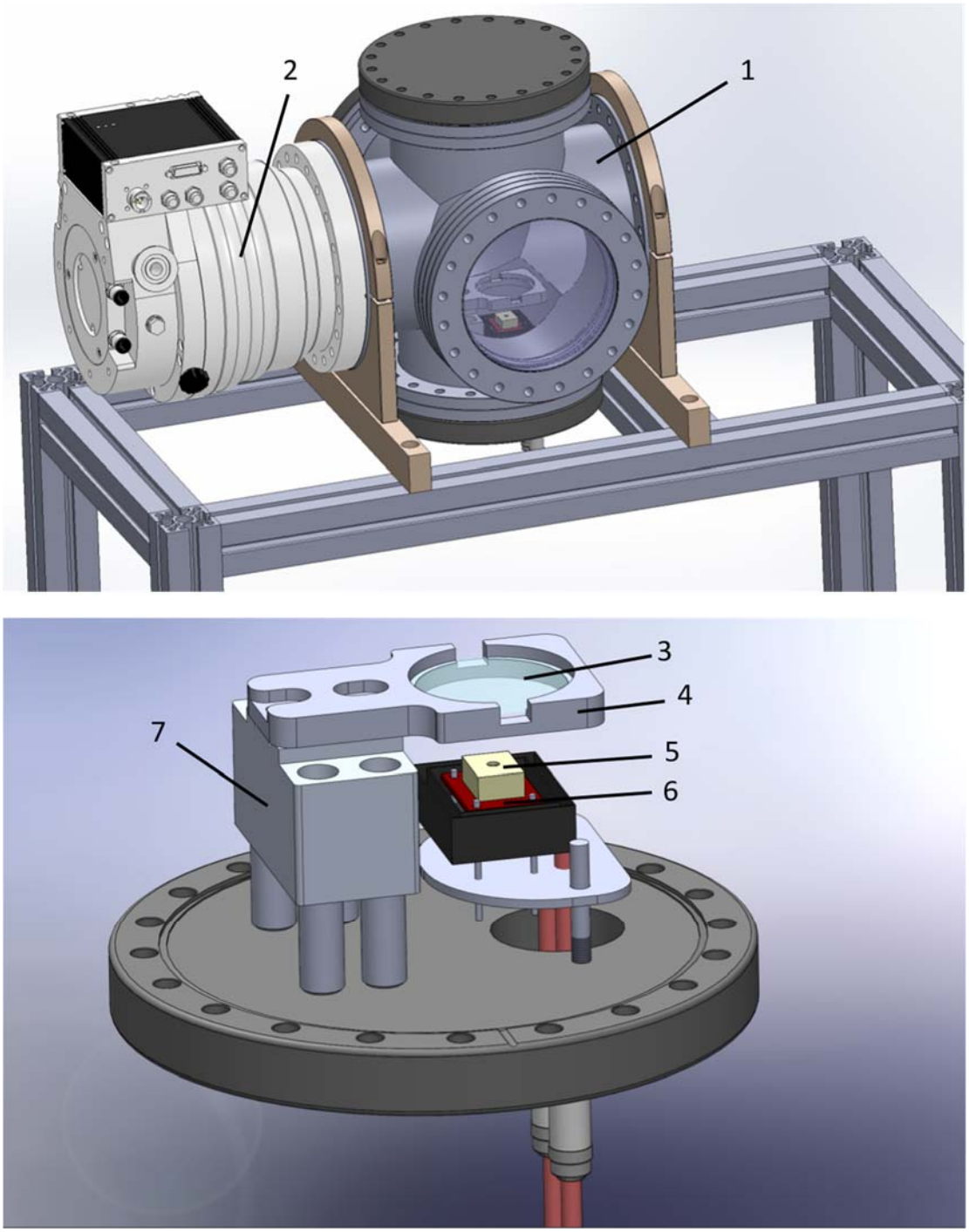

Figure S1. Evaporation chamber built by Philipp Knöpfel for evaporation studies of peptides in Basel: (top) Whole chamber; (bottom) inside view. 1) Vacuum chamber (*VAb*, DKCF160, 33.4 × 33.4 cm); 2) turbo pump (*Pfeifer*, *Turbo HiPace* 700, DN 160 CF-F); 3) glass plate for sample collection; 4) glass plate holder, 5) evaporation crucible (pyrolytic boron nitride); 6) heating unit (*tectra*, *Boralectric heater HTR* 1001); 7) Cooling block (aluminium), not shown: pre vacuum pump (*edwards*, scroll pump nXDS10i).

Supplementary Information for:

Tailoring the volatility and stability of oligopeptides

Jonas Schätti[1], Ugur Sezer[2], Sebastian Pedalino[2], J. P. Cotter[2], Markus Arndt[2*], Marcel Mayor[1,3] and Valentin Köhler[1*]

[1]University of Basel, Department of Chemistry, Basel, 4056, Switzerland

[2]University of Vienna, Faculty of Physics, Vienna, 1090, Austria

[3]Karlsruhe Institute of Technology, Institute for Nanotechnology, Karlsruhe, 76021, Germany

*markus.arndt@univie.ac.at, valentin.koehler@unibas.ch

Table of Contents

Chemicals and instrumentation

Chemicals were purchased from Sigma Aldrich, Fluorochem, Novabiochem, Bachem or P&M-Invest and used as received unless otherwise noted. UPLC experiments were performed with an Acquity UPLC H Class Bio from Waters equipped with a PDA and a SQ detector 2 with the following column: ACQUITY UPLC, HSS T3 1.8 µm, 2.1 x 100 mm. Solvents were water and acetonitrile, respectively, each containing 0.1 % formic acid, later on referred to as (A) and (B). The flow rate was set to 0.61 ml/min and the temperature to 40 °C. Method 1: 0 min – 100% A; 1 min – 100% A; 3 min – 80% A; 13.5 min – 20% A. Method 2: 0 min – 50% A; 1 min – 50% A; 7 min – 20% A; 10 min – 10% A. Mass detection was performed in scan mode for positive ions (Cone Voltage 40 V, Desolvation temperature: 600°C). A Water Prep LC 4000 System equipped with a Waters 2487: Dual λ Absorbance Detector as UV-Vis detector was used for preparative separations with the following column: Agilent: XDB-C18, 21.2 x 150 mm, 5 µm. Ultra pure water was prepared by means of an Ultra Ionic system from Milli-Q. ESI-HRMS experiments were conducted with Bruker maXis 4G. MALDI was recorded on a Bruker Daltonics Ultraflex II at the Molecular & Biomolecular Analysis Laboratory ETH Zürich. NMR experiments were performed at 20°C or 25°C on Bruker Avance III NMR spectrometers operating at 600, 500 or 400 MHz proton frequency. NMR spectrometers were equipped with direct (400 MHz) or inverse (600 MHz ,500 MHz) dual channel, broadband probe heads with *z* -gradients. ^{13}C and overlapping ^{1}H shifts were determined by 2D NMR experiments (COSY, HMBC and HMQC). ^{13}C shifts for CF_2 and CF_3 groups were not determined. TFA = trifluoroacetic acid; DIPEA = *N*,*N*-diisopropylethylamine; DMF = *N*,*N*-dimethylformamide; PyBOP = (Benzotriazol-1-yloxy)tripyrrolidinophosphonium hexafluorophosphate; NHS = *N*-hydroxysuccinimide; HSTU = *N*,*N*,*N'*,*N'*-tetramethyl-*O*-(*N*-succinimidyl)uronium hexafluorophosphate, HFIP = 1,1,1,3,3,3-hexafluoro-2-propanol.

General procedure 1: Ala-Trp-Ala **1**[1]

2-Chlorotrityl chloride resin (1 mmol/g, 700 mg) was placed in a plastic syringe equipped with a filter frit. The resin was washed with CH_2Cl_2 (~4 ml). Subsequently the syringe was filled with CH_2Cl_2 (~4 ml) and placed on a shaker for 15 min. The CH_2Cl_2 was exchanged and DIPEA (6.0 eq, 0.70 ml, 4.2 mmol), and Fmoc-ala-OH (2.00 eq., 436 mg, 1.40 mmol) were added. Note: equivalents refer to chlorotrityl groups on the resin (1 mmol/g). After the sample was agitated on a shaker for 1.5 h the reaction mixture was removed and the resin was washed with CH_2Cl_2 (~4 ml) and DMF (~4 ml). The unreacted binding sites on the resin were capped by adding MeOH-solution (~5 ml, 15% MeOH, 5% DIPEA, 80% CH_2Cl_2) followed by 15 min agitation. Subsequently the sample was washed with CH_2Cl_2 (~4 ml) and DMF (~4 ml). Next Fmoc deprotection solution (20 % piperidine in DMF) was added and shaking continued for 5 mins. This step was repeated three times. Note: In the following this procedure will be referred to as *Fmoc deprotection*. The sample was washed with DMF (~4 ml) and CH_2Cl_2 (~4 ml) and again with DMF (~4 ml). Between the different washing steps the sample was agitated on the shaker for ~30 sec. Note: In the following this procedure will be referred to as *washing.* After the *washing* DMF (~4 ml), DIPEA (6.0 eq, 0.70 ml, 4.2 mmol), Fmoc-Trp(Boc)-OH (2.00 eq. 737 mg, 1.40 mmol) and PyBOP (2.00 eq., 729 mg, 1.40 mmol) were

added. The mixture was agitated on a shaker for 2 h. Note: In the following this procedure will be referred to as *peptide coupling*. This was followed by *washing*, *Fmoc deprotection* and another *washing*. For the next peptide coupling DIPEA (6.0 eq., 0.70 ml, 4.2 mmol), Fmoc-Ala-OH (2.00 eq., 436 mg, 1.40 mmol) and PyBOP (2.00 eq., 729 mg, 1.40 mmol) were used. After *washing*, *Fmoc- deprotection* and another *washing* the resin was rinsed with CH_2Cl_2 (3 × ~4 ml) before the cleavage solution (5 ml, 96 % TFA, 3 % triisopropylsilane, 3 % H_2O) was added. For the cleavage procedure the mixture was agitated on the shaker for 1 h. Subsequently the cleavage solution was removed and the resin washed with TFA (1 ml). The TFA solution was concentrated on the rotary evaporator. Ice cold Et_2O (50 ml) was added and the formed precipitate collected by centrifugation (4400 rpm). Washing was repeated three times with Et_2O (20 ml) and the product obtained after drying as a white powder (195 mg, 0.564 mmol, 81 %).

UPLC-MS: Method 1, T_R = 3.61 min; m/z MS (ES+): 116.4 [50%], 258.4 [25%], 347.3 [100%, M + H^+], 369.2 [70 %, M + Na^+], 383.2 [25%, M + K^+].

ESI-HRMS: calculated for $C_{17}H_{23}N_4O_4^+$: 347.1714; found: 347.1719.

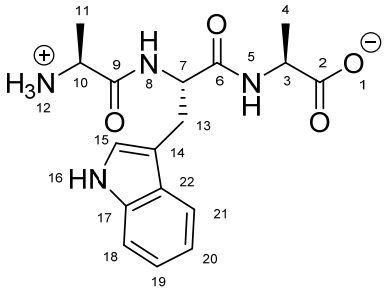

^{1}H-NMR (500 MHz, DMSO-d_6, 298 K): δ = 10.85 (d, $^3J_{H\text{-}H}$ = 2.2 Hz, 1 H, H-16), 8.52 (d, $^3J_{H\text{-}H}$ = 8.1 Hz, 1 H, H-8), 8.26 (d, $^3J_{H\text{-}H}$ = 7.0 Hz, 1 H, H-5), 7.66 (d, $^3J_{H\text{-}H}$ = 7.9 Hz, 1 H, H-21), 7.32 (dt, $^3J_{H\text{-}H}$ = 8.1 Hz, $^4J_{H\text{-}H}$ = 0.9 Hz, $^5J_{H\text{-}H}$ = 0.9 Hz, 1 H, H-18), 7.18 (d, $^3J_{H\text{-}H}$ = 2.2, 1 H, H-15), 7.06 (ddd, $^3J_{H\text{-}H}$ = 8.1 Hz, $^3J_{H\text{-}H}$ = 7.0Hz , $^4J_{H\text{-}H}$ = 1.2 Hz, 1 H, H-19), (ddd, $^3J_{H\text{-}H}$ = 8.0 Hz, $^3J_{H\text{-}H}$ = 7.0 Hz , $^4J_{H\text{-}H}$ = 0.9 Hz, 1 H, H-20), 4.59 (ddd , $^3J_{H\text{-}H}$ = 9.3 Hz, $^3J_{H\text{-}H}$ = 8.1 Hz, $^3J_{H\text{-}H}$ = 4.4 Hz, 1 H, H-7), 4.14 (p, $^3J_{H\text{-}H}$ = 7.1Hz, 1 H, H-3), 3.67 (q, $^3J_{H\text{-}H}$ = 6.9Hz, 1 H, H-10), 3.17 (dd, $^2J_{H\text{-}H}$ = 14.8 Hz, $^3J_{H\text{-}H}$ = 4.4 Hz, 1 H, H-13), 2.96 (dd, $^2J_{H\text{-}H}$ = 14.8 Hz, $^3J_{H\text{-}H}$ = 9.3 Hz, 1 H, H-13), 1.29 (d, $^3J_{H\text{-}H}$ = 7.0 Hz, 1 H, H-11), 1.27 (d, $^3J_{H\text{-}H}$ = 7.2 Hz, 1 H, H-4).

^{13}C δ = 174.1 (C-2), 171.1 (C-6), 170.9 (C-9), 136.6 (C-17), 127.6 (C-22), 123.7 (C-15), 120.6 (C-19), 118.3 (C-21), 118.0 (C-20), 111.1 (C-18), 110.1 (C-14), 53.1 (C-7), 48.1 (C-10), 47.7 (C-3), 27.5 (C-13), 17.3 (C-11), 17.2 (C-4).

General procedure 2: Ac-Ala-Trp-Ala-NH_2

Rink amid resin (0.54 mmol/g, 900 mg) was placed in a plastic syringe equipped with a filter frit. The resin was washed with CH_2Cl_2 (~4 ml). Then CH_2Cl_2 (~4 ml) was added and the syringe placed on a shaker for 15 min. Subsequently DMF (~4 ml), DIPEA (6.0 eq, 0.48 ml, 2.9 mmol), Fmoc-ala-OH (3.01 eq., 455 mg, 1.46 mmol) and PyBOP (3.00 eq., 760 mg, 1.46 mmol) were added. Note: Equivalents refer to the amine groups on the resin (0.54 mmol/g). The syringe was placed on a shaker and the mixture agitated

for 2 h. In the following this procedure will be referred to as *peptide coupling*. *Peptide coupling* was followed by *washing*, *Fmoc* deprotection and another *washing*. The second peptide coupling was performed with DIPEA (6.0 eq, 0.48 ml, 2.9 mmol), Fmoc-Trp(Boc)-OH (3.00 eq., 769 mg, 1.46 mmol) and PyBOP (3.00 eq., 760 mg, 1.46 mmol) followed by *washing*, *Fmoc deprotection* and another *washing*. The last peptide coupling was performed with DIPEA (6.0 eq, 0.48 ml, 2.9 mmol), Fmoc-Ala-OH (3.01 eq., 455 mg, 1.46 mmol) and PyBOP (3.00 eq., 760 mg, 1.46 mmol). After *washing*, *Fmoc deprotection* and another *washing*, capping solution (4 ml, 10 % acetic anhydride in DMF) and DIPEA (0.5 ml) were added and the mixture agitated for 5 min. The capping step was repeated once. After another *washing* the resin was rinsed with CH_2Cl_2 (3 × ~4 ml) before the cleavage solution (5 ml, 96 % TFA, 3 % triisopropylsilane, 3 % H_2O) was added. For the cleavage procedure the mixture was agitated on the shaker for 1 h. Subsequently the cleavage solution was collected and the resin washed with TFA (1 ml). The TFA solution was concentrated on the rotary evaporator. Ice cold Et_2O (50 ml) was added to the peptide solution and the precipitate was collected by centrifugation (4400 rpm). After washing with Et_2O (4 × 20 ml) and drying Ac-Ala-Trp-Ala-NH_2 was obtained as a white powder. (143 mg, 0.369 mmol, 76 %).

UPLC-MS: Method 1, T_R = 5.54 min; m/z MS (ES+): 371.3 [100%], 388.3 [40%, M + H^+], 410.4 [50 %, M + Na^+], 383.2 [25%, M + K^+].

ESI-HRMS: calculated for $C_{19}H_{26}N_5O_4^+$: 388.1979; found: 388.1979.

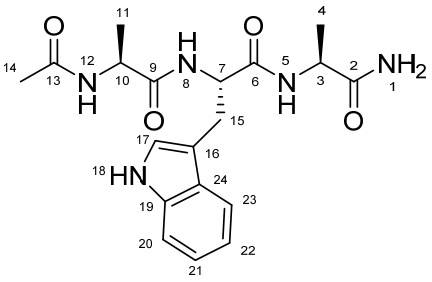

^{1}H-NMR (500 MHz, DMSO-d_6, 298 K): δ = 10.82 (d, $^3J_{H\text{-}H}$ = 2.3 Hz, 1 H, H-18), 8.04 (d, $^3J_{H\text{-}H}$ = 7.1 Hz, 1 H, H-12), 7.90 (d, $^3J_{H\text{-}H}$ = 7.7 Hz, 1 H, H-8), 7.80 (d, $^3J_{H\text{-}H}$ = 7.5 Hz, 1 H, H-5), 7.55 (dd, $^3J_{H\text{-}H}$ = 7.8 Hz, $^4J_{H\text{-}H}$ = 0.9 Hz, 1 H, H-23), 7.30 (dt, $^3J_{H\text{-}H}$ = 8.0, $^4J_{H\text{-}H}$ = 0.9 Hz, $^5J_{H\text{-}H}$ = 0.9 Hz, 1 H, H-20), 7.16 (s, 1 H, H-1), 7.14 (d, $^3J_{H\text{-}H}$ 2.4 Hz, 1 H, H-17), 7.05 (ddd, $^3J_{H\text{-}H}$ = 8.2 Hz, $^3J_{H\text{-}H}$ = 7.0 Hz, $^4J_{H\text{-}H}$ = 1.2 Hz, 1 H, H-21), 7.01 (s, 1 H, H-1), 6.96 (ddd, $^3J_{H\text{-}H}$ = 7.9 Hz, $^3J_{H\text{-}H}$ = 6.9 Hz, $^4J_{H\text{-}H}$ = 1.0 Hz, 1 H, H-22), 4.46 (td, $^3J_{H\text{-}H}$ = 8.4 Hz, $^3J_{H\text{-}H}$ = 4.6 Hz, 1 H, H-7), 4.19 (p, $^3J_{H\text{-}H}$ = 6.9 Hz, 1 H, H-10), 4.18 (p, $^3J_{H\text{-}H}$ = 7.2 Hz, 1 H, H-3), 3.15(dd, $^2J_{H\text{-}H}$ = 14.8 Hz, $^3J_{H\text{-}H}$ = 4.6 Hz, 1 H, H-15), 2.95 (dd, $^2J_{H\text{-}H}$ = 14.8 Hz, $^3J_{H\text{-}H}$ = 8.8 Hz, 1 H, H-15), 1.79 (s,3 H, H-14), 1.16 (d, $^3J_{H\text{-}H}$ = 7.1 Hz, 3 H, H-4), 1.13 (d, $^3J_{H\text{-}H}$ = 7.1 Hz, 3 H, H-11).

^{13}C δ = 173.8 (C-2), 172.3 (C-9), 170.6 (C-6), 196.2(C-13), 135.8 (C-19), 127.1 (C-24), 123.4 (C-17), 120.6 (C-22), 118.1 (C-23), 118.0 (C-21), 111.0 (C-20), 109.6 (C-16), 53.2 (C-7), 48.2 (C-10), 47.8 (C-3), 26.8 (C-15), 22.3 (C-14), 18.0 (C-4), 17.4 (C-11).

General procedure 3: Ac-N^{α}-Me-Ala-N^{α}-Me-Trp(Me)-N^{α}-Me-Ala-N(Me)$_2$ **2**[2]

NaH (25.0 eq., 465 mg, 19.4 mmol) was added to DMSO (14 mL). The suspension was heated to 90 °C for 60 min (until H_2 formation ceased) and allowed to cool to room temperature. The formed dimsyl-solution was added to a solution of Ac-Ala-Trp-Ala-NH_2 (1.00 eq., 300 mg, 0.774 mmol) in DMSO (5 ml). After 2 min methyl iodide (75.0 eq., 3.61 ml, 58.1 mmol) was added slowly under strong stirring. After 2 h H_2O (50 ml) was added to the reaction mixture and stirring continued for another 10 minutes. The product was extracted with chloroform (30 ml, 2 × 15 ml). The combined organic layers were washed with brine (2 × 25 ml) and H_2O (2 × 25 ml). The solvent was removed by means of a rotary evaporator and the crude product obtained as a brown oil. The product was purified by means of preparative HPLC using an isocratic flow of water (0.1 % TFA) /acetonitrile (0.1 % TFA) in a ratio of 75:25 with a flow rate of 19 ml (T_R = 11 min.). After lyophilisation Ac-N^{α}-Me-Ala-N^{α}-Me-Trp(Me)-N^{α}-Me-Ala-N(Me)$_2$ was isolated as a pale yellow solid (120 mg, 0.255 mmol, 33 %).

UPLC-MS: Method 1, T_R = 6.85 min; m/z MS (ES+): 342.3 [100%, M - (C-terminal Ala)$^-$], 427.4 [30%, M - NMe_2^-], 494.4 [50%, M + Na^+].

ESI-HRMS: calculated for $C_{25}H_{37}N_5NaO_4^+$: 494.2743; found: 494.2744.

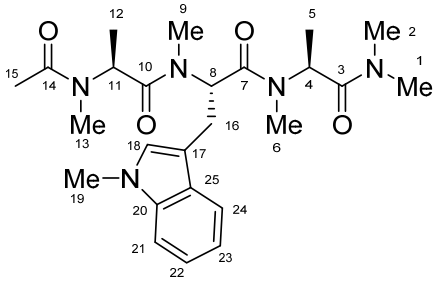

^{1}H-NMR (500 MHz, $CDCl_3$, 298 K): δ = 7.76 (dt, $^3J_{H\text{-}H}$ = 7.9 Hz, $^4J_{H\text{-}H}$ = 1.0, $^5J_{H\text{-}H}$ = 1.0 Hz, 1 H, H-24), 7.25 (dt, $^3J_{H\text{-}H}$ = 8.0 Hz, $^4J_{H\text{-}H}$ = 0.9 Hz, $^5J_{H\text{-}H}$ = 0.9 Hz, 1 H, H-21), 7.20 (ddd , $^3J_{H\text{-}H}$ = 8.1 Hz, $^3J_{H\text{-}H}$ = 6.9 Hz, $^4J_{H\text{-}H}$ = 1.2 Hz, 1 H, H-22), 7.11 (ddd , $^3J_{H\text{-}H}$ = 8.0 Hz, $^3J_{H\text{-}H}$ = 6.9 Hz, $^4J_{H\text{-}H}$ = 1.1 Hz, 1 H, H-23), 6.93 (s, 1 H, H-18), 5.88 (t, $^3J_{H\text{-}H}$ = 7.7, 1 H, H-8), 5.48 (q, $^3J_{H\text{-}H}$ = 6.9 Hz, 1 H, H-11), 5.40 (q, $^3J_{H\text{-}H}$ = 6.9 Hz, 1 H, H-4), 3.70 (s, 3 H, H-19), 3.30 (dd, $^2J_{H\text{-}H}$ = 14.5 Hz, $^3J_{H\text{-}H}$ = 7.7 Hz, 1 H, H-16), 3.09 (dd, $^2J_{H\text{-}H}$ = 14.5 Hz, $^3J_{H\text{-}H}$ = 8.1 Hz, 1 H, H-16), 2.98 (s, 3 H, H-9), 2.84 (s, 3 H, H-1 or H-2), 2.82(s, 3 H, H-6), 2.60 (s, 3 H, H-1 or H-2), 2.36 (s, 3 H, H-13), 1.90 (s, 3 H, H-15), 1.24 (d, $^3J_{H\text{-}H}$ = 6.8 Hz, 3 H, H-5), 1.20 (d, $^3J_{H\text{-}H}$ = 6.8 Hz, 3 H, H-12).

^{13}C δ = 171.2 (C-10), 170.6 (C-3 and C-14), 196.5 (C-7), 136.7 (C-20), 128.0 (C-18 and C-25), 121.7 (C-22), 119.1 (C-23), 118.8 (C-24), 109.3 (C-17), 109.0 (C-21), 53.7 (C-8), 49.3 (C-4), 48.8 (C-11), 36.2 (C-1 or C-2), 35.8 (C-1 or C-2), 32.5 (C-19), 30.2 (C-9), 30.0 (C-13), 29.9 (C-6), 24.8 (C-16), 21.5 (C-15), 14.4 (C-5 and C-12).

(2*H*,2*H*,3*H*,3*H*-perfluorooctanoyl)-Ala-Trp-Ala-NH_2 **3**

The synthesis was performed in analogy to general procedure 2. Rink amid resin (900 mg) was placed in a plastic syringe equipped with a filter frit. The resin was washed with CH_2Cl_2 (~4 ml). Subsequently CH_2Cl_2 (~4 ml) was added and the mixture agitated on a shaker for 15 min. *Peptide coupling* was performed with Fmoc-Ala-OH (3.01 eq., 455 mg, 1.46 mmol) and the respective reagents as described for the Rink amid resin procedure above. Note: The equivalents refer to the amine groups on the resin (0.54 mmol/g). *Peptide coupling* was followed by *washing*, *Fmoc-deprotection* and another *washing*. The second *peptide coupling* was performed with Fmoc-Trp(Boc)-OH (3.00 eq., 769 mg, 1.46 mmol) and the respective reagents, followed by *washing*, *Fmoc-deprotection* and another *washing*. The final peptide coupling was performed Fmoc-Ala-OH (3.01 eq., 455 mg, 1.46 mmol) and the respective reagents and washing and deprotection steps. 2*H*,2*H*,3*H*,3*H*-perfluorooctanoic acid (3.00 eq., 499 mg, 1.46 mmol) was coupled with the peptide coupling procedure employing a reaction time of 4 hours. After *washing* the resin was rinsed with CH_2Cl_2 (3 × ~4 ml), cleavage performed and the acylated peptide obtained after precipitation and washing with Et_2O as described above. (235 mg, 0.338 mmol, 70 %).

UPLC-MS: Method 2, T_R = 1.89 min; m/z MS (ES+): 582.0 [10%], 653.1 [100%, M - NH_2^-], 670.0 [30%, M + H^+], 692.2 [80 %, M + Na^+].

ESI-HRMS: calculated for $C_{25}H_{27}F_{11}N_5O_4^+$: 670.1882; found: 670.1882.

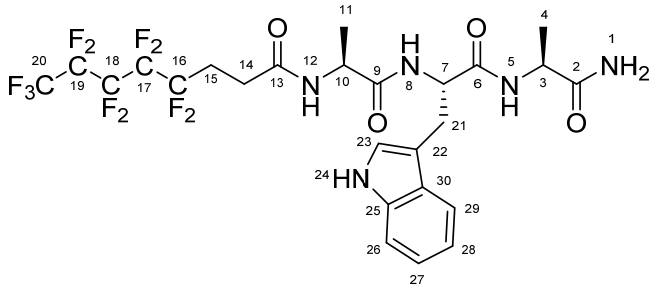

^{1}H-NMR (500 MHz, DMSO-d_6, 298 K): δ = 10.81 (d, $^3J_{H\text{-}H}$ = 2.4 Hz, 1 H, H-24), 8.26 (d, $^3J_{H\text{-}H}$ = 7.0 Hz, 1 H, H-12), 7.96 (d, $^3J_{H\text{-}H}$ = 7.7 Hz, 1 H, H-8), 7.79 (d, $^3J_{H\text{-}H}$ = 7.5 Hz, 1 H, H-5), 7.59 (dd, $^3J_{H\text{-}H}$ = 7.9 Hz, $^4J_{H\text{-}H}$ = 1.1 Hz, 1 H, H-29), 7.30 (dt, $^3J_{H\text{-}H}$ = 8.1, $^4J_{H\text{-}H}$ = 0.9 Hz, $^5J_{H\text{-}H}$ = 0.9 Hz, 1 H, H-26), 7.15 (s, 1 H, H-1), 7.13 (d, $^3J_{H\text{-}H}$ = 2.4 Hz, 1 H, H-23), 7.04 (ddd, $^3J_{H\text{-}H}$ = 8.2 Hz, $^3J_{H\text{-}H}$ = 7.0 Hz, $^4J_{H\text{-}H}$ = 1.2 Hz, 1 H, H-27), 7.02 (s, 1 H, H-1), 6.96 (ddd, $^3J_{H\text{-}H}$ = 8.0 Hz, $^3J_{H\text{-}H}$ = 7.0 Hz, $^4J_{H\text{-}H}$ = 1.0 Hz, 1 H, H-28), 4.47 (td, $^3J_{H\text{-}H}$ = 8.2, $^3J_{H\text{-}H}$ = 4.8 Hz, 1 H, H-7), 4.23 (p, $^3J_{H\text{-}H}$ = 6.9 Hz, 1 H, H-10), 4.18 (p, $^3J_{H\text{-}H}$ = 7.2 Hz, 1 H, H-3), 3.16 (dd, $^2J_{H\text{-}H}$ = 14.9, $^3J_{H\text{-}H}$ = 4.5 Hz, 1 H, H-21), 2.95 (dd, $^2J_{H\text{-}H}$ = 14.9 Hz, $^3J_{H\text{-}H}$ = 8.6 Hz, 1 H, H-21), 2.50-2.33 (m, 4 H, H-14 and H-15), 1.17 (d, $^3J_{H\text{-}H}$ = 7.2 Hz, 3 H, H-4), 1.16 (d, $^3J_{H\text{-}H}$ = 7.0 Hz, 3 H, H-11).

^{13}C δ = 174.4 (C-2), 172.0(C-9), 170.5 (C-6), 169.0 (C-13), 135.7 (C-25), 126.9(C-30), 123.5 (C-23), 120.7 (C-27), 118.3 (C-29), 118.1 (C-28), 111.2 (C-26), 109.5 (C-22), 53.3 (C-7), 48.4 (C-10), 47.9 (C-3), 26.9 (C-21), 25.6 (C-14), 25.6 (C-15), 17.9 (C-4), 17.6 (C-11).

(2*H*,2*H*,3*H*,3*H*-perfluorooctanoyl)-Ala-Trp-Ala

The synthesis was performed in analogy to general procedure 1 with the following quantities for the loading of the resin: 2-chlorotrityl chloride resin (700 mg), DIPEA (6.0 eq, 0.70 ml, 4.2 mmol), and Fmoc-ala-OH (2.00 eq., 436 mg, 1.40 mmol) were added. Note: The equivalents refer to the chlorotrityl groups on the resin. After the sample was agitated on a shaker for 1.5 h liquids were removed by filtration and the resin washed with CH_2Cl_2 (~4 ml) and DMF (~4 ml). The unreacted binding sites on the resin were capped by adding MeOH-solution (~5 ml, 15% MeOH, 5% DIPEA, 80% CH_2Cl_2) under agitation for 15 minutes. After *washing*, *Fmoc-deprotection* and another *washing, peptide coupling* was started with DIPEA (6.0 eq, 0.70 ml, 4.2 mmol), Fmoc-Trp(Boc)-OH (2.00 eq., 737 mg, 1.40 mmol) and PyBOP (2.00 eq., 729 mg, 1.40 mmol). This was followed by *washing*, *Fmoc-deprotection* and another *washing*. For the next *peptide coupling* the following quantities of DIPEA (6.0 eq, 0.70 ml, 4.2 mmol), Fmoc-ala-OH (2.00 eq., 436 mg, 1.40 mmol) and PyBOP (2.00 eq., 729 mg, 1.40 mmol) were used, followed by *washing*, *Fmoc-deprotection* and another *washing*. The last *peptide coupling* was performed with DIPEA (6.0 eq, 0.70 ml, 4.2 mmol) , 2*H*,2*H*,3*H*,3*H*-perfluorooctanoic acid (2.00 eq., 479 mg, 1.40 mmol), PyBOP (2.00 eq., 729 mg, 1.40 mmol) and a reaction time of 4 h. After *washing* the resin was washed with CH_2Cl_2 (3 × ~4 ml) before the cleavage solution (5ml, 96 % TFA, 3 % triisopropylsilane, 3 % H_2O) was added. Cleavage, precipitation and washing with Et_2O were performed as described in general procedure 1. The product was obtained as a white powder (310 mg, 0.462 mmol, 66%).

UPLC-MS: Method 1, T_R = 9.90 min; m/z MS (ES+): 582.2 [20%], 671.2 [100%, M + H^+], 693.2 [50%, M + Na^+], 709.0 [10 %, M + K^+].

ESI-HRMS: calculated for $C_{25}H_{26}F_{11}N_4O_5^+$: 671.1722; found: 671.1716.

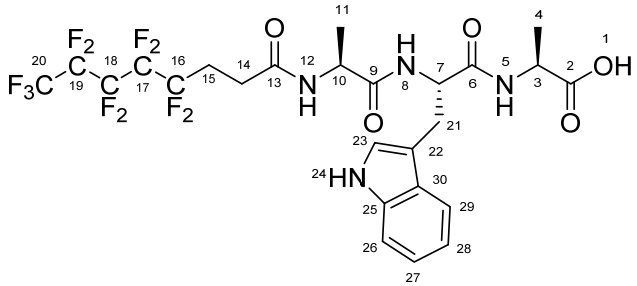

^{1}H-NMR (500 MHz, DMSO-d_6, 298 K): δ = 12.52 (s, 1 H, H-1), 10.80 (d, $^3J_{H\text{-}H}$ = 2.3 Hz, 1 H, H-24), 8.21 (d, $^3J_{H\text{-}H}$ = 7.2 Hz, 1 H, H-12), 8.11 (d, $^3J_{H\text{-}H}$ = 7.1 Hz, 1 H, H-5), 7.90 (d, $^3J_{H\text{-}H}$ = 8.2 Hz, 1 H, H-8), 7.59 (dd, $^3J_{H\text{-}H}$ = 8.0 Hz, $^4J_{H\text{-}H}$ = 1.2 Hz, 1 H, H-29), 7.30 (dt, $^3J_{H\text{-}H}$ = 8.0 Hz, $^4J_{H\text{-}H}$ = 0.9 Hz, $^5J_{H\text{-}H}$ = 0.9 Hz, 1 H, H-26), 7.13 (d, $^3J_{H\text{-}H}$ = 2.3 Hz, 1 H, H-23), 7.04 (ddd, $^3J_{H\text{-}H}$ = 8.1 Hz, $J^3_{H\text{-}H}$ = 7.0 Hz, $^4J_{H\text{-}H}$ = 1.2 Hz, 1 H, H-27), 6.96 (ddd, $^3J_{H\text{-}H}$ = 8.0 Hz, $^3J_{H\text{-}H}$ = 7.0 Hz, $^4J_{H\text{-}H}$ = 1.0 Hz, 1 H, H-28), 4.53 (td, $^3J_{H\text{-}H}$ = 8.7 Hz, $^3J_{H\text{-}H}$ = 4.4 Hz, 1 H, H-7), 4.43 (p, $^3J_{H\text{-}H}$ = 7.1 Hz, 1 H, H-10), 4.41 (p, $^3J_{H\text{-}H}$ = 7.3 Hz, 1 H, H-3), 3.17 (dd, $^2J_{H\text{-}H}$ = 14.9 Hz, $^3J_{H\text{-}H}$ = 4.4 Hz, 1 H, H-21), 2.95 (dd, $^2J_{H\text{-}H}$ = 14.9 Hz, $^3J_{H\text{-}H}$ = 8.7 Hz, 1 H, H-21), 2.50-2.33 (m, 4 H, H-14 and H-15), 1.26 (d, $^3J_{H\text{-}H}$ = 7.3 Hz, 3 H, H-4), 1.13 (d, $^3J_{H\text{-}H}$ = 7.1 Hz, 3 H, H-11).

^{13}C δ = 173.7 (C-2), 171.6 (C-9), 170.6 (C-6), 169.0 (C-13), 135.7 (C-25), 127.1 (C-30), 123.5 (C-23), 120.6 (C-27), 118.3 (C-29), 118.0 (C-28), 111.1 (C-26), 109.7 (C-22), 52.8 (C-7), 48.2 (C-10), 47.3 (C-3), 27.1 (C-21), 25.5 (C-14), 25.5 (C-15), 17.7 (C-11), 16.9 (C-4).

(2*H*,2*H*,3*H*,3*H*-perfluoroundecanoyl)-Ala-Trp-Ala

Identical procedure as for (2*H*,2*H*,3*H*,3*H*-perfluorooctanoyl)-Ala-Trp-Ala but employing 2*H*,2*H*,3*H*,3*H*-perfluoroundecanoic acid (2.00 eq., 688 mg, 1.40 mmol) instead of 2*H*,2*H*,3*H*,3*H*-perfluorooctanoic acid. White powder. (395 mg, 0.482 mmol, 68.8%). The product contained possibly another compound or conformer (see Figure S4, Top).

UPLC-MS: Method 2, T_R = 4.30 min; m/z MS (ES+): 159.3 [20%], 276.2 [20%] 732.0 [20%], 821.1 [100%, M + H^+], 843.1 [80%, M + Na^+].

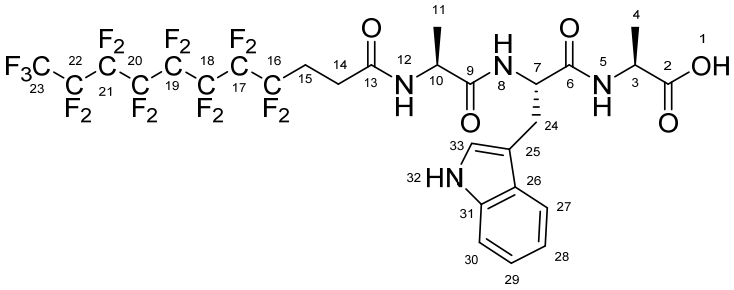

^{1}H-NMR (500 MHz, DMSO-d_6, 298 K): δ = 12.56 (s, 1 H, H-1), 10.80 (d, $^3J_{H\text{-}H}$= 2.4 Hz, 1 H, *H-32),* 8.20 (d, $^3J_{H\text{-}H}$ = 7.2 Hz, 1 H, H-12), 8.12 (d, $^3J_{H\text{-}H}$ = 7.2, Hz, 1 H, H-5), 7.88 (d, $^3J_{H\text{-}H}$ = 8.2 Hz, 1 H, H-8), 7.58 (dd, $^3J_{H\text{-}H}$ = 7.9 Hz, $^4J_{H\text{-}H}$= 1.0 Hz, 1 H, H-27), 7.30(dt, $^3J_{H\text{-}H}$ = 8.1 Hz, $^4J_{H\text{-}H}$= 1.0 Hz, $^5J_{H\text{-}H}$ = 1.0 Hz, 1 H, H-30), 7.13 (d, $^3J_{H\text{-}H}$ = 2.4 Hz, 1 H, H-33), 7.04 (ddd, $^3J_{H\text{-}H}$ = 8.1 Hz, 6.9 Hz, $^4J_{H\text{-}H}$= 1.0 Hz, 1 H, H-29), 6.95 (ddd, $^3J_{H\text{-}H}$ = 8.0 Hz, 6.9 Hz, $^4J_{H\text{-}H}$= 1.0 Hz, 1 H, H-28), 4.53 (td, $^3J_{H\text{-}H}$ = 8.7 Hz, 4.5 Hz, 1 H, H-7), 4.23 (p, $^3J_{H\text{-}H}$ = 7.2 Hz, 1 H, H-10), 4.21 (p, $^3J_{H\text{-}H}$ = 7.1 Hz, 1 H, H-3), 3.16 (dd, $^2J_{H\text{-}H}$ = 14.8 Hz, $^3J_{H\text{-}H}$ = 4.5 Hz, 1 H, H-24), 2.95 (dd, $^2J_{H\text{-}H}$ = 14.8 Hz, $^3J_{H\text{-}H}$ = 8.7 Hz, 1 H, H-24), 2.50-2.35 (m, 4 H, H-14 and H-15), 1.26 (d, $^3J_{H\text{-}H}$ = 7.2 Hz, 3 H, H-4), 1.13 (d, $^3J_{H\text{-}H}$ = 7.1 Hz, 3 H, H-11).

^{13}C δ = 173.6(C-2), 171.5 (C-9), 170.7 (C-6), 168.9 (C-13), 135.7 (C-31), 127.1(C-26), 123.4 (C-33), 120.6 (C-29), 118.3 (C-27), 117.9 (C-28), 111.0 (C-30), 109.6 (C-25), 52.8 (C-7), 47.5 (C-3 and C-10), 27.1 (C-24), 25.5 (C-14 and C-15), 17.7 (C-11), 16.9 (C-4).

(2*H*,2*H*,3*H*,3*H*-perfluoroundecanoyl)-Trp-Ala-Ala

Identical procedure as for (2*H*,2*H*,3*H*,3*H*-perfluoroundecanoyl)-Ala-Trp-Ala. White powder. (412 mg, 0.502 mmol, 72%).

UPLC-MS: Method 2, T_R = 4.46 min; m/z MS (ES+): 161.3 [20%], 731.9 [40%], 821.1 [100%, M + H^+], 843.0 [80%, M + Na^+].

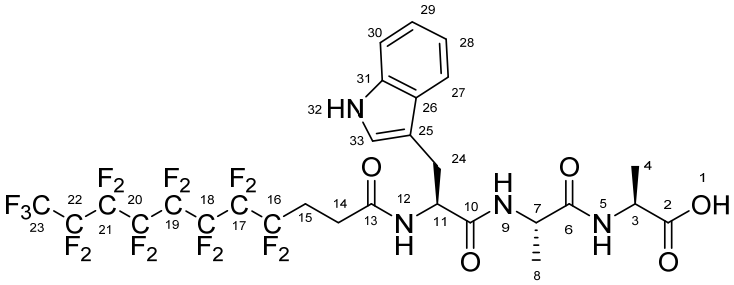

^{1}H-NMR (500 MHz, DMSO-d_6, 298 K): δ = 12.53 (s, 1 H, H-1), 10.79 (d, $^3J_{H\text{-}H}$= *2.4 Hz,* 1 H, H-32), 8.23 (d, $^3J_{H\text{-}H}$ = 8.1 Hz, 1 H, H-12), 8.11 (d, $^3J_{H\text{-}H}$ = 7.5, Hz, 1 H, H-9), 8.05 (d, $^3J_{H\text{-}H}$ = 7.2 Hz, 1 H, H-5), 7.60 (dd, $^3J_{H\text{-}H}$ = 7.9 Hz, $^4J_{H\text{-}H}$= 1.0 Hz, 1 H, H-27), 7.30(dd, $^3J_{H\text{-}H}$ = 8.1 Hz, $^4J_{H\text{-}H}$= 1.0 Hz, 1 H, H-30), 7.13 (d, $^3J_{H\text{-}H}$ = 2.4 Hz, 1 H, H-33), 7.04 (ddd, $^3J_{H\text{-}H}$ = 8.1 Hz, 7.0 Hz, $^4J_{H\text{-}H}$= 1.0 Hz, 1 H, H-29), 6.95 (ddd, $^3J_{H\text{-}H}$ = 7.9 Hz, 6.9 Hz, $^4J_{H\text{-}H}$= 1.0 Hz, 1 H, H-28), 4.56 (td, $^3J_{H\text{-}H}$ = 8.7 Hz, 4.6 Hz, 1 H, H-11), 4.31 (p, $^3J_{H\text{-}H}$ = 7.1 Hz, 1 H, H-7), 4.19 (p, $^3J_{H\text{-}H}$ = 7.3Hz, 1 H, H-3), 3.16 (dd, $^2J_{H\text{-}H}$ = 14.8 Hz, $^3J_{H\text{-}H}$ = 4.6 Hz, 1 H, H-24), 2.95 (dd, $^2J_{H\text{-}H}$ = 14.8 Hz, $^3J_{H\text{-}H}$ = 8.7 Hz, 1 H, H-24), 2.46-2.23 (m, 4 H, H-14 and H-15), 1.26 (d, $^3J_{H\text{-}H}$ = 7.3 Hz, 3 H, H-4), 1.20 (d, $^3J_{H\text{-}H}$ = 7.1 Hz, 3 H, H-8).

^{13}C δ = 173.8(C-2), 171.6 (C-6), 170.8 (C-10), 169.1 (C-13), 135.9 (C-31), 127.3(C-26), 123.5 (C-33), 120.6 (C-29), 118.3 (C-27), 117.9 (C-28), 111.0 (C-30), 109.9 (C-25), 53.4 (C-11), 47.6(C-7), 47.2 (C-3), 27.5 (C-24), 25.5 (C-14 and C-15), 17.8 (C-8), 16.8 (C-4).

(2*H*,2*H*,3*H*,3*H*-perfluoroundecanoyl)-Ala-Ala-Trp

Identical procedure as for (2*H*,2*H*,3*H*,3*H*-perfluoroundecanoyl)-Ala-Trp-Ala. White powder. (362 mg, 0.441 mmol, 63 %).

UPLC-MS: Method 2, T_R = 3.15 min; m/z MS (ES+): 205.2 [40%], 276.2 [20%], 821.1 [100%, M + H^+], 843.1 [70%, M + Na^+].

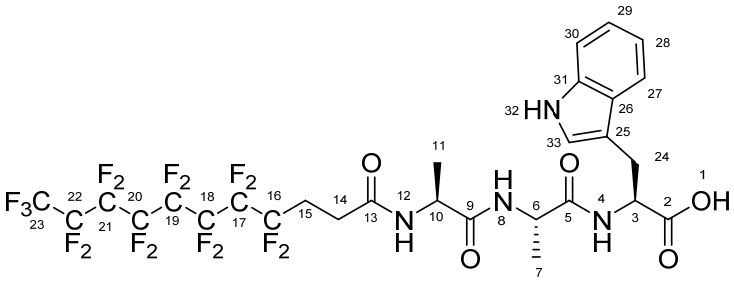

^{1}H-NMR (500 MHz, DMSO-d_6, 298 K): δ = 12.62 (s, 1 H, H-1), 10.84 (d, $^3J_{H\text{-}H}$= 2.4 Hz, 1 H, H-32), 8.23 (d, $^3J_{H\text{-}H}$ = 7.4 Hz, 1 H, H-12), 7.9 (d, $^3J_{H\text{-}H}$ = 7.7, Hz, 1 H, H-8), 7.97 (d, $^3J_{H\text{-}H}$ = 7.5 Hz, 1 H, H-4), 7.51 (dd, $^3J_{H\text{-}H}$ = 8.0

Hz, $^{4}J_{H\text{-}H}$= 1.0 Hz, 1 H, H-27), 7.32(dt, $^{3}J_{H\text{-}H}$ = 8.1 Hz, $^{4}J_{H\text{-}H}$= 1.0 Hz, $^{5}J_{H\text{-}H}$= 1.0 Hz, 1 H, H-30), 7.14 (d, $^{3}J_{H\text{-}H}$ = 2.4 Hz, 1 H, H-33), 7.05 (ddd, $^{3}J_{H\text{-}H}$ = 8.1 Hz, 6.9 Hz, $^{4}J_{H\text{-}H}$= 1.0 Hz, 1 H, H-29), 6.97 (ddd, $^{3}J_{H\text{-}H}$ = 8.0 Hz, 6.9 Hz, $^{4}J_{H\text{-}H}$= 1.0 Hz, 1 H, H-28), 4.60 (td, $^{3}J_{H\text{-}H}$ = 7.6 Hz, 5.4 Hz, 1 H, H-3), 4.30 (p, $^{3}J_{H\text{-}H}$ = 7.1 Hz, 1 H, H-6), 4.29 (p, $^{3}J_{H\text{-}H}$ = 7.0Hz, 1 H, H-10), 3.28 (dd, $^{2}J_{H\text{-}H}$ = 14.8 Hz, $^{3}J_{H\text{-}H}$ = 5.4 Hz, 1 H, H-24), 3.18 (dd, $^{2}J_{H\text{-}H}$ = 14.8 Hz, $^{3}J_{H\text{-}H}$ = 7.1 Hz, 1 H, H-24), 2.50-2.40 (m, 4 H, H-14 and H-15), 1.19 (d, $^{3}J_{H\text{-}H}$ = 7.1 Hz, 3 H, H-7), 1.15 (d, $^{3}J_{H\text{-}H}$ = 7.1 Hz, 3 H, H-11).

^{13}C δ = 173.5(C-2), 172.7 (C-5), 172.0 (C-9), 169.6 (C-13), 135.9 (C-31), 127.1(C-26), 123.4 (C-33), 120.7 (C-29), 118.1 (C-28), 117.9 (C-27), 111.1 (C-30), 109.4 (C-25), 52.6 (C-3), 47.8 (C-6 and C-10), 26.7 (C-24), 25.5 (C-14 and C-15), 17.9 (C-7), 17.8 (C-11).

(2*H*,2*H*,3*H*,3*H*-perfluorooctanoyl)-*N*$^{\alpha}$-Me-Ala-*N*$^{\alpha}$-Me-Trp(Me)-*N*$^{\alpha}$-Me-Ala-N(Me)$_2$ **4**

The dimsyl-anion was prepared in identical quantities and concentrations as described above for compound **2** and combined with a solution of (2*H*,2*H*,3*H*,3*H*-perfluorooctanoyl)-Ala-Trp-Ala-NH_2 (1.00 eq., 516 mg, 0.770 mmol) in DMSO (5 ml). Addition of MeI (75 eq., 3.6 ml, 58 mmol), quench with water, extraction and purification were performed as described above. The product was isolated as a pale brown oil (183 mg, 0.243 mmol, 31 %).

UPLC-MS: Method 2, T_R = 5.48 min; m/z MS (ES+): 624.3 [100%, M - (C-terminal Ala)$^-$], 709.3 [30%, M - NMe_2^-], 776.0 [80%, M + Na^+].

ESI-HRMS: calculated for $C_{31}H_{38}F_{11}N_5NaO_4^+$: 776.2640; found: 776.2651.

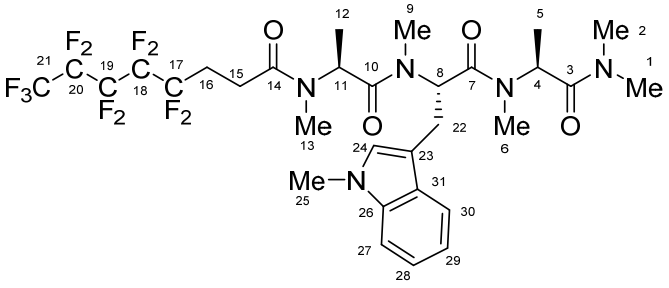

^{1}H-NMR (500 MHz, $CDCl_3$, 298 K): δ = 7.64 (dt, $^{3}J_{H\text{-}H}$ = 8.0 Hz, $^{4}J_{H\text{-}H}$ = 1.0 Hz, $J^{5}_{H\text{-}H}$ = 1.0 Hz, 1 H, H-30), 7.26 (dt, $^{3}J_{H\text{-}H}$ = 8.3 Hz, $^{4}J_{H\text{-}H}$ = 1.0 Hz, $^{5}J_{H\text{-}H}$ = 1.0 Hz 1 H, H-27), 7.20 (ddd , $^{3}J_{H\text{-}H}$ = 8.1 Hz, $^{3}J_{H\text{-}H}$ = 6.9 Hz, $^{4}J_{H\text{-}H}$ = 1.0 Hz, 1 H, H-28), 7.10 (ddd , $^{3}J_{H\text{-}H}$ = 8.0 Hz, $^{3}J_{H\text{-}H}$ = 6.9 Hz, $^{4}J_{H\text{-}H}$ = 1.0 Hz, 1 H, H-29), 6.93 (s, 1 H, H-24), 5.88 (dd, $^{3}J_{H\text{-}H}$ = 7.2 Hz, $^{3}J_{H\text{-}H}$ = 8.5 Hz, 1 H, H-8), 5.46 (q, $^{3}J_{H\text{-}H}$ = 6.9 Hz, 1 H, H-11), 5.41 (q, $^{3}J_{H\text{-}H}$ = 6.9 Hz, 1 H, H-4), 3.70 (s, 3 H, H-25), 3.26 (dd, $^{2}J_{H\text{-}H}$ = 14.7 Hz, $^{2}J_{H\text{-}H}$ = 7.3 Hz, 1 H, H-22), 3.13 (dd, $^{2}J_{H\text{-}H}$ = 14.7 Hz, $^{3}J_{H\text{-}H}$ = 8.4 Hz, 1 H, H-22), 2.98 (s, 3 H, H-9), 2.86 (s, 6 H, (H-1 or H-2) and H-6), 2.65 (s, 3 H, H-1 or H-2), 2.52-2.40 (m, 2 H, H-16), 2.40-2.20 (m, 2 H, H-15), 2.30 (s, 3 H, H-13), 1.25 (d, $^{3}J_{H\text{-}H}$ = 6.9 Hz, 3 H, H-5), 1.19 (d, $^{3}J_{H\text{-}H}$ = 6.9 Hz, 3H, H-12).

^{13}C δ = 171.1(C-10), 170.7 (C-3), 169.7 (C-7), 169.5 (C-14), 136.7 (C-26), 128.0 (C-31), 127.9 (C-24), 121.7 (C-28), 119.1 (C-29), 118.7 (C-30), 109.3 (C-23), 109.2 (C-27), 53.9 (C-8), 49.2 (C-4), 49.1 (C-11), 36.3 (C-1 or C-2), 35.7 (C-1 or C-2), 32.4 (C-25), 30.2 (C-9), 29.9 (C-6), 29.0 (C-13), 26.4 (C-16), 24.6 (C-22), 24.2 (C-15), 14.4 (C-5 and C-12).

General procedure 4: (2*H*,2*H*,3*H*,3*H*-perfluorooctanoyl)-Ala-Trp-Ala-(2*H*,2*H*,3*H*,3*H*-perfluorodecylamid) **5**

(2*H*,2*H*,3*H*,3*H*-perfluorooctanoyl)-Ala-Trp-Ala (1.00 eq., 2.50 g, 3.73 mmol), PyBOP (1.50 eq., 2.91 g, 5.59 mmol) and 1*H*,1*H*,2*H*,2*H*-heptadecafluorodecylamine (1.50 eq., 2.59 g, 5.59 mmol) were dissolved in DMF (250 ml) and stirred for 3 h. Then H_2O (250 ml) was added and the precipitate collected by centrifugation (4400 rpm). The precipitate was washed with DMF (2 × 10 ml), H_2O (2 × 30 ml) and MeCN (4 × 30 ml). The crude product was dissolved in hot DMF (75 °C) and then reprecipitated by addition of ice cold water. After washing with H_2O (2 × 30 ml) and MeCN (4 × 30 ml) followed by drying (2*H*,2*H*,3*H*,3*H*-perfluorooctanoyl)-Ala-Trp-Ala-(2*H*,2*H*,3*H*,3*H*-perfluorodecylamin) was isolated as a white powder (1.82 g, 1.63 mmol, 44 %).

UPLC-MS: Method 2, T_R = 8.05 min; m/z MS (ES+): 653.1 [30%], 1116.1 [40%, M + H^+], 1138.0 [100%, M + Na^+], 1154.1 [10%, M + K^+].

ESI-HRMS: calculated for $C_{35}H_{30}F_{28}N_5O_4^+$: 1116.1845; found: 1116.1848.

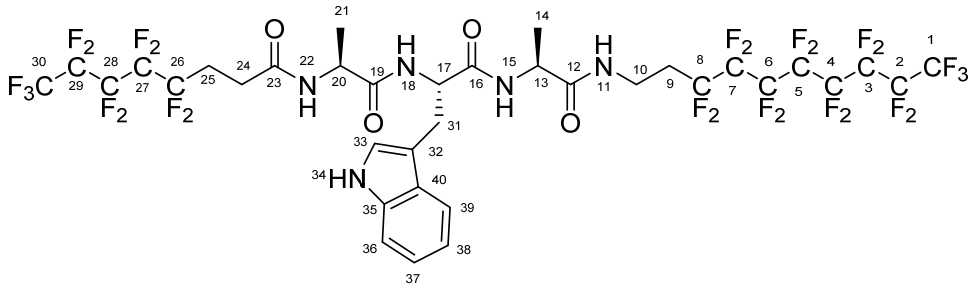

^{1}H-NMR (500 MHz, DMSO-d_6, 298 K): δ = 10.75 (s, 1H, H-34), 8.25 (d, $^3J_{H\text{-}H}$ = 6.6 Hz, 1 H, H-22), 7.89 (d, $^3J_{H\text{-}H}$ = 7.7 Hz, 1 H, H-18), 7.82 (d, $^3J_{H\text{-}H}$ = 7.2 Hz, 1 H, H-15), 7.76 (t, $^3J_{H\text{-}H}$ = 5.8 Hz, 1 H, H-11), 7.53 (d, $^3J_{H\text{-}H}$ = 7.9 Hz, 1 H, H-39), 7.28 (d, $^3J_{H\text{-}H}$ = 8.1 Hz, 1 H, H-36), 7.11 (s, 1 H, H-33), 7.01 (t, $^3J_{H\text{-}H}$ = 7.5 Hz, 1 H, H-37), 6.93 (t, $^3J_{H\text{-}H}$ = 7.5 Hz, 1 H, H-38), 4.48 (ddd, $^3J_{H\text{-}H}$ = 8.6 Hz, $^3J_{H\text{-}H}$ = 7.7 Hz , $^3J_{H\text{-}H}$ = 5.0 Hz, 1 H, H-17), 4.21-4.11 (m, 2 H, H-20 and H-13), 3.38-3.26 (m, 2 H, H-10), 3.16 (dd, $^2J_{H\text{-}H}$ = 14.9, Hz, $^3J_{H\text{-}H}$ = 5.0 Hz, 1 H, H-31), 3.00 (dd, $^2J_{H\text{-}H}$ = 14.9, Hz, $^3J_{H\text{-}H}$ = 8.6 Hz, 1 H, H-31), 2.50-2.23 (m, 6 H, H-9, H-24, H-25), 1.13 (d, $^3J_{H\text{-}H}$ = 7.1 Hz, 6 H, H-21, H-14).

^{13}C δ = 173.2 (C-19), 172.9 (C-12), 171.7 (C-16), 170.4 (C-23), 136.8 (C-35), 128.0 (C-40), 124.0 (C-33), 121.2 (C-37), 118.8 (C-39), 118.7 (C-38), 111.7 (C-36), 110.6 (C-32), 54.0 (C-17), 49.5 (C-20), 48.8 (C-13), 31.4 (C-10), 30.0 (C-9), 27.3 (C-31), 26.1 (C-24), 26.1 (C-25), 17.7 (C-14,C-21).

(2*H*,2*H*,3*H*,3*H*-perfluoroundecanoyl)-Ala-Trp-Ala-(2*H*,2*H*,3*H*,3*H*-perfluorodecylamid) **6**

Identical procedure as for (2H,2H,3H,3H-perfluorooctanoyl)-Ala-Trp-Ala-(2H,2H,3H,3H-perfluorodecylamid) but employing (2*H*,2*H*,3*H*,3*H*-perfluoroundecanoyl)-Ala-Trp-Ala instead of (2*H*,2*H*,3*H*,3*H*-perfluorooctanoyl)-Ala-Trp-Ala. White powder (710 mg, 0.561 mmol, 46 %).

UPLC-MS: Method 2, T_R = 9.65 min; m/z MS (ES+): 803.0 [20%], 1265.9 [20%, M + H^+], 1288.0 [100%, M + Na^+], 1303.8 [10%, M + K^+].

ESI-HRMS: calculated for $C_{38}H_{30}F_{34}N_5O_4^+$: 1266.1749; found: 1266.1739.

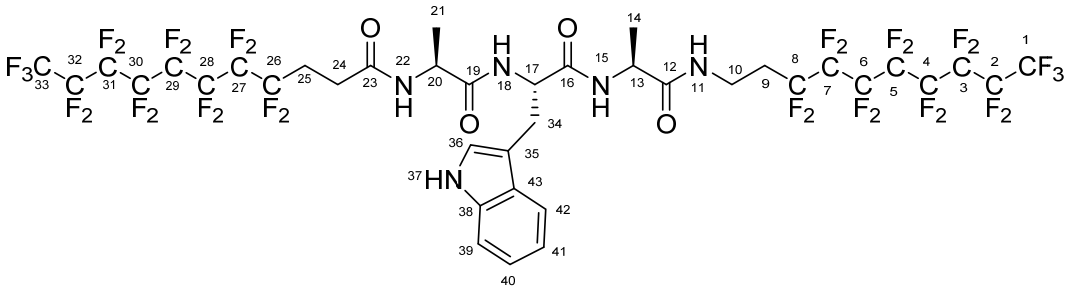

^{1}H-NMR (600 MHz, DMF-d_7, 333 K): δ = 10.73 (s, 1 H, H-37), 8.20 (d, $^3J_{H\text{-}H}$ = 6.2 Hz, 1 H, H-22), 7.82 (d, $^3J_{H\text{-}H}$ = 7.3 Hz, 1 H, H-18), 7.63 (d, $^3J_{H\text{-}H}$ = 7.5 Hz, 1 H, H-15), 7.60 (d, $^3J_{H\text{-}H}$ = 8.0 Hz, 1 H, H-42), 7.58 (t, $^3J_{H\text{-}H}$ = 5.7 Hz, 1 H, H-11), 7.39 (d, $^3J_{H\text{-}H}$ = 8.1 Hz, 1 H, H-39), 7.24 (d, $^3J_{H\text{-}H}$ = 2.3 Hz, 1 H, H-36), 7.08 (ddd, $^3J_{H\text{-}H}$ = 8.0 Hz, $^3J_{H\text{-}H}$ = 7.2 Hz, $^4J_{H\text{-}H}$ = 1.2 Hz, 1 H, H-40), 7.01 (ddd, $^3J_{H\text{-}H}$ = 8.0 Hz $^3J_{H\text{-}H}$ = 7.0 Hz, $^4J_{H\text{-}H}$ = 1.0 Hz, 1 H, H-41), 4.60 (td, $^3J_{H\text{-}H}$ = 7.6 Hz, $^3J_{H\text{-}H}$ = 5.3 Hz, 1 H, H-17), 4.33 (p, $^3J_{H\text{-}H}$ = 7.1 Hz, 1 H, H-13), 4.30 (p, $^3J_{H\text{-}H}$ = 7.0 Hz, 1 H, H-20), 3.54-3.43 (m, 2 H, H-10), 3.30 (dd, $^2J_{H\text{-}H}$ = 14.8 Hz, $^3J_{H\text{-}H}$ = 5.2 Hz, 1 H, H-34), 3.18 (dd, $^2J_{H\text{-}H}$ = 14.8 Hz, $^3J_{H\text{-}H}$ = 8.1 Hz, 1 H, H-34), 2.63-2.43 (m, 6 H, H-24, H-25 and H-9), 1.29 (d, $^3J_{H\text{-}H}$ = 7.1 Hz, 3 H, H-21), 1.24 (d, $^3J_{H\text{-}H}$ = 7.1 Hz, 3 H, H-14).

^{13}C δ = 172.9 (C-19), 172.4 (C-12), 171.1(C-16), 170.2 (C-23), 136.7 (C-38), 127.7 (C-43), 123.8(C-36), 121.0 (C-40), 118.6 (C-41), 118.4 (C-42), 111.3 (C-39), 110.3 (C-35), 54.4 (C-17), 50.0 (C-20), 49.0 (C-13), 31.4 (C-10), 30.3 (C-9), 27.0 (C-34), 26.1 (25 and 24), 17.1 (C-14), 16.8 (C-21).

(2*H*,2*H*,3*H*,3*H*-perfluoroundecanoyl)-Trp-Ala-Ala-(2*H*,2*H*,3*H*,3*H*-perfluorodecylamid) **7**

Identical procedure as for (2H,2H,3H,3H-perfluorooctanoyl)-Trp-Trp-Ala-(2H,2H,3H,3H-perfluorodecylamid) but employing (2*H*,2*H*,3*H*,3*H*-perfluoroundecanoyl)-Trp-Ala-Ala instead of (2*H*,2*H*,3*H*,3*H*-perfluorooctanoyl)-Ala-Trp-Ala. White powder (615 mg, 0.486 mmol, 40 %).

UPLC-MS: Method 2, T_R = 9.51 min; m/z MS (ES+): 803.0 [30%], 1266.0 [20%, M + H^+], 1288.0 [100%, M + Na^+], 1303.9 [10%, M + K^+].

ESI-HRMS: calculated for $C_{38}H_{30}F_{34}N_5O_4^+$: 1266.1749; found: 1266.1741.

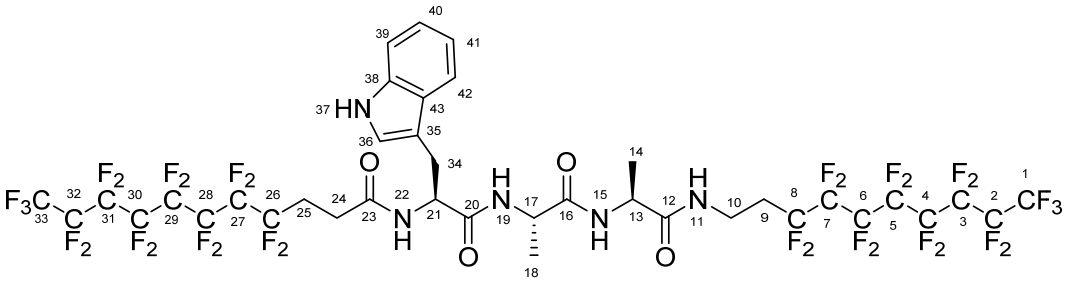

^{1}H-NMR (600 MHz, DMF-d_7, 333 K): δ = 10.70 (s, 1 H, H-37), 8.13 (d, $^3J_{H\text{-}H}$ = 6.9 Hz, 1 H, H-22), 7.96 (d, $^3J_{H\text{-}H}$ = 6.7 Hz, 1 H, H-19), 7.77 (t, $^3J_{H\text{-}H}$ = 5.7 Hz, 1 H, H-11), 7.63 (d, $^3J_{H\text{-}H}$ = 7.7 Hz, 1 H, H-15), 7.62 (d, $^3J_{H\text{-}H}$ = 7.8 Hz, 1 H, H-42), 7.40 (d, $^3J_{H\text{-}H}$ = 8.1 Hz, 1 H, H-39), 7.28 (d, $^3J_{H\text{-}H}$ = 2.3 Hz, 1 H, H-36), 7.09 (ddd, $^3J_{H\text{-}H}$ = 8.1 Hz, $^3J_{H\text{-}H}$ = 6.9 Hz, $^4J_{H\text{-}H}$ = 1.1 Hz, 1 H, H-40), 7.01 (ddd, $^3J_{H\text{-}H}$ = 8.0 Hz, $^3J_{H\text{-}H}$ = 6.9 Hz, $^4J_{H\text{-}H}$ = 1.0 Hz, 1 H, H-41), 4.67 (td, $^3J_{H\text{-}H}$ = 7.6 Hz, $^3J_{H\text{-}H}$ = 5.3 Hz, 1 H, H-21), 4.33 (p, $^3J_{H\text{-}H}$ = 7.1 Hz, 1 H, H-13), 4.32 (p, $^3J_{H\text{-}H}$ = 7.1 Hz, 1 H, H-17), 3.56-3.51 (m, 2 H, H-10), 3.32 (dd, $^2J_{H\text{-}H}$ = 14.8 Hz, $^3J_{H\text{-}H}$ = 5.2 Hz, 1 H, H-34), 3.18 (dd, $^2J_{H\text{-}H}$ = 14.8 Hz, $^3J_{H\text{-}H}$ = 8.0 Hz, 1 H, H-34), 2.67-2.48 (m, 6 H, H-24, H-25 and H-9), 1.31 (d, $^3J_{H\text{-}H}$ = 7.1 Hz, 3 H, H-21), 1.25 (d, $^3J_{H\text{-}H}$ = 7.1 Hz, 3 H, H-14).

^{13}C δ = 172.3 (C-38), 171.9 (C-16 and C-20), 170.3 (C-23), 136.7 (C-38), 127.8 (C-43), 123.8 (C-36), 120.9 (C-40), 118.3 (C-41 and C-42), 111.3 (C-39), 110.2 (C-35), 55.1 (C-21), 49.4 (C-17), 48.8 (C-13), 31.5 (C-10), 30.5 (C-9), 27.4 (C-37), 26.3 (C-24 and C-25), 17.2 (C-14), 16.8 (C-18).

(2*H*,2*H*,3*H*,3*H*-perfluoroundecanoyl)-Ala-Ala-Trp-(2*H*,2*H*,3*H*,3*H*-perfluorodecylamid) **8**

Identical procedure as for (2H,2H,3H,3H-perfluorooctanoyl)-Ala-Trp-Ala-(2H,2H,3H,3H-perfluorodecylamid) but employing (2*H*,2*H*,3*H*,3*H*-perfluoroundecanoyl)-Ala-Ala-Trp instead of (2*H*,2*H*,3*H*,3*H*-perfluorooctanoyl)-Ala-Trp-Ala. White powder (1.12 g, 0.885 mmol, 73 %).

UPLC-MS: Method 2, T_R = 9.60 min; m/z MS (ES+): 650.0 [20%], 1265.9 [30%, M + H^+], 1288.0 [100%, M + Na^+].

ESI-HRMS: calculated for $C_{38}H_{30}F_{34}N_5O_4^+$: 1266.1749; found: 1266.1745.

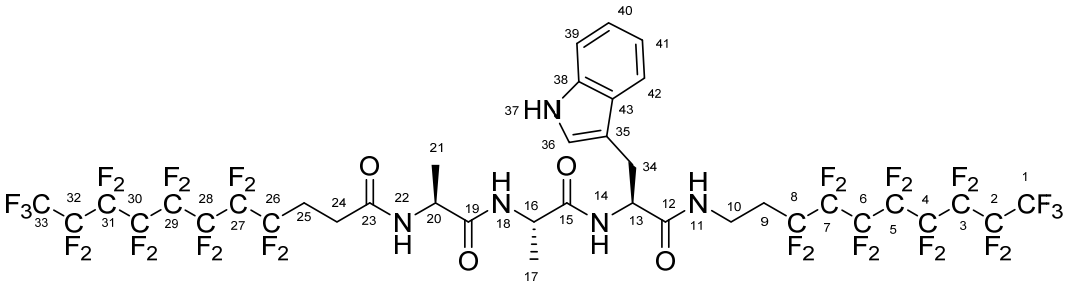

14

^{1}H-NMR (600 MHz, DMF-d_7, 333 K): δ = 10.67 (s, 1 H, H-37), 8.17 (d, $^{3}J_{H\text{-}H}$ = 6.5 Hz, 1 H, H-22), 8.00 (d, $^{3}J_{H\text{-}H}$ = 7.6 Hz, 1 H, H-18), 7.73 (t, $^{3}J_{H\text{-}H}$ = 5.7 Hz, 1 H, H-11), 7.61 (d, $^{3}J_{H\text{-}H}$ = 7.9 Hz, 1 H, H-42), 7.60 (d, $^{3}J_{H\text{-}H}$ = 7.9 Hz, 1 H, H-14), 7.38 (d, $^{3}J_{H\text{-}H}$ = 8.1 Hz, 1 H, H-39), 7.20 (d, $^{3}J_{H\text{-}H}$ = 2.3 Hz, 1 H, H-36), 7.08 (t, $^{3}J_{H\text{-}H}$ = 7.5 Hz, 1 H, H-40), 7.00 (t, $^{3}J_{H\text{-}H}$ = 7.4 Hz, 1 H, H-41), 4.60 (td, $^{3}J_{H\text{-}H}$ = 7.6 Hz, $^{3}J_{H\text{-}H}$ = 5.7 Hz, 1 H, H-13), 4.36 (dq, $^{3}J_{H\text{-}H}$ = 7.0 Hz, 1 H, H-20), 4.30 (dq, $^{3}J_{H\text{-}H}$ = 7.0 Hz, 1 H, H-16), 3.53-3.41 (m, 2 H, H-10), 3.28 (dd, $^{2}J_{H\text{-}H}$ = 14.6 Hz, $^{3}J_{H\text{-}H}$ = 5.8 Hz, 1 H, H-34), 3.18 (dd, $^{2}J_{H\text{-}H}$ = 14.6 Hz, $^{3}J_{H\text{-}H}$ = 7.6 Hz, 1 H, H-34), 2.66-2.55 (m, 4 H, H-24 and H-25), 2.42-2.34 (m, 2 H, H-9), 1.30 (d, $^{3}J_{H\text{-}H}$ = 7.1 Hz, 3 H, H-21), 1.27(d, $^{3}J_{H\text{-}H}$ = 7.1 Hz, 3 H, H-17).

^{13}C δ = 172.7 (C-19), 172.0 (C-15), 171.6 (C-12), 170.0 (C-23), 136.8 (C-38), 127.8(C-43), 123.6 (C-36), 121.0 (C-40), 118.5 (C-42), 118.3 (C-41), 111.2 (C-39), 110.4 (C-35), 54.2 (C-13), 49.6 (C-20), 49.5 (C-16), 31.5 (C-10), 30.5 (C-9), 28.5 (C-34), 26.3 (C-24 and C-25), 17.0 (C-21), 16.9 (C-17).

NHS-ester of *2H,2H,3H,3H*-perfluorodecanoic acid[3]

2H,2H,3H,3H-perfluorodecanoic acid (1.00 eq., 15.0 g, 30.5 mmol) was dissolved in THF (500 ml), then HSTU (1.50 eq., 13.8 g, 45.8 mmol) and DIPEA (1.49 eq., 7.50 ml, 45.4 mmol) were added and the solution was stirred overnight. The solvent was removed under reduced pressure and the crude product dissolved in EtOAc (1 l) and washed with 0.1 M HCl (2 $\times$ 200 ml), brine (200 ml) and H_2O (200 ml). After removal of volatiles under reduced pressure the crude product was purified by column chromatography (EtOAc/cyclohexane (1:1)). The product was obtained as a white solid (16.1 g, 27.4 mmol, 90 %).

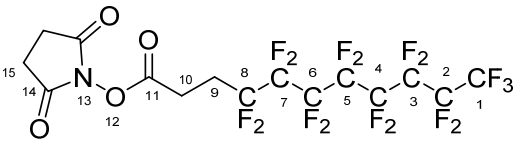

^{1}H-NMR ($CDCl_3$, 500 MHz, 293 K): δ = 3.03 – 2.92 (m, 2 H, H-10), 2.86 (s, 4 H, H-15), 2.68-2.45 (m, 2 H, H-9).

^{13}C δ = 168.7 (C-14), 166.7 (C-11), 117.3(C-8), 26.2(C-9), 25.5 (C-15), 22.8 (C-10).

Trp-Lys-Trp-Lys-Trp-Lys-Trp-Lys-Trp

2-chlorotrityl chloride resin (200 mg) was placed in a plastic syringe equipped with a filter frit. The CH_2Cl_2 was exchanged and DIPEA (2.4 eq, 20 µl, 0.12 mmol), and Fmoc-Trp(boc)-OH (1.00 eq., 26.3 mg, 49.9 µmol) were added. After the sample was agitated on a shaker for 2.5 h liquids were removed by filtration and the resin washed with CH_2Cl_2 (~4 ml) and DMF (~4 ml). The unreacted binding sites on the resin were capped by adding MeOH-solution (~5 ml, 15% MeOH, 5% DIPEA, 80% CH_2Cl_2) followed by agitation for 30 minutes. The peptide coupling steps were performed using a (intavis multi pep RSI) peptide synthesizer and employing 5.00 eq. of Fmoc-amino acids, PyBOP and DIPEA with a reaction time of first

45 min followed be a 2nd coupling step for 90 min. Fmoc-deprotection was carried out with piperidine (20 %, 4 × 5 min). In between coupling and Fmoc-deprotection the syringes were washed 5 times with DMF. In the end the syringe was washed with CH_2Cl_2 (5 × ~2 ml) before the cleavage solution (5ml, 96 % TFA, 3 % triisopropylsilane, 3 % H_2O) was added. Cleavage, precipitation and washing (Et_2O) were performed as described above. The product was isolated as a white solid (64 mg, 44 μmol, 88 %).

UPLC-MS: Method 1, T_R = 4.82 min; m/z MS (ES+): 488.4 [100 %, M + $3H^+$],731.4 [60 %, M + $2H^+$],1462.3 [25%, M + H^+].

ESI-HRMS: calculated for : $C_{79}H_{103}N_{18}O_{10}^{3+}$: 487.9363; found: 487.9367.

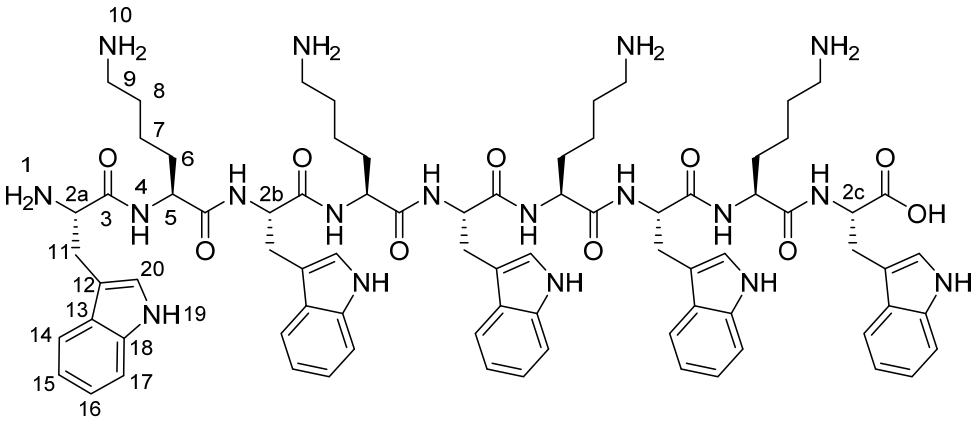

^{1}HNMR (DMSO, 500 MHz, 293 K): δ = 10.94 (s, 1 H, H-19), 10.82 (s, 1 H, H-19),10.78-10.71 (m, 3 H, H-19), 8.20-7.90 (m, 8 H, H-4), 7.90-7.70 (b, 10 H, H-1 and H-10), 7.64 (d, $^3J_{H\text{-}H}$ = 7.9 Hz, 1 H, H-14), 7.60 (d, $^3J_{H\text{-}H}$ = 7.9 Hz, 1 H, H-14) 7.57 (d, $^3J_{H\text{-}H}$ = 8.0 Hz, 1 H, H-14), 7.56 (d, $^3J_{H\text{-}H}$ = 7.9 Hz, 1 H, H-14), 7.52 (d, $^3J_{H\text{-}H}$ = 8.0 Hz, 1 H, H-14), 7.35 (d, $^3J_{H\text{-}H}$ = 8.2 Hz, 1 H, H-17), 7.32-7.27 (m, 4 H, H-17), 7.17 (d, $^3J_{H\text{-}H}$ = 2.4, 1 H, H-20), 7.15- 7.09 (m, 4 H, H-20), 7.07-7.00 (m, 5 H, H-16), 6.99-6.86 (m, 5 H, H-15), 4.65-4.55 (m, 3 H, H-2b), 4.50-4.40 (m, 1 H, H-2c), 4.35-4.20 (m, 4 H, H-5), 4.02-3.93 (1 H, H-2a), 3.20-2.90 (m, 10 H, H-11), 2.75-2.65 (m, 8 H, H-9), 1.68-1.41 (m, 16 H, H-6 and H-8), 1.32-1.15 (m, 8 H, H-7).

^{13}C ((RR'*C*=O) not detected) δ = 136.5 (5 C, C-18), 127.8 (5 C, C-13), 125.5 (C-20), 124.1 (4 C, C-20), 121.4 (5 C, C-16), 119.0 (5 C, C-14), 118.7 (5 C, C-15)111.8 (5 C, C-17), 110.3 (C-12), 53.7 (4 C, C-2b and C-2c), 52.9 (5 C, C-5 and C-2a), 39.1 (4 C, C-9), 32.0 (4 C, C-6), 28.2 (5 C, C-11), 27.1 (4 C, C-8), 22.5 (4 C, C-8).

Compound **9**

Trp-Lys-Trp-Lys-Trp-Lys-Trp-Lys-Trp (1.00 eq., 120 mg, 82.1 μmol) and *1H,1H,2H,2H*-perfluorodecanoic acid NHS ester (10.0 eq., 482 mg, 0.821 mmol) were dissolved in DMF (200ml), then DIPEA (20 eq., 0.30 ml, 1.6 mmol) was added and the solution was stirred for 56 h at 50°C. Subsequently the mixture was concentrated to 25 mL under reduced pressure and water (175 ml) was added. The precipitate was collected and washed with acetone (3 × 50 ml). The product was obtained as a pale brown solid (245 mg, 64.0 μmol, 80 %).

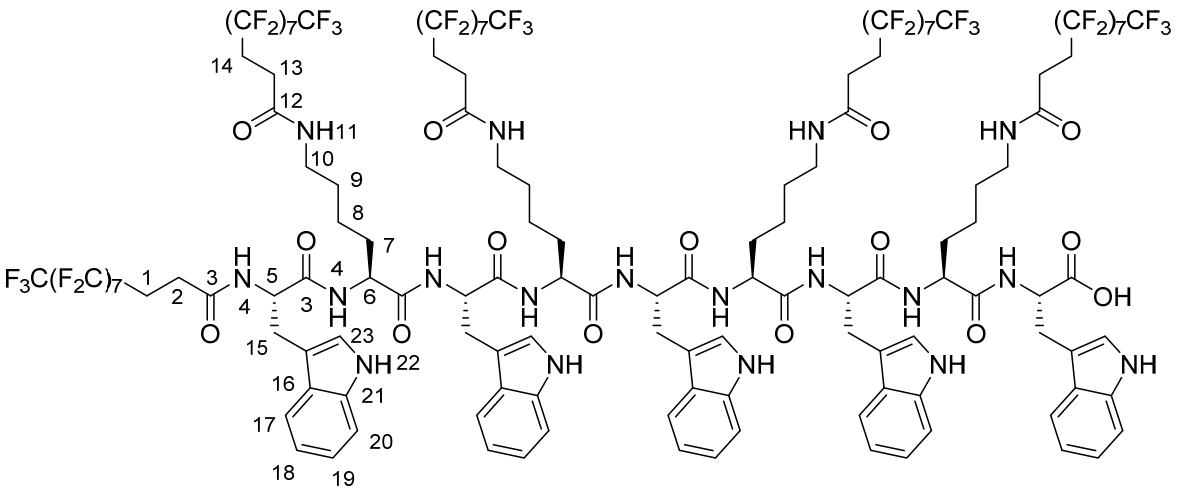

^{1}H NMR (HFIP-d_2 + 20 mol% H_2O, presat (water and OH-HFIP signal suppression, 500 MHz, 293 K): δ = 8.75 (s, 1 H, H-22), 8.74 (s, 1 H, H-22), 8.68 (s, 1 H, H-22), 8.65 (s, 1 H, H-22), 8.45 (s, 1 H, H-22), 7.66 (d, $^{3}J_{H\text{-}H}$ = 7.9 Hz, 1 H, H-17), 7.60 (d, $^{3}J_{H\text{-}H}$ = 8.2 Hz, 1H, H-17), 7.58 (d, $^{3}J_{H\text{-}H}$ = 8.3 Hz, 1 H, H-17), 7.54 (d, $^{3}J_{H\text{-}H}$ = 8.0 Hz, 1 H, H-17), 7.49 (d, $^{3}J_{H\text{-}H}$ = 7.9 Hz, 1 H, H-17), 7.46-7.37 (m, 4 H, H-17), 7.36 (s, 1 H, H-4), 7.33-7.12 (m, 13 H, 1 H, H-17, 5 H, H-18, 5 H, H-19, 2 H, H-4 (7.27 and 7.18 according to COSY), 7.10 (s, 1 H, H-23), 7.09 (s, 1 H, H-4), 7.08 (s, 1 H, H-23), 7.02 (s, 1 H, H-23), 7.01 (s, 1 H, H-23), 6.96 (s, 2 H, H-4), 6.90 (s, 1 H, H-23), 6.84 (s, 1 H, H-4), 6.56 (s, 1 H, H-4), 6.30-6.15 (m, 4 H, H-11), 4.82-4.76 (m, 1 H, H-5), 4.65-4.58 (m, 2 H,H-5), 4.58-4.50 (m, 2 H, H-5), 4.10 (t, $^{3}J_{H\text{-}H}$ = 6.9 Hz, 1 H, H-6), 4.05-3.98 (m, 2 H, H-6), 3.94-3.89 (m, 1 H, H-6), 3.50-2.95 (m,18 H, H-15 and H-10), 2.60-2.25 (m, 20 H, H-1 and H-2), 1.77-1.41 (m, 8 H, H-7), 1.41-1.25 (m, 8 H, H-8), 1.16-0.86 (m, 8 H, H-9).

^{13}C (no HMBC experiment was recorded - carbon atoms without hydrogen substituents were not detected) δ = 123.0 (C-23), 122.7 (C-23), 122.4 (3 C, C-23), 121.4 (5 C, C-19), 118.7 (5 C, C-18), 117.2 (C-17), 116.9 (2 C, C-17), 116.7 (2 C, C-17), 110.6 (5 C, C-20), 54.7 (C-6), 54.6 (C-6), 54.3 (C-6), 53.9 (2 C, C-5), 53.6 (2 C, C-5), 53.4 (C-6), 52.5 (C-5), 38.4 (4 C, C-10), 29.2 (4 C, C-7), 26.8 (C-8), 25.6 (10 C, C-1 and C-2), 25.2 (5 C, C-15), 21.2 (C-9).

MALDI: 3853.5 [M + Na^+].

^{1}H NMR spectra and LC chromatograms

Ala-Trp-Ala **1**

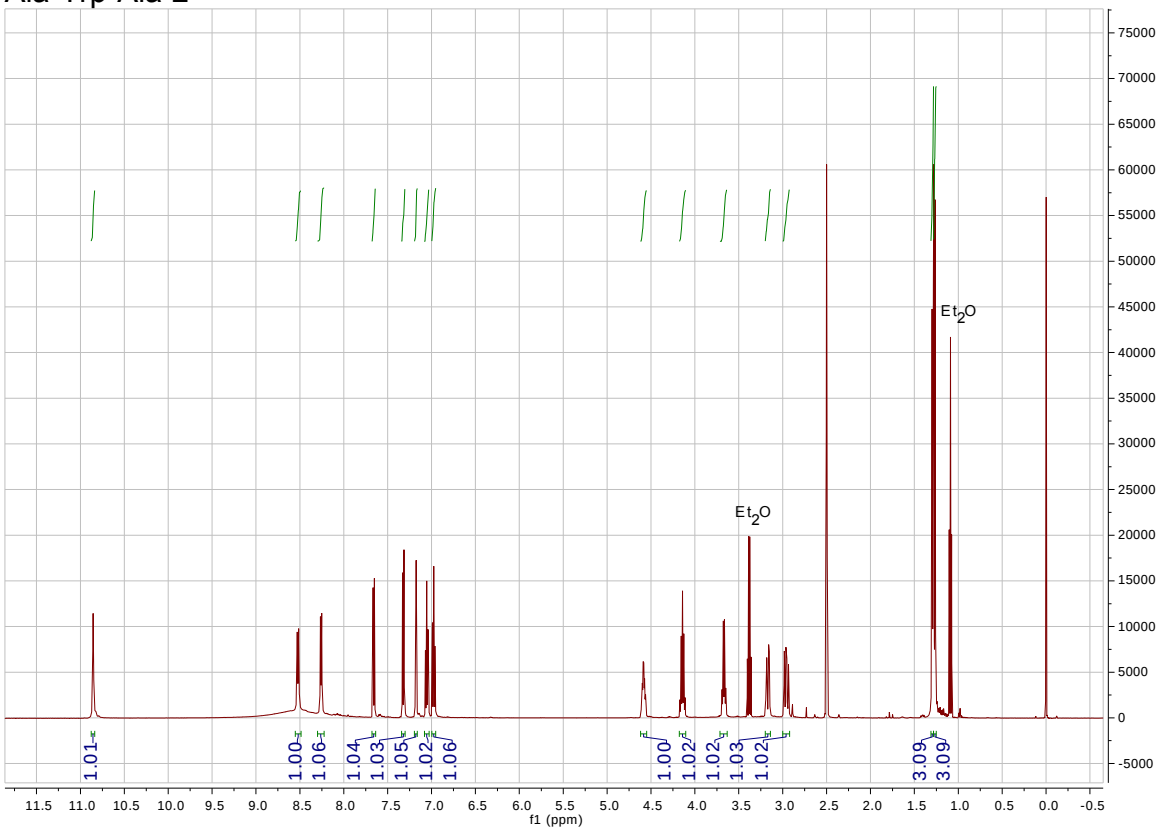

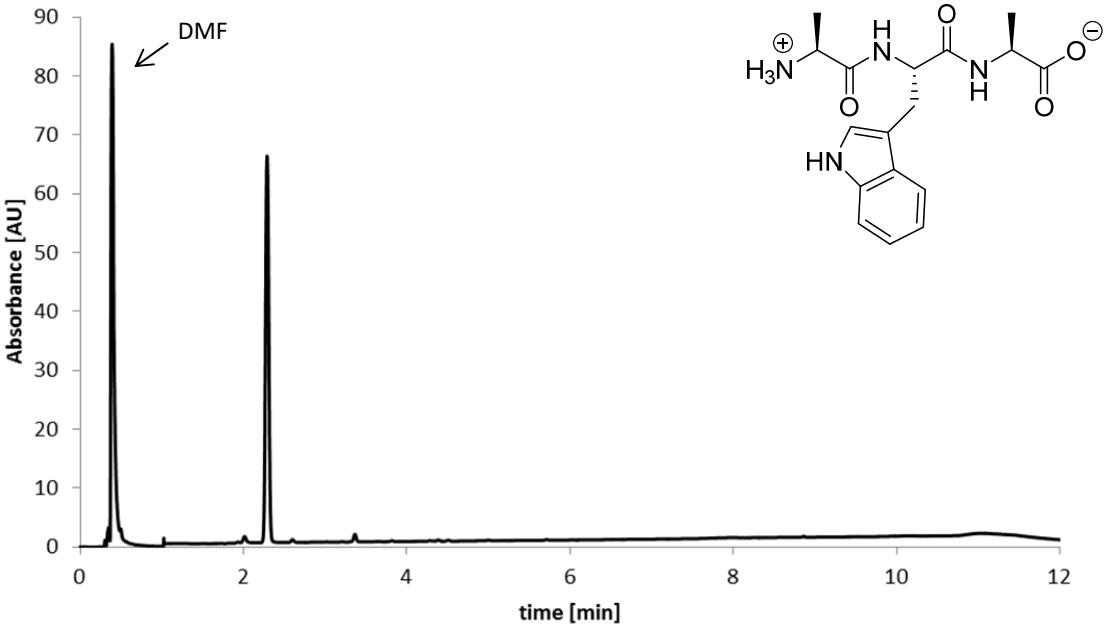

S1. Ala-Trp-Ala **1**. Top: ^{1}H-NMR (DMSO-d_6, 500 MHz, 293 K), Bottom: UV-Vis-trace 190-500 nm of UPLC chromatogram (Method 1).

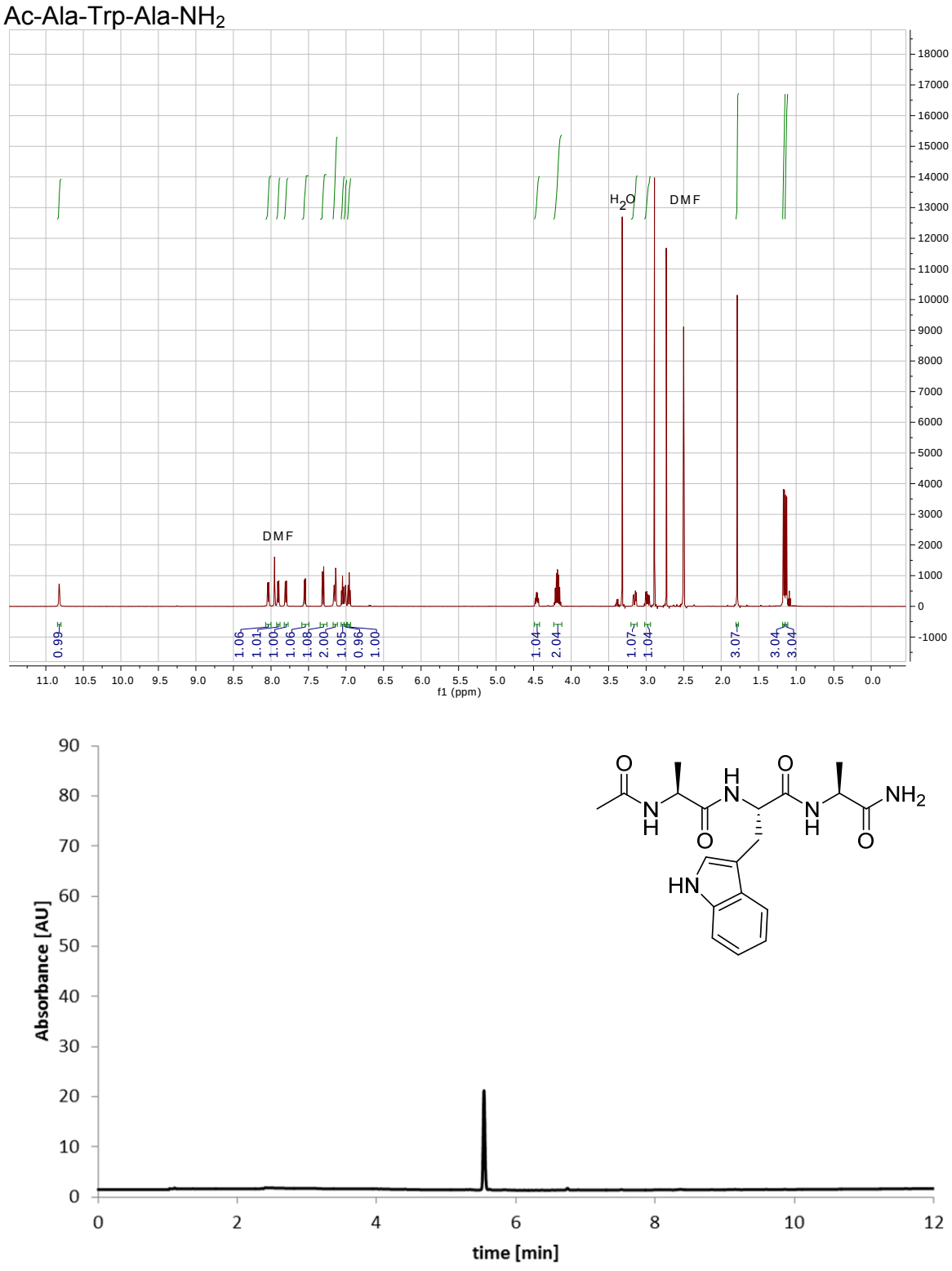

S2. Ac-Ala-Trp-Ala-NH_2. Top: ^{1}H-NMR (DMSO-d_6, 500 MHz, 293 K), Bottom: UV-Vis-trace 190-500 nm of UPLC chromatogram (Method 1).

(2*H*,2*H*,3*H*,3*H*-perfluorooctanoyl)-Ala-Trp-Ala

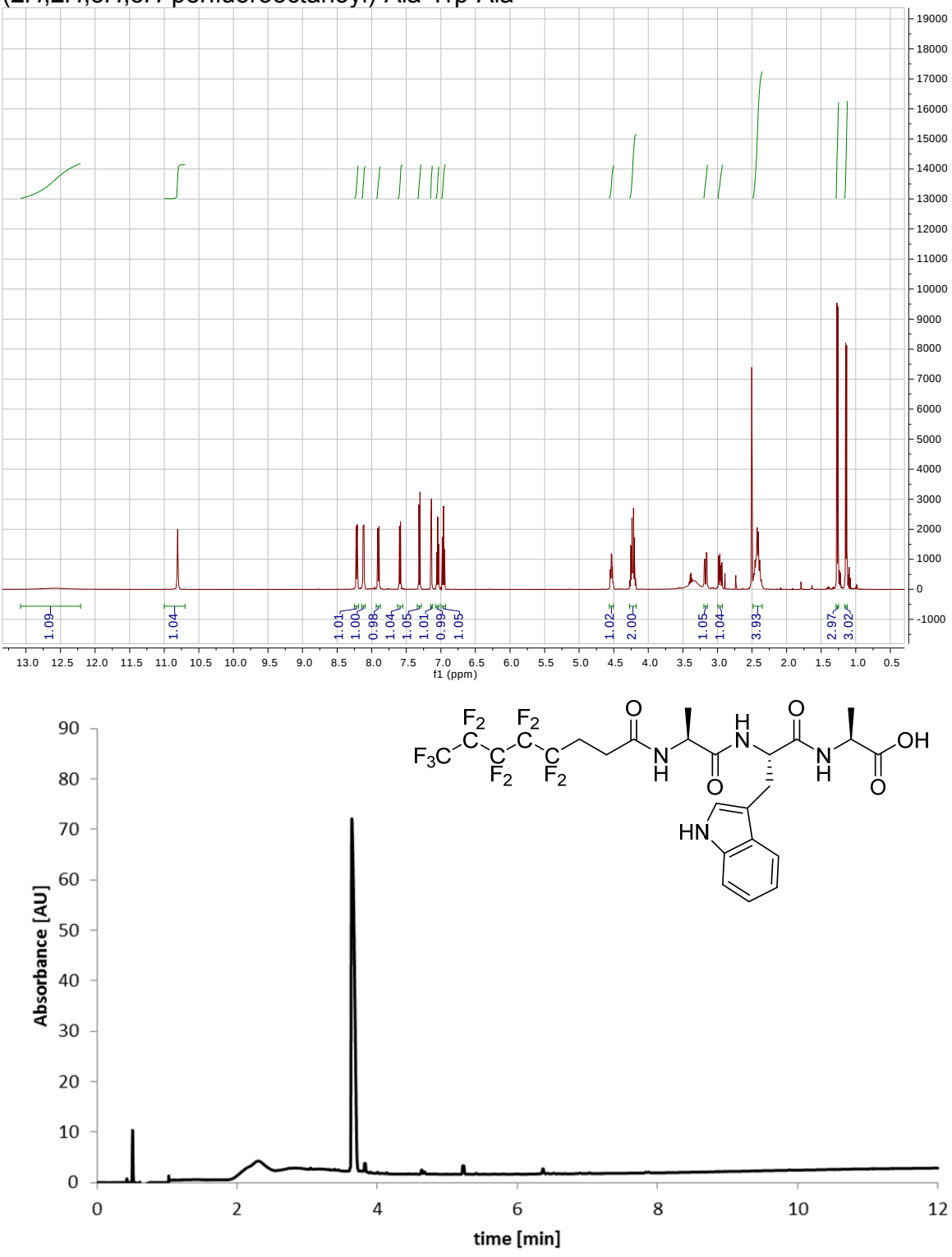

S3. (2*H*,2*H*,3*H*,3*H*-perfluorooctanoyl)-Ala-Trp-Ala. Top: ^{1}H-NMR (DMSO-d_6, 500 MHz, 293 K), Bottom: UV-Vis-trace 190-500 nm of UPLC chromatogram (Method 2).

(2*H*,2*H*,3*H*,3*H*-perfluoroundecanoyl)-Ala-Trp-Ala

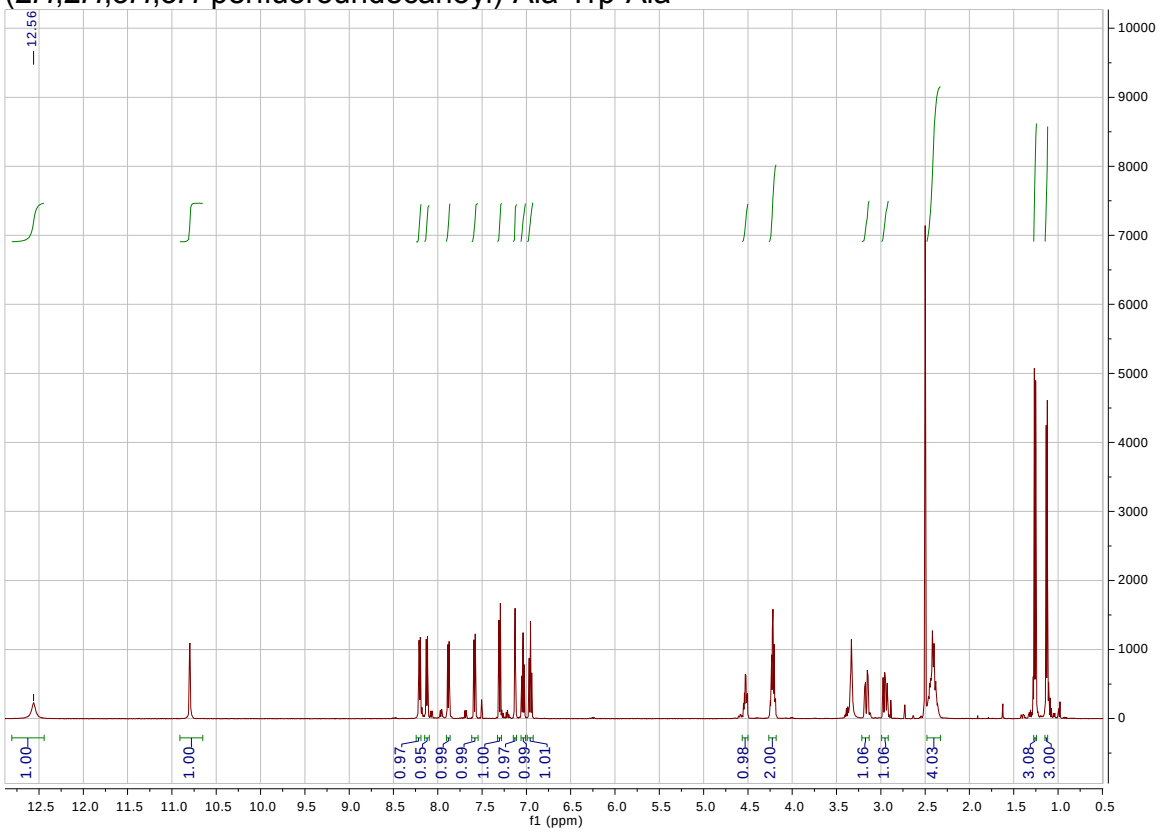

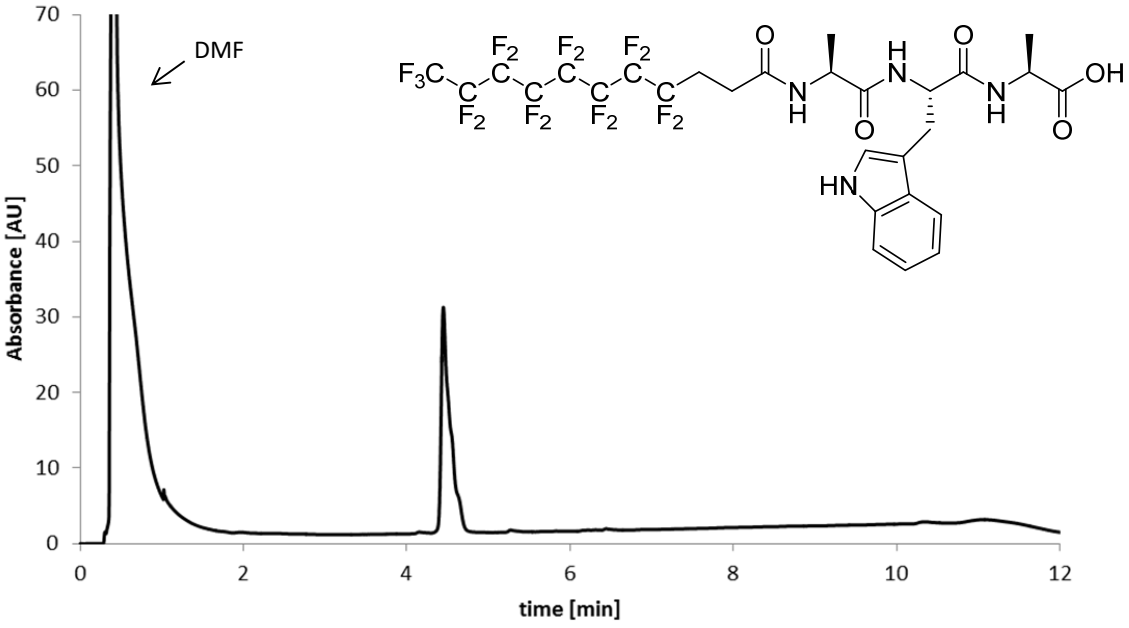

S4. (2*H*,2*H*,3*H*,3*H*-perfluoroundecanoyl)-Ala-Trp-Ala. Top: ^{1}H-NMR (DMSO-d_6, 500 MHz, 293 K), Bottom: UV-Vis-trace 190-500 nm of UPLC chromatogram (Method 2).

(2*H*,2*H*,3*H*,3*H*-perfluoroundecanoyl)-Trp-Ala-Ala

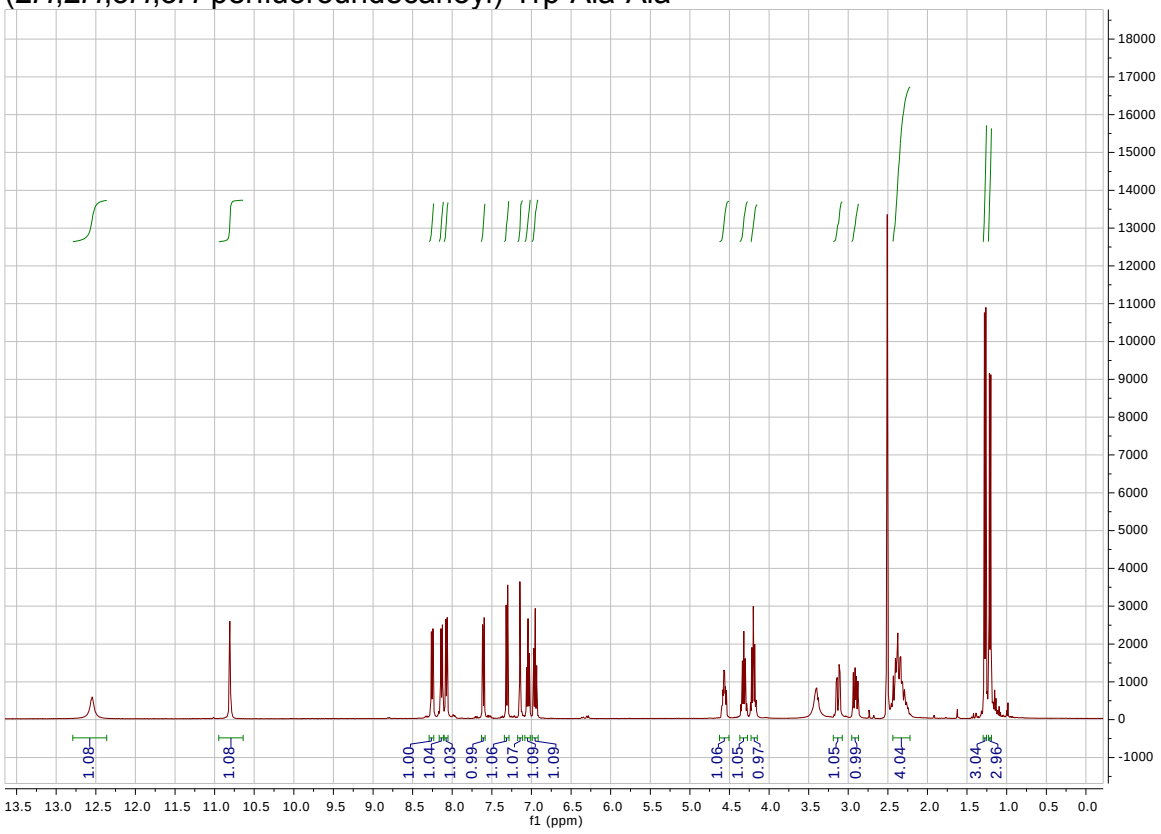

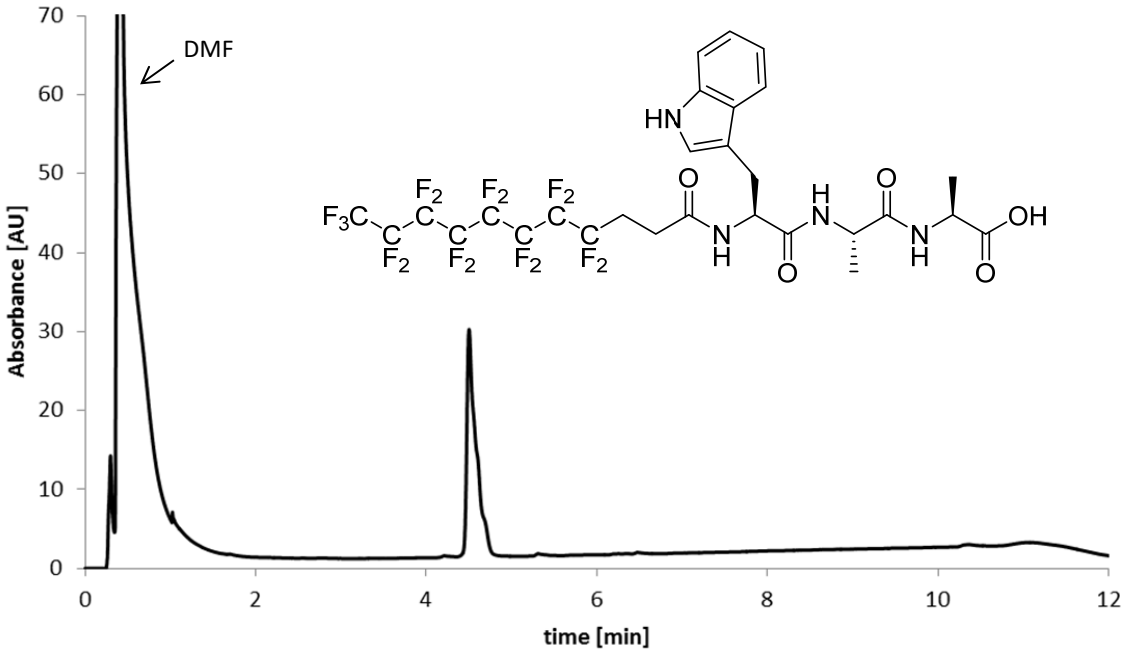

S5. (2*H*,2*H*,3*H*,3*H*-perfluoroundecanoyl)-Trp-Ala-Ala: Top: ^{1}H-NMR (DMSO-d_6, 500 MHz, 293 K), Bottom: UV-Vis-trace 190-500 nm of UPLC chromatogram (Method 2).

(2*H*,2*H*,3*H*,3*H*-perfluoroundecanoyl)-Ala-Ala-Trp

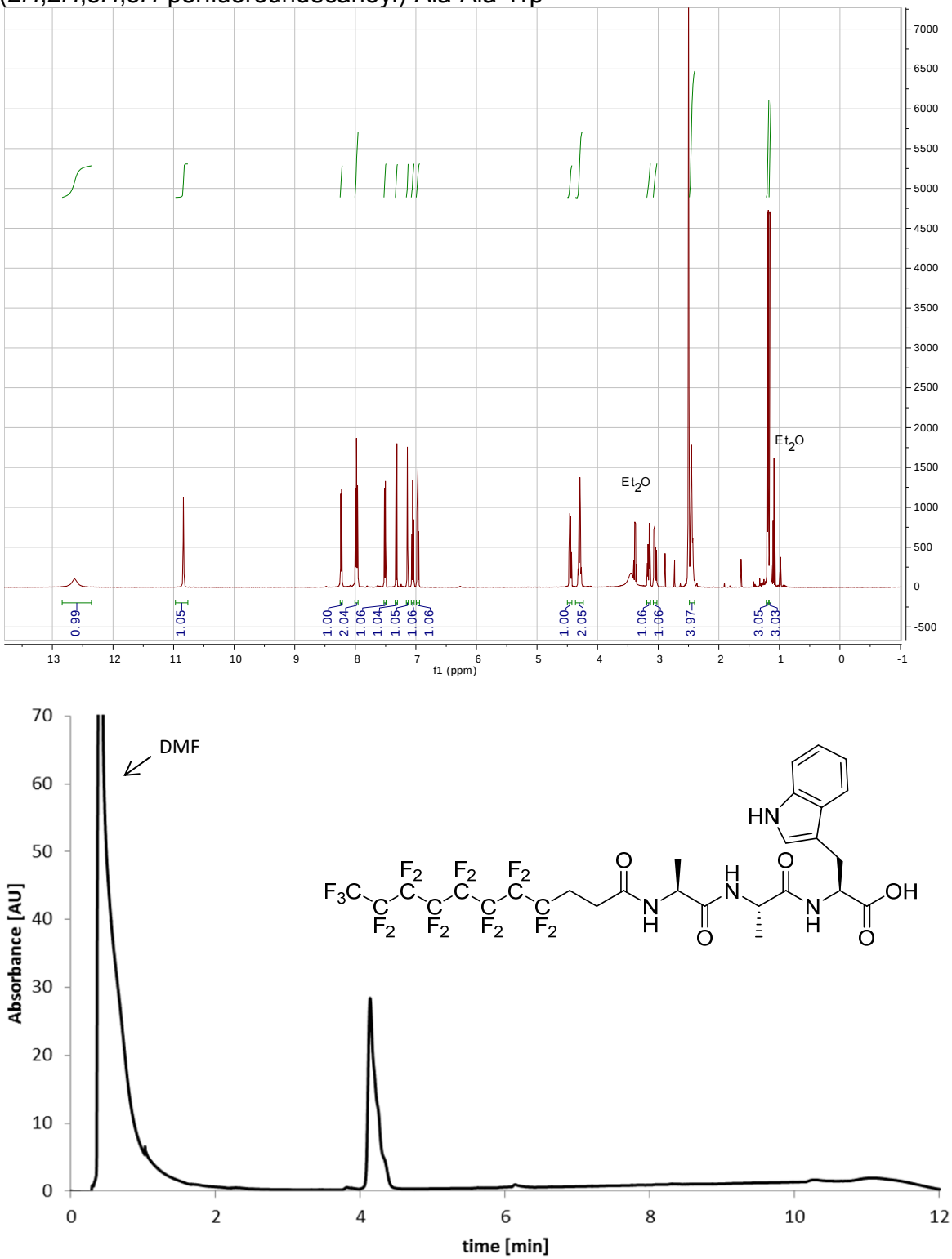

S6. (2*H*,2*H*,3*H*,3*H*-perfluoroundecanoyl)-Ala-Ala-Trp: Top: ^{1}H-NMR (DMSO-d_6, 500 MHz, 293 K), Bottom: UV-Vis-trace 190-500 nm of UPLC chromatogram (Method 2).

Ac-N^{α}-Me-Ala-N^{α}-Me-Trp(Me)-N^{α}-Me-Ala-N(Me)$_2$ **2**

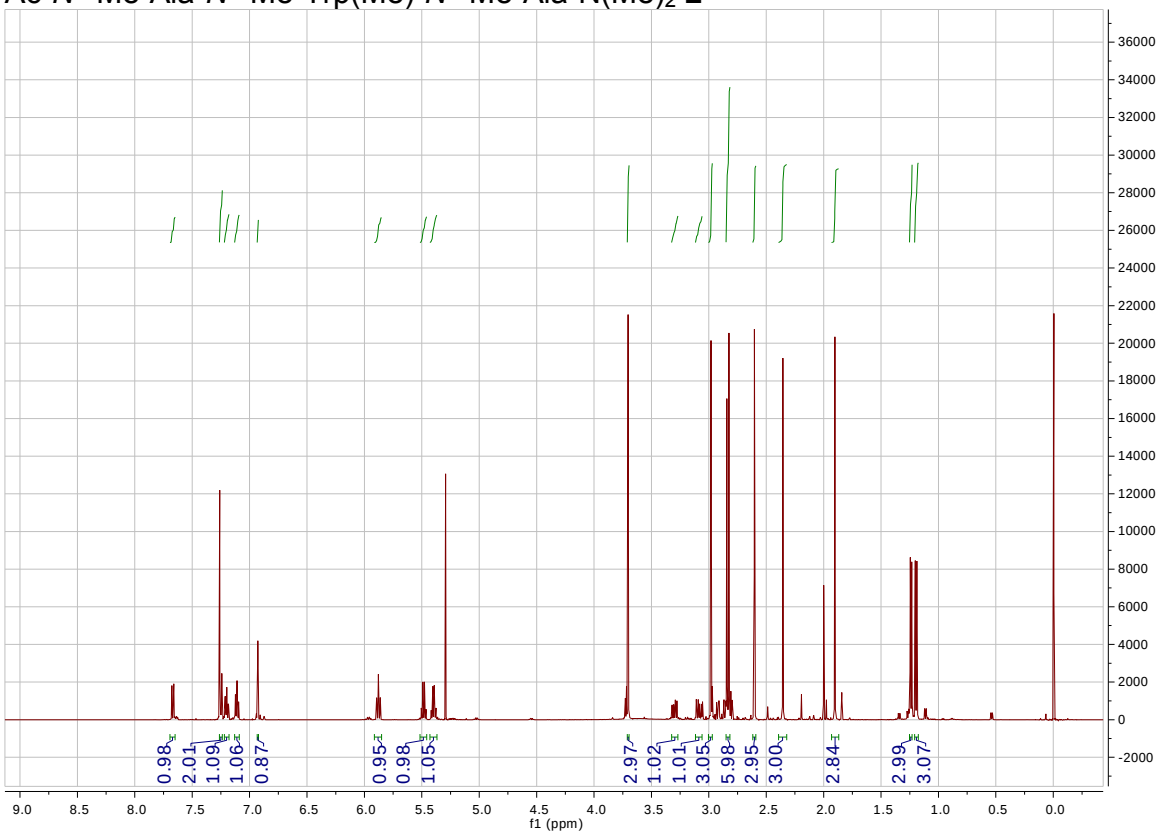

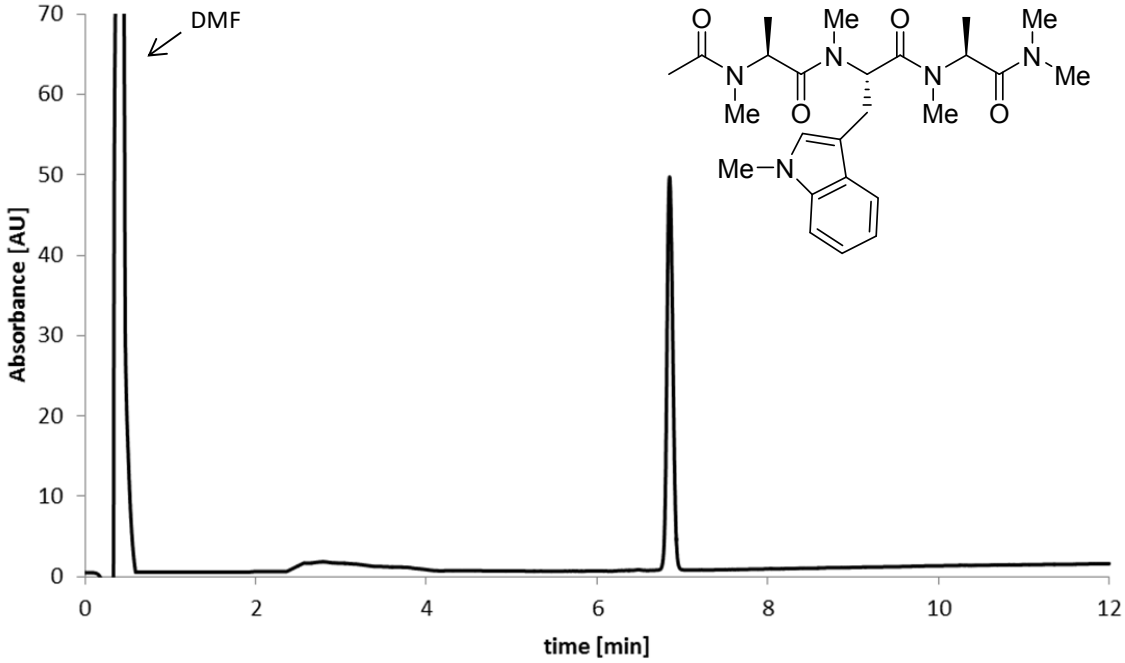

S7. Ac-N$^{\alpha}$-Me-Ala-N$^{\alpha}$-Me-Trp(Me)-N$^{\alpha}$-Me-Ala-N(Me)$_2$ **2**. Top: ^{1}H-NMR ($CDCl_3$, 500 MHz, 293 K), Bottom: UV-Vis-trace 190-500 nm of UPLC chromatogram (Method 2).

(2*H*,2*H*,3*H*,3*H*-perfluorooctanoyl)-Ala-Trp-Ala-NH_2 **3**

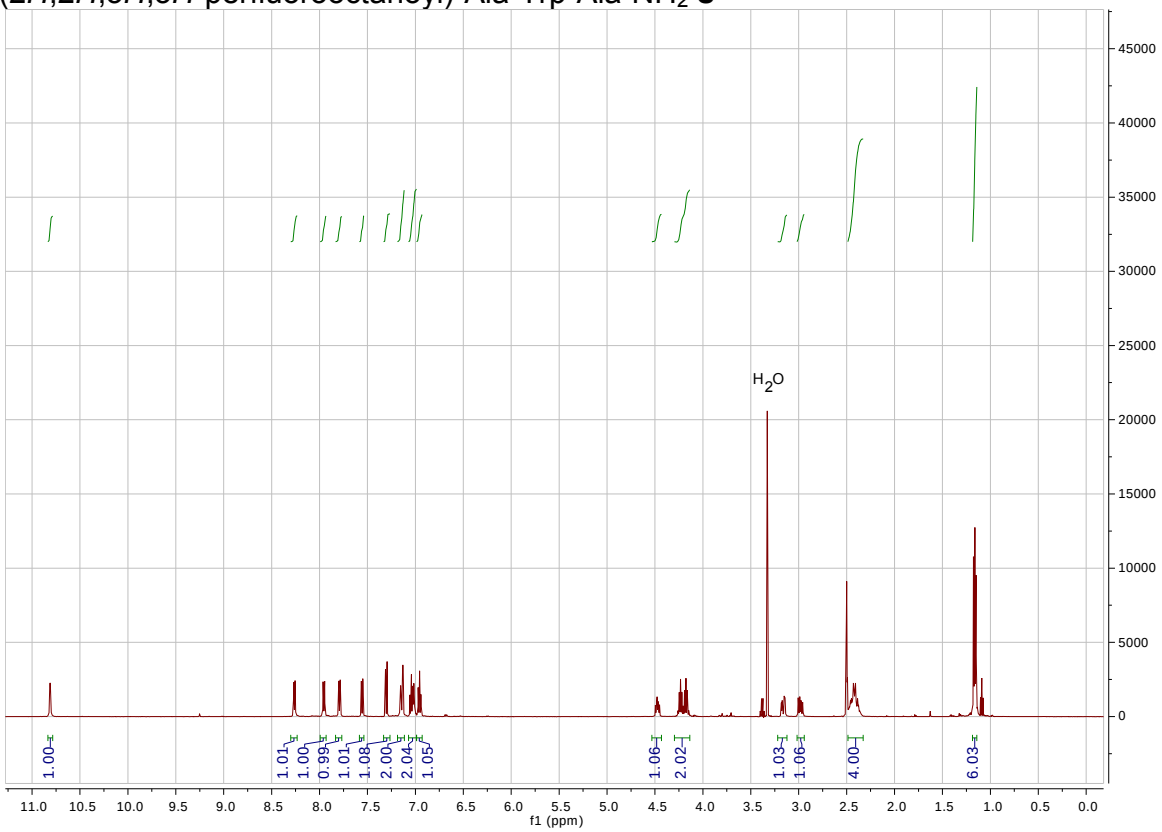

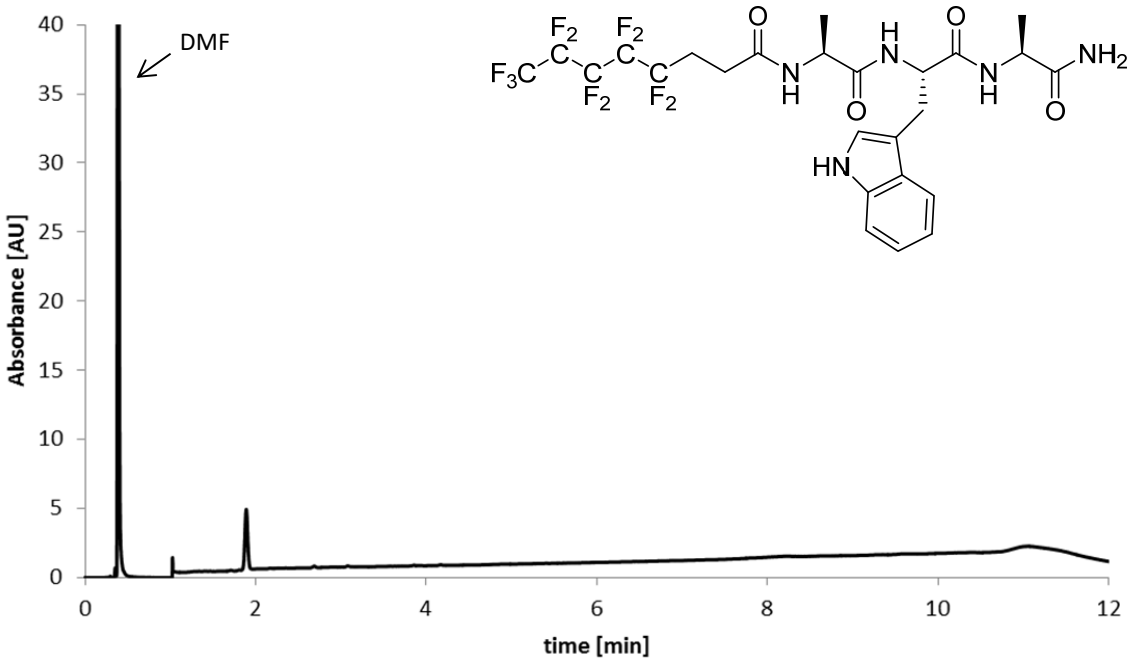

S8. (2*H*,2*H*,3*H*,3*H*-perfluorooctanoyl)-Ala-Trp-Ala-NH_2. Top: ^{1}H-NMR (DMSO-d_6, 500 MHz, 293 K), Bottom: UV-Vis-trace 190-500 nm of UPLC chromatogram (Method 2).

(2*H*,2*H*,3*H*,3*H*-perfluorooctanoyl)-N^{α}-Me-Ala-N^{α}-Me-Trp(Me)-N^{α}-Me-Ala-N(Me)$_2$ **4**

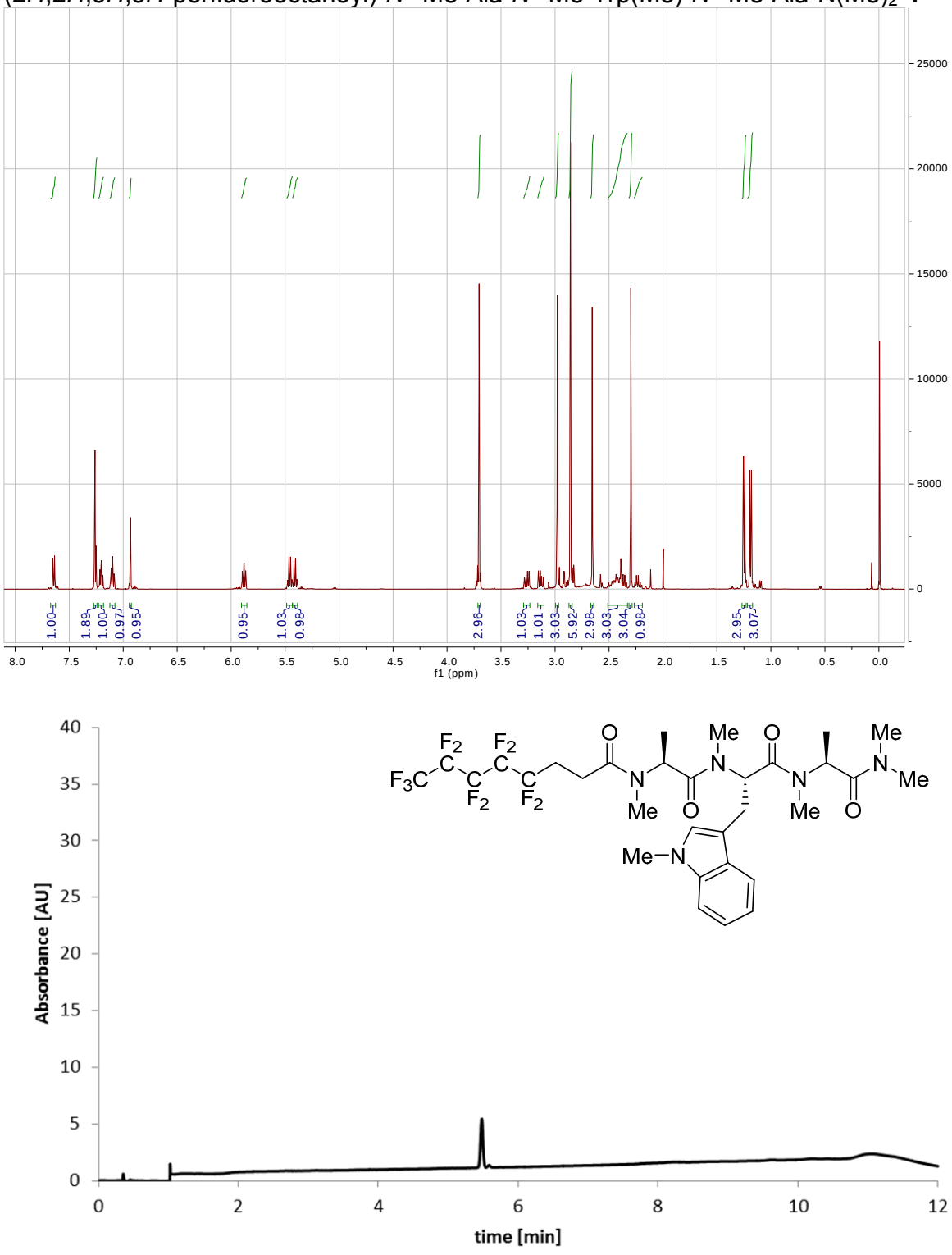

S9. (2*H*,2*H*,3*H*,3*H*-perfluorooctanoyl)-N^{α}-Me-Ala-N^{α}-Me-Trp(Me)-N^{α}-Me-Ala-N(Me)$_2$. Top: ^{1}H-NMR ($CDCl_3$, 500 MHz, 293 K), Bottom: UV-Vis-trace 190-500 nm of UPLC chromatogram (Method 2).

(2*H*,2*H*,3*H*,3*H*-perfluorooctanoyl)-Ala-Trp-Ala-(2*H*,2*H*,3*H*,3*H*-perfluorodecylamid) **5**

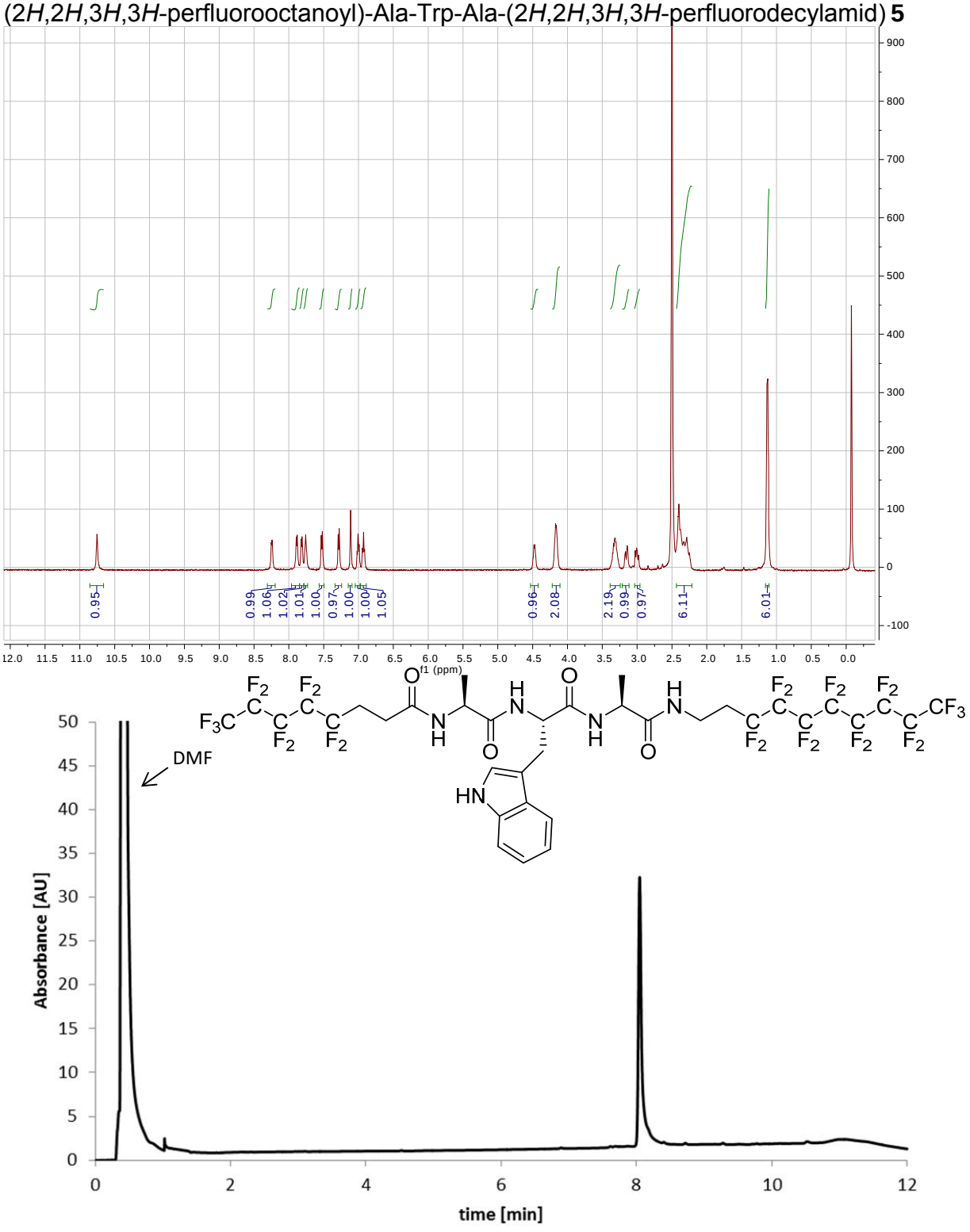

S9:

S10. (2*H*,2*H*,3*H*,3*H*-perfluorooctanoyl)-Ala-Trp-Ala-(2*H*,2*H*,3*H*,3*H*-perfluorodecylamid). Top: ^{1}H-NMR (DMSO-d_6, 500 MHz, 293 K), Bottom: UV-Vis-trace 190-500 nm of UPLC chromatogram (Method 2).

(2*H*,2*H*,3*H*,3*H*-perfluoroundecanoyl)-Ala-Trp-Ala-(2*H*,2*H*,3*H*,3*H*-perfluorodecylamid) **6**

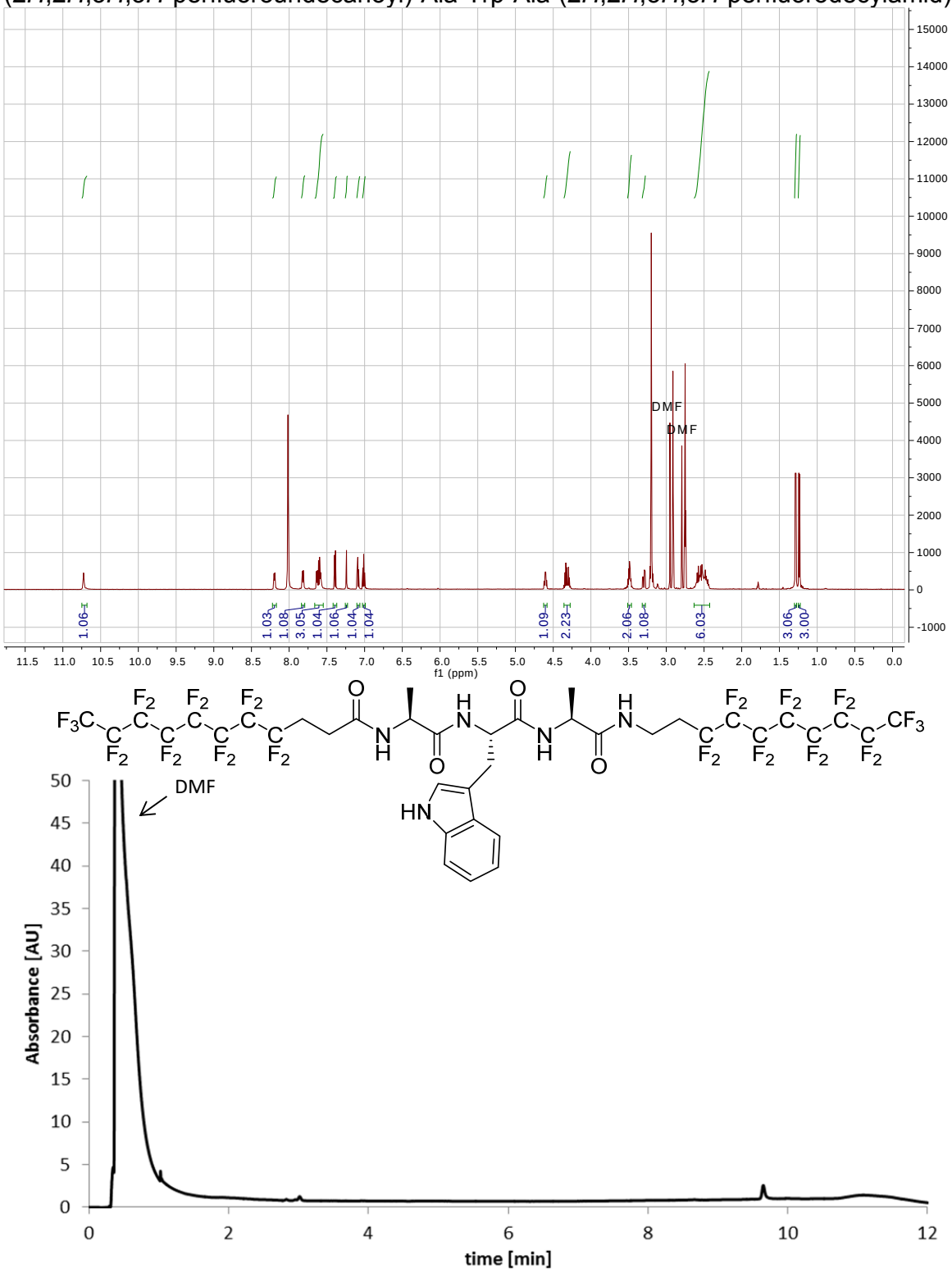

S11. (2*H*,2*H*,3*H*,3*H*-perfluoroundecanoyl)-Ala-Trp-Ala-(2*H*,2*H*,3*H*,3*H*-perfluorodecylamid) **6**. Top: ^{1}H-NMR (DMF-d_7, 600 MHz, 333 K), Bottom: UV-Vis-trace 190-500 nm of UPLC chromatogram (Method 2).

(2*H*,2*H*,3*H*,3*H*-perfluoroundecanoyl)-Trp-Ala-Ala-(2*H*,2*H*,3*H*,3*H*-perfluorodecylamid) **7**

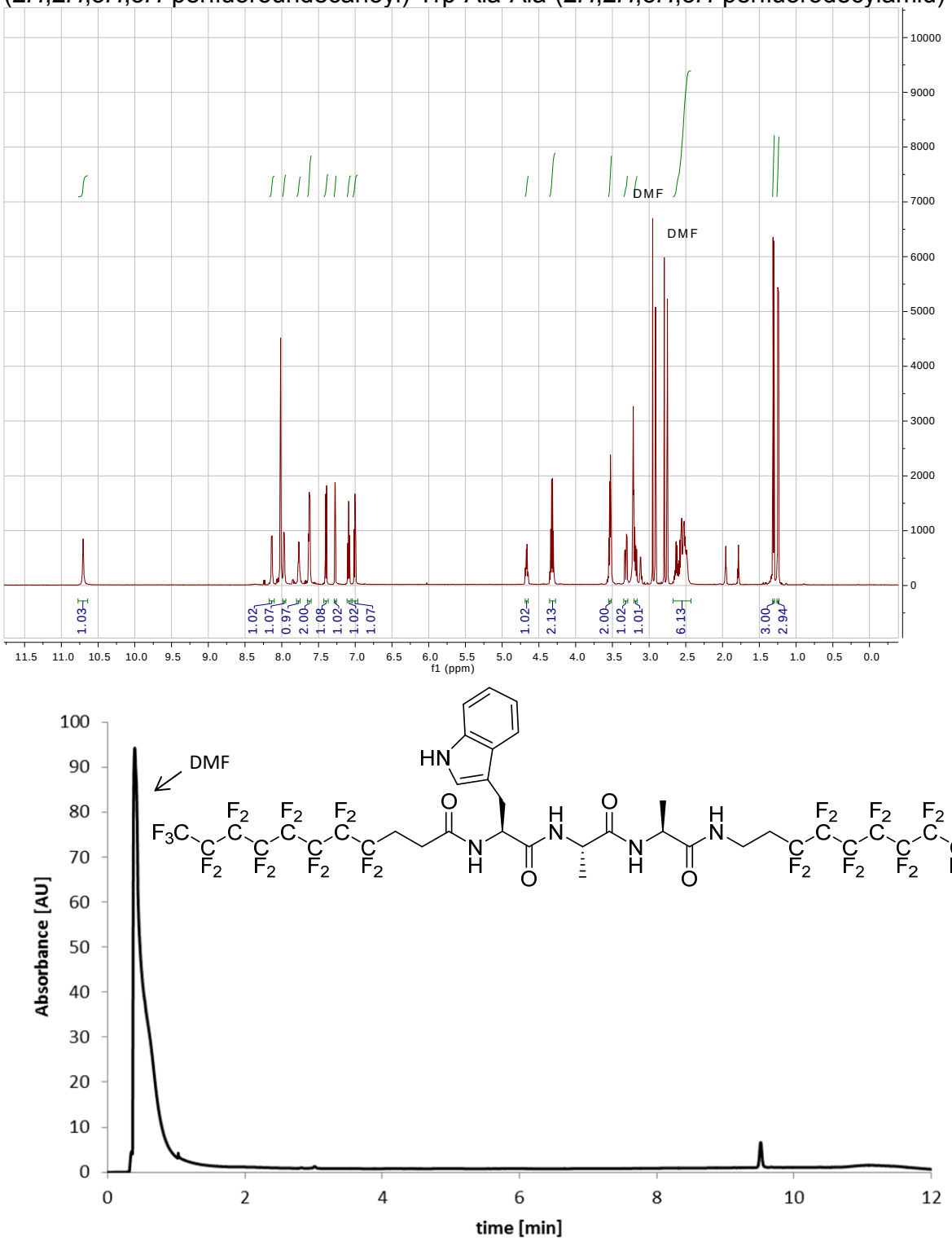

S12. (2*H*,2*H*,3*H*,3*H*-perfluoroundecanoyl)-Trp-Ala-Ala-(2*H*,2*H*,3*H*,3*H*-perfluorodecylamid) **7**. Top: ^{1}H-NMR (DMF-d_7, 600 MHz, 333 K), Bottom: UV-Vis-trace 190-500 nm of UPLC chromatogram (Method 2).

(2*H*,2*H*,3*H*,3*H*-perfluoroundecanoyl)-Ala-Ala-Trp-(2*H*,2*H*,3*H*,3*H*-perfluorodecylamid) **8**

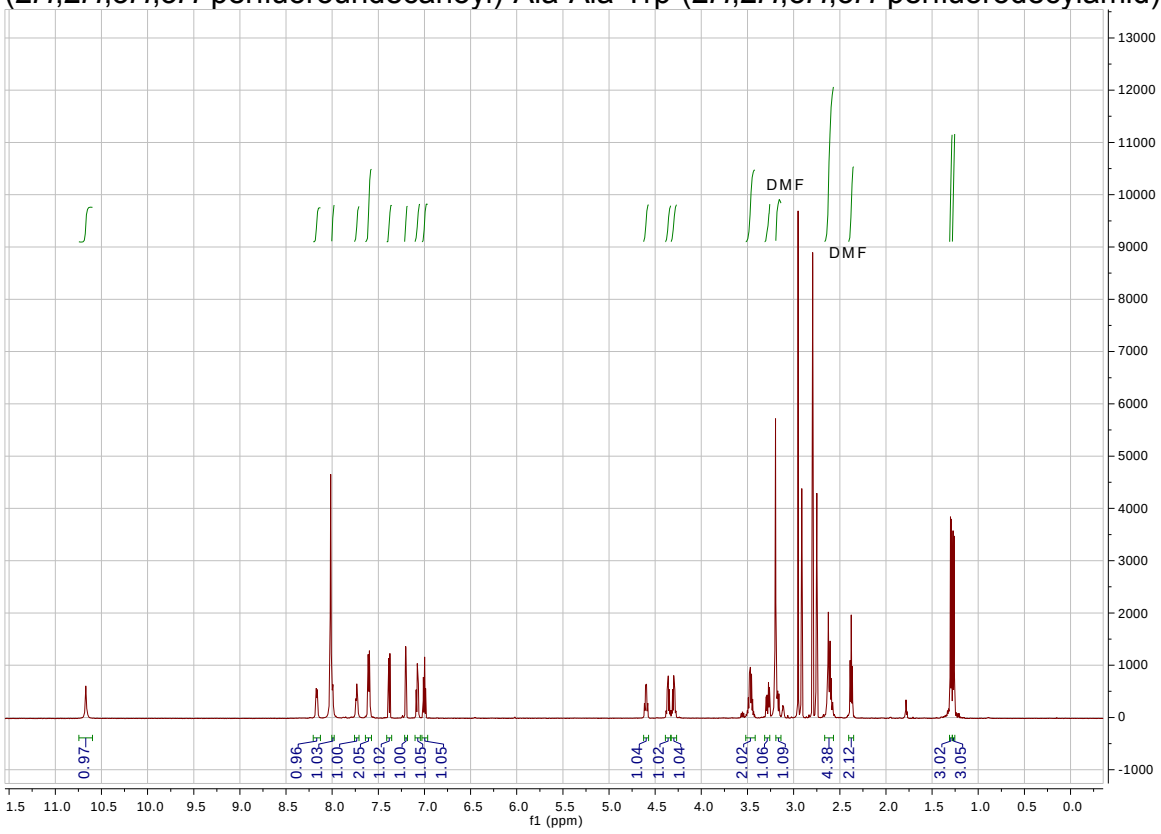

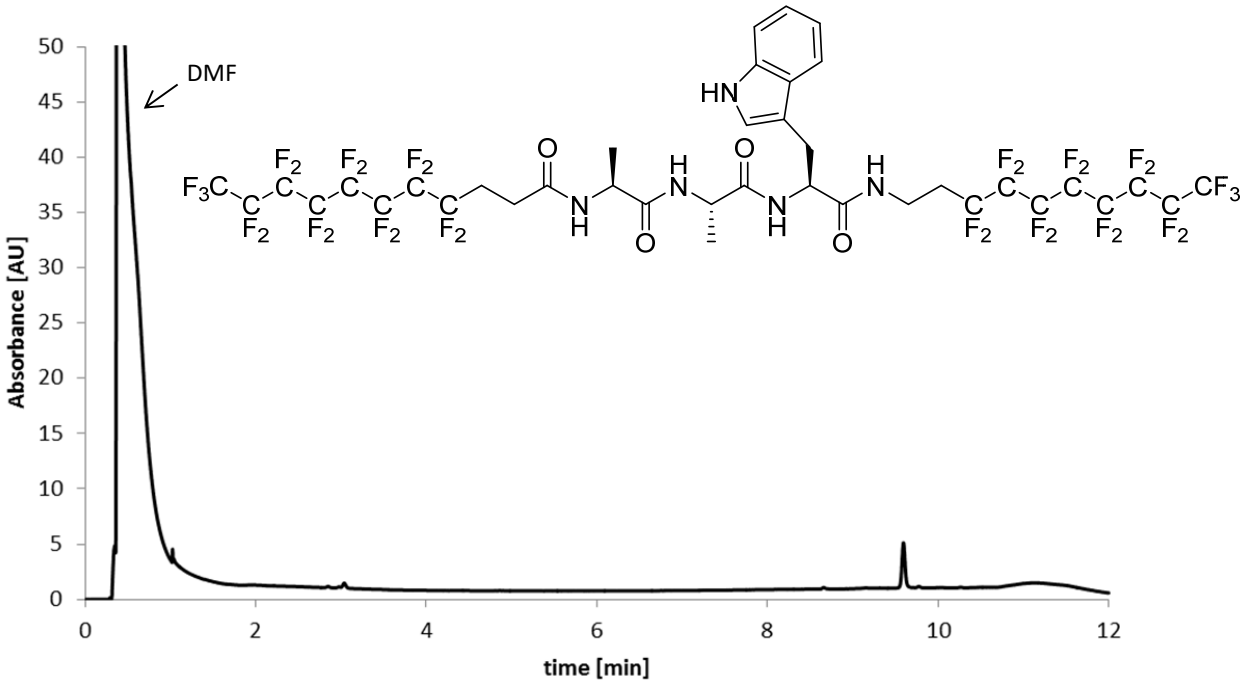

S13. (2*H*,2*H*,3*H*,3*H*-perfluoroundecanoyl) -Ala-Ala-Trp-(2*H*,2*H*,3*H*,3*H*-perfluorodecylamid) **8**. Top: ^{1}H-NMR (DMF-d_7, 600 MHz, 333 K), Bottom: UV-Vis-trace 190-500 nm (UPLC, Method 2).

NHS-ester of *2H,2H,3H,3H*-perfluorodecanoic acid

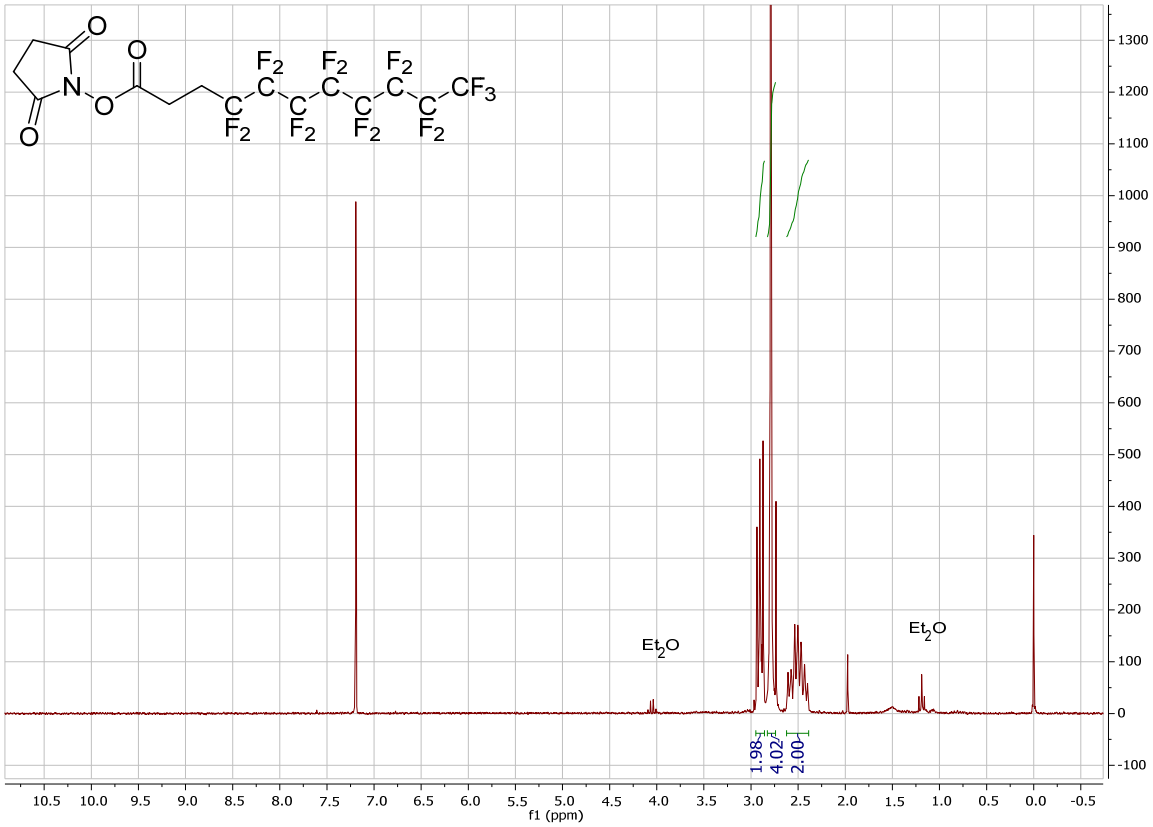

S14. *2H,2H,3H,3H*-perfluorodecanoic acid NHS ester. ^{1}H-NMR ($CDCl_3$, 500 MHz, 293 K).

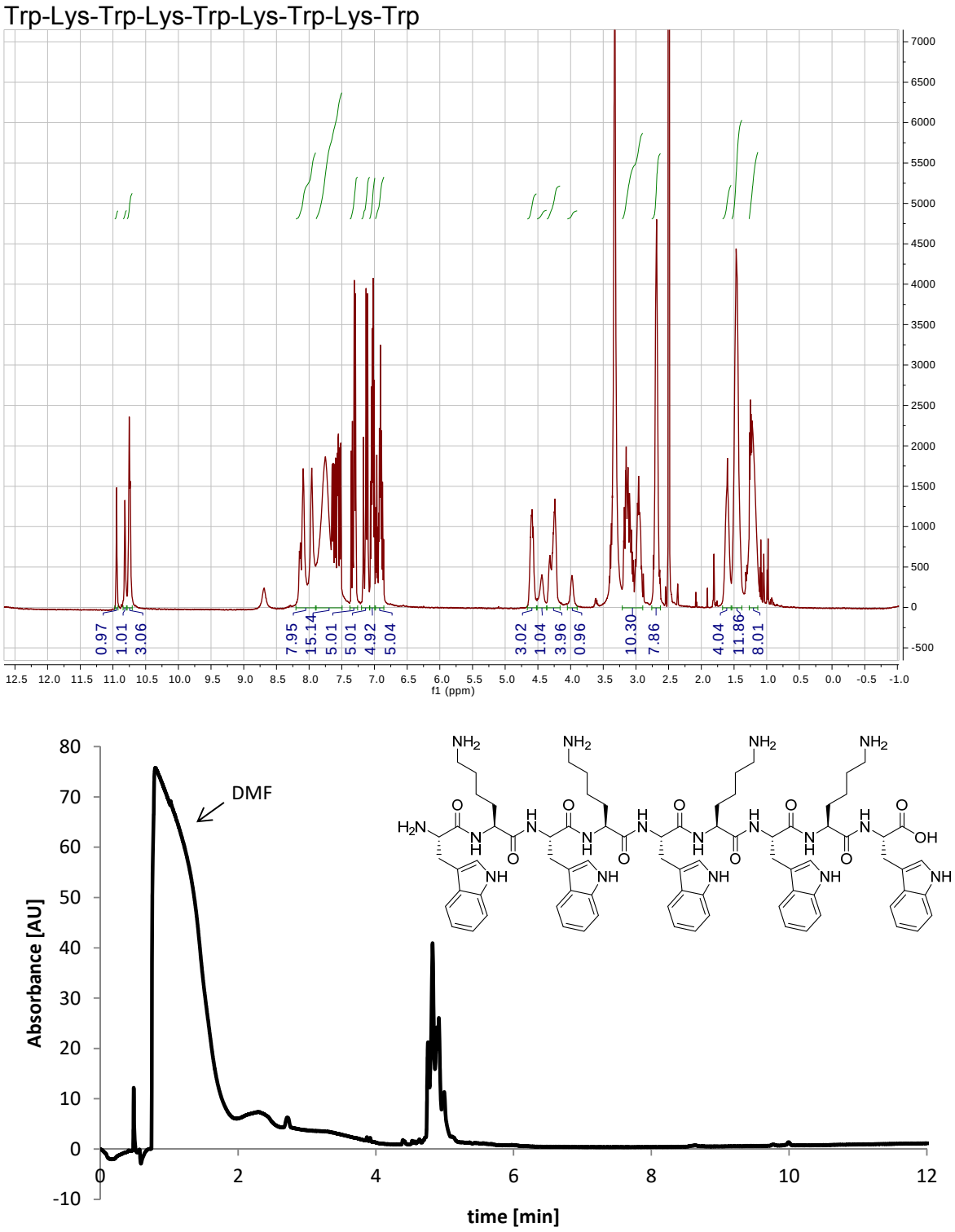

S15. Trp-Lys-Trp-Lys-Trp-Lys-Trp-Lys-Trp. Top: ^{1}H-NMR (DMSO-d_6, 500 MHz, 293 K), Bottom: UV-Vis-trace 190-500 nm of UPLC chromatogram (Method 1). The chromatogram shows multiple peaks with identical absorption and MS-spectra which are possibly caused by interconverting conformers.

Compound **9**

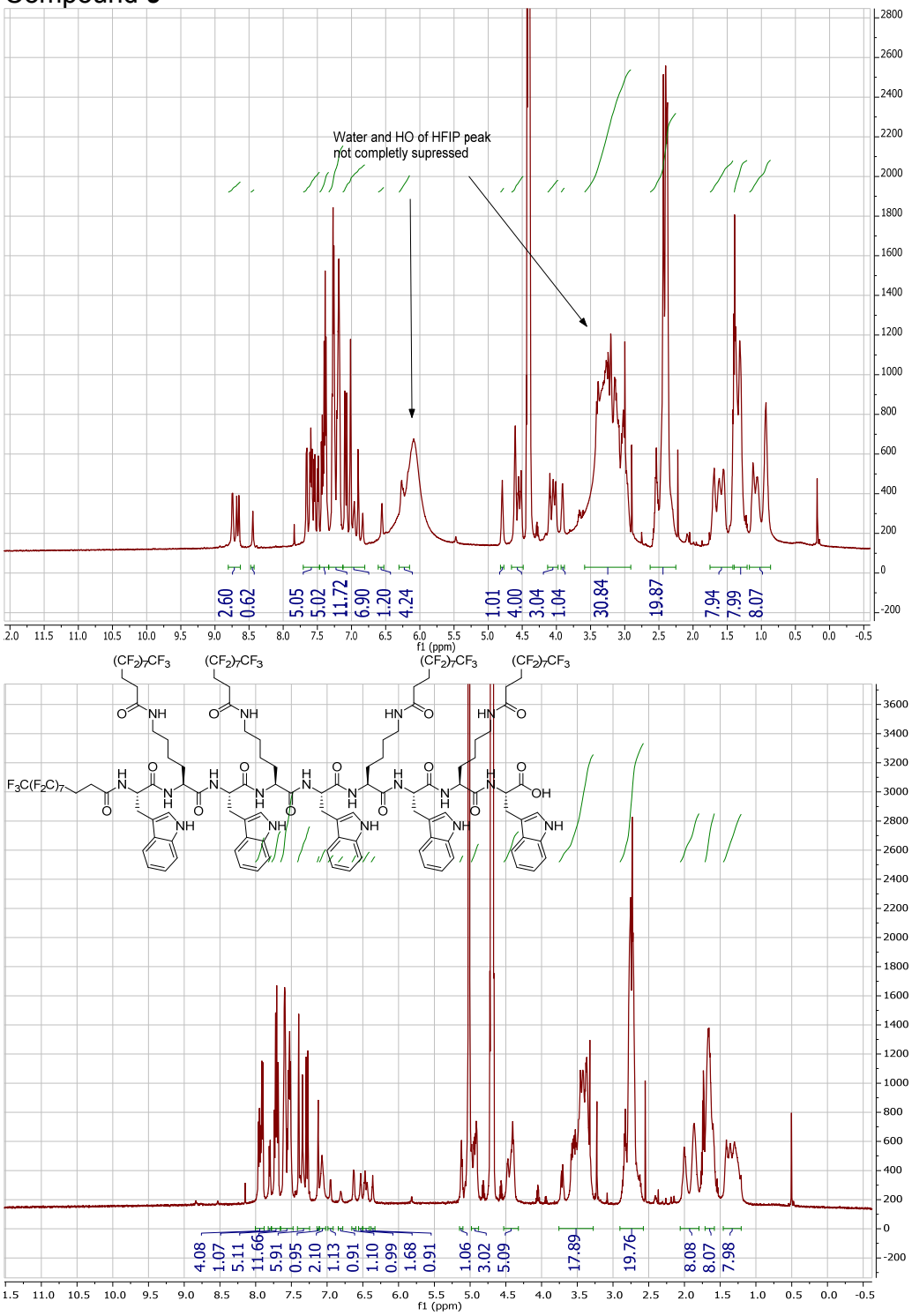

S16. Compound **9**. Top: ^{1}H-NMR (HFIP-d_2+ 20 mol% H2O, presat (water and OH-HFIP signal suppression, 600 MHz, 293 K), Bottom: : ^{1}H-NMR (HFIP-d_2, 600 MHz, 293 K).

References

[1] M. Amblard, J.-A. Fehrentz, J. Martinez, G. Subra, Methods and protocols of modern solid phase peptide synthesis. *Mol. Biotechnol.* **2006**, *33*, 239-254.

[2] H. R. Morris, D. H. Williams, R. P. Ambler, Determination of the sequences of protein-derived peptides and peptide mixtures by mass spectrometry. *Biochem. J.* **1971**, *125*, 189-201.

[3] Malik, L., Nygaard, J., Hoiberg-Nielsen, R., Arleth, L., Hoeg-Jensen, T., Jensen, K. J. Perfluoroalkyl Chains Direct Novel Self-Assembly of Insulin. *Langmuir* **2012**, *28*, 593-603.

Chapter 2. Matter-wave interference of modified tripeptides

Compounds **4**-**7** were described in chapter 1.[1]

Modified Trp-Lys-Gly 8

The unmodified Lys-Trp-Gly was synthesized on a rink-amid resin (2.7 g, 0.54 mmol/g) following known procedures.[1] The protected amino acids (3.00 eq., 4.37 mmol), PyBOP (3.00 eq., 2.27 g, 4.37 mmol) and DIPEA (6.00 eq., 1.45 mL, 8.74 mmol) were used with a reaction time of 2 h per coupling. After cleavage of the resin with TFA and precipitation from Et_2O, the unmodified crude peptide (435 mg, 1.12 mmol, 77%) was obtained. It was directly dissolved in DMF (50 mL) and coupled to the NHS-ester of perfluoro-2*H,*2*H,*3*H,*3*H*-undecanoic acid (4.00 eq., 317 mg, 3.36 mmol) under stirring for 5 h at room temperature. The solvent was reduced to 20 mL, and water (20 mL) was added. The crude precipitate was reprecipitated twice from DMF by addition of water. The modified tripeptide **8** was obtained in moderate purity (524 mg, 506 µmol, 45%). UPLC-MS: Method 2, T_R = 4.32 min; MS (ESI+) m/z: 1037.6 [100%, M + H^+].

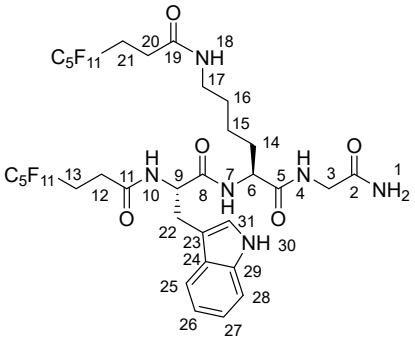

8

^{1}H-NMR (DMSO-d_6, 500 MHz, 293 K) δ: 10.91 (s, 1 H, H-30), 8.88-8.80 (m, 1 H, H-10), 8.78-8.70 (m, 1 H, H-7), 8.23-8.18 (m, 1 H, H-4), 8.18-8.11 (m, 1 H, H-18), 7.51 (d, $^3J_{H\text{-}H}$ = 7.6 Hz, 1 H, H-28), 7.30 (d, $^3J_{H\text{-}H}$ = 7.6 Hz, 1 H, H-25), 7.27 (s, 1 H, H-1), 7.14 (d, $^3J_{H\text{-}H}$ = 2.3 Hz, 1 H, H-31), 7.06 (s, 1 H, H-1), 7.03 (t, $^3J_{H\text{-}H}$ = 7.6 Hz, 1 H, H-26), 6.94 (t, $^3J_{H\text{-}H}$ = 7.4 Hz, 1 H, H-27), 4.57-4.51 (m, 1 H, H-9), 4.18-4.11 (m, 1 H, H-6), 3.62 (dd, $^2J_{H\text{-}H}$ = 16.8 Hz, $^3J_{H\text{-}H}$ = 6.1 Hz, 1 H, H-3), 3.55 (dd, $^2J_{H\text{-}H}$ = 16.8 Hz, $^3J_{H\text{-}H}$ = 5.7 Hz, 1 H, H-3), 3.15 (dd, $^2J_{H\text{-}H}$ = 14.7 Hz, $^3J_{H\text{-}H}$ = 4.8 Hz, 1 H, H-22), 3.02 (q, $^3J_{H\text{-}H}$ = 6.6 Hz, 2 H, H-17), 2.94 (dd, $^2J_{H\text{-}H}$ = 14.7 Hz, $^3J_{H\text{-}H}$ = 9.4 Hz, 1 H, H-22), 2.47-2.25 (H-12,H-13, H-20 and H-21), 1.71-1.52 (m, 2 H, H-14), 1.42-1.21 (m, 4 H, H-15 and H-16). ^{13}C-NMR δ: 171.9 (C-8), 171.7 (C-5), 170.8 (C-2), 169.3 (C-11), 168.8 (C-19), 135.8 (C-29), 127.1 (C-24), 123.4 (C-31), 120.5 (C-26), 118.4 (C-28), 117.9 (C-27), 111.0 (C-25), 110.0 (C-23), 54.1 (C-9), 53.0 (C-6), 41.8 (C-3), 38.2 (C-17), 30.9 (C-14), 28.4 (C-16), 27.4 (C-22), 25.5 (C-12, C-13, C-20 and C-21), 22.4 (C-15), all fluorinated carbon atoms were not detected.

Modified Trp-Gly-Lys 9

Tripeptide **9** was prepared following the procedure described for the preparation of **8**. The unmodified peptide (398 mg, 1.02 mmol, 70%) was collected after precipitation and converted into **9** (465 mg of material with moderate purity, 449 µmol, 44%). UPLC-MS: Method 2, T_R = 4.29 min; MS (ESI+) m/z: 1037.5 [100%, M + H^+].

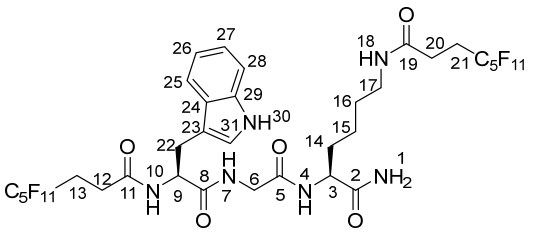

9

^{1}H-NMR (DMSO-d_6, 500 MHz, 293 K) δ: 10.91 (d, $^3J_{H\text{-}H}$ = 2.4 Hz, 1 H, H-30), 8.78 (d, $^3J_{H\text{-}H}$ = 7.8 Hz, 1 H, H-4), 8.72 (d, $^3J_{H\text{-}H}$ = 7.7 Hz, 1 H, H-4), 8.38 (t, $^3J_{H\text{-}H}$ = 5.9 Hz, 1 H, H-7), 8.19 (t, $^3J_{H\text{-}H}$ = 5.6 Hz, 1 H, H-18), 7.53 (d, $^3J_{H\text{-}H}$ = 7.9 Hz, 1 H, H-28), 7.30 (d, $^3J_{H\text{-}H}$ = 8.1 Hz, 1 H, H-25), 7.25 (s, 1 H, H-1), 7.14 (d, $^3J_{H\text{-}H}$ = 2.3 Hz, 1 H, H-31), 7.07 (s, 1 H, H-1), 7.03 (t, $^3J_{H\text{-}H}$ = 7.6 Hz, 1 H, H-26), 6.94 (t, $^3J_{H\text{-}H}$ = 7.4 Hz, 1 H, H-27),4.46-4.40 (m, 1 H, H-9), 4.18-4.11 (m, 1 H, H-3), 3.66 (dd, $^2J_{H\text{-}H}$ = 16.8 Hz, $^3J_{H\text{-}H}$ = 6.2 Hz, 1 H, H-6), 3.51 (dd, $^2J_{H\text{-}H}$ = 16.8 Hz, $^3J_{H\text{-}H}$ = 5.4 Hz, 1 H, H-6), 3.16 (dd, $^2J_{H\text{-}H}$ = 14.7 Hz, $^3J_{H\text{-}H}$ = 4.9 Hz, 1 H, H-22), 3.05-2.91 (m, 3 H, H-17 and H-22), 2.47-2.25 (H-12, H-13, H-20 and H-21), 1.55-1.40 (m, 2 H, H-14), 1.36-1.07 (m, 4 H, H-15 and H-16). ^{13}C-NMR δ: 171.9 (C-11), 171.7 (C-8), 170.8 (C-2), 169.6 (C-5), 169.0 (C-19), 135.9 (C-29), 127.2 (C-24), 123.4 (C-31), 120.3 (C-26), 118.0 (C-28), 117.8 (C-27), 110.9 (C-25), 110.0 (C-23), 53.7 (C-9), 53.0 (C-3), 41.7 (C-6), 37.8 (C-17), 31.0 (C-14), 28.2 (C-16), 26.6 (C-22), 25.5 (C-12, C-13, C-20 and C-21), 22.2 (C-15) all fluorinated carbon atoms were not detected.

Modified Tyr-Gly-Trp 10

The unmodified Tyr-Gly-Trp was synthesized on a 2-chlorotrityl chloride resin (2.10 g, 1 mmol/g) following known procedures.[1] The protected amino acids (3.00 eq., 6.30 mmol), PyBOP (3.00 eq., 3.28 g, 6.30 mmol) and DIPEA (6.00 eq., 2.09 mL, 12.6 mmol) were used with a reaction time of 2 h per coupling. Perfluoro-2*H*,2*H*,3*H*,3*H*-undecanoic acid (2.00 eq., 2.07 g, 4.20 mmol) was coupled to the N-terminus of the still resin-bond peptide with PyBOP (2.00 eq., 2.19 g, 4.20 mmol) and DIPEA (4.00 eq., 1.40 mL, 8.40 mmol) for overnight. Afterward, the peptide was cleaved from the resin with TFA and precipitated from Et_2O yielding the crude N-terminal modified peptide (725 mg, 807 µmol, 38%). To a solution of this peptide in DMF (100 mL) perfluoro-1*H*,1*H*,2*H*,2*H*-decan-1-amine (3.00 eq., 1.04 g, 2.42 mmol), HATU (3.00 eq., 920 mg, 2.42 mmol) and DIPEA (6.00 eq., 800 µl, 4.84 mmol) were added and the mixture was stirred overnight at room temperature. The solvent was reduced to 20 mL, and water (20 mL) was added. The crude precipitate was reprecipitated twice from DMF by addition

of water. The modified tripeptide **10** was obtained in moderate purity (835 mg, 635 µmol, 79%). UPLC-MS: Method 2, T_R = 4.94 min; MS (ESI+) m/z: 1366.3 [100%, M + Na^+].

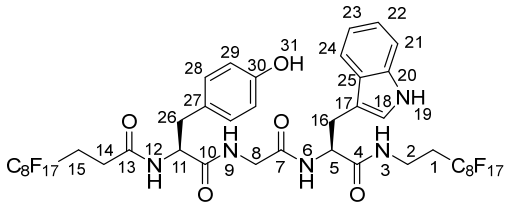

10

^{1}H-NMR (DMSO-d_6, 500 MHz, 293 K) δ: 10.81 (s, 1 H, H-19), 9.15 (s, 1 H, H-31), 8.42 (d, $^3J_{H\text{-}H}$ = 7.5 Hz, 1 H, H-12), 7.51 (d, $^3J_{H\text{-}H}$ = 7.8 Hz, 1 H, H-24), 8.33 (t, $^3J_{H\text{-}H}$ = 5.4 Hz, 1 H, H-9), 7.93 (d, $^3J_{H\text{-}H}$ = 8.2 Hz, 1 H, H-6), 7.75 (t, $^3J_{H\text{-}H}$ = 5.4 Hz, 1 H, H-3) 7.29 (d, $^3J_{H\text{-}H}$ = 8.1 Hz, 1 H, H-21), 7.12 (d, $^3J_{H\text{-}H}$ = 2.4 Hz, 1 H, H-18), 7.03-6.97 (m, 2 H, H-22 and H-28), 6.92 (t, $^3J_{H\text{-}H}$ = 7.5 Hz, 1 H, H-23), 6.63 (d, $^3J_{H\text{-}H}$ = 8.5 Hz, 2 H, H-29), 4.43 (q, $^3J_{H\text{-}H}$ = 8.1 Hz, 1 H, H-5), 4.30 (q, $^3J_{H\text{-}H}$ = 7.5 Hz, 1 H, H-11), 3.87 (dd, $^2J_{H\text{-}H}$ = 16.7 Hz, $^3J_{H\text{-}H}$ = 6.5 Hz, 1 H, H-8), 3.48-3.38 (m, 3 H, H-2 and H-8), 3.32-3.22 (m, 2 H, H-2), 3.15-3.08 (m, 1 H, H-16), 2.97-291 (m, 1 H, H-16), 2.73-2.59 (m, 2 H, H-26), 2.43-2.10 (m, 6 H, H-1, H-14 and H-15). ^{13}C-NMR δ: 160.8 (C-4), 155.7 (C-30), 135.9 (C-20), 129.7 (C-28), 127.2 (C-27), 127.8 (C-25), 123.3 (C-18), 120.4 (C-22), 117.9 (C-24), 117.8 (C-23), 114.6 (C-29), 110.9 (C-21), 109.7 (C-17), 54.9 (C-11), 53.7 (C-5), 41.9 (C-8), 35.8 (C-26), 30.8 (C-2), 29.2 (C-1), 26.8 (C-16), 25.6 (C-14 and C-15), C-7, C-10, C-13 and all fluorinated carbon atoms were not detected.

Modified Tyr-Gly-Trp 11

Tripeptide **11** was prepared following the procedure for **10**. The N-terminal modified peptide (820 mg, 913 µmol, 43%) was collected after precipitation and converted into **11.** The product was obtained after precipitation in moderate purity (932 mg, 694 µmol, 76%). UPLC-MS: Method 2, T_R = 4.93 min; MS (ESI+) m/z: 1366.3 [100%, M + Na^+].

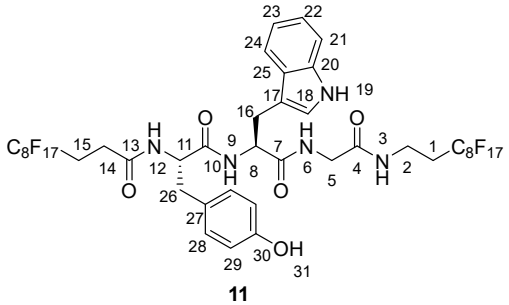

11

^{1}H-NMR (DMSO-d_6, 500 MHz, 293 K) δ: 10.84 (d, $^3J_{H\text{-}H}$ = 2.3 Hz, 1 H, H-19), 9.12 (s, 1 H, H-31), 8.20-8.11 (m, 3 H, H-6, H-9 and H-12), 7.87 (t, $^3J_{H\text{-}H}$ = 5.8 Hz, 1 H, H-3) 7.54 (d, $^3J_{H\text{-}H}$ = 7.9 Hz, 1 H, H-24), 7.32 (d, $^3J_{H\text{-}H}$ = 8.1 Hz, 1 H, H-21), 7.15 (d, $^3J_{H\text{-}H}$ = 2.3 Hz, 1 H, H-18), 7.06 (t, $^3J_{H\text{-}H}$ = 8.0 Hz, 1 H, H-22), 6.97 (t,

$^{3}J_{H\text{-}H}$ = 8.1 Hz, 1 H, H-23), 6.89 (d, $^{3}J_{H\text{-}H}$ = 8.5 Hz, 2 H, H-28), 6.55 (d, $^{3}J_{H\text{-}H}$ = 8.5 Hz, 2 H, H-29), 4.43 (q, $^{3}J_{H\text{-}H}$ = 6.9 Hz, 1 H, H-8), 4.33-4.27 (m, 1 H, H-11), 3.78 (dd, $^{2}J_{H\text{-}H}$ = 16.7 Hz, $^{3}J_{H\text{-}H}$ = 6.4 Hz, 1 H, H-5), 3.50 (dd, $^{2}J_{H\text{-}H}$ = 16.7 Hz, $^{3}J_{H\text{-}H}$ = 5.1 Hz, 1 H, H-5), 3.33 (m, 2 H, H-2), 3.19 (dd, $^{2}J_{H\text{-}H}$ = 14.7 Hz, $^{3}J_{H\text{-}H}$ = 5.5 Hz, 1 H, H-16), 3.02 (dd, $^{2}J_{H\text{-}H}$ = 14.7 Hz, $^{3}J_{H\text{-}H}$ = 8.3 Hz, 1 H, H-16), 2.81 (dd, $^{2}J_{H\text{-}H}$ = 14.1 Hz, $^{3}J_{H\text{-}H}$ = 4.7 Hz, 1 H, H-26), 2.58 (dd, $^{2}J_{H\text{-}H}$ = 14.1 Hz, $^{3}J_{H\text{-}H}$ = 9.6 Hz, 1 H, H-26), 2.45-2.24 (m, 6 H, H-1, H-14 and H-15). ^{13}C-NMR δ: 171.5 (C-7), 169.2 (C-13), 168.7 (C-4), 155.6 (C-30), 135.9 (C-20), 129.6 (C-28), 127.4 (C-27), 127.2 (C-25), 123.1 (C-18), 120.5 (C-22), 118.0 (C-24), 117.8 (C-23), 114.5 (C-29), 111.0 (C-21), 109.6 (C-17), 54.7 (C-11), 53.6 (C-8), 41.8 (C-5), 36.0 (C-26), 30.5 (C-2), 29.3 (C-1), 26.6 (C-16), 25.5 (C-14 and C-15), C-10 and all fluorinated carbon atoms were not detected.

Modified Trp-Pro-Ala 12

Tripeptide **12** was prepared following the procedures for **10**. The N-terminal modified peptide (697 mg, 823 µmol, 39%) was collected after precipitation and converted into **12**. The product was obtained after precipitation in moderate purity (752 mg, 582 µmol, 71%). UPLC-MS: Method 2, T_R = 5.15 min; MS (ESI+) m/z: 1314.5 [100%, M + Na^+].

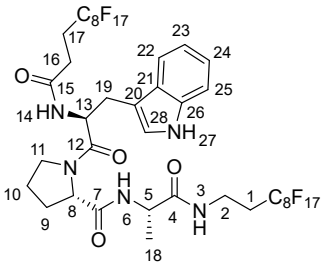

12

There are two rotamers present in solution indicated with R1 and R2 behind the atom number. ^{1}H-NMR (DMF-d_7, 500 MHz, 293 K) δ: 11.01 (d, $^{3}J_{H\text{-}H}$ = 2.4 Hz, 1 H, H-27, R1),), 10.93 (d, $^{3}J_{H\text{-}H}$ = 2.4 Hz, 1 H, H-27, R2), 8.71 (d, $^{3}J_{H\text{-}H}$ = 6.6 Hz, 1 H, H-14 , R1), 8.44 (d, $^{3}J_{H\text{-}H}$ = 7.5 Hz, 1 H, H-14, R2), 8.24 (d, $^{3}J_{H\text{-}H}$ = 7.5 Hz, 1 H, H-6, R1), 8.00 (d, $^{3}J_{H\text{-}H}$ = 7.3 Hz, 1 H, H-6 , R2), 7.97 (t, $^{3}J_{H\text{-}H}$ = 5.8 Hz, 1 H, H-3 , R2), 7.92 (t, $^{3}J_{H\text{-}H}$ = 5.9 Hz, 1 H, H-3 , R1),)), 7.66 (d, $^{3}J_{H\text{-}H}$ = 7.9 Hz, 1 H, H-22 , R2), 7.56 (d, $^{3}J_{H\text{-}H}$ = 7.9 Hz, 1 H, H-22 , R1), 7.43 (d, $^{3}J_{H\text{-}H}$ = 8.6 Hz, 1 H, H-25 , R1), 7.41 (d, $^{3}J_{H\text{-}H}$ = 8.2 Hz, 1 H, H-25 , R2), 7.35 (d, $^{3}J_{H\text{-}H}$ = 2.4 Hz, 1 H, H-28 , R2), 7.32 (d, $^{3}J_{H\text{-}H}$ = 2.4 Hz, 1 H, H-28 , R1), 7.14-7,07 (m, 1 H, H-24), 7.05-6.99 (m, 1 H, H-23), 4.97 (td, , $^{3}J_{H\text{-}H}$ = 7.9 Hz, $^{3}J_{H\text{-}H}$ = 5.1 Hz, 1 H, H-13, R2), 4.97 (dt, , $^{3}J_{H\text{-}H}$ = 8.9 Hz, $^{3}J_{H\text{-}H}$ = 6.5 Hz, 1 H, H-13, R1), 4.40 (dd, $^{3}J_{H\text{-}H}$ = 8.3 Hz, $^{3}J_{H\text{-}H}$ = 4.7 Hz, 1 H, H-8, R2), 4.37-4.22 (m, 1 H, H-5), 3.83 (dd, $^{3}J_{H\text{-}H}$ = 8.3 Hz, $^{3}J_{H\text{-}H}$ = 1.7 Hz, 1 H, H-8, R2) 3.79-3.73 (m, 1 H, H-11, R2), 3.66-3.58 (m, 1 H, H-11, R2), 3.57-3.44 (m, 1 H, H-2), 3.44-3.36 (m, 1 H, H-11, R1) 3.33-3.26 (m, 2 H, H-11, R1 and H-19, R2), 3.22-3.11 (m, 2 H, H-19, R1, 3.10-3.00 (m, 1 H, H-19, R2), 2.64-2.32 (m, 6 H, H-1, H-16 and H-17), 2.18-2.08 (m,

1 H, H-9 , R2), 2.01-1.93 (m, 2 H, H-9, R2 and H-10, R2), 189-1.81 (m, 1 H, H-10, R2), 1.78-1.70 (m, 1 H, H-9 , R1), 1.56-1.49 (m, 2 H, H-10 , R1, 1.35-1.30 (m, 3 H, H-18), 0.96-0.86 (m, 1 H, H-9, R1). ^{13}C-NMR δ: 172.7 (C-4), 171.7 (C-12, R2), 171.6 (C-7 , R2), 171.5 (C-7, R1), 171.2 (C-12, R1), 170.0 (C-15, R1, 169.8 (C-15, R2, 136.9 (C-26), 127.9 (C-21, R2), 127.6 (C-21, R1), 124.4 (C-28, R1), 124.1 (C-28, R2), 121.2 (C-24), 118.7 (C-22, R1), 118.6 (C-23), 118.3 (C-22, R2), 111.6 (C-25), 110.3 (C-20, R2), 109.6 (C-20, R1), 61.1 (C-8, R2), 60.5 (C-8, R1), 53.1 (C-13, R1), 52.6 (C-13, R2), 49.7 (C-5, R1), 49.2 (C-5, R2), 47.4 (C-11, R2), 46.5 (C-11, R1), 31.6 (C-2), 30.6 (C-9, R1), 30.2 (C-1), 28.9 (C-9, R2), 28.5 (C-19, R1), 27.3 (C-19, R2), 26.3 (C-16 and C-17), 24.9 (C-10, R2), 21.8 (C-10, R1), 17.4 (C-18), all fluorinated carbon atoms were not detected.

Modified Trp-Pro-Ala 13

Tripeptide **13** was produced following the procedures for **10**. The N-terminal modified peptide (734 mg, 878 µmol, 42%) was collected after precipitation and converted into **13.** The product was obtained after precipitation in moderate purity (628 mg, 486 µmol, 55%). UPLC-MS: Method 2, T_R = 5.12 min; MS (ESI+) m/z: 1314.8 [100%, M + Na^+].

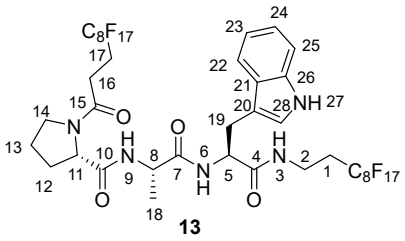

13

Two rotamers are present in solution that give rise to broad signals. ^{1}H-NMR (DMF-d_7, 500 MHz, 293 K) δ: 10.09 (b, 1 H, H-27), 8.35 (b, 1 H, H-9), 7.82 (b, 1H, H-3), 7.70-7.56 (m, 2 H, H-6 and H-22), 7.39 (b, 1 H, H-25), 7.21 (b, 1 H, H-28), 7.09 (b, 1 H, H-24), 7.00 (b, 1 H, H-23), 4.70-4.30 (m, 2 H, H-5 and H-11), 4.22 (b, 1 H, H-8), 3.70 (b, 2 H, H-14), 3.47 (b, 2 H, H-2), 3.37-3.12 (m, 2 H, H-19), 2.72-2.24 (m, 6 H, H-1, H-16 and H-17), 2.19-1.81 (m, 4 H, H-12 and H-13), 1.35-1.17 (m, 3 H, H-18). ^{13}C-NMR δ: 172.5 (C-7), 137.0 (C-26), 127.8 (C-21), 121.0 (C-24), 123.7 (C-28), 121.1 (C-24), 118.5 (C-22 and C-23), 111.5 (C-25), 110.6 (C-20), 61.0 (C-11), 54.2 (C-5), 50.0 (C-8), 47.3 (C-14), 31.4 (C-2), 30.1 (C-2), 29.6 (C-12), 25.9 (C-16 or C-17) 25.2 (C-16 or C-17), 24.6 (C-13), 16.7 (C-18). C-4, C-10, C-15 and all fluorinated carbon atoms were not detected.

References

1. J. Schätti; U. Sezer; S. Pedalino; J. P. Cotter; M. Arndt; M. Mayor; V. Köhler, Tailoring the volatility and stability of oligopeptides. *J. Mass Spectrom.* **2017,** *52* (8), 550-556.

Chapter 3. Pushing the mass limit for intact launch and photoionization of large neutral biopolymers

J. Schätti; P. Rieser; U. Sezer; G. Richter; P. Geyer; G. G. Rondina; D. Häussinger; M. Mayor; A. Shayeghi; V. Köhler; M. Arndt, *Chem. Commun.,* **2018,** *1* (1), 93

Supplementary Methods

Acronyms used

- **aa:** amino acid
- **^{13}C-NMR:** Carbon NMR
- **^{19}F-NMR**: Fluorine NMR
- **^{1}H-NMR:** Proton NMR
- **2D NMR:** 2-Dimensional NMR
- **COSY:** Correlation spectroscopy
- **DHB:** 2,5-Dihydroxybenzoic acid
- **DIPEA:** *N*,*N*-diisopropylamine
- **DMF:** *N*,*N*-dimethylformamide
- **DMSO:** Dimethyl sulfoxide
- **DMSO-d_6:** Hexadeuterodimethyl sulfoxide
- **Et_2O:** Diethylether
- **EtOAc:** Ethyl acetate
- **Fmoc-**: Fluorenylmethoxycarbonyl-
- **HFIP:** 1,1,1,3,3,3-Hexafluoroisopropanol
- **HFIP-d_2:** Dideutero-1,1,1,3,3,3-hexafluoroisopropanol
- **HMBC:** Heteronuclear multiple bond correlation spectroscopy
- **HMQC:** Heteronuclear multiple-quantum correlation spectroscopy
- **HPLC:** High performance liquid chromatography
- **HRMS:** High resolution mass spectrometry
- **HSQC:** Heteronuclear single quantum coherence spectroscopy
- **MALDI:** Matrix assisted laser desorption/ionization
- **MALDI-TOF:** Matrix assisted laser desorption/ionization time of flight mass spectrometry
- **NHS-ester:** *N*-hydroxysuccinimide ester
- **NMR:** Nuclear magnetic resonance spectroscopy
- **NOESY:** Nuclear Overhauser effect spectroscopy
- **PDA detector:** Photo diode array detector
- **QCI-F Probe:** Quadruple resonance cryoprobe
- **SEC:** Size exclusion chromatography
- **SQ detector:** Single quadrupole detector
- **TFA:** Trifluoroacetic acid
- **UPLC:** Ultraperformance liquid chromatography

Synthetic procedures and characterization of compounds

Overall strategy

Peptides were assembled with standard solid phase peptide synthesis methods (for details see general procedure 1 below) employing Fmoc-chemistry while long coupling times and a high excess of coupling reagents were applied to realize a near quantitative conversion.[1] Amidation reactions for the introduction of perfluoroalkylchains at lysine side chains and the N-terminus of the assembled peptide were performed after cleavage from the resin with NHS ester **P1** (for details see general procedure 2).[2]

General Information

Chemicals were purchased from Sigma Aldrich, Fluorochem, Novabiochem or Bachem and used as received unless otherwise noted. UPLC experiments were performed with an Acquity UPLC-H Class Bio from Waters equipped with a PDA and a SQ detector 2 with the following column: ACQUITY UPLC, HSS T3 1.8 µm, 2.1 × 100 mm. Solvents for UPLC analysis were water and acetonitrile, each containing 0.1 % formic acid, later on referred to as (A) and (B). The flow rate was set to 0.61 ml/min and the column temperature to 40 °C. Method: 0 min – 100 % A; 1 min – 100 % A; 4 min – 100 % B; 4.5 min – 100 % B; 5.0 min 100% A; 5.5 min – 100 % A. Mass detection for UPLC analysis was performed in scan mode for positive ions (cone voltage 40 V, desolvation temperature: 600°C). A Varian PrepStar with an Ultimate 3000 RS Variable Wavelength Detector was used for preparative HPLC with the following column: Dr. Maisch Reprospher 100 C18-DE, 5 µm, 150 × 40 mm. Ultrapure water was prepared by means of an Ultra Ionic system from Milli-Q. Size exclusion chromatography was performed with a Shodex GPC HFIP-803 column, 10 µm, 300 × 8 mm, in 1,1,1,3,3,3-hexafluoro-2-propanol (HFIP) at a flow rate of 0.75 ml/min and 40°C column temperature. HRMS experiments were conducted on a Bruker maXis 4G. MALDI experiments were carried out on a Bruker microflex LRF, which was calibrated with Bruker protein calibration standard 1 and 2 (1: insulin, ubiquitin I, cytochrom C, myoglobin; 2: trypsinogen, protein A, albumin-bovine). NMR experiments were performed at 25 °C on Bruker Avance III NMR spectrometers operating at 500 or 600 MHz proton frequency. The NMR spectrometers were equipped with inverse or direct observe broadband probe heads or with a four-channel cryogenic QCI-F probe (600 MHz) all with self-shielded *z*-gradients. ^{13}C shifts were determined by 2D NMR experiments (HMBC and HMQC). ^{1}H and ^{13}C signals were assigned by 2D NMR (COSY, NOESY, HMBC, HMQC). Chemical shifts are reported in δ values (ppm) and are relative to the solvent residual signal (for samples in HFIP-d_2, $\delta(^1H)$ = 4.41 ppm; $\delta(^{13}C)$ = 68.07 ppm; DMF-d_7, $\delta(^1H)$ = 2.75 ppm; $\delta(^{13}C)$ = 29.76 ppm; for samples in $CDCl_3$, $\delta(^1H)$ = 7.26 ppm; $\delta(^{13}C)$ = 77.0 ppm; for samples in DMSO-d_6 $\delta(^1H)$ = 2.50 ppm; $\delta(^{13}C)$ = 39.5 ppm). The trifluoroacetic acid (TFA) content of peptides with free amino groups was determined by comparison of the integrals of the TFA signal in the $^{19}F\{^1H\}$ NMR spectra of samples before and after spiking with a defined amount of TFA. The preparation of **P1** and **P2** has been described previously.[3]

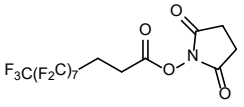

P1

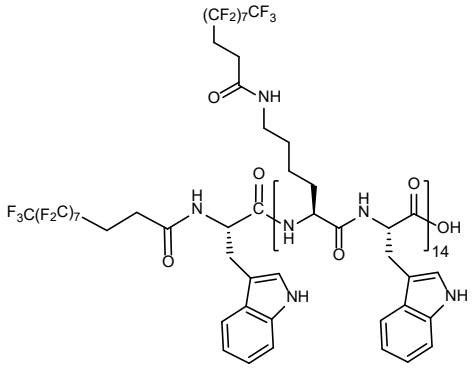

P2

General procedure 1 – Synthesis of the Lys-Trp oligomers and related compounds

2-chlorotrityl chloride resin (200 mg) was placed in a plastic syringe equipped with a filter frit. The resin was washed with CH_2Cl_2 (~2 ml). Fresh CH_2Cl_2 (~2 ml) was added and DIPEA (20 µl, 0.12 mmol, 2.4 eq.), and Fmoc-amino acid (1.0 eq., 50 µmol) were added. After the sample was agitated on a shaker for 2 h liquids were removed by filtration and the resin washed with CH_2Cl_2 (~4 ml) and DMF (~4 ml). The unreacted binding sites on the resin were capped by treatment with a capping mix (5 ml, 15 % MeOH, 5 % DIPEA, 80 % CH_2Cl_2) under agitation for 30 minutes. Peptide coupling steps were performed using a peptide synthesizer (intavis multi pep RSI) employing Fmoc-amino acids (5.0 eq.), PyBOP (5.0 eq.) and DIPEA (5.0 eq.) with a reaction time of first 45 min followed by a 2nd coupling step with identical reagent loadings for 90 min. For peptides longer than 15 amino acids (**P4**, **P5**) the coupling times were extended to 90 minutes and 180 minutes respectively for aa > 15. Fmoc-deprotection was performed with piperidine (20 % piperidine in DMF, 3 cycles (1 ml) of 5 min. each). The resin was washed with CH_2Cl_2 (5 × ~2 ml) before the cleavage solution (5 ml, 96 % TFA, 3 % triisopropylsilane, 3 % H_2O) was added and the mixture agitated for 1 h. Subsequently, the cleavage solution was removed by filtration and the resin washed with TFA (1 ml). The combined TFA solutions were concentrated under reduced pressure until the mixture started to become viscous. Ice cold Et_2O (50 ml) was added and the resulting precipitate collected by centrifugation (4650 g). The precipitate was washed with Et_2O (3 × 20 ml) and the product obtained after drying as a colorless solid.

H-(Lys-Trp)$_{10}$-OH × 11 CF_3CO_2H (P3)

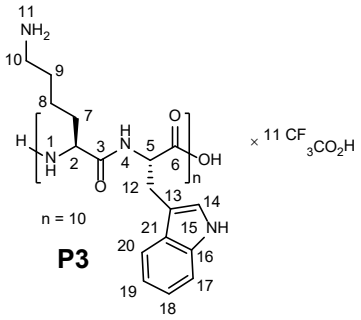

P3 was isolated as a white solid (122 mg, 27.6 µmol, 55 %).

UPLC-MS:, T_R = 2.75 min; MS (ES+) m/z: 452.9 [100 %, M+7H$^+$], 528.0 [100 %, M+6H$^+$], 633.5 [60 %, M+5H$^+$]. HRMS: calculated for: $C_{170}H_{227}N_{40}O_{21}^{5+}$: 632.9579; found: 632.9586. ^{1}H-NMR (DMSO-d_6, 500 MHz, 293 K) δ 10.85-10.66 (m, 10 H, H-15), 8.36-7.66 (m, 52 H, H-1, H-4 and H-11), 7.65-7.45 m, 10 H, H-20), 7.35-7.25 (m, 10 H, H-17), 7.17- 7.06 (m, 10 H, H-14), 7.06-6.96 (m, 10 H, H-18), 6.96-6.83 (m, 10 H, H-19), 4.64-4.46 (m, 9 H, H-5), 4.43-3.94 (m, 11 H, 10 H-2 and H-5), 3.25-2.90 (m, 20 H, H-12), 2.70-2.55 (m, 20 H, H-10), 1.70-1.30 (m, 40 H, H-7 and H-9), 1.25-1.10 (m, 20 H, H-8). ^{13}C-NMR (chemical shifts determined by 2D NMR, C=O was not detected) δ 136 (C-16), 127 (C-21), 123 (C-14), 121 (C-18), 118 (C-20 and C-19), 111 (C-17), 110 (C-13), 53 (C-2), 52 (C-5), 38 (C-10), 31 (C-7), 27 (C-12 and C-9), 22 (C-8).

H-Trp-(Lys-Trp)$_{14}$-OH × 15 CF_3CO_2H (P4)

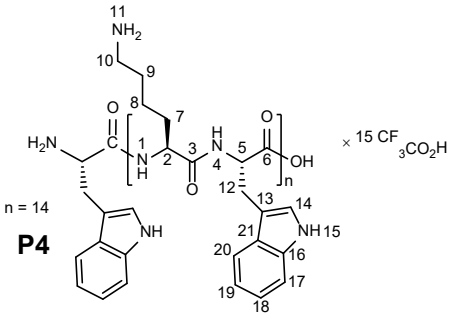

P4 was isolated as a pale yellow solid (175 mg, 28.2 µmol, 56 %).

UPLC-MS: T_R = 2.78 min; MS (ES+) m/z: 513.0 [80 %, M+9H$^+$], 576.8 [100 %, M+8H$^+$], 659.0 [60 %, M+7H$^+$]. HRMS: calculated for: $C_{249}H_{328}N_{58}O_{30}^{8+}$: 576.3235; found: 576.3225. ^{1}H-NMR (DMSO-d_6, 500 MHz, 293 K) 10.95 (s, 1 H, H-15), 10.85-10.78 (m, 2 H, H-15), 10.78-10.66 (m, 12 H, H-15), 8.35-7.60 (m, 73 H, H-1, H-4 and H-11), 7.60-7.48 (m, 15 H, H-20), 7.37-7.26 (m, 15 H, H-17), 7.20-6.81 (m, 45 H, H-14, H-18 and H-19) 4.73-4.48 (m, 14 H, H-5), 4.34-4.10 (m, 14 H, H-2), 3.75 (b, 1 H, H-5), 3.16-2.88 (m, 30 H, H-12), 2.77-2.60 (m, 28 H, H-10), 1.70-1.30 (m, 56 H, H-7 and H-9), 1.30-1.07 (m, 28 H, H-8). ^{13}C-NMR (chemical shifts determined by 2D NMR experiments, only CH_n (n=1-3) resonances detected) δ 123 (C-14), 121 (C-18), 118 (C-20 and C-19), 111 (C-17), 53 (C-2), 52 (C-5), 38 (C-10), 31 (C-7), 27 (C-12 and C-9), 22 (C-8).

H-(Lys-Trp)$_{25}$-OH × 26 CF_3CO_2H (P5)

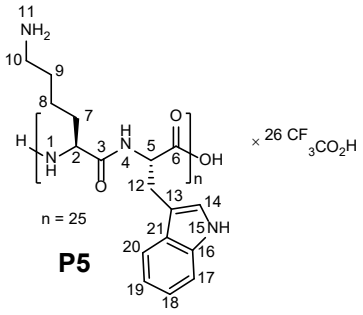

P5 was isolated as a yellow solid (220 mg, 20.3 µmol, 41 %) after precipitation from ether and was either used as such or further purified by preparative HPLC. Following lyophilization H-(Lys-Trp)$_{25}$-OH × 26 CF_3CO_2H was isolated as a white powder (85 mg, 7.8 µmol, 16 % yield after purification by preparative HPLC).

UPLC-MS: T_R = 2.86 min; MS (ES+) m/z: 788.5 [50 %, M+10H$^+$], 876.2 [70 %, M+9H$^+$], 985.5 [80 %, M+8H$^+$], 1126.1 [100 %, M+7H$^+$], 1313.8 [30 %, M+6H$^+$]. HRMS: calculated for: $C_{425}H_{563}N_{100}O_{51}^{11+}$: 716.7683 ; found 716.6757. ^{1}H-NMR (DMSO-d_6, 500 MHz, 293 K) δ 10.88-10.80 (m, 4 H, H-15), 10.80-10.66 (m, 21 H, H-15), 8.59 (d, $^3J_{H\text{-}H}$ = 7.5 Hz, 1 H, H-1 or H-4), 8.31 (d, $^3J_{H\text{-}H}$ = 7.8 Hz, 1 H, H-1 or H-4), 8.21-7.70 (m, 125 H, H-1, H-4 and H-11), 7.66 (d, $^3J_{H\text{-}H}$ = 8.0 Hz, 1 H, H-20), 7.60-7.51 (m, 24 H, H-20), 7.35-7.25 (m, 25 H, H-17), 7.19- 6.83 (m, 75 H, H-14 , H-18 and H-19) 4.64-4.46 (m, 24 H, H-5), 4.34-4.10 (m, 24 H, H-2), 4.06-4.02 (m, 1 H, H-5), 3.75-3.70 (m, 1 H, H-2), 3.25-2.90 (m, 50 H, H-12), 2.77-2.60 (m, 50 H, H-10), 1.70-1.35 (m, 100 H, H-7 and H-9), 1.32-1.07 (m, 50 H, H-8). ^{13}C-NMR (chemical

shifts determined by 2D NMR experiments, only CH_n (n=1-3) resonances detected) δ 123 (C-14), 121 (C-18), 118 (C-20 and C-19), 111 (C-17), 53 (C-2), 52 (C-5), 38 (C-10), 31 (C-7), 27 (C-12 and C-9), 22 (C-8).

H-(Lys-Trp)$_{15}$-OH × 16 CF_3CO_2H (P6)

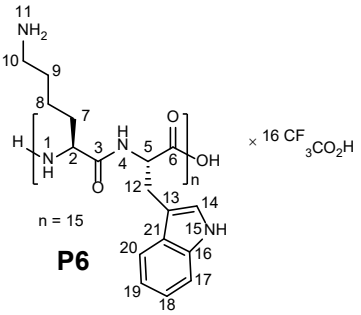

P6

P6 was isolated as a pale yellow solid (164 mg, 25.0 µmol, 50 %).

UPLC-MS: T_R = 2.79 min; MS (ES+) m/z: 527.1 [80 %, M+9H$^+$], 592.9 [100 %, M+8H$^+$], 677.3 [80 %, M+7H$^+$], 791.5 [30 %, M+6H$^+$]. HRMS: calculated for: $C_{255}H_{339}N_{60}O_{31}^{7+}$: 676.8108; found: 676.8109. ^{1}H-NMR (DMSO-d_6, 500 MHz, 293 K) 10.88-10.80 (m, 3 H, H-15), 10.80-10.66 (m, 12 H, H-15), 8.59 (d, $^3J_{H-H}$ = 7.4 Hz, 1 H, H-1 or H-4), 8.31 (d, $^3J_{H-H}$ = 7.9 Hz, 1 H, H-1 or H-4), 8.21-7.70 (m, 75 H, H-1, H-4 and H-11), 7.66 (d, $^3J_{H-H}$ = 7.9 Hz, 1 H, H-20), 7.60-7.51 (m, 14 H, H-20), 7.35-7.25 (m, 15 H, H-17), 7.19- 6.83 (m, 45 H, H-14, H-18 and H-19) 4.64-4.46 (m, 14 H, H-5), 4.34-4.10 (m, 14 H, 10 H-2), 4.03 (q, $^3J_{H-H}$ = 7.0 Hz, 1 H, H-5), 3.71 (b, 1 H, H-2), 3.25-2.90 (m, 30 H, H-12), 2.77-2.60 (m, 30 H, H-10), 1.70-1.35 (m, 60 H, H-7 and H-9), 1.32-1.07 (m, 30 H, H-8). ^{13}C-NMR (chemical shifts determined by 2D NMR experiments, C=O was not detected) δ 123 (C-14), 121 (C-18), 118 (C-20 and C-19), 111 (C-17), 53 (C-2), 52 (C-5), 38 (C-10), 31 (C-7), 27 (C-12 and C-9), 22 (C-8).

Decatryptophan × CF_3CO_2H (2 × CF_3CO_2H)

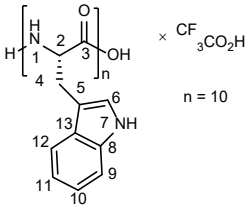

2

Decatryptophan (**2**) was prepared as its trifluoroacetate salt according to general procedure 1 with the following modifications: a resin loading of 125 µmol/g resin was chosen and peptide coupling times on the peptide synthesizer were extended to 2 hours and 4 hours, respectively. The final peptide product was precipitated from the cleavage solution by addition of Et_2O without prior concentration.

UPLC-MS: T_R = 3.84 min; MS (ES+) m/z: 941.1 [100 %, M+2 H$^+$], 1881.1 [50 %, M+1 H$^+$], 1903.1 [20 %, M+1 Na$^+$]. HRMS: calculated for: $C_{119}H_{103}N_{20}O_{11}^+$: 1879.8110 ; found 1879.8084. ^{1}H-NMR (DMF-d_7, 500 MHz, 293 K) δ 11.02 (d, $^3J_{H-H}$ = 2.4 Hz, 1 H, H-7) 10.84-10.81 (m, 2 H, H-7), 10.79 (d, $^3J_{H-H}$ = 2.4 Hz, 1 H, H-7), 10.77 (d, $^3J_{H-H}$ = 2.4 Hz, 1 H, H-7), 10.74 (d, $^3J_{H-H}$ = 2.4 Hz, 1 H, H-7), 10.71 (d, $^3J_{H-H}$ = 2.4 Hz, 1 H, H-7), 10.70-10.66 (m, 3 H, H-7), 9.09 (d, $^3J_{H-H}$ = 7.5 Hz, 1 H, H-1), 8.43 (b, 3 H, H-1 (N-terminus), 8.33 (d,

$^{3}J_{H\text{-}H}$ = 7.5 Hz, 1 H, H-1), 8.21-7.98 (m, 7 H, H-1), 7.76 (d, $^{3}J_{H\text{-}H}$ = 7.9 Hz, 1 H, H-12) 7.66-7.52 (m, 9 H, H-12), 7.46-7.33 (m, 10 H, H-9), 7.27-7.10 (m, 10 H, H-6), 7.09- 6.90 (m, 20 H, H-10, H-11), 4.88-4.64 (m, 9 H, H-2), 4.46-4.40 (m, 1 H, H-2), 3.34-3.06 (m, 20 H, H-4). ^{13}C-NMR (chemical shifts were determined by 2D NMR experiments; not all carbon atoms were detected) δ 124 (C-6), 121 (C-10), 119 (C-11 and C-12), 111 (C-9), 54.6 (3 × C-2), 54.5 (3 × C-2), 54.1 (C-2), 53.8 (C-2), 53.5 (C-2), 28 (C-4).

Ac-(Lys-Trp)$_5$-OH × 5 CF_3CO_2H (3 × 5 CF_3CO_2H)

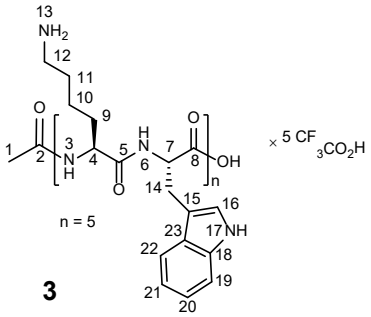

3

Ac-(Lys-Trp)$_5$-OH (**3**) × 5 CF_3CO_2H was prepared according to general procedure 1 with the following modification: Following the final Fmoc-deprotection the N-terminus was capped with acetic anhydride (4 ml, 10 % in DMF with 1 % DIPEA) for 15 min.

UPLC-MS: T_R = 2.87 min; MS (ES+) m/z: 327.5 [50 %, M+5 H^+], 545.1 [100 %, M+4 H^+], 545.1 [20 %, M+3H^+], 816.6 [10 %, M+2H^+]. HRMS: calculated for: $C_{87}H_{116}N_{20}O_{12}^{2+}$: 816.4535; found 816.4543. ^{1}H-NMR (DMSO, 500 MHz, 293 K) δ 10.80 (s, 1 H, H-17) 10.78-10.73 (m, 3 H, H-17), 10.71 (s, 1 H, H-17), 8.17- 7.59 (m, 25 H, H-3, H-6 and H-13), 7.58-7.50 (m, 5 H, H-22), 7.33-7.26 (m, 5 H, H-19), 7.15- 7.07 (m, 5 H, H-16), 7.06-7.00 (m, 5 H, H-20), 6.98-6.88 (m, 5 H, H-21), 4.61-4.48 (m, 9 H, H-7), 4.30-4.02 (m, 11 H, 10 × H-3 and 1 × H-7), 3.25-2.93 (m, 10 H, H-14), 2.70-2.60 (m, 10 H, H-12), 1.81 (s, 3 H, H-1), 1.69-1.30 (m, 20 H, H-9 and H-11), 1.25-1.09 (m, 10 H, H-10). ^{13}C-NMR (chemical shifts were determined by 2D NMR experiments, C=O was not detected) δ 136 (C-18), 127 (C-23), 123 (C-16), 121 (C-20), 118 (C-22 and C-21), 111 (C-19), 110 (C-15), 53 (C-4), 52 (C-7), 38 (C-12), 31 (C-9), 27 (C-14) 26 (C-11), 22.1 (C-1), 22 (C-10).

General procedure 2 – Amidation of Lys-Trp oligomers with NHS-fluoroalkyl-ester P1

The lysine-tryptophan oligomer (1.00 eq) and NHS-ester **P1** (2.00 eq for every NH_2-group of the peptide) were dissolved in DMF (200 ml). DIPEA (4.0 eq. for every NH_2-group of the peptide) was added and the mixture stirred for 56 hours at 50 °C. Subsequently the mixture was concentrated under reduced pressure. The formed precipitate was isolated by filtration, washed with cold DMF (2 × 25 ml), EtOAc (2 × 25 ml), Et_2O (2 × 25 ml) and dried under reduced pressure.

(*2H*,*2H*,*3H*,*3H*-perfluoroundecanoyl)-(Lys(*2H*,*2H*,*3H*,*3H*-perfluoroundecanoyl)-Trp)$_{10}$-OH (4)

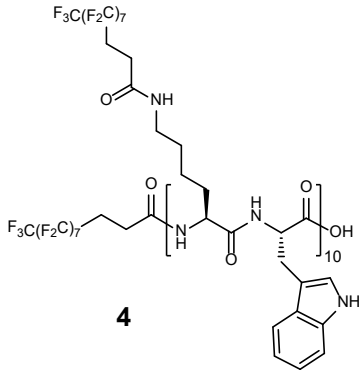

4

P3 (1.00 eq., 250 mg, 56.6 µmol) was converted according to general procedure 2. 5 was obtained as an orange solid (295 mg, 35.2 µmol, 62 %). SEC HFIP: T_r: 11.1 min; MALDI: 8399.1 [M + Na^+]. Unambiguous assignment of the NMR-data was not possible with a reasonable effort due to signal overlap in 1D-^{1}H and 2D-NMR spectra. A representative 1D-^{1}H, as well as HSQC, NOESY and COSY NMR spectra, a size exclusion chromatography trace and a MALDI-TOF MS spectrum are shown in Supplementary Figures 14-21.

(*2H*,*2H*,*3H*,*3H*-perfluoroundecanoyl)-Trp-(Lys(*2H*,*2H*,*3H*,*3H*-perfluoroundecanoyl)-Trp)$_{14}$-OH (5)

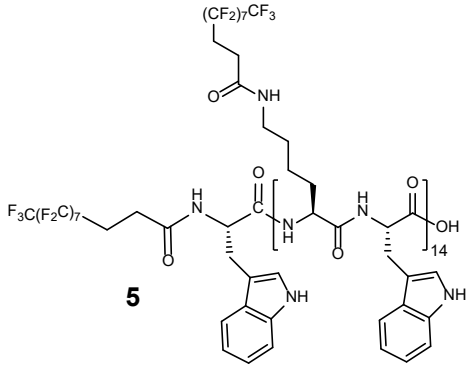

5

P4 (1.00 eq., 300 mg, 65.1 µmol) was converted according to general procedure 2. **5** was obtained as a brown solid (385 mg, 32.9 µmol, 51 %). SEC HFIP: T_r: 10.1 min; MALDI: 11740 [M+Na^+]. Unambiguous assignment of the NMR-data was not feasible with a reasonable effort. A representative size exclusion chromatography trace and a MALDI-TOF MS spectrum are shown in Supplementary Figures 22-25.

(*2H*,*2H*,*3H*,*3H*-perfluoroundecanoyl)-(Lys(*2H*,*2H*,*3H*,*3H*-perfluoroundecanoyl)-Trp)$_{25}$-OH (6)

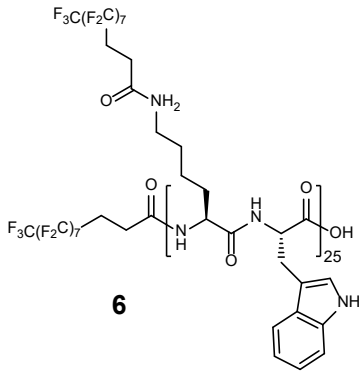

6

P5 (1.00 eq., 300 mg, 27.7 µmol) was converted according to general procedure 2. **6** was obtained as a brown solid (280 mg, 13.9 µmol, 50 %). A second batch was prepared with H-(Lys-Trp)$_{25}$-OH × 26 CF_3CO_2H, **P5** that was purified by preparative HPLC (1.00 eq., 75 mg, 6.9 µmol) following the same procedure but employing only half volumes of all solvents. The product was obtained as a brown solid (115 mg, 5.7 µmol, 83 %). Both batches were tested in laser desorption/postionization studies and the second batch was used for characterization. SEC HFIP: T_r : 9.5 min; MALDI: 20224 [M+Na$^+$]. Unambiguous assignment of the NMR-data was not feasible with a reasonable effort. A representative 1D-^{1}H NMR spectrum, a size exclusion chromatography trace and a MALDI-TOF MS spectrum are shown in Supplementary Figures 26-29.

(*2H*,*2H*,*3H*,*3H*-perfluoroundecanoyl)-(Lys(*2H*,*2H*,*3H*,*3H*-perfluoroundecanoyl)-Trp)$_{15}$-OH (P7)

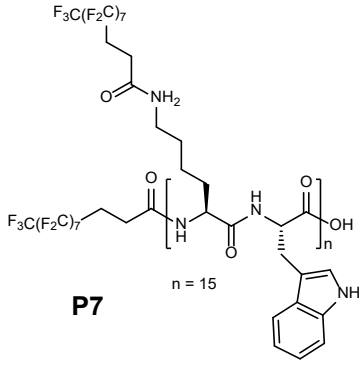

P7

P6 (1.00 eq., 300 mg, 45.7 µmol) was converted according to general procedure 2. **P7** was obtained as a brown solid (330 mg, 26.8 µmol, 59 %). SEC HFIP: T_r : 10.2 min; MALDI: 12342 [M+Na$^+$]. Unambiguous assignment of the NMR-data was not feasible with a reasonable effort. 1D-^{1}H NMR spectrum, a size exclusion chromatography trace and a MALDI-TOF MS spectrum are shown in Supplementary Figures 30-32.

Supplementary Note 1. Determination of the TFA content in peptide products

A comparison of the integral values for the trifluoroacetate signal in the ^{19}F-NMR spectrum of the respective compound (4.0 mg) in DMSO-d_6 (0.5 mL) before and after spiking with a defined amount of trifluoroacetic acid (1.0 µl, 13 µmol) was used to estimate the trifluoroacetate equivalents a in the original sample (compound name × a CF_3CO_2H) as follows and is here exemplified for compound **P3**.

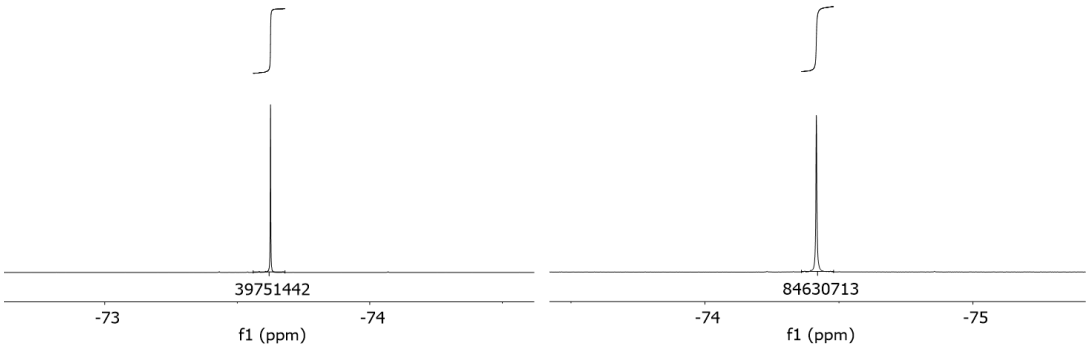

Supplementary Figure 1. ^{19}F-NMR (DMSO-d_6, 471 MHz, 298 K, D1 = 4s) of **P3** × a CF_3CO_2H (4.0 mg) in DMSO-d_6 (0.50 ml) before (left) and after (right) addition of trifluoroacetic acid (1.0 µl, 13 µmol).

$$a = \frac{n_{CF_3CO_2H} \cdot M_{w(P2free)}}{m - n_{CF_3CO_2H} \cdot M_{w(CF_3CO_2H)}} \quad (1)$$

with

$$n_{CF_3CO_2H} = \frac{I_{bs} \cdot n_{CF_3CO_2H(s)}}{(I_{as} - I_{bs})} \quad (2)$$

where

$n_{CF_3CO_2H}$ is the amount of substance of CF_3CO_2H before spiking;

I_{bs} is the integral of the CF_3CO_2H signal *before* spiking;

$n_{CF_3CO_2H(s)}$ is the amount of substance of CF_3CO_2H added for spiking (13 µmol);

I_{as} is the integral of the CF_3CO_2H signal *after* spiking;

$M_{w(P2free)}$ is the theoretical molecular weight of **P3**, which is free of CF_3CO_2H (3161.91 g/mol);

m is the weight of **P3** × a CF_3CO_2H employed in the experiment (4.0 mg);

$M_{w(CF_3CO_2H)}$ is the molecular weight of CF_3CO_2H (114.02 g/mol);

The results for compounds **3**, **P3**-**P5** are given in Supplementary Table 1.

compound	theoretical M_w of CF_3CO_2H free compound	a calculated	number of basic amine units in molecule
3	1632.00 g/mol	6.3	5
P3	3161.91 g/mol	13.6	11
P4	4605.67 g/mol	17.4	15
P5	7877.74 g/mol	28.0	26

Supplementary Table 1. CF_3CO_2H equivalents contained per formular unit for compounds **3, P3** - **P5**. The calculated values match reasonably well with the number of basic amine units of the molecules.

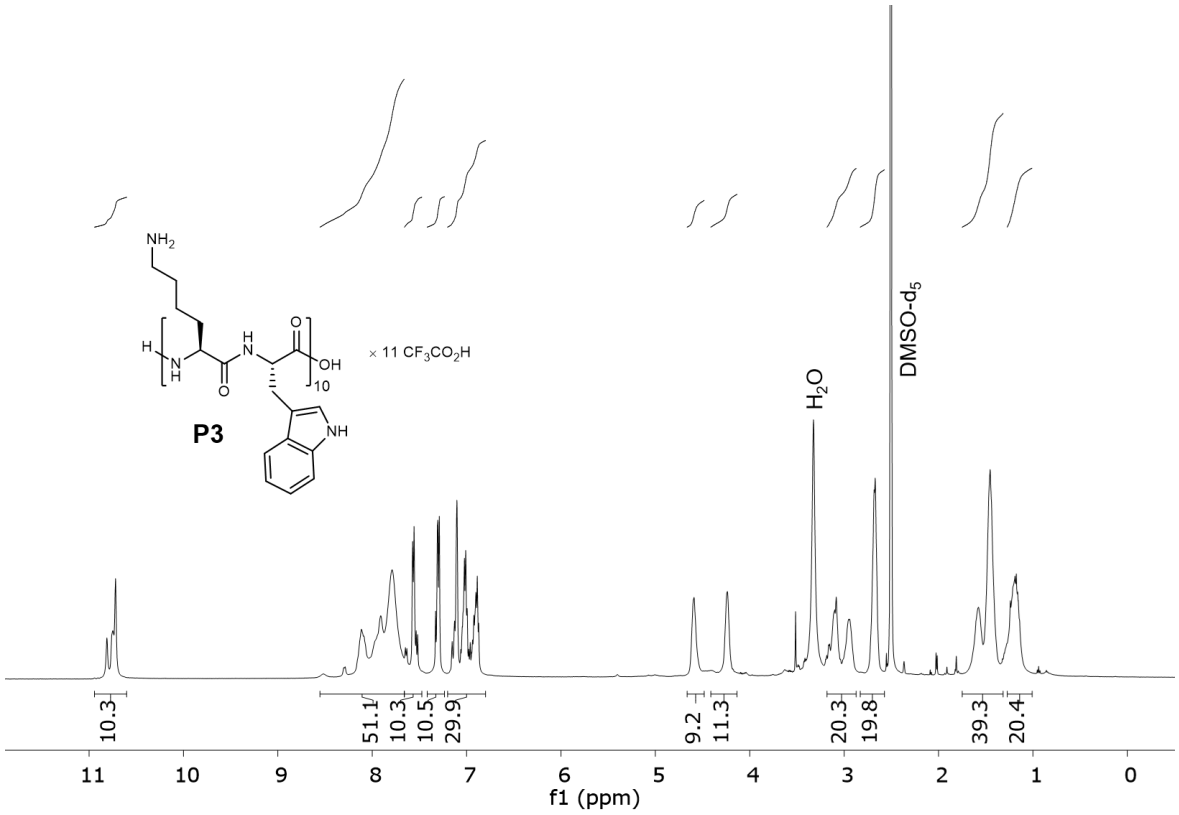

Supplementary Figure 2. ^{1}H-NMR spectrum of compound **P3** × 11 CF_3CO_2H: DMSO-d_6, 500 MHz, 298 K.

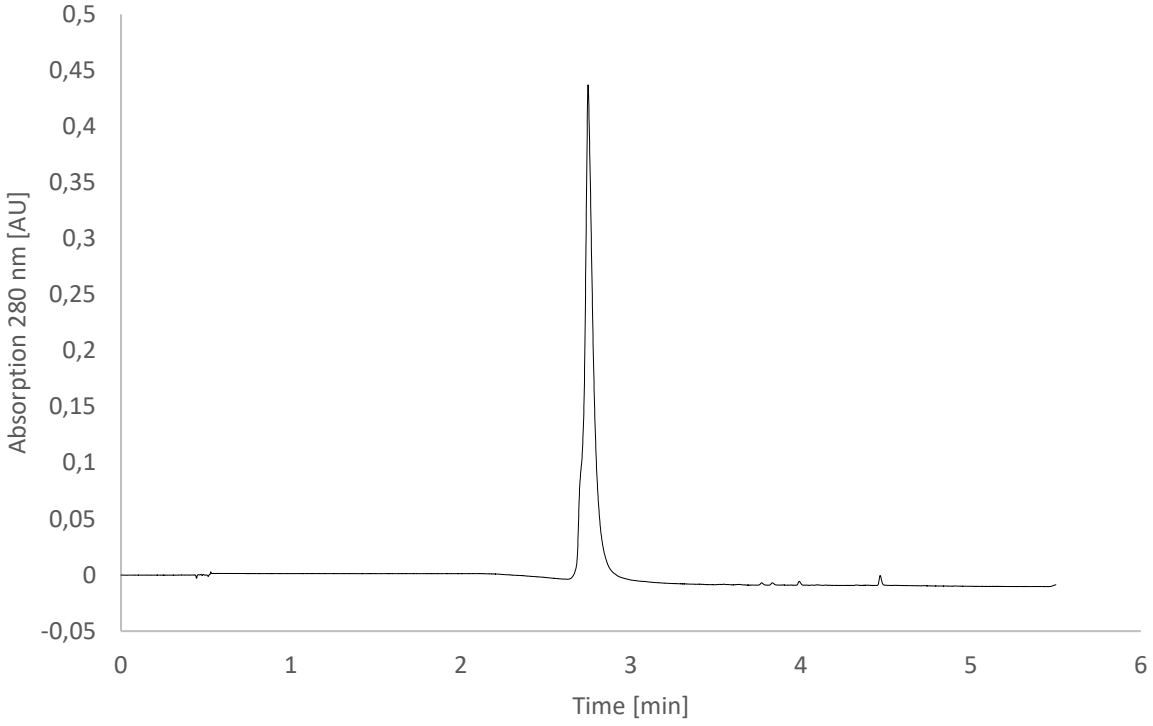

Supplementary Figure 3. UPLC-chromatogram for compound **P3**.

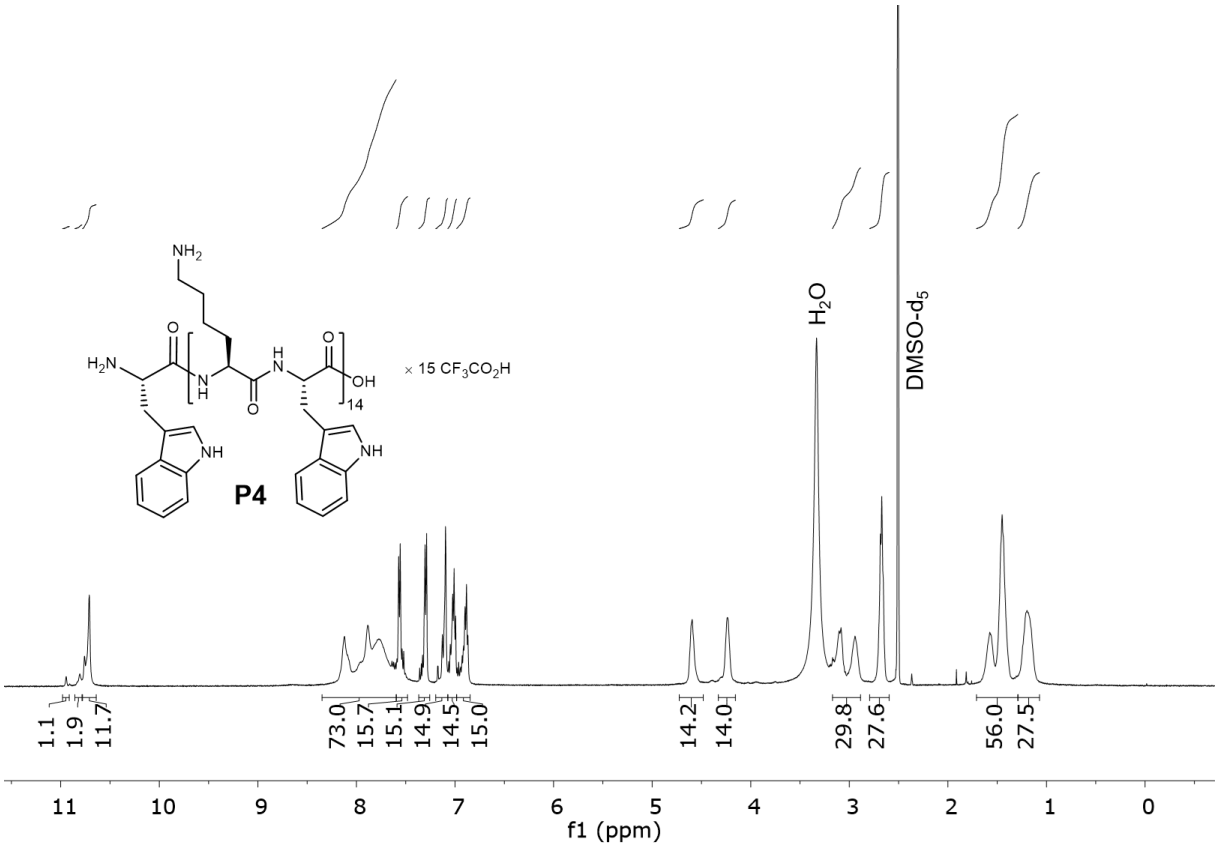

Supplementary Figure 4. ^{1}H-NMR (DMSO-d_6, 500 MHz, 298 K), compound **P4** × 16 CF_3CO_2H.

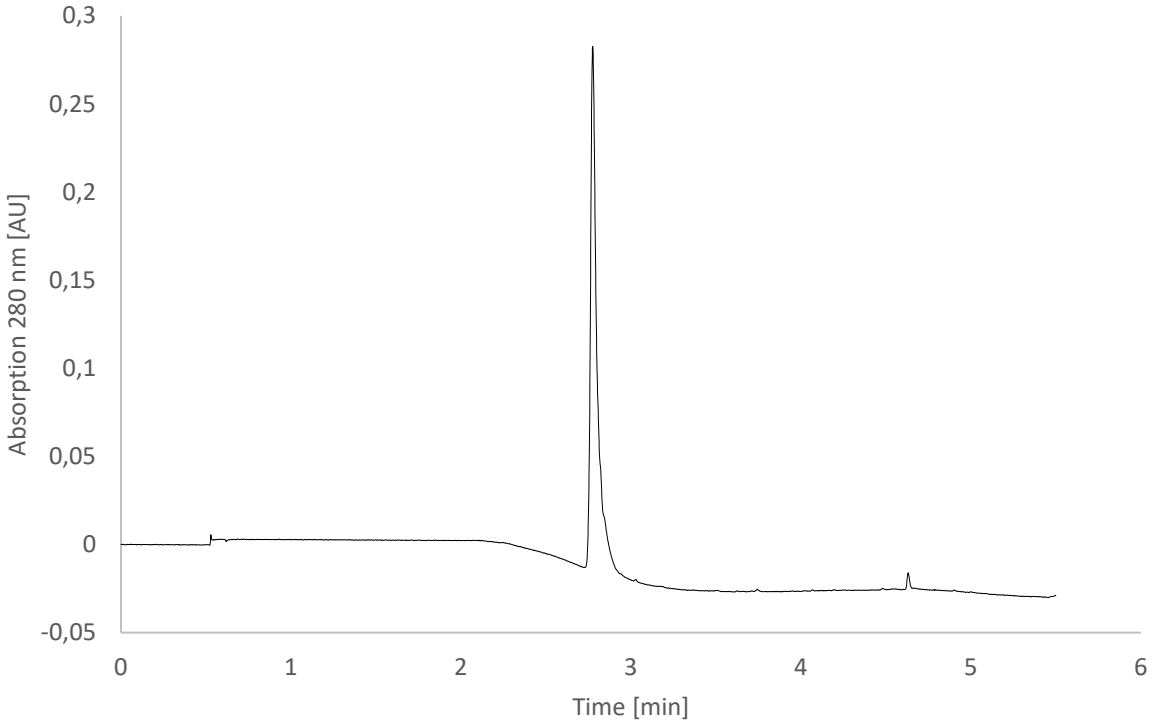

Supplementary Figure 5. UPLC-chromatogram for compound **P4**.

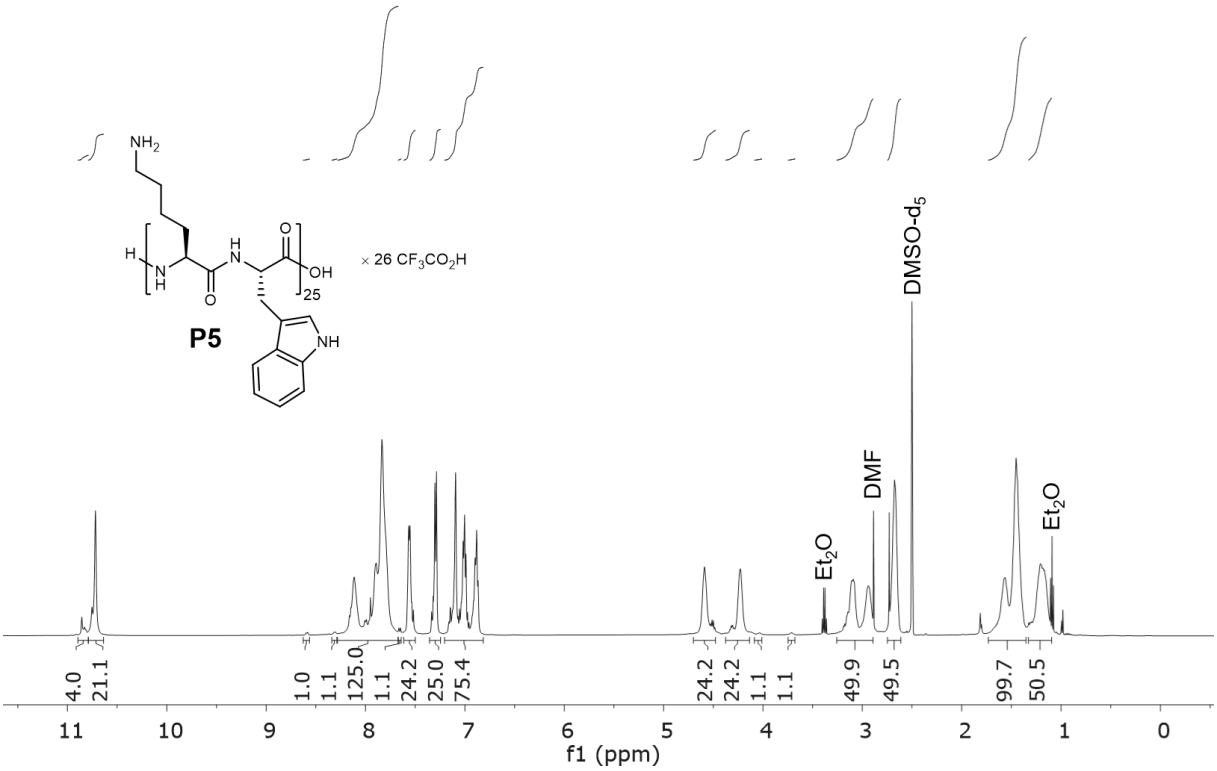

Supplementary Figure 6. ^{1}H-NMR (DMSO-d_6, 500 MHz, 298 K) of compound **P5** × 26 CF_3CO_2H.

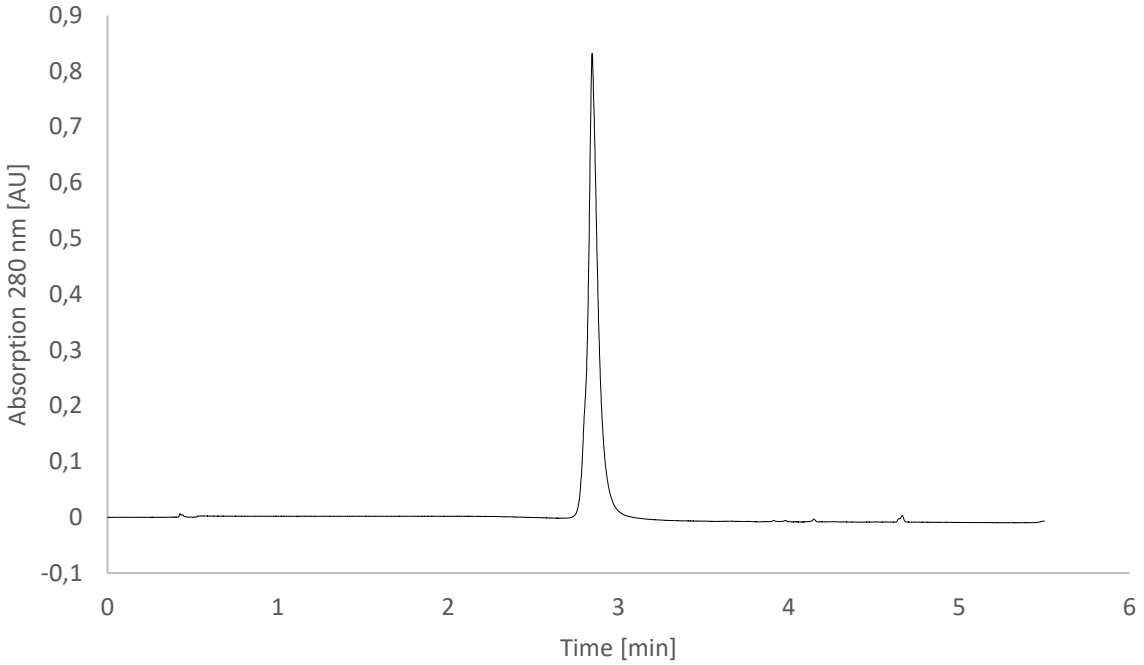

Supplementary Figure 7. UPLC-chromatogram for compound **P5**.

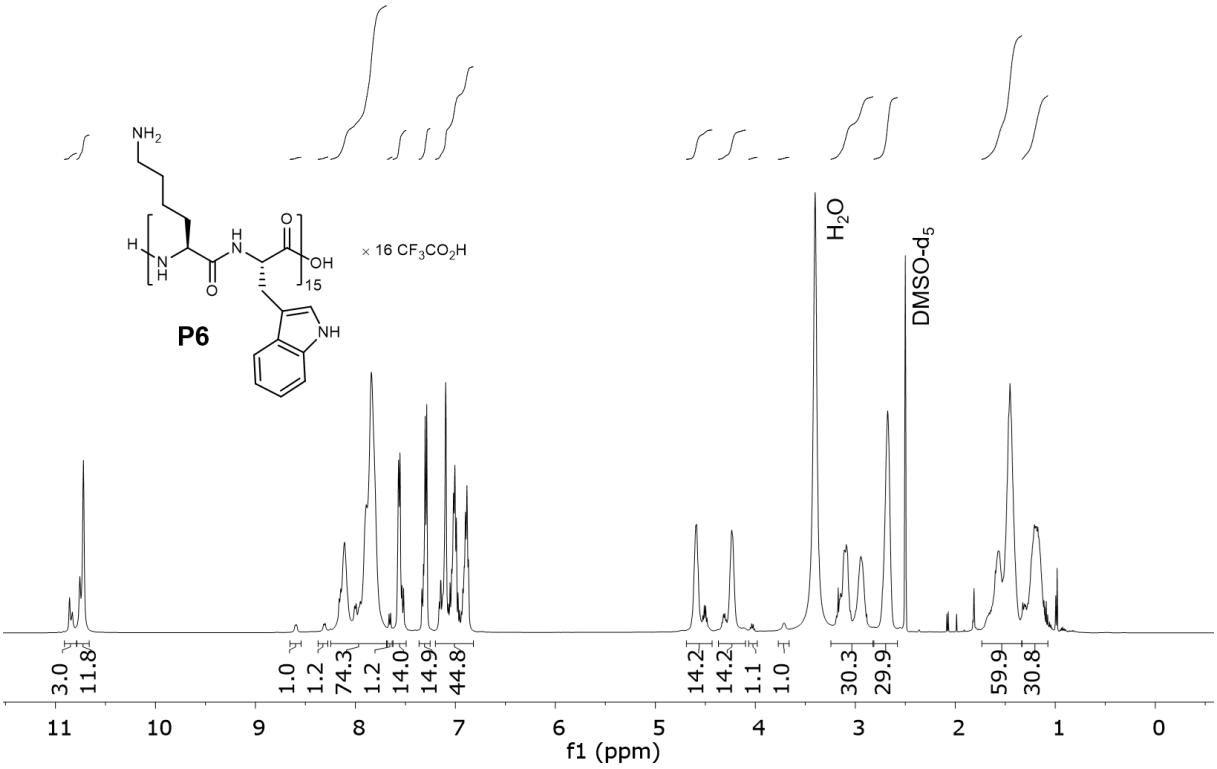

Supplementary Figure 8. ^{1}H-NMR (DMSO-d_6, 500 MHz, 298 K) of compound **P6** × 16 CF_3CO_2H.

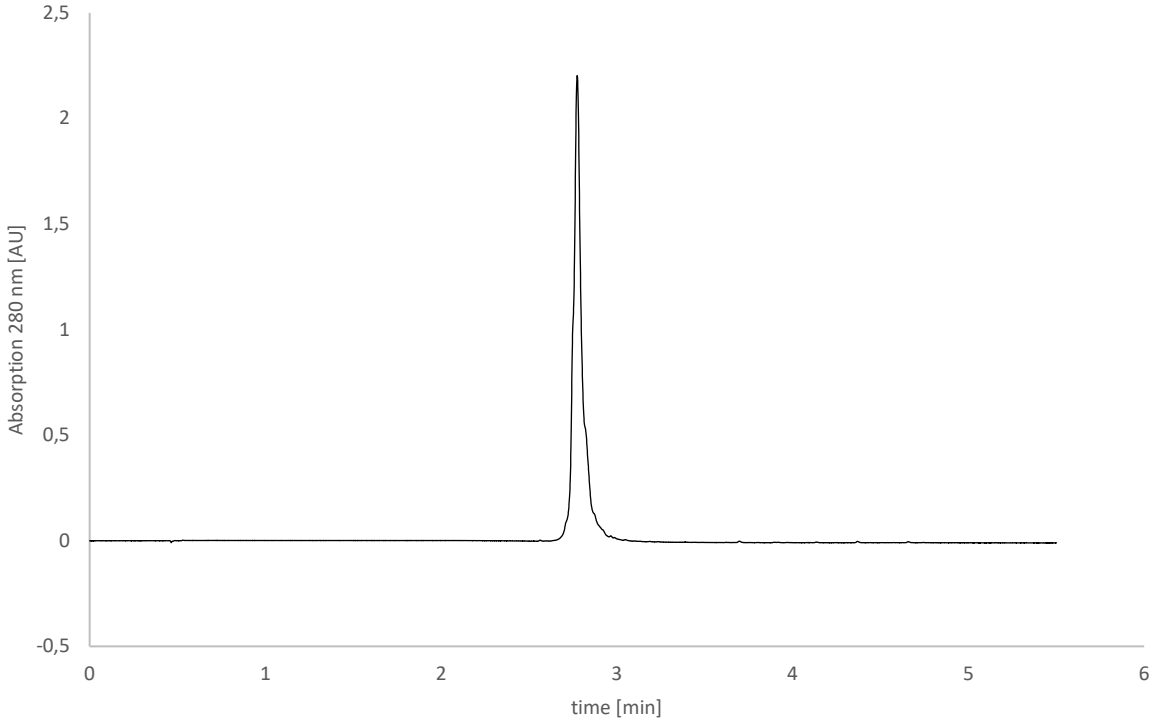

Supplementary Figure 9: UPLC-chromatogram for compound **P6**.

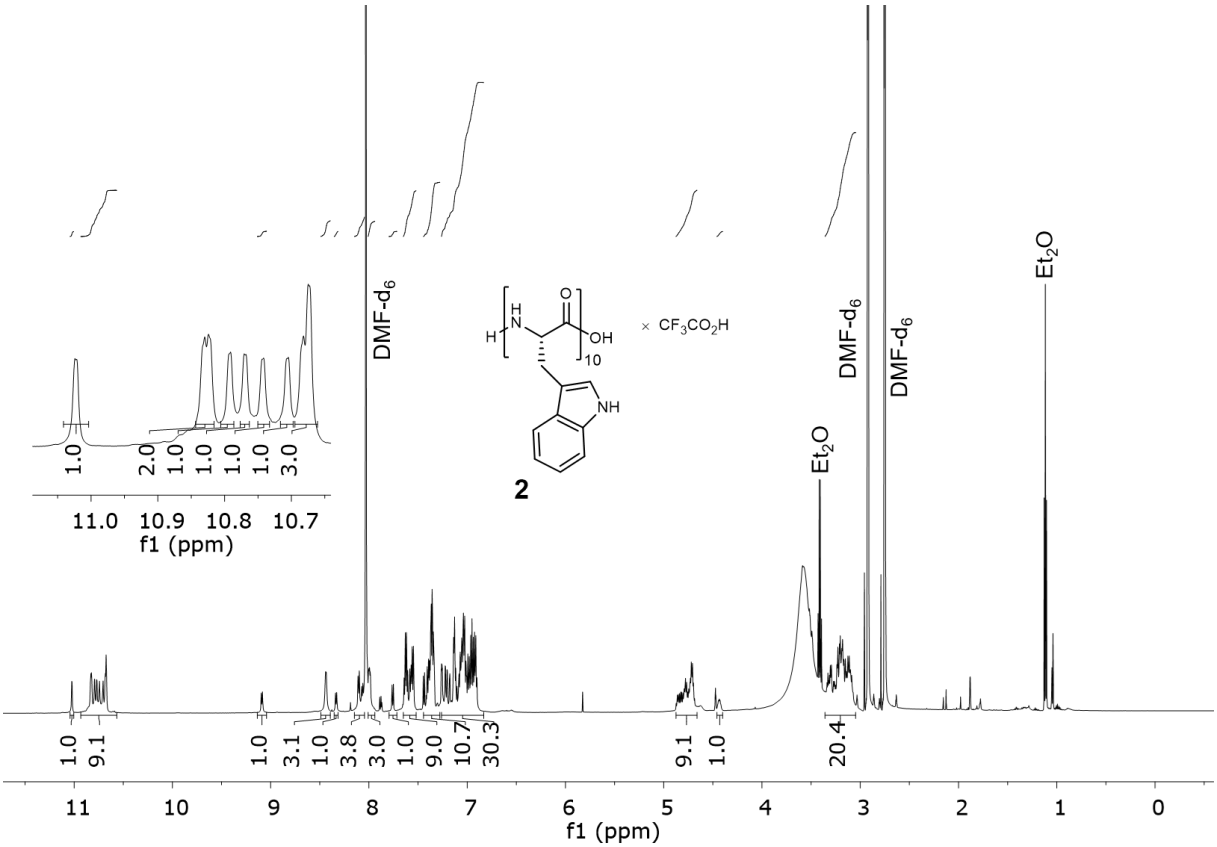

Supplementary Figure 10. ^{1}H-NMR (DMF-d_7, 600 MHz, 298 K) of decatryptophan **2** × CF_3CO_2H. The insert shows the signals of the N*H* protons of the indole rings.

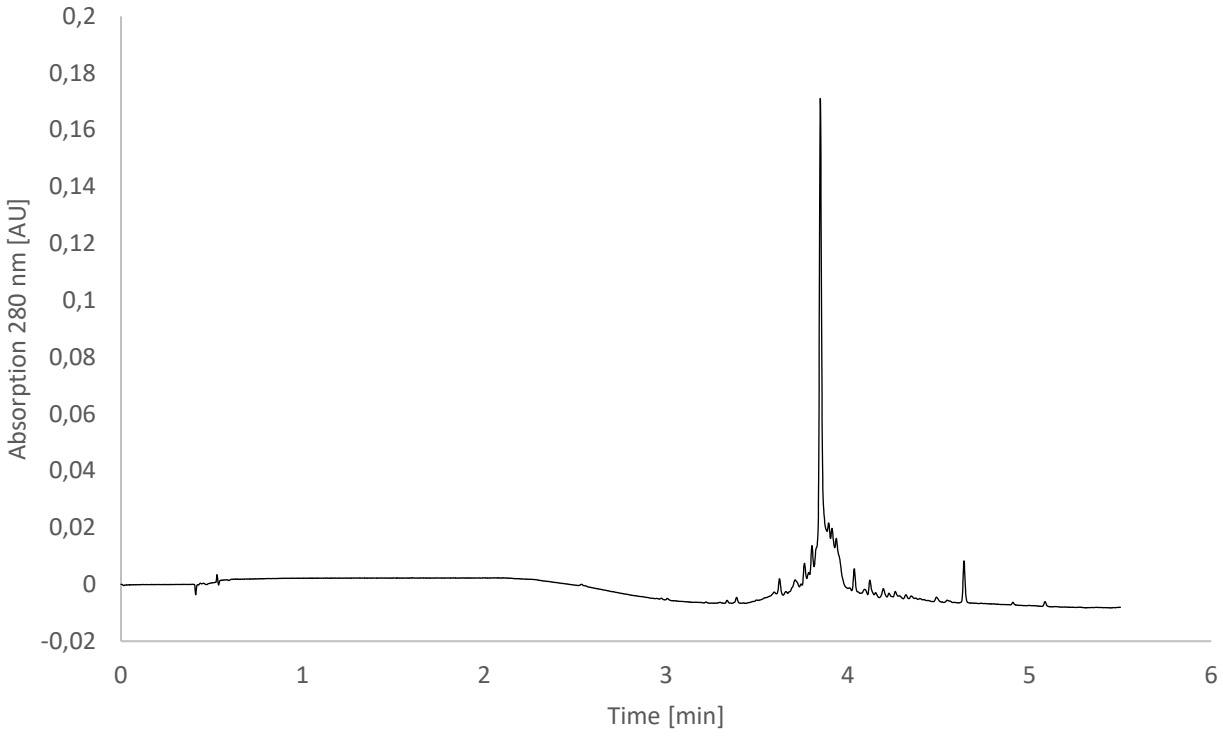

Supplementary Figure 11. UPLC-chromatogram for decatryptophan **2**.

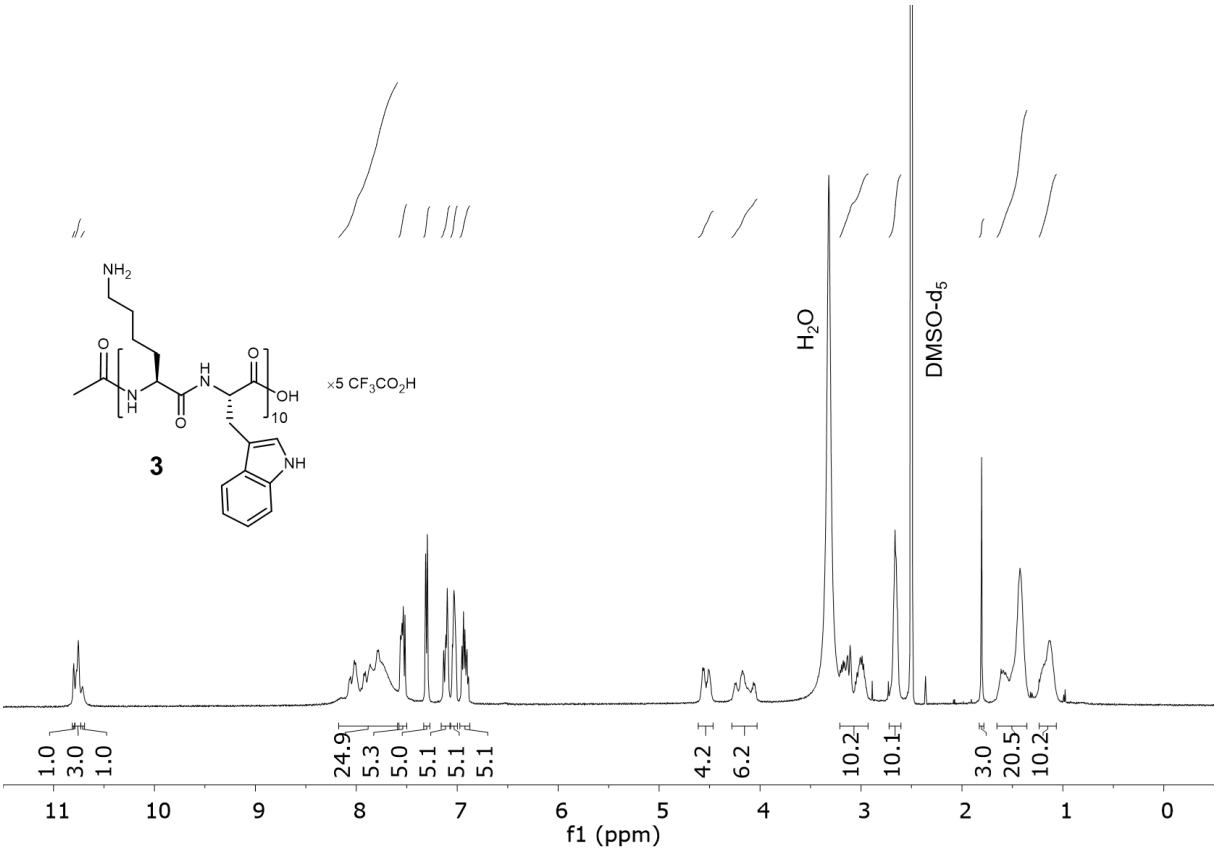

Supplementary Figure 12. ^{1}H-NMR (DMSO-d_6, 500 MHz, 298 K) of compound **3** × 5 CF_3CO_2H.

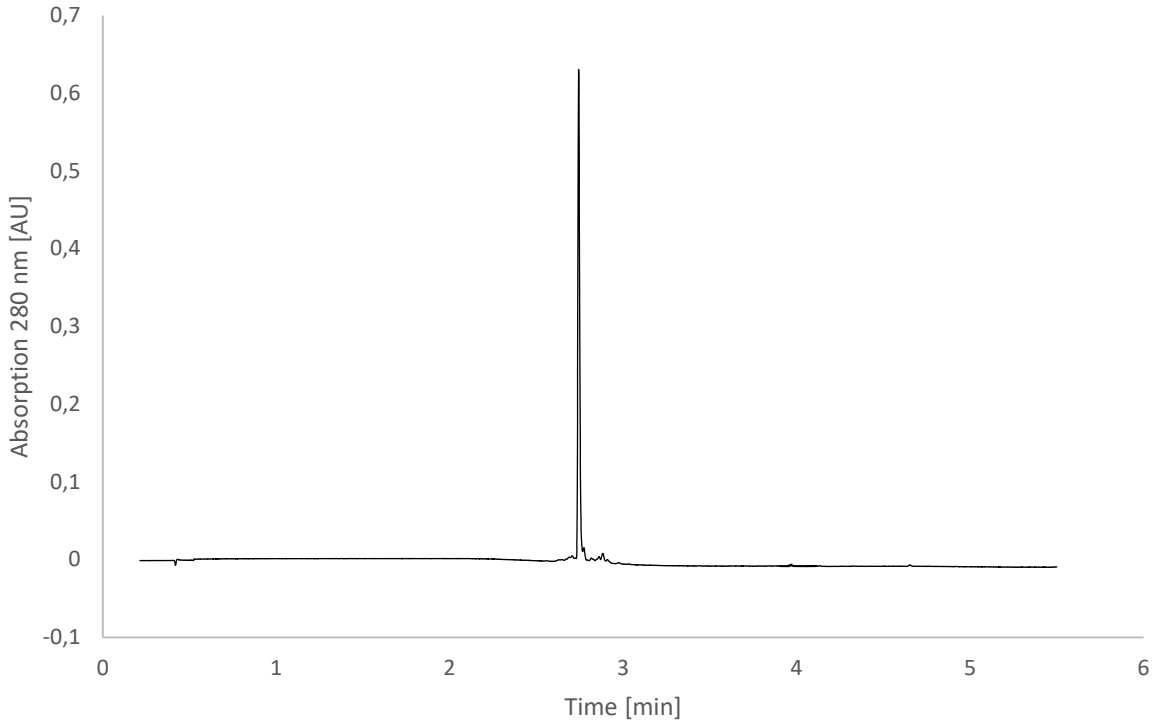

Supplementary Figure 13. UPLC-chromatogram for compound **3**.

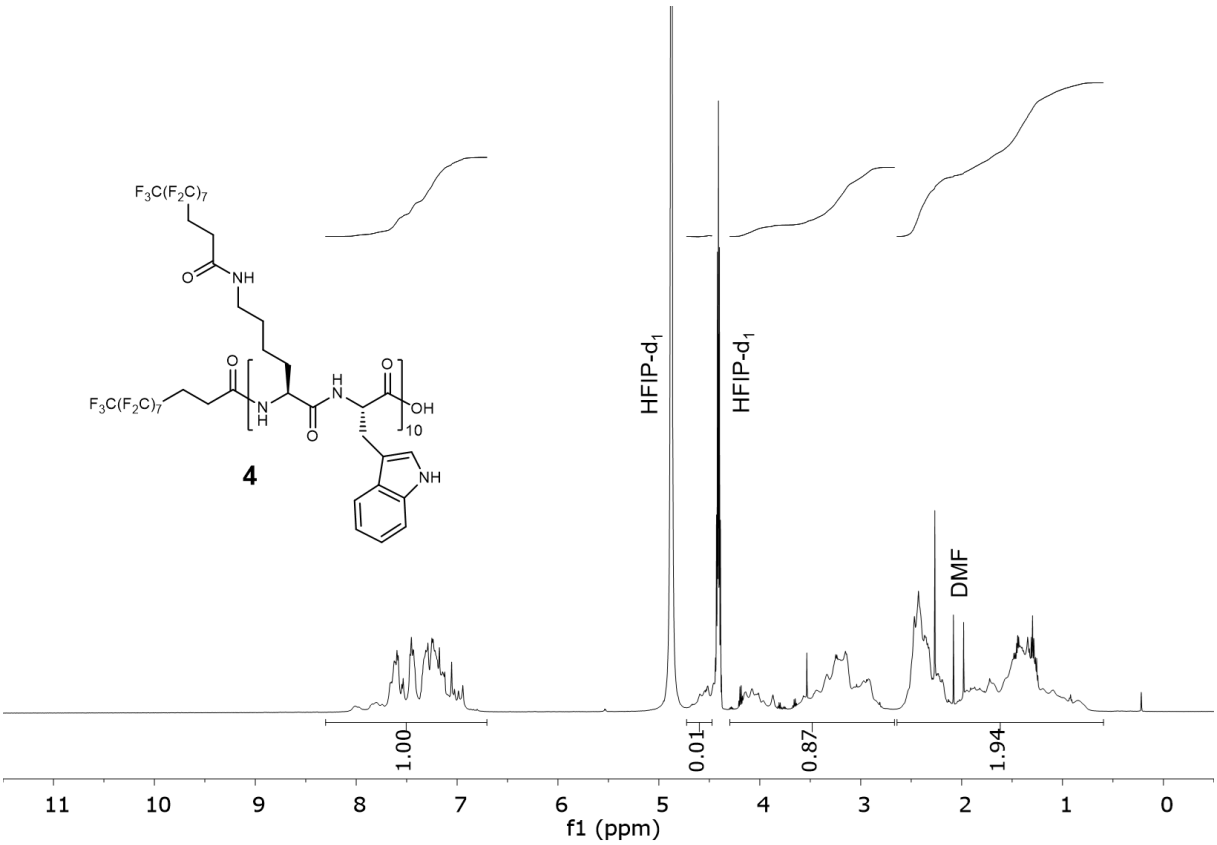

Supplementary Figure 14. ^{1}H-NMR (HFIP-d_2, 600 MHz, 298 K) of compound **4**.

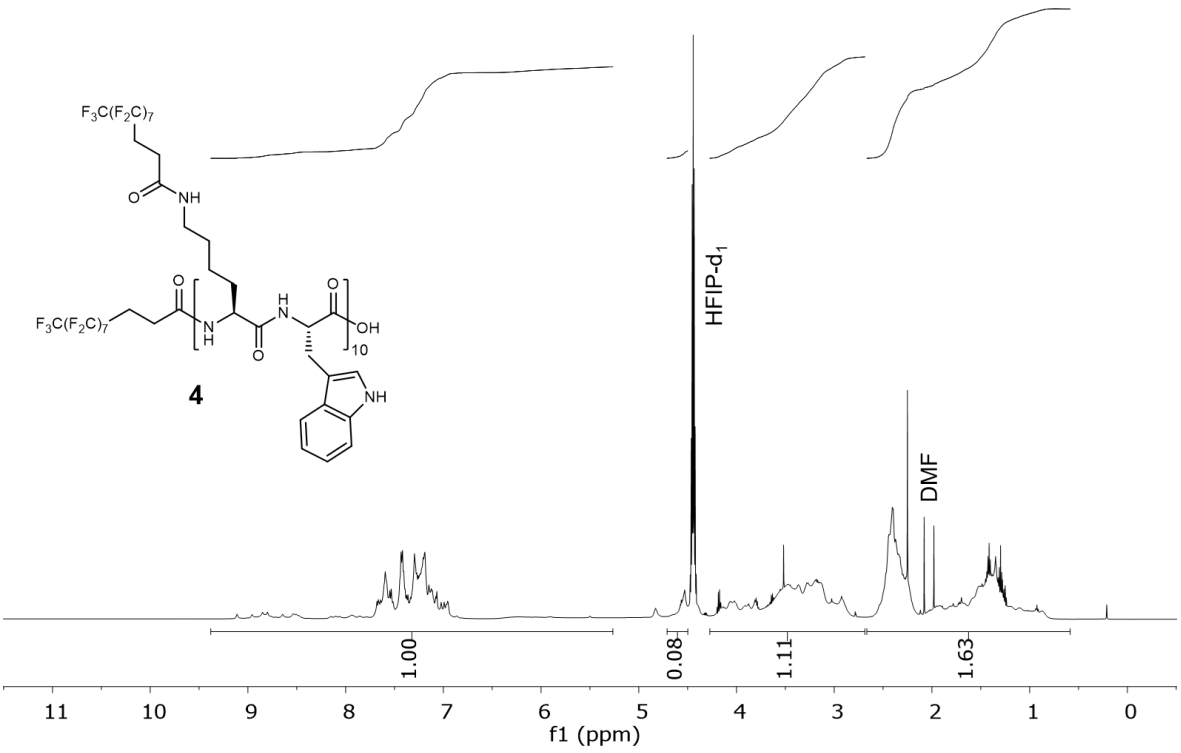

Supplementary Figure 15. ^{1}H-NMR (HFIP-d_2, 600 MHz, 298 K), compound **4** after addition of 10% H_2O recorded with presaturation (water and *H*O-CD$(CF_3)_2$ signal suppression). The addition of H_2O enables observation of the NH-signals. Note that the deuterium to protium exchange is only partial.

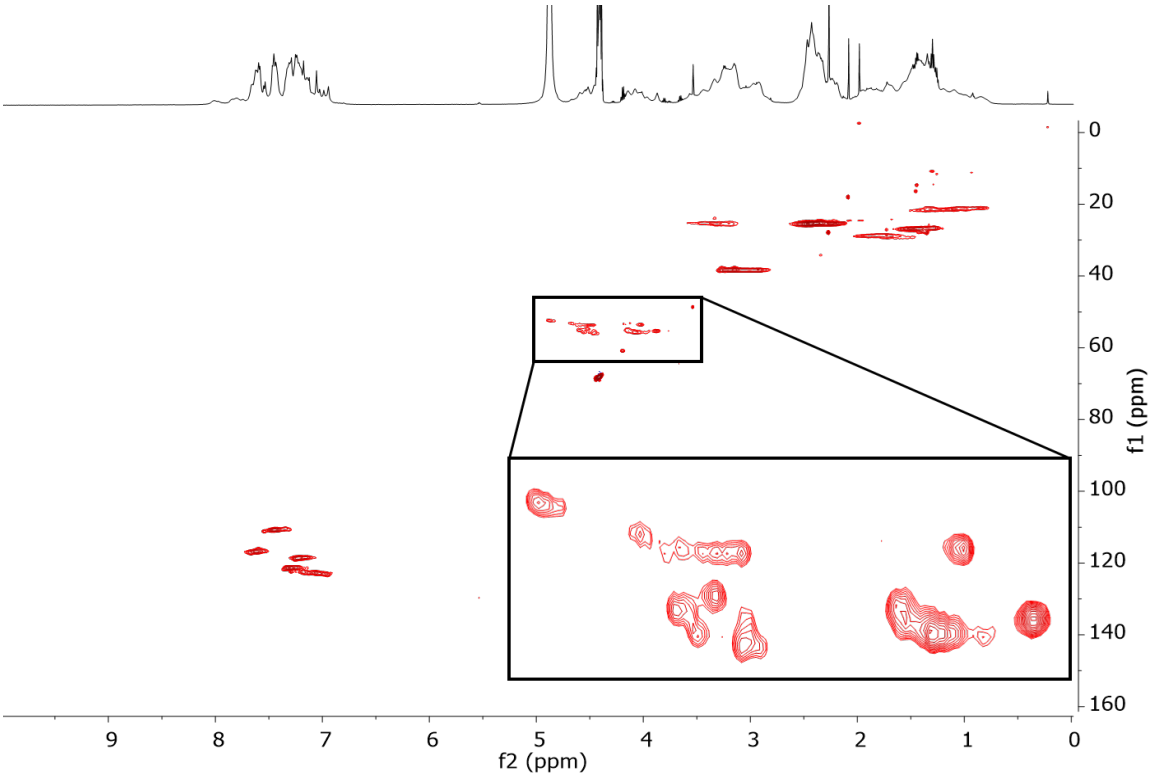

Supplementary Figure 16. HSQC of compound **4** in HFIP-d_2. The inset shows a zoom into the C_α-region. However, a conclusive determination of the number of individual C_α-atoms and accordingly amino acid units was not possible with this experiment due to overlapping signals.

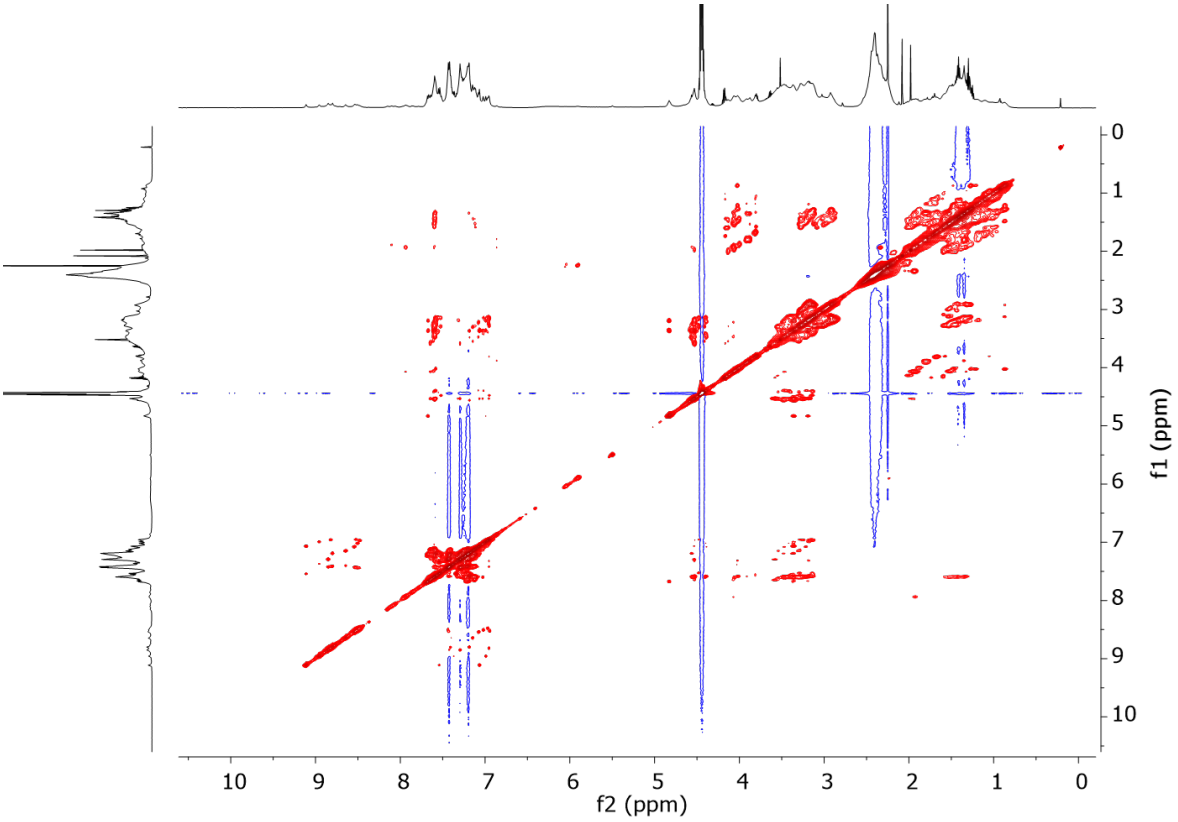

Supplementary Figure 17. NOESY of compound **4** in HFIP-d_2 after addition of 10% H_2O recorded with presaturation (water and *H*O-CD$(CF_3)_2$ signal suppression).

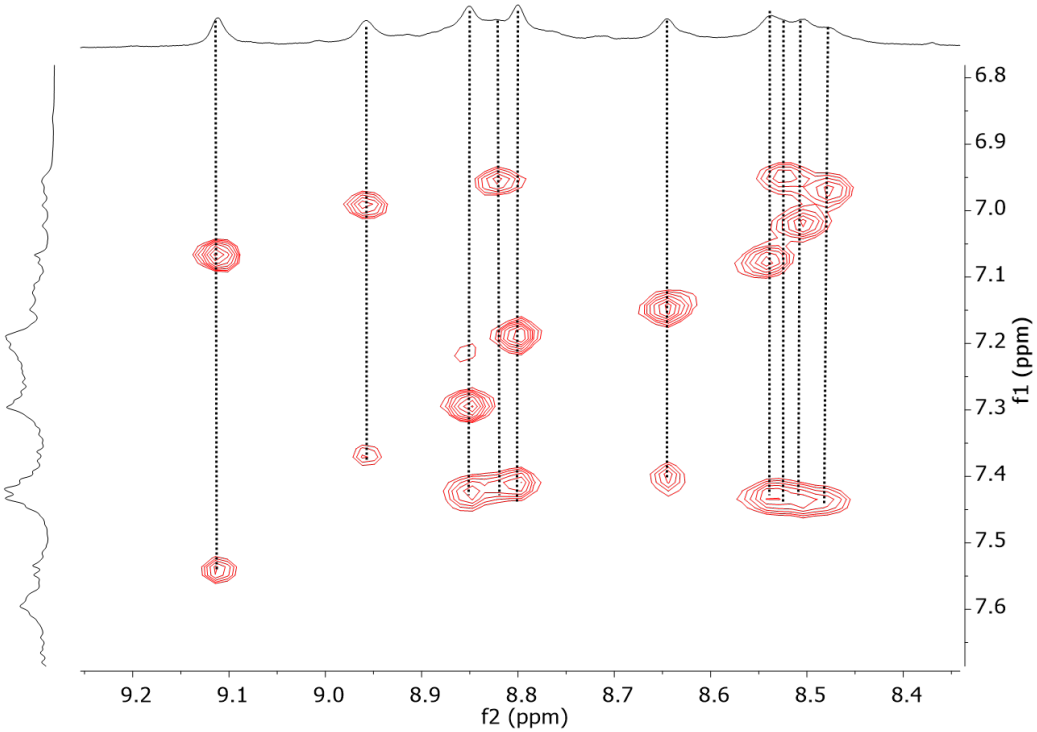

Supplementary Figure 18. Zoom into the indole NH region of NOESY spectrum of compound **4** shown in Supplementary Figure 17. 10 different indol N*H* moieties can be distinguished by indol CH correlations.

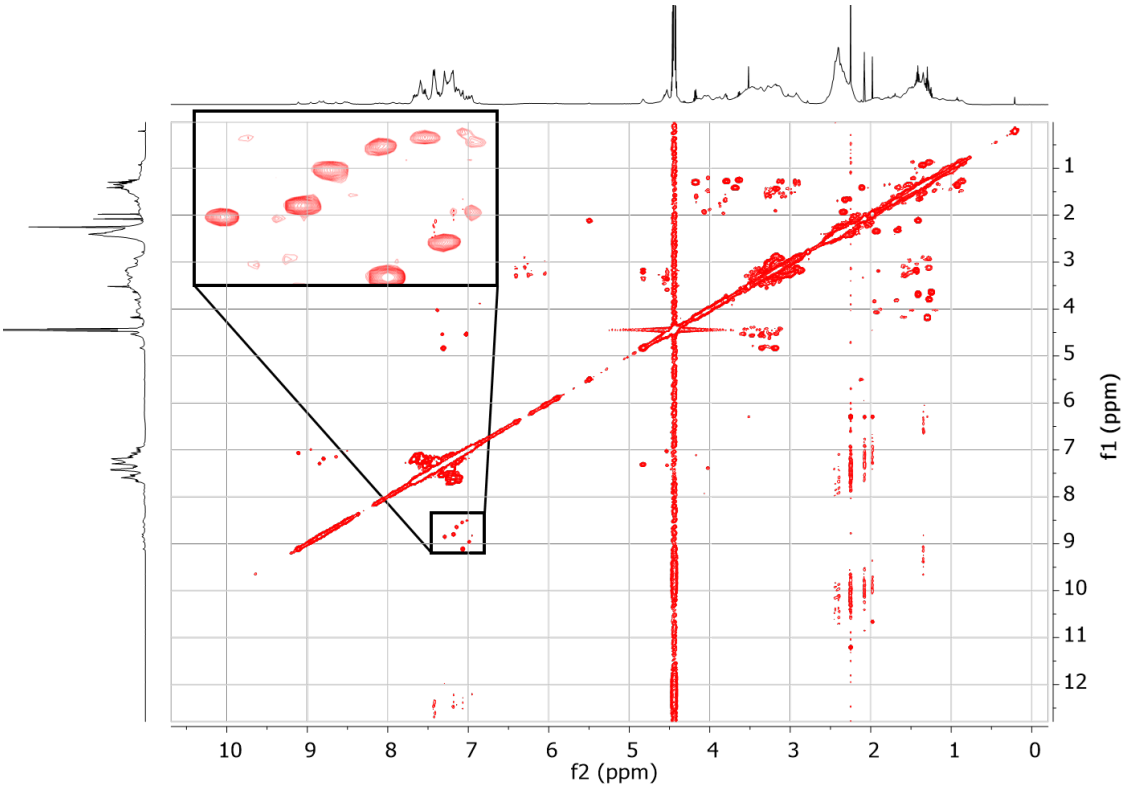

Supplementary Figure 19. COSY of compound **4** in HFIP-d_2 after addition of 10% H_2O, recorded with presaturation (water and *H*O-CD$(CF_3)_2$ signal suppression). The inset shows a zoom of the indole NH region revealing 10 individual indol NH-groups.

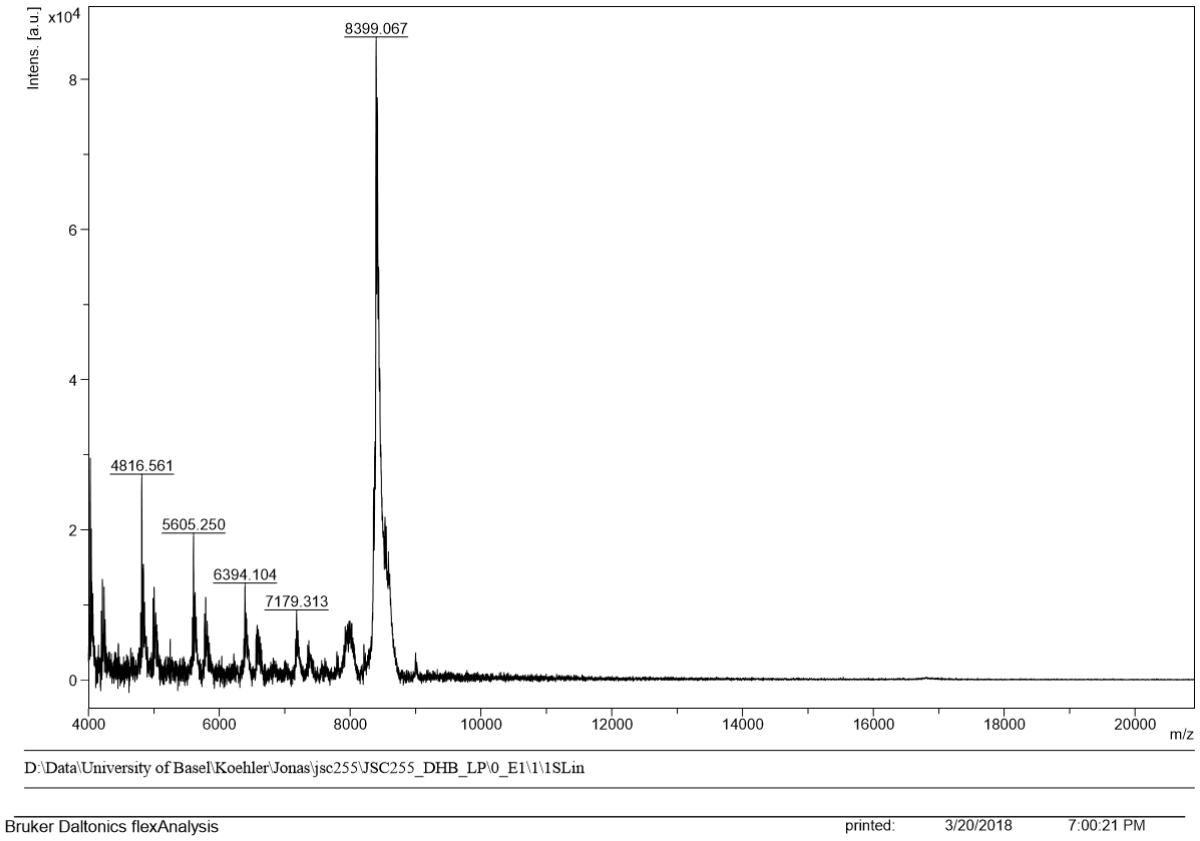

Supplementary Figure 20. MALDI-TOF spectra of compound **4** recorded with DHB as matrix.

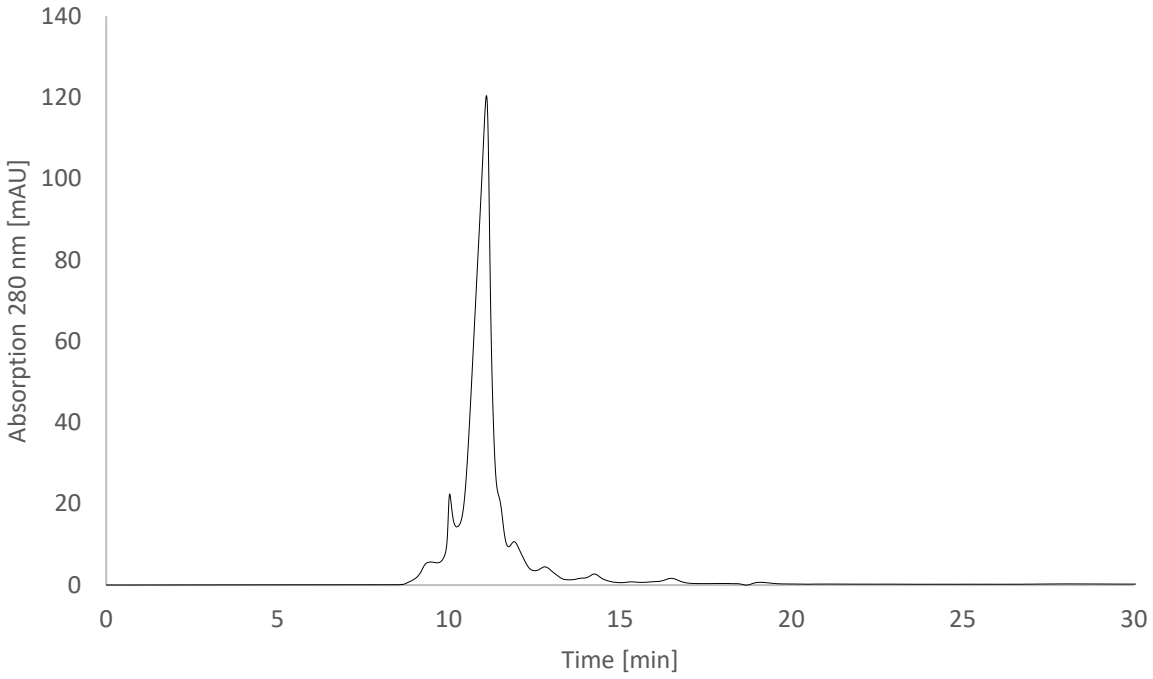

Supplementary Figure 21. Size exclusion chromatogram of compound **4**.

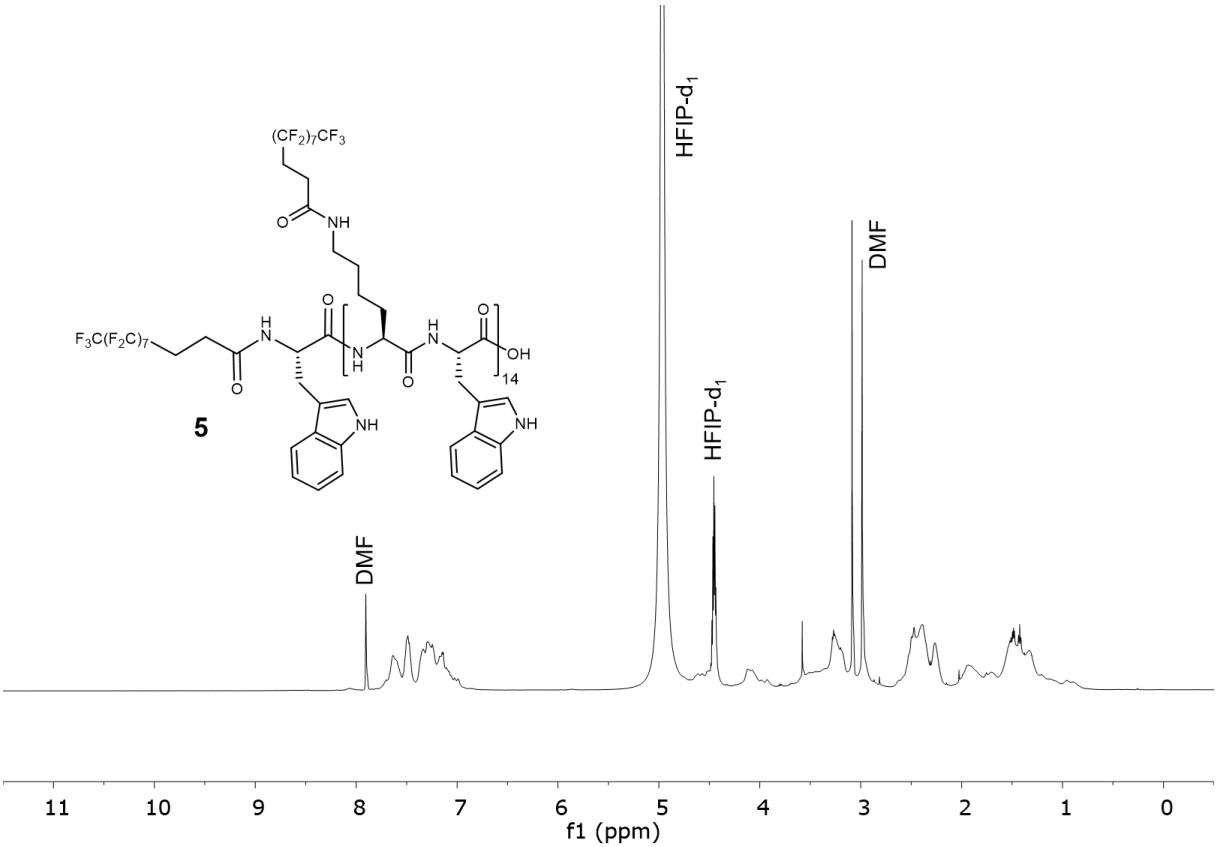

Supplementary Figure 22. ^{1}H-NMR (HFIP-d_2, 600 MHz, 298 K) of compound **5**.

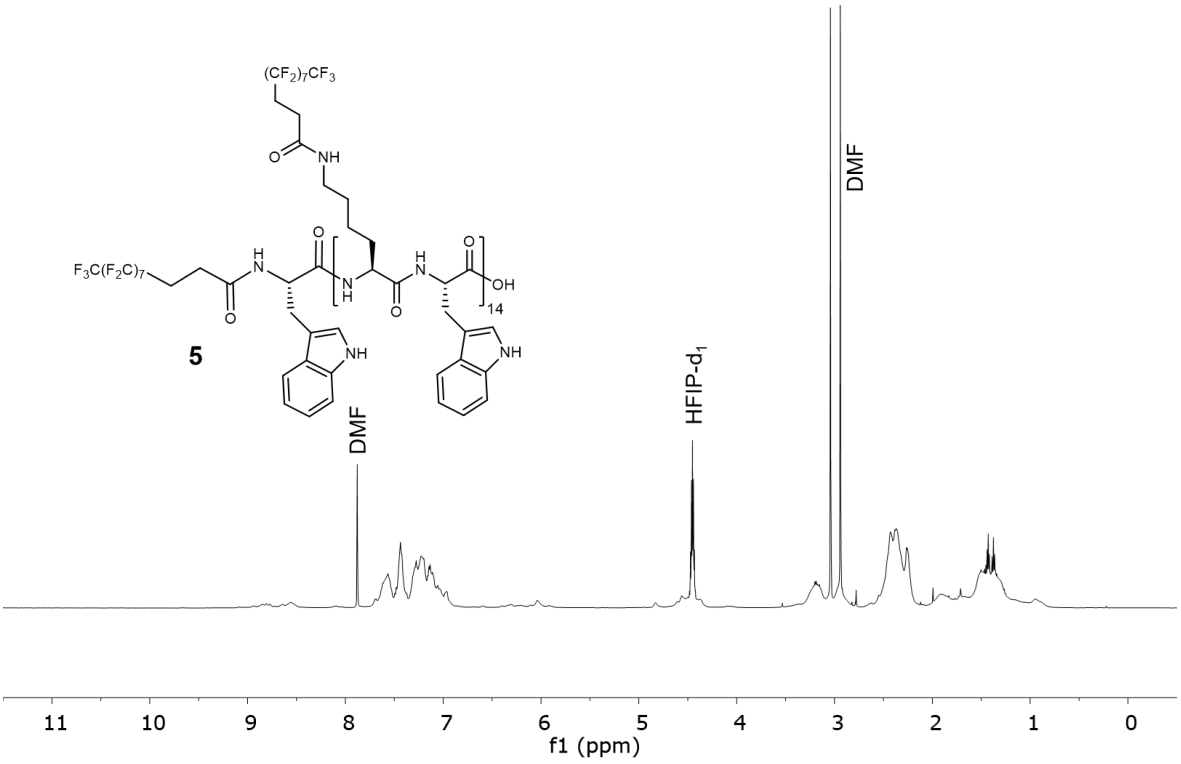

Supplementary Figure 23. ^{1}H-NMR (HFIP-d_2, 600 MHz, 298 K), compound **5** after addition of 10% H_2O recorded with presaturation (water and *HO*-CD$(CF_3)_2$ signal suppression). The addition of H_2O enables observationof the NH-signals. Note that the deuterium to protium exchange is only partial.

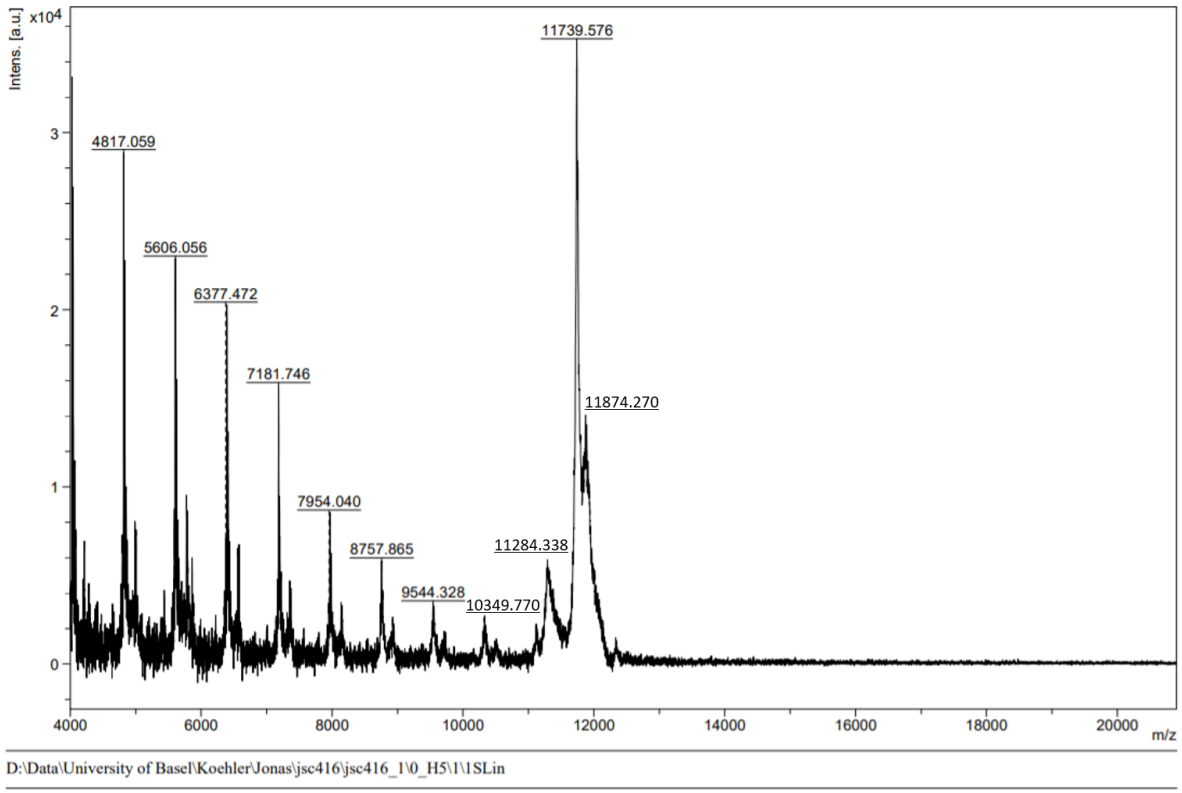

Supplementary Figure 24. MALDI-TOF Mass spectrum of compound **5** recorded with DHB as a matrix.

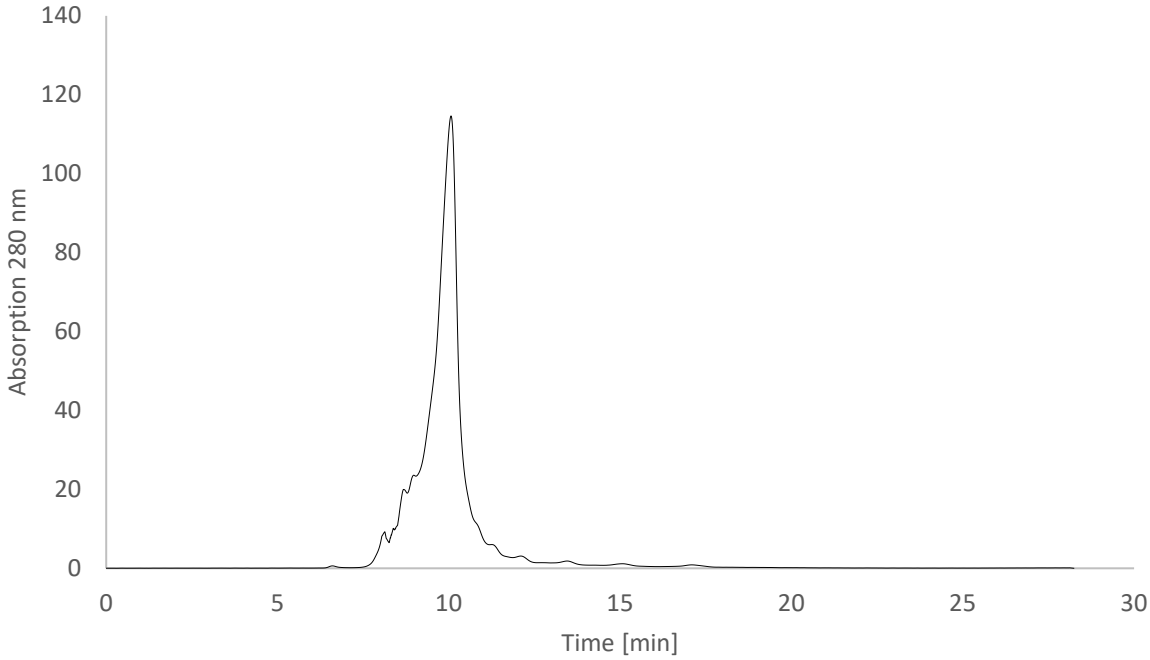

Supplementary Figure 25. Size exclusion chromatogram of compound **5**.

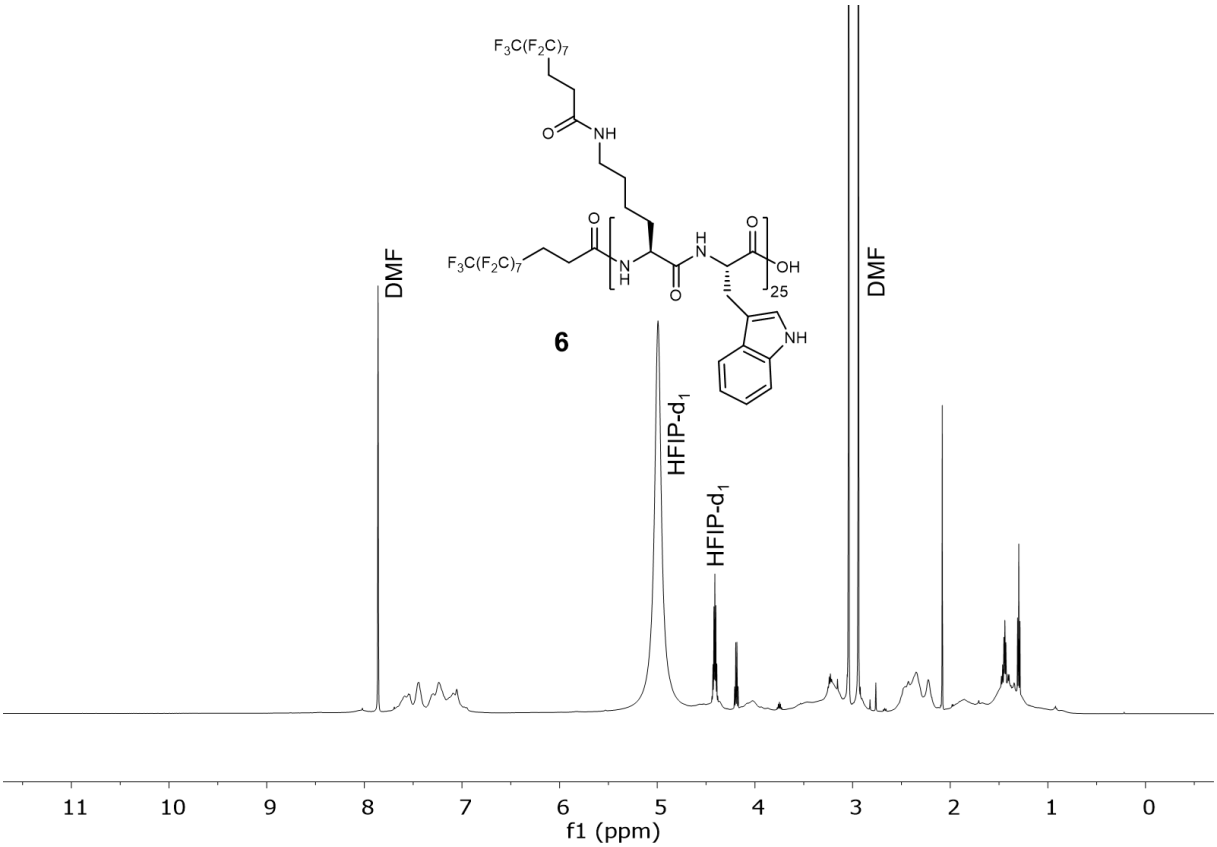

Supplementary Figure 26. ^{1}H-NMR (HFIP-d_2, 600 MHz, 298 K) of compound **6**.

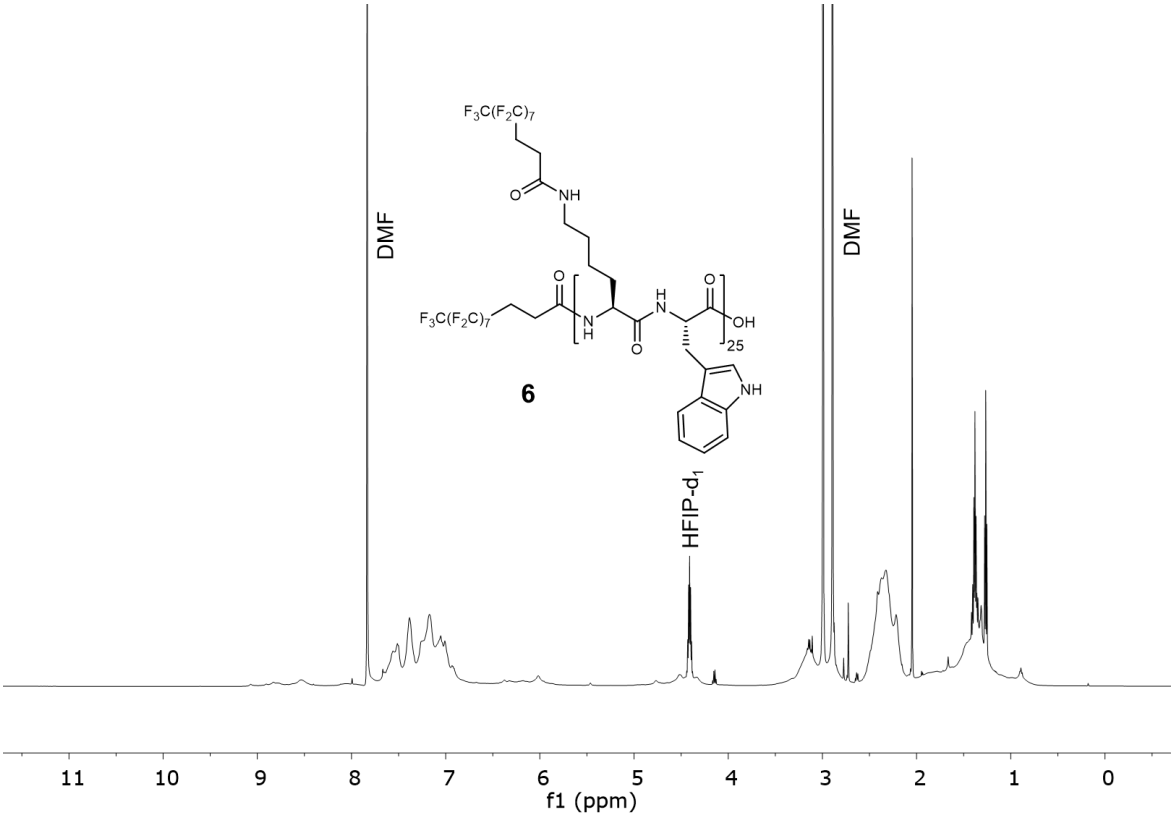

Supplementary Figure 27. ^{1}H-NMR (HFIP-d_2, 600 MHz, 298 K), compound **6** after addition of 10% H_2O recorded with presaturation (water and *HO*-CD$(CF_3)_2$ signal suppression). The addition of H_2O enables observation of the NH-signals. Note that the deuterium to protium exchange is only partial.

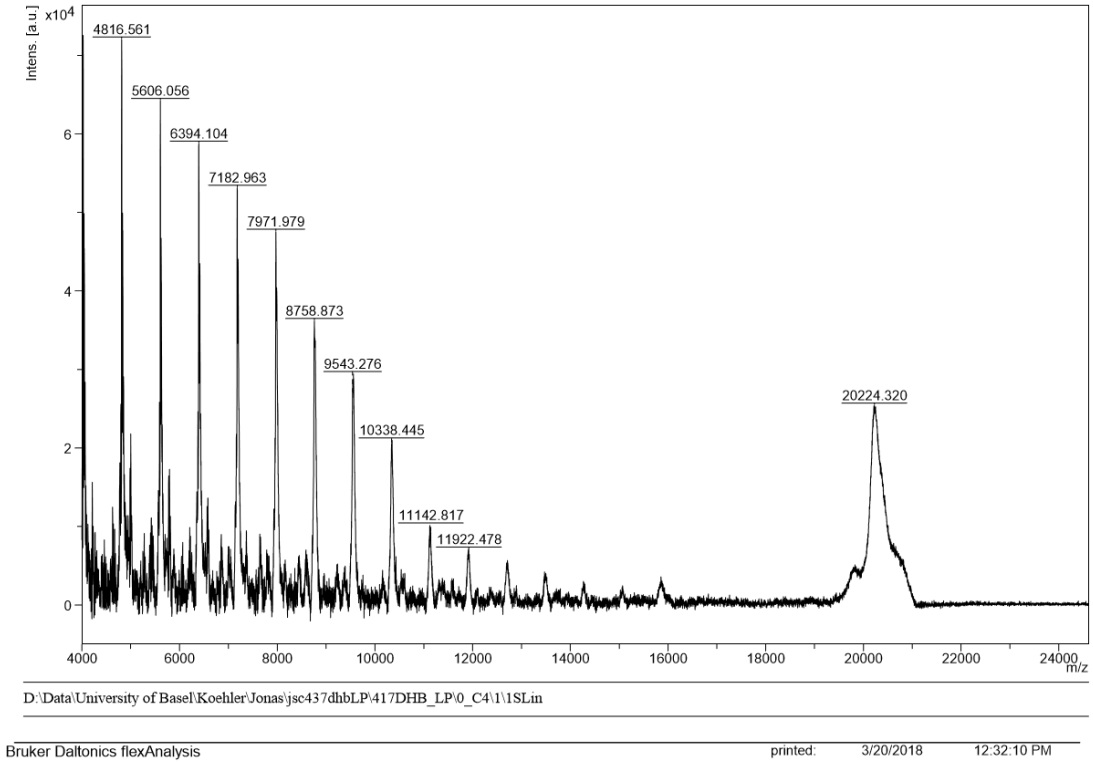

Supplementary Figure 28. MALDI-TOF spectrum of compound **6** recorded with DHB as a matrix.

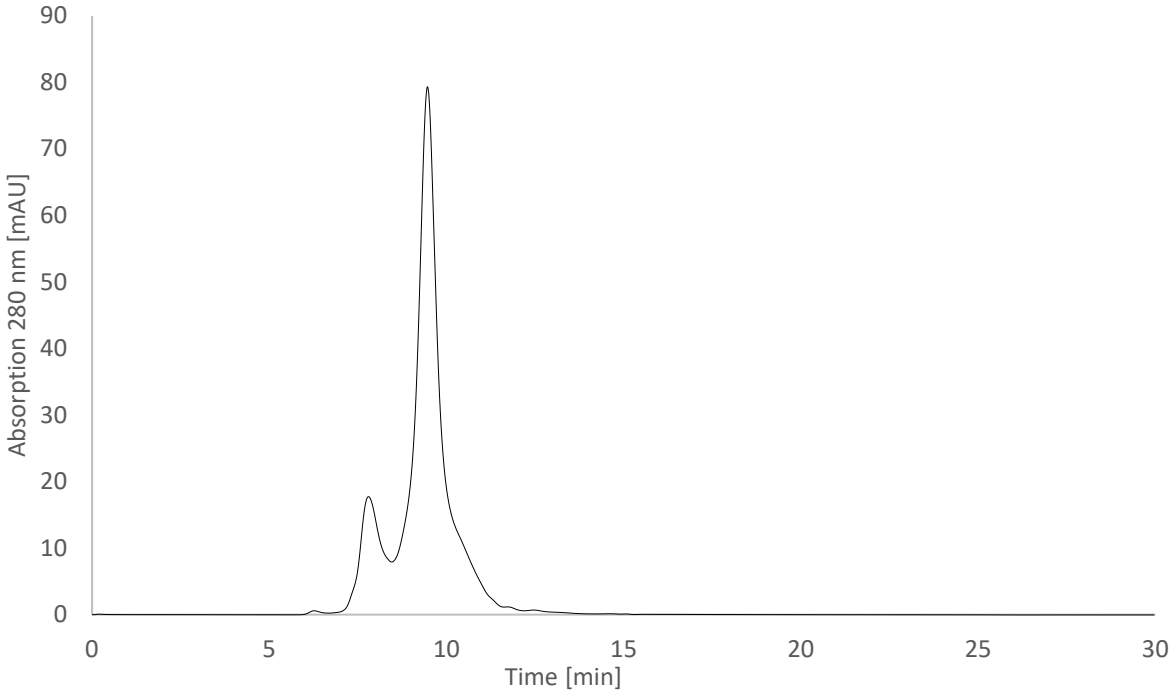

Supplementary Figure 29. Size exclusion chromatogram of compound **6**.

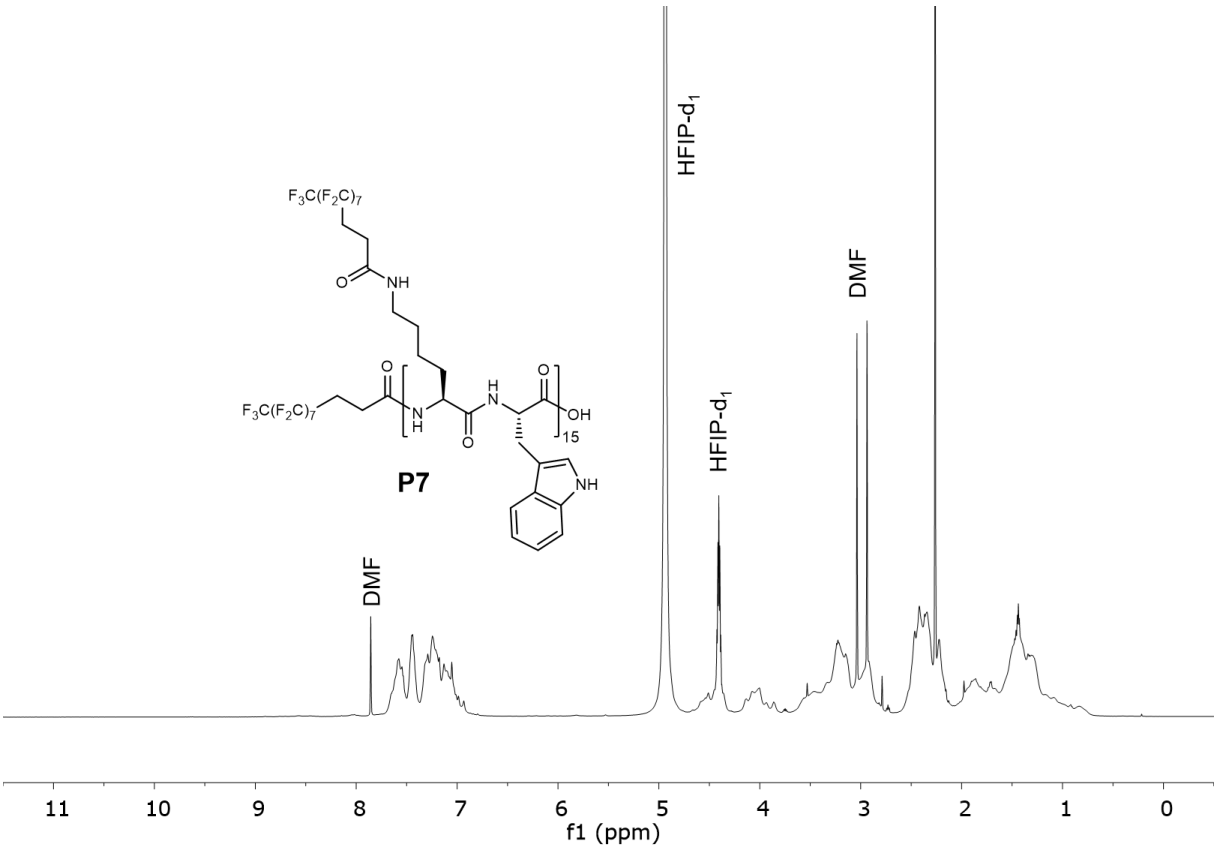

Supplementary Figure 30. ^{1}H-NMR (HFIP-d_2, 600 MHz, 298 K) of compound **P7**.

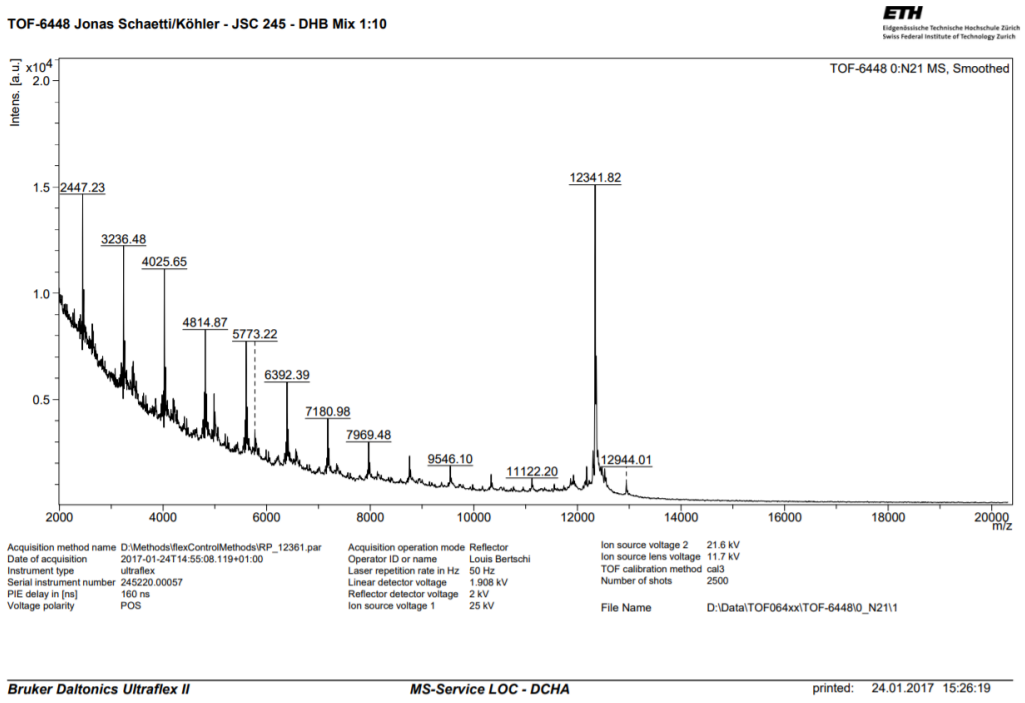

Supplementary Figure 31. MALDI-TOF Mass spectrum of compound **P7** recorded with DHB as a matrix.

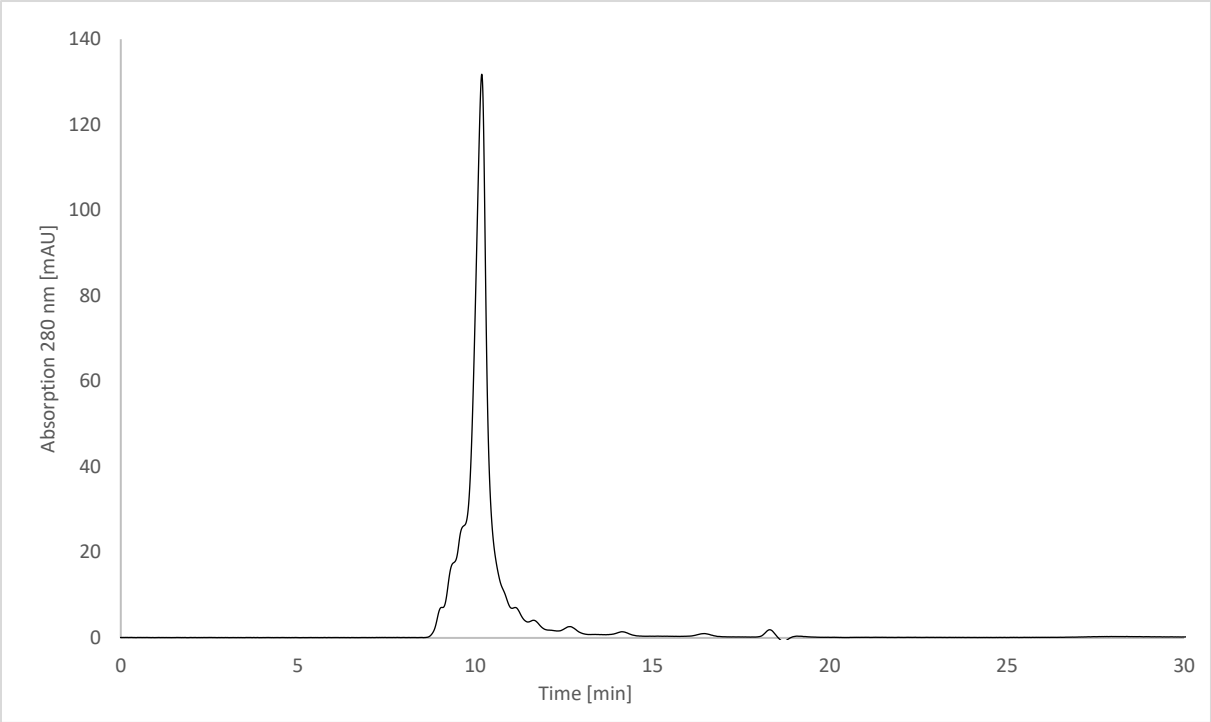

Supplementary Figure 32. Size exclusion chromatogram of compound **P7**.

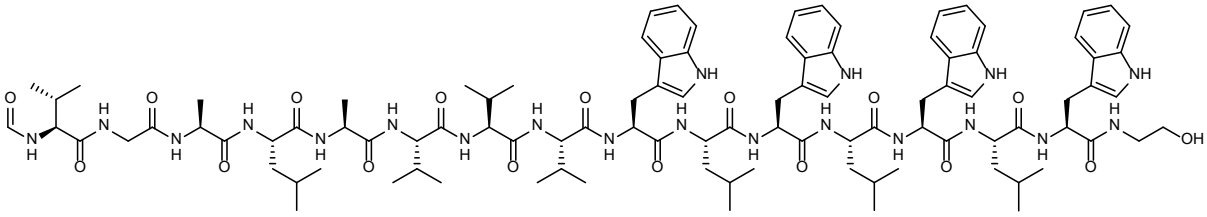

1 (1882 amu)

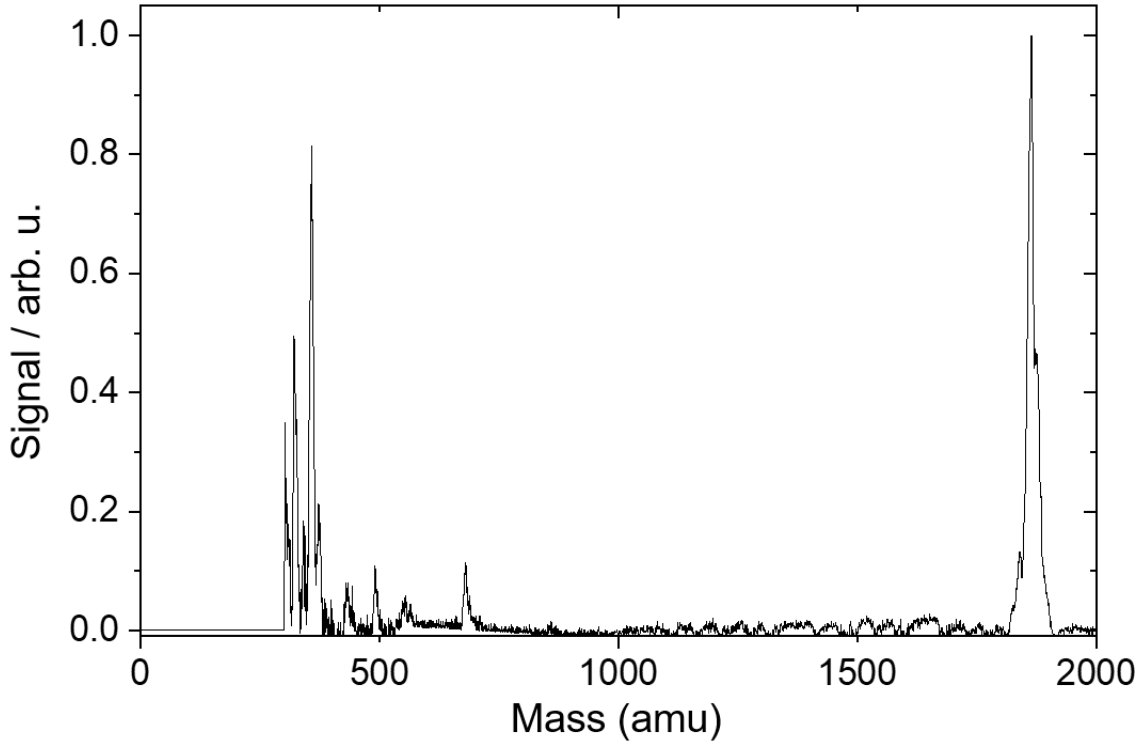

Supplementary Figure 33. Laser desorption/photoionization TOF mass spectrum of commercial Gramicidin D (Sigma Aldrich, purity as delivered, main component A1), recorded after shortpulse infrared laser desorption (7 ns, 1064 nm). The peaks below 500 amu are noise, unrelated to the desorbed molecule.

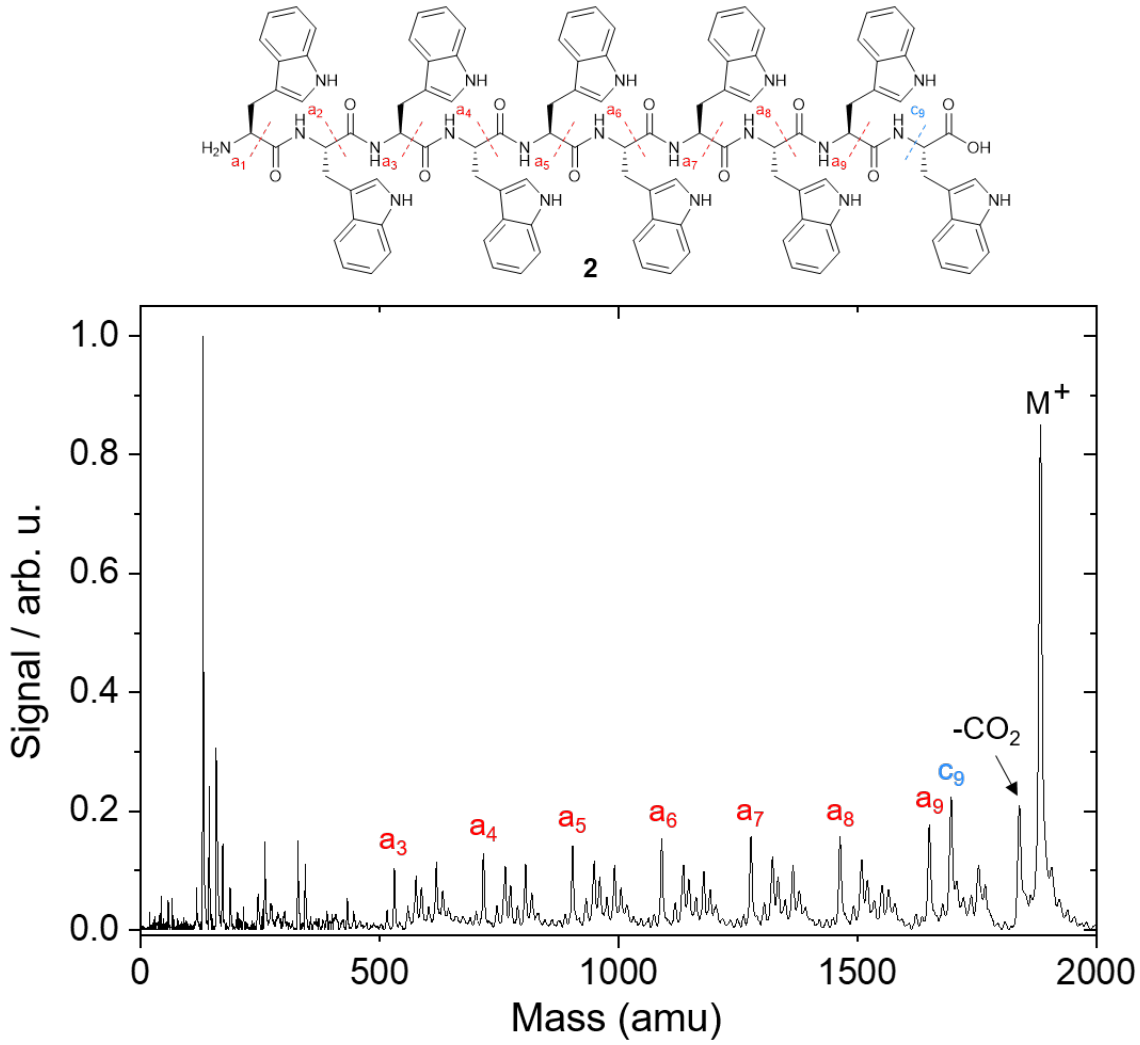

Supplementary Figure 34. Laser desorption/photoionization TOF mass spectrum of the TFA salt of decatryptophan **2** recorded after shortpulse infrared laser light desorption (7 ns, 1064 nm).

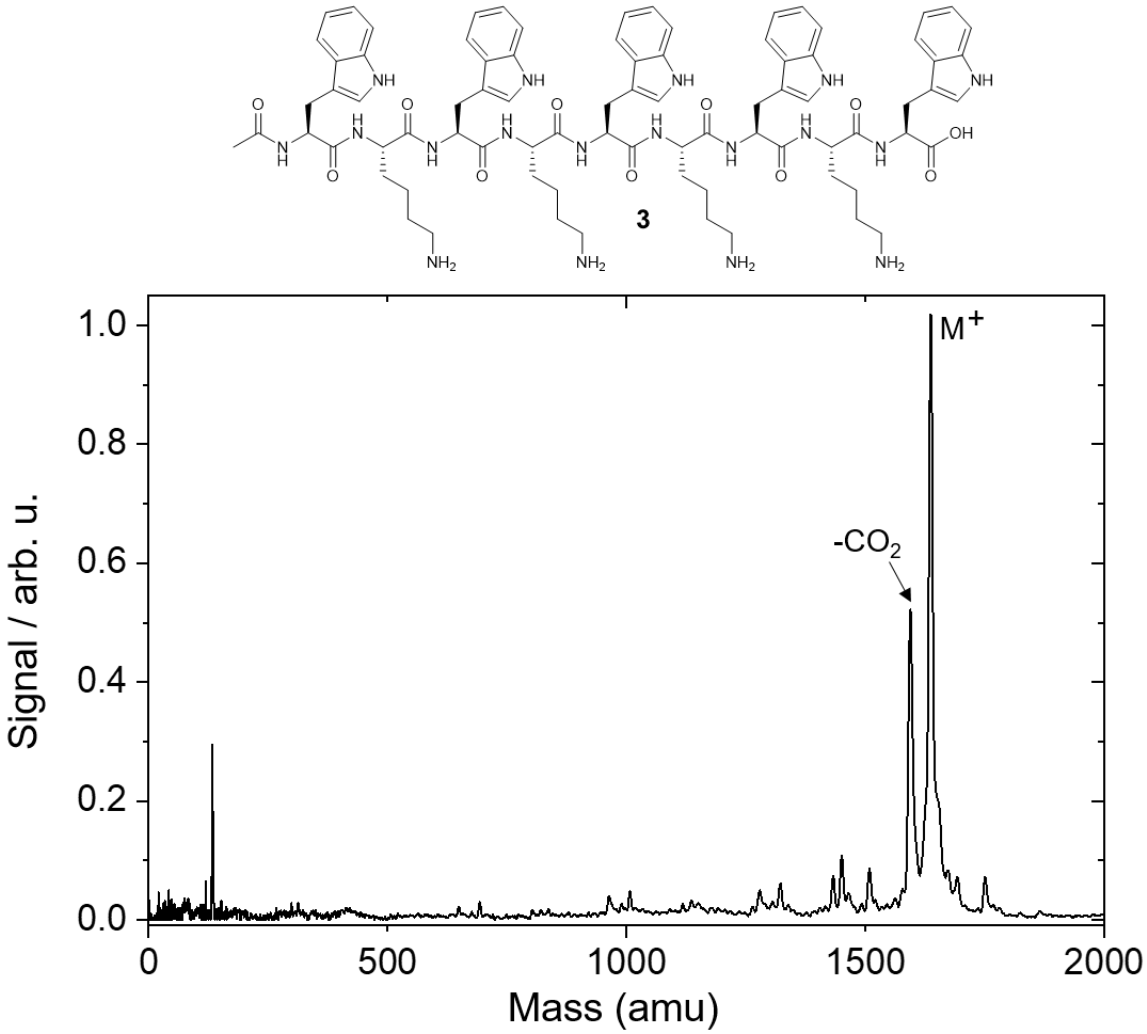

Supplementary Figure 35. Laser desorption/photoionization TOF mass spectrum of the TFA salt of compound **3** recorded after short-pulse infrared laser light desorption (7 ns, 1064 nm).

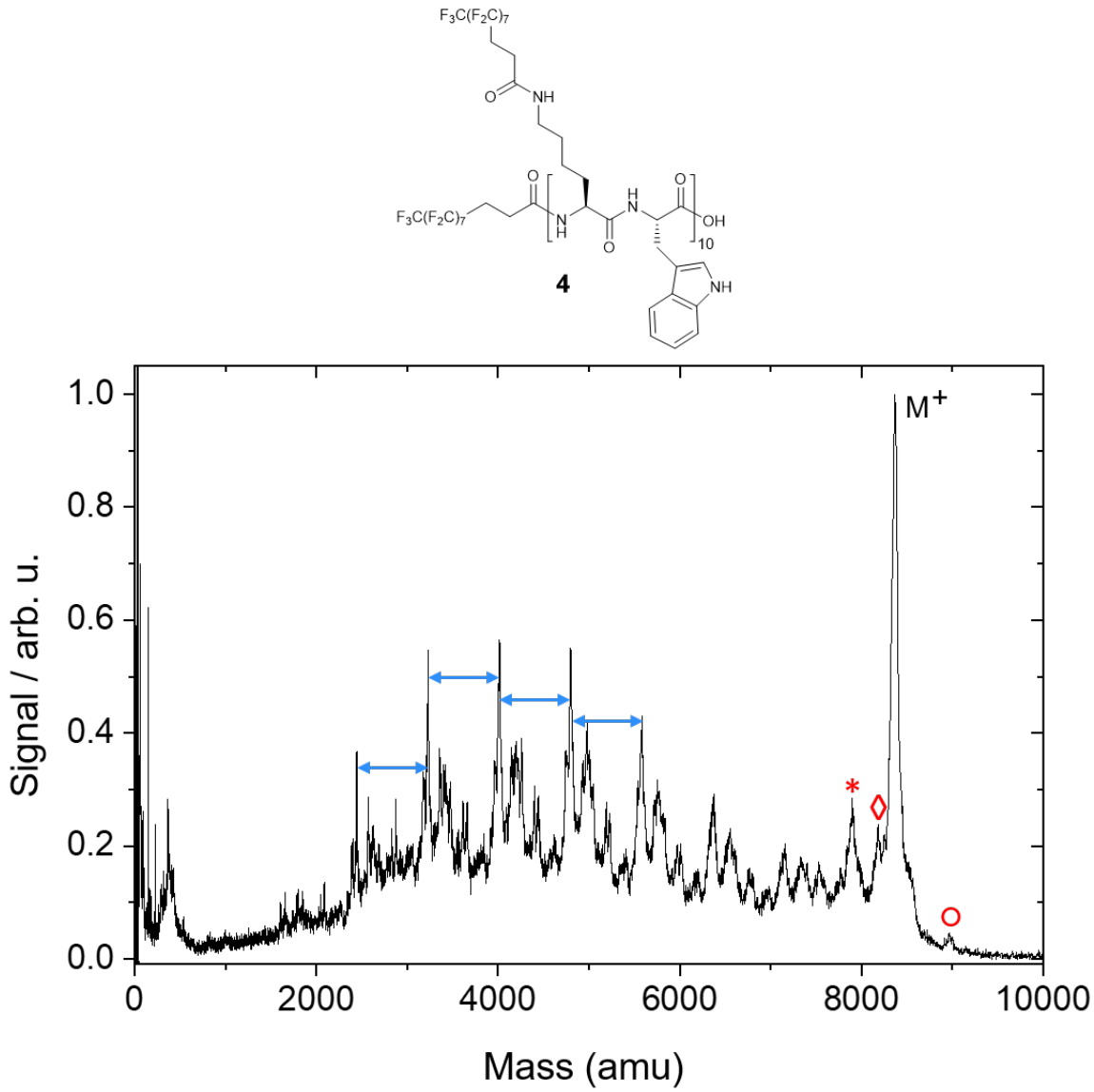

Supplementary Figure 36. Laser desorption/photoionization TOF mass spectra of compound (**4**), using 266 nm laser desorption from Trp matrix and carried by a T = 115 K Argon supersonic gas jet. The blue arrows indicate the mass difference of Trp-Lys(*2H*,*2H*,*3H*,*3H*-perfluoroundecanoyl) units (788 amu) between fragments. * corresponds to the loss of a 2*H*,2*H*,3*H*,3H-perfluoroundecanoyl unit (475 amu); ◊ corresponds to the loss of the C-terminal tryptophan unit (188 amu); ○ is likely caused by an impurity which results from incorporation of an additional Lys(*2H*,*2H*,*3H*,*3H*-perfluoroundecanoyl) unit (602 amu) during synthesis.

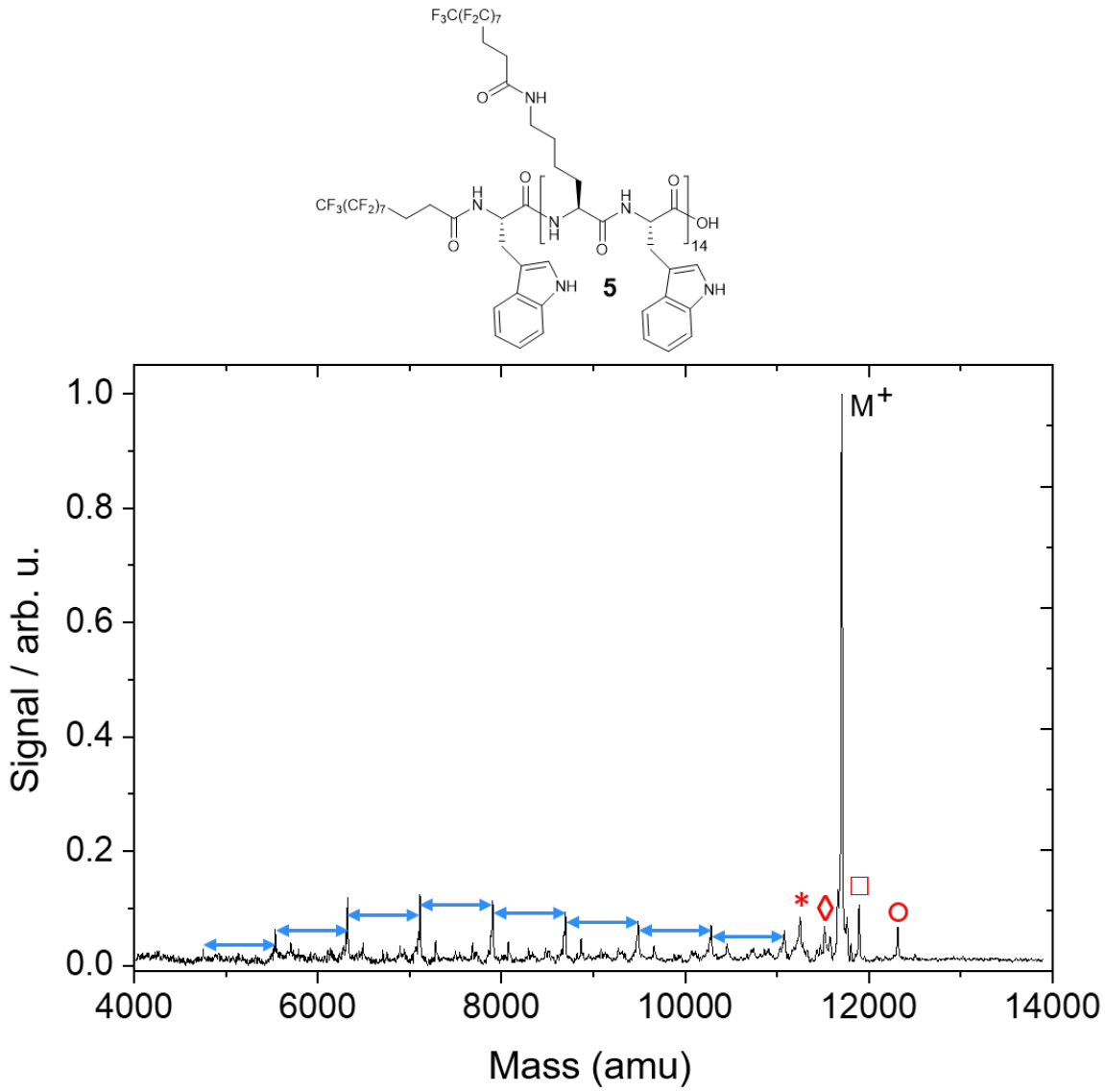

Supplementary Figure 37. Laser desorption/photoionization TOF mass spectra of compound **5** recorded after 343 nm laser desorption (E = 15 μJ, τ = 292 fs) from Trp matrix at T = 300 K. The blue arrows indicate the mass difference of Trp-Lys(*2H*,*2H*,*3H*,*3H*-perfluoroundecanoyl) units (788 amu) between fragments. * corresponds to the loss of a 2H,2H,3H,3H-perfluoroundecanoyl unit (475 amu); ◊ corresponds to the loss of the C-terminal tryptophan unit (188 amu); □ and ○ are likely caused by impurities which result from incorporation of an additional Trp (186 amu) or Lys(*2H*,*2H*,*3H*,*3H*-perfluoroundecanoyl) unit (602 amu) during synthesis.

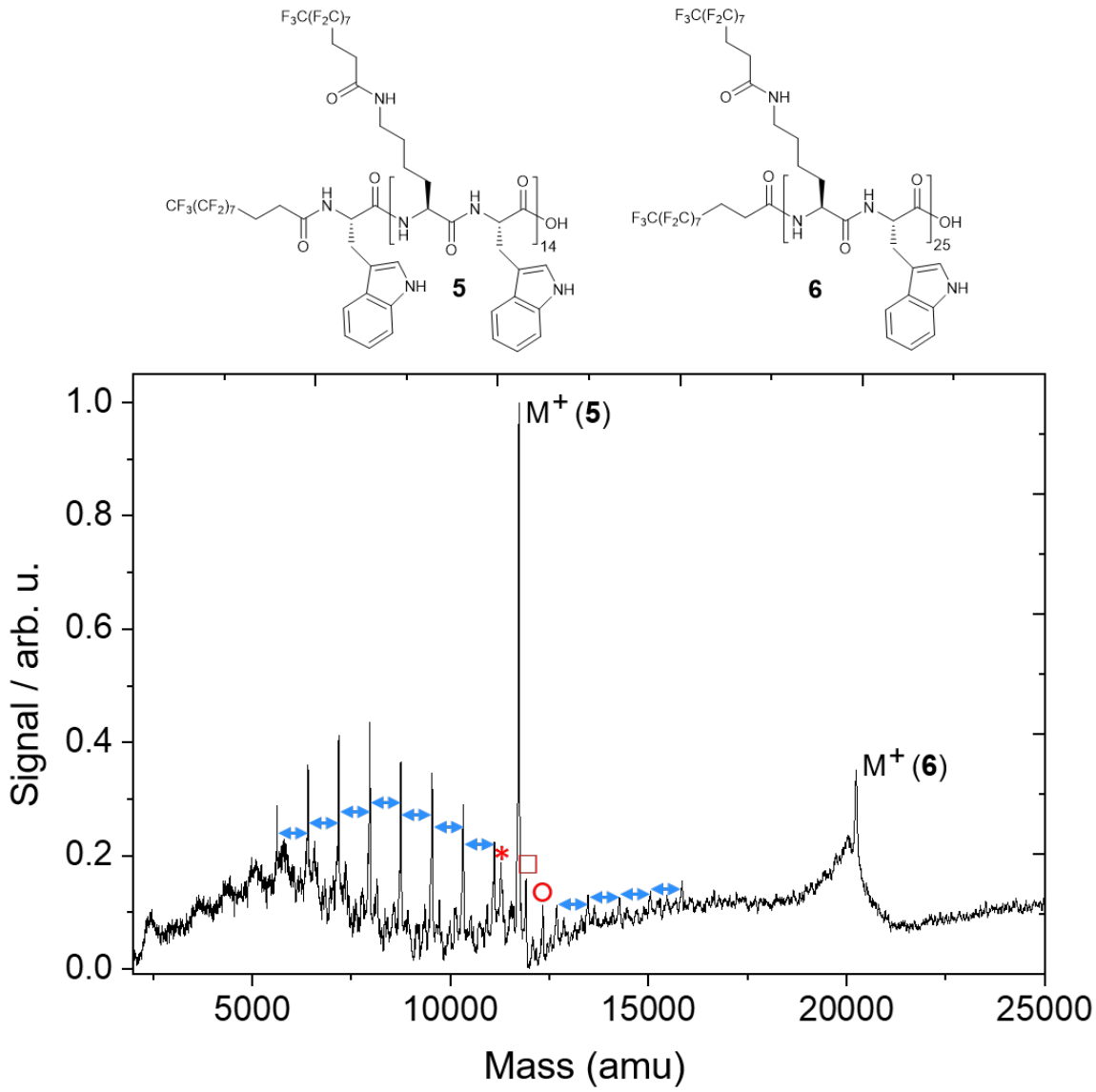

Supplementary Figure 38. Laser desorption/photoionization TOF mass spectra of a mixture of compound **5** and **6** (ratio 3 : 28) recorded after 343 nm laser desorption (E = 15 μJ, τ = 292 fs). The blue arrows indicate the mass difference of Trp-Lys(*2H*,*2H*,*3H*,*3H*-perfluoroundecanoyl) units (788 amu) between fragments. * corresponds to the loss of a 2H,2H,3H,3H-perfluoroundecanoyl unit (475 amu) from **5**; □ and ○ are likely caused by impurities which result from incorporation of an additional Trp (186 amu) or Lys(*2H*,*2H*,*3H*,*3H*-perfluoroundecanoyl) unit (602 amu) during synthesis.

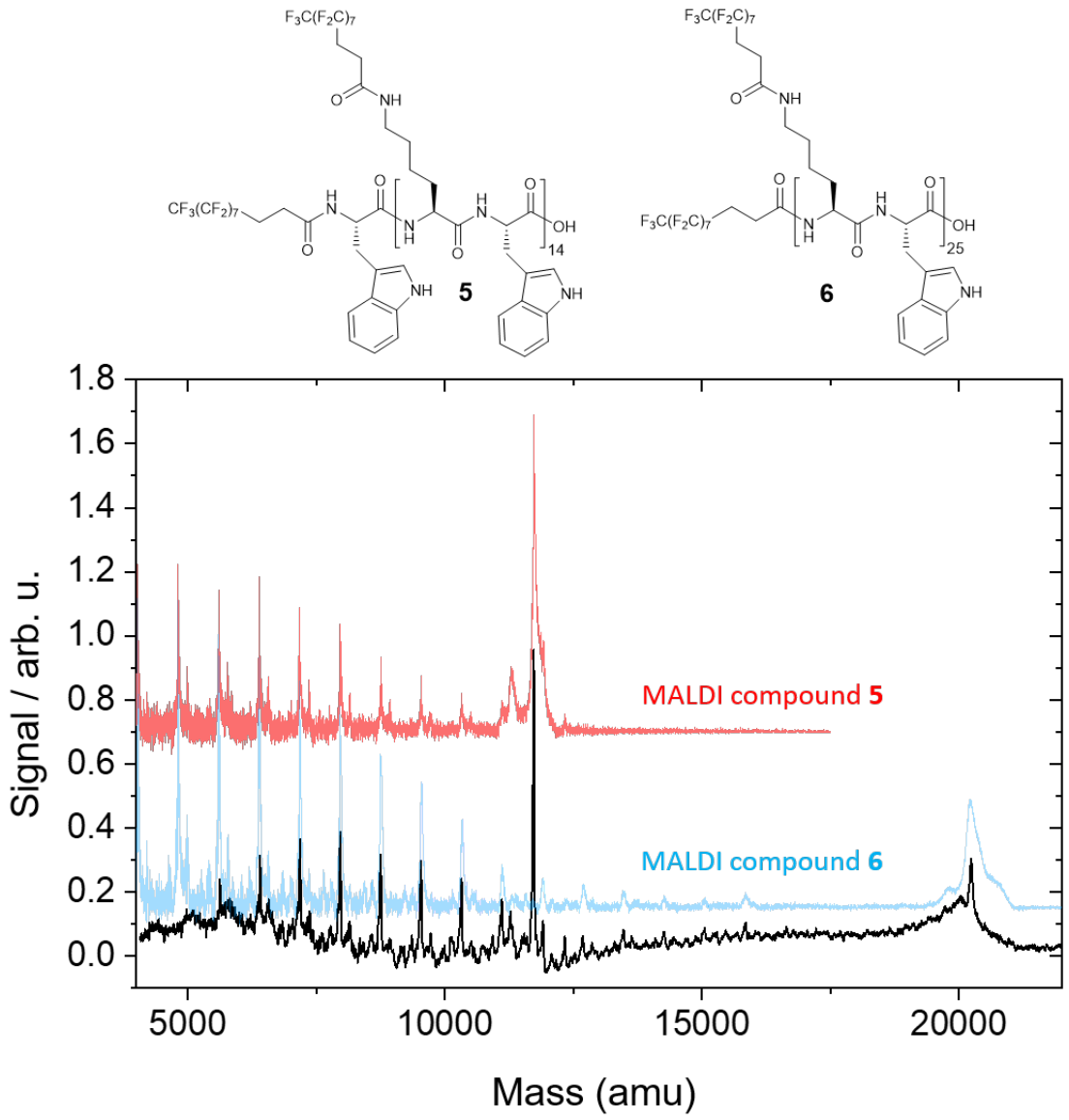

Supplementary Figure 39. Calibration of the high mass spectra. Overlay of MALDI-TOF mass spectra for compounds **5** and **6** and laser desorption/VUV postionization experiment depicted in Supplementary Figure 38, which was conducted with a mixture of compound **5** and **6**. An offset has been applied to highlight the match between the observed signals in the three spectra. Comparing the spectra allowed unambiguous calibration of the laser desorption/VUV postionization experiment. The MALDI instrument was calibrated with protein standards as specified in the synthesis section of the Supplementary Methods section.

Supplementary Note 2. Computational details

A single molecule of the artificial protein (**6**) was simulated in GROMACS 2018.1 using a vacuum setup, i.e. periodic boundary conditions switched off, the box is ignored, and no distance cut-offs employed when evaluating interatomic interactions. The GROMOS force-field version 54B7 was used as the force-field of the Lysine and Tryptophan residues,[4,5] while the force-field for the fluoroalkyl chains was obtained using the Automated Topology Builder methodology, based on automated parametrization employing the GROMOS force-field and optimal partial charge assignment aided by ab-initio quantum calculations.[6,7] Canonical-ensemble (NVT) molecular dynamics simulations were performed over the temperature range 10-400K in steps of 10K. The temperature coupling method employed was velocity rescaling with a stochastic term.[8] The length of the bonds involving hydrogen atoms was constrained with the LINCS algorithm.[9] The leapfrog integrator with a time step of 1 fs was employed. At each temperature, 200 runs of 2 ns each were performed. Each run started from the same stretched configuration, but with different initial velocities randomly assigned from a Maxwell distribution at each given temperature. Thus, simulations at each temperature spanned a combined length of 400 ns. For each temperature, the quantities of interest were averaged over the last 100 ps of each run, and then the pool of averages were re-averaged and the standard deviation was calculated. The average end-to-end distance, $\langle R_e \rangle$, was calculated between the terminus of the amino acids at the ends of the backbone. The average solvent surface accessible area, <SASA>, was calculated using the method descried in Ref. 10.[10]

Compound	(1)	(2)	(3)	(4)	(5)	(6)	(P2)	(P7)
MW / amu	1882	1880	1631	8377	11716	20201	3832	12320
Molecular beam								
Backing gas	Ar/Ne/Ne/Ne	Argon	Argon	Argon	Argon	Argon	Argon	Neon
Backing pressure /bar	20 / 28 / 28 / 28	20	30	48	48	48	48	48
Gas temperature / K	300	300	300	90	300	300	300	115
Source pressure/mbar	10^{-4}	10^{-4}	10^{-4}	10^{-4}	10^{-5}	10^{-5}	10^{-4}	10^{-4}
Trp. admixture	none	none	none	1:20	none	none	none	1:20
Desorption								
Dersorption λ / nm	1064 / 266 / 1040 / 343	1064	1064	266	343	343	1064	266
Dersorption τ	7 ns / 7 ns / 290 fs / 290 fs	7 ns	7 ns	7 ns	290 fs	290 fs	7 ns	7 ns
Desorption E	32 mJ / 4 mJ / 15 µJ / 15 µJ	32 mJ	32 mJ	1.77 mJ, 2.64 mJ, 4 mJ, 5.44 mJ	15 µJ	15 µJ	32 mJ	1.77 mJ, 2.64 mJ, 4 mJ, 5.44 mJ, 8.53 mJ
Circular spot diameter	3 mm / 3 mm / 100 µm / 100 µm	3 mm	3 mm	3 mm	100 µm	100 µm	3 mm	3 mm
Repetition rate / Hz	10 / 10 / 20 & 100 / 20 & 100	10	10	10	100	100	10	10
Ionization								
Wavelength λ / nm	157.6	157.6	157.6	157.6	157.6	157.6	157.6	157.6
Pulse duration τ / ns	10	10	10	10	10	10	10	10
Energy E / mJ	0.8	0.8	0.8	0.528, 0.8	1.6	1.6	0.8	0.528, 0.8
Spot size / mm x mm	3 x 1	3 x 1	3 x 1	3 x 1	3 x 1	3 x 1	3 x 1	3 x 1
Averaging / shots	500	500	300	500	5000	5000	600	1000

Supplementary Table 2. Desorption and ionization efficiency. Experimental parameters used in the laser desorption/photoionization experiments.

Supplementary Note 3. The influence of the desorption laser wavelength and pulse length on the character of the mass spectrum

Throughout this work, various laser wavelengths and pulse durations were explored to optimize the desorption conditions. As illustrated in Figure 5 of the main text, the final mass spectra for compound **(5)** resemble each other in almost all detail, even when comparing nanosecond and femtosecond desorption. The process differs, however, in the efficiency of the molecular individualization.

Here we complement this information by comparing six different desorption settings for gramicidin D, namely *nanosecond* desorption 1064 nm and 266 nm as well as *femtosecond* desorption with 1030 nm and 343 nm and repetition rates of 10, 20 and 100 Hz. This is shown in Supplementary Figure 40. While one finds different absolute numbers of molecules, the overall mass spectrum remains largely unchanged for gramicidin D.

However, UV desorption becomes important for high-mass compounds, such as (**4**) and (**5**), and the 20 kDa polypeptides (**6**) could only be seen after fs desorption at 343 nm. Both shorter wavelength and shorter pulses go along with a reduced penetration depth of the laser light. This is consistent with the observation of fewer molecular aggregates in the vacuum chamber.

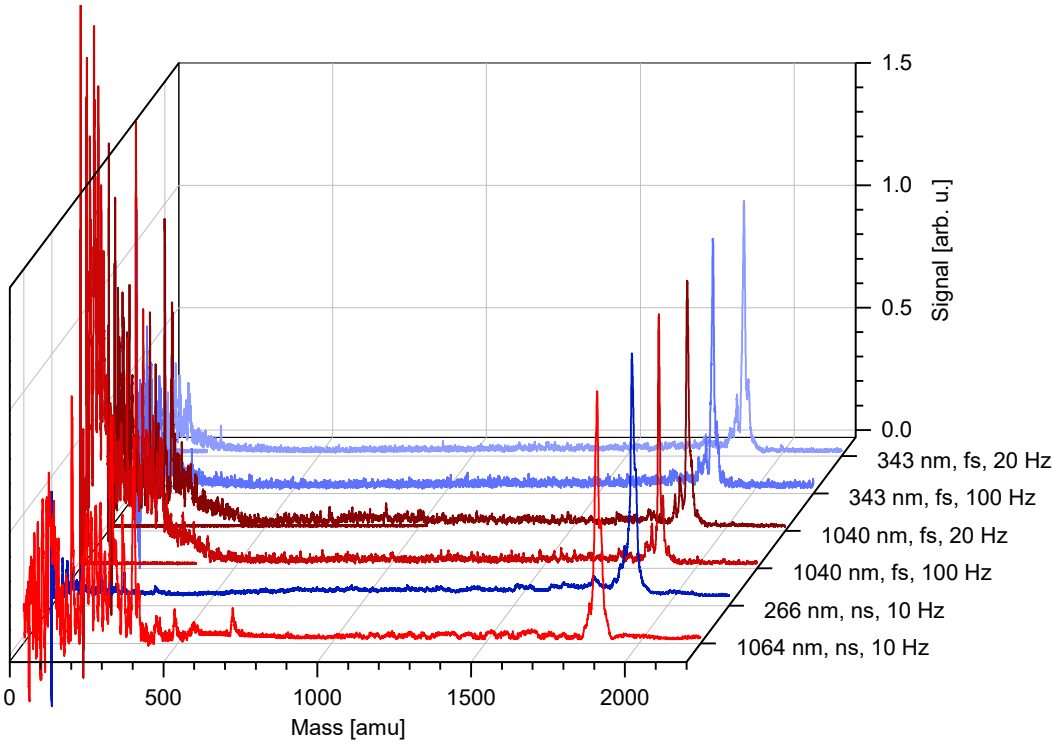

Supplementary Figure 40. Mass spectra of gramicidin D, recorded for different laser conditions as tabulated in Supplementary Table 2. Even under vastly different desorption conditions – from pulse durations between 290 fs to 7 ns and, energies between 40 µJ and 30 mJ and wavelengths between 343 nm and 1064 nm, the changing laser settings *significantly influence the number of released molecules but much less their mass spectrum*. The signals are normalized to the gramicidin peak. The noise below 500 amu is also present without the molecular beam. As described in the main text, the key difference between the different laser conditions is in the number of aggregates that are released by the pulses. They decide about the economy of the desorption process, but are too massive to be detected by the TOF-MS.

Supplementary Note 4. The influence of the desorption energy/fluence

When varying the desorption laser power, we observe the threshold behavior and saturation seen in Supplementary Figure 41. It suggests that all accessible material has been volatilized, that high power light facilitates the occurrence of large aggregates – which would not show up in TOF-MS - or that fragmentation processes start to compete with the intact volatilization process. The latter can be essentially excluded, when comparing signals differing more than 3-fold in desorption energy in Supplementary Figure 42.

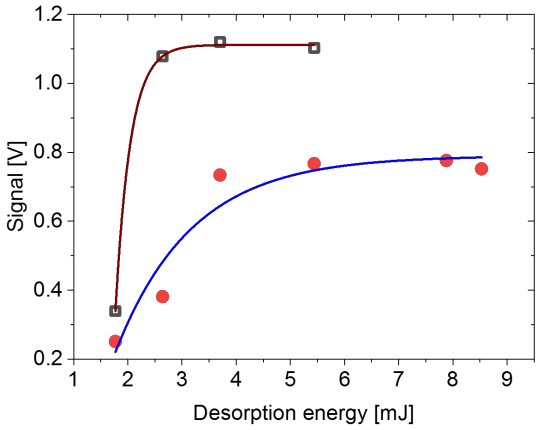

Supplementary Figure 41. The signal increases with **increasing desorption laser energy**, as is illustrated here for the high-mass polymers **(4)** with 8377 amu and **(P7)** with 12320 amu. They are represented by grey squares and red circles, respectively**.** The experimental data are fitted by exponential growth curves to guide the eye. The compounds were desorbed using 266 nm light with 7 ns pulse duration at 10 Hz repetition rate and ionized with 157.6 nm and 0.8 mJ pulse energy (see Supplementary Table 2).

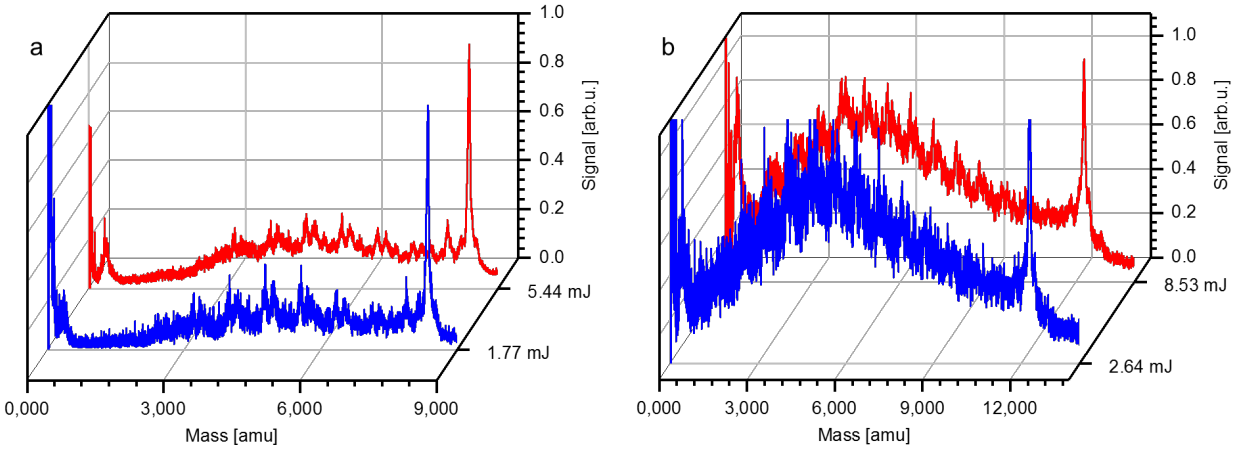

Supplementary Figure 42. Mass spectra of (a) compound (**4**) and (b) compound (**P7**) for different desorption energies. The mass spectra for low desorption energies have been scaled to show that the desorption process does not induce any additional major fragmentation even when the energy is increased by a factor of 3. The compounds were desorbed using 266 nm light with 7 ns pulse duration at 10 Hz repetition rate and ionized with 157.6 nm and 0.8 mJ pulse energy (see Supplementary Table 2).

Supplementary Note 5. The influence of the ionization energy/fluence on the normalized mass peak

The ionization laser pulse energy obviously affects the ion signal of the principle mass and to first order one would expect a linear dependence for a single-photon ionization processes, as observed for cold clusters of tryptophan[11]. On the other hand, it is justified to assume that the total absorption cross section grows linearly with the number of chromophores, i.e. here with the length of the peptide chain.

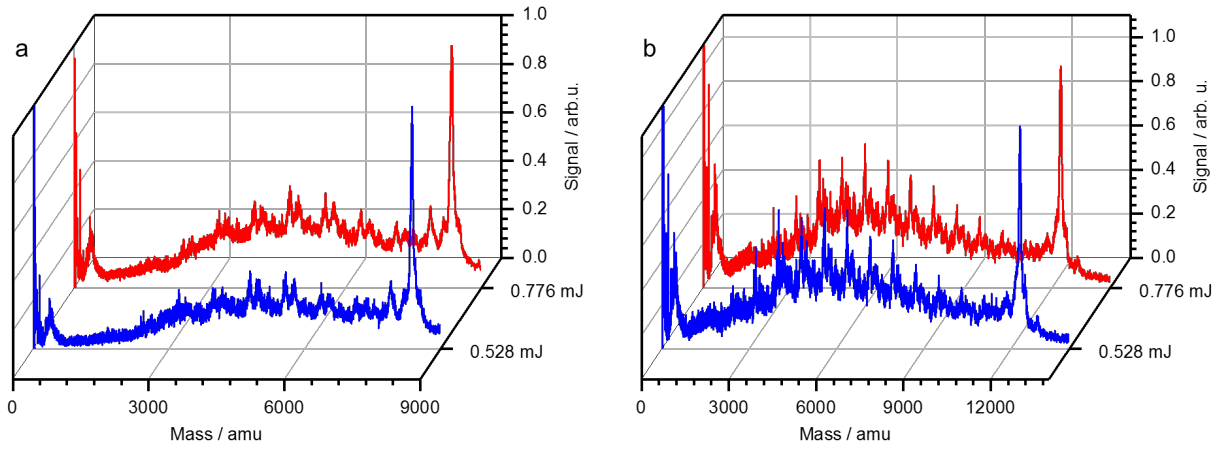

Supplementary Figure 43. Mass spectra of (a) compound (**4**) and (b) compound (**P7**) for different **ionization energies**. The mass spectra for low ionization energy have been scaled by a factor of 1.4. Within the 50% power variation, the overall molecular beam intensity follows linearly the laser energy while the mass peak distribution does not change substantially. The data are shown without adaptive baseline correction. The experimental conditions are given in Supplementary Table 2 with 4 mJ desorption pulse energy.

Supplementary References

[1] Chan WC, White PD. *Fmoc Solid Phase Peptide Synthesis*. Oxford University Press, Oxford (2000).

[2] Malik L, Nygaard J, Hoiberg-Nielsen R, Arleth L, Hoeg-Jensen T, Jensen KJ. Perfluoroalkyl chains direct novel self-assembly of insulin. *Langmuir* **28**, 593-603 (2012).

[3] Schätti J, Sezer U, Pedalino S, Cotter JP, Arndt M, Mayor M, Köhler V. Tailoring the volatility and stability of oligopeptides. *J Mass Spectrom* **52**, 550-556 (2017).

[4] Poger D, Mark AE, van Gunsteren WF. A new force field for simulating phosphatidylcholine bilayers. *J Comput Chem* **31**, 1117-1125 (2010).

[5] Schmid N, Eichenberger AP, Choutko A, Riniker S, Winger M, Mark AE, van Gunsteren WF. Definition and testing of the GROMOS force-field versions 54A7 and 54B7. *Eur Biophys J* **40**, 843-856 (2011).

[6] Malde AK, Zuo L, Breeze M, Stroet M, Poger D, Nair PC, Oostenbrink C, Mark AE. An Automated force field Topology Builder (ATB) and repository: version 1.0. *J Chem Theory Comput* **7**, 4026-4037 (2011).

[7] Koziara KB, Stroet M, Malde AK, Mark AE. Testing and validation of the Automated Topology Builder (ATB) version 2.0: prediction of hydration free enthalpies. *J Comput Aid Mol Des* **28**, 221-233 (2014).

[8] Bussia G, Donadio D, Parrinello M. Canonical sampling through velocity rescaling. *J Chem Phys* **126**, 014101 (2007).

[9] Hess B, Bekker H, Berendsen HJC, Fraaije JGEM. LINCS: A linear constraint solver for molecular simulations. *J Comput Chem* **18** 1463-1472 (1997).

[10] Eisenhaber F, Lijnzaad P, Argos P, Sander, C, Scharf M. The double cubic lattice method: Efficient approaches to numerical integration of surface area and volume and to dot surface contouring of molecular assemblies. *J Comput Chem* **16**, 273-284 (1995).

[11] M. Marksteiner, P. Haslinger, M. Sclafani, H. Ulbricht, M. Arndt, UV and VUV Ionization of Organic Molecules, Clusters, and Complexes, *J. Phys. Chem.* **A 113**, 9952-9957 (2009).

[12] S. Gerlich, S. Eibenberger, M. Tomandl, S. Nimmrichter, K. Hornberger, P. Fagan, J. Tüxen, M. Mayor, M. Arndt, Quantum interference of large organic molecules, *Nature Communs* **2**, 263 (2011).

Chapter 4. Gene-encoded tryptophan-rich tags and synthetic tags for protein photoionization

Laser desorption/photoionization experiments for gramicidin and $(Trp\text{-}Lys)_n$ constructs modified by amidation with fluoroalkyl chains were described before.[1] The same experiments were also successfully conducted on unmodified $(Trp\text{-}Lys)_{10}$ which has a molecular weight of 3160 amu. This likely constitutes the largest unmodified peptide that has been successfully photoionized with table-top lasers. Ionization of cytochrome c with synchrotron radiation at 80 nm has been reported previously.[2] The analytical data for $(Trp\text{-}Lys)_{10}$ can be found in the supplementary information for chapter 3 as a precursor to its fluorinated equivalent.

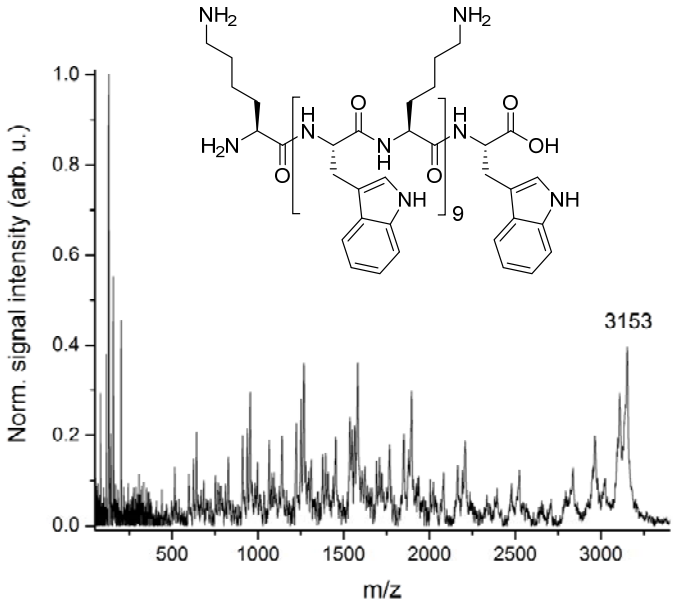

Figure S1. Laser desorption postionization spectra of $(Trp\text{-}Lys)_{10}$. Desorption was performed with 1064 nm laser light (Nd:YAG laser), photoionization at 157 nm (fluorine laser). For detailed conditions see supplementary Table 2, row 3 (chapter3).

2,5-Dioxopyrrolidin-1-yl-2-(pyren-1-yl)acetate (2)

The compound was prepared in analogy to a published procedure.[3] 1-Pyreneacetic acid (**6**) (1.00 eq., 500 mg, 1.92 mmol) was dissolved in dry THF (10 mL), DIPEA (1.20 eq., 381 µl, 2.30 mmol) and TSTU (1.20 eq., 694 mg, 2.30 mmol) were added and the solution was stirred overnight at room temperature. Volatiles were removed under reduced pressure and the crude mixture was dissolved in EtOAc (50 mL) and washed with aq. HCl (50 mL, 0.1 M) and water (50 mL). Succinimidyl ester **2** was isolated after flash column chromatography (EtOAc/cyclohexane 1:3) as a golden solid (205 mg, 574 µmol, 30%).

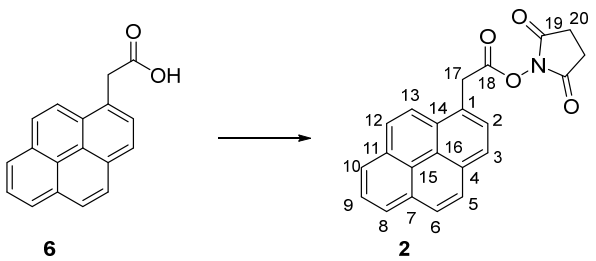

^{1}H-NMR (DMSO-d_6, 500 MHz, 293 K) δ: 8.35- 8.31 (m, 2 H, H-8, and H-10 or H-12), 8.31-8.26 (m, 3 H, H-3, H-13 and H-12 or H-10), 8.22-8.17 (m, 2 H, H-5 and H-6), 8.13 (d, $^{3}J_{H\text{-}H}$ = 7.8 Hz, 1 H and H-2), 8.10 (t, $^{3}J_{H\text{-}H}$ = 7.6 Hz, 1 H, H-9), 4.53 (s, 2 H, H-17), 2.80 (s, 4 H, H-20). ^{13}C-NMR δ: 170.6 (C-19), 168.1 (C-18), 131.7 (C-7), 131.0 (C-4), 130.3 (C-11), 129.4 (C-14), 128.5 (C-2), 127.7 (C-10 or C-12), 127.2 (C-5 and C-6), 127.0 (C-1), 126.2 (C-9), 125.9 (-15), 125.3 (C-8), 125.2 (C-3), 124.8 (C-10 or C-12), 124.3 (C-16), 123.0 (C-13), 34.7 (C-17), 25.2 (C-20).

2,5-Dioxopyrrolidin-1-yl 2-(naphthalen-1-yl)acetate (3)

The compound was prepared in analogy to a published procedure. [3] 1-Naphtalenacetic acid (**7**) (1.00 eq., 501 mg, 2.69 mmol) was dissolved in dry THF (10 mL), DIPEA (1.20 eq., 534 µl, 3.23 mmol) and TSTU (1.20 eq., 972 mg, 3.23 mmol) were added and the solution was stirred overnight at room temperature. Volatiles were removed under reduced pressure and the residue was dissolved in EtOAc (50 mL) and washed with aq. HCl (50 mL, 0.1 M) and water (50 mL). Succinimidyl ester **2** was isolated after flash column chromatography (EtOAc/cyclohexane 1:1) as a white solid (365 mg, 1.29 mmol, 48%).

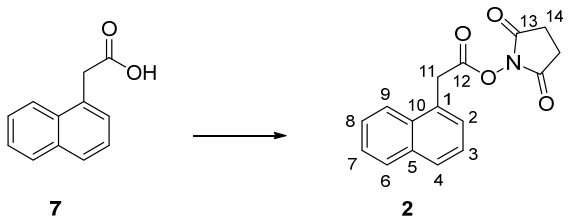

^{1}H-NMR (DMSO-d_6, 500 MHz, 293 K) δ: 8.01 (d, $^{3}J_{H\text{-}H}$ = 8.1 Hz, 1 H, H-6), 7.97 (dd, $^{3}J_{H\text{-}H}$ = 7.9 Hz, $^{4}J_{H\text{-}H}$ = 1.5 Hz 1 H, H-4), 7.92 (d, $^{3}J_{H\text{-}H}$ = 8.2 Hz, 1 H, H-9), 7.63-7.54 (m, 3 H, H-2, H-3 and H-7), 7.51 (dd, $^{3}J_{H\text{-}H}$ = 8.1 Hz, $^{3}J_{H\text{-}H}$ = 7.0 Hz, 1 H, H-8), 4.60 (s, 2 H, H-11), 2.80 (s, 4 H, H-14). ^{13}C-NMR δ: 170.0 (C-13), 167.3 (C-12), 133.0 (C-5), 131.3 (C-10), 129.0 (C-1), 128.2 (C-4), 128.0 (C-9), 127.9 (C-2), 126.1 (C-3), 125.9 (C-7), 125.2 (C-8), 123.4 (C-6), 34.1 (C-11), 25.1 (C-14).

Insulin modification

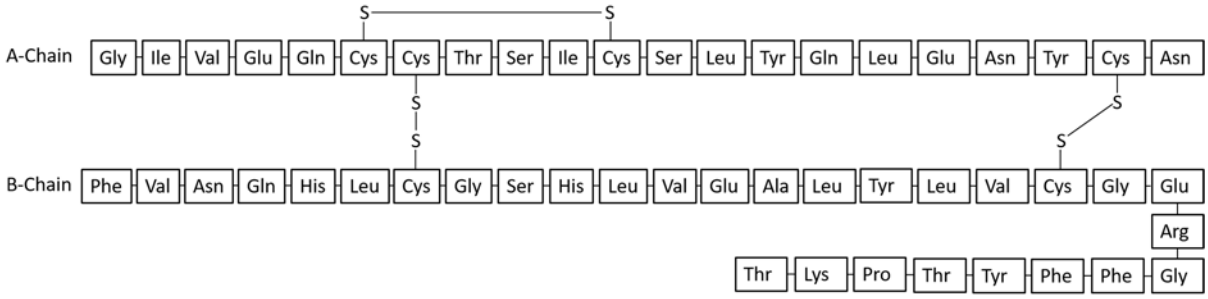

Figure S2. Amino acid sequence of human insulin used for the following experiments.

1-Pyrenylacetylation of insulin

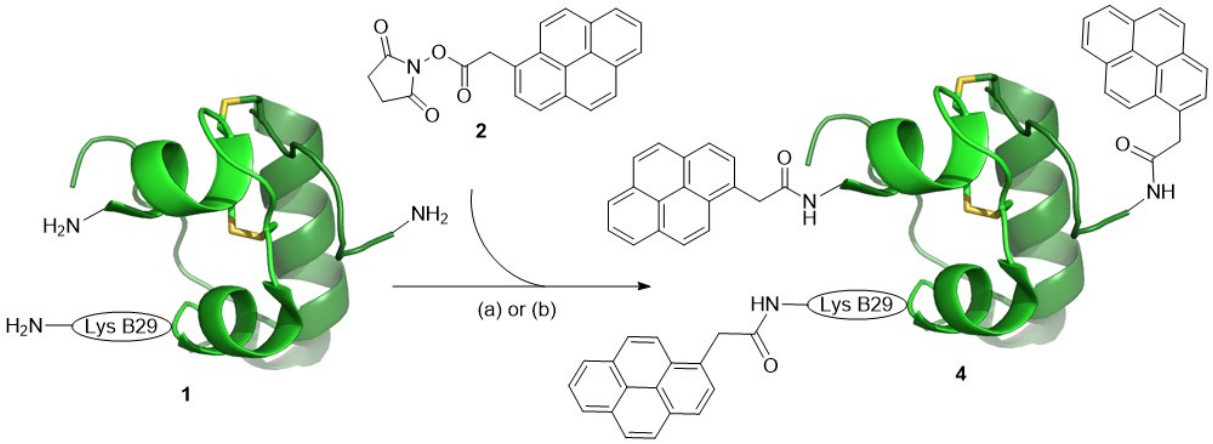

Human insulin **1** (1.00 eq., 125 mg, 35.0 µmol) was dissolved in Na_2CO_3 buffer (30 mL, 0.1 M, pH 8.5), the NHS-ester **2** (75.0 eq., 153 mg, 540 µmol) dissolved in THF (30 mL) was added and the solution stirred for 2 h. The solvent was removed by lyophilization and the crude mixture was purified by preparative HPLC yielding 3-fold pyrenylacetylated insulin **4** (12.0 mg, 1.29 µmol, 14%). UPLC-MS: Method 3, T_R = 4.99 min; MS (ESI+) m/z: 1099.2 [20%, M + 6 H^+], 1307.7 [100%, M + 5 H^+], 1634.6 [70%, M + 4 H^+].2179.0 [20%, M + 3 H^+].

1-Naphthylacetylation of insulin

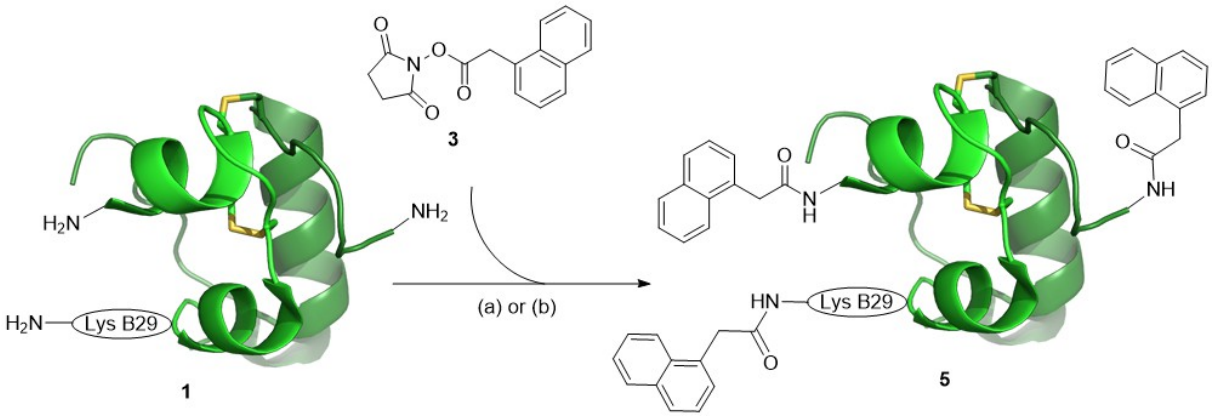

Human insulin **1** (1.00 eq., 42.0 mg, 7.23 µmol) was dissolved in aq. Na_2CO_3 buffer (30 mL, 0.1 M, pH 8.5). The NHS-ester **3** (75.0 eq., 153 mg, 540 µmol) dissolved in MeCN (20 mL) was added, and the solution was stirred for 2 h. UPLC analysis of the reaction mixture revealed the presence of various insulin containing species with up to six naphthylacetylations. To convert the different insulin species into three- and fourfold modified insulin, TFA (2.5 mL) was added, and the solution was stirred for 15 min. Finally, the reaction was quenched by addition of aq. NH_3 (5 mL, 32%). After 2 min the pH was adjusted to pH 7, and the modified insulin was purified by preparative HPLC, yielding threefold naphthylacetylated insulin **5** (14.0 mg, 2.14 µmol, 30%). UPLC-MS: Method 3, T_R = 4.33 min; MS (ESI+) m/z: 1263.4 [100%, M + 5 H^+], 1579.0 [80%, M + 4 H^+], 2105.0 [20%, M + 3 H^+].

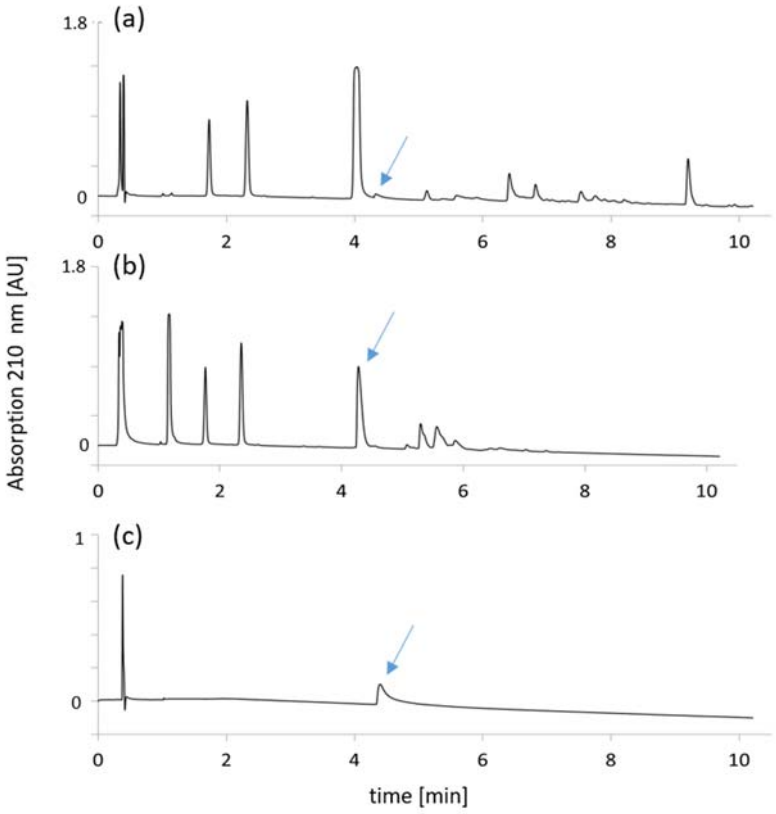

Figure S3. UPLC chromatograms of the insulin modification with NHS-ester **3**. (a) Crude material; (b) after treatment with TFA, followed by quenching with aq. ammonia; (c) after purification by preparative HPLC. The blue arrows indicate the signal for threefold modified insulin **5**.

Disulfide bond reduction of modified insulin 4

Modified insulin **4** (1 mg) was dissolved in reduction buffer (8 M urea, 50 mM Tris-HCl, 5 mM DTT, pH 7.8) and incubated for 45 min at 37 °C before the fragments were analyzed by UPLC-MS. Method: 0 min – 100% A; 1 min – 100% A; 3 min – 20% B; 13.5 min – 80% B; 13.5 min – 100% B; A H_2O with 0.1% formic acid; B MeCN with 0.1% formic acid.

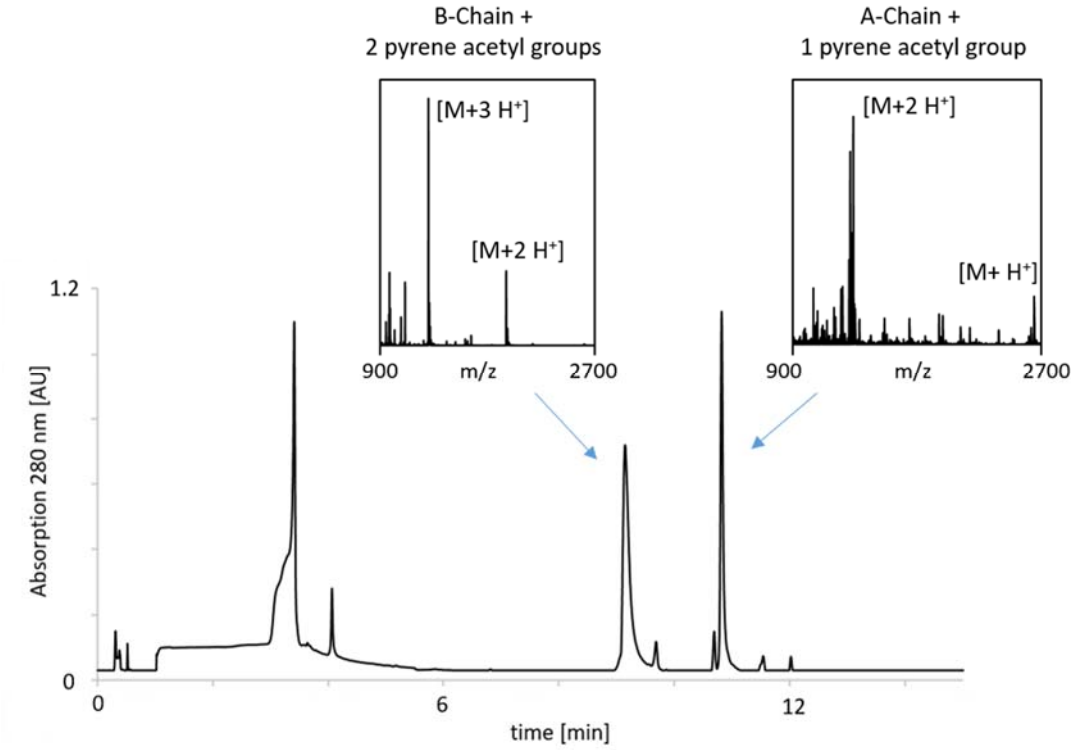

Figure S4. UPLC-MS chromatogram of three-fold pyrenylacetyl-modified insulin (**4**) after reduction of the disulfide bonds with DTT. The two peptide chains can be separated nicely, and their identity and degree of modification can be determined by MS. The B-chain with two pyrene chromophores (3914 amu) has a retention time of 9.1 min. The A-chain with one pyrenylacetly group (2626 amu) has a retention time of 10.8 min.

Transformation into chemically competent cells

The pET24a plasmids for all constructs were ordered from *GeneScript* and diluted with elution buffer (*Macherey-Nagel*, 40 µL) to reach plasmid concentrations between 100 and 150 ng/µl. The chemically competent cells (*E. coli* BL21 (DE3)) were prepared by Juliane Klehr following the Hanahan method[4] and stored as 50 µl-aliquots at -80 °C. First, the cells were allowed to thaw for 10 min on ice. Then 1 µl of plasmid was added, and the cells were incubated for 20 min on ice before heating them for 30 sec to 42 °C. After the heating LB medium (250 µL) was added, and the cells were incubated (1 h at 37 °C, 210 rpm). Finally, the cells were spread on kanamycin-containing agar plates and incubated overnight.

Small-scale expression

One colony was transferred from the agar plate to autoinduction medium (5 mL, 50 µg/mL kanamycin) and incubated for 24 h at 37 °C. The cells were harvested by centrifugation (30 min, 4000 g) followed by resuspension of the cell pellet in MOPS buffer (90 µL, pH 7.4, 50 mmol). Cell lysis was accomplished by adding *BugBuster®* (12 µL) and DNAse solution (2 µl, 1 mg/mL) and leaving the suspension for 30 min on ice. Expression was checked by tricine SDS-PAGE of either the cell-suspension (all expressed proteins) or the supernatant (soluble proteins).

Large-scale expression

One colony was transferred to LB-medium (5 mL, 50 µg/mL kanamycin) and incubated overnight. 1.5 mL off the preculture was transferred to autoinduction medium (2 L, 50 µg/mL kanamycin) and incubated in a 5-liter shaking flask (36 h at 28 °C, 200 rpm). The cells were harvested by centrifugation (30 min, 4000 g) and the cells were frozen at -80 °C for 2 h. The cells were thawed, resuspended in lysis buffer (60 mL) and lysed for 45 min at 0 °C. The cell-free extract was gained by centrifugation (30 min, 4000 g).

Protein purification (Ubi-1, wt)

The cell lysate (60 mL) was heated to 70 °C for ubiquitin respectively 80 °C for S6 for 30 min. The precipitate was removed by centrifugation, and the supernatant was diluted 1:1 with *miliQ* water and dialyzed (3 × 24 h) against *miliQ* water using *Spectra/Pro®* dialysis membrane (MWCO: 3.5 kDa). The proteins were obtained after lyophilization as a white powder.

Protein purification (Ubi-3 -W_5)

(i) The cell lysate (60 mL) was heated to 60 °C for 30 min. The precipitate was removed by centrifugation, and the supernatant was diluted 1:1 with *miliQ* water and dialyzed (3 × 24 h) against *miliQ* water using *Spectra/Pro®* dialysis membrane with a MWCO of 3.5 kDa. The precipitate formed during dialysis was collected by centrifugation, washed with *miliQ* water (2 × 10 mL) and dried by lyophilization.

(ii) The cell lysate (60 mL) was heated to 80 °C for 30 min. The precipitate was collected by centrifugation and redissolved in aq. urea (100 mL, 8 M). The solution was dialyzed (3 × 24 h) against *miliQ* water using *Spectra/Pro®* dialysis membrane (MWCO: 3.5 kDa). The precipitate formed during dialysis was collected by centrifugation (30 min, 4000 g), washed with miliQ water (2 × 10 mL) and dried by lyophilization.

With both purification methods, a certain amount of DNA is coprecipitating with **Ubi-3**. The DNA can be removed on a small scale by means of DNA miniprep cartridges (MN, NucleoSpin® Plasmid): **Ubi-3**

(0.2 mg) was dissolved in aq. urea (500 µl, 1 M) and applied on a DNA miniprep cartridge. The flow-through did not contain any DNA fragments according to an ethidium bromide stained agarose gel.

Chromatograms and mass spectra of the purified protein constructs

The protein constructs were analyzed by revers phase UPLC-MS on a C4 column (Aeris Widepore, 3.6 u, C4, 50×2-4 mm). Method: 0 min – 95% A; 0.1 min – 95% A; 2.5 min – 55% A; 4.0 min – 90% B; 5.5 min – 95% A; A H_2O with 0.1% formic acid; B MeCN with 0.1% formic acid.

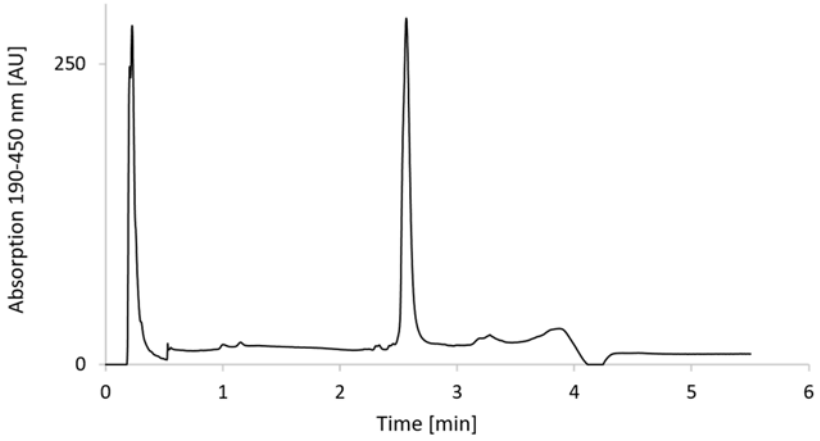

Figure S5. UPLC Chromatogram of **S6-1** (wt).

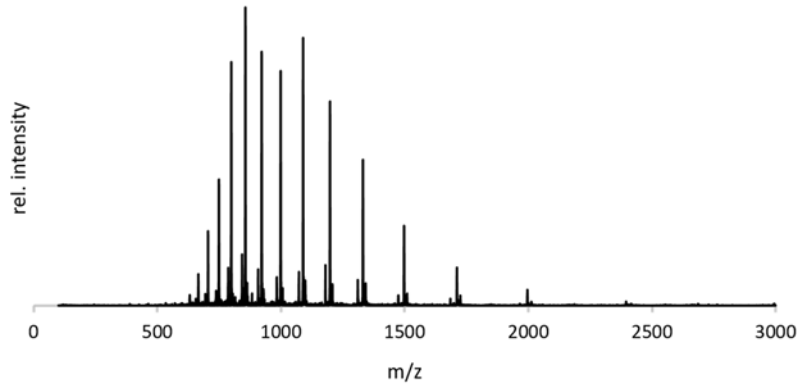

Figure S6. Mass spectrum of **S6-1** (wt).

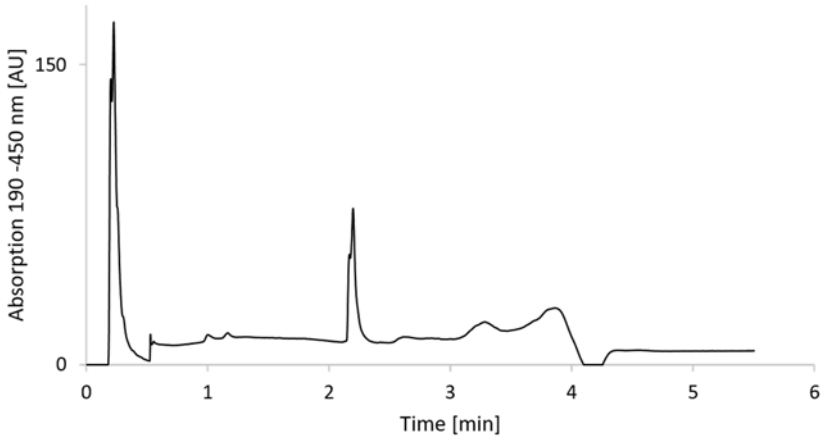

Figure S7. UPLC Chromatogram of **Ubi-1** (wt).

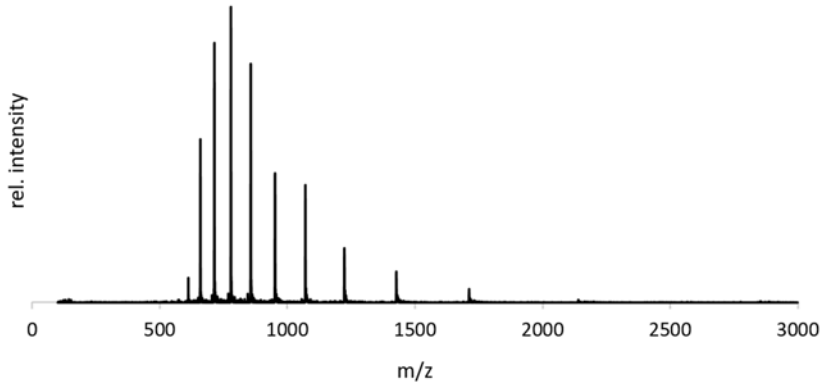

Figure S8. Mass spectrum of **Ubi-1** (wt).

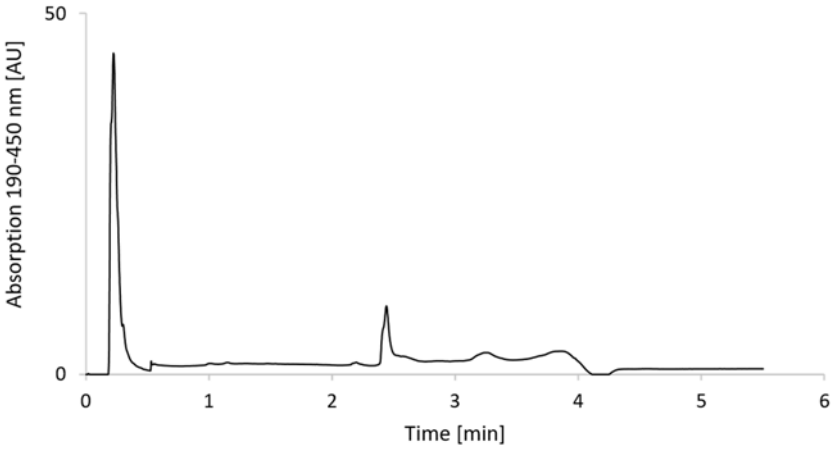

Figure S9. UPLC Chromatogram of **Ubi-3** (Ubi-W_5).

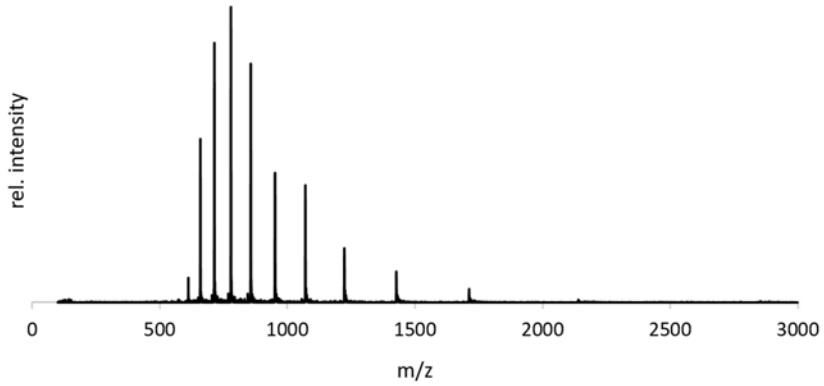

Figure S10. Mass spectrum of **Ubi-3** (Ubi-W_5).

Recipes for media, buffers and gels

Name	Composition
LB-medium	1% tryptone, 0.5% yeast extract and 1% NaCl in distilled water and autoclaved.
Autoinduction-medium	Modified ZYP-5052 Medium[5] : 1% tryptone, 1% (v/v) glycerol, 0.5% yeast extract, 0.4% lactose, 50 mM KH_2PO_4, 50 mM Na_2HPO_4, 25 mM $(NH_4)_2SO_4$, 5.6 mM glucose-monohydrate, 4.0 mM $MgSO_4$ in distilled water and autoclaved.
Lysis buffer	10 mM Tris-HCl, , 1 mg/mL lysozyme, 10 ug/mL DNAse, pH 7.4
Agarose gel	1% agarose, 0.5 µg/mL ethidium bromide in TBE buffer (100 mM Tris-HCl, 90 mM boric acid, 25 µM Na_2EDTA)
Agar plate	1.5% Agar in LB media, autoclave, cool down to 50 °C add kanamycin to a final concentration of 50 µg/mL, pour plates.
SDS-PAGE	Tricine SDS-PAGE[6]: Tricine SDS-PAGE has better separation properties for small Proteins below 15 kDa compared to standard SDS-PAGE.
Anode buffer	10 mM Tris-HCl, 2.25 mM HCl, pH 8.9
Cathode buffer	10 mM Tris-HCl, 10 mM Tricine, 1% SDS, pH 8.25
Gel buffer	3.0 M Tris-HCl, 1.0 M HCl, 0.3% SDS, pH 8.45
Stacking gel (4.5%)	1.5 mL acrylamide (30%), 1.5 mL gel buffer, 7 mL miliQ water, 100 µl APS, 15 µl TEMED
Running gel (15%)	8 mL acrylamide (30%), 6.5 mL gel buffer, 1.5 mL glycerol, 100 µl APS, 15 µl TEMED

Table S1. Media, buffers and gels used for protein expression, purification, and characterization

Gene sequences

#	construct	gene sequence
Ubi-1	Ubiquitin (wt)	ATG CAA ATT TTT GTT AAA ACG TTG ACT GGG AAG ACA ATC ACT TTA GAA GTC GAA TCT TCG GAT ACT ATC GAT AAT GTG AAA TCG AAA ATC CAG GAC AAG GAA GGG ATA CCG CCC GAC CAA CAA CGT TTG ATA TTC GCT GGT AAA CAA CTG GAG GAC GGT AGA ACA TTG TCA GAC TAC AAC ATT CAA AAG GAA AGT ACC CTT CAT TTG GTC CTG CGG TTA CGC GGC GGG TAA TAA
Ubi-2	Ubi R→K	ATG CAA ATT TTC GTC AAG ACT CTT ACA GGA AAA ACT ATA ACC CTT GAA GTC GAA AGTTCT GAT ACG ATT GAT AAC GTA AAG TCG AAA ATT CAG GAC AAG GAG GGG ATT CCC CCA GAC CAG CAG AAG CTT ATA TTC GCT GGA AAA CAA CTT GAA GAT GGG AAA ACC TTG TCA GAC TAC AAC ATA CAA AAA GAA AGC ACT CTG CAC CTG GTG CTG AAA TTA AAA GGT GGC TAA TAA
Ubi-3	Ubi-W_5	ATG CAA ATT TTT GTT AAA ACG TTG ACT GGG AAG ACA ATC ACT TTA GAA GTC GAA TCT TCG GAT ACT ATC GAT AAT GTG AAA TCG AAA ATC CAG GAC AAG GAA GGG ATA CCG CCC GAC CAA CAA CGT TTG ATA TTC GCT GGT AAA CAA CTG GAG GAC GGT AGA ACA TTG TCA GAC TAC AAC ATT CAA AAG GAA AGT ACC CTT CAT TTG GTC CTG CGG TTA CGC GGC GGG TGG TGG TGG TGG TGG TAA TAA
Ubi-4	Ubi-$(KW)_5$	ATG CAA ATT TTT GTT AAA ACG TTG ACT GGG AAG ACA ATC ACT TTA GAA GTC GAA TCT TCG GAT ACT ATC GAT AAT GTG AAA TCG AAA ATC CAG GAC AAG GAA GGG ATA CCG CCC GAC CAA CAA CGT TTG ATA TTC GCT GGT AAA CAA CTG GAG GAC GGT AGA ACA TTG TCA GAC TAC AAC ATT CAA AAG GAA AGT ACC CTT CAT TTG GTC CTG CGG TTA CGC GGC GGG AAA TGG AAA TGG AAA TGG AAA TGG AAA TGG TAA TAA
Ubi-5	Ubi-$(LW)_5$	ATG CAA ATT TTT GTT AAA ACG TTG ACT GGG AAG ACA ATC ACT TTA GAA GTC GAA TCT TCG GAT ACT ATC GAT AAT GTG AAA TCG AAA ATC CAG GAC AAG GAA GGG ATA CCG CCC GAC CAA CAA CGT TTG ATA TTC GCT GGT AAA CAA CTG GAG GAC GGT AGA ACA TTG TCA GAC TAC AAC ATT CAA AAG GAA AGT ACC CTT CAT TTG GTC CTG CGG TTA CGC GGC GGG CTG TGG CTG TGG CTG TGG CTG TGG CTG TGG TAA TAA
Ubi-7	Ubi-W_{10}	ATG CAA ATT TTT GTT AAA ACG TTG ACT GGG AAG ACA ATC ACT TTA GAA GTC GAA TCT TCG GAT ACT ATC GAT AAT GTG AAA TCG AAA ATC CAG GAC AAG GAA GGG ATA CCG CCC GAC CAA CAA CGT TTG ATA TTC GCT GGT AAA CAA CTG GAG GAC GGT AGA ACA TTG TCA GAC TAC AAC ATT CAA AAG GAA AGT ACC CTT CAT TTG GTC CTG CGG TTA CGC GGC GGG TGG TGG TGG TGG TGG TGG TGG TGG TGG TGG TAA TAA CTG TAT TTT CAG AGC CAT CAT CAT CAT CAT CAT CAT TAA TAA
Ubi-8	Ubi-GGGGS-W_5-GGGGS	ATG CAA ATT TTT GTT AAA ACG TTG ACT GGG AAG ACA ATC ACT TTA GAA GTC GAA TCT TCG GAT ACT ATC GAT AAT GTG AAA TCG AAA ATC CAG GAC AAG GAA GGG ATA CCG CCC GAC CAA CAA CGT TTG ATA TTC GCT GGT AAA CAA CTG GAG GAC GGT AGA ACA TTG TCA GAC TAC AAC ATT CAA AAG GAA AGT ACC CTT CAT TTG GTC CTG CGG TTA CGC GGC GGG GGT GGA GGC GGG TCA TGG TGG TGG TGG TGG GGT GGA GGC GGG TCA TAA TAA CTG TAT TTT CAG AGC CAT CAT CAT CAT CAT CAT CAT TAA TAA

Ubi-9	Ubi-GGGGS-W_{10}-GGGGS	ATG CAA ATT TTT GTT AAA ACG TTG ACT GGG AAG ACA ATC ACT TTA GAA GTC GAA TCT TCG GAT ACT ATC GAT AAT GTG AAA TCG AAA ATC CAG GAC AAG GAA GGG ATA CCG CCC GAC CAA CAA CGT TTG ATA TTC GCT GGT AAA CAA CTG GAG GAC GGT AGA ACA TTG TCA GAC TAC AAC ATT CAA AAG GAA AGT ACC CTT CAT TTG GTC CTG CGG TTA CGC GGC GGG GGT GGA GGC GGG TCA TGG TGG TGG TGG TGG TGG TGG TGG TGG TGG GGT GGA GGC GGG TCA TAA TAA CTG TAT TTT CAG AGC CAT CAT CAT CAT CAT CAT CAT TAA TAA
Ubi-10	Ubi-EAAAK-W_5-EAAAK	ATG CAA ATT TTT GTT AAA ACG TTG ACT GGG AAG ACA ATC ACT TTA GAA GTC GAA TCT TCG GAT ACT ATC GAT AAT GTG AAA TCG AAA ATC CAG GAC AAG GAA GGG ATA CCG CCC GAC CAA CAA CGT TTG ATA TTC GCT GGT AAA CAA CTG GAG GAC GGT AGA ACA TTG TCA GAC TAC AAC ATT CAA AAG GAA AGT ACC CTT CAT TTG GTC CTG CGG TTA CGC GGC GGG GAA GCT GCT GCG AAA TGG TGG TGG TGG TGG GAA GCT GCT GCG AAA TAA TAA CTG TAT TTT CAG AGC CAT CAT CAT CAT CAT CAT CAT TAA TAA
Ubi-11	Ubi-EAAAK-W_{10}-EAAAK	ATG CAA ATT TTT GTT AAA ACG TTG ACT GGG AAG ACA ATC ACT TTA GAA GTC GAA TCT TCG GAT ACT ATC GAT AAT GTG AAA TCG AAA ATC CAG GAC AAG GAA GGG ATA CCG CCC GAC CAA CAA CGT TTG ATA TTC GCT GGT AAA CAA CTG GAG GAC GGT AGA ACA TTG TCA GAC TAC AAC ATT CAA AAG GAA AGT ACC CTT CAT TTG GTC CTG CGG TTA CGC GGC GGG GAA GCT GCT GCG AAA TGG TGG TGG TGG TGG TGG TGG TGG TGG TGG GAA GCT GCT GCG AAA TAA TAA CTG TAT TTT CAG AGC CAT CAT CAT CAT CAT CAT CAT TAA TAA
Ubi-12	Ubi-W_5-GGGGS-W_5-GGGGS	ATG CAA ATT TTT GTT AAA ACG TTG ACT GGG AAG ACA ATC ACT TTA GAA GTC GAA TCT TCG GAT ACT ATC GAT AAT GTG AAA TCG AAA ATC CAG GAC AAG GAA GGG ATA CCG CCC GAC CAA CAA CGT TTG ATA TTC GCT GGT AAA CAA CTG GAG GAC GGT AGA ACA TTG TCA GAC TAC AAC ATT CAA AAG GAA AGT ACC CTT CAT TTG GTC CTG CGG TTA CGC GGC GGG TGG TGG TGG TGG TGG GGT GGA GGC GGG TCA TGG TGG TGG TGG TGG GGT GGA GGC GGG TCA TAA TAA CTG TAT TTT CAG AGC CAT CAT CAT CAT CAT CAT CAT TAA TAA
Ubi-13	Ubi-W_5-EAAAK-W_5-EAAAK	ATG CAA ATT TTT GTT AAA ACG TTG ACT GGG AAG ACA ATC ACT TTA GAA GTC GAA TCT TCG GAT ACT ATC GAT AAT GTG AAA TCG AAA ATC CAG GAC AAG GAA GGG ATA CCG CCC GAC CAA CAA CGT TTG ATA TTC GCT GGT AAA CAA CTG GAG GAC GGT AGA ACA TTG TCA GAC TAC AAC ATT CAA AAG GAA AGT ACC CTT CAT TTG GTC CTG CGG TTA CGC GGC GGG TGG TGG TGG TGG TGG GGT GGA GGC GGG TCA TGG TGG TGG TGG TGG GGT GGA GGC GGG TCA TAA TAA CTG TAT TTT CAG AGC CAT CAT CAT CAT CAT CAT CAT TAA TAA
Ubi-14	W_5-Ubi	TGG TGG TGG TGG TGG ATG CAA ATT TTT GTT AAA ACG TTG ACT GGG AAG ACA ATC ACT TTA GAA GTC GAA TCT TCG GAT ACT ATC GAT AAT GTG AAA TCG AAA ATC CAG GAC AAG GAA GGG ATA CCG CCC GAC CAA CAA CGT TTG ATA TTC GCT GGT AAA CAA CTG GAG GAC GGT AGA ACA TTG TCA GAC TAC AAC ATT CAA AAG GAA AGT ACC CTT CAT TTG GTC CTG CGG TTA CGC GGC GGG TAA TAA CTG TAT TTT CAG AGC CAT CAT CAT CAT CAT CAT CAT TAA TAA

#	construct	gene sequence
Ubi-15	W_5-Ubi-W_5	TGG TGG TGG TGG TGG ATG CAA ATT TTT GTT AAA ACG TTG ACT GGG AAG ACA ATC ACT TTA GAA GTC GAA TCT TCG GAT ACT ATC GAT AAT GTG AAA TCG AAA ATC CAG GAC AAG GAA GGG ATA CCG CCC GAC CAA CAA CGT TTG ATA TTC GCT GGT AAA CAA CTG GAG GAC GGT AGA ACA TTG TCA GAC TAC AAC ATT CAA AAG GAA AGT ACC CTT CAT TTG GTC CTG CGG TTA CGC GGC GGG TGG TGG TGG TGG TGG TAA TAA CTG TAT TTT CAG AGC CAT CAT CAT CAT CAT CAT CAT TAA TAA
Ubi-16	Ubi-$(WS)_{10}$	ATG CAA ATT TTT GTT AAA ACG TTG ACT GGG AAG ACA ATC ACT TTA GAA GTC GAA TCT TCG GAT ACT ATC GAT AAT GTG AAA TCG AAA ATC CAG GAC AAG GAA GGG ATA CCG CCC GAC CAA CAA CGT TTG ATA TTC GCT GGT AAA CAA CTG GAG GAC GGT AGA ACA TTG TCA GAC TAC AAC ATT CAA AAG GAA AGT ACC CTT CAT TTG GTC CTG CGG TTA CGC GGC GGG TGG AGC TGG TCG TGG AGC TGG TCC TGG TCA TGG TCC TGG TCC TGG AGC TGG TCG TGG TCA TAA TAA CTG TAT TTT CAG AGC CAT CAT CAT CAT CAT CAT CAT TAA TAA
Ubi-17	Ubi-$(WKWE)_5$	ATG CAA ATT TTT GTT AAA ACG TTG ACT GGG AAG ACA ATC ACT TTA GAA GTC GAA TCT TCG GAT ACT ATC GAT AAT GTG AAA TCG AAA ATC CAG GAC AAG GAA GGG ATA CCG CCC GAC CAA CAA CGT TTG ATA TTC GCT GGT AAA CAA CTG GAG GAC GGT AGA ACA TTG TCA GAC TAC AAC ATT CAA AAG GAA AGT ACC CTT CAT TTG GTC CTG CGG TTA CGC GGC GGG TGG AAG TGG GAA TGG AAA TGG GAG TGG AAG TGG GAG TGG AAA TGG GAG TGG AAA TGGGAG TAA TAA CTG TAT TTT CAG AGC CAT CAT CAT CAT CAT CAT CAT TAA TAA
S6-1	S6-W_5	ATG CGT CGC TAT GAA GTG AAT ATT GTG CTG AAT CCG AAT CTG GAT CAG AGT CAG CTG GCA CTG GAA AAA GAA ATT ATT CAG CGT GCC CTG GAA AAT TAT GGT GCA CGT GTT GAA AAA GTT GAA GAA CTG GGT CTG CGT CGT CTG GCA TAT CCG ATT GCA AAA GAT CCG CAG GGT TAT TTT CTG TGG TAT CAG GTT GAA ATG CCG GAA GAT CGT GTT AAT GAT CTG GCA CGT GAA CTG CGT ATT CGT GAT AAT GTT CGT CGT GTT ATG GTT GTG AAA AGC CAA GAA CCG TTT CTG GCA AAT GCC TGG TGG TGG TGG TGG TAA TAA
S6-2	S6 R→K	ATG AAA AAA TAC GAG GTG AAC ATC GTG CTG AAT CCG AAT CTG GAT CAG AGT CAG CTG GCA CTG GAA AAA GAA ATT ATT CAG AAA GCC CTG GAA AAC TAC GGT GCC AAA GTT GAA AAA GTG GAA GAA CTG GGT CTG AAA AAA CTG GCA TAT CCG ATT GCA AAA GAT CCG CAG GGT TAT TTT CTG TGG TAT CAG GTT GAA ATG CCG GAA GAT AAA GTT AAC GAT CTG GCC AAA GAG CTG AAA ATC AAA GAT AAC GTG AAA AAA GTG ATG GTG GTG AAA AGC CAA GAA CCG TTT CTG GCA AAT GCC TAA TAA
S6-3	S6-W_5	ATG CGT CGC TAT GAA GTG AAT ATT GTG CTG AAT CCG AAT CTG GAT CAG AGT CAG CTG GCA CTG GAA AAA GAA ATT ATT CAG CGT GCC CTG GAA AAT TAT GGT GCA CGT GTT GAA AAA GTT GAA GAA CTG GGT CTG CGT CGT CTG GCA TAT CCG ATT GCA AAA GAT CCG CAG GGT TAT TTT CTG TGG TAT CAG GTT GAA ATG CCG GAA GAT CGT GTT AAT GAT CTG GCA CGT GAA CTG CGT ATT CGT GAT AAT GTT CGT CGT GTT ATG GTT GTG AAA AGC CAA GAA CCG TTT CTG GCA AAT GCC TGG TGG TGG TGG TGG TAA TAA

#	construct	gene sequence
S6-4	S6-$(KW)_5$	ATG CGT CGC TAT GAA GTG AAT ATT GTG CTG AAT CCG AAT CTG GAT CAG AGT CAG CTG GCA CTG GAA AAA GAA ATT ATT CAG CGT GCC CTG GAA AAT TAT GGT GCA CGT GTT GAA AAA GTT GAA GAA CTG GGT CTG CGT CGT CTG GCA TAT CCG ATT GCA AAA GAT CCG CAG GGT TAT TTT CTG TGG TAT CAG GTT GAA ATG CCG GAA GAT CGT GTT AAT GAT CTG GCA CGT GAA CTG CGT ATT CGT GAT AAT GTT CGT CGT GTT ATG GTT GTG AAA AGC CAA GAA CCG TTT CTG GCA AAT GCC AAA TGG AAA TGG AAA TGG AAA TGG AAA TGG TAA TAA
S6-5	S6-$(LW)_5$	ATG CGT CGC TAT GAA GTG AAT ATT GTG CTG AAT CCG AAT CTG GAT CAG AGT CAG CTG GCA CTG GAA AAA GAA ATT ATT CAG CGT GCC CTG GAA AAT TAT GGT GCA CGT GTT GAA AAA GTT GAA GAA CTG GGT CTG CGT CGT CTG GCA TAT CCG ATT GCA AAA GAT CCG CAG GGT TAT TTT CTG TGG TAT CAG GTT GAA ATG CCG GAA GAT CGT GTT AAT GAT CTG GCA CGT GAA CTG CGT ATT CGT GAT AAT GTT CGT CGT GTT ATG GTT GTG AAA AGC CAA GAA CCG TTT CTG GCA AAT GCC CTG TGG CTG TGG CTG TGG CTG TGG CTG TGG TAA TAA
S6-6	S6-$(KW)_{10}$	ATG CGT CGC TAT GAA GTG AAT ATT GTG CTG AAT CCG AAT CTG GAT CAG AGT CAG CTG GCA CTG GAA AAA GAA ATT ATT CAG CGT GCC CTG GAA AAT TAT GGT GCA CGT GTT GAA AAA GTT GAA GAA CTG GGT CTG CGT CGT CTG GCA TAT CCG ATT GCA AAA GAT CCG CAG GGT TAT TTT CTG TGG TAT CAG GTT GAA ATG CCG GAA GAT CGT GTT AAT GAT CTG GCA CGT GAA CTG CGT ATT CGT GAT AAT GTT CGT CGT GTT ATG GTT GTG AAA AGC CAA GAA CCG TTT CTG GCA AAT GCC AAA TGG AAA TGG AAA TGG AAA TGG AAA TGG AAA TGG AAA TGG AAA TGG AAA TGG AAA TGG TAA TAA
S6-8	S6-GGGGS-W_5-GGGGS	ATG CGT CGC TAT GAA GTG AAT ATT GTG CTG AAT CCG AAT CTG GAT CAG AGT CAG CTG GCA CTG GAA AAA GAA ATT ATT CAG CGT GCC CTG GAA AAT TAT GGT GCA CGT GTT GAA AAA GTT GAA GAA CTG GGT CTG CGT CGT CTG GCA TAT CCG ATT GCA AAA GAT CCG CAG GGT TAT TTT CTG TGG TAT CAG GTT GAA ATG CCG GAA GAT CGT GTT AAT GAT CTG GCA CGT GAA CTG CGT ATT CGT GAT AAT GTT CGT CGT GTT ATG GTT GTG AAA AGC CAA GAA CCG TTT CTG GCA AAT GCC GGT GGA GGC GGG TCA TGG TGG TGG TGG TGG GGT GGA GGC GGG TCA TAA TAA CTG TAT TTT CAG AGC CAT CAT CAT CAT CAT CAT CAT TAA TAA
S6-10	S6-EAAAK-W_5-EAAAK	ATG CGT CGC TAT GAA GTG AAT ATT GTG CTG AAT CCG AAT CTG GAT CAG AGT CAG CTG GCA CTG GAA AAA GAA ATT ATT CAG CGT GCC CTG GAA AAT TAT GGT GCA CGT GTT GAA AAA GTT GAA GAA CTG GGT CTG CGT CGT CTG GCA TAT CCG ATT GCA AAA GAT CCG CAG GGT TAT TTT CTG TGG TAT CAG GTT GAA ATG CCG GAA GAT CGT GTT AAT GAT CTG GCA CGT GAA CTG CGT ATT CGT GAT AAT GTT CGT CGT GTT ATG GTT GTG AAA AGC CAA GAA CCG TTT CTG GCA AAT GCC GAA GCT GCT GCG AAA TGG TGG TGG TGG TGG GAA GCT GCT GCG AAA TAA TAA CTG TAT TTT CAG AGC CAT CAT CAT CAT CAT CAT CAT TAA TAA

Table S2. Gene sequence used for the expression of ubiquitin and ribosomal protein S6 constructs. (blue) Sequence coding for the wild type protein core; (red) sequence coding for the Trp-rich tag (for **Ubi-2** and **S6-2** the R→ K mutations are marked); (black) stop codon; (green) sequence for a possible introduction of a His-tag for purification; including protease cleavage site for cleaving of the His-tag after purification. His-tag purification was not performed in the scope of the thesis.

References

1. J. Schätti; P. Rieser; U. Sezer; G. Richter; P. Geyer; G. G. Rondina; D. Häussinger; M. Mayor; A. Shayeghi; V. Köhler; M. Arndt, Pushing the mass limit for intact launch and photoionization of large neutral biopolymers. *Commun. Chem.* **2018,** *1* (1), 93.
2. A. R. Milosavljevic; C. Nicolas; J. Lemaire; C. Dehon; R. Thissen; J.-M. Bizau; M. Refregiers; L. Nahon; A. Giuliani, Photoionization of a protein isolated in vacuo. *Phys. Chem. Chem. Phys.* **2011,** *13* (34), 15432-15436.
3. L. Malik; J. Nygaard; R. Hoiberg-Nielsen; L. Arleth; T. Hoeg-Jensen; K. J. Jensen, Perfluoroalkyl Chains Direct Novel Self-Assembly of Insulin. *Langmuir* **2012,** *28* (1), 593-603.
4. D. Hanahan, Studies on transformation of Escherichia coli with plasmids. *J. Mol. Biol.* **1983,** *166* (4), 557-580.
5. F. W. Studier, Protein production by auto-induction in high-density shaking cultures. *Protein Expr. Purif.* **2005,** *41* (1), 207-234.
6. H. Schagger, Tricine-SDS-PAGE. *Nat. Protocols* **2006,** *1* (1), 16-22.

Chapter 5. Tailored photocleavable peptides: fragmentation and neutralization pathways in high vacuum

M. Debiossac; J. Schätti; M. Kriegleder; P. Geyer; A. Shayeghi; M. Mayor; M. Arndt; V. Kohler, *Phys.Chem.Chem.Phys.,* **2018***, 20,* 11412-11417.

Supporting Information for:

Tailored photocleavable peptides: fragmentation and neutralization pathways in high vacuum

M. Debiossac,[a] J. Schätti,[b] M. Kriegleder,[a] P. Geyer,[a] A. Shayeghi,[a] M. Mayor,[c,d,e] M. Arndt,[a] and V. Köhler[b]

[a] Vienna Center for Quantum Science and Technology, Faculty of Physics, University of Vienna, Boltzmanngasse 5, A-1090 Vienna, Austria
[b] Department of Chemistry, University of Basel, Mattenstrasse 24a, BPR 1096, CH-4058 Basel
[c] Department of Chemistry, University of Basel, St. Johannsring 19, CH-4056 Basel, Switzerland
[d] Institute of Nanotechnology (INT), Karlsruhe Institute of Technology (KIT), Hermann-von-Helmholtz-Platz 1, D-76344 Eggenstein-Leopoldshafen, Germany
[e] Lehn Institute of Functional Materials (LIFM), Sun Yat-Sen University (SYSU), Xingang Rd. W., Guangzhou, China

Contents

Synthesis

General

Chemicals were purchased from Sigma Aldrich, Fluorochem, Novabiochem or Bachem and used as received unless otherwise noted. UPLC experiments were performed with an Acquity UPLC-H Class Bio from Waters equipped with a PDA and a SQ detector 2 with the following column: ACQUITY UPLC, HSS T3 1.8 µm, 2.1 x 100 mm. Solvents were water and acetonitrile, respectively, each containing 0.1 % formic acid, later on referred to as (A) and (B). The flow rate was set to 0.61 ml/min and the temperature to 40 °C. Method 1: 0 min – 90 % A; 1 min – 90 % A; 6 min – 100 % B; 7.5 min – 100 % B. Method 2: 0 min – 100 % A; 1 min – 100 % A; 3 min – 80 % A; 13.5 min – 20 % A. Method 3: 0 min – 100 % A; 1 min – 100 % A; 7.5 min – 10 % A. Mass detection was performed in scan mode for positive ions (cone voltage 40 V, desolvation temperature: 600°C). A Water Prep LC 4000 System equipped with a Waters 2487: Dual λ Absorbance Detector was used for preparative separations with the following column: Agilent: XDB-C18, 21.2 x 150 mm, 5 µm. HRMS experiments were conducted with a Bruker maXis 4G. NMR experiments were performed at 25°C on Bruker Avance III NMR spectrometers operating at 250, 500 or 600 MHz proton frequency. The NMR spectrometers were equipped with inverse or direct observe, broadband probe heads or with a four-channel cryogenic QCI-F probe (600 MHz) all with self-shielded *z*-gradients. ^{13}C shifts were determined by 2D NMR experiments (HMBC and HMQC). ^{1}H and ^{13}C signals were assigned by 2D NMR experiments (COSY, HMBC, HMQC and ^{19}F-^{13}C HSQC for **1b**). Chemical shifts are reported in δ values (ppm) and are relative to the solvent residual signal (for samples in $CDCl_3$ ^{1}H = 7.26; ^{13}C = 77.0 ppm; for samples in DMSO-d_6 ^{1}H = 2.50 ppm; ^{13}C = 39.5 ppm). ^{19}F chemical shifts are referenced externally to CCl_3F in $CDCl_3$ (= 0 ppm).

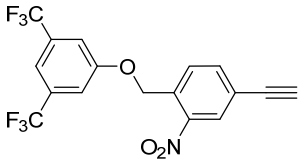

S1

S1. The synthesis of the precursor alkyne for attachment of the photocleavable unit by click chemistry to the peptide followed a procedure published previously. [1]

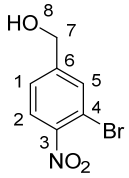

S2

S2. 3-bromo-4-nitrobenzoic acid (800 mg, 3.25 mmol, 1.00 eq.) was dissolved in a solution of BH_3 in THF (1 M BH_3 in THF, 26.0 ml, 26.0 mmol, 8.00 eq.) and the resulting mixture heated to 50 °C for 4 h. The solvent was removed under reduced pressure and the residue subjected to column chromatography (cyclohexane /ethyl acetate 3:1). **S2** was isolated as a pale yellow solid (580 mg, 77 %). ^{1}H-NMR: (500 MHz, $CDCl_3$, 298 K) δ 7.85 (d, $^{3}J_{H\text{-}H}$ = 8.3 Hz, 1 H, H-2), 7.76 (m, 1 H, H-5), 7.43 (m, 1 H, H-1), 4.78 (d, $^{3}J_{H\text{-}H}$ = 5.5 Hz, 2 H, H-7), 2.03 (t, $^{3}J_{H\text{-}H}$ = 5.5 Hz, 1 H, H-8); δ ^{13}C (determined by HMQC and HMBC experiments) 148.5 (C-3), 146.9 (C-6), 132.6 (C-5), 125.8 (C-1, C-2),

114.7 (C- 4), 63.2 (C-7); UPLC Method 1, T_R = 3.85 min; HRMS (ESI-) calcd. for $C_7H_5BrNO_3^-$ ($M-H^+$): 229.9458, found: 229.9461.

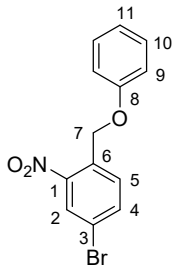

S3

S3. *General procedure 1.* The reaction was performed in analogy to the preparation of **S1** and under exclusion of light.[1] (3-Bromo-4-nitrophenyl)methanol (1.20 g, 5.17 mmol, 1.00 eq.), phenol (584 mg, 6.20 mmol, 1.20 eq.) and triphenylphosphine (1.63 g, 6.20 mmol, 1.20 eq.) were dissolved in dry THF and cooled to 0°C. Diisopropyl azodicarboxylate (1.52 ml, 7.76 mmol, 1.50 eq.) was added dropwise over 15 min. After completed addition the reaction was allowed to warm to room temperature and stirring continued overnight. For work up volatiles were removed under reduced pressure and the remaining residue subjected to column chromatography (cyclohexane /ethyl acetate 20:1). **S3** was isolated as a pale yellow solid (542 mg, 1.76 mmol, 34 %). ^{1}H-NMR (500 MHz, DMSO-d_6, 298 K) δ 8.30 (d, $^4J_{H\text{-}H}$ = 2.1 Hz, 1 H, H-2), 7.99 (dd, $^3J_{H\text{-}H}$ = 8.3 Hz, $^4J_{H\text{-}H}$ = 2.1 Hz, 1 H, H-4), 7.72 (d, $^3J_{H\text{-}H}$ = 8.3 Hz, 1 H, H-5), 7.35-7.29 (m, 2 H, H-10), 7.02- 6.96 (m, 3 H, H-9 and H-11), 5.40 (s, 2 H, H-7); δ ^{13}C (determined by HMQC and HMBC experiments) 157.3 (C-8), 147.8 (C-1), 136.2 (C-4), 131.7 (C-6), 130.6 (C-5), 129.4 (C-10), 127.0 (C-2), 121.0 (C-9), 120.6 (C-3),114.4 (C-11), 65.5 (C-7); UPLC Method 1, T_R = 5.88 min; HRMS (ESI-) calcd. for $C_{13}H_9BrNO_3^-$ ($M-H^+$): 305.9771, found: 305.9775.

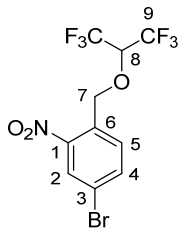

S4

S4. The synthesis followed the protocol described for **S3** (*General procedure 1*) with 1,1,1,3,3,3-hexafluoropropan-2-ol (652 µl, 6.20 mmol, 1.20 eq.) instead of phenol. **S4** was obtained as a pale yellow solid and contained 21 wt% diisopropyl azodicarboxylate (DIAD) as judged by ^{1}H NMR (858 mg, 1.77 mmol, 34 % corrected yield). ^{1}H-NMR (500 MHz, $CDCl_3$, 298 K) δ 8.31 (d, $^4J_{H\text{-}H}$ = 2.0 Hz, 1 H, H-2), 7.84 (dd, $^3J_{H\text{-}H}$ = 8.4 Hz, $^4J_{H\text{-}H}$ = 2.0 Hz, 1 H, H-4), 7.71 (d, $^3J_{H\text{-}H}$ = 8.4 Hz, 1 H, H-5), 5.27 (s, 2 H, H-7), 4.34 (hept, $^3J_{H\text{-}F}$ = 5.8 Hz, 1 H, H-8); δ ^{13}C (determined by HMQC and HMBC experiments) 146.9 (C-1), 137.3 (C-4), 131.1 (C-6), 129.9 (C-5), 128.1 (C-2), 122.3 (C-3), 121.3 (q, C-9), 76.5 (C-8), 72.7 (C-7); UPLC Method 1, T_R = 5.79 min; HRMS (ESI-) calcd. for $C_{10}H_5BrF_6NO_3^-$ ($M-H^+$): 379.9362, found: 379.9368.

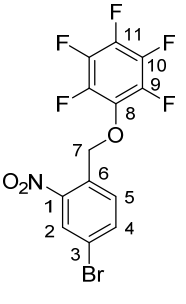

S5

S5. The synthesis followed the protocol described for **S3** (*General procedure 1*) with pentafluorophenol (1.14 g, 6.20 mmol, 1.20 eq.) instead of phenol and has been previously reported.[2] **S5** was isolated as a slightly yellow solid (925 mg, 2.32 mmol, 45 %). ^{1}H-NMR (500 MHz, $CDCl_3$, 298 K) δ 8.32 (d, $^4J_{H\text{-}H}$ = 1.4 Hz, 1 H, H-2), 7.89-7.85 (m, 2 H, H-4 and H-5), 5.54 (s, 2 H, H-7); δ ^{13}C (determined by HMQC and HMBC experiments, C-9, C-10 and C-11 were assigned in analogy to compound **1b**) 147.0 (C-1), 143.8 (C-11), 140.0 (C-9 or C-10), 137.5 (C-4), 136.2 (C-9 or C-10), 133.0 (C-8), 131.4 (C-6), 130.1 (C-5),

128.1 (C-2), 122.3 (C-3), 73.0 (C-7); ^{19}F-NMR (235 MHz, $CDCl_3$, 298 K) δ -156.1 (m, 2 F, 9-F), -161.7 (m, 1 F, 11-F), -162.5 (m, 2 F, 10-F); UPLC Method 1, T_R = 6.09 min; HRMS (ESI-) calcd. for $C_{13}H_4BrF_5NO_3^-$ (M-H$^+$): 395.9300, found: 395.9304.

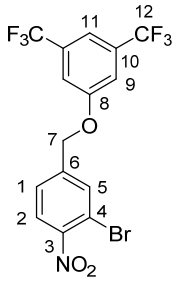

S6

S6. The synthesis followed the protocol described for **S3** (*General procedure 1*) starting with (3-bromo-4-nitrophenyl)methanol (541 mg, 2.33 mmol, 1.00 eq.) and 3,5-bis(trifluoromethyl)phenol (643 mg, 2.80 mmol, 1.20 eq). **S6** was isolated as a pale yellow solid (592 mg, 1.33 mmol, 57 %). ^{1}H-NMR (500 MHz, $CDCl_3$, 298 K) δ 7.91 (d, $^3J_{H\text{-}H}$ = 8.3 Hz, 1 H, H-2), 7.87-7.86 (m, 1 H, H-5), 7.55-7.52 (m, 2 H, H-1 and H-11), 7.41 (s, 2 H, H-9), 5.20 (s, $^3J_{H\text{-}H}$ = 5.5 Hz, 2 H, H-7); δ ^{13}C (determined by HMQC and HMBC experiments) 158.3 (C-8), 149.3 (C-3), 141.3 (C-6), 133.4 (C-5), 133.2 (C-10), 126.5 (C-1), 126.0 (C-2), 123.0 (q, C-12), 115.1 (C-4), 115.4 (C-11), 115.1 (C-9), 68.5 (C-7); UPLC-MS: Method 1, T_R = 6.24 min; m/z MS (ES-): 444.8, 442.7 [100%, M$^-$], 229.1 [40 %, $(CF_3)_2C_6H_3O^-$]; HRMS (ESI-) calcd. for $C_{15}H_7BrF_6NO_3^-$ (M-H$^+$): 441.9519, found: 441.9520.

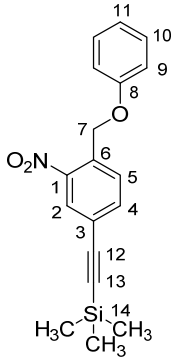

S7

S7. *General procedure 2*. The synthesis followed the procedure reported for the preparation of **S1**, but employed a twofold loading of catalyst.[1] The reaction flask was wrapped in aluminium foil to exclude light before 4-bromo-2-nitro-1-(phenoxymethyl)benzene (400 mg, 1.30 mmol, 1.00 eq.) was dissolved in triethylamine (15 ml). The solution was degassed by bubbling with nitrogen for 20 min before CuI (5.0 mg, 2 mol% and tetrakis-(triphenylphosphine)palladium (15 mg, 1 mol%) were added and the reaction mixture degassed for another 10 min. Trimethylsilylacetylene (277 µl, 2.00 mmol, 1.54 eq.) was added and the reaction stirred under reflux overnight. After filtration through Celite, *tert*-butyl methyl ether (100 ml) was added and the solution was washed with water (2 × 100 ml) and brine (100 ml). Volatiles were removed under reduced pressure and the residue purified by column chromatography (cyclohexane / ethyl acetate 40 : 1). **S7** was isolated as a slightly yellow solid which contained 32 wt% starting material **S3** (253 mg, 0.53 mmol, 41 % corrected yield). ^{1}H-NMR (500 MHz, DMSO-d_6, 298 K) δ 8.13 (d, $^4J_{H\text{-}H}$ = 1.7 Hz, 1 H, H-2), 7.83 (dd, $^3J_{H\text{-}H}$ = 8.1 Hz, $^4J_{H\text{-}H}$ = 1.7 Hz, 1 H, H-4), 7.78 (d, $^3J_{H\text{-}H}$ = 8.1 Hz, 1 H, H-5), 7.33-7.28 (m, 2 H, H-10), 7.03-6.96 (m, 3 H, H-9 and H-11), 5.45 (s, 2 H, H-7), 0.26 (s, 9 H, H-14); δ ^{13}C (determined by HMQC and HMBC experiments) 157.4 (C-8), 147.0 (C-1), 136.1 (C-4), 133.0 (C-6), 129.4 (C-10), 129.2 (C-5), 127.2 (C-2), 122.3 (C-3), 121.0 (C-9), 114.5 (C-11), 101.9 (C-12), 96.9 (C-13), 65.7 (C-7), -0.7 (C-14); UPLC Method 1, T_R = 6.66 min; HRMS (ESI-) calcd. for $C_{18}H_{18}NO_3Si^-$ (M-H$^+$): 324.1061, found: 324.1065.

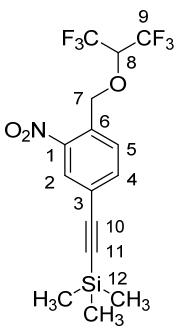

S8

S8. The synthesis followed the protocol described for the synthesis of **S7** (*General procedure 2*) employing **S4** (250 mg, 654 μmol, 1.00 eq., the DIAD impurity was not considered in the calculation). **S8** was isolated as a pale yellow solid 89 mg, 0.22 mmol, 34 %. ^{1}H-NMR (500 MHz, DMSO-d_6, 298 K) δ 8.13 (d, $^{4}J_{H\text{-}H}$ = 1.7 Hz, 1 H, H-2), 7.89 (dd, $^{3}J_{H\text{-}H}$ = 8.1 Hz, $^{4}J_{H\text{-}H}$ = 1.7 Hz, 1 H, H-4), 7.72 (d, $^{3}J_{H\text{-}H}$ = 8.1 Hz, 1 H, H-5), 5.77 (hept, $^{3}J_{H\text{-}F}$ = 6.4 Hz, 1 H, H-8), 5.30 (s, 2 H, H-7), 0.26 (s, 9 H, H-12); δ ^{13}C (determined by HMQC and HMBC) 146.9 (C-1), 136.5 (C-4), 132.0 (C-6), 129.0 (C-5), 127.3 (C-2), 122.8 (C-3), 121.6 (q, C-9), 102.0 (C-10), 97.3 (C-11), 74.0 (C-8), 71.7 (C-7), -0.7 (C-12); UPLC Method 1, T_R = 6.53 min; HRMS (ESI-) calcd. for $C_{15}H_{14}F_6NO_3Si^-$ (M-H$^+$): 398.0653, found: 398.0655.

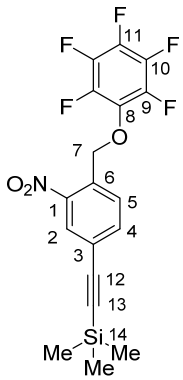

S9

S9. The synthesis followed the protocol for the synthesis of **S7** (*General procedure 2*) employing **S5** (250 mg, 628 μmol, 1.00 eq.). **S9** was isolated as a pale yellow solid (106 mg, 0.26 mmol, 39 %); ^{1}H-NMR (500 MHz, DMSO-d_6, 298 K) δ 8.15 (d, $^{4}J_{H\text{-}H}$ = 1.7 Hz, 1 H, H-2), 7.91 (dd, $^{3}J_{H\text{-}H}$ = 8.0 Hz, $^{4}J_{H\text{-}H}$ = 1.7 Hz, 1 H, H-4), 7.86 (d, $^{3}J_{H\text{-}H}$ = 8.0 Hz, 1 H, H-5), 5.61 (s, 2 H, H-7), 0.26 (s, 9 H, H-14); ^{13}C NMR (126 MHz, DMSO-d_6, 298 K, C-9, C-10, C-11 were assigned in analogy to compound **1b**) 146.9 (C-1), 142.1 (C-9 or C-10), 140.1 (C-9 or C-10), 136.5 (C-4), 136.4 (C-11), 132.4 (C-8), 131.4 (C-6), 129.8 (C-5), 127.3 (C-2), 123.0 (C-3), 101.7 (C-12), 97.4 (C-13), 72.6 (C-7), -0.7 (C-14); UPLC Method 1, T_R = 6.78 min; HRMS (ESI-) calcd. for $C_{18}H_{13}F_5NO_3Si^-$ (M-H$^+$): 414.0590, found: 414.0592.

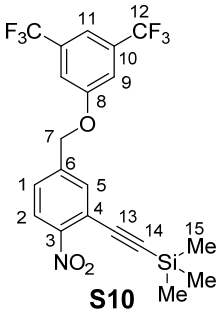

S10

S10. The synthesis followed the protocol for the synthesis of **S7** (*General procedure 2*) employing **S6** (200 mg, 0.450 mmol, 1.00 eq.). **S10** was isolated as a pale yellow solid (126 mg, 0.27 mmol, 61 %). ^{1}H-NMR (500 MHz, $CDCl_3$, 298 K) δ 8.08 (d, $^{3}J_{H\text{-}H}$ = 8.5 Hz, 1 H, H-2), 7.75-7.73 (m, 1 H, H-5), 7.54 (s, 1 H, H-11), 7.53-7.50 (m, 1 H, H-1), 7.40 (s, 2 H, H-9), 5.18 (s, 2 H, H-7), 0.29 (s, 9 H, H-15); δ ^{13}C (determined by HMQC and HMBC experiments) 158.5 (C-8), 149.7 (C-3), 140.6 (C-6), 133.4 (C-5), 133,0 (C-10), 127.1 (C-1), 125.1 (C-2), 123.0 (q, C-12), 119.0 (C-4), 115.3 (C-11), 115.1 (C-9), 104.7 (C-14), 98.6 (C-13), 68.8 (C-7), -0.5 (C-15); UPLC-MS: Method 1, T_R = 6.78 min; m/z MS (ES-): 460.9 [100%, M - H$^+$], 229.5 [80%, $(CF_3)_2C_6H_3O^-$]; HRMS (ESI-) calcd. for $C_{20}H_{16}F_6NO_3Si^-$ (M-H$^+$):460.0809, found: 460.0817.

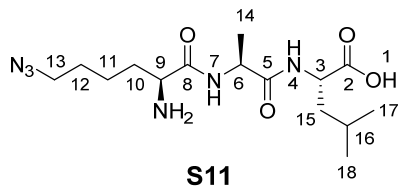

S11

S11. 2-Chlorotrityl chloride resin (1 mmol/g, 700 mg) was placed in a plastic syringe equipped with a filter frit. The resin was washed with CH_2Cl_2 (ca. 4 ml). Subsequently the syringe was filled with CH_2Cl_2 (ca. 4 ml) and placed on a shaker for 15 min. The CH_2Cl_2 was exchanged and DIPEA (150 μl, 0.908 mmol, 2.00 eq.), and Fmoc-Leu-OH (160 mg, 0.453 mmol, 1.00 eq.) were added.

After the sample was agitated on the shaker for 1.5 h the liquid phase was removed by filtration and the resin washed with CH_2Cl_2 (ca. 4 ml) and DMF (ca. 4 ml). The unreacted binding sites on the resin were capped by adding a basic MeOH-solution in dichloromethane (ca. 5 ml, 80 % CH_2Cl_2; 15 % MeOH, 5 % *N*,*N*-diisopropylethylamine) followed by 15 min agitation. Subsequently the sample was washed with CH_2Cl_2 (ca. 4 ml) and DMF (ca. 4 ml). For Fmoc deprotection a solution of piperidine in DMF (20 % piperidine, ca. 4 ml) was added and shaking continued for 5 mins. This step was repeated three times. Note: In the following, this procedure will be referred to as *Fmoc deprotection*. The sample was washed with DMF (ca. 4 ml) and CH_2Cl_2 (ca. 4 ml) and again with DMF (ca. 4 ml). Between the different washing steps the sample was agitated on a shaker for ca. 30 sec. Note: In the following this procedure will be referred to as *washing.* After the *washing*, DMF (ca. 4 ml), *N*,*N*-diisopropylethylamine (750 µl, 4.54 mmol, 10.0 eq.), Fmoc-Ala-OH (705 mg, 2.26 mmol, 5.00 eq.) and PyBOP (1.18 g, 2.27 mmol, 5.01 eq.) were added. The mixture was agitated on a shaker for 2 h. Note: In the following this procedure will be referred to as *peptide coupling*. This was followed by *washing*, *Fmoc deprotection* and another *washing*. For the next peptide coupling step DIPEA (300 µl, 1.81 mmol, 4.01 eq.), Fmoc-azidolysine (411 mg, 0.906 mmol, 2.00 eq.) and PyBOP (471 mg, 0.905 mmol, 2.00 eq.) were used. After *washing*, *Fmoc- deprotection* and another *washing* the resin was rinsed with CH_2Cl_2 (3 × ca. 4 ml) before a cleavage solution of trifluoro acetic acid, triisopropylsilane and water (5 ml, 92 % TFA, 5 % triisopropylsilane, 3 % H_2O) was added. For the cleavage procedure, the mixture was agitated on the shaker for 1 h. Subsequently the cleavage solution was removed and the resin washed with TFA (1 ml). The TFA containing filtrates were combined and concentrated under reduced pressure to ca. 0.5 ml. Ice cold Et_2O (50 ml) was added and the formed precipitate was collected by centrifugation (4400 rpm). The precipitated trifluoroacetate salt was washed with Et_2O (3 × 20 ml) and obtained after drying as a white powder (108 mg, 0.230 mmol, 51 %). ^{1}H-NMR: (500 MHz, DMSO-d_6, 298 K) δ 8.56 (d, $^3J_{H\text{-}H}$ = 7.7 Hz, 1 H, H-7), 8.16 (d, $^3J_{H\text{-}H}$ = 8.1 Hz, 1 H, H-4), 4.39 (quint, $^3J_{H\text{-}H}$ = 7.1 Hz, 1 H, H-6), 4.21 (q, $^3J_{H\text{-}H}$ = 7.9 Hz, 1 H, H-3), 3.71 (t, $^3J_{H\text{-}H}$ = 6.5 Hz, 1 H, H-9), 3.35-3.25 (m, 2 H, H-13), 1.72-1.58 (m, 3 H, H-10 and H-16), 1.54-1.45 (m, 4 H, H-12 and H-15), 1.35 (quint, $^3J_{H\text{-}H}$ = 7.2 Hz, 2 H, H-11), 1.24 (d, $^3J_{H\text{-}H}$ = 7.0 Hz, 3 H, H-14), 0.88 (d, $^3J_{H\text{-}H}$ = 6.5 Hz, 3 H, H-17 or H-18), 0.83 (d, $^3J_{H\text{-}H}$ = 6.5 Hz, 3 H, H-17 or H-18); ^{13}C NMR (126 MHz, DMSO-d_6, 298 K) 173.7 (C-2), 171.3 (C-5), 168.1 (C-8), 51.7 (C-9), 50.1 (C-13), 49.9 (C-3), 47.5 (C-6), 40.0 (C-15), 30.5 (C-10), 27.5 (C-12) 24.3 (C-16), 22.6 (C-17 or C-18), 21.2 (C-11), 21.1 (C-17 or C-18), 18.0 (C-14); UPLC-MS Method 2, T_R = 4.88 min; m/z MS (ESI+): 357.3 [100 %, M + H^+], 226.3 [65 %]; HRMS (ESI+) calcd. for $C_{15}H_{29}F_6O_4^+$ ($M+H^+$): 357.2245, found: 357.2249.

S5

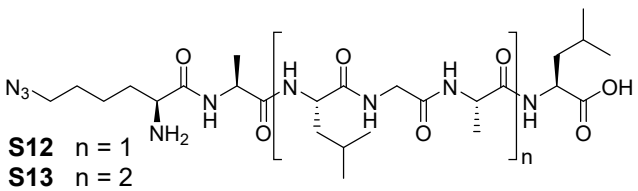

S12 n = 1
S13 n = 2
S14 n = 3

General procedure 3. 2-chlorotrityl chloride resin (1 mmol/g, 200 mg) was loaded with Fmoc-Leu-OH (18 mg, 51 μmol, 1.0 eq.) and unreacted binding sites capped as described above. Peptide coupling steps were performed by means of a peptide synthesizer (Intavis multi pep RSI) with Fmoc-amino acids (5.00 eq.), PyBOP (5.00 eq.), and DIPEA (5.00 eq.) in DMF (1.6 ml) at room temperature, with a reaction time of 45 min followed by a 2nd coupling of 90 min duration and identical concentrations. Fmoc-deprotection was performed with piperidine (20 % in DMF, 0.8 ml , 4 × 5 min) after the syringes were washed with DMF (5 × 1 ml). The coupling of Fmoc-azidolysine was performed with 1.50 eq. of Fmoc-amino acids, PyBOP and *N*,*N*-diisopropylethylamine in DMF (1.6 ml) for 2 h followed by another 8 h after exchange of the coupling reagents. In the end the resin was washed CH_2Cl_2 (5 × 1.6 ml) before cleavage. Cleavage, precipitation and washing in Et_2O were performed as described for **S11**. The trifluoroacetate salts of the products were isolated as white solids.

S12. 25 mg (contains ca. 5 wt% Et_2O, 65 % corrected yield). ^{1}H-NMR (500 MHz, DMSO-d_6, 298 K) δ 8.60 (d, $^3J_{H\text{-}H}$ = 7.4 Hz, 1 H, NH), 8.16- 8.06 (m, 5 H, NH and NH_2), 7.88 (d, $^3J_{H\text{-}H}$ = 7.6 Hz, 1 H, NH), 4.40 (quint, $^3J_{H\text{-}H}$ = 7.1 Hz, 1 H, H-C_α), 4.35-4.26 (m, 2 H, H-C_α), 4.19 (m, 1 H, H-C_α), 3.82-3.62 (m, 3 H, H-C_α), 3.33-3.28 (m, 2 H, H-$C_{\varepsilon(Lys)}$), 1.71-1.45 (m, 10 H, H-$C_{\beta(Lys)}$, H-$C_{\delta\ (lys)}$, H-$C_{\beta(leu)}$, H-$C_{\gamma(leu)}$), 1.39-1.31 (m, 2 H, H-$C_{\gamma(lys)}$), 1.24 (d, $^3J_{H\text{-}H}$ = 7.0 Hz, 3 H, H-$C_{\beta(ala)}$), 1.20 (d, $^3J_{H\text{-}H}$ = 7.0 Hz, 3 H, H-$C_{\beta(ala)}$), 0.89 (d, $^3J_{H\text{-}H}$ = 6.4 Hz, 3 H, H-$C_{\delta(leu)}$), 0.87 (d, $^3J_{H\text{-}H}$ = 6.4 Hz, 3 H, 0.83 (d, $^3J_{H\text{-}H}$ = 6.4 Hz, 3 H, H-$C_{\delta(leu)}$), 0.83 (d, $^3J_{H\text{-}H}$ = 6.4 Hz, 3 H, H-$C_{\delta(leu)}$). UPLC-MS Method 3, T_R = 4.18 min; m/z MS (ES+): 598.2 [100 %, M + H^+], 299.7 [60 %, M + 2 H^+]; HRMS (ESI+) calcd. for $C_{26}H_{48}N_9O_7^+$ (M+H^+): 598.3671, found: 598.3681.

S13. 30 mg (62 %). ^{1}H-NMR: (500 MHz, DMSO-d_6, 298 K): 8.60 (d, $^3J_{H\text{-}H}$ = 7.4 Hz, 1 H, amide NH), 8.16- 8.03 (m, 6 H, 4 amide NH and amine NH_2), 7.99 (d, $^3J_{H\text{-}H}$ = 7.9 Hz, 1 H, amide NH), 7.95 (d, $^3J_{H\text{-}H}$ = 7.2 Hz, 1 H, amide NH), 7.84 (d, $^3J_{H\text{-}H}$ = 7.5 Hz, 1 H, amide NH), 4.40 (quint., $^3J_{H\text{-}H}$ = 7.1 Hz, 1 H, H-C_α), 4.35-4.16 (m, 5 H, H-C_α), 3.81-3.62 (m, 5 H, H-C_α), 3.34-3.25 (m, 2 H, H-$C_{\varepsilon(Lys)}$), 1.71-1.43 (m, 13 H, H-$C_{\beta(lys)}$, H-$C_{\delta\ (lys)}$, H-$C_{\beta(leu)}$, H-$C_{\gamma(leu)}$), 1.39-1.31 (m, 2 H, H-$C_{\gamma(lys)}$), 1.24 (d, $^3J_{H\text{-}H}$ = 7.0 Hz, 3 H, H-$C_{\beta(ala)}$), 1.21 (d, $^3J_{H\text{-}H}$ = 7.0 Hz, 3 H, H-$C_{\beta(ala)}$), 1.20 (d, $^3J_{H\text{-}H}$ = 7.1 Hz, 3 H, H-$C_{\beta(ala)}$), 0.90-0.86 (m, 9 H, H-$C_{\delta(leu)}$), 0.85-0.83 (m, 9 H, H-$C_{\delta(leu)}$); UPLC-MS Method 3, T_R = 4.51 min; m/z MS (ES+): 839.2 [100 %, M + H^+], 420.4 [60 %, M + 2 H^+]; HRMS (ESI+) calcd. for $C_{37}H_{67}N_{12}O_{10}^+$ (M+H^+): 839.5098, found: 839.5096.

S14. 36 mg (contains ca. 4 wt% Et_2O, 57 % corrected yield). ^{1}H-NMR: (500 MHz, DMSO-d_6, 298 K): 8.59 (d, $^3J_{H\text{-}H}$ = 7.5 Hz, 1 H, amide NH), 8.14- 7.82 (m, 12 H, 10 amide NH and amine NH_2), 4.41 (quint, $^3J_{H\text{-}H}$ = 7.1

Hz, 1 H, H-C_α), 4.35-4.16 (m, 7 H, H-C_α), 3.80-3.62 (m, 7 H, H-C_α), 3.34-3.25 (m, 2 H, H-$C_{\varepsilon(Lys)}$), 1.71-1.43 (m, 16 H, H-$C_{\beta(lys)}$, H-$C_{\delta\ (lys)}$, H-$C_{\beta(leu)}$, H-$C_{\gamma(leu)}$), 1.39-1.31 (m, 2 H, H-$C_{\gamma(lys)}$), 1.24 (d, $^3J_{H\text{-}H}$ = 7.0 Hz, 3 H, H-$C_{\beta(ala)}$), 1.22-1.18 (m, 9 H, H-$C_{\beta(ala)}$), 0.90-0.86 (m, 12 H, H-$C_{\delta(leu)}$), 0.85-0.83 (m, 12 H, H-$C_{\delta(leu)}$); UPLC-MS Method 3, T_R = 4.78 min; m/z MS (ES+): 1080.2 [100 %, M + H^+], 540.9 [60 %, M + 2 H^+]; HRMS (ESI+) calcd. for $C_{48}H_{86}N_{15}O_{13}^+$ (M+H^+): 1080.6524, found: 1080.6516.

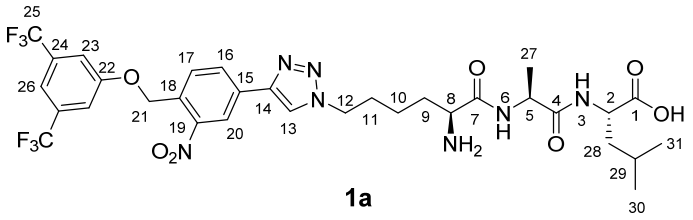

1a

1a. *General procedure 4*. To a suspension of **S1** (43.6 mg, 112 μmol, 1.00 eq.) and the trifluoroacetate salt of **S11** (40.0 mg, 85.1 μmol, 0.760 eq.) in water / *tert*-butanol (1 : 1, 10 ml) was added aq. sodium ascorbate (1 M, 400 μl, 3.57 eq.) and aq. $CuSO_4$ (1 M, 40 μl, 0.36 eq.) and the resulting mixture was stirred for 4 h at 55 °C. Subsequently volatiles were removed under reduced pressure and the resulting residue was purified by reversed phase HPLC. The trifluoroacetate salt of the **1a** was obtained as a white powder after lyophilisation (22 mg, 23 %). ^{1}H-NMR (500 MHz, DMSO-d_6, 298 K) δ 8.91 (s, 1 H, H-13), 8.59 (d, $^4J_{H\text{-}H}$ = 1.7 Hz, 1 H, H-20), 8.25 (dd, $^3J_{H\text{-}H}$ = 8.1 Hz, $^4J_{H\text{-}H}$ = 1.7 Hz, 1 H, H-16), 8.24 (d, $^3J_{H\text{-}H}$ = 7.0, 1 H, H-6), 7.94 (d, $^3J_{H\text{-}H}$ = 8.3 Hz, 1 H, H-3), 7.92 (d, $^3J_{H\text{-}H}$ = 8.1 Hz, 1 H, H-17), 7.76 (s, 2 H, H-23), 7.70 (s, 1 H, H-26), 5.69 (s, 2 H, H-21), 4.42 (t, $^3J_{H\text{-}H}$ = 7.0 Hz, 2 H, H-12), 4.30 (quint, $^3J_{H\text{-}H}$ = 7.0 Hz, 1 H, H-5), 4.10 (td, $^3J_{H\text{-}H}$ = 8.2 Hz, $^3J_{H\text{-}H}$ = 5.7 Hz, 1 H, H-2), 3.29 (t, $^3J_{H\text{-}H}$ = 6.2 Hz, 1 H, H-8), 1.88 (quint, $^3J_{H\text{-}H}$ = 7.1 Hz, 2 H, H-11), 1.71-1.62 (m, 1 H, H-9), 1.65-1.57 (m, 1 H, H-29), 1.52-1.43 (m, 3 H, H-9, H-28), 1.37-1.29 (m, 2 H, H-10), 1.19 (d, $^3J_{H\text{-}H}$ = 7.0 Hz, 3 H, H-27), 0.85 (d, $^3J_{H\text{-}H}$ = 6.6 Hz, 3 H, H-30 or H-31), 0.82 (d, $^3J_{H\text{-}H}$ = 6.5 Hz, 3 H, H-30 or H-31); δ ^{13}C (determined by HMQC and HMBC experiments) 173.6 (C-1), 171.4 (C-4), 158.6 (C-22), 147.8 (C-19), 143.6 (C-14), 132.6 (C-24), 132.0 (C-15), 130.2 (C-18), 130.1 (C-17), 129.8 (C-16), 122.9 (q, C-25), 122.6 (C-13), 120.7 (C-20), 115.8 (C-23), 114.3 (C-26), 67.1 (C-21), 53.5 (C-8), 50.8 (C-2), 49.3 (C-12), 47.6 (C-5), 40.4 (C-28), 33.1 (C-9), 29.1 (C-11), 24.2 (C-29), 22.8 (C-30 or C-31), 21.6 (C-10), 21.5 (C-30 or C-31), 18.2 (C-27), (C-7 was not detected); UPLC-MS Method 3, T_R = 6.10 min; m/z MS (ES+): 746.1 [100 %, M + H^+], 394.5 [40 %]; HRMS (ESI+) calcd. for $C_{32}H_{38}F_6N_7O_7^+$ (M+H^+): 746.2731, found: 746.2737.

2a. The synthesis followed the protocol for the synthesis of **1a** (*General procedure 4*) starting with **S1** (23 mg, 50 μmol, 1.0 eq.) and the trifluoroacetate salt of **S12** (30 mg, 40 μmol, 0.80 eq.). The modified peptide was isolated as a white solid (8 mg, 7 μmol, 18 %). ^{1}H-NMR (600 MHz, DMSO-d_6, 298 K) δ 12.51 (br, 1 H, COOH), 8.83 (s, 1 H, H-1), 8.60-8.57 (m, 2 H, H-8 and amide NH), 8.24 (dd, $^3J_{H\text{-}H}$ = 8.0 Hz, $^4J_{H\text{-}H}$ = 1.8 Hz, 1 H, H-4), 8.16- 8.04 (m, 5 H, 3 amide NH, amine NH_2), 7.93 (d, $^3J_{H\text{-}H}$ = 8.1 Hz, 1 H, H-5), 7.89 (d, $^3J_{H\text{-}H}$ = 7.5 Hz, 1 H, amide NH), 7.76 (s, 2 H, H-11), 7.71 (s, 1 H, H-13), 5.70 (s, 2 H, H-9), 4.44-4.35 (m, 3 H, 2 H-$C_{\varepsilon(Lys)}$ and H-C_α), 4.35-4.26 (m, 2 H, H-C_α), 4.19 (m, 1 H, H-C_α), 3.77-3.62 (m, 3 H, H-C_α), 1.89 (quint, $^3J_{H\text{-}H}$ = 7.3 Hz, 2 H,

H-$C_{\delta\,(lys)}$), 1.75-1.69 (m, 2 H, H-$C_{\beta(lys)}$), 1.66-1.57 (m, 2 H, H-$C_{\gamma(leu)}$), 1.56-1.43 (m, 4 H, H-$C_{\beta(leu)}$), 1.38-1.31 (m, 2 H, H-$C_{\gamma(lys)}$), 1.24 (d, $^3J_{H\text{-}H}$ = 7.1 Hz, 3 H, H-$C_{\beta(ala)}$), 1.19 (d, $^3J_{H\text{-}H}$ = 7.2 Hz, 3 H, H-$C_{\beta(ala)}$), 0.89-0.85 (m, 6 H, H-$C_{\delta(leu)}$), 0.83-0.81 (m, 6 H, H-$C_{\delta(leu)}$).UPLC-MS: Method 3, T_R = 6.12 min; m/z MS (ES+): 987.0 [100 %, M + H^+], 856.4 [40 %], 494.1 [40 %, M + 2 H^+]; HRMS (ESI+) calcd. for $C_{43}H_{57}F_6N_{10}O_{10}^+$ (M+H^+): 987.4158, found: 987.4172.

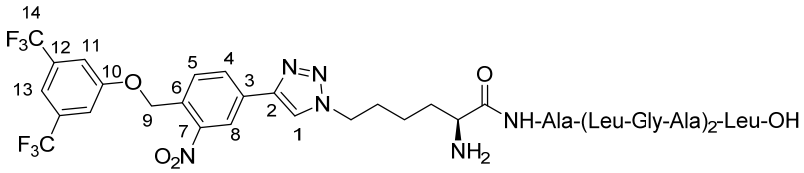

3a

3a. The synthesis followed the protocol for the synthesis of **1a** (*General procedure 4*) starting with **S1** (23 mg, 50 μmol, 1 eq.) and the trifluoroacetate salt of **S13** (42 mg, 44 μmol, 0.88 eq.). The trifluoroacetate salt of the modified peptide was isolated as a white solid (7 mg, 5 μmol, 12 %). ^{1}H-NMR (600 MHz, DMSO-d_6, 298 K) δ 12.44 (br, 1 H, COOH), 8.83 (s, 1 H, H-1), 8.60-8.57 (m, 2 H, H-8 and amide NH), 8.24 (dd, $^3J_{H\text{-}H}$ = 8.0 Hz, $^4J_{H\text{-}H}$ = 1.8 Hz, 1 H, H-4), 8.11- 8.03 (m, 6 H, 4 amide NH, amine NH_2), 8.00 (d, $^3J_{H\text{-}H}$ = 7.9 Hz, 1 H, amide NH), 7.96 (d, 1 H, $^3J_{H\text{-}H}$ = 7.2 Hz, amide NH), 7.93 (d, $^3J_{H\text{-}H}$ = 8.1 Hz, 1 H, H-5), 7.85 (d, $^3J_{H\text{-}H}$ = 7.5 Hz, 1 H, amide NH), 7.76 (s, 2 H, H-11), 7.71 (s, 1 H, H-13), 5.70 (s, 2 H, H-9), 4.44-4.36 (m, 3 H, 2 H-$C_{\varepsilon(Lys)}$ and H-C_α), 4.35-4.14 (m, 5 H, H-C_α), 3.77-3.62 (m, 5 H, H-C_α), 1.89 (quint, $^3J_{H\text{-}H}$ = 7.1 Hz, 2 H, H-$C_{\delta\,(lys)}$), 1.76-1.60 (m, 2 H, H-$C_{\beta(lys)}$), 1.66-1.57 (m, 3 H, H-$C_{\gamma(leu)}$), 1.54-1.42 (m, 6 H, H-$C_{\beta(leu)}$), 1.40-1.32 (m, 2 H, H-$C_{\gamma(lys)}$), 1.24 (d, $^3J_{H\text{-}H}$ = 7.1 Hz, 3 H, H-$C_{\beta(ala)}$), 1.20 (d, $^3J_{H\text{-}H}$ = 7.2 Hz, 6 H, H-$C_{\beta(ala)}$), 0.89-0.85 (m, 9 H, H-$C_{\delta(leu)}$), 0.83-0.81 (m, 9 H, H-$C_{\delta(leu)}$); UPLC-MS Method 3, T_R = 6.47 min; m/z MS (ES+): 1250.1 [40 %, M + Na^+], 1228.2 [100 %, M + H^+], 614.9 [40 %, M + 2 H^+]; HRMS (ESI+) calcd. for $C_{54}H_{76}F_6N_{13}O_{13}^+$ (M+H^+): 1228.5584, found: 1228.5582.

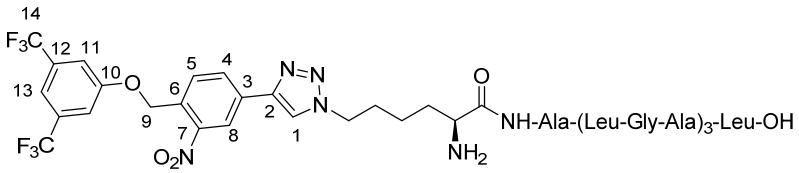

4a

4a. The synthesis followed the protocol for the synthesis of **1a** (*General procedure 4*) starting with **S1** (14 mg, 30 μmol, 1.0 eq.) and the trifluoroacetate salt of **S14** (32 mg, 26 μmol, 0.86 eq.). The trifluoroacetate salt of the modified peptide was isolated as a white solid (6.9 mg, 17 %). The modified peptide was isolated as a white solid (6.9 mg, 9.0 %). ^{1}H-NMR (500 MHz, DMSO-d_6, 298 K) δ 12.51 (br, 1 H, COOH), 8.83 (s, 1 H, H-1), 8.59 (m, 2 H, H-8 and amid), 8.24 (dd, $^3J_{H\text{-}H}$ = 8.1 Hz, $^4J_{H\text{-}H}$ = 1.7 Hz, 1 H, H-4), 8.14- 8.02 (m, 8 H, 6 amide, amine NH_2), 8.02-7.88 (m, 5 H, H-5 and amide NH), 7.84 (d, $^3J_{H\text{-}H}$ = 7.5 Hz, 1 H, amide NH), 7.76 (s, 2 H, H-11), 7.71 (s, 1 H, H-13), 5.70 (s, 2 H, H-9), 4.44-4.36 (m, 3 H, 2 H-$C_{\varepsilon(Lys)}$ and H-C_α), 4.35-4.14 (m, 7 H, H-C_α), 3.78-3.62 (m, 7 H, H-C_α), 1.89 (quint, $^3J_{H\text{-}H}$ = 7.1 Hz, 2 H, H-$C_{\delta\,(lys)}$), 1.76-1.69 (m, 2 H, H-$C_{\beta(lys)}$), 1.66-1.57 (m, 4 H, H-$C_{\gamma(leu)}$), 1.54-1.42 (m, 8 H, H-$C_{\beta(leu)}$), 1.40-1.32 (m, 2 H, H-$C_{\gamma(lys)}$), 1.24 (d, $^3J_{H\text{-}H}$ = 7.1 Hz, 3 H, H-$C_{\beta(ala)}$), 1.20 (d, $^3J_{H\text{-}H}$ = 7.2

Hz, 9 H, H-$C_{\beta(ala)}$), 0.90-0.80 (m, 24 H, H-$C_{\delta(leu)}$); UPLC-MS: Method 4, T_R = 7.02 min; m/z MS (ES+): 1467.2 [100 %, M + H^+], 733.4 [40 %, M + 2 H^+]; HRMS (ESI+) calcd. for $C_{65}H_{95}F_6N_{16}O_{16}^+$ (M+H^+): 1469.7011, found: 1469.7005.

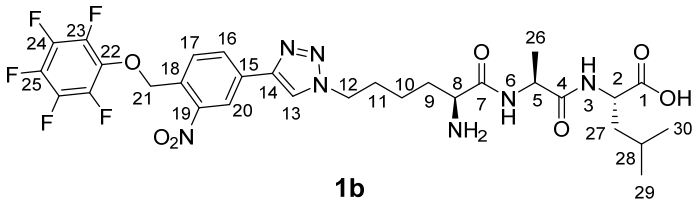

1b

1b. *General procedure 5*. The trimethylsilyl-protected alkyne **S9** was deprotected *in situ*. **S9** (51 mg, 0.12 mmol, 1.0 eq.) and the trifluoroacetate salt of **S11** (44 mg, 94 μmol, 0.78 eq.) were suspended in water/*tert*-butanol (1:1, 10 ml). Aq. sodium ascorbate (1.00 M, 200 μl, 1.63 eq.), aq. $CuSO_4$ (1.00 M, 20 μl, 0.16 eq.) and TBAF (1 M in THF, 369 μl, 0.369 mmol, 3.00 eq.) were added and the mixture was stirred for 4 h at 55 °C. Subsequently volatiles were removed under reduced pressure and the residue purified by reversed phase preparative HPLC. The trifluoroacetate salt of the product was obtained as a white powder after lyophilisation. (8.0 mg, 11 %). ^{1}H-NMR (600 MHz, DMSO-d_6, 298 K) δ 8.85 (s, 1 H, H-13), 8.59 (d, $^3J_{H\text{-}H}$ = 7.5 Hz, 1 H, H-6), 8.57 (d, $^4J_{H\text{-}H}$ = 1.8 Hz, 1 H, H-20), 8.28 (dd, $^3J_{H\text{-}H}$ = 8.1 Hz, $^4J_{H\text{-}H}$ = 1.8 Hz, 1 H, H-16), 8.22 (d, $^3J_{H\text{-}H}$ = 8.1 Hz, 1 H, H-3), 7.94 (d, $^3J_{H\text{-}H}$ = 8.1 Hz, 1 H, H-17), 5.63 (s, 2 H, H-21), 4.47-4.35 (m, 3 H, H-12 and H-5), 4.22 (ddd, $^3J_{H\text{-}H}$ = 9.2 Hz, $^3J_{H\text{-}H}$ = 8.0 Hz, $^3J_{H\text{-}H}$ = 5.4 Hz, 1 H, H-2), 3.77 (t, $^3J_{H\text{-}H}$ = 6.5 Hz, 1 H, H-8), 1.89 (quint, $^3J_{H\text{-}H}$ = 7.2 Hz, 2 H, H-11), 1.76-1.69 (m, 2 H, H-9), 1.67-1.58 (m, 1 H, H-28), 1.56-1.47 (m, 2 H, H-27), 1.40-1.32 (m, 2 H, H-10), 1.25 (d, $^3J_{H\text{-}H}$ = 7.1 Hz, 3 H, H-26), 0.88 (d, $^3J_{H\text{-}H}$ = 6.6 Hz, 3 H, H-29 or H-30), 0.82 (d, $^3J_{H\text{-}H}$ = 6.5 Hz, 3 H, H-29 or H-30); ^{13}C NMR (150 MHz, DMSO-d_6, 298 K) δ 173.9 (C-1), 171.7 (C-4), 168.1 (C-7), 147.9 (C-19), 144.0 (C-14), 141.4 (C-23), 137.5 (C-24), 137.0 (C-25), 132.5 (C-15), 130.9 (C-17), 130.1 (C-18), 130.0 (C-16), 122.8 (C-13), 120.9 (C-20), 73.1 (C-21), 51.9 (C-8), 50.1 (C-2), 49.5 (C-12), 48.0 (C-5), 39.9 (C-27), 30.6 (C-9), 29.0 (C-11), 24.3 (C-28), 22.9 (C-29 or C-30), 21.3 (C-29 or C-30), 21.2 (C-10), 18.2 (C-26), C-22 was not detected; ^{19}F-NMR (565 MHz, DMSO-d_6, 298 K) δ -73.5 (s, trifluoroacetate), -156.1 (m, 2 F, 9-F), -161.7 (m, 1 F, 11-F), -162.5 (m, 2 F, 10-F); UPLC-MS Method 3, T_R = 5.59 min; m/z MS (ES+): 700.4 [100 %, M + H^+]; HRMS (ESI+) calcd. for $C_{30}H_{35}F_5N_7O_7^+$ (M+H^+): 700.2513, found: 700.2519.

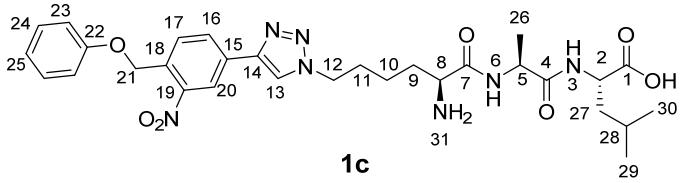

1c

1c. The synthesis followed the protocol for the synthesis of **1b** (*General procedure 5*) employing **S7** (27 mg, 57 μmol, 1.0 eq.) and the trifluoroacetate salt of **S11** (30 mg, 64 μmol, 1.1 eq.). The trifluoroacetate salt of the product was isolated as a white solid (3 mg, 7 %); ^{1}H-NMR (500 MHz, DMSO-d_6, 298 K) δ 8.81 (s, 1 H, H-13), 8.59 (d, $^3J_{H\text{-}H}$ = 8.0 Hz, 1 H, H-6), 8.55(d, $^4J_{H\text{-}H}$ = 1.5 Hz, 1 H, H-20), 8.25-8.20 (m, 2 H, H-16 and H-3), 8.05 (br s, 2 H, H-31), 7.88 (d, $^3J_{H\text{-}H}$ = 8.1 Hz, 1 H, H-17), 7.34-7.30 (m, 2 H, H-24), 7.05-7.01 (m, 2 H, H-23), 7.00-6.95 (m, 1 H, H-25), 5.48 (s, 2 H, H-21), 4.45-4.35 (m, 3

H, H-12 and H-5), 4.25-4.18 (m, 1 H, H-2), 3.78-3.73 (m, 1 H, H-8), 1.93-1.84 (m, 2 H, H-11), 1.76-1.69 (m, 2 H, H-9), 1.67-1.60 (m, 1 H, H-28), 1.57-1.46 (m, 2 H, H-27), 1.39-1.30 (m, 2 H, H-10), 1.25 (d, $^{3}J_{H\text{-}H}$ = 6.9 Hz, 3 H, H-26), 0.88 (d, $^{3}J_{H\text{-}H}$ = 6.1 Hz, 3 H, H-29 or H-30), 0.82 (d, $^{3}J_{H\text{-}H}$ = 6.1 Hz, 3 H, H-29 or H-30). δ ^{13}C (determined by HMQC and HMBC experiments) 171.3 (C-4), 167.7 (C-7), 157.5 (C-22), 147.7 (C-19), 143.6 (C-14), 131.3 (C-15 and C-18), 129.7 (C-17), 129.4 (C-16), 129.2 (C-24), 122.2 (C-13), 120.9 (C-25), 120.5 (C-20), 114.4 (C-23), 65.8 (C-21), 51.5 (C-8), 49.9 (C-2), 49.0 (C-12), 47.7 (C-26), 39.5 (C-27), 30.1 (C-9), 28.7 (C-11), 23.9 (C-28), 22.4 (C-29 or C-30), 20.9 (C-29 or C-30), 20.8 (C-10), 17.7 (C-26), C-1 was not detected; UPLC-MS Method 3, T_R = 5.25 min; m/z MS (ES+): 610.1 [100 %, M + H$^+$], 326.3 [40 %], 305.8 [40 %, M + 2 H$^+$]; HRMS (ESI+) calcd. for $C_{30}H_{40}N_7O_7^+$ (M+H$^+$): 610.2984, found: 610.2989.

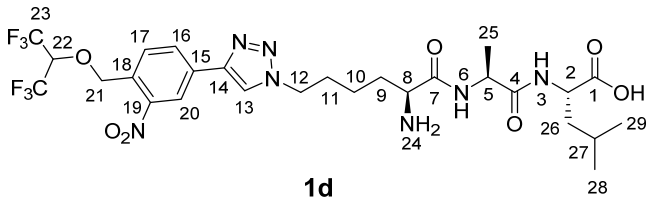

1d

1d. The synthesis followed the protocol for the synthesis of **1b** (*General procedure 5*) starting from **S8** (30 mg, 75 μmol, 1.0 eq.) and the trifluoroacetate salt of **S11** (27 mg, 57 μmol, 0.76 eq.) The trifluoroacetate of the product was isolated as a white solid (5 mg, contains 23 wt% of a tetrabutylammonium salt, which was considered as the trifluoroacetate, corrected yield 8 %). ^{1}H-NMR (600 MHz, DMSO-d$_6$, 298 K) δ 12.57 (br, 1 H), 8.83 (s, 1 H, H-13), 8.61 (d, $^{3}J_{H\text{-}H}$ = 7.5 Hz, 1 H, H-6), 8.54 (d, $^{4}J_{H\text{-}H}$ = 1.8 Hz, 1 H, H-20), 8.28 (dd, $^{3}J_{H\text{-}H}$ = 8.1 Hz, $^{4}J_{H\text{-}H}$ = 1.8 Hz, 1 H, H-16), 8.22 (d, $^{3}J_{H\text{-}H}$ = 8.0 Hz 1 H, H-3), 8.09 (s, 2 H, H-24), 7.82 (d, $^{3}J_{H\text{-}H}$ = 8.1 Hz, 1 H, H-17), 5.78 (hept, $^{3}J_{H\text{-}F}$ = 6.4 Hz, 1 H, H-22), 5.32 (s, 2 H, H-21), 4.46-4.36 (m, 3 H, H-12 and H-5), 4.22 (ddd, $^{3}J_{H\text{-}H}$ = 9.7 Hz, $^{3}J_{H\text{-}H}$ = 8.0 Hz, $^{3}J_{H\text{-}H}$ = 5.4 Hz, 1 H, H-2), 3.77 (t, $^{3}J_{H\text{-}H}$ = 6.4 Hz, 1 H, H-8), 1.89 (quint, $^{3}J_{H\text{-}H}$ = 7.2 Hz, 2 H, H-11), 1.75-1.70 (m, 2 H, H-9), 1.67-1.58 (m, 1 H, H-27), 1.56-1.47 (m, 2 H, H-26), 1.40-1.32 (m, 2 H, H-10), 1.25 (d, $^{3}J_{H\text{-}H}$ = 7.1 Hz, 3 H, H-25), 0.88 (d, $^{3}J_{H\text{-}H}$ = 6.6 Hz, 3 H, H-28 or H-29), 0.82 (d, $^{3}J_{H\text{-}H}$ = 6.6 Hz, 3 H, H-28 or H-29); ^{13}C NMR (150 MHz, DMSO-d$_6$, 298 K) δ 174.0 (C-1), 171.7 (C-4), 168.1 (C-8), 147.7 (C-19), 144.0 (C-14), 132.2 (C-15), 130.5 (C-18), 130.1 (C-17), 130.0 (C-16), 122.8 (C-13), 121.7 (q, $^{1}J_{C\text{-}F}$ ≈ 284 Hz, C-23), 120.9 (C-20), 74.2 (sept, $^{3}J_{H\text{-}F}$ = 32 Hz, C-22), 72.2 (C-21), 51.9 (C-8), 50.2 (C-2), 49.5 (C-12), 48.1 (C-5), 39.9 (C-26), 30.6 (C-9), 29.0 (C-11), 24.3 (C-27), 22.9 (C-28 or C-29), 21.3 (C-28 or C-29), 21.2 (C-10), 18.2 (C-25); UPLC-MS Method 3, T_R = 5.32 min; m/z MS (ES+): 683.9 [100 %, M + H$^+$], 363.9 [40 %]; HRMS (ESI+) calcd. for $C_{27}H_{36}F_6N_7O_7^+$ (M+H$^+$): 684.2575, found: 684.2576.

p-**1a**. The synthesis followed the protocol described for **1b** (*General procedure 5*) starting from **S10** (30 mg, 65 μmol, 1.0 eq.) and the trifluoroacetate salt of **S11** (23 mg, 49 μmol, 0.76 eq.). The trilfuoroacetate salt of the product was isolated as a white solid (5 mg, 9 %). ^{1}H-NMR (500 MHz, DMSO-d$_6$, 298 K) δ 12.57 (br, 1H), 8.61 (d, $^{3}J_{H\text{-}H}$ = 7.5 Hz, 1 H, H-6), 8.51 (s, 1 H, H-13), 8.22 (d, $^{3}J_{H\text{-}H}$ = 8.1 Hz, 1 H, H-3), 8.09 (d, $^{3}J_{H\text{-}H}$ =

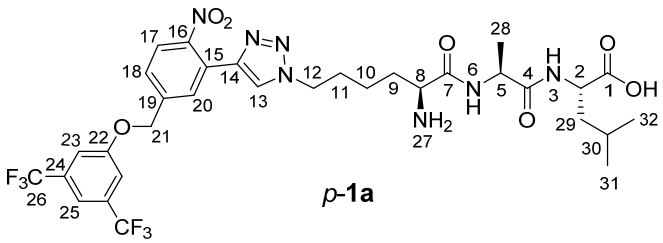

5.4 Hz, 2 H, H-27), 7.99 (d, $^{3}J_{H\text{-}H}$ = 8.3, 1 H, H-17), 7.97 (d, $^{4}J_{H\text{-}H}$ = 1.8 Hz, 1 H, H-20), 7.76 (s, 2 H, H-23), 7.72 (dd, $^{3}J_{H\text{-}H}$ = 8.3 Hz, $^{4}J_{H\text{-}H}$ = 1.8 Hz, 1 H, H-18), 7.70 (s, 1 H, H-25), 5.46 (s, 2 H, H-21), 4.43-4.35 (m, 3 H, H-5 and H-12), 4.23 (ddd, $^{3}J_{H\text{-}H}$ = 9.4 Hz, $^{3}J_{H\text{-}H}$ = 8.1 Hz, $^{3}J_{H\text{-}H}$ = 5.8 Hz, 1 H, H-2), 3.29 (m, 1 H, H-8), 1.88 (quint, $^{3}J_{H\text{-}H}$ = 7.3 Hz, 2 H, H-11), 1.76-1.70 (m, 2 H, H-9), 1.65-1.57 (m, 1 H, H-30), 1.52-1.46 (m, 2 H, H-29), 1.37-1.29 (m, 2 H, H-10), 1.25 (d, $^{3}J_{H\text{-}H}$ = 7.0 Hz, 3 H, H-28), 0.87 (d, $^{3}J_{H\text{-}H}$ = 6.6 Hz, 3 H, H-31 or H-32), 0.82 (d, $^{3}J_{H\text{-}H}$ = 6.5 Hz, 3 H, H-31 or H-32); δ ^{13}C (determined by HMQC and HMBC experiments) 173.6 (C-1), 171.3 (C-4), 167.8 (C-7), 158.7 (C-22), 147.2 (C-16), 141.0 (C-14), 140.5 (C-19), 131.4 (C-24), 128.6 (C-20), 127.8 (C-18), 124.1 (C-17), 123.7 (C-15), 123.2 (C-13), 122.7 (q, $^{3}J_{C\text{-}F}$ = 273 Hz, C-26), 115.8 (C-23), 114.0 (C-25), 68.7 (C-21), 51.5 (C-8), 49.8 (C-2), 49.2 (C-12), 47.7 (C-5), 39.6 (C-29), 30.3 (C-9), 29.0 (C-11), 24.1 (C-30), 22.8 (C-31 or C-32), 20.9 (C-31 or C-32), 20.8 (C-10), 17.8 (C-28); UPLC-MS: Method 3, T_R = 5.93 min; m/z MS (ES+): 746.5 [100 %, M + H$^+$], 394.4 [40 %], 373.9 [40 %]; HRMS (ESI+) calcd. for $C_{32}H_{38}F_6N_7O_7^+$ (M+H$^+$): 746.2731, found: 746.2738.

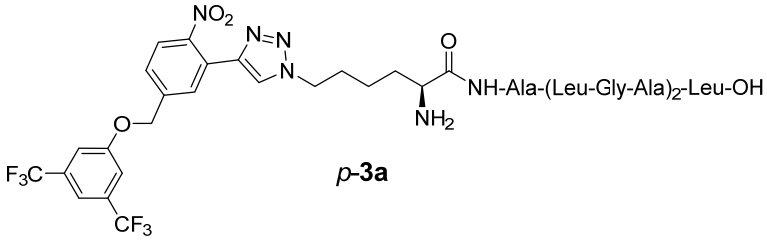

p-**3a**. The synthesis followed the protocol described for the synthesis of **1b** (*General procedure 5*) starting from **S10** (20 mg, 50 μmol, 1.0 eq.) and the trifluoroacetate salt of **S13** (42 mg, 44 μmol, 0.88 eq.). The trifluoroacetate salt of the modified peptide was isolated as a white solid (4 mg, 7%). ^{1}H-NMR (500 MHz, DMSO-d$_6$, 298 K) δ 12.49 (br, 1 H), 8.61 (d, $^{3}J_{H\text{-}H}$ = 7.2 Hz, 1 H, amid), 8.51 (s, 1 H, H-1), 8.13-8.03 (m, 6 H, 4 amide NH and amine NH$_2$), 8.02- 7.91 (m, 4 H, H-5, H-8 and 2 amid), 7.84 (d, $^{3}J_{H\text{-}H}$ = 7.5 Hz, 1 H, amide NH), 7.76 (s, 2 H, H-11), 7.72 (dd, $^{3}J_{H\text{-}H}$ = 8.5 Hz, $^{4}J_{H\text{-}H}$ = 2.0 Hz, 1 H, H-6), 7.70 (s, 1 H, H-13), 5.47 (s, 2 H, H-9), 4.44-4.36 (m, 3 H, 2 H-C$_{\varepsilon(Lys)}$ and H-C$_\alpha$), 4.35-4.14 (m, 5 H, H-C$_\alpha$), 3.77-3.62 (m, 5 H, H-C$_\alpha$), 1.87 (quint, $^{3}J_{H\text{-}H}$ = 7.1 Hz, 2 H, H-C$_{\delta\ (lys)}$), 1.76-1.70 (m, 2 H, H-C$_{\beta(lys)}$), 1.66-1.57 (m, 3 H, H-C$_{\gamma(leu)}$), 1.54-1.42 (m, 6 H, H-C$_{\beta(leu)}$), 1.40-1.32 (m, 2 H, H-C$_{\gamma(lys)}$), 1.24 (d, $^{3}J_{H\text{-}H}$ = 7.1 Hz, 3 H, H-C$_{\beta(ala)}$), 1.21 (d, $^{3}J_{H\text{-}H}$ = 7.2 Hz, 6 H, H-C$_{\beta(ala)}$), 0.89-0.85 (m, 9 H, H-C$_{\delta(leu)}$), 0.83-0.81 (m, 9 H, H-C$_{\delta(leu)}$); UPLC-MS Method 1, T_R = 4.57 min; m/z MS (ES+): 1250.1 [10 %, M + Na$^+$], 1228.2 [80 %, M + H$^+$], 614.9 [100 %, M + 2 H$^+$]. HRMS (ESI+) calcd. for $C_{54}H_{76}F_6N_{13}O_{13}^+$ (M+H$^+$): 1228.5584, found: 1228.5574.

Sample preparation for MS experiments

For the electrospray and depletion experiments 1 mg of peptide was added in dry form to 2 ml of a mixture of deionized water, methanol and ammonia (25 %) in a ratio of 1:1:0.001, resulting in a pH value of approximately 8.3. The electrospray was operated at a flow rate of 5 μl/min.

Kinetic rate equations

Figure S1: *idealized absorption scheme in the peptide photo-depletion experiments. The letter M designates a molecular electronic ground state, M* an excited state, while D_1 and D_2 refer to depletion states. The absorption cross section σ is weighted by the probability γ to require more than a single-photon process for successful beam depletion. We assume the dominant beam depletion process to be cleavage rather than electron detachment.*

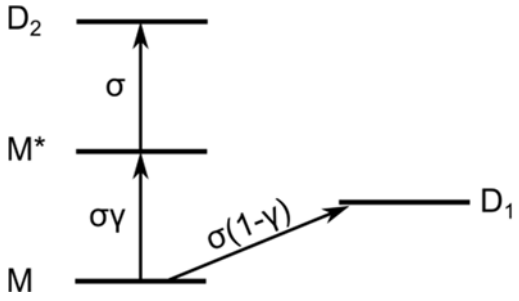

Our derivation of the UV photo depletion and fragment yield, equation (1) in the main text, follows [3]. We assume a sequential 2-photon absorption, as illustrated in Figure S1, which can be generalized to the case of N photons: The populations of all levels change in dependence of the laser fluence F.

$$\frac{dM}{dF} = -\sigma M \qquad Eq.(S2)$$

$$\frac{dM^*}{dF} = \sigma\gamma M - \sigma M^*$$

$$\frac{dD_1}{dF} = \sigma(1-\gamma)M$$

$$\frac{dD_2}{dF} = \sigma M^*$$

With the initial condition $M(F=0)=1$, we obtain

$$M = e^{-\sigma F} \qquad Eq.(S3)$$

$$M^* = \gamma\sigma F e^{-\sigma F}$$

$$D_1 = (1-\gamma)(1-e^{-\sigma F})$$

$$D_2 = \gamma(1-(1+\sigma F)e^{-\sigma F})$$

The depletion of the intact molecular mass peak M is given by the *ultraviolet photo-depletion probability*

$$UVPD = 1 - D_1 - D_2 = 1 - \alpha + \alpha(1+\gamma\sigma F)e^{-\sigma F} \quad (Eq.S3),$$

where we have introduced the *beam overlap* α. It measures the fraction of the molecular beam overlapping with the depleting laser beam. The fragment yield is the sum of all fragment channels and given by

$$FY = D_1 + D_2 = \eta_{det}\alpha(1-(1+\gamma\sigma F)e^{-\sigma F}) \qquad (Eq.S4)$$

where η_{det} includes losses due to the limited detection efficiency for fragment ions as well as electron photodetachment as a depletion channel that does not generate new mass peaks.

UV photodepletion of nonapeptide 3a and dodecapeptide 4a

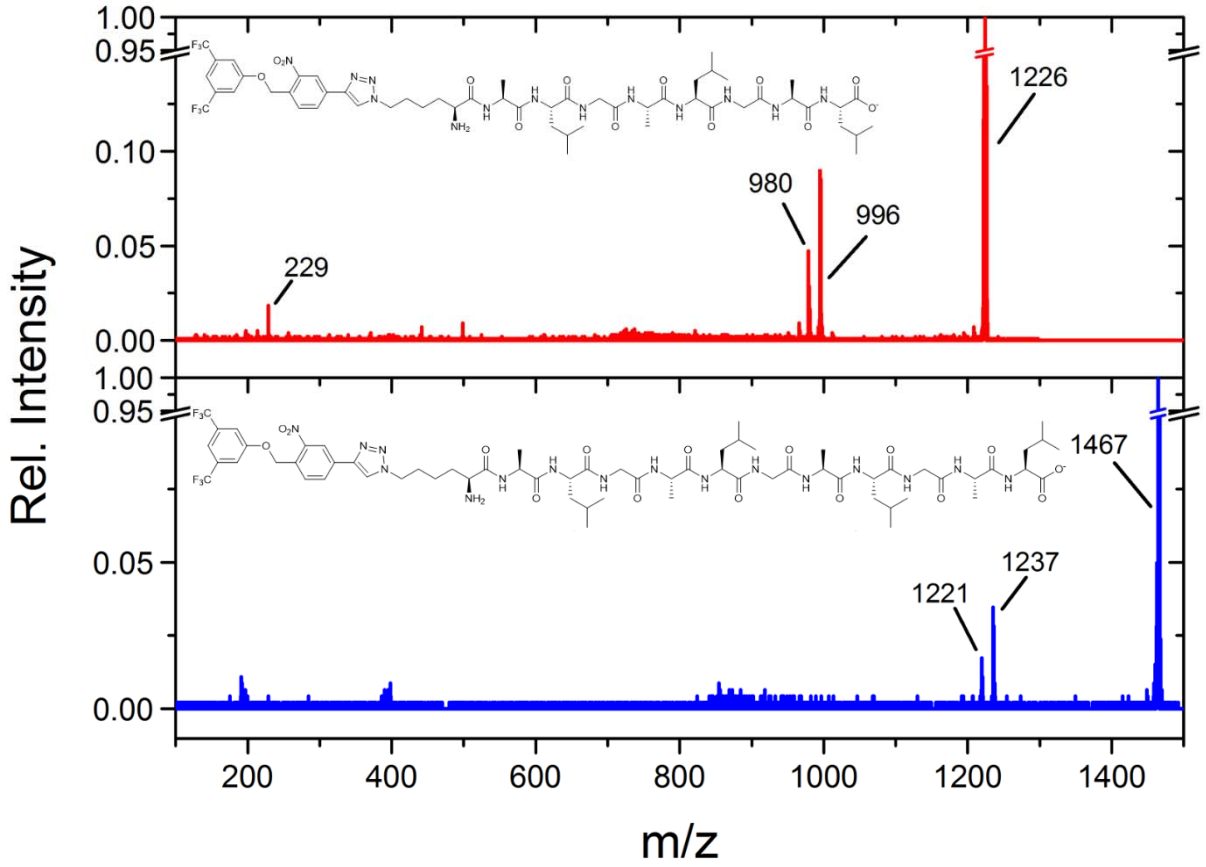

Figure S2: *UVPD mass spectra for the tagged nonapeptide **3a** (LG-PCG-Lys-Ala-Leu-Gly-Ala-Leu-Gly-Ala-Leu, upper panel) and the tagged dodecapeptide **4a** (LG-PCG-Lys-Ala-Leu-Gly-Ala-Leu-Gly-Ala-Leu-Gly-Ala-Leu, lower panel). Again, bond-selective heterolytic photocleavage can be observed, but the probability for this process shrinks with peptide length, while homolytic cleavage emerges.*

At an average laser power of 200 mW in a circular beam of 2 mm diameter, delivered in 10 ns pulses at a repetition rate of 250 Hz, we see again bond-selective photocleavage. The delay between the laser pulse and the mass spectrometer extraction voltage (ion pusher) was set to maximize the detection of the high mass fragment to assess the total depletion rate. In both cases, the dominant fragments appear at m/z=(M-230) u/e and (M-246) u/e, with M the mass of the parent peak. The fragment at (M-230) u/e can be assigned to homolytic cleavage and proton transfer to the LG. The UVPD mass spectrum of peptide **3a** still shows a small signal for the leaving group **a**, which is absent in the spectrum of the longer peptide **4a**.

Temperature dependence of the UVPD curves of hexapeptide 2a

We have studied the UVPD curves for the hexapeptide **2a** at 300 K and 60 K (Figure S3) to explore the influence of the molecular heat capacity. The depletion curves exhibit a clear multiphoton behaviour at both temperatures and the best fit is obtained for a sequential absorption of 2 photons (with $\gamma = 1$). In this model we use the same absorption cross section as for the tripeptide **1a**.

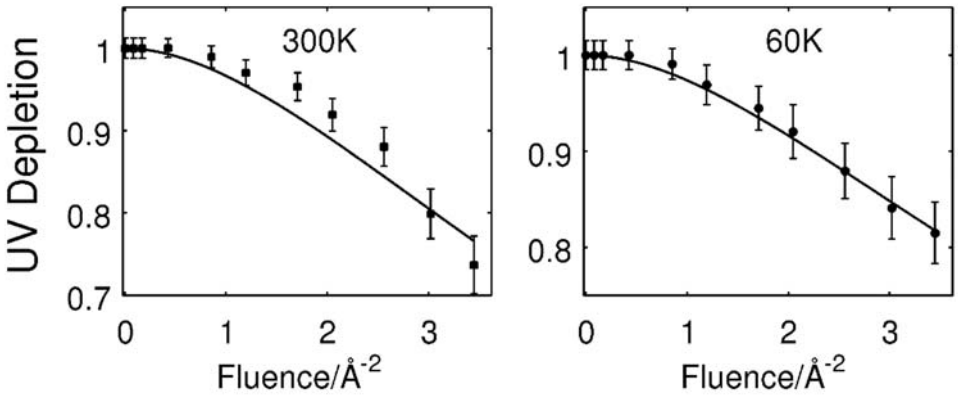

Figure S3: *Temperature dependence of the UV photodepletion curves for the hexapeptide* ***2a*** *at 300 K* ***(left)*** *and 60 K* ***(right)****. Points and error bars represent experimental values. Lines are fits assuming a multiphoton process and the same absorption cross section as for the tripeptide* ***1a****. The best fit parameters are found for a pure 2 sequential photons absorption (γ = 1).*

UVPD mass spectra of tripeptides 1b, 1c, 1d

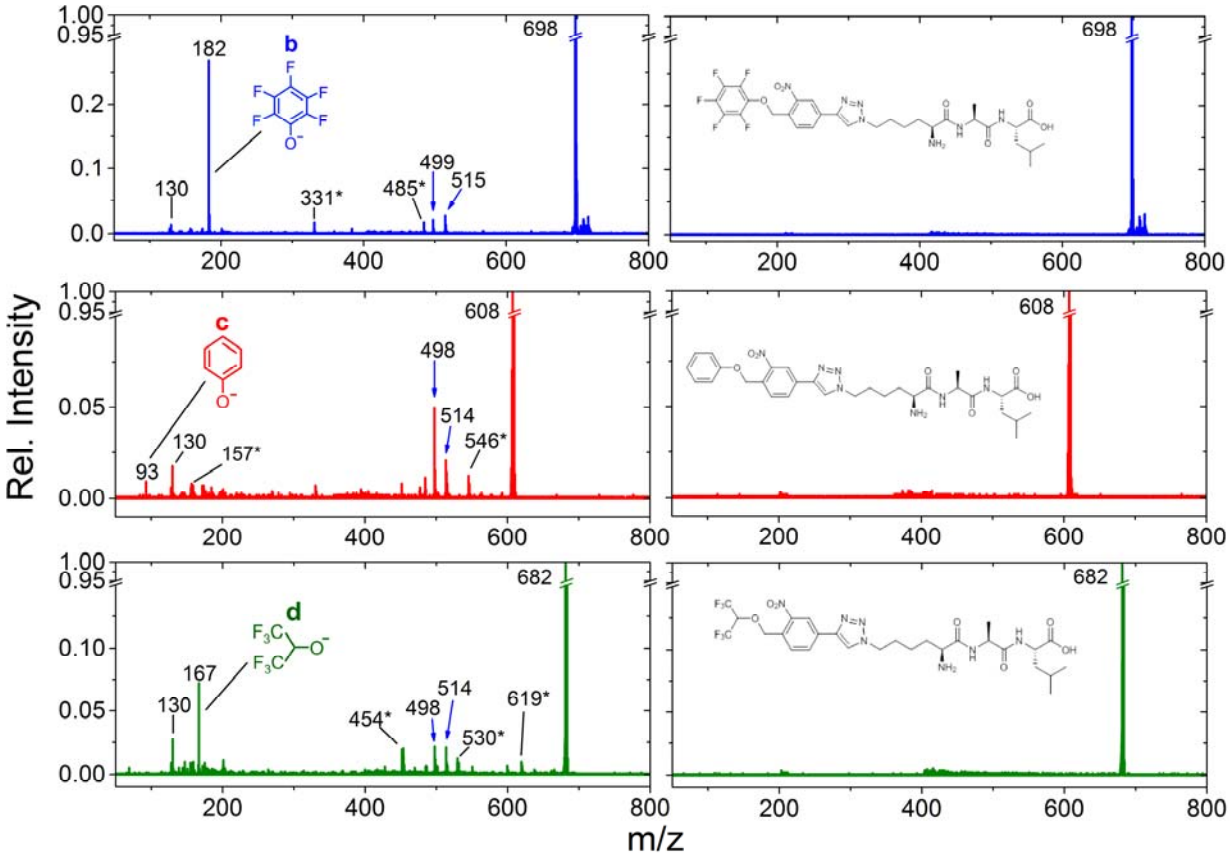

Figure S4: *Comparison of the UVPD mass spectra of tripeptide* ***1b, 1c, 1d*** *with* ***(left)*** *and without* ***(right)*** *laser radiation. This shows that signal-to-noise and mass-selectivity is good enough for the smallest peaks to be unambiguously assigned to the photo-cleavage process, even with peak amplitudes below 1% of the parent peak.*

To unambiguously establish that all observed fragments are caused by the incident laser radiation, we have recorded the UVPD mass spectra of three differently tagged tripeptides **1b, 1c, 1d** (see Figure **3b**) and compared them with their mass spectra in the absence of any laser light (see Figure S4, right column).

For tripeptide **1b**, the leaving group is expected at m/z = 182 u/e, for tripeptide **1c** at 93 u/e and for tripeptide **1d** at 167 u/e. The blue arrows indicate the proton transfer fragments (as depicted in Scheme 1 of the main text), which can be observed in all three cleavage processes. The fragment with m/z = 130 u/e is present in all spectra and arises from dissociation of the peptide backbone, that is common to all tested molecules. Note, that the dominant fragment of tripeptide **1d** is the proton transfer fragment, rather than the leaving group **d**. The fragments marked with an asterix * are assigned to backbone fragments.

Collison-induced dissociation mass spectra of peptides 1a-4a

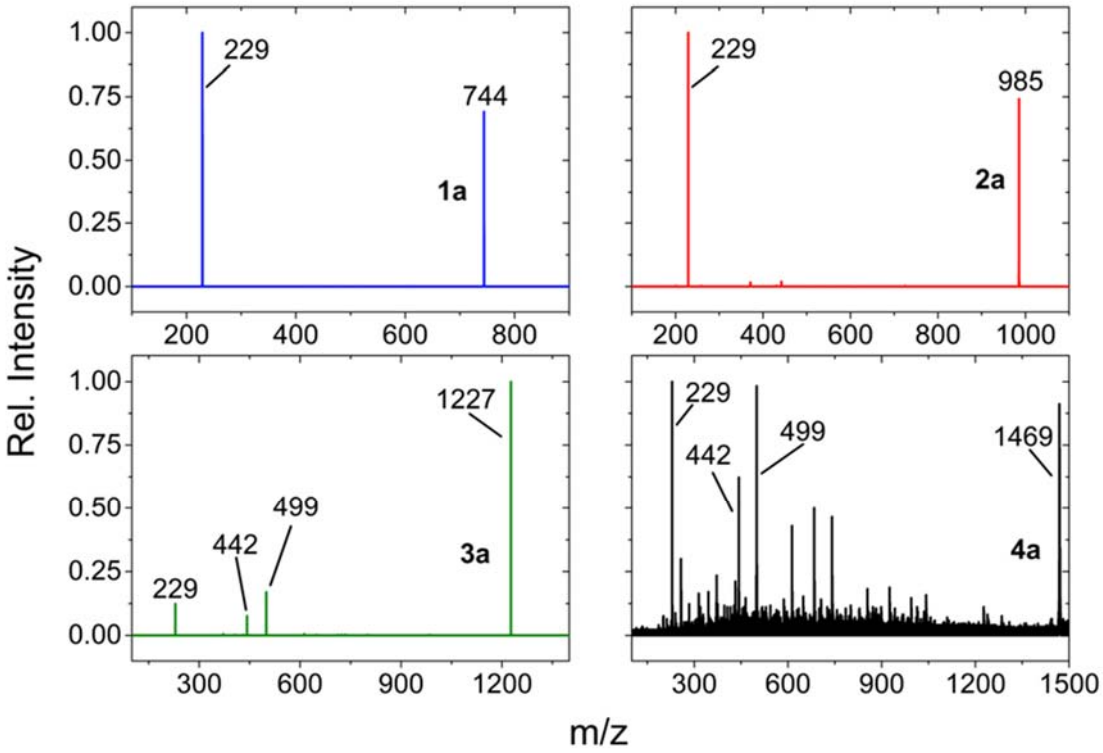

Figure S5: *Collision-induced dissociation mass spectra of peptides **1a** - **4a**. **Top left**: tagged tripeptide **1a**, **top right**: tagged hexapeptide **2a**, **bottom left**: tagged nonapeptide **3a**, **bottom right:** tagged dodecapeptide **4a**. The designed leaving group is always observed. At a given collision energy, the fragment yield decreases with increasing peptide length (33-73 eV, see Figure S6).*

The thermal nature of the selective bond cleavage can be explored by studying the collision-induced dissociation (CID) mass spectra of the peptides **1a**, **2a**, **3a** and **4a.** They were recorded at room temperature (300 K), with neutral argon atoms as the collision gas. The gas pressure is estimated to be 10^{-4} mbar. The spectra were recorded at kinetic energies between 33 and 73 eV (see Figure 2 of the main text), to achieve that each peptide parent peak is depleted by 90%. We find identical fragments, namely only the leaving group **a** in the CID and UVPD spectra of peptides **1a** and **2a.** Additional fragments arise in the CID spectra of the peptides **3a** and **4a**. They are attributed to backbone fragments whose probability increases with peptide length. Peptide **4a** has a smaller fragment yield. The scaled signal thus shows increased background noise. Figure S6 shows that the depletion of the parent peptide by CID requires a kinetic energy which increases linearly with peptide length.

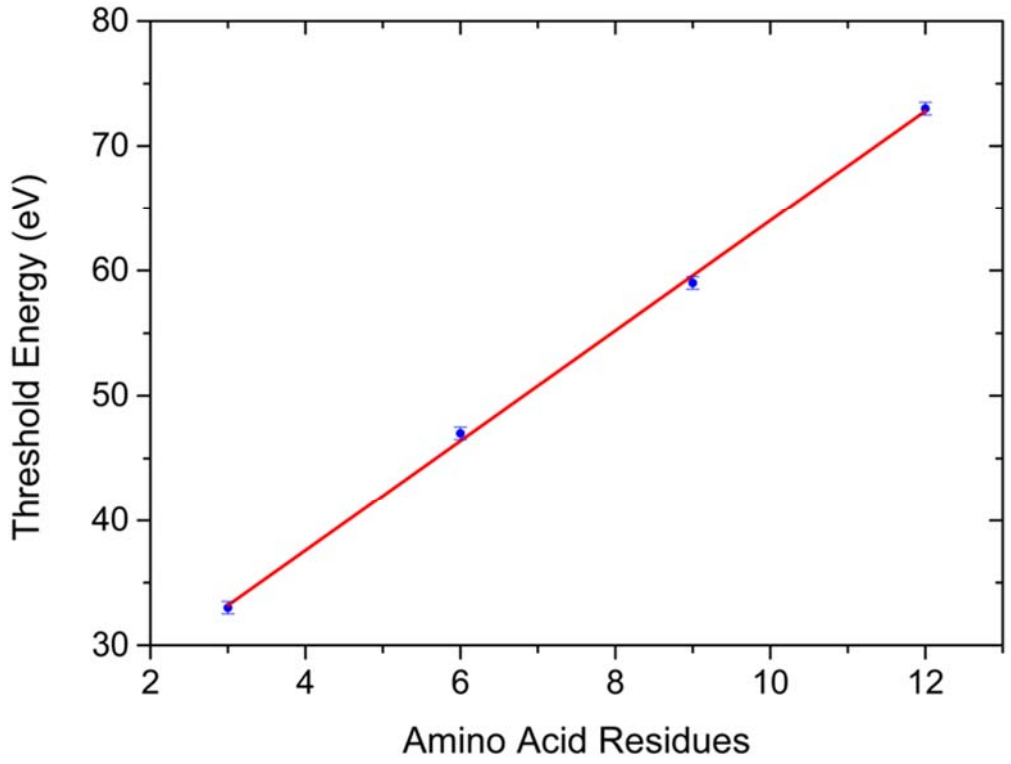

Figure S6: *CID threshold energy as function of the number of amino acid residues per tagged peptide (from tripeptide **1a** to dodecapeptide **4a**). The number shown on the y-axis is the threshold kinetic energy of the peptide ions in collision with the thermal (300 K) argon gas to achieve 90% depletion of the molecular parent peak. The heat capacity increases linearly with peptide length, and so does the CID threshold energy. A linear fit to the data finds a slope of 4.4 ± 0.1 eV/residue and a linear regression coefficient of R^2=0.998. The error bars represent the uncertainty in the energy setting.*

Computational Information

AIMD: Short ab initio molecular dynamics (AIMD) simulations are performed to additionally scan the conformational space of the peptides for structural candidates that are used in the following computations. Using the AIMD module of NWChem v6.6 [4] the nuclear motion of the peptides is integrated with the velocity-Verlet algorithm, while the electronic potential is provided by DFT at the PBE0/3-21G [5, 6] level of theory. Due to the high computational costs of AIMD simulations, we have only calculated several tens of picoseconds using a small basis set for a scan of the potential energy surface (PES). Starting peptide conformations are manually generated and dynamics are run at 300 K in 1 fs time steps using a stochastic velocity rescaling thermostat [7] to control the temperature with a relaxation time of 0.1 ps. The small basis set size can be justified since binding- and torsion angles, which are the relevant

geometric parameters for our scan, are generally less sensitive to basis set sizes than bond lengths, and because the peptides are further locally optimized at a higher level of theory.

DFT: Structural candidates extracted from the AIMD trajectories are further geometry optimized using the Gaussian09 program package [8] at the PBE0/Def2TZVP level of theory [5, 9]. Harmonic frequencies are calculated for the lowest energy conformations to ensure true minima on the PES. Conformations that converge to transition states are distorted along their imaginary modes and re-optimized. In case they do not converge to minima, they are excluded from further investigations. The computed harmonic frequencies are further used to estimate mean thermal energies derived by the frequency model [10] using known beam temperatures of 60 K and 300 K in the buffer gas from the knowledge of all 3*N*-6 harmonic modes:

$$\langle E \rangle_T = \sum_{i=1}^{3N-6} \frac{\hbar\omega_i}{\exp\left(\frac{\hbar\omega_i}{k_B T}\right) - 1}$$

BDE: The tripeptide anions, here named as complex AB^-, are locally relaxed (AB^-_{eq}) and then split heterolytically to evaluate the energies of the fragments A (a neutral zwitterion) and B^- (the negatively charged leaving group) from single-point calculations using the geometries of the fragments within the complex: BDE = E(A) + E(B^-) – E(AB^-_{eq}). Heterolytic bond dissociation energies are generally higher than typical homolytic values due to the additional coulomb attraction between fragments of opposite charge [11]. Adiabatic bond dissociation energies: Here, the fragments A and B^- were further relaxed to the next local minimum found in geometry optimization using tight convergence criteria in Gaussian09: BDE = (A_{eq}) + E(B^-_{eq})– E(AB^-_{eq}). The difference between BDE and adiabatic BDE may be considered as a maximum reorganization energy while the adiabatic values are representative for the strength of the interaction of the monomers A and B^- forming the complex AB^-.

VDE: Vertical electron detachment energies are calculated from the energies of the optimized tripeptide anions AB^-_{eq} and single-point energies after detachment of one electron within the geometries of the anions: VDE = E(AB) – E(AB^-_{eq}). Adiabatic detachment energies (ADE) for the tripeptide anions can be calculated by further relaxing the neutralized complexes: ADE = E(AB_{eq}) – E(AB^-_{eq}). However, any attempt to calculate the ADE leads to decarboxylation of the neutralized tripeptides and therefore E(AB_{eq}) could not be evaluated. In order to study the electron detachment process in more detail, Mulliken orbital population analysis was performed to estimate partial charges. Here, the smaller Def2SVP basis set was used to counter a common problem of predicting unphysical charges when using diffuse basis functions. Single-point calculations using the Def2SVP basis set for geometries optimized with the larger basis set Def2TZVP were performed for the deprotonated tripeptides AB^- and their respective neutral products AB within the geometry of the anion AB^-. Then partial charges were evaluated and the change in partial

charge between these two geometries was studied showing that the biggest change in partial charge by vertical electron detachment is found for the COO^- group in the complex AB^-.

Additionally, basis set superposition errors (BSSE) were estimated by computing counterpoise corrections [12], which tend to slightly reduce the calculated BDE (-0.1 eV). The influence of dispersion effects has also been tested using Grimmes D3 correction [13] leading to an increase in BDE (+0.1 eV) thereby counteracting the effect of BSSE corrections. Additional calculations using the CAM-B3LYP functional [14] provided slightly higher VDE (+0.2 eV) and significantly higher BDE (+1.0 eV). Binding energies for the homolytic dissociation case i.e. the proton transfer pathway were not calculated although they would be very interesting values to know for comparison purposes. However, due to the yet unknown mechanism of the proton transfer route BDE could not be evaluated.

Table S1: *Comparison of pK_a values [15] and experimental fragment yields for the differently tagged tripeptides* ***1a-1d****, with calculated VDE and BDE values and thermal energies at 300 K. All energies are given in eV. For all species the thermal energy at 60 K is below 0.1 eV and therefore negligible compared to the photon energy at 266 nm. All energies are obtained by DFT at the PBE0/Def2TZVP level of theory. BDE values calculated after geometry relaxation of the fragments are shown in parentheses.*

PCT	pK_a	Yield	VDE	BDE	$\langle E \rangle_{300K}$
1a	8.0	0.12	4.6	6.9 (3.7)	1.4
1b	5.5	0.10	4.6	6.7 (3.5)	1.2
1c	9.8	0.01	4.6	7.8 (4.5)	1.2
1d	9.9	0.02	4.6	7.5 (4.4)	1.4

TDDFT: For every tripeptide, TDDFT calculations have been performed at the PBE0/Def2TZVP level of theory using the Gaussian09 package. For every tripeptide 100 excited states have been considered. The calculated line spectra are presented as Gaussian convolutions with Gaussian functions with a FWHM=0.33 eV. Natural transition orbitals [16] of the main optical transitions are analyzed. UV transitions including the weak transitions around 350 nm show mainly contributions of the PCT and the transitions mainly consist of one or two pairs of NTOs with significant contributions. Figure S7 shows the NTOs with largest contribution for the transitions closest to 266 nm for tripeptides **1a**-**1d**.

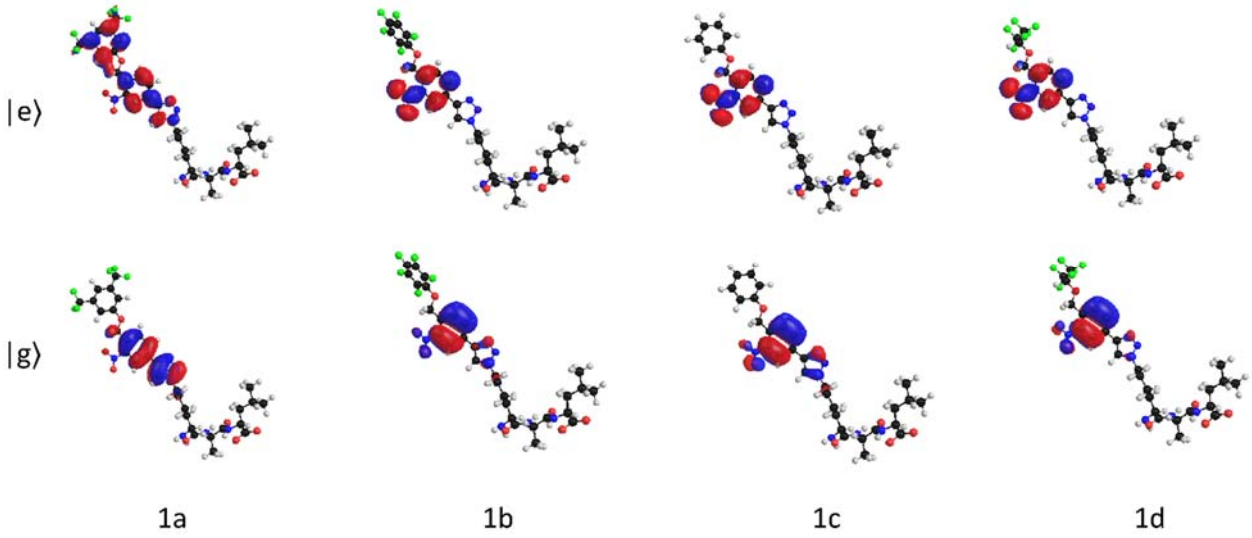

Figure S7: *NTO obtained by TDDFT at the PBE0/Def2TZVP level of theory for the tripeptides* ***1a***-***1d****. Only NTOs with the largest contributions to the calculated transitions closest to the experimental wavelength of 266 nm are shown. While only the NTO of* ***1a*** *shows a charge transfer towards the LG, all NTOs show that close to 266 nm only the PCT is the dominant absorber.*

Solution phase cleavage of 1a and *p*-1a

1a (3 mg, 4 μmol) or *p*-**1a**, respectively were dissolved in DMSO-d_6 (0.5 mL), placed in a standard 3.5 mL quartz cuvette and irradiated overnight in a TLC viewing chamber at 254 nm by positioning the cuvette directly in front of the lamp unit. NMR spectra of the samples were recorded before and after irradiation (Figure S8).

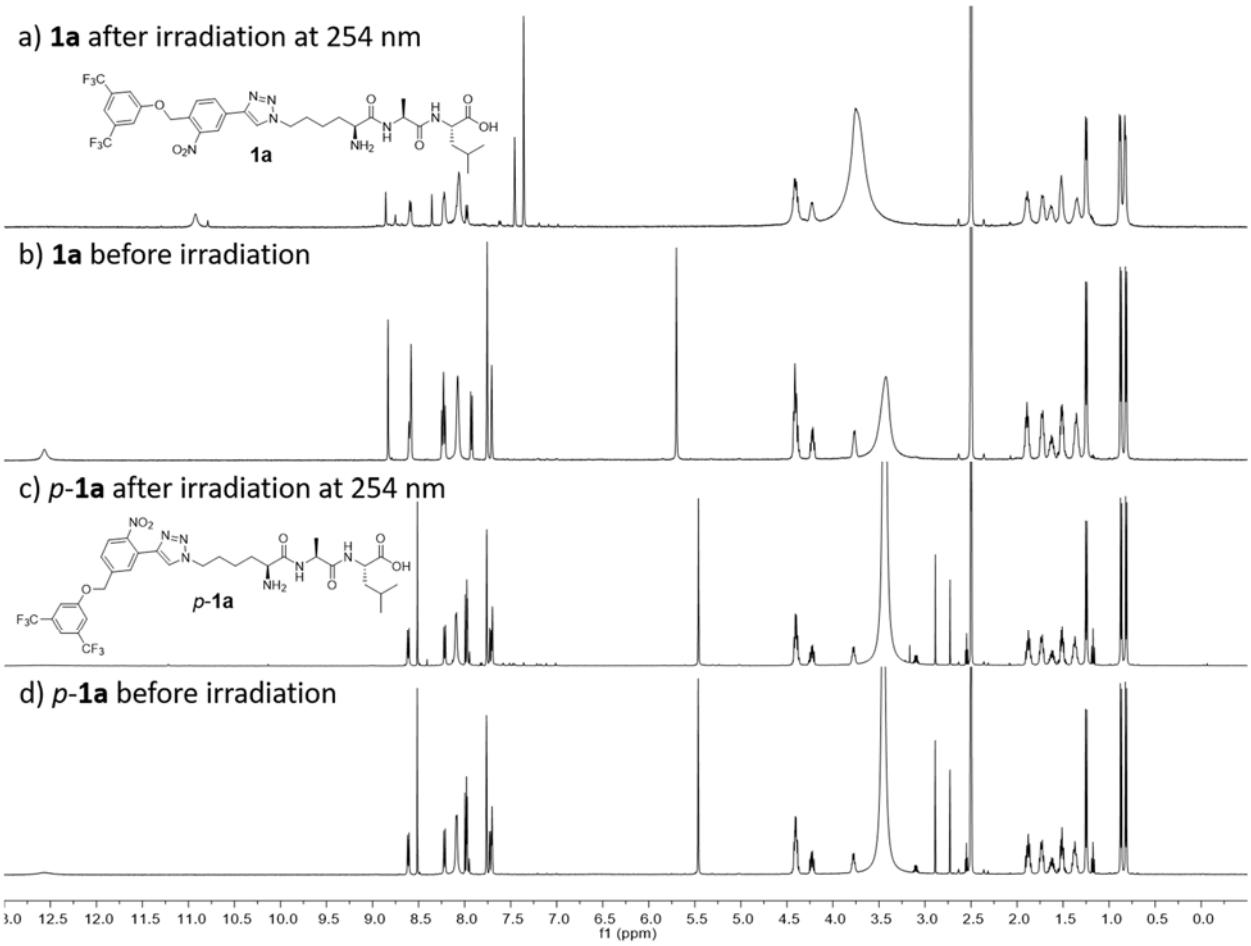

Figure S8. ^{1}H NMR spectra (500 MHz, DMSO-d_6, 298K) of solution phase irradiation experiments and references. a) **1a** after irradiation overnight; b) sample of **1a** before irradiation; c) *p*-**1a** after irradiation overnight d) sample of *p*-**1a** before irradiation. Only **1a,** which has the nitro-group in *ortho*-position to the aryl ether function, cleaves upon irradiation, whereas *p*-**1a** with the nitro-group in *para*-position to the aryl ether function does not cleave.

NMR-spectra and LC-traces of compounds synthesized

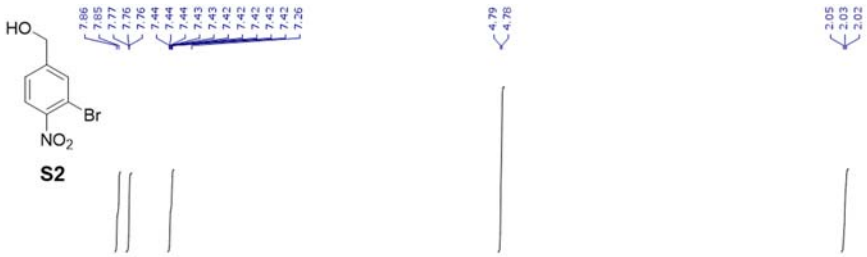

^{1}H-NMR ($CDCl_3$, 500 MHz, 298 K)

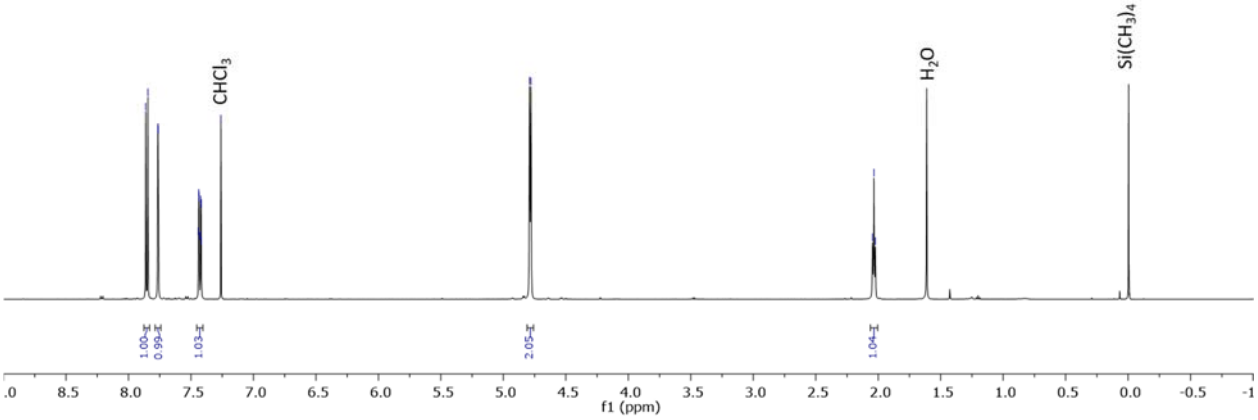

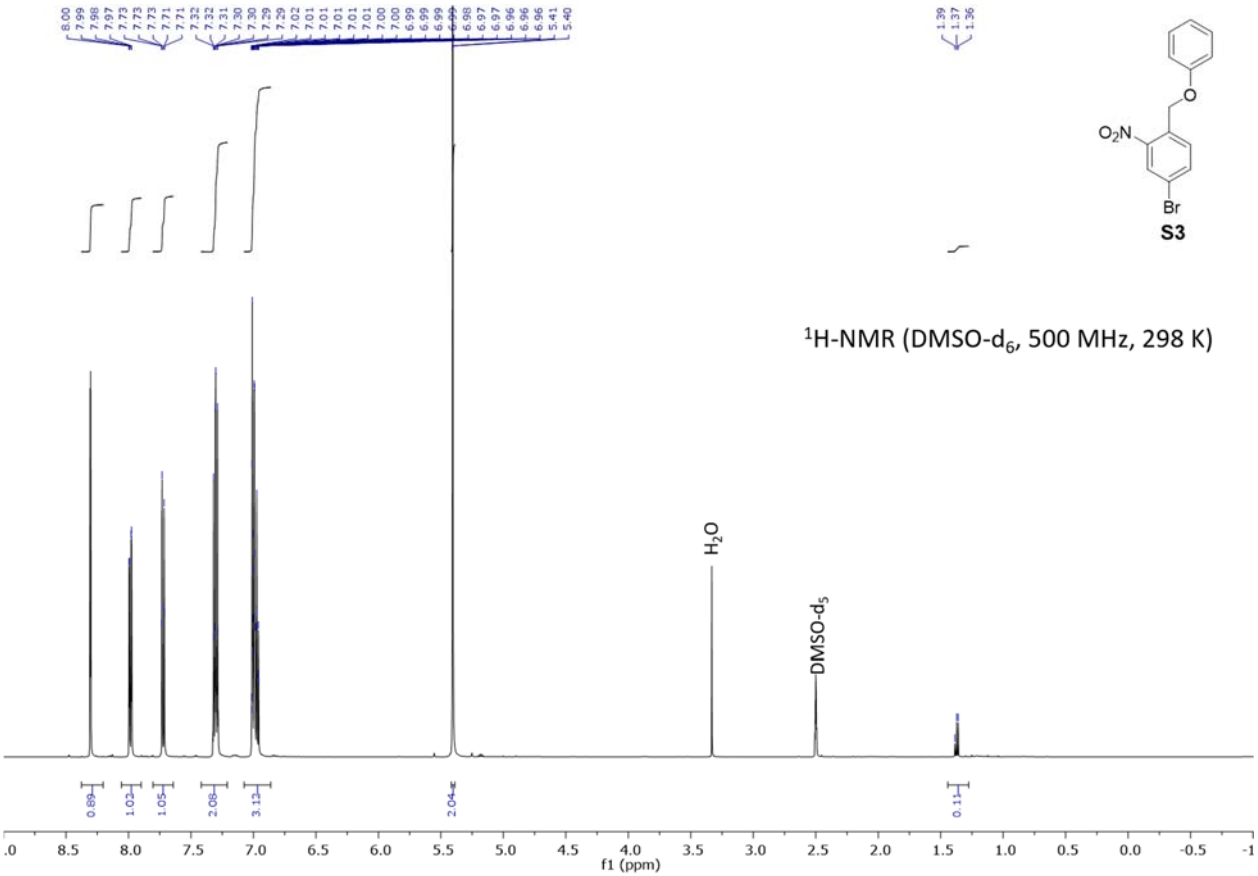

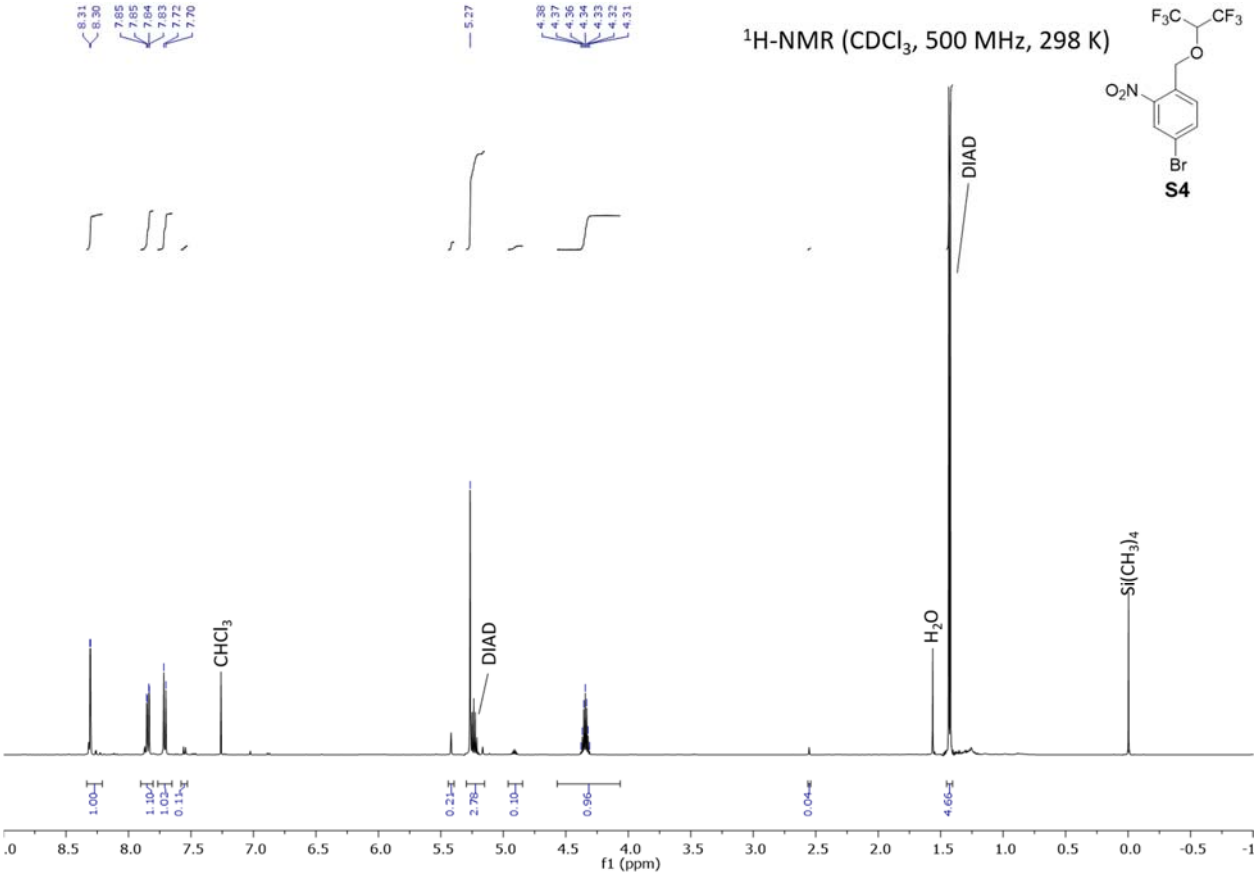

DIAD = diisopropyl azodicarboxylate

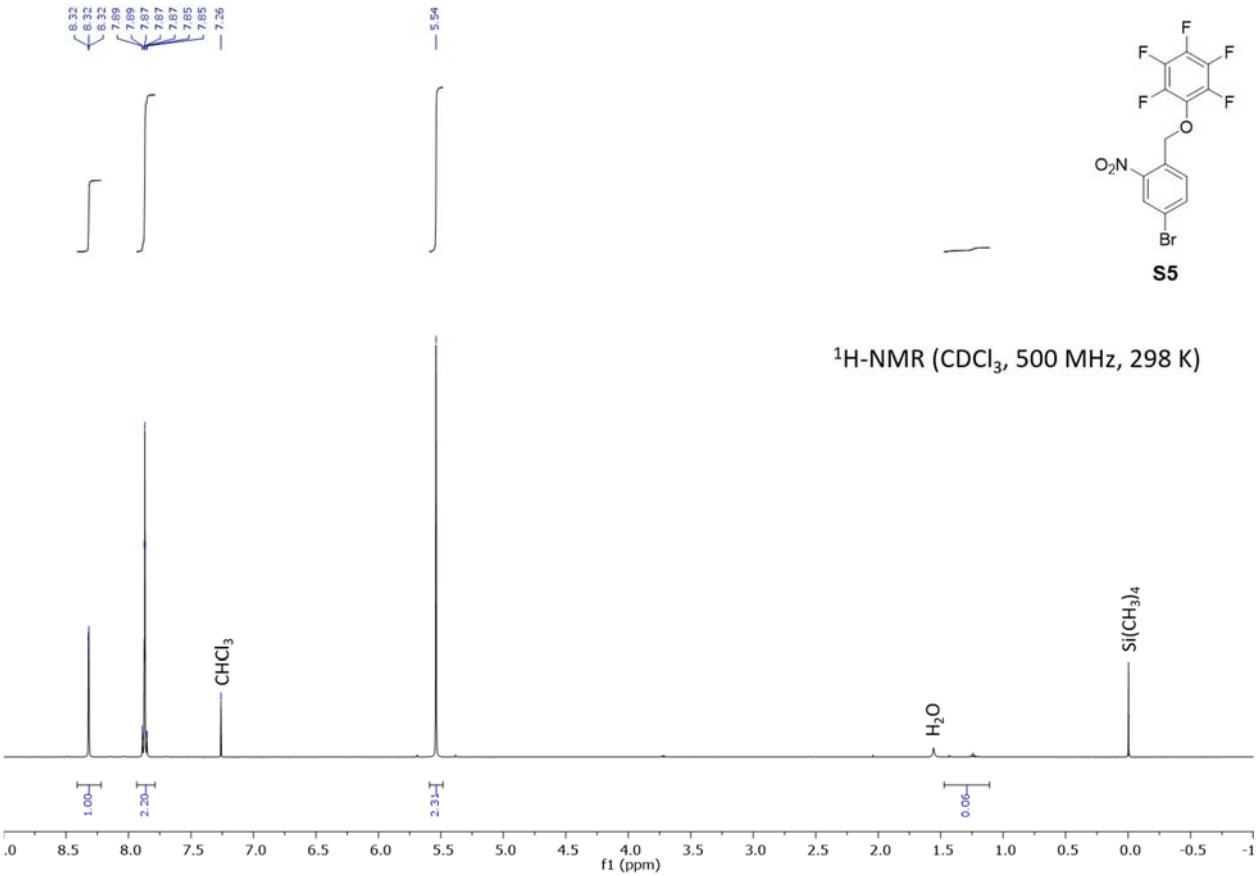
S5
^{1}H-NMR ($CDCl_3$, 500 MHz, 298 K)
$CHCl_3$
H_2O
$Si(CH_3)_4$
f1 (ppm)

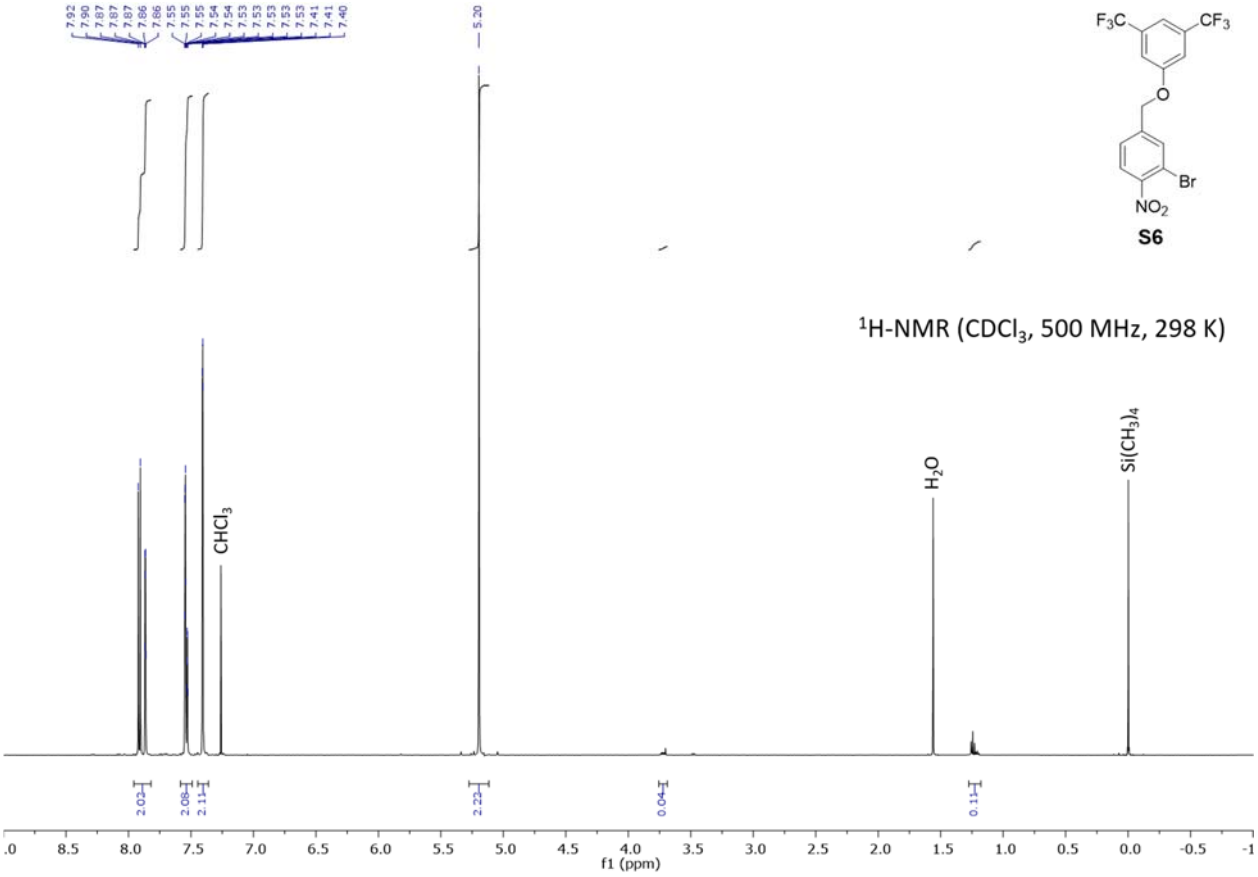
S6
^{1}H-NMR ($CDCl_3$, 500 MHz, 298 K)
$CHCl_3$
H_2O
$Si(CH_3)_4$
f1 (ppm)

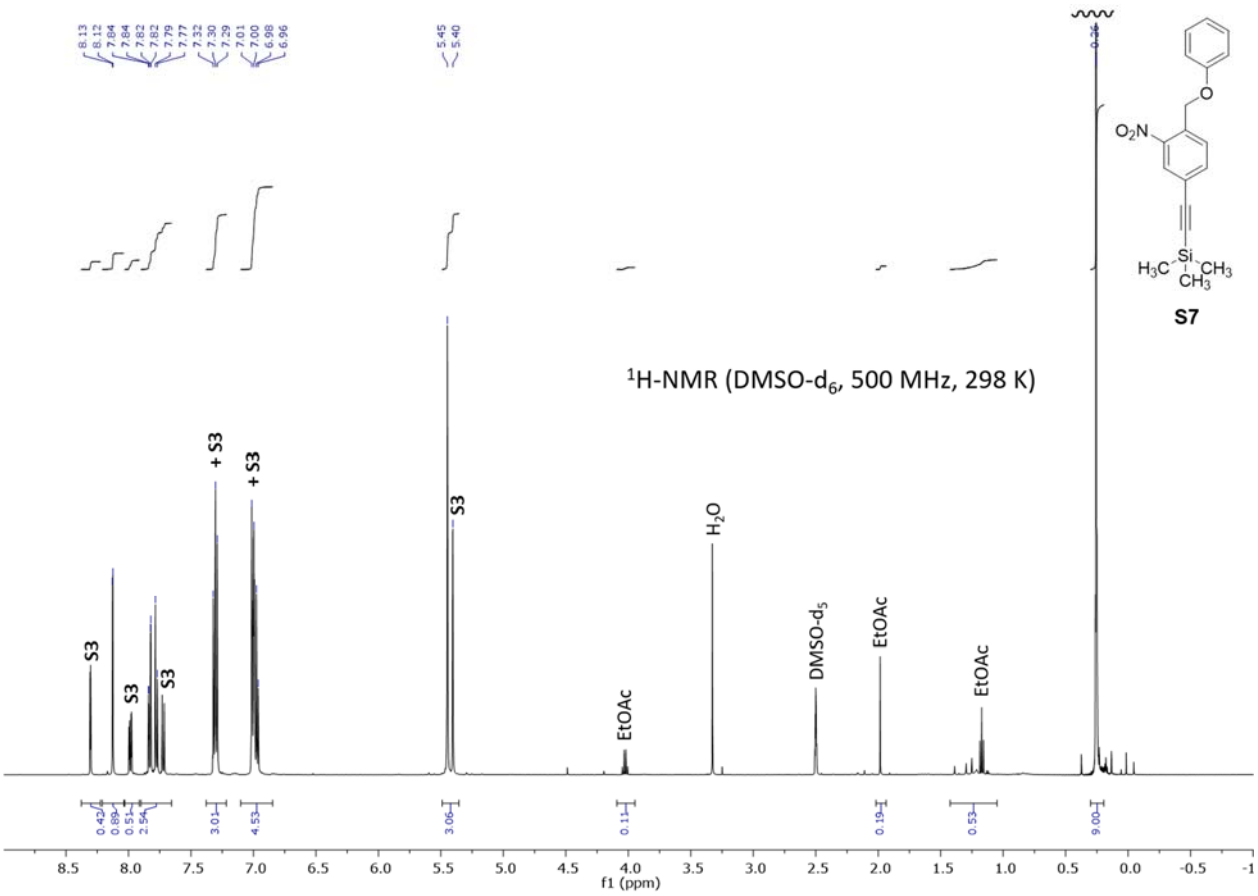
S7
^{1}H-NMR (DMSO-d$_6$, 500 MHz, 298 K)
S3
+ S3
+ S3
S3
S3
S3
EtOAc
H$_2$O
DMSO-d$_5$
EtOAc
EtOAc
f1 (ppm)

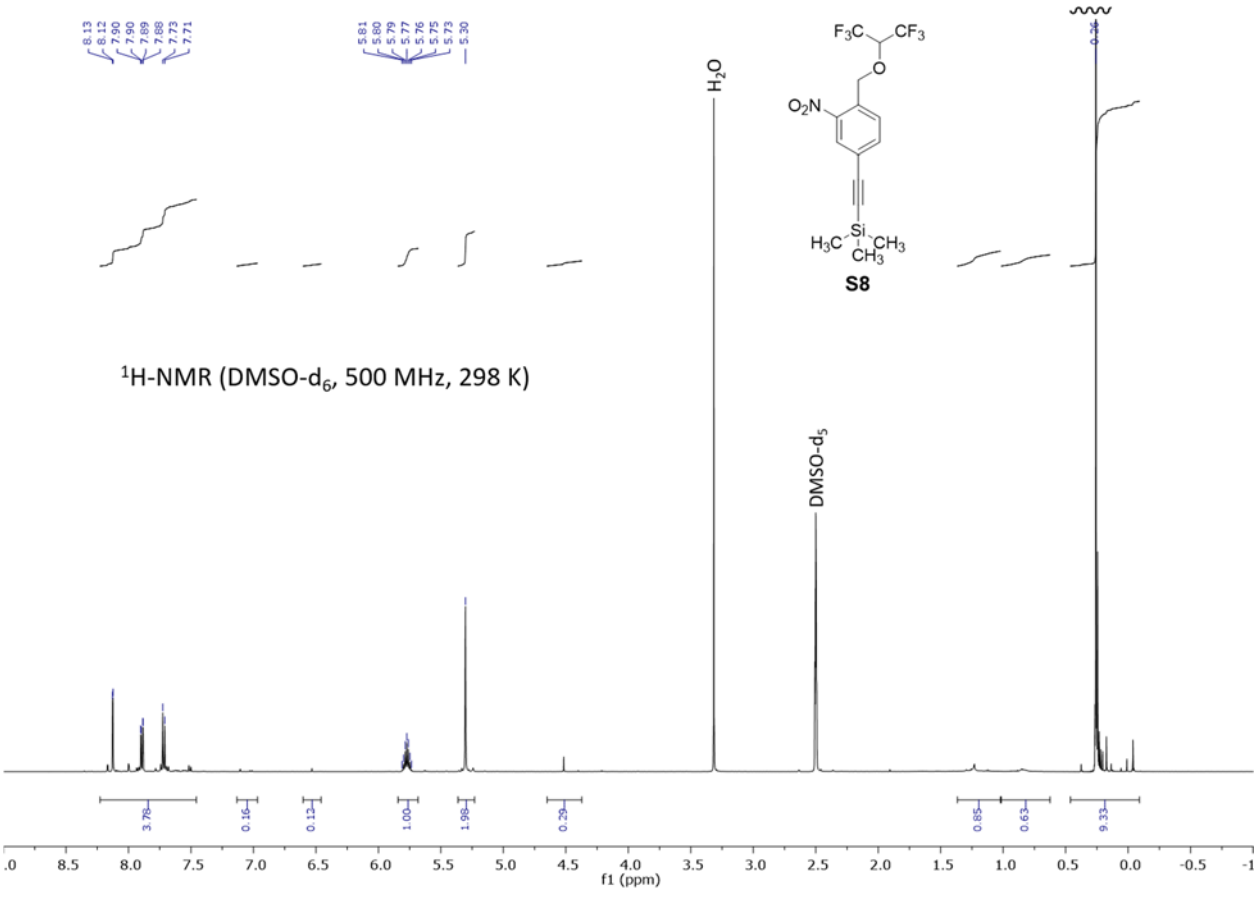
S8
^{1}H-NMR (DMSO-d$_6$, 500 MHz, 298 K)
H$_2$O
DMSO-d$_5$
f1 (ppm)

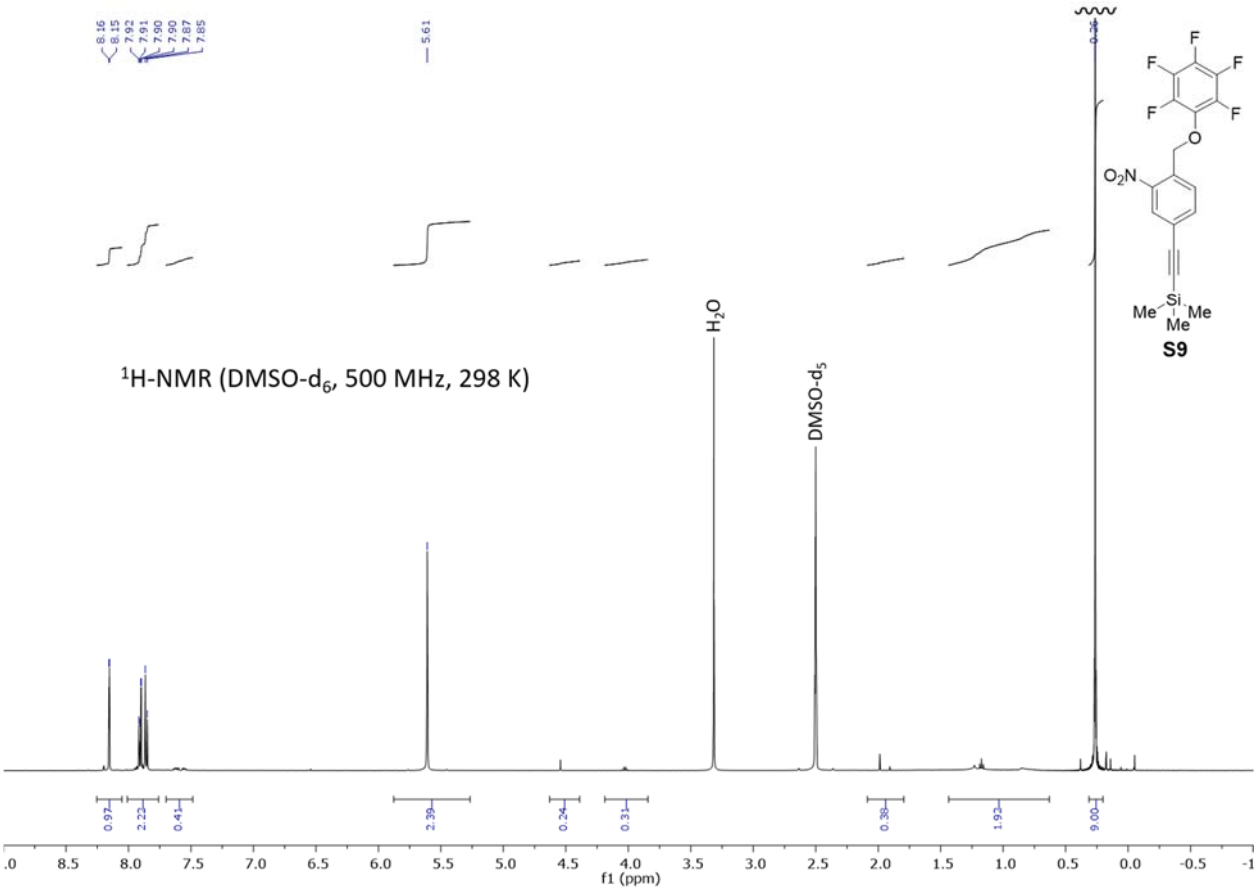
8.16
8.15
7.92
7.91
7.90
7.90
7.87
7.85
5.61
0.26
H2O
DMSO-d5
1H-NMR (DMSO-d6, 500 MHz, 298 K)
F
F
F
F
F
O
O2N
Si
Me
Me
Me
S9
0.97
2.23
0.41
2.39
0.24
0.31
0.38
1.93
9.00
f1 (ppm)

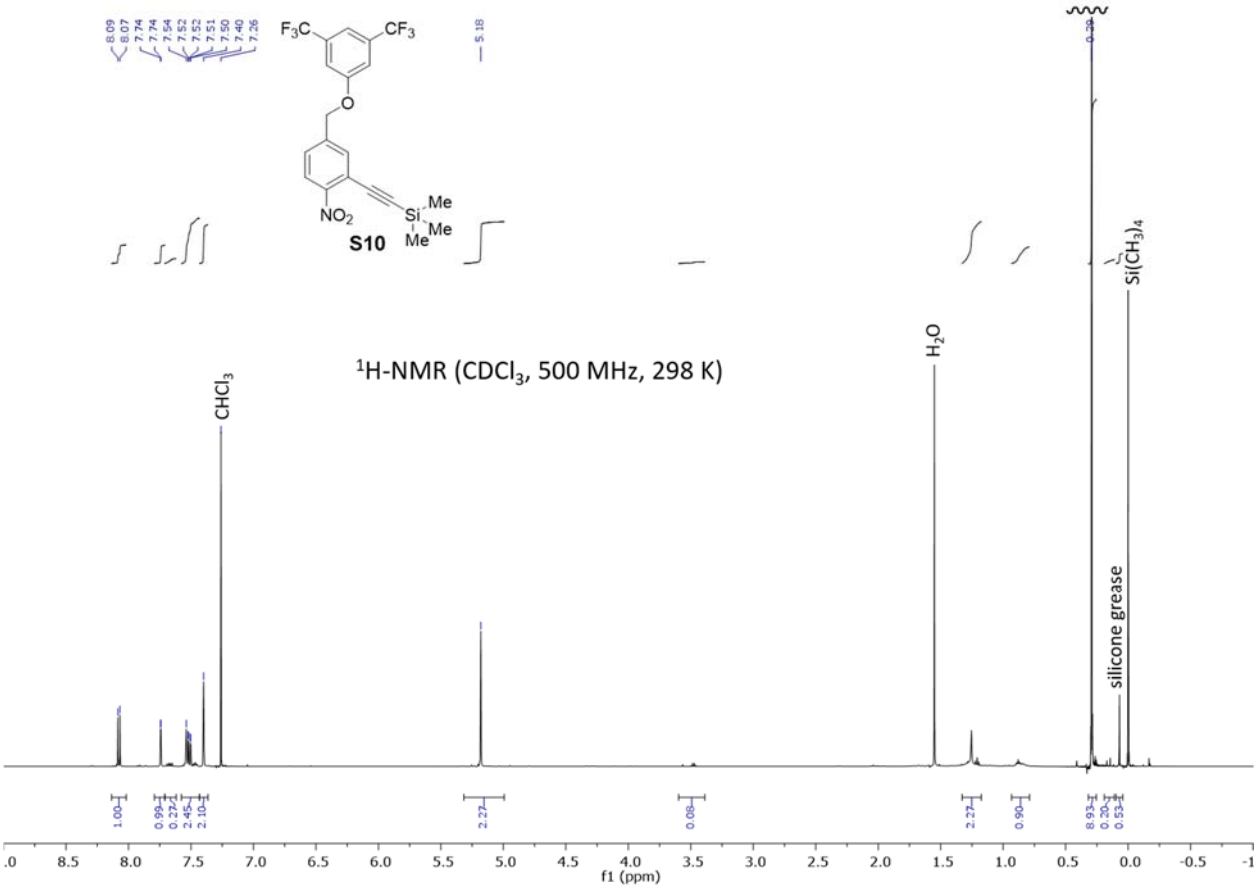
S10
^{1}H-NMR ($CDCl_3$, 500 MHz, 298 K)
$CHCl_3$
H_2O
$Si(CH_3)_4$
silicone grease
f1 (ppm)

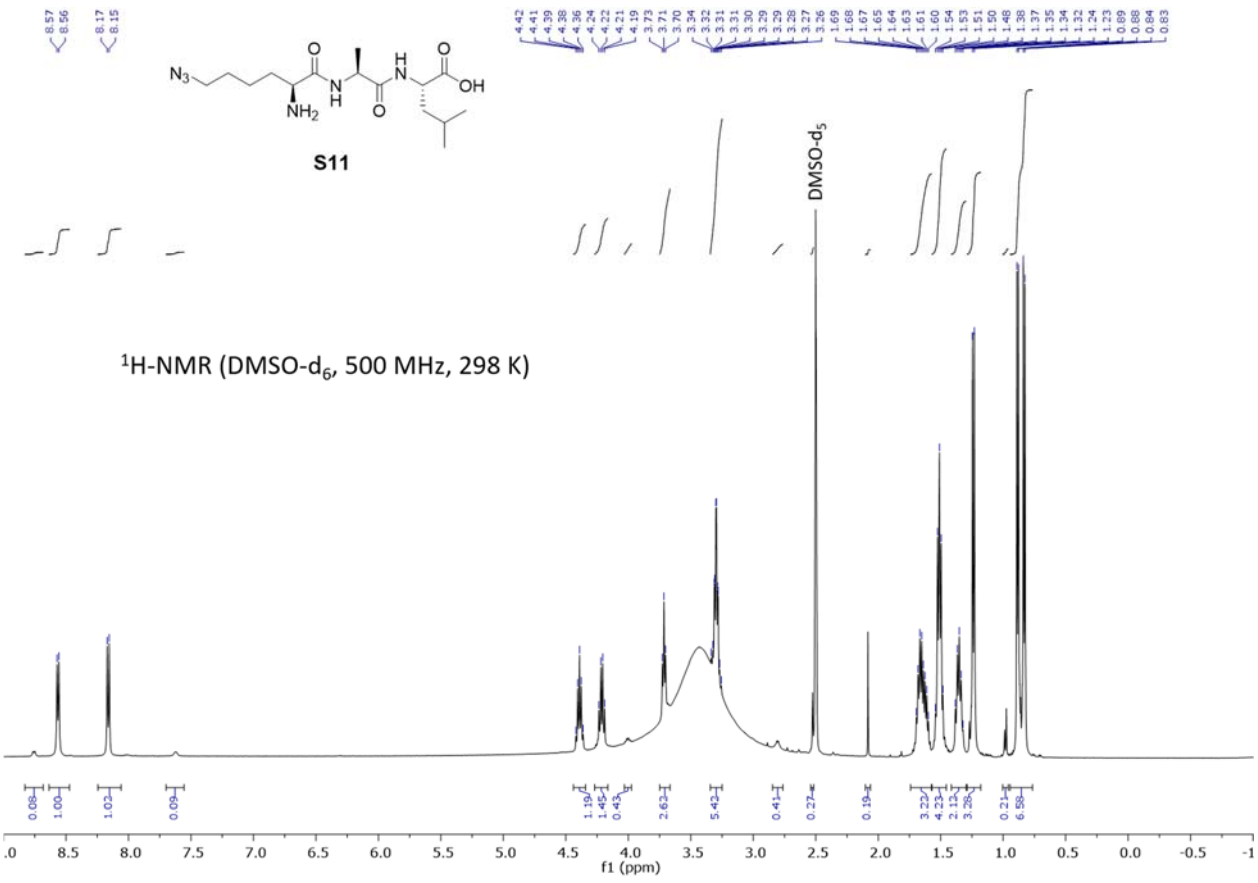
S11
^{1}H-NMR (DMSO-d_6, 500 MHz, 298 K)
DMSO-d_5
f1 (ppm)

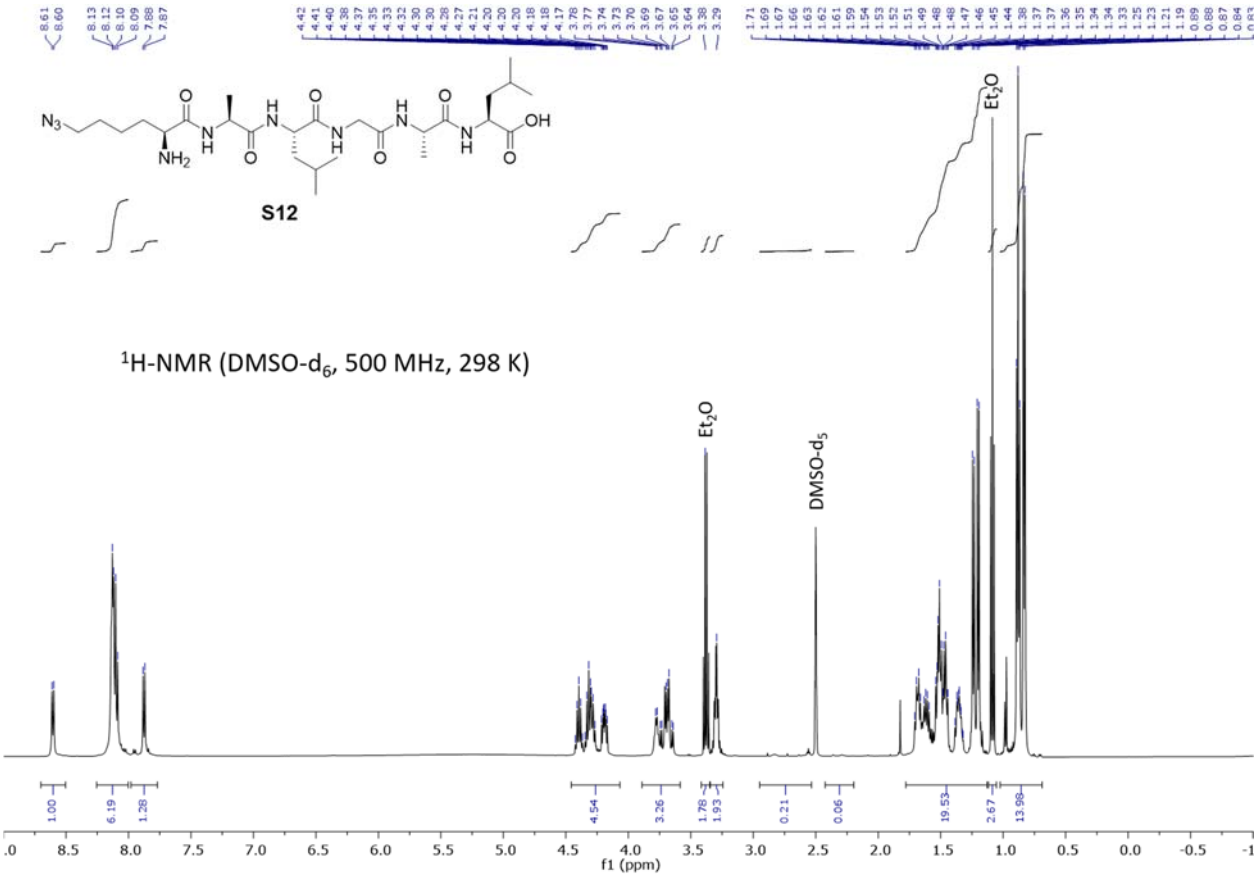
S12
^{1}H-NMR (DMSO-d$_6$, 500 MHz, 298 K)
Et$_2$O
DMSO-d$_5$
f1 (ppm)

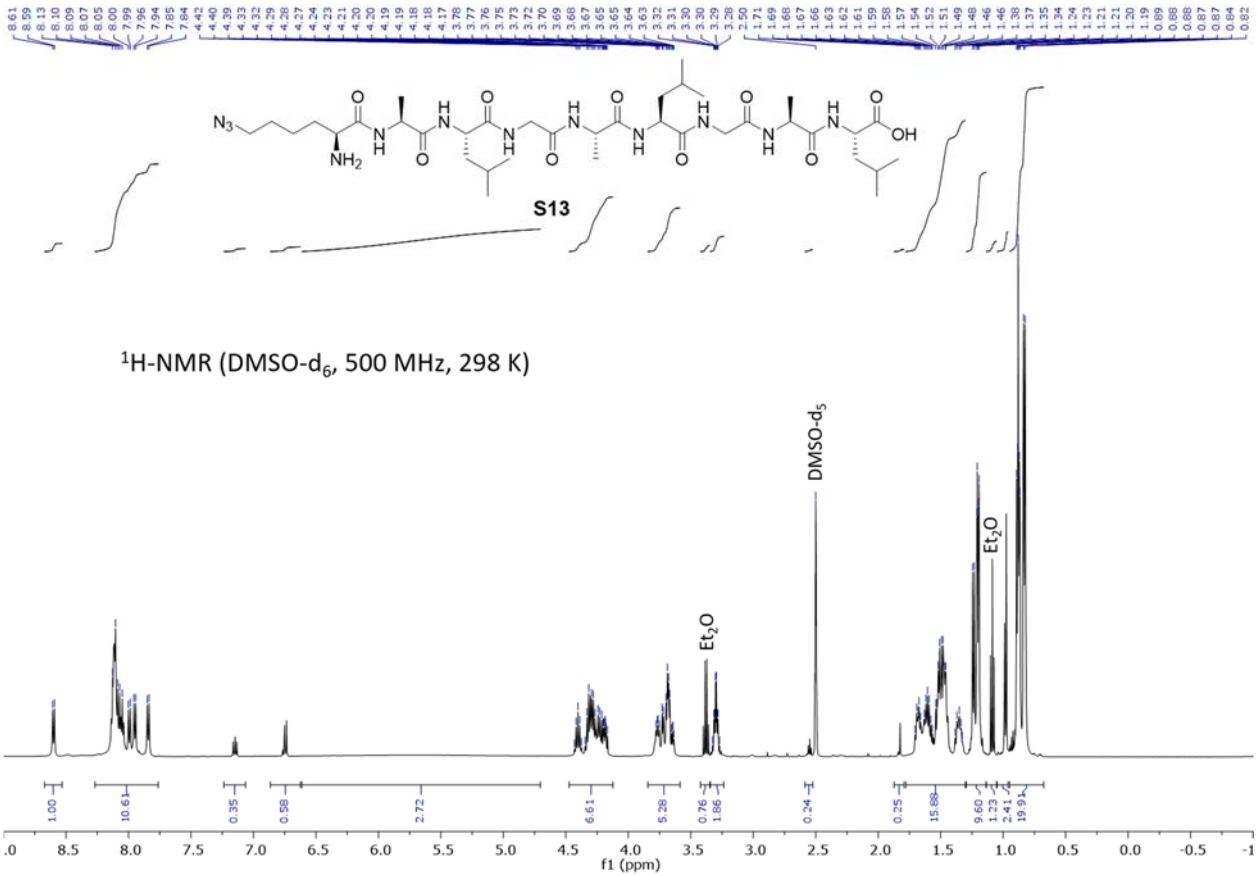
S13
^{1}H-NMR (DMSO-d$_6$, 500 MHz, 298 K)
DMSO-d$_5$
Et$_2$O
Et$_2$O
f1 (ppm)

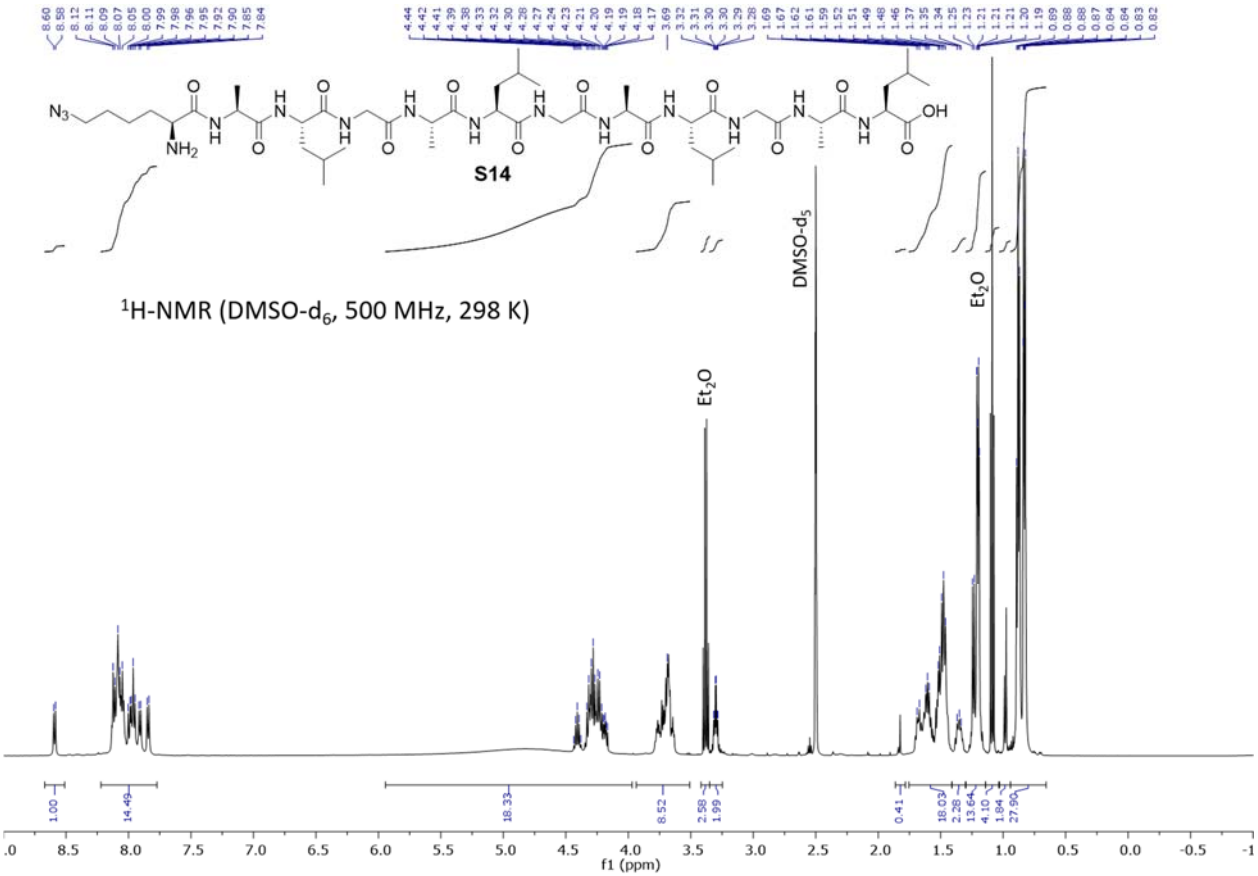

S29

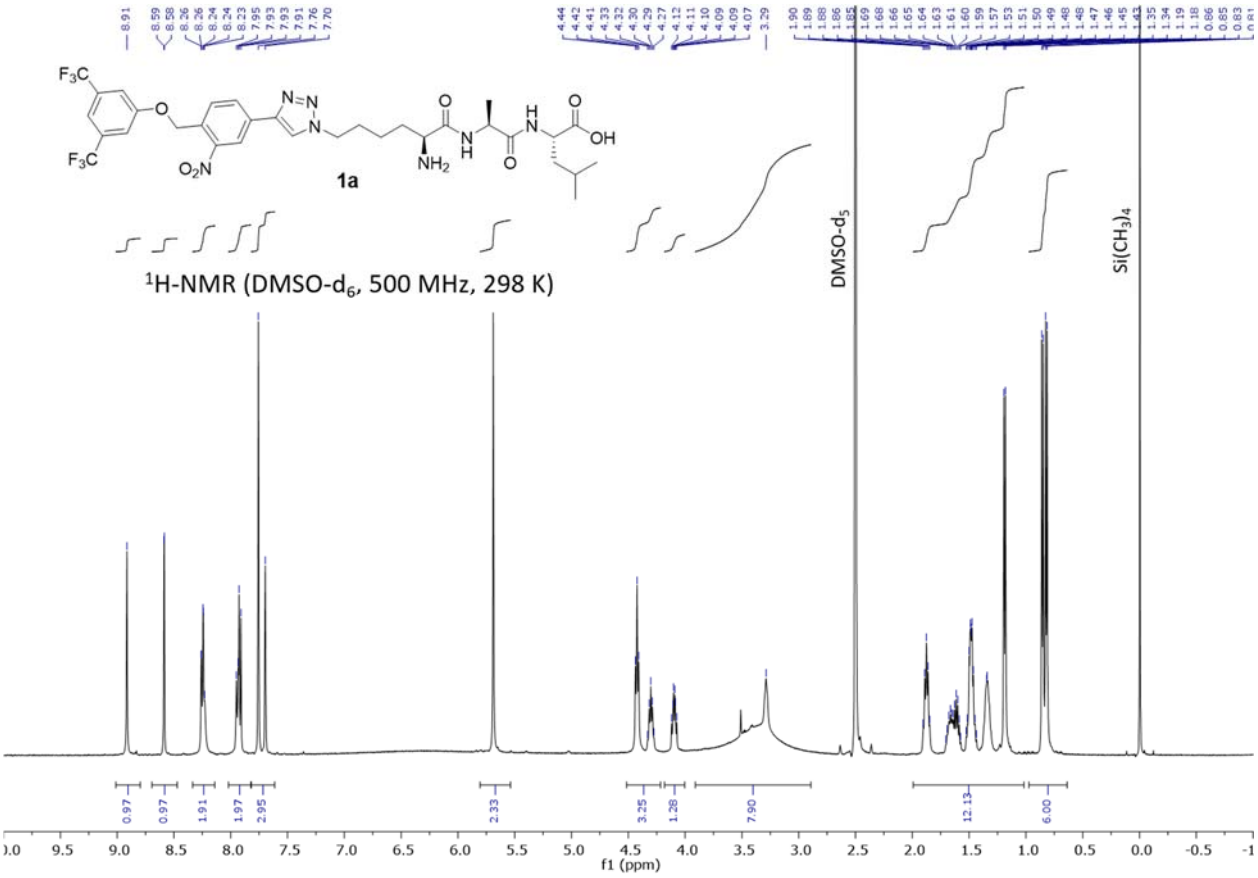
1a
^{1}H-NMR (DMSO-d$_6$, 500 MHz, 298 K)
DMSO-d$_5$
Si(CH$_3$)$_4$
f1 (ppm)

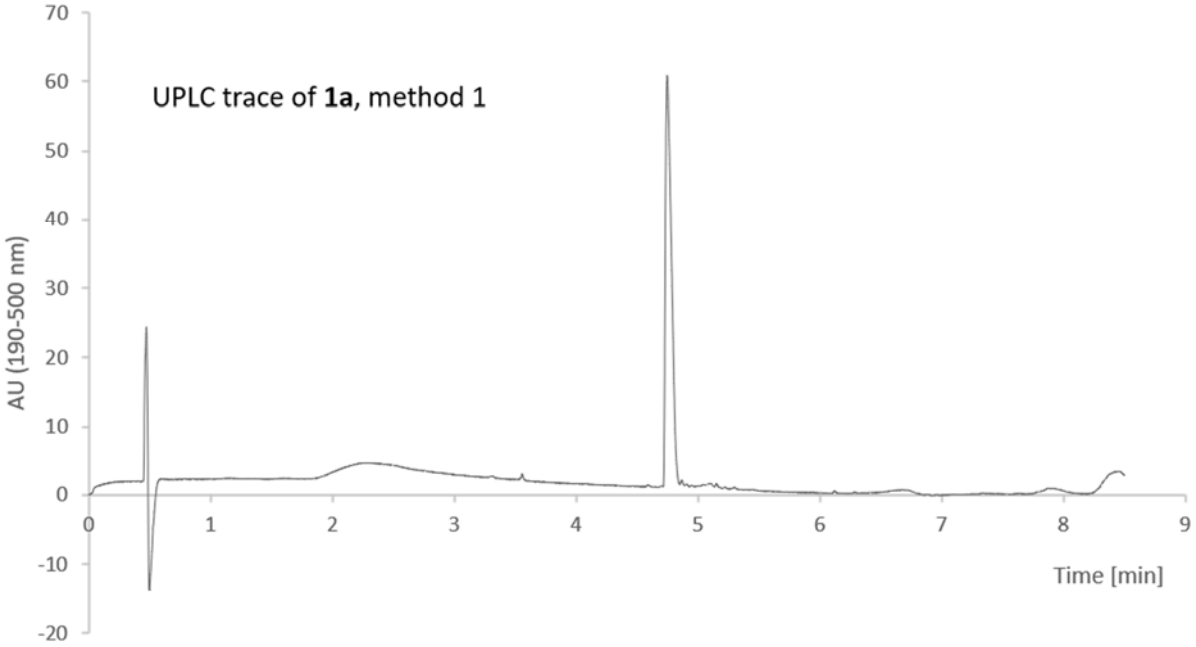
UPLC trace of **1a**, method 1
AU (190-500 nm)
Time [min]

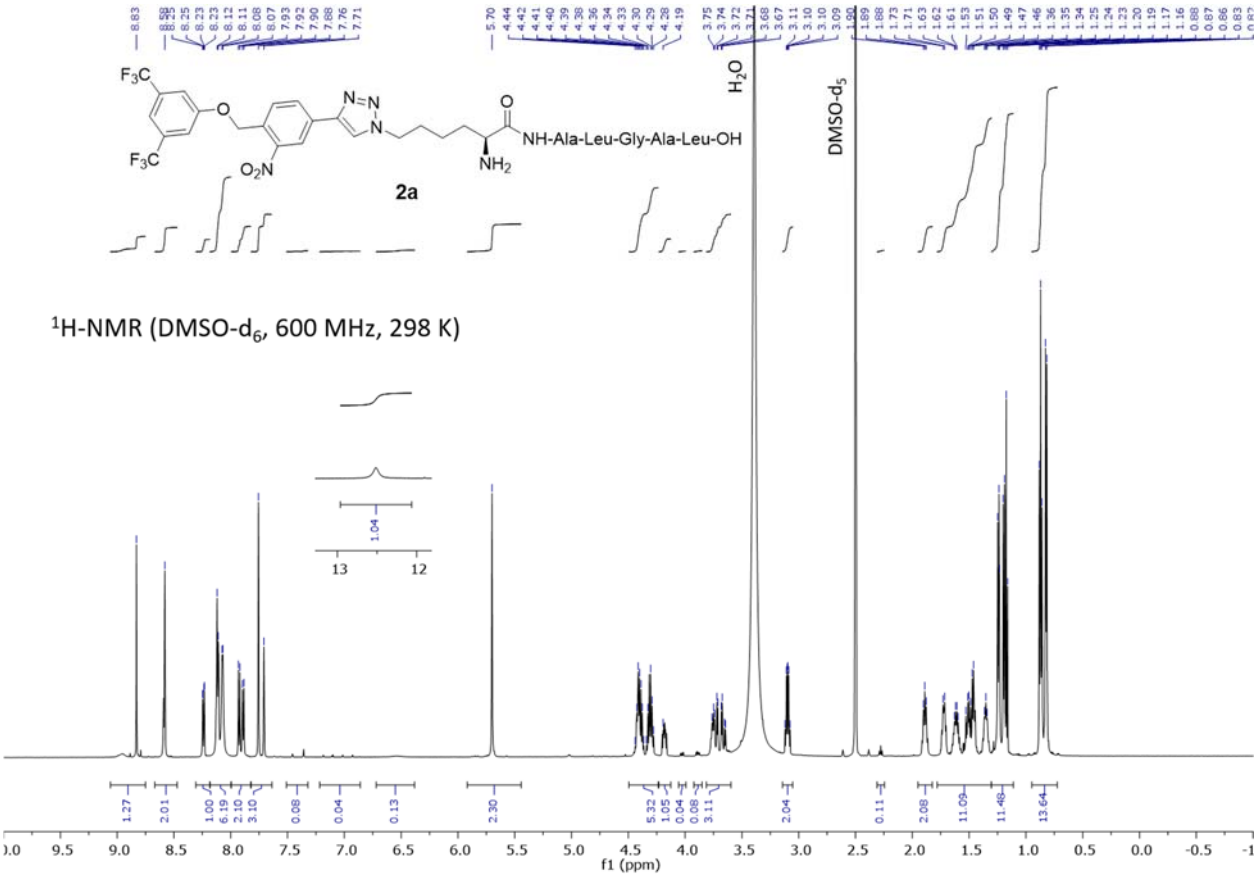
2a
NH-Ala-Leu-Gly-Ala-Leu-OH
H2O
DMSO-d5
1H-NMR (DMSO-d6, 600 MHz, 298 K)
f1 (ppm)

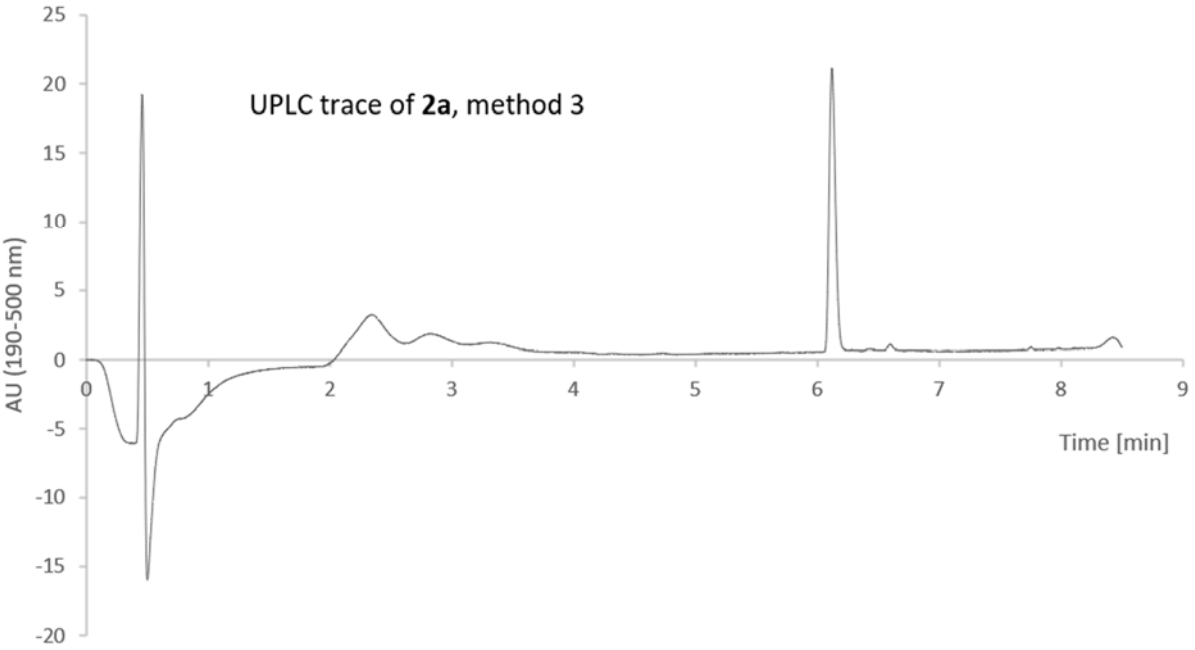
UPLC trace of 2a, method 3
AU (190-500 nm)
Time [min]

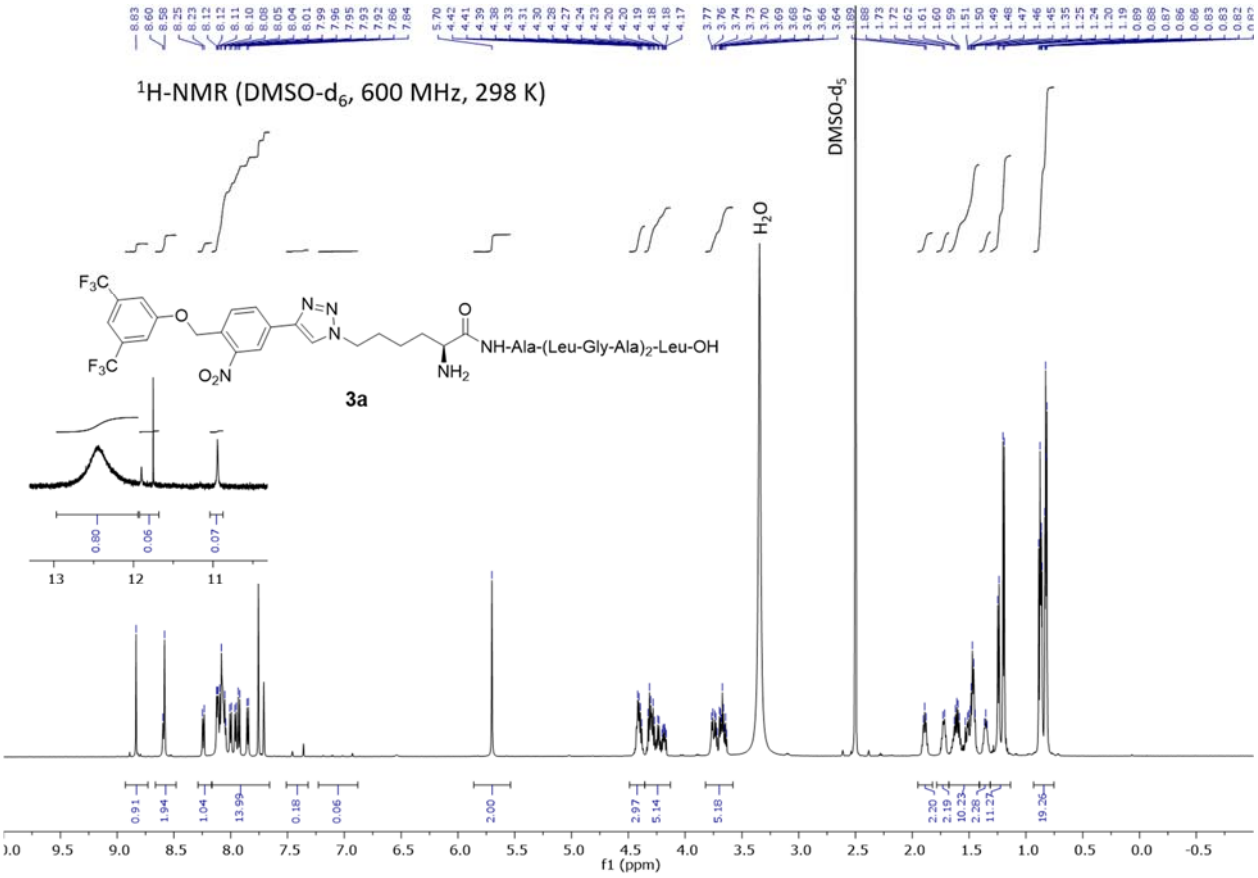
^{1}H-NMR (DMSO-d$_6$, 600 MHz, 298 K)
DMSO-d$_5$
H$_2$O
NH-Ala-(Leu-Gly-Ala)$_2$-Leu-OH
3a
f1 (ppm)

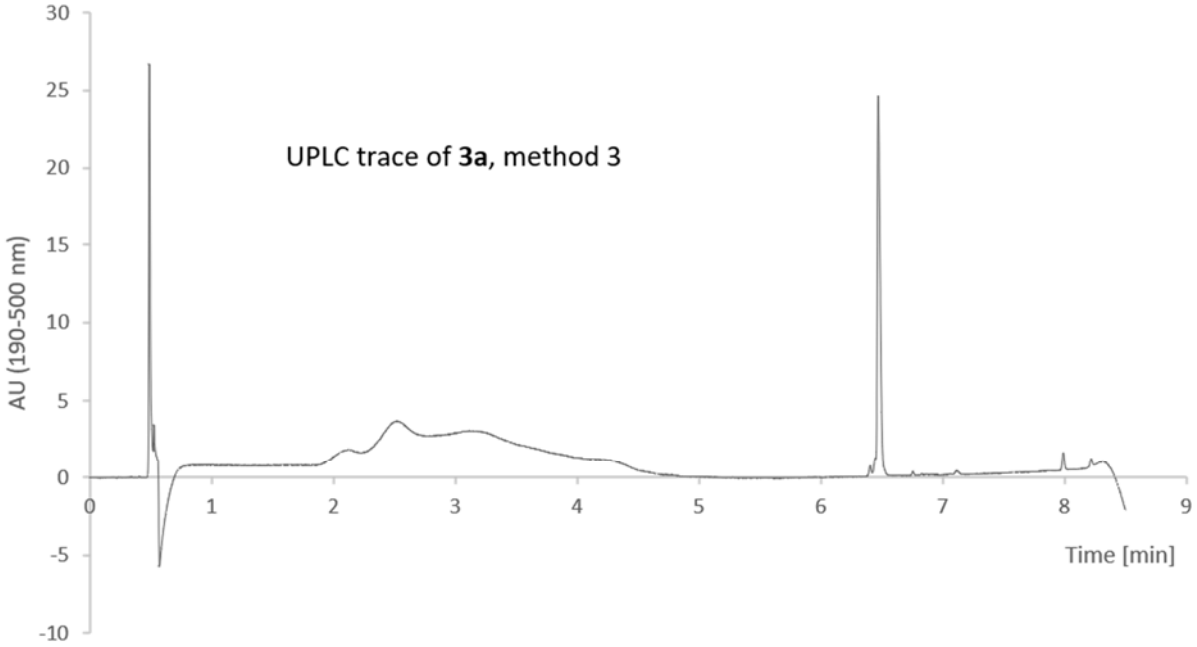
UPLC trace of **3a**, method 3
AU (190-500 nm)
Time [min]

S32

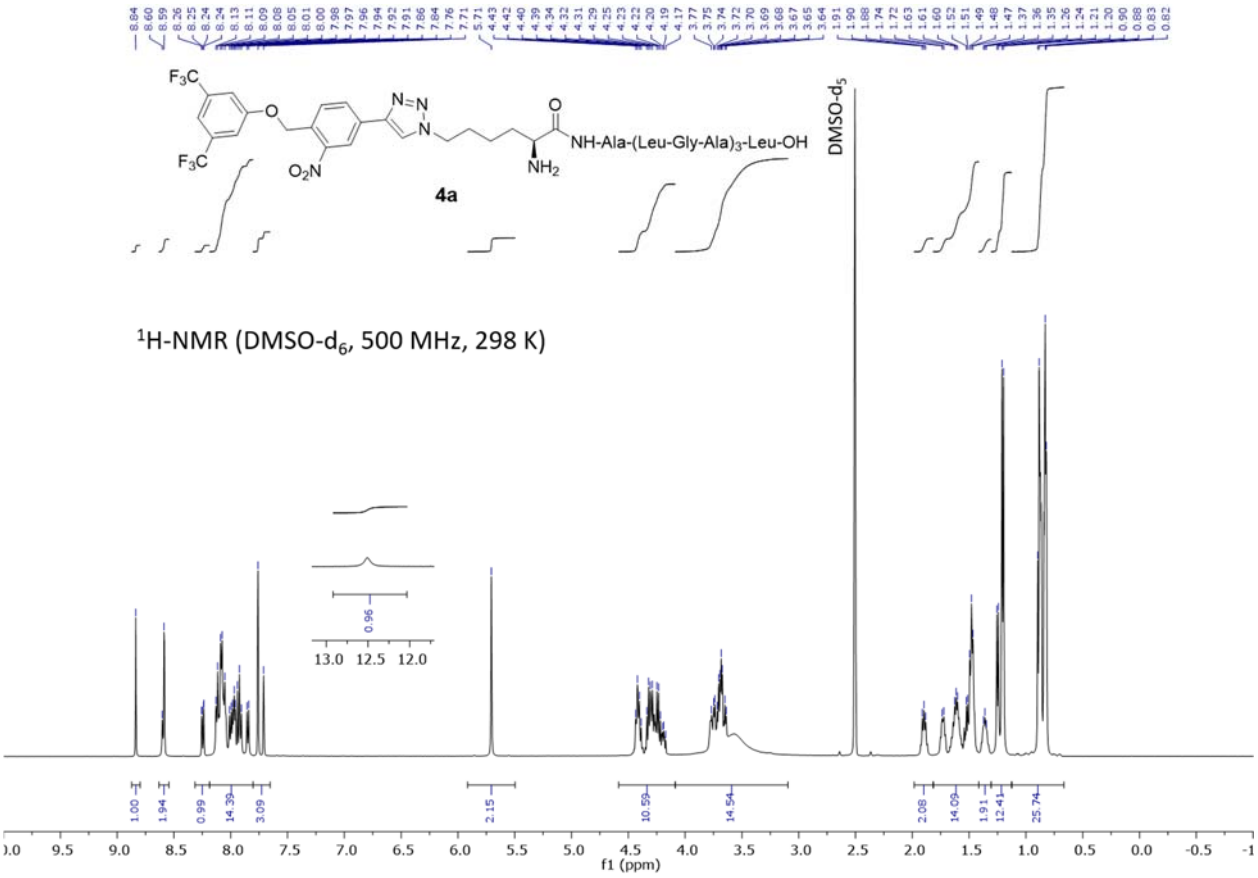
F3C
F3C
O2N
NH-Ala-(Leu-Gly-Ala)3-Leu-OH
NH2
4a
DMSO-d5
1H-NMR (DMSO-d6, 500 MHz, 298 K)
f1 (ppm)

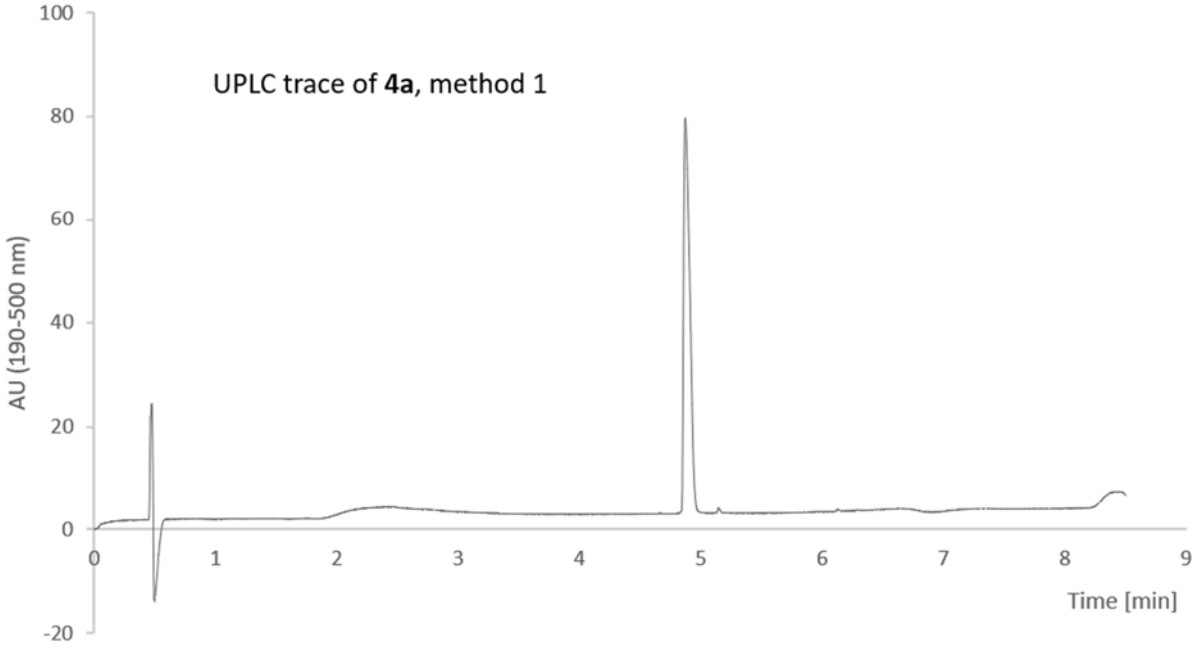
UPLC trace of 4a, method 1
AU (190-500 nm)
Time [min]

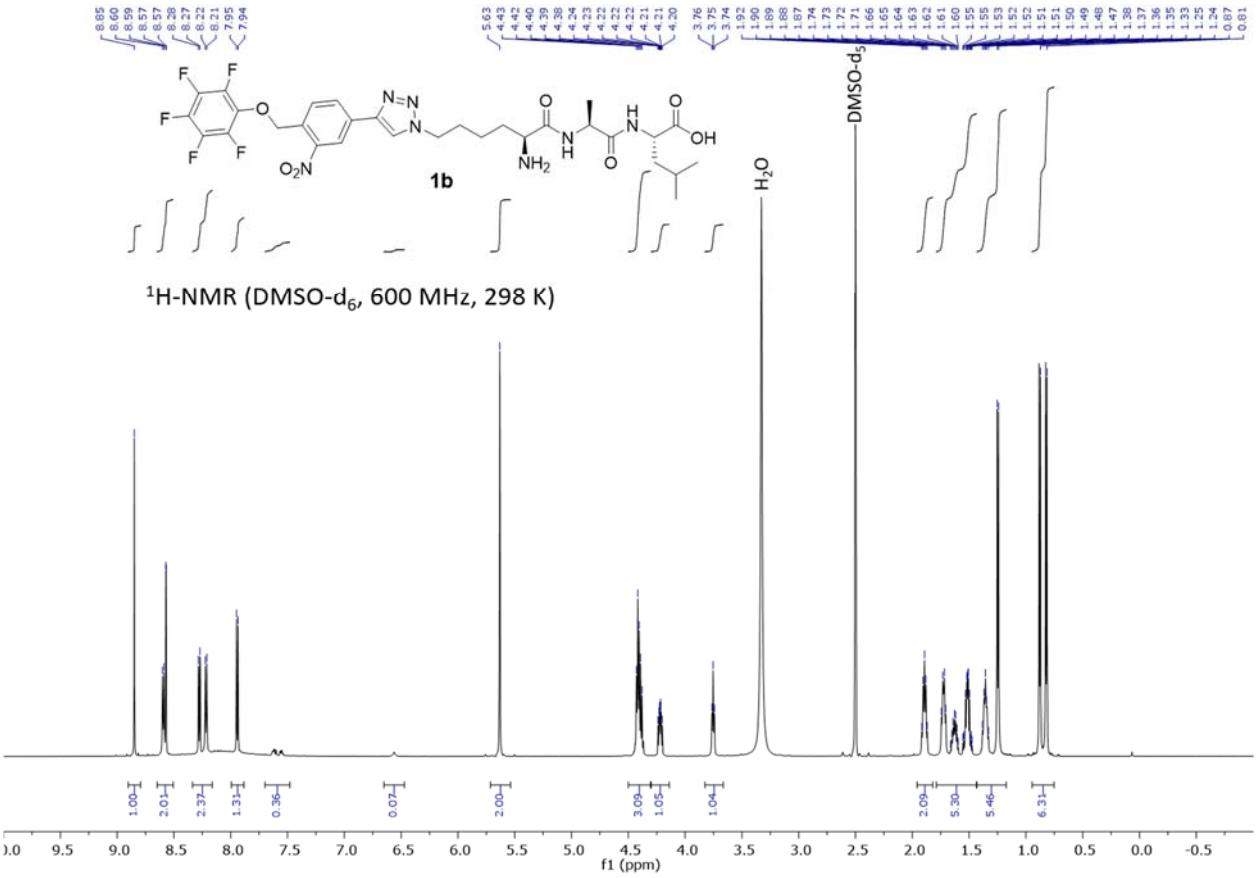
1b
^{1}H-NMR (DMSO-d$_6$, 600 MHz, 298 K)
DMSO-d$_5$
H$_2$O
f1 (ppm)

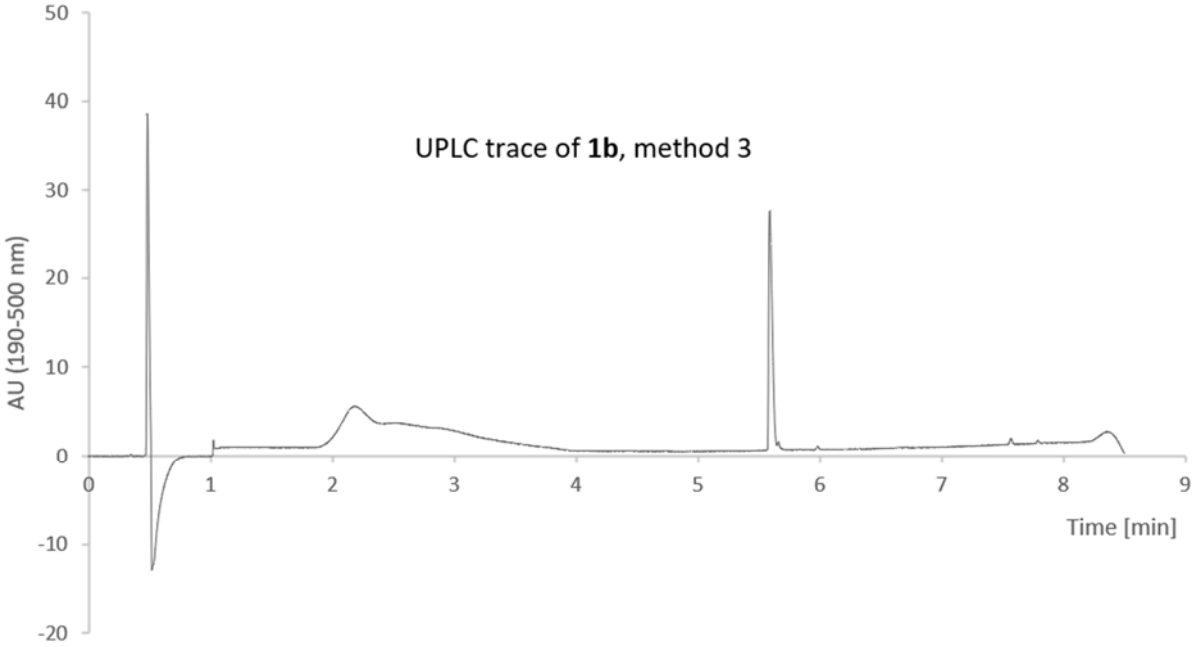
UPLC trace of **1b**, method 3
AU (190-500 nm)
Time [min]

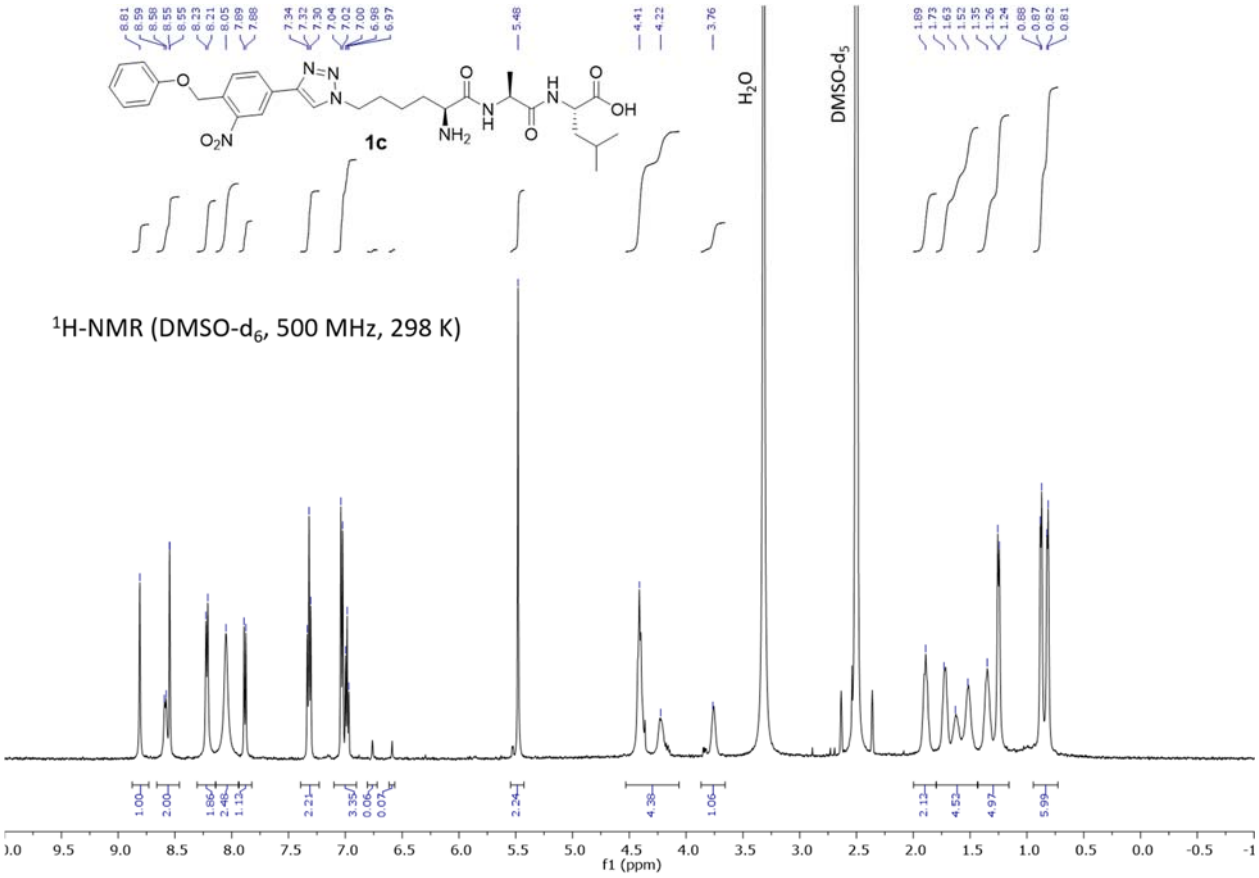
1c
^{1}H-NMR (DMSO-d$_6$, 500 MHz, 298 K)
H$_2$O
DMSO-d$_5$
f1 (ppm)

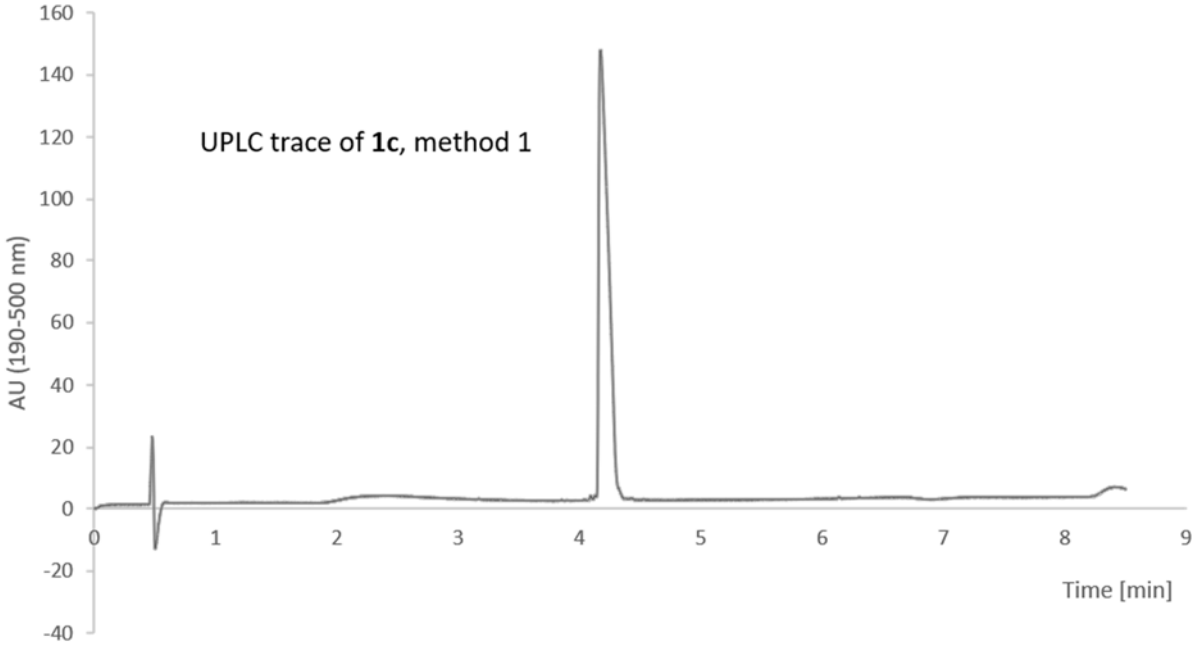
UPLC trace of **1c**, method 1
AU (190-500 nm)
Time [min]

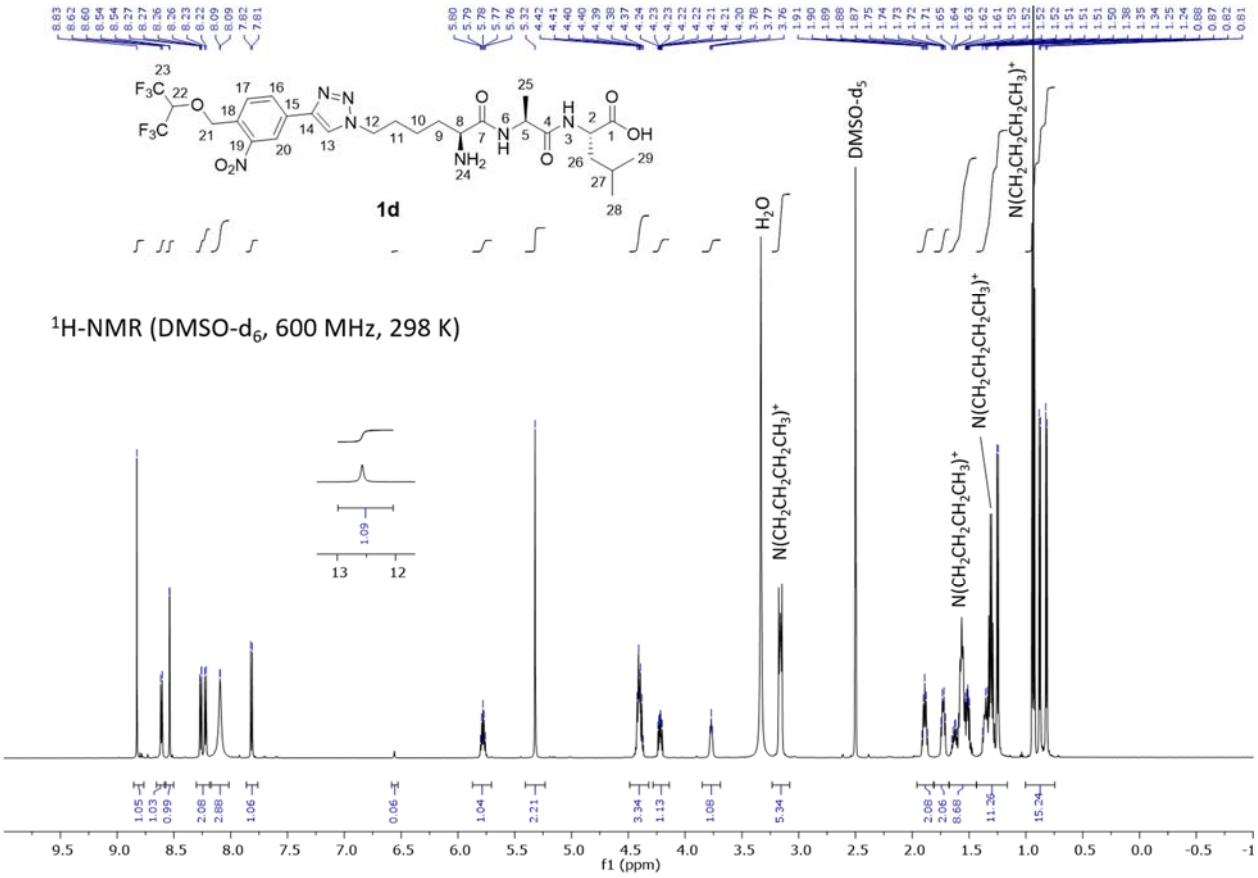
1d
^{1}H-NMR (DMSO-d$_6$, 600 MHz, 298 K)
H$_2$O
DMSO-d$_5$
N(CH$_2$CH$_2$CH$_2$CH$_3$)$^+$
f1 (ppm)

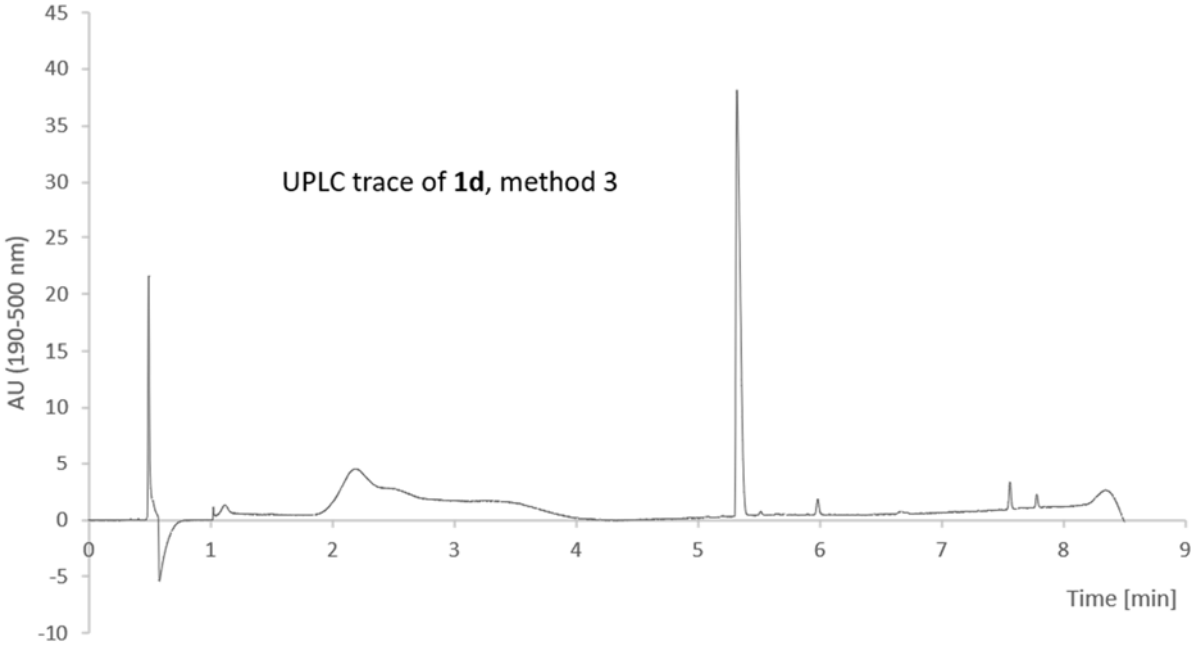
UPLC trace of **1d**, method 3
AU (190-500 nm)
Time [min]

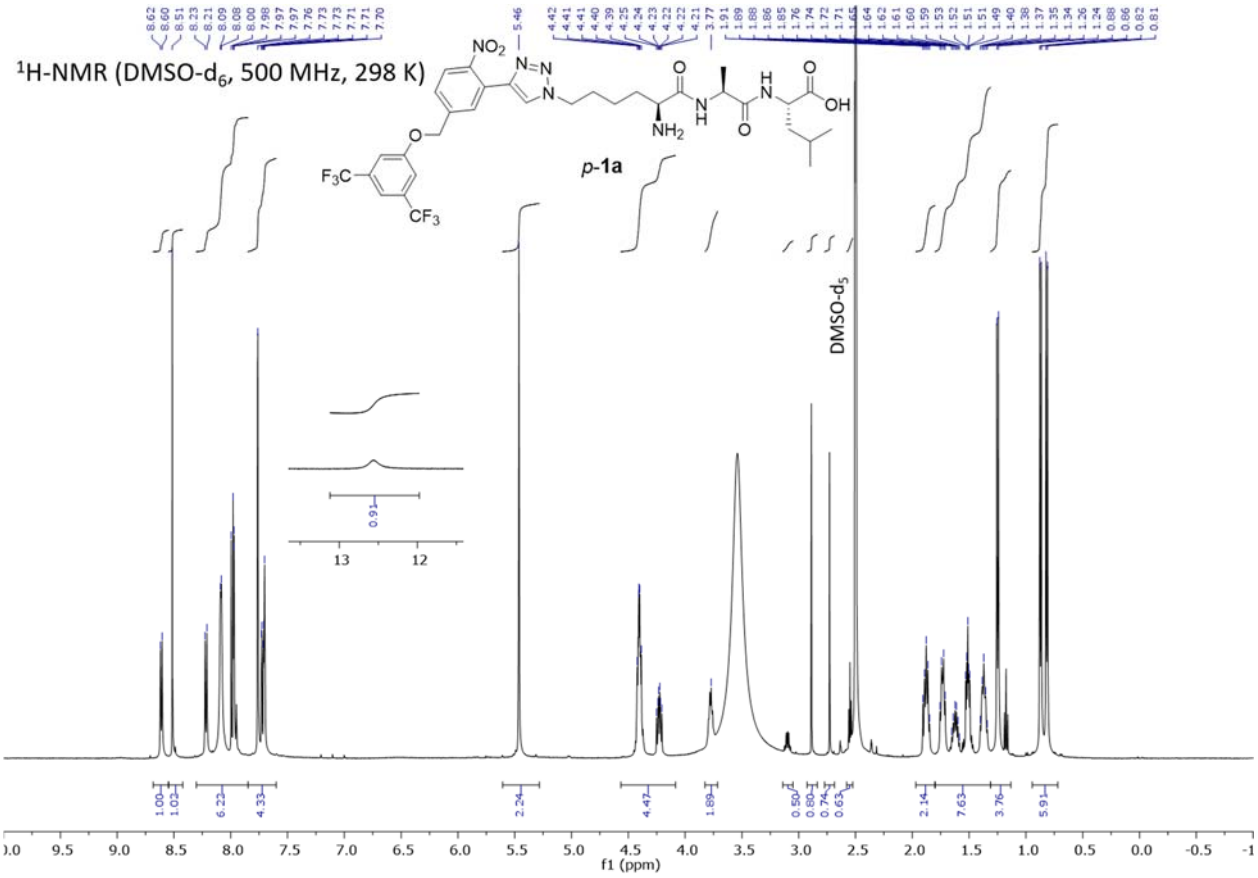
^{1}H-NMR (DMSO-d$_6$, 500 MHz, 298 K)
p-1a
DMSO-d$_5$
f1 (ppm)

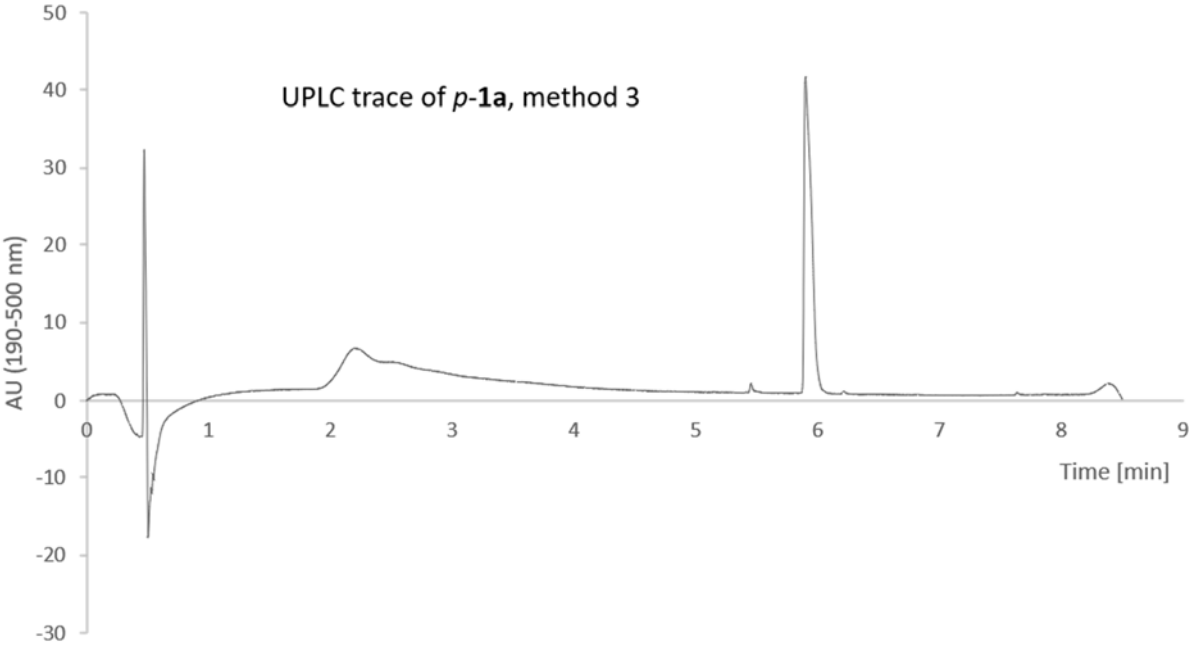
UPLC trace of p-1a, method 3
AU (190-500 nm)
Time [min]

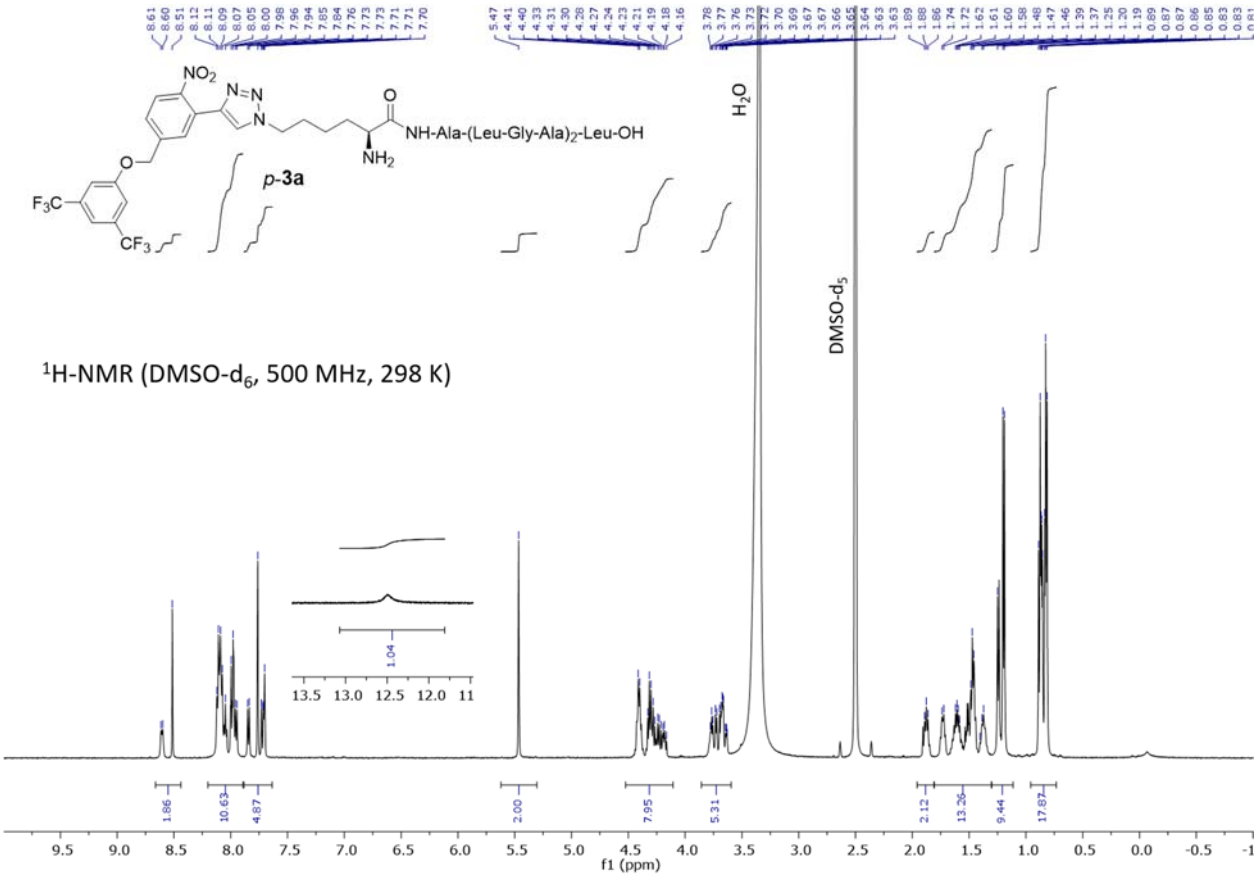
p-3a
NH-Ala-(Leu-Gly-Ala)2-Leu-OH
H2O
DMSO-d5
1H-NMR (DMSO-d6, 500 MHz, 298 K)
f1 (ppm)

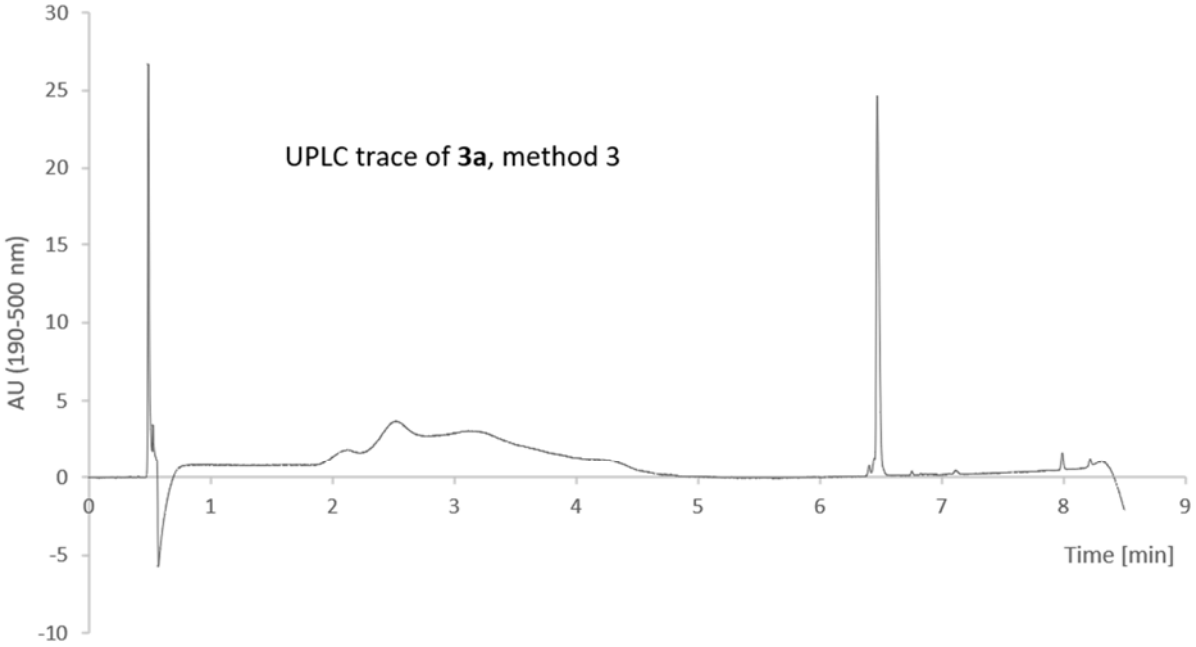
UPLC trace of 3a, method 3
AU (190-500 nm)
Time [min]

References

1. Sezer, U.; Geyer, P.; Kriegleder, M.; Debossiac, M.; Shayeghi, A.; Arndt, M.; Felix, L.; Mayor, M. *Beilstein J. Nanotechnol.*, **2017**, *8*, 325–333.
2. Felix, L., PhD thesis, University of Basel, **2016**.
3. Friedrich, J.; Gilb, S.; Ehrler, O. T.; Behrendt, A.; Kappes, M. M.; *J. Chem. Phys.* **2002,** *117*, 2635-2644.
4. Valiev, M.; Bylaska, E. J.; Govind, N.; Kowalski, K.; Straatsma, T. P.; Van Dam, H. J. J.; Wang, D.; Nieplocha, J.; Apra, E.; Windus, T. L.; de Jong, W. A. *Comput. Phys. Commun.* **2010**, *181*, 1477-1489.
5. Adamo, C.; Barone, V. J. *J. Chem. Phys.* **1999**, *110*, 6158-6170.
6. Binkley, J. S.; Pople, J. A.; Hehre, W. J. *J. Am. Chem. Soc.*, **1980**, *102,* 939-947.
7. Bussi, G.; Donadio, D.; Parinello, M. *J. Chem. Phys.* **2007**, *126*, 014101.
8. Frisch, M. J.; et al., Revision A.1 ed., Gaussian Inc., Wallingford, CT, **2009**.
9. Weigend, F.; Ahlrichs, R. *Phys. Chem. Chem. Phys*. **2005**, *7*, 3297-3305.
10. Drahos, L. and Ve´key, K. *J. Am. Soc. Mass Spectrom*. **1999**, *10*, 323–328.
11. Coimbra, J. T. S.; Neves, R. P. P.; Passos, Ó.; Jarukanont, D.; Fernandes, P. A.; Patel, S.; Garcia, M. E.; Ramos, M. J.; *Chem. Phys. Lett.*, **2014**, *615*, 75-82.
12. Boys, S. F.; Bernardi, F.; *Mol. Phys.*, **1970**, *19*, 553-556.
13. Grimme, S.; Antony, J.; Ehrlich, S.; Krieg, H.; *J. Chem. Phys*. **2010**, *132*, 154104.
14. Yanai, T.; Tew, D. P.; Handy, N. C. *Chem. Phys. Lett.* **2004**, *393*, 51-57.
15. calculated using Advanced Chemistry Development (ACD/Labs) Software V11.02
16. Martin, R. L. *J. Chem. Phys.,* **2003**, *118*, 4775-4777.

Chapter 6. Ionic tags for photo-induced charge control and neutralization of proteins in the gas-phase

J. Schätti; M. Kriegleder; M. Debiossac; M. Kerschbaum; Philipp Geyer; Armin Shayeghi; Marcel Mayor; Markus Arndt; Valentin Köhler.

Experimental Parameters

All modified peptides and insulin were prepared in a mixture of 50:50 methanol and deionized water. 1 mg of powder was dissolved in 1 mL of solvent. We added 1% of formic acid to the positive samples and 1% of ammonia to the negative samples to increase ion count. The injection flow of the solution was set to 5 µL/min for all experiments. The electrospray was optimized to maximize ion counts for each species, but the capillary voltage was set to 3.5 kV for positive and -3 kV for measurements in the negative mode.

All photo cleavage experiments were performed using a frequency quadrupled Nd:YAG laser emitting at a wavelength of 266 nm, width a pulse width of 10 ns. The laser beam is aligned counter-propagating to the molecular beam, clipped with a pinhole at the entrance to 2 mm diameter. The other parameters are contained in the following table:

Peptide & charge state	Laser power (mW)	Repetition rate (Hz)	Integration time (sec)
1-neg-LG^{-}	94	250	120
2-neg-LG^{-}	94	250	120
3-neg-LG^{-}	442	500	120
3-neg-LG^{2-}	442	500	120
4-neg-LG^{-}	442	500	120
1-pos-LG^{+}	94	250	240
3-pos-LG^{+}	94	250	240
3-pos-LG^{2+}	94	250	240
neg-ins^{2-}	560	1000	240
neg-ins^{2-}	560	1000	240
neg-ins^{3-}	560	1000	240
neg-ins^{4-}	560	1000	240
neg-ins^{5-}	560	1000	240
neg-ins^{6-}	560	1000	240
neg-ins^{7-}	560	1000	240
pos-ins^{3+}	560	1000	240
pos-ins^{4+}	560	1000	240
pos-ins^{5+}	560	1000	240
pos-ins^{6+}	560	1000	240
pos-ins^{7+}	560	1000	240

Tabel S1. Measurement parameter for the displayed cleaving experiments; laserpower, repetition rate and integration time.

Additional MS-data for UV cleavage

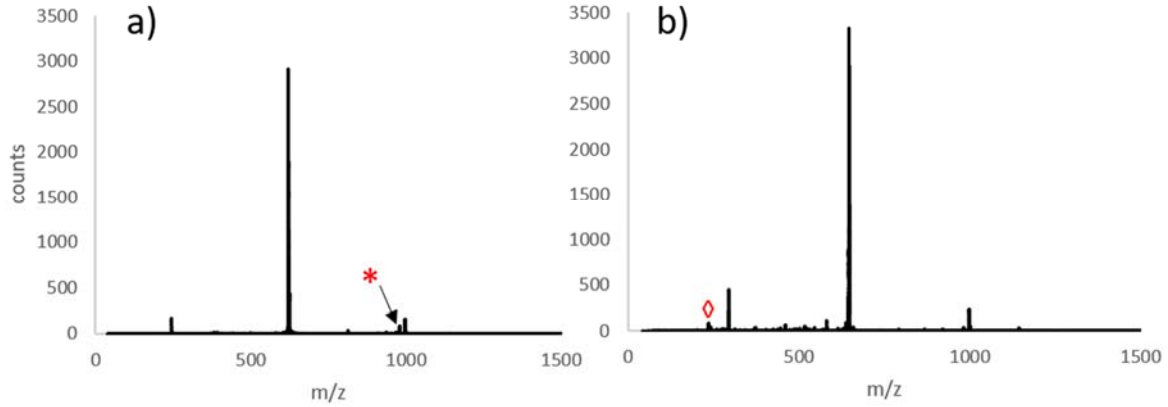

Figure S1. MS-TOF of a) doubly charged **3-neg-LG** and b) **3-pos-LG** upon laser radiation at 266 nm. The asterisk indicates the loss of 16 amu of singly charged peptide moiety after cleavage. The diamond indicates the loss of NMe_3 from the leaving group fragment.

MS-data for collision induced dissociation.

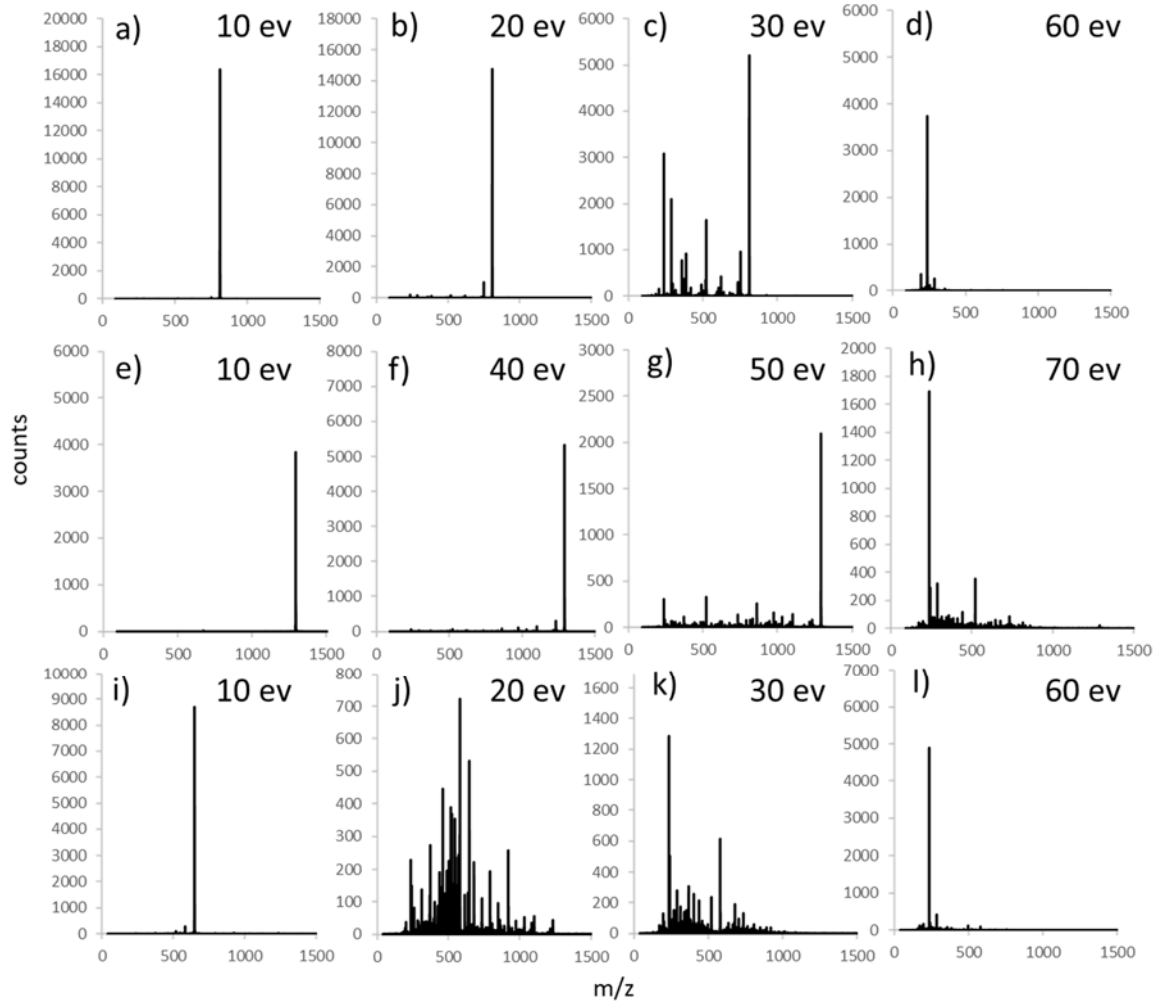

Figure S2. Mass spectra after CID at various collision energies for positively charged peptides **1-pos-LG** (singly charged, a-d); **3-pos-LG** (singly charged, e-h), **3-pos-LG** (doubly charged, i-l).

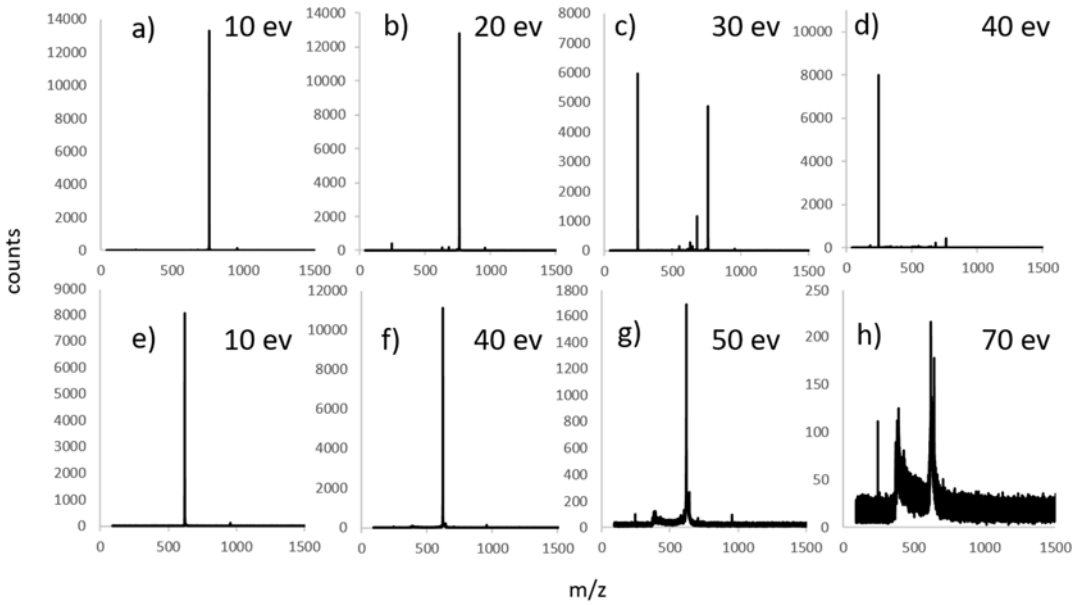

Fgure S3. Mass spectra after CID for various collision energies of negatively charged **1-neg-LG** (singly charged, a-d); **3-neg-LG** (doubly charged, e-h).

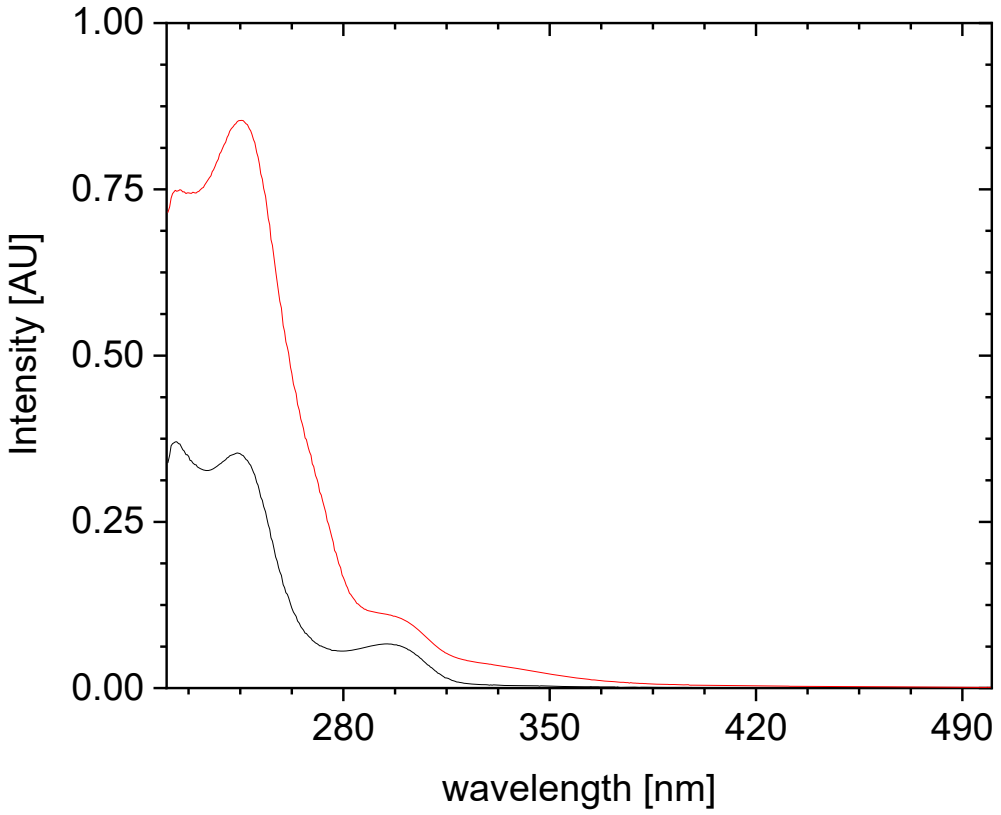

Figure S4. Absorption spectra of unmodified insulin (black line) and **neg-ins**, which carries 3 negatively charged leaving groups (red line) at a concentration of 0.03 mg/mL in 50:50 MeCN / aq. NaOH (0.1 M). Insulin (0.6 mg) and **neg-ins** (0.6 mg) respectively, were dissolved in 1 mL 50:50 MeCN / aq. NaOH (0.1 M). The solutions for the measurement were prepared by a 1 to 20 dilution of a stock solution. Absorption at 266 nm was determined as 0.090 AU for insulin and 0.398 AU for **neg-ins.** The absorption of the modified insulin **neg-ins** is ca. 4 times higher at 266 nm compared to unmodified insulin.

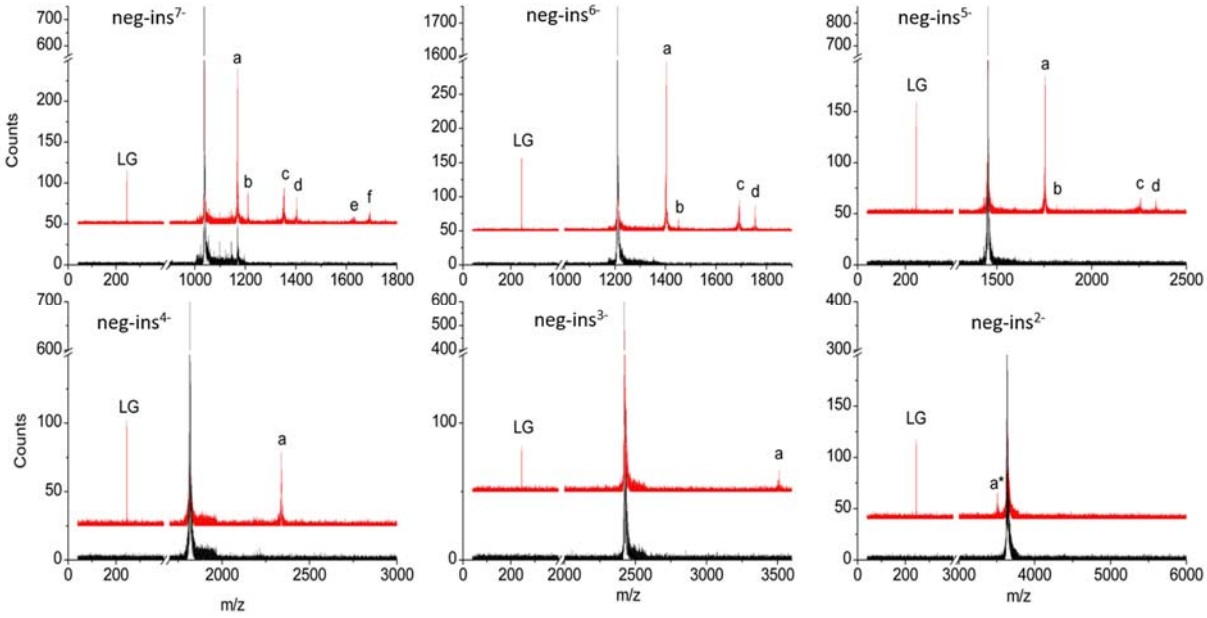

Figure S5. Mass spectra of mass selected **neg-ins** for charge states -2 to -7. (black) before irradiation; (red) after irradiation; LG = leaving group; (a) $[M^{n-} -LG]^{(n-1)-}$, (b) $[M^{n-}-e]^{(n-1)-}$, (c) $[M^{n-} -2\ LG]^{(n-2)-}$, (d) $[M^{n-} -LG -e]^{(n-2)-}$, (e) $[M^{n-} -3\ LG]^{(n-3)-}$, (f) $[M^{n-} -2\ LG -e]^{(n-3)-}$, (a*)$[M^{2-}-LG-H]^{2-}$ at a low charge state the LG can be partially protonated, therefore the loss of a neutral LG fragment is possible.

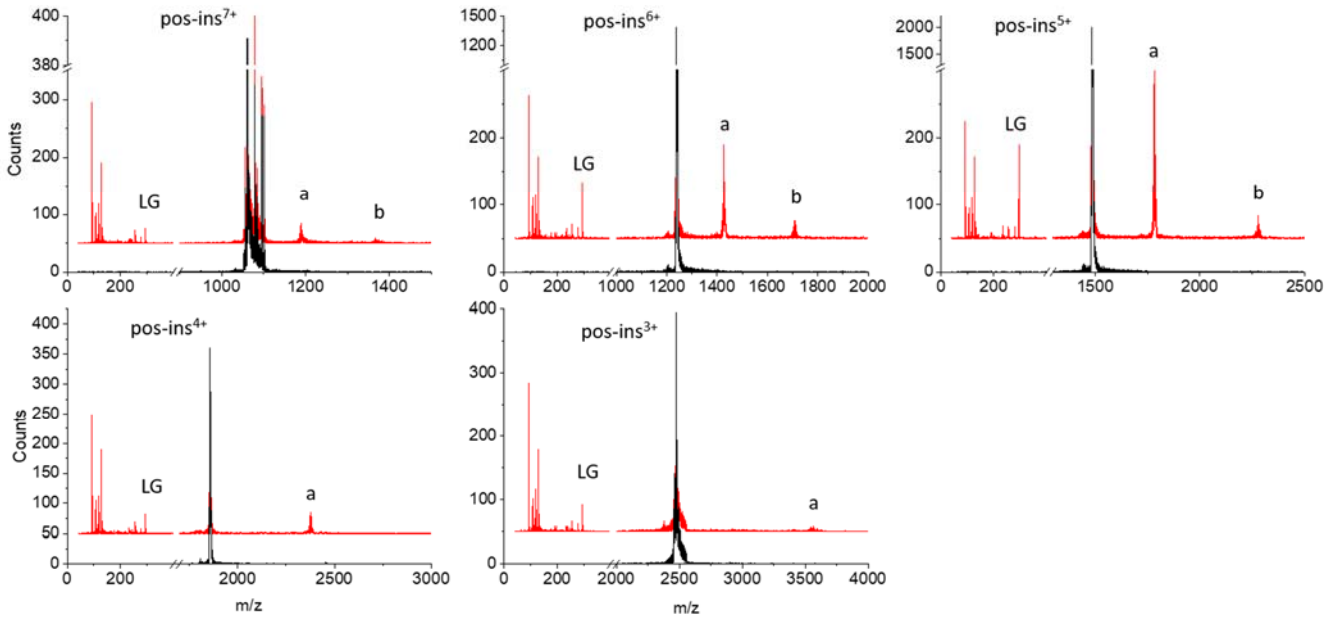

Figure S6. Mass spectra of mass selected **pos-ins** for charge states +3 to +7. (black) before irradiation; (red) after irradiation; LG = leaving group; (a) $[M^{n+} -LG]^{(n-1)+}$, (b) $[M^{n+} - 2\ LG]^{(n-2)+}$. The signals below the mass of the LG were not assigned.

General

Chemicals were purchased from Sigma Aldrich, Fluorochem, Novabiochem or Bachem and used as received unless otherwise noted. UPLC experiments were performed with an Acquity UPLC-H Class Bio from Waters equipped with a PDA and a SQ detector 2 with the following column: ACQUITY UPLC, HSS T3 1.8 µm, 2.1 x 100 mm. Solvents were water and acetonitrile, respectively, each containing 0.1% formic acid, later on referred to as (A) and (B). The flow rate was set to 0.61 mL/min and the temperature to 40 °C. Method 1: 0 min – 90% A; 1 min – 90% A; 6 min – 100% B; 7.5 min – 100% B. Method 2: 0 min – 100% A; 1 min – 100% A; 6 min – 100% B; 7.5 min – 100% B. Mass detection was performed in scan mode for positive ions (cone voltage 40 V, desolvation temperature: 600°C). A Water Prep LC 4000 System equipped with a Waters 2487: Dual λ Absorbance Detector was used for preparative separations with the following column: Agilent: XDB-C18, 21.2 x 150 mm, 5 µm. Ultra pure water was prepared by means of an Ultra Ionic system from Milli-Q. HRMS experiments were conducted with a Bruker maXis 4G. NMR experiments were performed at 25°C on Bruker Avance III NMR spectrometers operating at 600, 500 or 400 MHz proton frequency. NMR spectrometers were equipped with direct (400 MHz) or inverse (600 MHz ,500 MHz) dual channel, broadband probe heads with *z* -gradients. ^{13}C shifts were determined by 2D NMR experiments (HMBC and HMQC). ^{1}H and ^{13}C signals were assigned by 2D NMR (COSY, HMBC, HMQC).

Synthesis

The synthesis of the peptides **S1** and **S2** were synthesized by standard Fmoc-SPPS followed a procedure published previously.[1]

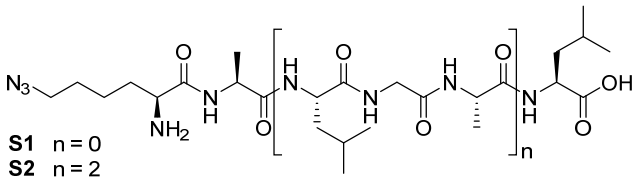

Peptide **S3** and **S4** were synthesized by standard Fmoc-SPPS using rink amid resin.

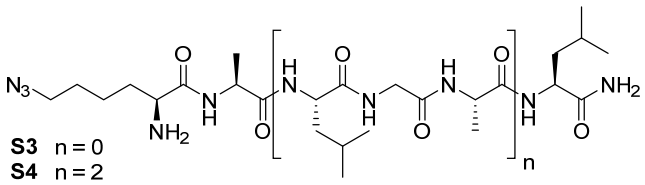

Rink amide-resin (200 mg, loading: 0.45 mmol/g resin) was placed in a plastic syringe equipped with a filter frit. The resin was washed with CH_2Cl_2 (~2 mL). Peptide coupling steps were performed using a peptide synthesizer (intavis multi pep RSI) employing Fmoc-amino acids (5.0 eq.), PyBOP (5.0 eq.) and DIPEA (5.0 eq.) with a reaction time of first 45 min followed by a 2nd coupling step with identical reagent

loadings for 90 min. Fmoc-deprotection was performed with piperidine (20% piperidine in DMF, 3 cycles (1 mL) of 5 min. each). Before and after the Fmoc-deprotection the resin was washed with DMF (5 × ~2 mL). In the end the resin was washed with CH_2Cl_2 (5 × ~2 mL) before the cleavage solution (5 mL, 96% TFA, 3% triisopropylsilane, 3% H_2O) was added and the mixture agitated for 1 h. Subsequently, the cleavage solution was removed by filtration and the resin washed with TFA (3 × ~2 mL). The combined TFA solutions were concentrated under reduced pressure until the mixture started to become viscous. Ice cold Et_2O (50 mL) was added and the resulting precipitate collected by centrifugation (4650 g). The precipitate was washed with Et_2O (3 × 20 mL) and the product obtained after drying as a colorless solid as the TFA salt.

Peptide S3

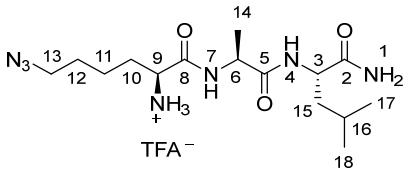

28.2 mg (62.2 μmol, 69%).

UPLC-MS: Method 1, T_R = 2.38 min; m/z MS (ES+): 356.3 [100%, M + H+], 339.5 [20%]; HRMS: calculated for: $C_{15}H_{30}N_7O_3^+$: 356.2405; found 356.2405. ^{1}H-NMR: (500 MHz, DMSO-d_6, 298 K) δ 8.60 (d, $^3J_{H\text{-}H}$ = 7.5 Hz, 1 H, H-7), 7.96 (d, $^3J_{H\text{-}H}$ = 8.4 Hz, 1 H, H-4), 7.33 (s, 1 H, H-1), 6.97 (s, 1 H, H-1), 4.39 (p, $^3J_{H\text{-}H}$ = 7.1 Hz, 1 H, H-6), 4.21 (td, $^3J_{H\text{-}H}$ = 8.5 Hz, $^3J_{H\text{-}H}$ = 6.2 Hz, 1 H, H-3), 3.76 (t, $^3J_{H\text{-}H}$ = 6.4 Hz, 1 H, H-9), 3.35-3.25 (m, 2 H, H-13), 1.75-1.64 (m, 2 H, H-10), 1.63-1.48 (m, 3 H, H-12 and H-16), 1.47-1.41 (m, 2 H, H-15) 1.40-1.31 (m, 2 H, H-11), 1.24 (d, $^3J_{H\text{-}H}$ = 7.0 Hz, 3 H, H-14), 0.87 (d, $^3J_{H\text{-}H}$ = 6.6 Hz, 3 H, H-17 or H-18), 0.83 (d, $^3J_{H\text{-}H}$ = 6.5 Hz, 3 H, H-17 or H-18); δ ^{13}C (determined by HMQC and HMBC experiments) 173.5 (C-2), 170.9(C-5), 167.8 (C-8), 51.6 (C-9), 50.4 (C-3), 49.9 (C-13), 47.8 (C-6), 40.9 (C-15), 30.4 (C-10), 27.4 (C-12) 24.0 (C-16), 22.6 (C-17 or C-18), 21.2 (C-17 or C-18), 21.0 (C-11), 17.7 (C-14).

Peptide S4

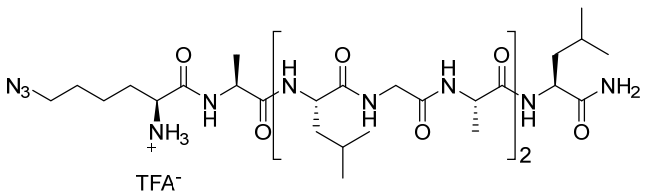

70.0 mg (75.0 μmol, 83%).

UPLC-MS Method 1, T_R = 2.84 min; m/z MS (ES+): 838.2 [100%, M + H^+], 821.7 [10%], 420.1 [60%, M + 2 H^+], 411.2 [30%]; HRMS: calculated for: $C_{37}H_{68}N_{13}O_9^+$: 838.5257; found 838.5253; ^{1}H-NMR: (500 MHz, DMSO-d_6, 298 K) δ 8.56 (d, $^3J_{H\text{-}H}$ = 7.5 Hz, 1 H, amide), 8.16- 8.10 (m, 2 H, amide), 8.07 (t, $^3J_{H\text{-}H}$ = 5.6 Hz, 1 H, amide), 7.99 (d, $^3J_{H\text{-}H}$ = 7.7 Hz, 1 H, amide), 7.97 (d, $^3J_{H\text{-}H}$ = 7.2 Hz, 1 H, amide), 7.94 (d, $^3J_{H\text{-}H}$ = 7.0 Hz, 1 H, amide), 7.15 (s, 1 H, amid C-terminus), 6.96 (s, 1 H, amid C-terminus), 4.40 (p, $^3J_{H\text{-}H}$ = 7.1 Hz, 1 H, H-C_α), 4.33-4.14 (m, 5 H, H-C_α), 3.77-3.64 (m, 5 H, H-C_α), 3.34-3.25 (m, 2 H, H-$C_{\varepsilon(Lys)}$), 1.71-1.43 (m, 13 H, H-$C_{\beta(lys)}$, H-$C_{\delta\ (lys)}$, H-$C_{\beta(leu)}$, H-$C_{\gamma(leu)}$), 1.39-1.31 (m, 2 H, H-$C_{\gamma(lys)}$), 1.24 (d, $^3J_{H\text{-}H}$ = 7.0 Hz, 3 H, H-$C_{\beta(ala)}$), 1.21 (d, $^3J_{H\text{-}H}$ = 7.0 Hz, 6 H, H-$C_{\beta(ala)}$), 0.90-0.86 (m, 9 H, H-$C_{\delta(leu)}$), 0.85-0.83 (m, 9 H, H-$C_{\delta(leu)}$).

Compound S5

(3-Bromo-4-nitrophenyl)methanol (348 mg, 1.50 mmol, 1.00 eq.) was dissolved in triethylamine (15 mL). The solution was degassed by bubbling with nitrogen for 20 min before CuI (5.7 mg, 2 mol% and tetrakis-(triphenylphosphine)palladium (17.3 mg, 1 mol%) were added and the reaction mixture degassed for another 10 min. Trimethylsilylacetylene (320 µl, 2.25 mmol, 1.50 eq.) was added and the reaction stirred under reflux overnight. After filtration through Celite, *tert*-butyl methyl ether (100mL) was added and the solution was washed with water (2 × 100 mL) and brine (100 mL). Volatiles were removed under reduced pressure and the residue purified by column chromatography (cyclohexane /ethyl acetate, 10:1). **S5** was isolated as a slightly yellow solid (267 mg, 1.07 mmol, 71%).

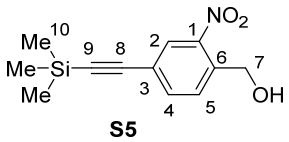

S5

^{1}H-NMR (500 MHz, MeOH-d_4, 298 K) δ 8.04 (s , 1 H, H-2), 7.83 (d, $^3J_{H\text{-}H}$ = 8.1 Hz, 1 H, H-5), 7.72 (d, $^3J_{H\text{-}H}$ = 8.1 Hz, 1 H, H-4), 4.93 (s, 2 H, H-7), 0.26 (s, 9 H, H-14); δ ^{13}C (determined by HMQC and HMBC experiments) δ 148.0 (C-1), 139.2 (C-6), 137.0 (C-4), 129.4 (C-5), 127.9 (C-2), 123.9 (C-3), 103.0 (C-8), 96.8 (C-9), 61.3(C-7), -0.6 (C-10).

Compound S6

S5 (249 mg, 1.00 mmol, 1.00 eq.), sodium 2,3,5,6-tetrafluoro-4-hydroxybenzenesulfonate (268 mg, 1.00 mmol, 1.00 eq.) and triphenylphosphine (315 mg, 1.20 mmol, 1.20 eq.) were dissolved in dry DMF and cooled to 0°C. Diisopropyl-azodicarboxylate (294 µl, 1.50 mmol, 1.50 eq.) was added dropwise over 15 min. After completed addition the reaction was allowed to warm to room temperature and stirring continued overnight. For work up volatiles were removed under reduced pressure and the remaining residue subjected to prep HPLC. After lyophilisation **S6** was isolated as a brown solid (155 mg, 0.325 mmol, 33%).

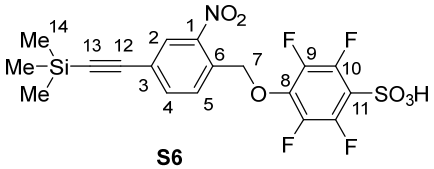

S6

UPLC-MS Method 1, T_R = 5.47 min; m/z MS (ES-): 476.8 [100%, M - H^+]. ^{1}H-NMR (500 MHz, DMSO-d_6, 298 K) δ 8.15 (d, $^4J_{H\text{-}H}$ = 1.6 Hz, 1 H, H-2), 7.89 (dd, $^3J_{H\text{-}H}$ = 8.1 Hz, $^4J_{H\text{-}H}$ = 1.6 Hz, 1 H, H-4), 7.85 (d, $^3J_{H\text{-}H}$ = 8.1 Hz, 1 H, H-5), 5.65 (s, 2 H, H-7), 0.26 (s, 9 H, H-14); δ ^{13}C (determined by HMQC and HMBC experiments) δ 147.1 (C-1), 144.1 (C-9 or C-10), 142.1 (C-9 or C-10), 136.5 (C-4), 136.2 (C-8), 132.0 (C-6), 130.1 (C-5), 127.6 (C-2), 123.3 (C-3), 121.4 (C-11) 102.1 (C-12), 97.8 (C-13), 72.4 (C-7), -0.3 (C-14).

Compound S7

2-*N,N,N*-trimethylammonium ethylamine × TFA was synthesized as described elsewhere.[2]

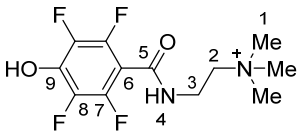

S7

2-*N,N,N*-trimethylammonium ethylamine × TFA (1.51 g, 7.00 mmol, 1.00 eq.), 2,3,5,6-tetrafluoro-4-hydroxybenzoic acid (1.47 g, 7.00 mmol, 1.00 eq.), HBTU (2.92 g, 7.70 mmol, 1.10 eq.) and DIPEA (5.78 mL, 35.0 mmol, 5.00 eq.) were dissolved in DMF (200 mL) and stirred overnight at room temperature. Full conversion was proved by UPLC-MS. The solvent was removed under reduced pressure and the crude was directly used for the next step without purification. For analytical batch the crude was purified by preparative revers phase HPLC.

UPLC-MS method 2, T_R = 3.41 min; m/z MS (ES+): 294.9 [100%, M^+], 589.3 [10%, 2 M^+-H^+]; HRMS: calculated for: $C_{12}H_{15}F_4N_2O_2^+$: 295.1064; found 295.1066; ^{1}H-NMR (500 MHz, DMSO-d_6, 298 K) δ 9.06 (t, $^3J_{H\text{-}H}$ = 5.7 Hz, 1 H, H-4), 3.70 (td, $^3J_{H\text{-}H}$ = 6.8 Hz, $^3J_{H\text{-}H}$ = 5.7 Hz, 2 H, H-3), 3.49 (t, $^3J_{H\text{-}H}$ = 6.8 Hz, 2 H, H-2), 3.13 (s, 9 H, H-1); ^{13}C (determined by HMQC and HMBC experiments) δ 158.2 (C-5), 63.0 (C-2), 52.3 (C-1), 33.2 (C-3), C-6, C-7, C-8 and C-9 not visible.

Compound S8

S7 (crude, 1.60 g, 1.90 mmol. 1.00 eq.), **S5** (474 mg, 1.90 mmol, 1.00 eq.) and PPh_3 (648 mg, 2.47 mmol, 1.30 eq.) were dissolved in dry DMF and cooled down to 0 °C, then DIAD (560 µl, 2.85 mmol, 1.50 eq.) were added slowly and the reaction was stirred at room temperature for 5 h. The solvent was removed under reduced pressure and the crude was purified by preparative revers phase HPLC. After lyophilisation **S8** was isolated as a brown solid (98.0 mg, 0.186 mmol, 10%).

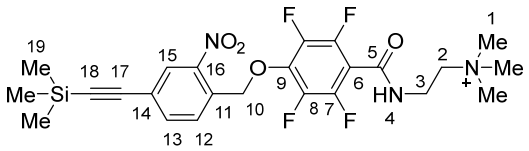

S8

UPLC-MS method 1, T_R = 4.82 min; m/z MS (ES+): 526.2 [100%, M^+], 1051.7 [10%, 2 M^+-H^+]; HRMS: calculated for: $C_{24}H_{28}F_4N_3O_4Si^+$: 526.1780; found 526.1780; ^{1}H-NMR (500 MHz, DMSO-d_6, 298 K) δ 9.21 (t, $^3J_{H\text{-}H}$ = 5.8 Hz, 1 H, H-4), 8.17 (d, $^4J_{H\text{-}H}$ = 1.7 Hz, 1 H, H-15), 7.93 (dd, $^3J_{H\text{-}H}$ = 8.0 Hz, $^4J_{H\text{-}H}$ = 1.7 Hz, 1 H, H-13), 7.87 (d, $^3J_{H\text{-}H}$ = 8.0 Hz, 1 H, H-11), 5.72 (s, 2 H, H-10), 3.73 (td, $^3J_{H\text{-}H}$ = 6.8 Hz, $^3J_{H\text{-}H}$ = 5.8 Hz, 2 H, H-3), 3.49 (t, $^3J_{H\text{-}H}$ = 6.8 Hz, 2 H, H-2), 3.14 (s, 9 H, H-1), 0.26 (s, 9 H, H-19); ^{13}C (determined by HMQC and HMBC experiments) δ 157.7 (C-5), 147.3 (C-16), 137.5 (C-8), 136.5 (C-13), 131.6 (C-11), 130.0 (C-12), 127.6 (C-15), 123.4 (C-14), 101.8 (C-17), 97.8 (C-18), 72.4 (C-10), 63.0 (C-2), 52.4 (C-1), 33.5 (C-3), -0.5 (C-19), C-6, C-7, C-8 and C-9 not visible.

Photocleavable tripeptide 1-neg-LG

General procedure 1. To a suspension of **S1** (20.0 mg, 56.2 µmol, 2.00 eq.) and **S6** (13.9 mg, 28.1 µmol, 1.00 eq.) in water / *tert*-butanol (1 : 1, 5 mL) was added aq. sodium ascorbate (1 M, 200 µl, 7.12 eq.) and aq. $CuSO_4$ (1 M, 20 µl, 0.71 eq.) and the resulting mixture was stirred for 4 h at 55 °C. Subsequently volatiles were removed under reduced pressure and the resulting residue was purified by reversed phase HPLC. The product was obtained as a white powder after lyophilisation (6.4 mg, 8.4 µmol, 30%).

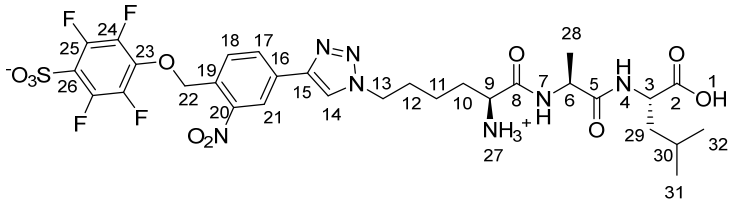

UPLC-MS Method 1, T_R = 3.52 min; m/z MS (ES-): 760.9 [100%, M - H^+], 380.2 [20%, M - 2H^+]; HRMS: calculated for: $C_{30}H_{35}F_4N_7NaO_{10}S^+$: 784.1994; found 784.2001. ^{1}H-NMR (500 MHz, DMSO-d_6, 298 K) δ 8.83 (s, 1 H, H-14), 8.58 (d, $^3J_{H\text{-}H}$ = 7.6 Hz, 1 H, H-7), 8.56 (d, $^4J_{H\text{-}H}$ = 1.8 Hz, 1 H, H-21), 8.25 (dd, $^3J_{H\text{-}H}$ =-8.0 Hz, $^4J_{H\text{-}H}$ = 1.8 Hz, 1 H, H-17), 8.22 (d, $^3J_{H\text{-}H}$ = 8.1 Hz, 1 H, H-4), 8.04 (b, 3 H, H-27), 7.92 (d, $^3J_{H\text{-}H}$ = 8.1 Hz, 1 H, H-18), 5.68 (s, 2 H, H-22), 4.45-4.36 (m, 3 H, H-13 and H-6), 4.23 (ddd ($^3J_{H\text{-}H}$ =9.3 Hz, $^3J_{H\text{-}H}$ =8.0 Hz, $^3J_{H\text{-}H}$ = 5.8 Hz, 1 H, H-3), 3.75 (b, 1 H, H-9), 1.89 (p, $^3J_{H\text{-}H}$ = 7.1 Hz, 2 H, H-12), 1.75-1.69 (m, 2 H, H-10), 1.67-1.59 (m, 1 H, H-30), 1.57-1.47 (m, 2 H, H-29), 1.38-1.29 (m, 2 H, H-11), 1.25 (d, $^3J_{H\text{-}H}$ = 7.0 Hz, 3 H, H-28), 0.88 (d, $^3J_{H\text{-}H}$ = 6.6 Hz, 3 H, H-31 or H-32), 0.83 (d, $^3J_{H\text{-}H}$ = 6.5 Hz, 3 H, H-31 or H-32); ^{13}C (determined by HMQC and HMBC experiments) δ 173.5 (C-2), 171.3 (C-5), 167.8 (C-8), 147.7 (C-20), 143.7 (C-15), 132.2 (C-16), 130.7 (C-18), 129.9 (C-19), 129.6 (C-17), 122.5 (C-14), 120.6 (C-21), 72.2 (C-22), 51.6 (C- 9), 49.9 (C-3), 49.2 (C-13), 47.7 (C-6), 39.6 (C-29), 30.4 (C-10), 28.7 (C-12), 24.1 (C-30), 22.6 (C-31 or C-32), 21.0 (C-31 or C-32), 20.9 (C-11), 17.9 (C-28). C-23, 24, 25 and 26 are not visible).

Photocleavable tripeptide 2-neg-LG

The synthesis followed the protocol for the synthesis of **1-neg-LG** (*General procedure 1*) starting with **S3** (20 mg, 56.2 μmol, 2.00 eq.). The modified peptide was isolated as a white solid (6.0 mg, 7.9 μmol, 28%).

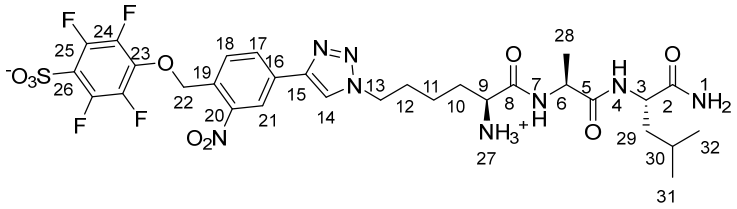

UPLC-MS method 1, T_R = 3.40 min; m/z MS (ES-): 760.1 [100%, M - H^+], 379.7 [20%, M - $2H^+$]; HRMS: calculated for: $C_{30}H_{36}F_4N_8NaO_9S^+$: 783.2154; found 783.2142; ^{1}H-NMR (500 MHz, DMSO-d_6, 298 K) δ 8.83 (s, 1 H, H-14), 8.58 (d, $^3J_{H\text{-}H}$ = 7.6 Hz, 1 H, H-7), 8.56 (d, $^4J_{H\text{-}H}$ = 1.8 Hz, 1 H, H-21), 8.25 (dd, $^3J_{H\text{-}H}$ = 8.0 Hz, $^4J_{H\text{-}H}$ = 1.8 Hz, 1 H, H-17), 8.04 (b, 3 H, H-27), 7.95 (d, $^3J_{H\text{-}H}$ = 8.4 Hz, 1 H, H-4), 7.92 (d, $^3J_{H\text{-}H}$ = 8.1 Hz, 1 H, H-18), 7.34 (b, 1 H, H-1), 6.98 (b, 1 H, H-1), 5.68 (s, 2 H, H-22), 4.46-4.32 (m, 3 H, H-13 and H-6), 4.30-4.20 (m, 1 H, H-3), 3.75 (b, 1 H, H-9), 1.89 (p, $^3J_{H\text{-}H}$ = 7.1 Hz, 2 H, H-12), 1.75-1.69 (m, 2 H, H-10), 1.62-1.53 (m, 1 H, H-30), 1.48-1.41 (m, 2 H, H-29), 1.38-1.29 (m, 2 H, H-11), 1.24 (d, $^3J_{H\text{-}H}$ = 7.0 Hz, 3 H, H-28), 0.87 (d, $^3J_{H\text{-}H}$ = 6.6 Hz, 3 H, H-31 or H-32), 0.83 (d, $^3J_{H\text{-}H}$ = 6.5 Hz, 3 H, H-31 or H-32). ^{13}C (determined by HMQC and HMBC experiments) δ 173.4 (C-2), 170.8 (C-5), 167.7(C-8), 147.7 (C-20), 143.7 (C-15), 132.2 (C-16), 130.7 (C-18), 129.9 (C-19), 129.6 (C-17), 122.5 (C-14), 120.6 (C-21), 72.2 (C-22), 51.6 (C- 9), 50.5 (C-3), 49.2 (C-13), 47.9 (C-6), 40.7 (C-29), 30.4 (C-10), 28.7 (C-12), 23.8 (C-30), 22.8 (C-31 or C-32), 21.3 (C-31 or C-32), 20.8 (C-11), 17.8 (C-28). C-23, C-24, C-25 and C-26 are not visible).

Photoclevable nonapeptide 3-neg-LG

The synthesis followed the protocol for the synthesis of **1-neg-LG** (*General procedure 1*) starting with **S2** (34.0 mg, 40.5 μmol, 2.00 eq.). The modified peptide was isolated as a white solid (7.0 mg, 5.5 μmol, 27%).

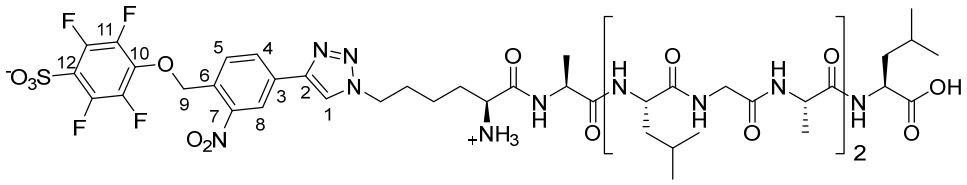

UPLC-MS Method 1, T_R = 3.67 min; m/z MS (ES+): 1243.3 [100%, M + H^+], 621.5 [30%, M + $2H^+$]; HRMS: calculated for: $C_{52}H_{73}F_4N_{13}NaO_{16}S^+$: 1266.4847; found 1266.4842; ^{1}H-NMR (500 MHz, DMSO-d_6, 298 K) δ 8.83 (s, 1 H, H-1), 8.57 (d, $^3J_{H\text{-}H}$ = 7.6 Hz, 1 H, amid), 8.56 (d, $^4J_{H\text{-}H}$ = 1.8 Hz, 1 H, H-8) 8.25 (dd, $^3J_{H\text{-}H}$ = 8.0 Hz, $^4J_{H\text{-}H}$ = 1.8 Hz, 1 H, H-4), 8.14 - 8.00 (m, 7 H, 4 amide, 3 amonium), 7.99 (d, $^3J_{H\text{-}H}$ = 7.8 Hz,

1 H, amid), 7.95 (d, $^{3}J_{H\text{-}H}$ = 7.4 Hz, 1 H, amid),7.92 (d, $^{3}J_{H\text{-}H}$ = 8.1 Hz, 1 H, H-5), 7.84 (d, $^{3}J_{H\text{-}H}$ = 7.6 Hz, 1 H, amid), 5.68 (s, 2 H, H-9), 4.44-4.35 (m, 3 H, 2 H-$C_{\varepsilon(Lys)}$ and H-C_{α}), 4.35-4.16 (m, 5 H, H-C_{α}), 3.77-3.62 (m, 5 H, H-C_{α}), 1.89 (p, $^{3}J_{H\text{-}H}$ = 7.3 Hz, 2 H, H-$C_{\delta\ (lys)}$), 1.75-1.67 (m, 2 H, H-$C_{\beta(lys)}$), 1.66-1.57 (m, 3 H, H-$C_{\gamma(leu)}$), 1.56-1.43 (m, 6 H, H-$C_{\beta(leu)}$), 1.38-1.31 (m, 2 H, H-$C_{\gamma(lys)}$), 1.24 (d, $^{3}J_{H\text{-}H}$ = 7.1 Hz, 3 H, H-$C_{\beta(ala)}$), 1.20(d, $^{3}J_{H\text{-}H}$ = 7.2 Hz, 6 H, H-$C_{\beta(ala)}$), 0.91-0.85 (m, 9 H, H-$C_{\delta(leu)}$), 0.85-0.80 (m, 9 H, H-$C_{\delta(leu)}$).

Photocleavable nonapeptide 4-neg-LG

The synthesis followed the protocol for the synthesis of **1-neg-LG** (*General procedure 1*) starting with **S4** (17.0 mg, 40.6 μmol, 2.00 eq.). The modified peptide was isolated as a white solid (6.0 mg, 4.7 μmol, 23%).

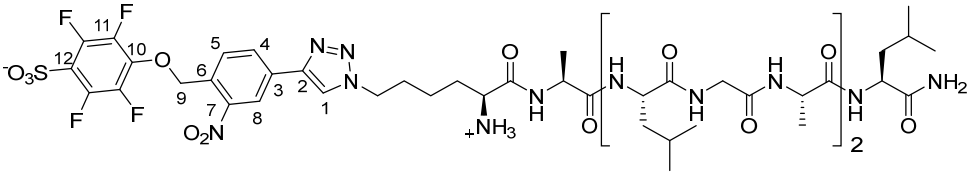

UPLC-MS Method 1, T_R = 3.70 min; m/z MS (ES+): 1242.5 [100%, M + H^+], 621.1 [20%, M + $2H^+$]; HRMS: calculated for: $C_{52}H_{74}F_4N_{14}NaO_{15}S^+$: 1265.5007; found 1265.5004; ^{1}H-NMR (500 MHz, DMSO-d_6, 298 K) δ 8.83 (s, 1 H, H-1), 8.58 (d, $^{3}J_{H\text{-}H}$ = 7.8 Hz, 1 H, amid), 8.56 (d, $^{4}J_{H\text{-}H}$ = 1.8 Hz, 1 H, H-8) 8.25 (dd, $^{3}J_{H\text{-}H}$ = 8.0 Hz, $^{4}J_{H\text{-}H}$ = 1.8 Hz, 1 H, H-4), 8.14 - 7.90 (m, 6 H, 4 amide, 3 ammonium), 7.99 (d, $^{3}J_{H\text{-}H}$ = 7.8 Hz, 1 H, amid), 7.97 (d, $^{3}J_{H\text{-}H}$ = 7.1 Hz, 1 H, amid),7.94 (d, $^{3}J_{H\text{-}H}$ = 7.4 Hz, 1 H, amid) 7.92 (d, $^{3}J_{H\text{-}H}$ = 8.2 Hz, 1 H, H-5), 7.78 (d, $^{3}J_{H\text{-}H}$ = 8.4 Hz, 1 H, amid), 7.14 (s, 1 H, $CONH_2$), 6.96 (s, 1 H, $CONH_2$), 5.68 (s, 2 H, H-9), 4.47-4.13 (m, 9 H, 2 H-$C_{\varepsilon(Lys)}$ and 7 H-C_{α}), 3.79-3.64 (m, 4 H, H-C_{α}), 1.93-1.85 (m, 2 H, H-$C_{\delta\ (lys)}$), 1.74-1.67 (m, 2 H, H-$C_{\beta(lys)}$), 1.64-1.54 (m, 3 H, H-$C_{\gamma(leu)}$), 1.52-1.43 (m, 6 H, H-$C_{\beta(leu)}$), 1.38-1.29 (m, 2 H, H-$C_{\gamma(lys)}$), 1.24 (d, $^{3}J_{H\text{-}H}$ = 7.1 Hz, 3 H, H-$C_{\beta(ala)}$), 1.20 (d, $^{3}J_{H\text{-}H}$ = 7.2 Hz, 6 H, H-$C_{\beta(ala)}$), 0.91-0.85 (m, 9 H, H-$C_{\delta(leu)}$), 0.85-0.80 (m, 9 H, H-$C_{\delta(leu)}$).

Photocleavable tripeptide 1-pos-LG

The synthesis followed the protocol for the synthesis of **1-neg-LG** (*General procedure 1*) starting with **S1** (20.0 mg, 56.2 μmol, 2.00 eq.) and **S8** (14.8 mg, 28.1 μmol, 1.00 eq.). The modified peptide was isolated as a white solid (4.5 mg, 4.5 μmol, 16%).

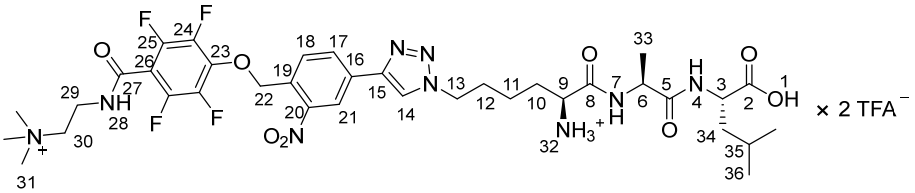

UPLC-MS Method 2, T_R = 4.24 min; m/z MS (ES+): 810.4 [60%, M^+], 405.6 [100%, M^+ + H^+]; HRMS: calculated for: $C_{36}H_{48}F_4N_9O_8^+$: 810.3556; found 810.3564; ^{1}H-NMR (500 MHz, DMSO-d_6, 298 K) δ 9.25

(t, $^{3}J_{H\text{-}H}$ = 5.8 Hz, 1 H, H-28), 8.85 (s, 1 H, H-14), 8.60 (d, $^{3}J_{H\text{-}H}$ = 7.5 Hz, 1 H, H-7), 8.58 (d, $^{4}J_{H\text{-}H}$ = 1.8 Hz, 1 H, H-21), 8.29 (dd, $^{3}J_{H\text{-}H}$ = 8.1 Hz, $^{4}J_{H\text{-}H}$ = 1.8 Hz, 1 H, H-17), 8.23 (d, $^{3}J_{H\text{-}H}$ = 8.0 Hz, 1 H, H-4), 8.09 (b, 3 H, H-32), 7.96 (d, $^{3}J_{H\text{-}H}$ = 8.1 Hz, 1 H, H-18), 5.74 (s, 2 H, H-22), 4.46-4.36 (m, 3 H, H-13 and H-6), 4.22 (ddd, $^{3}J_{H\text{-}H}$ = 9.4 Hz, $^{3}J_{H\text{-}H}$ = 8.0 Hz, $^{3}J_{H\text{-}H}$ = 5.6 Hz, 1 H, H-3), 3.77 (b, 1 H, H-9), 3.73 (td, , $^{3}J_{H\text{-}H}$ = 6.9 Hz , $^{3}J_{H\text{-}H}$ = 5.8 Hz, 2 H, H-29), 3.50 (t , $^{3}J_{H\text{-}H}$ = 6.9 Hz, 2 H, H-30), 3.14 (s, 9 H, H-31), 1.93-1.85 (m, 2 H, H-12), 1.77-1.70 (m, 2 H, H-10), 1.66-1.58 (m, 1 H, H-35), 1.55-1.49 (m, 2 H, H-34), 1.40-1.33 (m, 2 H, H-11), 1.25 (d, $^{3}J_{H\text{-}H}$ = 7.0 Hz, 3 H, H-33), 0.88 (d, $^{3}J_{H\text{-}H}$ = 6.6 Hz, 3 H, H-36), 0.82 (d, $^{3}J_{H\text{-}H}$ = 6.5 Hz, 3 H, H-36);^{13}C (determined by HMQC and HMBC experiments) δ 173.7 (C-2), 171.4 (C-5), 167.7 (C-8), 157.6 (C-27), 147.7 (C-20), 143.6 (C-15), 137.6 (C-23), 132.3 (C-16), 130.6 (C-18), 129.8 (C-17 and C-19), 122.5 (C-14), 120.7 (C-21), 72.6 (C-22), 62.7 (C-30), 52.4 (C-31), 51.6 (C-9), 49.9 (C-3), 49.1 (C-13), 47.7 (C-6), 39.7 (C-34), 33.4 (C-29), 30.3 (C-10), 28.8 (C-12), 24.1 (C-35), 22.6 (C-36), 21.0 (C-36), 20.9 (C-11), 17.9 (C-33).

Photocleavable nonapeptide 3-pos-LG

The synthesis followed the protocol for the synthesis of **1-neg-LG** (*General procedure 1*) starting with **S1** (25.5 mg, 30.4 μmol, 2.00 eq.) and **S8** (8.0 mg, 15.2 μmol, 1.00 eq.). The modified peptide was isolated as a white solid (5.7 mg, 3.8 μmol, 25%).

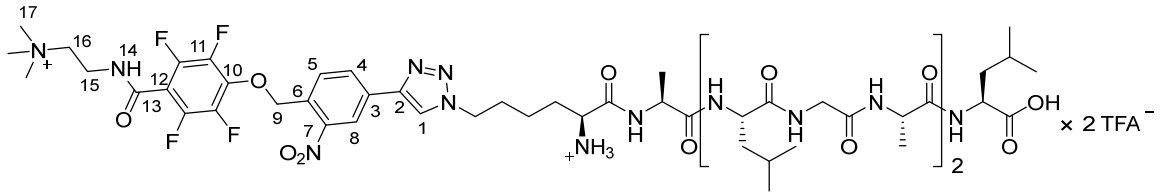

UPLC-MS Method 2, T_R = 4.44 min; m/z MS (ES+): 1292.6 [50%, M^+], 646.9 [100%, $M^+ + H^+$], 431.7 [80%, $M^+ + 2\ H^+$]; HRMS: calculated for: $C_{58}H_{86}F_4N_{15}O_{14}^+$: 1292.6409; found 1292.6384; ^{1}H-NMR (500 MHz, DMSO-d_6, 298 K) δ 9.23 (t, 1 H, H-14), 8.85 (s, 1 H, H-1), 8.59 (d, $^{3}J_{H\text{-}H}$ = 6.5 Hz, 1 H, amide), 8.58 (d, $^{4}J_{H\text{-}H}$ = 1.8 Hz, 1 H, H-8) 8.29 (dd, $^{3}J_{H\text{-}H}$ = 8.0 Hz, $^{4}J_{H\text{-}H}$ = 1.8 Hz, 1 H, H-4), 8.16- 8.02 (m, 8 H, 4 amide, 3 ammonium), 8.00 (d, $^{3}J_{H\text{-}H}$ = 7.8 Hz, 1 H, amide), 7.98-7.93 (m, 2 H, H-5 and amide), 7.85 (d, $^{3}J_{H\text{-}H}$ = 7.5 Hz, 1 H, amide), 5.75 (s, 2 H, H-9), 4.46-4.37 (m, 3 H, 2 H-$C_{\varepsilon(Lys)}$ and H-C_{α}), 4.35-4.16 (m, 5 H, H-C_{α}), 3.77-3.62 (m, 7 H, H-C_{α} and H-16), 3.50 (t, $^{3}J_{H\text{-}H}$ = 6.9 Hz), 3.14 (s, 9 H, H-17), 1.93-1.85 (m, 2 H, H-$C_{\delta\ (lys)}$), 1.75-1.67 (m, 2 H, H-$C_{\beta(lys)}$), 1.66-1.42 (m, 9 H, H-$C_{\gamma(leu)}$, H-$C_{\beta(leu)}$), 1.41-1.32 (m, 2 H, H-$C_{\gamma(lys)}$), 1.25 (d, $^{3}J_{H\text{-}H}$ = 7.0 Hz, 3 H, H-$C_{\beta(ala)}$), 1.20(d, $^{3}J_{H\text{-}H}$ = 7.2 Hz, 6 H, H-$C_{\beta(ala)}$), 0.91-0.85 (m, 9 H, H-$C_{\delta(leu)}$), 0.85-0.80 (m, 9 H, H-$C_{\delta(leu)}$).

Compound S9

To a suspension of 2-azidoacetic acid (28.2 mg, 279 µmol, 1.50 eq.) and **S6** (88.8 mg, 186 µmol, 1.00 eq.) in water / *tert*-butanol (1 : 1, 10 mL) was added aq. sodium ascorbate (1.00 M, 186 µl, 1.00 eq.) and aq. $CuSO_4$ (1.00 M, 37.0 µl, 0.20 eq.) and the resulting mixture was stirred for 2 h at 55 °C. Subsequently volatiles were removed under reduced pressure and the resulting residue was purified by reversed phase HPLC. The product was obtained as a white powder after lyophilisation (26.0 mg, 49.2 µmol 27%).

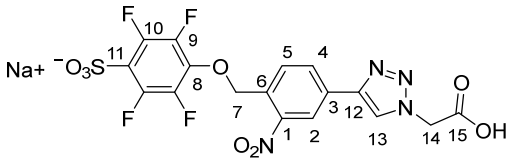

S9

UPLC-MS method 1, T_R = 3.40 min; m/z MS (ES-): 505.0 [100%, M - H^+], 251.9 [20%, M – 2 H^+]; ^{1}H-NMR (500 MHz, D_2O, 298 K) δ 8.52 (d, $^4J_{H\text{-}H}$ = 1.8 Hz, 1 H, H-2), 8.48 (s, 1 H, H-13), 8.12 (dd, $^3J_{H\text{-}H}$ = 8.1 Hz, $^4J_{H\text{-}H}$ = 1.8 Hz, 1 H, H-4), 7.87 (d, $^3J_{H\text{-}H}$ = 8.1 Hz, 1 H, H-5), 5.71 (s, 2 H, H-7), 5.40 (s, 2 H, H-14); ^{13}C (determined by HMQC and HMBC experiments) δ 171.4 (C-15), 148.0 (C-1), 145.7 (C-12), 139.1 (C-8), 132.0 (C-6), 131.9 (C-3), 131.6 (C-4), 131.5 (C-5), 125.1 (C-13), 122.7 (C-2), C-9, C-10 and C-11 are not visible.

Compound S10

To a suspension of 2-azidoacetic acid (115 mg, 1.00 mmol, 2.00 eq.) and **S8** (320 mg, 0.50 mmol, 1.00 eq.) in water / *tert*-butanol (1 : 1, 20 mL) was added aq. sodium ascorbate (1 M, 500 µl, 1.0 eq.) and aq. $CuSO_4$ (1 M, 100 µl, 0.2 eq.) and the resulting mixture was stirred for 2 h at 55 °C. Subsequently volatiles were removed under reduced pressure and the resulting residue was purified by reversed phase HPLC. The product was obtained as a white powder after lyophilisation (280 mg, 429 µmol, 86%).

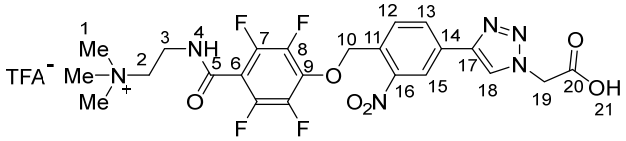

S10

UPLC-MS method 2, T_R = 4.34 min; m/z MS (ES+): 554.7 [100%, M^+], 251.9 [50%, M^+ + H^+]; HRMS: calculated for: $C_{23}H_{23}F_4N_6O_6^+$: 555.1610; found 555.1612; ^{1}H-NMR (500 MHz, DMSO-d_6, 298 K) δ 9.27 (t, $^3J_{H\text{-}H}$ = 5.7 Hz, 1 H, H-4), 8.82 (s, 1 H, H-18), 8.61 (d, $^4J_{H\text{-}H}$ = 1.8 Hz, 1 H, H-15), 8.32 (dd, $^3J_{H\text{-}H}$ = 8.0 Hz, $^4J_{H\text{-}H}$ = 1.8 Hz, 1 H, H-13), 7.95 (d, $^3J_{H\text{-}H}$ = 8.0 Hz, H-12), 5.75 (s, 2 H, H-10), 5.36 (s, 2 H, H-19), 3.73 (q, $^3J_{H\text{-}H}$ = 6.5 Hz, 2 H, H-3), 3.50 (t, $^3J_{H\text{-}H}$ = 6.8 Hz, 2 H, H-2), 3.14 (s, 9 H, H-1), ^{13}C (determined by HMQC and HMBC experiments) δ 168.9 (C-20), 158.3 (C-5), 148.4 (C-16), 144.3 (C-17), 138.2 (C-9), 131.5 (C-11), 130.6 (C-12), 129.7 (C-13), 124.0 (C-18), 120.6 (C-15), 72.5 (C-10), 62.8 (C-2), 52.2 (C-1), 50.7 (C-19), 33.4 (C-3), C-6, C-7 and C-8 are not visible.

Human insulin modified with negatively charged photocleavable groups

neg-ins

S9 (10.0 mg, 18.9 µmol, 3.84 eq.), TSTU (5.90 mg, 19.7 µmol, 4.00 eq.) and DIPEA (6.5 µl 39.4 µmol, 8.00 eq.), were dissolved in DMF (2 mL) and stirred for 1 h at room temperature. Then the solution was added to insulin (30.0 mg, 4.93 µmol, 1.00 eq.) dissolved in DMF(2 mL) and stirred for 2 h a room temperature afterwards the solvent was removed under reduced pressure and the crude was purified by preparative HPLC. **neg-ins** was isolated after lyophilisation (2.1 mg, 0.31 µmol, 18%).

UPLC-MS method 1, T_R = 4.00 min; m/z MS (ES+): 1455.7 [30%, M^{3-}+ 8 H^+], 1819.0 [80%, M^{3-}+ 7 H^+], 2425.2 [100%, M^{3-}+ 6 H^+].

Human insulin modified with positively charged photocleavable groups

pos-ins

S10 (9.3 mg, 14.2 µmol, 2.54 eq.), TSTU (5.1 mg, 16.8 µmol, 3.00 eq.), DIPEA (2.8 µl, 16.8 µmol, 3.00 eq.), were dissolved in DMF (1 mL) and stirred for 1 h at room temperature. Then the solution was added to insulin (32.5 mg, 5.60 µmol, 1.00 eq.) dissolved in DMF (10 mL) and stirred for 2 h a room temperature afterwards the solvent was removed under reduced pressure and the crude was purified by preparative HPLC. **pos-ins** was isolated after lyophilisation (3.4 mg, 0.46 µmol, 8%).

UPLC-MS method 1, T_R = 4.00 min; m/z MS (ES+): 928.2 [20%, M^{3+}+ 5 H^+], 1060.6 [60%, M^{3+}+ 4 H^+], 1237.1 [100%, M^{3+}+ 3 H^+], 1484.4 [60%, M^{3+}+ 2 H^+], 1855.5 [20%, M^{3+}+ H^+].

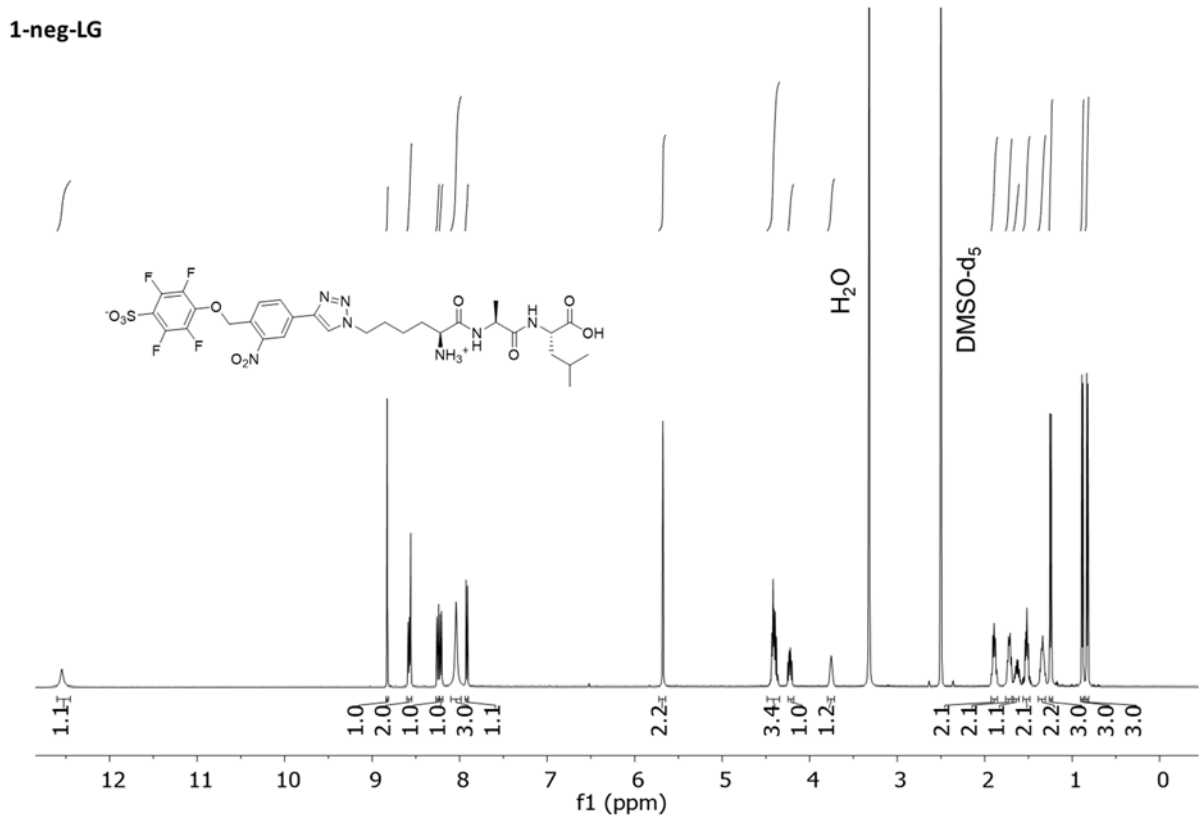

Figure S7. ^{1}H-NMR (DMSO-d_6, 500 MHz, 298 K) of **1-neg-LG.**

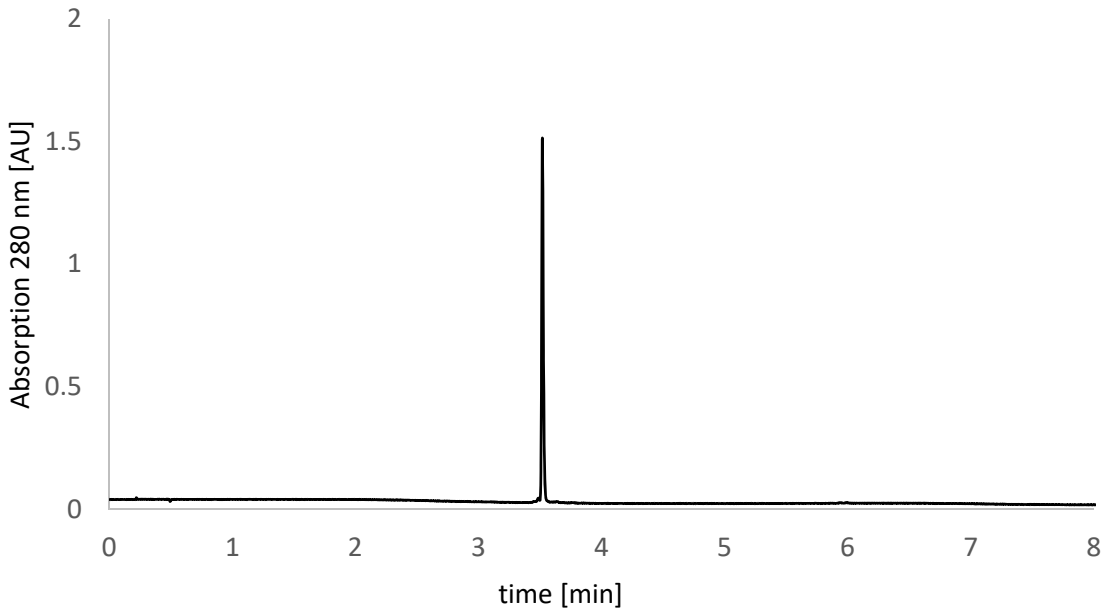

Figure S8. UPLC-chromatogram of **1-neg-LG.**

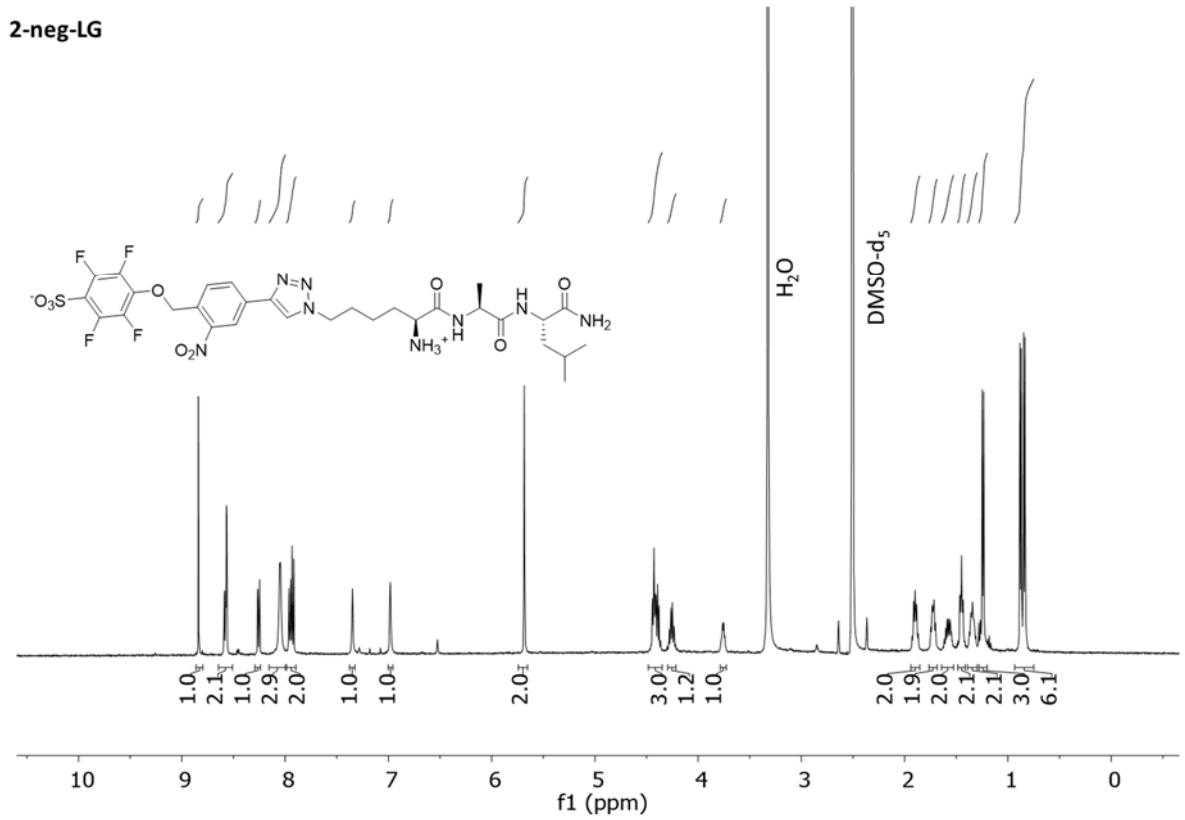

Figure S9. ^{1}H-NMR (DMSO-d_6, 500 MHz, 298 K) of **2-neg-LG.**

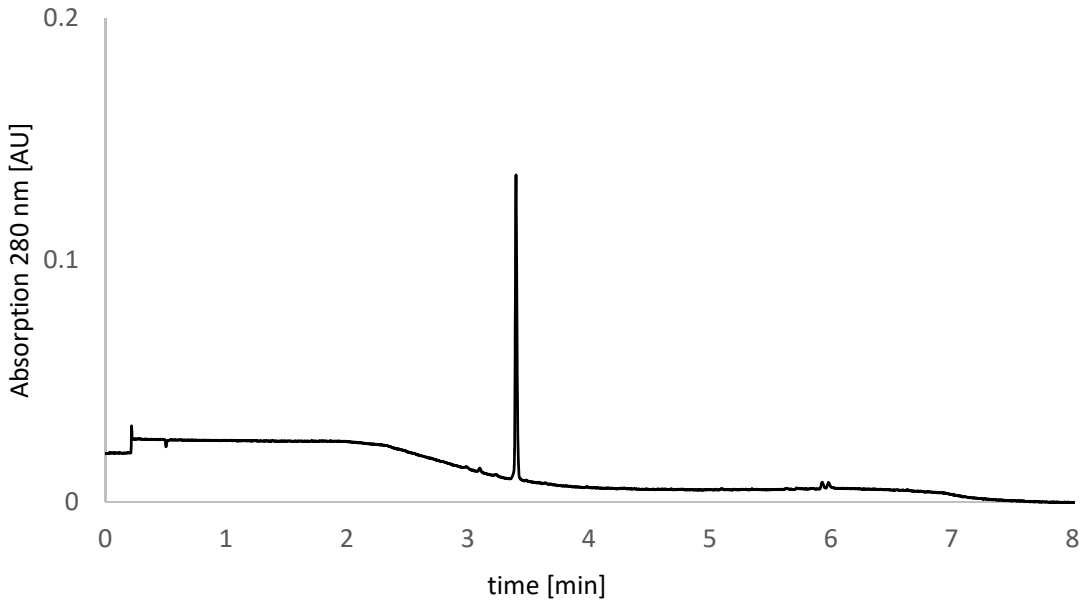

Figure S10. UPLC-chromatogram of **2-neg-LG.**

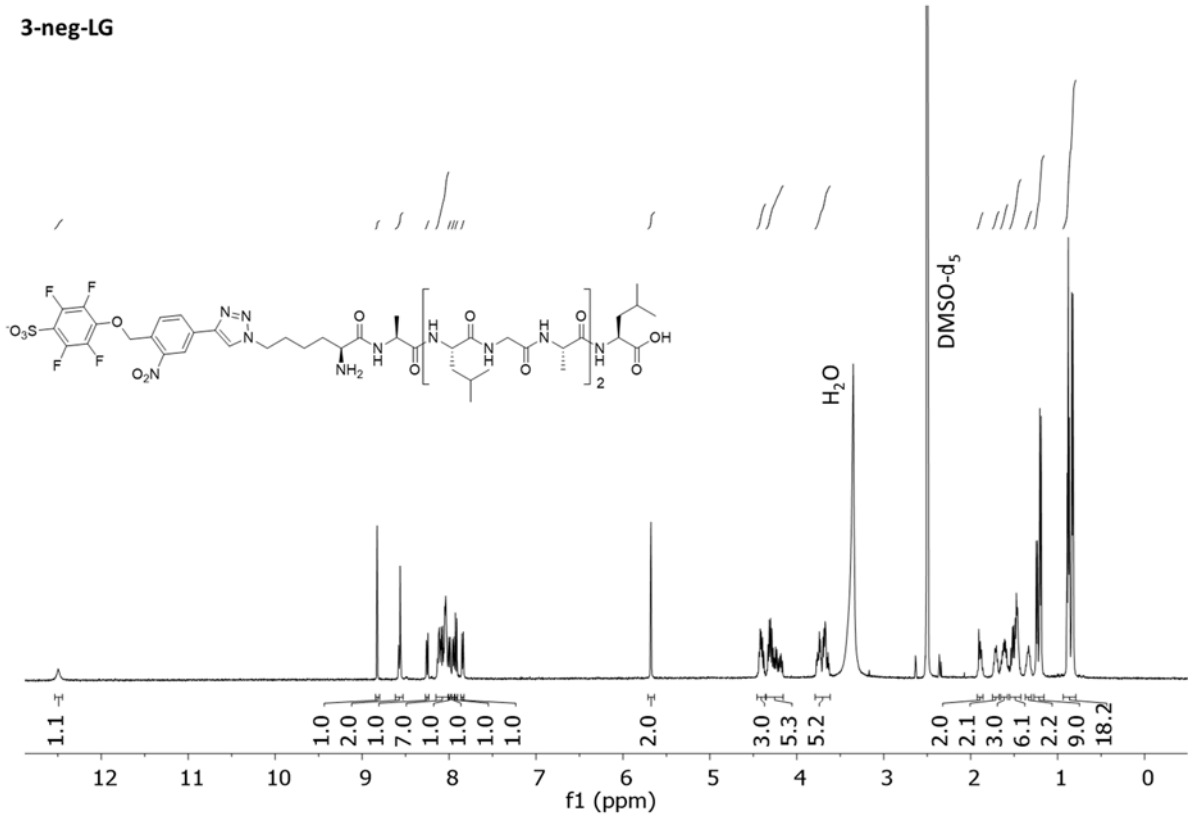

Figure S11. ^{1}H-NMR (DMSO-d_6, 500 MHz, 298 K) of **3-neg-LG.**

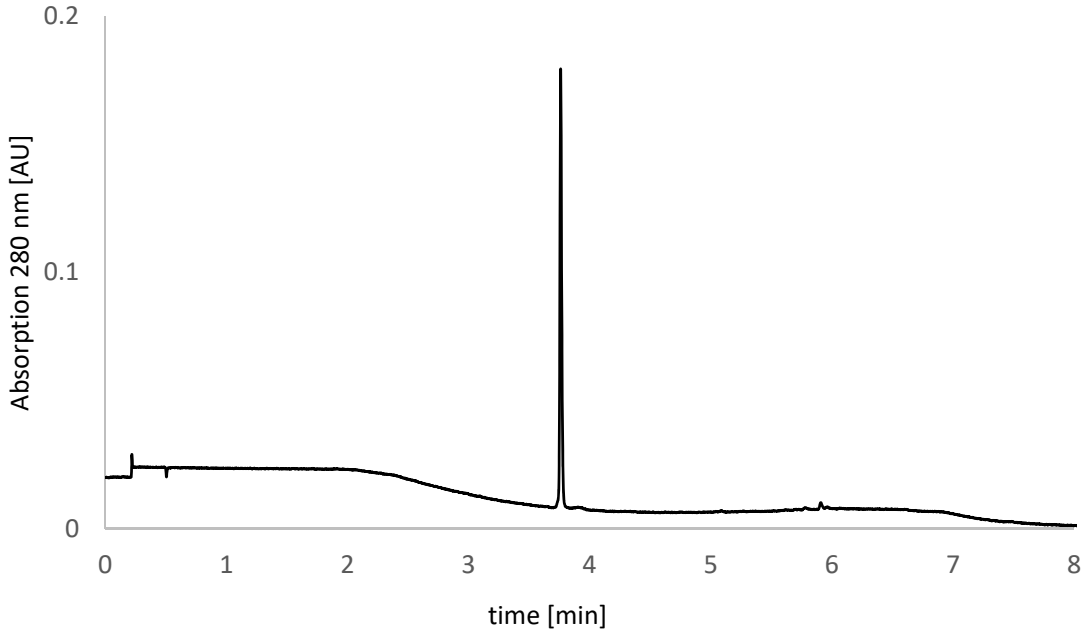

Figure S12. UPLC-chromatogram of **3-neg-LG.**

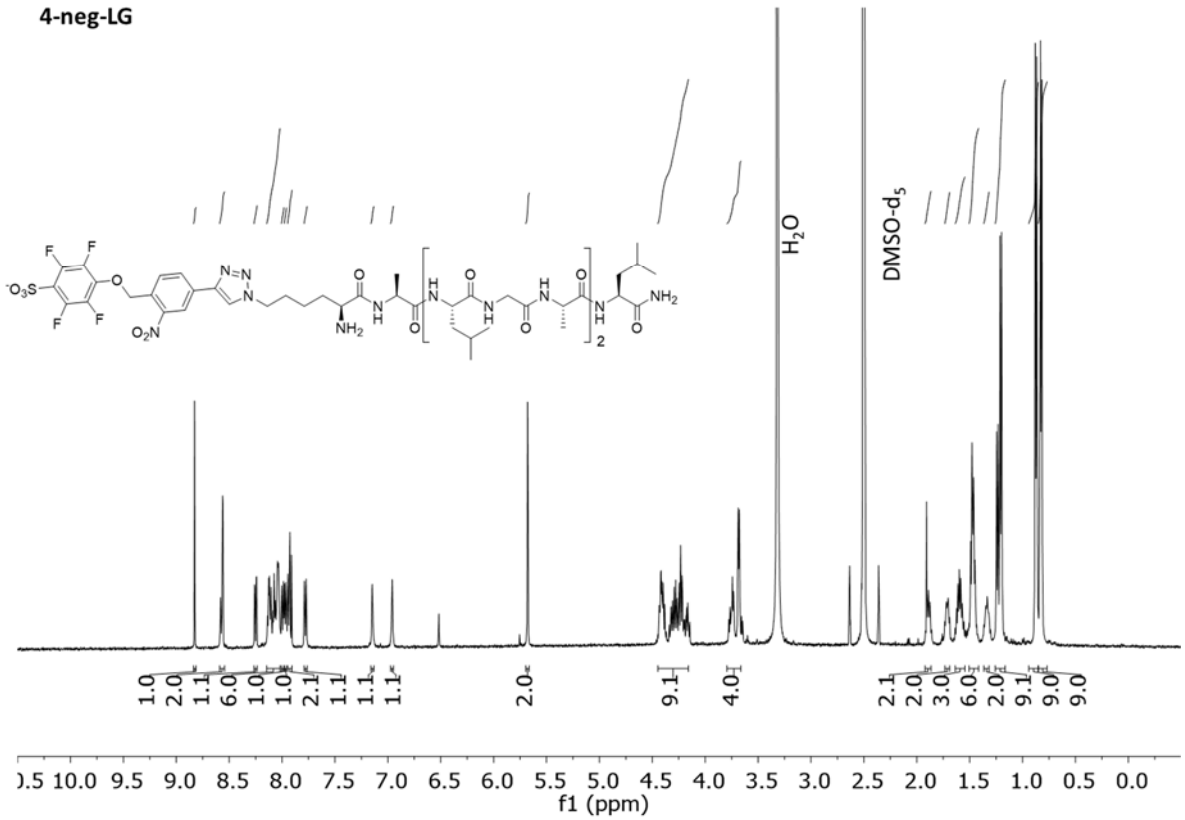

Figure S13. ^{1}H-NMR (DMSO-d_6, 500 MHz, 298 K) of **4-neg-LG.**

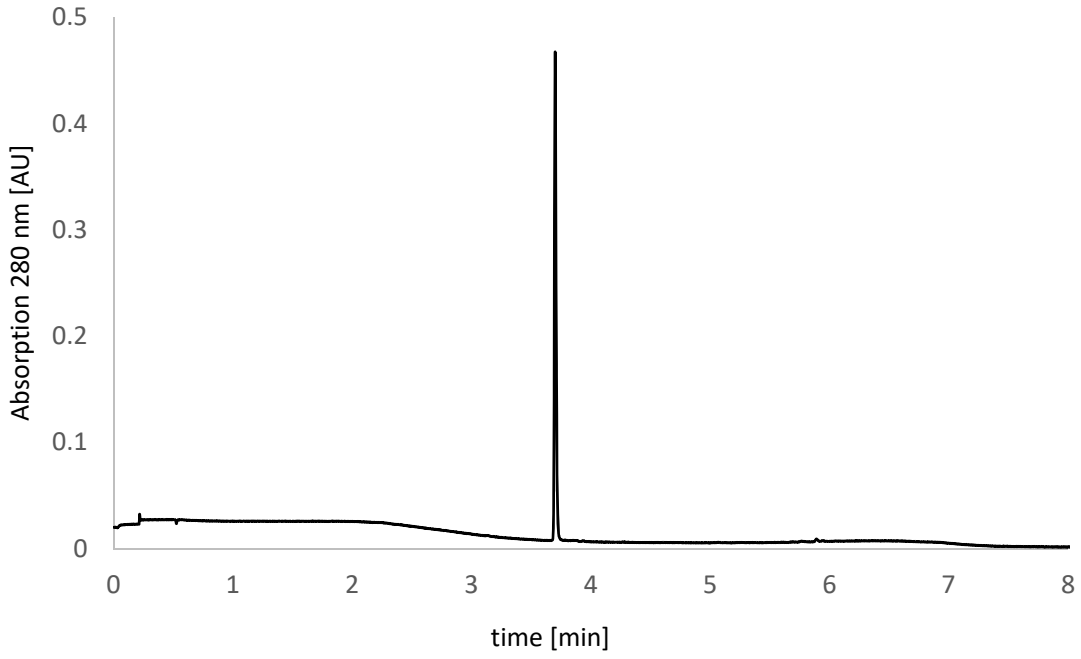

Figure S14. UPLC-chromatogram of **4-neg-LG.**

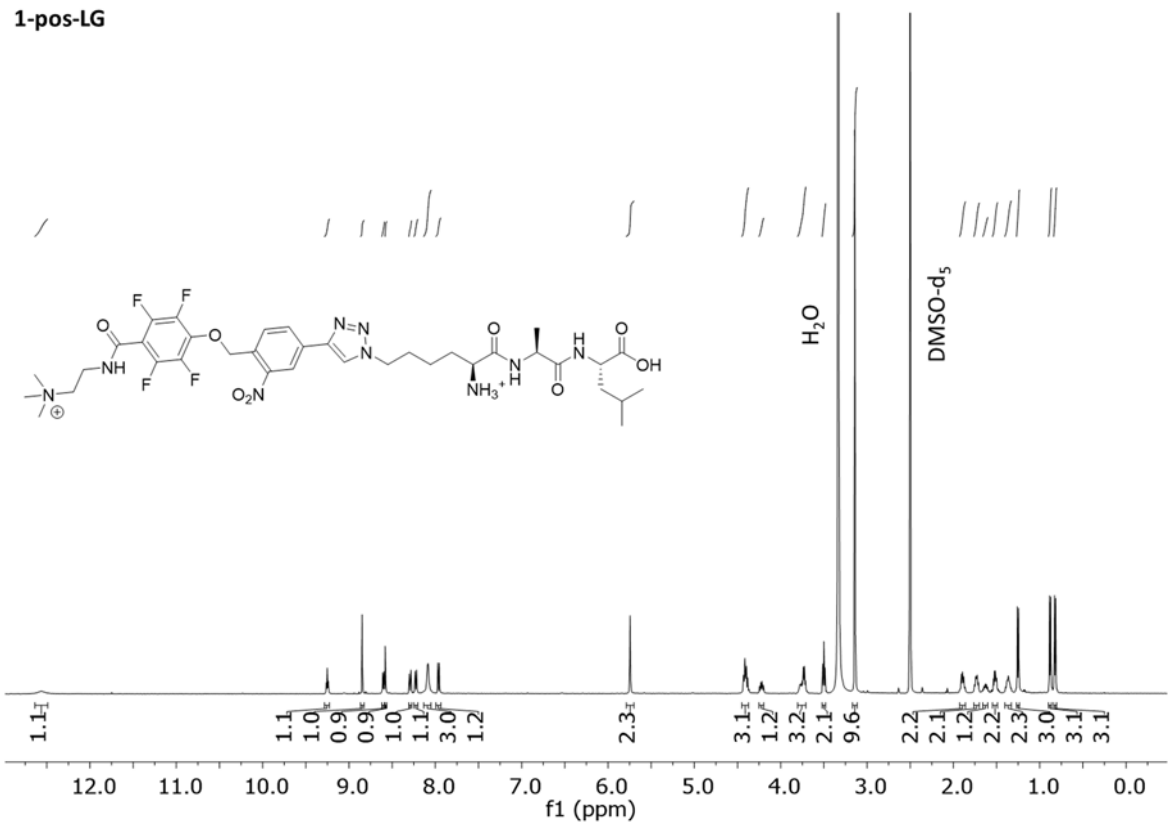

Figure S15. ^{1}H-NMR (DMSO-d_6, 500 MHz, 298 K) of **1-pos-LG.**

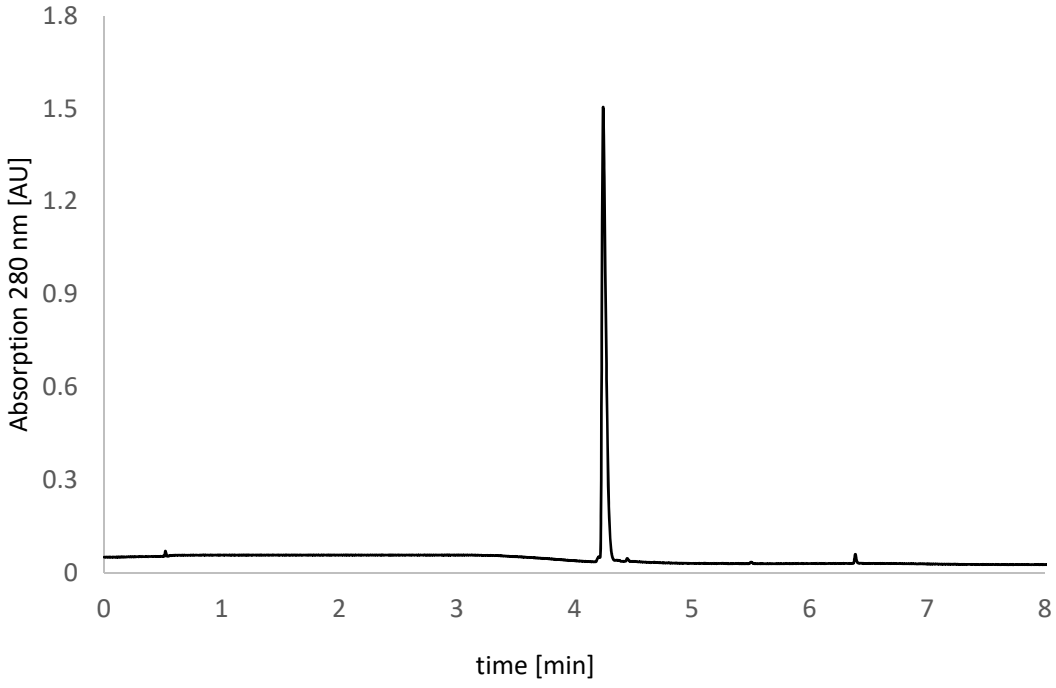

Figure S16. UPLC-chromatogram of **1-pos-LG.**

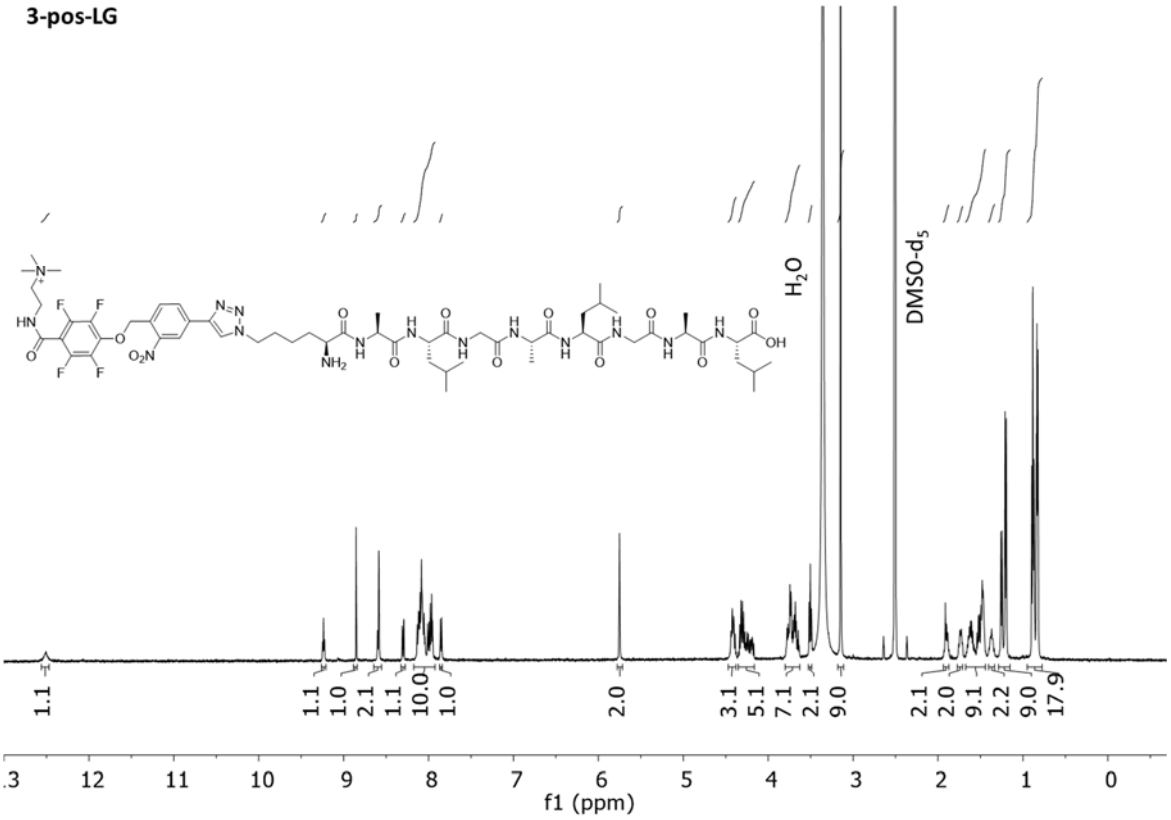

Figure S17. ^{1}H-NMR (DMSO-d_6, 500 MHz, 298 K) of **3-pos-LG.**

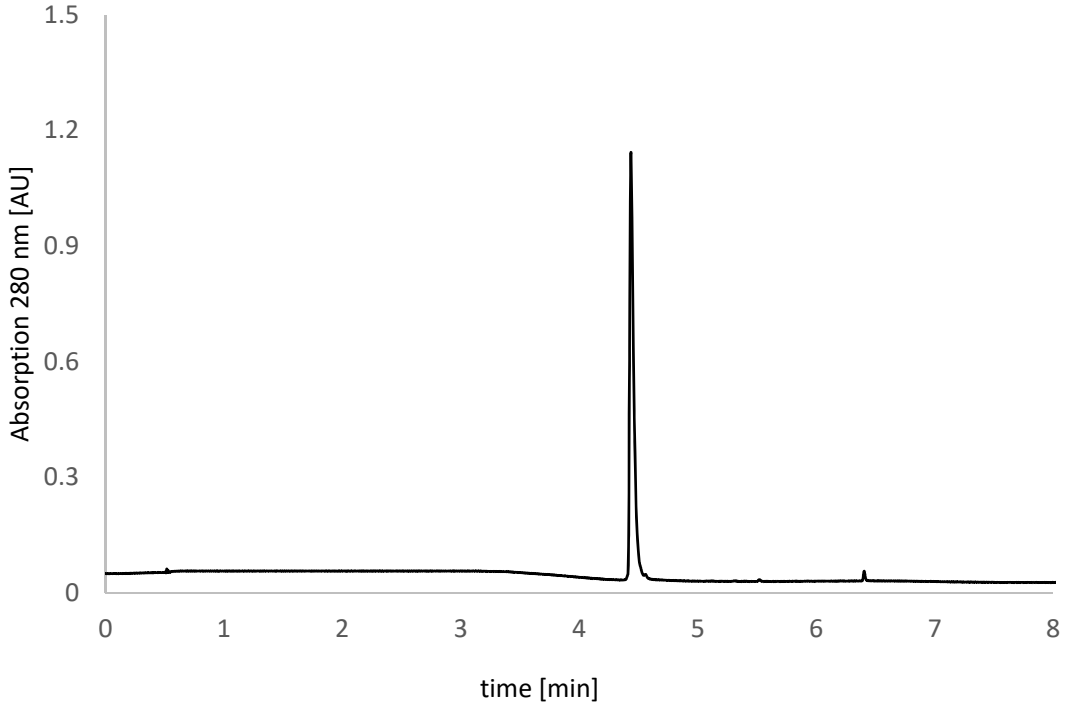

Figure S18. UPLC-chromatogram of **3-pos-LG.**

neg-ins

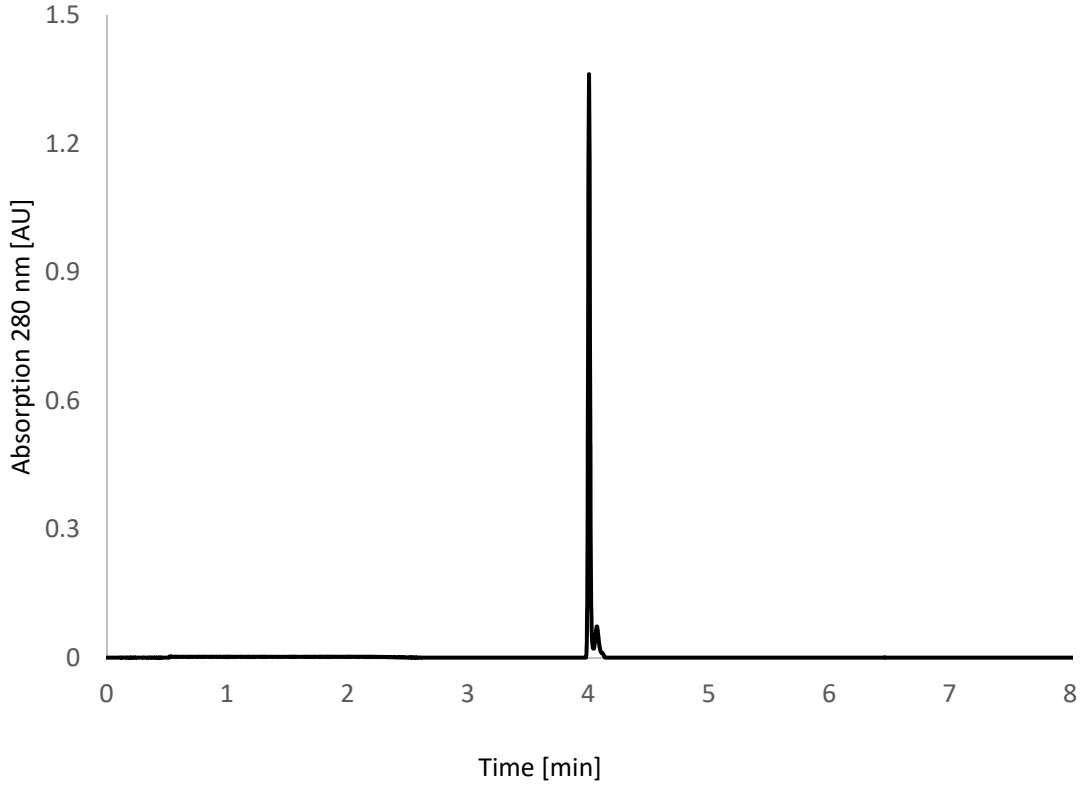

Figure S19. UPLC-chromatogram of **neg-ins.**

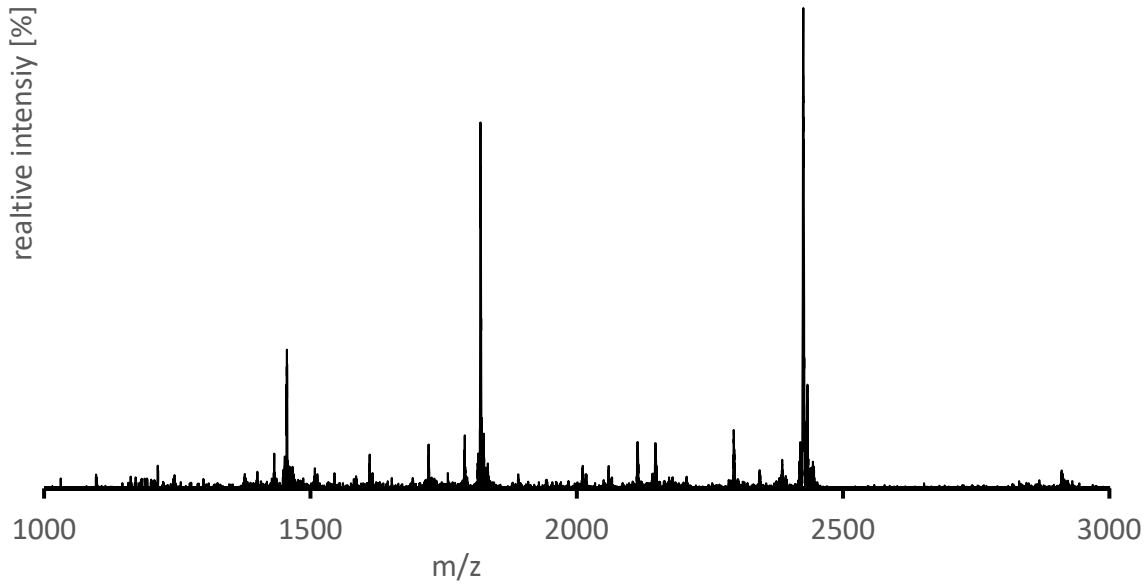

Figure S20. Mass spectra (ESI+) of **neg-ins.**

pos-ins

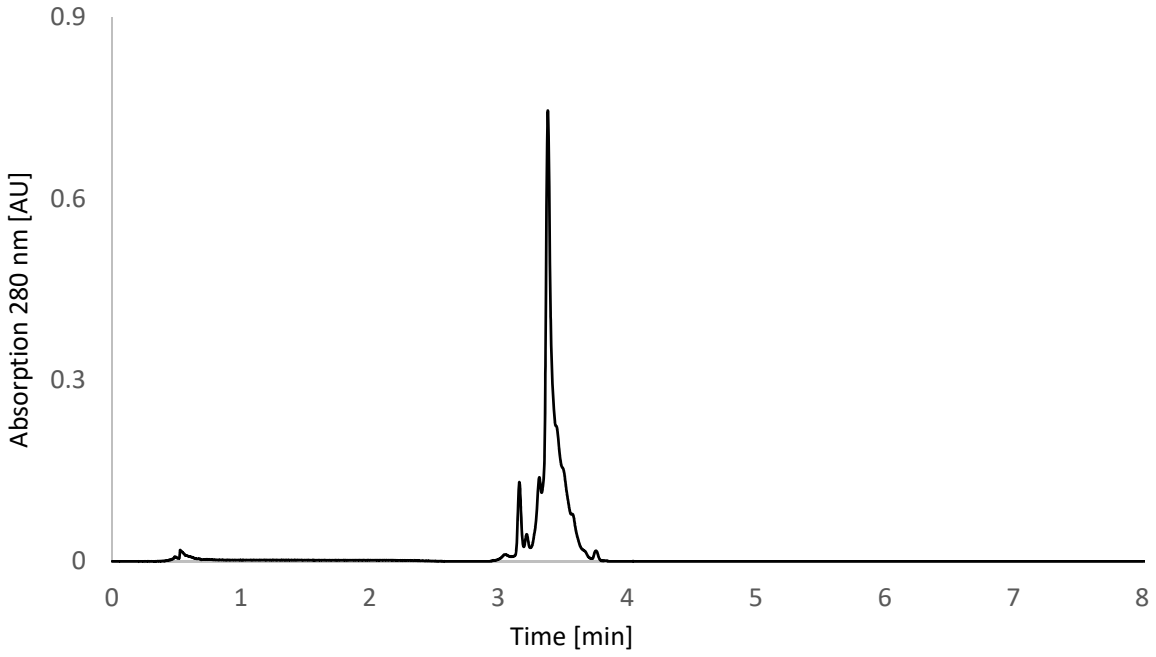

Figure S21. UPLC-chromatogram of **pos-ins.**

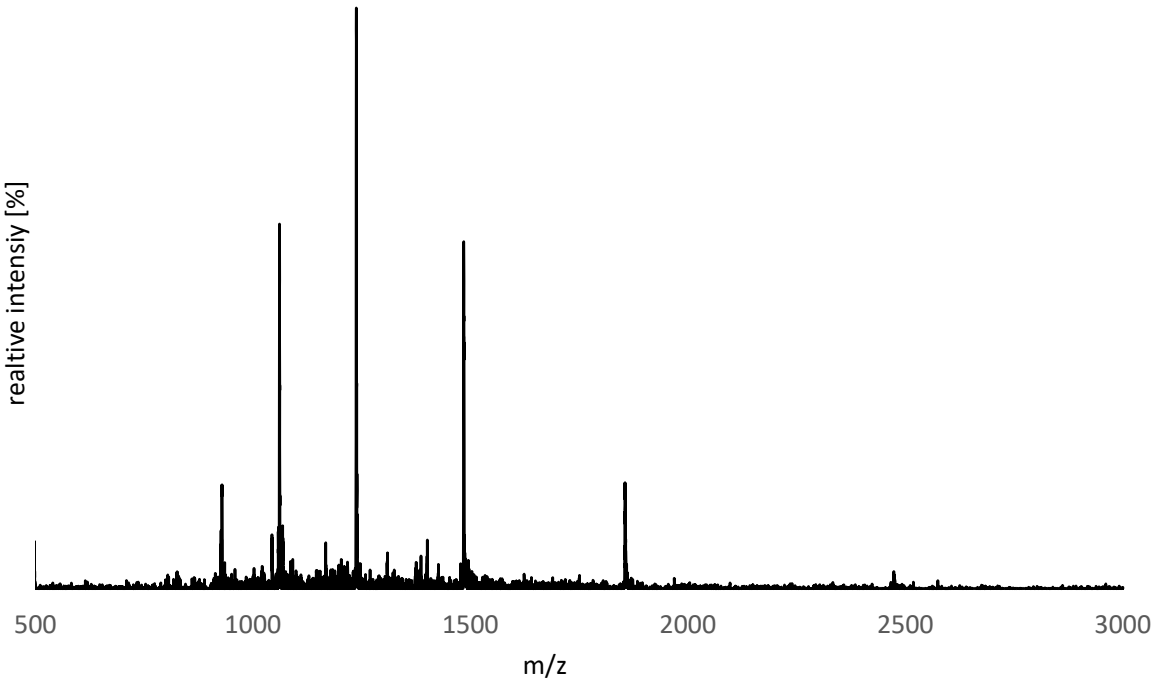

Figure S22. Mass spectra (ESI+) of **pos-ins.**

References

1. M. Debiossac; J. Schatti; M. Kriegleder; P. Geyer; A. Shayeghi; M. Mayor; M. Arndt; V. Kohler, Tailored photocleavable peptides: fragmentation and neutralization pathways in high vacuum. *Phys. Chem. Chem. Phys.* **2018**.
2. A. Saha; S. Panda; S. Paul; D. Manna, Phosphate bioisostere containing amphiphiles: a novel class of squaramide-based lipids. *Chem. Commun.* **2016,** *52* (60), 9438-9441.

Chapter 7. Wavelength-dependent photocleavage with visible light for neutralization followed by post-ionization.

8-Hydroxymethyl-1,3,4,4,5,7-hexamethyl-4-bora-3a,4a-diaza-*s*-indacene (9)

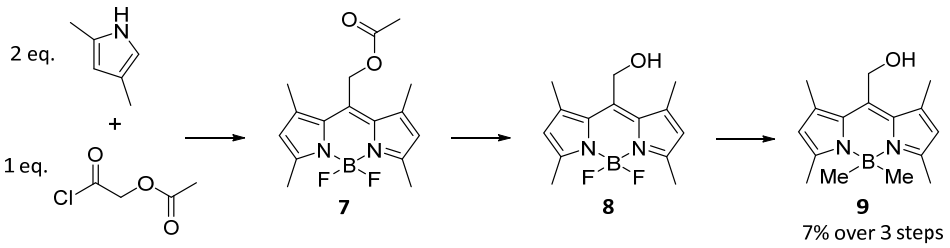

Hexamethyl-BODIPY **9** was prepared in a sequential synthesis starting from 2,4-dimethylpyrrole and 2-chloro-2-oxoethyl acetate according to a modified procedure from the group of Petr Klán. [1]

2,4-dimethylpyrrole (2.00 eq., 8.00 mL, 77.7 mmol) and acetoxyacetyl chloride (1.00 eq., 4.18 mL, 38.9 mmol) were dissolved in dry CH_2Cl_2 (750 mL) and stirred for 18 h at room temperature. DIPEA (4.00 eq., 25.7 mL, 155 mmol) was added, and the solution was stirred for another 25 min before $BF_3{\cdot}OEt_2$ (4.00 eq., 19.2 mL, 155 mmol) was added dropwise over 30 min. The reaction was stirred for another 20 min. Volatiles were removed under reduced pressure, and the residue was dissolved in acetonitrile (200 mL). Water (100 mL) was added, and the precipitate **7** was collected by filtration and used without further purification for the next step (3.52 g, 11.0 mmol).

Acetyl ester **7** (1.00 eq., 3.52 g, 11.0 mmol) was dissolved in dry THF (200 mL). Aq. LiOH (3.00 eq. 0.165 M, 200 mL, 33.0 mmol) was added, and the solution was stirred for 3 h. The solution was extracted with EtOAc (3×100 mL), the combined organic layers were washed with sat. aq. NH_4Cl (100 mL) and brine (100 mL). Volatiles were removed under reduced pressure, and the residue was redissolved in MeCN (100 mL). Water (100 mL) was added, and the precipitate **8** was collected by filtration and used without further purification for the next step (2.22 g, 22.0 mmol).

Alcohol **8** (1,00 eq., 1.11 g, 4.00 mmol) was dissolved in dry Et_2O (100 mL). A solution of methylmagnesium iodide in Et_2O (10.0 eq., 3 M, 13.3 mL, 40.0 mmol) was added slowly to the solution before stirring it for 1 h at room temperature. The reaction was quenched by slow addition of water (100 mL) followed by sat. aq. NH_4Cl (100 mL) and extracted with CH_2Cl_2 (3×100 mL). The combined organic layers were washed with brine (100 mL), and water (100 mL). Volatiles were removed under reduced pressure, and the residue was purified by flash column chromatography (cyclohexane/EtOAc 5:1→1:1). Hexamethyl-BODIPY **9** was isolated as an orange-green powder (354 mg, 1.31 mmol, 7% over 3 steps). Analytical data are in agreement with literature values and are not shown.[1]

2,6-Diiodo-8-hydroxymethyl-1,3,4,4,5,7-hexamethyl-4-bora-3a,4a-diaza-*s*-indacene (10)

Diiodo compound **10** was prepared following published procedures and used without further purification.[1] UPLC-MS: Method 1, T_R = 5.33 min; MS (ESI+) m/z: 507.0 [100%, M-Me$^-$].

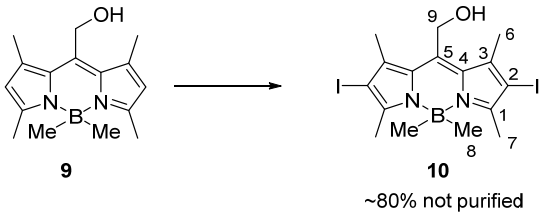

^{1}H-NMR ($CDCl_3$, 600 MHz, 293 K) δ: 4.98 (s, 2 H, H-9), 2.59 (s, 6 H, H-6), 2.54 (s, 6 H, H-7), 0.19 (s, 6 H, H-8). ^{13}C-NMR δ: 153.4 (C-1), 139.4 (C-3), 137.5 (C-5), 130.4 (C-4), 87.2 (C-2), 56.8 (C-9), 18.4 (C-6), 18.3 (C-7), 10.1 (C-8).

2,6-diiodo-8-(4-methoxy-succinic acid)-1,3,4,4,5,7-hexamethyl-4-bora-3a,4a-diaza-*s*-indacene (2):

The alcohol **10** (1.00 eq., 14.6 mg, 28.0 µmol), succinic anhydride (10.0 eq., 28.0 mg, 280 µmol) and DIPEA (10.0 eq., 46.3 µl, 280 µmol) were dissolved in chloroform (5 mL) and stirred for 1 h at 50 °C. Volatiles were removed under reduced pressure, and the residue was purified by reversed phase preparative HPLC. The cleavable **2** was isolated as a purple powder (12.0 mg, 19.3 µmol, 69%) UPLC-MS: Method 2, T_R = 5.10 min; MS (ESI+) m/z: 607.3 [100%, M-Me$^-$].

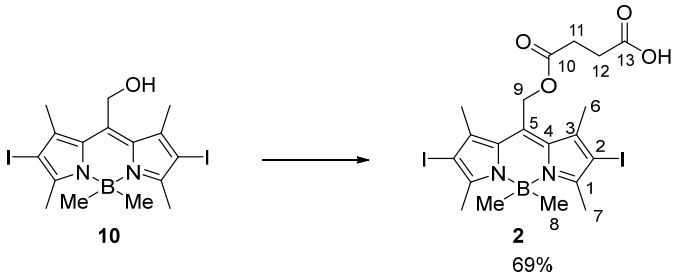

^{1}H-NMR ($CDCl_3$, 500 MHz, 293 K) δ: 5.39 (s, 2 H, H-9), 2.78-2.68 (m, 4 H, H-11 and H-12), 2.55 (s, 6 H, H-7), 2.40 (s, 6 H, H-6), 0.20 (s, 6 H, H-8). ^{13}C-NMR δ: 175.5 (C-13), 171.8 (C-10), 153.9 (C-1), 139.4 (C-3), 132.3 (C-5), 130.9 (C-4), 87.6 (C-2), 59.3 (C-9), 28.4 (C-11 or C-12), 28.3 (C-11 or C-12), 18.3 (C-7) 18.2 (C-6) 10.1 (C-8).

2,6-Diiodo-8-(2-(4-methoxy-4-oxobutanamido)-N,N,N-trimethylethan-1-aminium)-1,3,4,4,5,7-hexamethyl-4-bora-3a,4a-diaza-*s*-indacene (1)

Acid **2** (1.00 eq., 12.4 mg, 19.9 µmol), NH_3-CH_2-CH_2-$NMe_3^{2+}I^-TFA^-$ (3.00 eq., 20.7 mg, 60.0 µmol), EDC (3.00 eq., 11.5 mg, 60.0 µmol), DMAP (0.10 eq., 0.24 mg, 2.0 µmol) and DIPEA (6.00 eq., 19.8 µl, 12.0 µmol) were dissolved in DMF (10 mL) and stirred for 3 h at room temperature. Volatiles were removed under reduced pressure, and the residue was purified by reversed phase preparative HPLC.

The cationic cleavable **1** was isolated as a purple powder (4.5 mg, 5.6 µmol, 28%). UPLC-MS: Method 2, T_R = 4.21 min; MS (ESI+) m/z: 707.4 [100%, M^+].

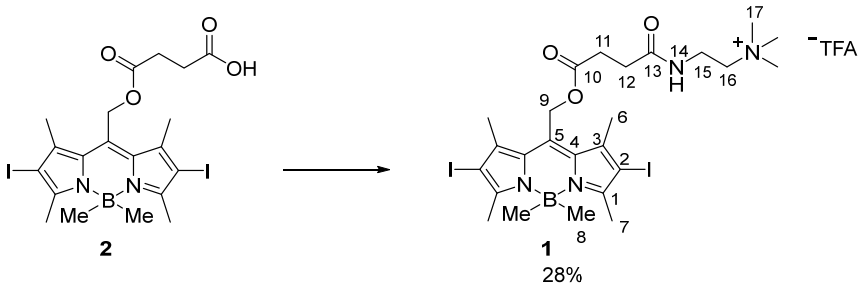

^{1}H-NMR ($CDCl_3$, 500 MHz, 293 K) δ: 9.01 (s, 1 H, H-14), 5.33 (s, 2 H, H-9), 3.89-3.62 (m, 4 H, H-15 and H-16), 3.24 (s, 9 H, H-17), 2.75-2.57 (m, 4 H, H-11 and H-12), 2.54 (s, 6 H, H-7), 2.40 (s, 6 H, H-6), 0.19 (s, 6 H, H-8). ^{13}C-NMR δ: 172.5 (C-10), 153.8 (C-1), 139.6 (C-3), 132.6 (C-5), 131.0 (C-4), 87.7 (C-2), 66.2 (C-16), 59.1 (C-9), 54.6(C-17), 34.5 (C-15), 29.9 (C-11 or C-12), 28.6 (C-11 or C-12), 18.3 (C-6 and C-7), 10.1 (C-8).

(*S*)-2,6-Diiodo-4,4'-dimethyl-8-(2-amino-3-phenylpropanoyl)methyl-1,3,5,7tetramethyl-4-bora-3a,4a-diaza-*s*-indacene (11)

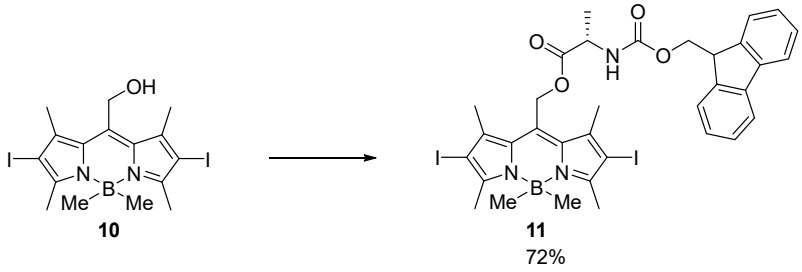

The modified alanine **11**was prepared following known procedures. Analytical data are in agreement with literature[1] and are not shown.

Fmoc deprotection of **11**

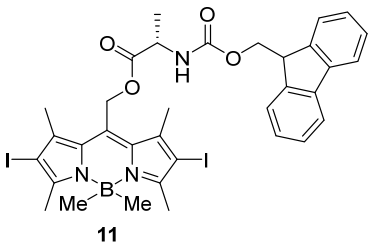

Various deprotection conditions were screened to remove the Fmoc protection group of **11**. No successful conditions were found; all tested condition lead to decomposition of **11**. Tried conditions are displayed in table S1.

#	Conditions	Time	Outcome
1	20% piperidine in DMF	30 min	Complete decomposition
2	20% piperidine in DMF	5 min	Complete decomposition
3	10% piperidine in DMF	5 min	Decomposition products and **11**
4	2% piperidine in DMF	30 min	Decomposition products and **11**
5	5% DBU in DMF	30 min	Complete decomposition
6	2% DBU in DMF	30 min	Complete decomposition
7	2% DBU in DMF	5 min	Decomposition products and **11**
8	10% Morpholine	5 min	Decomposition products and **11**
9	1.0 M NaOH, 30% dioxane	5 min	Complete decomposition
10	0.2 M NaOH, 30% dioxane	5 min	Complete decomposition
11	0.1 M NaOH, 30% dioxane	5 min	Complete decomposition

Table S1. Investigation of various conditions for the Fmoc-deprotection of **11**.

Tert-butyl (*E*)-3-(4-(((*tert*-butyldimethylsilyl)oxy)methyl)-7-(diethylamino)-2-oxo-2*H*-chromen-3-yl) acrylate (18)

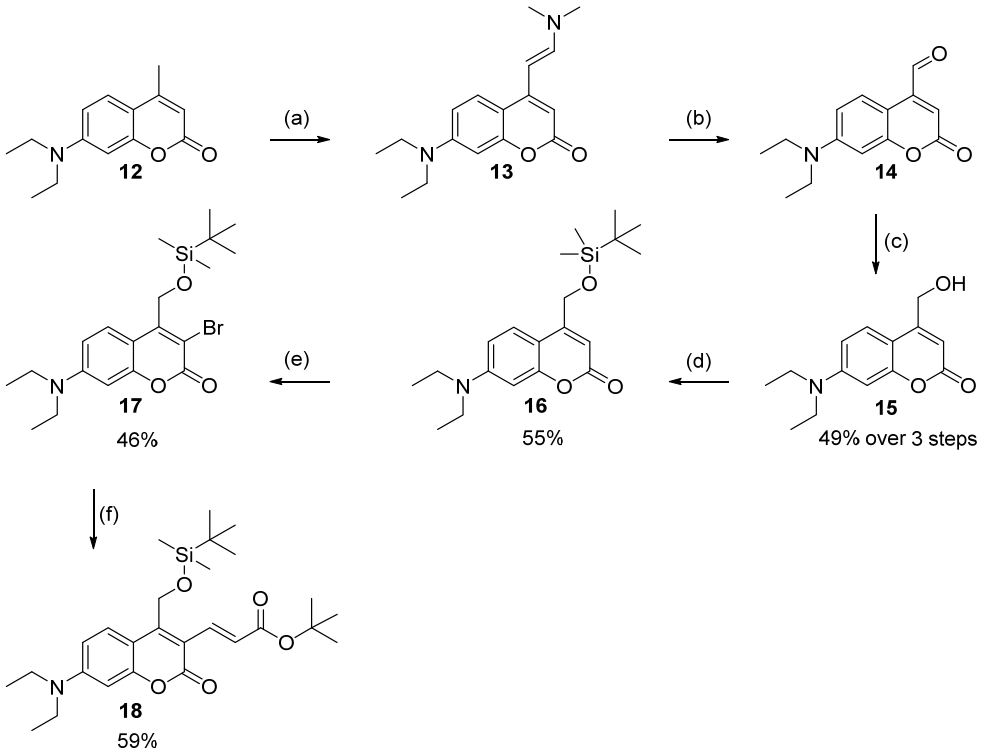

Scheme S1. Synthesis towards **18**. [2-3] (a) 2.0 eq. DMF-DMA, DMF, reflux, overnight. (b) 3.0 eq. $NaIO_4$, H_2O/THF (1:1), rt, 2 h. (c) 2.0 eq. $NaBH_4$, THF, 0 °C → rt, 2 h. (d) 1.2 eq. TBDMS-Cl, CH_2Cl_2, 0 °C → rt, 4 h. (e) 1.2 eq NBS, MeCN, 0 °C → rt , 1 h. (f) 3.0 eq. *tert*-butyl acrylate, LiCl, tetrabutylamonium chloride, $NaHCO_3$, $Pd(OAc)_2$, DMF, reflux, 1 h.

Compound **18** was synthesized according to published procedures. The NMR and MS data were in accordance with published data and are not shown.[2,3]

(*E*)-3-(7-(Diethylamino)-4-(hydroxymethyl)-2-oxo-2*H*-chromen-3-yl) acrylic acid (19)

Tert-butyl ether **18** (1.00 eq., 250 mg, 600 µmol) was dissolved in CH_2Cl_2/TFA (1:1, 20 mL) and stirred for 40 min. Volatiles were removed under reduced pressure, and the residue was redissolved in CH_2Cl_2 (20 mL). Volatiles were removed under reduced pressure, to remove last traces of TFA, and the residue was dissolved in THF (20 mL). A solution of TBAF in THF (5.00 eq. 3.00 mL, 3.00 mmol, 1 M) was added, and the reaction was stirred for 5 h at room temperature. H_2O (40 mL) were added and the solvent was extracted with EtOAc (4 × 30 mL) and the combined organic layers were dried over $MgSO_4$. Volatiles were removed under reduced pressure, and the residue was purified by flash column chromatography (CH_2Cl_2/MeOH, 99:1 →95:5). Acrylic acid **19** was isolated as an orange powder in good yield (118 mg, 479 µmol, 80%). UPLC-MS: Method 2, T_R = 3.44 min; MS (ESI+) m/z: 242.3 [100%], 318.0 [100%, M + H+].

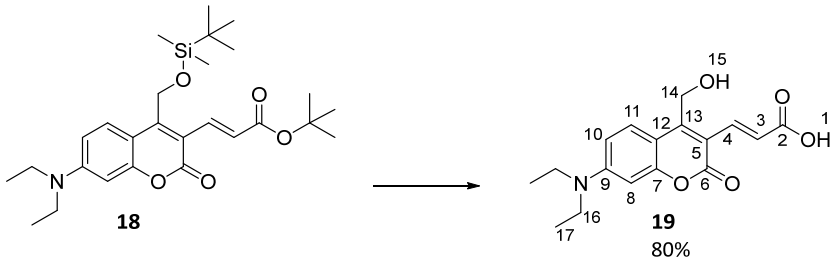

^{1}H-NMR (DMSO-d_6, 500 MHz, 293 K) δ: 7.80 (d, $^3J_{H\text{-}H}$ = 15.6 Hz, 1 H, H-4), 7.78 (d, $^3J_{H\text{-}H}$ = 9.3 Hz, 1 H, H-11), 6.91 (d, $^3J_{H\text{-}H}$ = 15.6 Hz, 1 H, H-3), 6.79 (dd, $^3J_{H\text{-}H}$ = 9.3 Hz, $^4J_{H\text{-}H}$ = 2.6 Hz, 1 H, H-10), 6.54 (d, $^4J_{H\text{-}H}$ = 2.6 Hz, 1 H, H-8), 5.62 (t, $^3J_{H\text{-}H}$ = 5.4 Hz, 1 H, H-15), 4.72 (d, $^3J_{H\text{-}H}$ = 5.4 Hz, 2 H, H-14), 3.47 (q, $^3J_{H\text{-}H}$ = 7.1 Hz, 4 H, H-16), 1.14 (t, $^3J_{H\text{-}H}$ = 7.0 Hz, 6 H, H-17). ^{13}C-NMR δ: 167.8 (C-2), 159.3 (C-6), 155.1(C-7), 153.3 (C-12), 150.8(C-9), 136.1 (C-4), 127.8 (C-11), 121.1 (C-3), 111.0(C-5), 109.3 (C-10), 107.1 (C-12), 95.9 (C-12), 54.9 (C-14), 43.9 (C-16), 12.0(C-17).

***tert*-Butyl (E)-(3-(7-(diethylamino)-4-(hydroxymethyl)-2-oxo-2*H*-chromen-3-yl)acryloyl)-*L*-alaninate (20)**

Acrylic acid **19** (1.00 eq., 246 mg, 1.00 mmol) was dissolved in CH_2Cl_2/MeCN (1:1, 20 mL) *L*-alanine *tert*-butyl ester hydrochloride (1.00 eq, 182 mg, 1.00 mmol), EDC (1.20 eq, 230 mg, 1.20 mmol) and DIPEA (2.00 eq., 331 µl, 2.00 mmol) were added and the solution was stirred for 2 h at room temperature. Volatiles were removed under reduced pressure, and the residue was purified by flash column chromatography (EtOAc/cyclohexane, 2:1). Alcohol **20** was isolated as an orange powder (198 mg, 530 µmol, 53%).

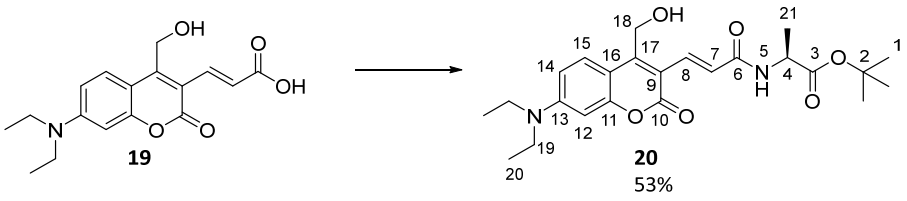

^{1}H-NMR ($CDCl_3$, 500 MHz, 293 K) δ: 7.84 (d, $^{3}J_{H\text{-}H}$ = 15.0 Hz, 1 H, H-8), 7.70 (d, $^{3}J_{H\text{-}H}$ = 9.2 Hz, 1 H, H-15), 7.30 (d, $^{3}J_{H\text{-}H}$ = 15.0 Hz, 1 H, H-7), 6.64 (dd, $^{3}J_{H\text{-}H}$ = 9.2 Hz, $^{4}J_{H\text{-}H}$ = 2.6 Hz, 1 H, H-14), 6.49 (d, $^{4}J_{H\text{-}H}$ = 2.6 Hz, 1 H, H-12), 6.29 (d, $^{3}J_{H\text{-}H}$ = 7.5 Hz, 1 H, H-5), 4.99 (s, 2 H, H-18), 4.59 (p, $^{3}J_{H\text{-}H}$ = 7.2 Hz, 1 H, H-4), 3.44 (q,$^{3}J_{H\text{-}H}$ = 7.1 Hz, 4 H, H-19), 1.48 (s, 9 H, H-1), 1.43 (d, $^{3}J_{H\text{-}H}$ = 7.1 Hz, 3 H, H-21), 1.22 (t, $^{3}J_{H\text{-}H}$ = 7.1 Hz, 6 H, H-20).^{13}C-NMR δ: 172.2 (C-3), 166.1 (C-6), 160.7 (C-10), 155.8 (C-11), 151.2 (C-13), 151.0 (C-17), 131.9 (C-8), 127.1 (C-15), 124.3 (C-7), 113.2 (C-9), 109.3 (C-14), 108.1 (C-16), 97.1 (C-12), 82.0 (C-2), 56.5 (C-18), 49.0 (C-4), 44.9 (C-19), 27.8 (C-1), 18.7 (C-21), 12.4 (C-20).

tert-Butyl-(*E*)-(3-(4-(acetoxymethyl)-7-(diethylamino)-2-oxo-2*H*-chromen-3-yl)acryloyl)-*L*-alaninate (21)

Alcohol **20** (1.00 eq., 200 mg, 536 µmol) was dissolved in CH_2Cl_2 (20 mL) acetic acid (3.00 eq., 93 µl, 1.61 mmol), EDC (3.00 eq., 308 mg, 1.61 mmol) and DMAP

(0.50 eq. 32.7 mg, 268 µmol) were added and the solution was stirred for 3 h at room temperature. Sat. aq. ammonium chloride (20 mL) was added, and the organic layer was separated and washed with H_2O (2×20 mL). Volatiles were removed under reduced pressure, and the residue was purified by flash column chromatography (EtOAc/cyclohexane 1:1). Acetyl ester **21** was isolated as an orange powder (155 mg, 373 µmol, 70%). UPLC-MS: Method 1, T_R = 5.49 min; MS (ESI+) m/z: 342.5 [80%, M-(ala-O-*t*bu)+ H^+], 431.5 [100%], 487.5 [100%, M + H^+], 509.0 [20%, M + Na^+].

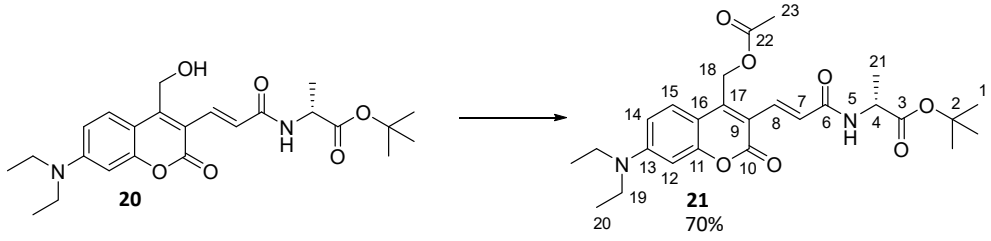

^{1}H-NMR ($CDCl_3$, 500 MHz, 293 K) δ: 7.80 (d, $^{3}J_{H\text{-}H}$ = 15.1 Hz, 1 H, H-8), 7.53 (d, $^{3}J_{H\text{-}H}$ = 9.2 Hz, 1 H, H-15), 7.31 (d, $^{3}J_{H\text{-}H}$ = 15.1 Hz, 1 H, H-7), 6.63 (dd, $^{3}J_{H\text{-}H}$ = 9.2 Hz, $^{4}J_{H\text{-}H}$ = 2.6 Hz, 1 H, H-14), 6.49 (d, $^{4}J_{H\text{-}H}$ = 2.6 Hz, 1 H, H-12), 6.28 (d, $^{3}J_{H\text{-}H}$ = 7.4 Hz, 1 H, H-5), 5.41 (s, 2 H, H-18), 4.61 (p, $^{3}J_{H\text{-}H}$ = 7.2 Hz, 1 H, H-4), 3.44 (q, $^{3}J_{H\text{-}H}$ = 7.1 Hz, 4 H, H-19), 2.09 (s, 3 H, H-23), 1.48 (s, 9 H, H-1), 1.43 (d, $^{3}J_{H\text{-}H}$ = 7.0 Hz, 3 H, H-21), 1.22 (t, $^{3}J_{H\text{-}H}$ = 7.1 Hz, 6 H, H-20). ^{13}C-NMR δ: 172.1 (C-3), 170.3 (C-22), 165.3 (C-6), 160.0 (C-10), 155.5 (C-11), 151.1 (C-13), 146.6 (C-17), 131.8 (C-8), 126.6 (C-15), 125.1 (C-7), 115.0 (C-9), 109.4 (C-14), 107.8 (C-16), 97.1 (C-12), 81.9 (C-2), 57.3 (C-18), 48.7 (C-4), 44.7 (C-19), 27.9 (C-1), 20.7 (C-23), 18.7 (C-21), 12.2 (C-20).

(*E*)-(3-(4-(acetoxymethyl)-7-(diethylamino)-2-oxo-2H-chromen-3-yl)acryloyl)-*L*-alanine (3)

Acetyl ester **21** (1.00 eq., 100 mg, 241 µmol) was dissolved in CH_2Cl_2/TFA (1:1, 10 mL) and stirred for 1 h. Volatiles were removed under reduced pressure, and the residue was redissolved in CH_2Cl_2 (1 mL). After removal of volatiles, the acid **3** was isolated as an orange powder (86 mg, 236 µmol, 99%). UPLC-MS: Method 2, T_R = 4.68 min; MS (ESI+) m/z: 431.9 [100%, M + H+], 454.3 [30%, M + Na^+].

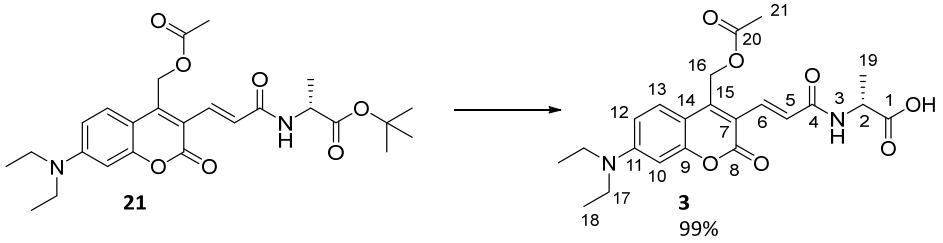

^{1}H-NMR ($CDCl_3$, 500 MHz, 293 K) δ: 7.88 (d, $^3J_{H\text{-}H}$ = 15.1 Hz, 1 H, H-6), 7.58 (d, $^3J_{H\text{-}H}$ = 9.3 Hz, 1 H, H-13), 7.48 (d, $^3J_{H\text{-}H}$ = 15.1 Hz, 1 H, H-5), 6.65 (dd, $^3J_{H\text{-}H}$ = 9.3 Hz, $^4J_{H\text{-}H}$ = 2.6 Hz, 1 H, H-12), 6.58 (d, $^3J_{H\text{-}H}$ = 6.2 Hz, 1 H, H-3), 6.51 (d, $^4J_{H\text{-}H}$ = 2.6 Hz, 1 H, H-10), 5.46-5.39 (m, 2 H, H-16), 4.67 (p, $^3J_{H\text{-}H}$ = 6.8 Hz, 1 H, H-2), 3.45 (q,$^3J_{H\text{-}H}$ = 7.1 Hz, 4 H, H-17), 2.10 (s, 3 H, H-21), 1.56 (d, $^3J_{H\text{-}H}$ = 7.1 Hz, 3 H, H-19), 1.23 (t, $^3J_{H\text{-}H}$ = 7.1 Hz, 6 H, H-18). ^{13}C-NMR δ: 173.1 (C-1), 170.4 (C-20), 168.2 (C-4), 160.6 (C-8), 155.6 (C-9), 151.5 (C-11), 147.6 (C-15), 133.3 (C-6), 126.9 (C-13), 123.4 (C-5), 114.1 (C-7), 109.8 (C-12), 108.0 (C-14), 97.1 (C-10), 57.3 (C-16), 49.1 (C-2), 44.9 (C-17), 20.7 (C-21), 17.1 (C-19), 12.4 (C-18).

(*S,E*)-2-(2-(3-(4-(acetoxymethyl)-7-(diethylamino)-2-oxo-*2H*-chromen-3-yl)acrylamido)propan-amido)-*N,N,N*-trimethylethan-1-aminium (5)

Acid **3** (1.00 eq. 40.0 mg, 92.9 µmol) was dissolved in DMF (5 mL), NH_3-CH_2-CH_2-$NMe_3^{2+}I^-TFA^-$ (1.20 eq. 38.3 mg, 112 µmol), EDC (1.20 eq., 21.4 mg, 112 µmol) and DIPEA (4.00 eq., 61.5 µl, 372 µmol) were added and the solution was stirred for 3 h at room temperature. Volatiles were removed under reduced pressure, and the residue was purified by reversed phase preparative HPLC. After lyophilization, the cationic cleavable **5** was isolated as an orange powder (3.0 mg, 4.9 µmol, 5%). UPLC-MS: Method 1, T_R = 3.10 min; MS (ESI+) m/z: 258.2 [100%, M^+ + H^+], 515.4 [60%, M^+].

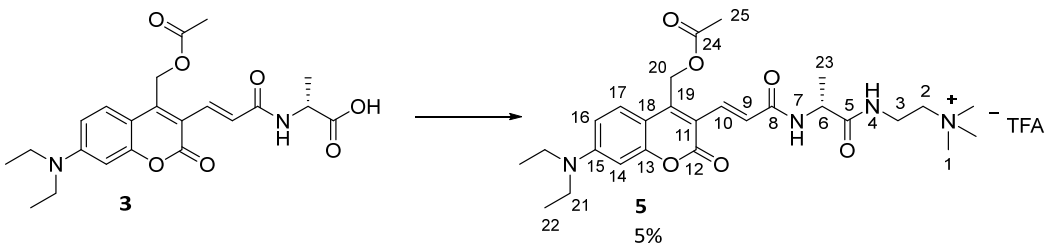

^{1}H-NMR (DMSO-d_6, 500 MHz, 293 K) δ: 8.54 (s, 1 H, H-7), 8.23 (s, 1 H, H-4), 7.65 (d, $^3J_{H\text{-}H}$ = 8.8 Hz, 1 H, H-17), 7.56 (d, $^3J_{H\text{-}H}$ = 15.2 Hz, 1 H, H-10), 7.20 (d, $^3J_{H\text{-}H}$ = 15.2 Hz, 1 H, H-9), 6.78 (d $^3J_{H\text{-}H}$ = 7.6 Hz, 1 H, H-16), 6.55 (s, 1 H, H-14), 5.35 (s, 2 H, H-20), 4.36-4.27 (m, 1 H, H-6), 3.60-3.30 (m, 8 H, H-2, H-3 and

H-21), 3.09 (s, 9 H, H-1), 2.04 (s, 3 H, H-25), 1.25 (d, $^{3}J_{H\text{-}H}$ = 7.2 Hz, 3 H, H-23), 1.13 (t, $^{3}J_{H\text{-}H}$ = 7.1 Hz, 6 H, H-22). ^{13}C-NMR δ: 172.7 (C-5), 169.7 (C-24), 165.1 (C-8), 159.0 (C-12), 154.9 (C-13), 151.0 (C-15), 146.6 (C-19), 130.5 (C-10), 127.2 (C-17), 125.4 (C-9), 113.3 (C-11), 109.5 (C-16), 106.8 (C-18), 96.1 (C-14), 63.5 (C-2), 57.4 (C-20), 52.4 (C-1), 48.5 (C-6), 43.9 (C-21), 33.0 (C-3), 20.3 (C-25), 17.3 (C-23), 12.2 (C-22).

tert-Butyl (_E_)-(3-(4-((3,5-bis(trifluoromethyl)phenoxy)methyl)-7-(diethylamino)-2-oxo-2_H_-chromen-3-yl)acryloyl)-_L_-alaninate (22)

Alcohol **20** (1.00 eq., 35.0 mg, 97.4 µmol) and 3,5-bis(trifluoromethyl)phenol (2.00 eq., 46.2 mg, 195 µmol) were dissolved in dry THF (5 mL) and cooled to 0 °C. DIAD (6.00 eq., 115 µl, 584 µmol) and PPh_3 (6.00 eq. 153 mg, 584 µmol) were added over 1 h in portions of one equivalent (the DIAD portions were added 5 min after the addition of PPh_3) until UPLC-MS showed full conversion. Volatiles were removed under reduced pressure, and the residue was purified by flash column chromatography (cyclohexane/EtOAc 10:1). Ether **22** was isolated as an orange powder (19 mg, 33 µmol, 34%) with DIAD as an impurity. The product was used without further purification. UPLC-MS: Method 2, T_R = 4.89 min; MS (ESI+) m/z: 511.8 [100%, M-(ala-O-*t*bu) + H^+], 657.5 [80%, M + H^+].

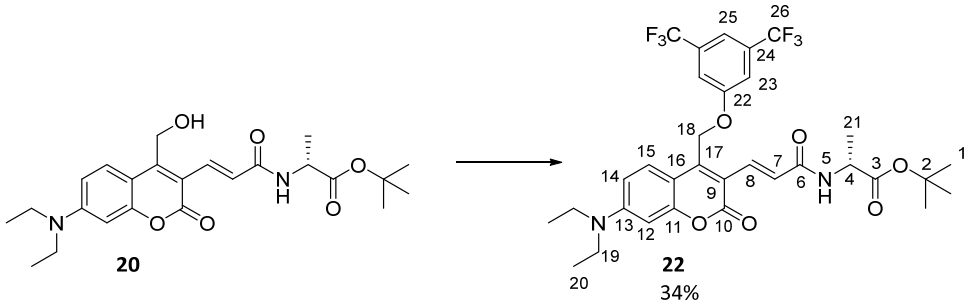

^{1}H-NMR ($CDCl_3$, 500 MHz, 293 K) δ: 7.77 (d, $^{3}J_{H\text{-}H}$ = 15.0 Hz, 1 H, H-8), 7.54 (s, 1 H, H-25), 7.42 (d, $^{3}J_{H\text{-}H}$ = 9.2 Hz, 1 H, H-15), 7.41 (s, 2 H, H-23), 7.32 (d, $^{3}J_{H\text{-}H}$ = 15.0 Hz, 1 H, H-7), 6.61 (dd, $^{3}J_{H\text{-}H}$ = 9.2 Hz, $^{4}J_{H\text{-}H}$ = 2.6 Hz, 1 H, H-14), 6.51 (d, $^{4}J_{H\text{-}H}$ = 2.6 Hz, 1 H, H-12), 6.28 (d, $^{3}J_{H\text{-}H}$ = 7.5 Hz, 1 H, H-5), 5.41-5.35 (m, 2 H, H-18), 4.56 (p, $^{3}J_{H\text{-}H}$ = 7.1 Hz, 1 H, H-4), 3.44 (q, $^{3}J_{H\text{-}H}$ = 7.1 Hz, 4 H, H-19), 1.47 (s, 9 H, H-1), 1.41 (d, $^{3}J_{H\text{-}H}$ = 7.1 Hz, 3 H, H-21), 1.22 (t, $^{3}J_{H\text{-}H}$ = 7.1 Hz, 6 H, H-20). ^{13}C-NMR δ: 172.1 (C-3), 165.6 (C-6), 160.1 (C-10), 158.5 (C-22), 155.6 (C-11), 151.3 (C-13), 145.4 (C-17), 131.2 (C-8), 126.5 (C-15), 125.8 (C-7), 115.4 (C-25), 115.0 (C-23), 114.8 (C-9), 109.5 (C-14), 108.0 (C-16), 97.2 (C-12), 82.1 (C-2), 62.2 (C-18), 48.7 (C-4), 44.8 (C-19), 27.9 (C-1), 18.7 (C-21), 12.2 (C-20), C-24 and C-26 not detected.

(_E_)-(3-(4-((3,5-bis(trifluoromethyl)phenoxy)methyl)-7-(diethylamino)-2-oxo-2_H_-chromen-3-yl)acryloyl)-_L_-alanine (4)

Ether **22** (1.00 eq., 15.0 mg, 26.2 µmol) was dissolved in CH_2Cl_2/TFA (1:1, 5 mL) and stirred for 1 h. Volatiles were removed under reduced pressure and the residue was redissolved in CH_2Cl_2 (5 mL). After

removal of the solvent, acid **4** could be isolated as an orange powder (13.3 mg, 25.8 µmol, 99%). UPLC-MS: Method 1, T_R = 5.77 min; MS (ESI+) m/z: 512.4 [30%, M-(ala-O-*t*bu) + H^+], 601.1 [100%, M + H^+].

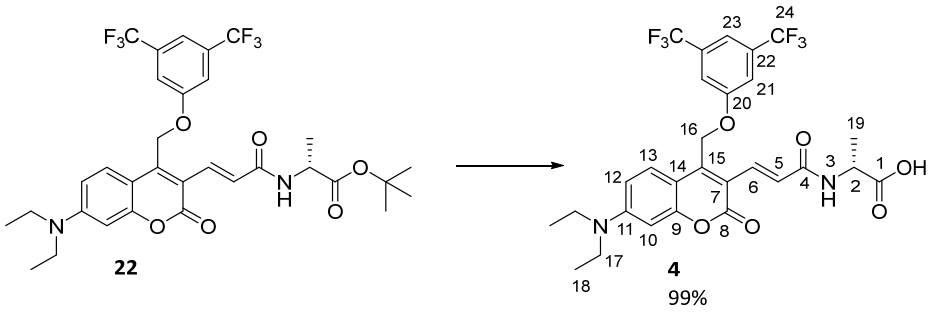

^{1}H-NMR ($CDCl_3$, 500 MHz, 293 K) δ: 7.80 (d, $^3J_{H\text{-}H}$ = 15.0 Hz, 1 H, H-6), 7.54 (s, 1 H, H-23), 7.53 (d, $^3J_{H\text{-}H}$ = 15.0 Hz, 1 H, H-5), 7.45 (d, $^3J_{H\text{-}H}$ = 9.2 Hz, 1 H, H-13), 7.43 (s, 2 H, H-21), 6.84 (s, 1 H, H-3), 6.63 (dd, $^3J_{H\text{-}H}$ = 9.2 Hz , $^4J_{H\text{-}H}$ = 2.6 Hz, 1 H, H-12), 6.53 (d, $^4J_{H\text{-}H}$ = 2.6 Hz, 1 H, H-10), 5.44-5.37 (m, 2 H, H-16), 4.65 (p, $^3J_{H\text{-}H}$ = 6.8 Hz, 1 H, H-2), 3.45 (q, $^3J_{H\text{-}H}$ = 7.1 Hz, 4 H, H-17), 1.53 (d, $^3J_{H\text{-}H}$ = 7.1 Hz, 3 H, H-19), 1.23 (t, $^3J_{H\text{-}H}$ = 7.1 Hz, 6 H, H-18). ^{13}C-NMR δ: 173.8 (C-1), 167.4 (C-4), 160.3 (C-8), 158.4 (C-20), 155.6 (C-9), 151.4 (C-11), 146.3 (C-15), 132.1 (C-6), 126.6 (C-13), 124.8 (C-5), 122.9 (C-22), 115.4 (C-23), 115.0 (C-21), 114.0 (C-7), 109.9 (C-12), 107.8 (C-14), 97.1 (C-10), 62.4 (C-16), 48.8 (C-2), 44.8 (C-17), 17.4 (C-19), 12.4 (C-18), C-24 was not detected.

(*S*,*E*)-2-(2-(3-(4-((3,5-bis(trifluoromethyl)phenoxy)methyl)-7-(diethylamino)-2-oxo-2*H*-chromen-3-yl)acrylamido)propanamido)-*N,N,N*-trimethylethan-1-aminium (6)

Acid **4** (1.00 eq. 15.0 mg, 25.0 µmol) was dissolved in DMF (5 mL), NH_3-CH_2-CH_2-$NMe_3^{2+}I^-TFA^-$ (2.00 eq. 17.2 mg, 50.0 µmol), HBTU (2.00 eq., 19.0 mg, 50.0 µmol) and DIPEA (4.00 eq., 16.5 µl, 100 µmol) were added and the solution was stirred for 3 h at room temperature. Volatiles were removed under reduced pressure and the residue was purified by reversed phase preperative HPLC. After lyophilisation, the cationic cleavable **6**was isolated as an orange powder (1.5 mg, 1.9 µmol, 8%). UPLC-MS: Method 1, T_R = 4.74 min; MS (ESI+) m/z: 343.1 [100%, M^++ H^+], 685.7 [50%, M^+].

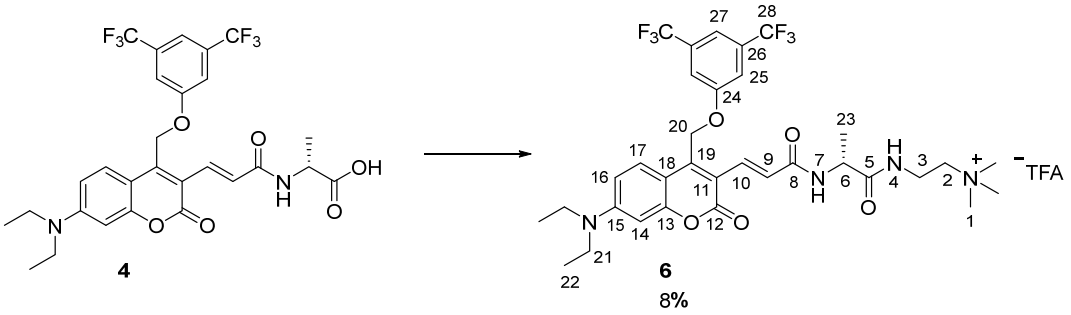

^{1}H-NMR (MeCN-d_3, 500 MHz, 293 K) δ: 7.67 (s, 1 H, H-27), 7.65 (d, $^{3}J_{H\text{-}H}$ = 15.2 Hz, 1 H, H-10), 7.61 (s, 2 H, H-25), 7.59 (d, $^{3}J_{H\text{-}H}$ = 9.3 Hz, 1 H, H-17), 7.46 (t, $^{3}J_{H\text{-}H}$ = 6.0 Hz, 1 H, H-4), 7.26 (d, $^{3}J_{H\text{-}H}$ = 6.8 Hz, 1 H, H-7), 7.19 (d, 15.2 Hz, 1 H, H-9), 6.72 (dd, $^{3}J_{H\text{-}H}$ = 9.3 Hz , $^{4}J_{H\text{-}H}$ = 2.6 Hz, 1 H, H-16), 6.55 (d, $^{4}J_{H\text{-}H}$ = 2.6 Hz, 1 H, H-14), 5.50-5.42 (m, 2 H, H-20), 4.31 (p, $^{3}J_{H\text{-}H}$ = 6.8 Hz, 1 H, H-6), 3.63-3.53 (m, 2 H, H-3), 3.47 (q,$^{3}J_{H\text{-}H}$ = 7.1 Hz, 4 H, H-21), 3.35 (t, $^{3}J_{H\text{-}H}$ = 6.1 Hz, 2 H, H-2), 3.03 (s, 9 H, H-1), 1.30 (d, $^{3}J_{H\text{-}H}$ = 7.2 Hz, 3 H, H-23), 1.18 (t, $^{3}J_{H\text{-}H}$ = 7.9 Hz, 6 H, H-22). ^{13}C-NMR δ: 173.5 (C-5), 166.1 (C-8), 160.0 (C-12), 159.0 (C-24), 155.7 (C-13), 151.6 (C-15), 146.2 (C-19), 132.2 (C-10), 127.7 (C-17), 126.0 (C-9) 123.4 (C-26), 116.7 (C-25), 115.8 (C-27), 114.7 (C-11), 107.6 (C-18), 65.4 (C-2), 63.9 (C-20), 54.1 (C-1), 34.3 (C-3), 17.4 (C-23), 11.7 (C-22).

References

1. T. Slanina; P. Shrestha; E. Palao; D. Kand; J. A. Peterson; A. S. Dutton; N. Rubinstein; R. Weinstain; A. H. Winter; P. Klan, In search of the perfect photocage: structure-reactivity relationships in meso-methyl BODIPY photoremovable protecting groups. *J. Am. Chem. Soc.* **2017,** *139* (42), 15168-15175.
2. W. Timo; G. Markus; G. Christian; P. Thomas; G. Michael, Synthesis of a Cytidine Phosphoramidite with Protected Nitroxide Spin Label for EPR Experiments with RNA. *Eur. J. Org. Chem.* **2017,** *2017* (3), 491-496.
3. J. P. Olson; H.-B. Kwon; K. T. Takasaki; C. Q. Chiu; M. J. Higley; B. L. Sabatini; G. C. R. Ellis-Davies, Optically Selective Two-Photon Uncaging of Glutamate at 900 nm. *J. Am. Chem. Soc.* **2013,** *135* (16), 5954-5957.

Abbreviation

Abbreviation	Name
2D NMR	2-Dimensional NMR
A	Alanine
aa	Amino acid
Ala	Alanine
AIMD	Ab initio molecular dynamics
APS	Ammonium peroxodisulfate
Boc-	*tert*-butyloxycarbonyl
BODIPY	Boron-dipyrromethene
BP	Base pair
$CDCl_3$	Deuterated chloroform
CH_2Cl_2	Dichloromethane
$CHCl_3$	Chloroform
CID	Collision-induced dissociation
^{13}C-NMR	Carbon NMR
COSY	Correlation spectroscopy
CREMS	Charge reduction electrospray mass spectrometry
DBU	Diazabicycloundecene
DIAD	Diisopropyl azodicarboxylate
DIPEA	*N,N*-Diisopropylethylamine
DMAP	4-Dimethylaminopyridine
DMF	*N,N*-Dimethylformamide
DMF-d_7	Heptadeutero-*N,N*-dimethylformamide
DMF-DMA	*N,N*-Dimethylformamide dimethyl acetal
DMSO-d_6	Hexadeuterodimethyl sulfoxide
DNA	Deoxyribonucleic acid
DTT	Dithiothreitol
E	Glutamate
EDC	1-Ethyl-3-(3-dimethylaminopropyl)carbodiimide
ESI	Electrospray ionization
Et_2O	Diethylether
EtOAc	Ethyl acetate
Fmoc-	Fluorenylmethoxycarbonyl-
FRET	Förster resonance energy transfer
G	Glycine
Gly	Glycine
HBTU	Hexafluorophosphate benzotriazole tetramethyl uronium
^{1}H-NMR	Proton NMR
HFIP	1,1,1,3,3,3-Hexafluoroisopropanol
HFIP-d_2	Dideutero-1,1,1,3,3,3-hexafluoroisopropanol
His-tag	Polyhistidine-tag
HMBC	Heteronuclear multiple-bond correlation spectroscopy
HMQC	Heteronuclear multiple-quantum correlation spectroscopy
HPLC	High-performance liquid chromatography
HSQC	Heteronuclear single quantum coherence spectroscopy
HRMS	High-resolution mass spectrometry
IMS-MS	Ion-mobility-spectrometry-mass spectrometry

Abbreviation	Name
K	Lysine
KDTL	Kapitza–Dirac–Talbot–Lau interferometer
L	Leucine
LG	Leaving group
LUMI	Long baseline universal matter-wave interferometer
Lys	Lysine
MALDI	Matrix assisted laser desorption/ionization
MeCN	Acetonitrile
MeMgBr	Methylmagnesium bromide
miliQ water	Ultrapure water gained by purification system from *Millipore Corporation*
MS	Mass spectrometry
MWCO	Molecular weight cut-off
NBS	*N*-Bromosuccinimide
Nd:YAG	Neodymium-doped yttrium aluminum garnet
NMR	Nuclear magnetic resonance spectroscopy
NOESY	Nuclear overhauser enhancement and exchange spectroscopy
NHS-ester	*N*-hydroxysuccinimide ester
NMR	Nuclear magnetic resonance spectroscopy
NOSEY	Nuclear Overhauser effect spectroscopy
PCT	Photocleavable tag
PDA detector	Photo diode array detector
PPh_3	Triphenylphosphine
Pro	Proline
PyBOP	Benzotriazol-1-yl-oxytripyrrolidinophosphonium hexafluorophosphate
QCI-F Probe	Quadruple resonance cryoprobe
QMS	Quadrupole mass spectrometer
rt	Room temperature
S	Serine
SEC	Size exclusion chromatography
SQ detector	Single quadrupole detector
SDS-PAGE	Sodium dodecyl sulfate polyacrylamide gel electrophoresis
TBAF	Tetra-*n*-butylammonium fluoride
TBDMS-Cl	*tert*-Butyldimethylsilyl chloride
TFA	Trifluoroacetic acid
TEMED	Tetramethylethylendiamine
THF	Tetrahydrofuran
TOF	Time of flight
Tris-HCl	Tris(hydroxymethyl)aminomethane hydrochloride
Trp	Tryptophan
Tyr	Tyrosine
TSTU	*N,N,N',N'*-Tetramethyl-*O*-(*N*-succinimidyl)uranium tetrafluorborate
UPLC	Ultra performance liquid chromatography
VUV	Vacuum ultraviolet
W	Tryptophan
wt	Wild type

Dr. Jonas Schaetti

Research Chemist

Steinbühlalle 41, 4054 Basel
Date of birth: 15.07.1990
Nationality: Swiss
E-Mail: jonas.schaetti@unibas.ch
LinkedIn: www.linkedin.com/in/jonas-schaetti

Profile

- PhD in nanoscience (magna cum laude)
- Main focus on preparative organic synthesis and solid-phase peptide synthesis
- Strong background in analytical chemistry

Technical expertise

- Analytical methods: UPLC-MS, prep. HPLC, SEC, UPC^2, GC-MS, SPPS, NMR including 2D-NMR)
- Experience in analytical method development
- Software applications: Microsoft Office (Word, Excel, PowerPoint), Chemdraw, Mestrenova, Origin, PyMOL, MassLynx, Chromeleon
- Broad experience in preparative organic synthesis and solid-phase peptide synthesis
- Cultivation and handling of *E. coli* cells including recombinant protein expression, isolation and purification

Education

2015 –2019 PhD at the University of Basel (Swiss Nanoscience Institute) in the Research group of **Prof. Dr. Marcel Mayor / Dr. Valentin Köhler**.The topic of my PhD thesis was «Towards matter-wave experiments with biomolecules: Generation and detection of neutral biomolecular beams». I was responsible for the synthesis and modification of peptides and proteins. A substantial part of my work was the complete characterization of complex peptides with NMR, UV/Vis and UPLC-MS.

2012–2014 Master in chemistry at the University of Basel, Master thesis in the Research group of **Prof. Dr. Thomas Ward**. The topic of my master thesis was « New catalytic activity arising from metallation of a putative facial triad motif within a lactonase». I expressed 10 different proteins baring a putative metal binding site (His-triad) and several point mutations. I performed an oxidation activity screening and measured Michaelis Menten kinetics.

2009-2012 Bachelor in chemistry at the University of Basel

Communication and presentation

- Clear and precise writing style, resulting in 4 First-authored research publications during my PhD
- Communication and presentation of my research results in various forms (talks and poster presentation) at group meetings as well as several international conferences

Management and teamwork

- Working together in different interdisciplinary research collaborations
- Learned in my PhD to manage my own research project including design and planning of the work, time-management of the day-to-day research in the lab and meeting of deadlines.
- Independently developed strategies to solve given problems. Carefully analyzed literature and experimental data, drew conclusions and successfully applied them to proceed with my research.

Teaching

- **Project supervision**, University of Basel, Switzerland
  Supervision of 8 research projects from bachelor and master students during my PhD.
- **Teaching Assistant**, University of Basel, Switzerland
  Supervising Chemistry practical courses for chemistry, biology and nanoscience students (6 Semester)
- **Group responsibility for HPLC's**, University of Basel, Switzerland
  Giving introductions and help to the use of UPLC-MS, HPLC and prep. HPLC

Language skills

- German (native speaker)
- English (full professional proficiency, written and spoken)
- French (limited working proficiency)

Hobbies and interests

- Strategy board games (member of a local chess club)
- Volleyball/ beach volleyball
- Outdoor sports (hiking, biking, skiing)

Publications

2019 J. Schaetti et al., *Chem. Commun.,* **2019**, 55, 12507-12510.

2018 J. Schaetti et al., *Commun. Chem.,* **2018**, *1 (1)*, 93.

2018 J. Schaetti, et al., *Phys. Chem. Chem. Phys.* **2018**, *20 (16)*, 11412-11417.

2017 J. Schaetti, et al., *J. Mass Spectrom.* **2017**, *52 (8)*, 550-556.

2015 N. Fujieda and J. Schaetti, et al., *Chem. Sci.,* **2015**, *6*, 4060–4065.